eCAM
Evidence-Based Complementary and Alternative Medicine

Neurobiological Mechanisms of Acupuncture

Guest Editors: Lijun Bai, Richard E. Harris, Jian Kong, Lixing Lao, Vitaly Napadow, and Baixiao Zhao

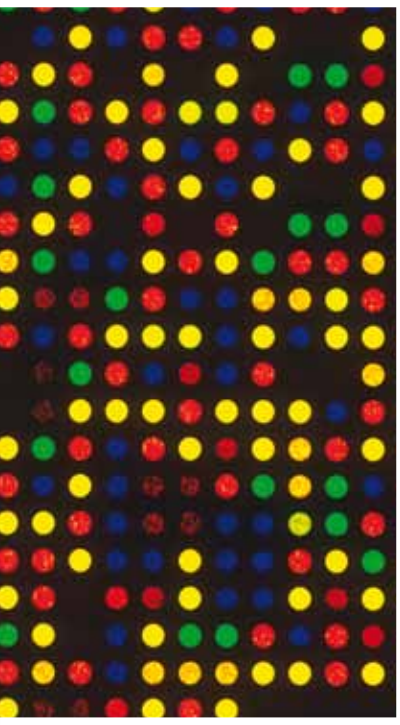

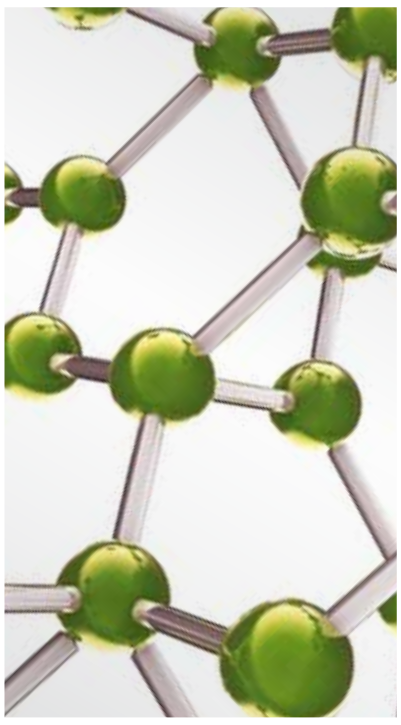


Neurobiological Mechanisms of Acupuncture

Evidence-Based Complementary and Alternative Medicine

Neurobiological Mechanisms of Acupuncture

Guest Editors: Lijun Bai, Richard E. Harris, Jian Kong, Lixing Lao, Vitaly Napadow, and Baixiao Zhao

Editorial Board

Contents

Neurobiological Mechanisms of Acupuncture, Lijun Bai, Richard E. Harris, Jian Kong, Lixing Lao, Vitaly Napadow, and Baixiao Zhao
Volume 2013, Article ID 652457, 2 pages

Effects of Pretreatment with a Combination of Melatonin and Electroacupuncture in a Rat Model of Transient Focal Cerebral Ischemia, Lingguang Liu and R. T. F. Cheung
Volume 2013, Article ID 953162, 12 pages

Electroacupuncture Stimulation at CV12 Inhibits Gastric Motility via TRPV1 Receptor, Zhi Yu, Xin Cao, Youbing Xia, Binbin Ren, Hong Feng, Yali Wang, Jingfeng Jiang, and Bin Xu
Volume 2013, Article ID 294789, 6 pages

Neural Encoding of Acupuncture Needling Sensations: Evidence from a fMRI Study, Xiaoling Wang, Suk-Tak Chan, Jiliang Fang, Erika E. Nixon, Jing Liu, Kenneth K. Kwong, Bruce R. Rosen, and Kathleen K. S. Hui
Volume 2013, Article ID 483105, 15 pages

Effect of Bee Venom Acupuncture on Oxaliplatin-Induced Cold Allodynia in Rats, Bong-Soo Lim, Hak Jin Moon, Dong Xing Li, Munsoo Gil, Joon Ki Min, Giseog Lee, Hyunsu Bae, Sun Kwang Kim, and Byung-Il Min
Volume 2013, Article ID 369324, 8 pages

Multivariate Granger Causality Analysis of Acupuncture Effects in Mild Cognitive Impairment Patients: An fMRI Study, Shangjie Chen, Lijun Bai, Maosheng Xu, Fang Wang, Liang Yin, Xuming Peng, Xinghua Chen, and Xuemin Shi
Volume 2013, Article ID 127271, 12 pages

Mechanisms of Electroacupuncture-Induced Analgesia on Neuropathic Pain in Animal Model, Woojin Kim, Sun Kwang Kim, and Byung-Il Min
Volume 2013, Article ID 436913, 11 pages

Electroacupuncture Could Regulate the NF-κB Signaling Pathway to Ameliorate the Inflammatory Injury in Focal Cerebral Ischemia/Reperfusion Model Rats, Wen-yi Qin, Yong Luo, Ling Chen, Tao Tao, Yang Li, Yan-li Cai, and Ya-hui Li
Volume 2013, Article ID 924541, 15 pages

Acupuncture-Evoked Response in Somatosensory and Prefrontal Cortices Predicts Immediate Pain Reduction in Carpal Tunnel Syndrome, Yumi Maeda, Norman Kettner, Jeungchan Lee, Jieun Kim, Stephen Cina, Cristina Malatesta, Jessica Gerber, Claire McManus, Jaehyun Im, Alexandra Libby, Pia Mezzacappa, Leslie R. Morse, Kyungmo Park, Joseph Audette, and Vitaly Napadow
Volume 2013, Article ID 795906, 13 pages

Placebo Acupuncture Devices: Considerations for Acupuncture Research, Dan Zhu, Ying Gao, Jingling Chang, and Jian Kong
Volume 2013, Article ID 628907, 9 pages

Hypothalamus-Related Resting Brain Network Underlying Short-Term Acupuncture Treatment in Primary Hypertension, Hongyan Chen, Jianping Dai, Xiaozhe Zhang, Kai Wang, Shuhua Huang, Qingtian Cao, Hong Wang, Yuhong Liang, Chuanying Shi, Mengyuan Li, Tingting Ha, Lin Ai, Shaowu Li, Jun Ma, Wenjuan Wei, Youbo You, Zhenyu Liu, Jie Tian, and Lijun Bai
Volume 2013, Article ID 808971, 9 pages

Acupuncture Effect and Central Autonomic Regulation, Qian-Qian Li, Guang-Xia Shi, Qian Xu, Jing Wang, Cun-Zhi Liu, and Lin-Peng Wang
Volume 2013, Article ID 267959, 6 pages

fMRI Evidence of Acupoints Specificity in Two Adjacent Acupoints, Hua Liu, Jian-Yang Xu, Lin Li, Bao-Ci Shan, Bin-Bin Nie, and Jing-quan Xue
Volume 2013, Article ID 932581, 5 pages

Visceral Nociceptive Afferent Facilitates Reaction of Subnucleus Reticularis Dorsalis to Acupoint Stimulation in Rats, Liang Li, Lingling Yu, Peijing Rong, Hui Ben, Xia Li, Bing Zhu, and Rixin Chen
Volume 2013, Article ID 931283, 7 pages

Neurobiological Foundations of Acupuncture: The Relevance and Future Prospect Based on Neuroimaging Evidence, Lijun Bai and Lixing Lao
Volume 2013, Article ID 812568, 9 pages

Effects of Moxa Smoke on Monoamine Neurotransmitters in SAMP8 Mice, Huanfang Xu, Baixiao Zhao, Yingxue Cui, Min Yee Lim, Ping Liu, Li Han, Hongzhu Guo, and Lixing Lao
Volume 2013, Article ID 178067, 6 pages

Enhanced Antidepressant-Like Effects of Electroacupuncture Combined with Citalopram in a Rat Model of Depression, Jian Yang, Yu Pei, Yan-Li Pan, Jun Jia, Chen Shi, Yan Yu, Jia-Hui Deng, Bo Li, Xiao-Li Gong, Xuan Wang, Xiao-Min Wang, and Xin Ma
Volume 2013, Article ID 107380, 12 pages

Modulation of Brain Electroencephalography Oscillations by Electroacupuncture in a Rat Model of Postincisional Pain, Jing Wang, Jing Wang, Xuezhu Li, Duan Li, Xiao-Li Li, Ji-Sheng Han, and You Wan
Volume 2013, Article ID 160357, 11 pages

Long-Term Stimulation with Electroacupuncture at DU20 and ST36 Rescues Hippocampal Neuron through Attenuating Cerebral Blood Flow in Spontaneously Hypertensive Rats, Gui-Hua Tian, Kai Sun, Ping Huang, Chang-Man Zhou, Hai-Jiang Yao, Ze-Jun Huo, Hui-Feng Hao, Lei Yang, Chun-Shui Pan, Ke He, Jing-Yu Fan, Zhi-Gang Li, and Jing-Yan Han
Volume 2013, Article ID 482947, 10 pages

Spinal Serotonergic and Opioid Receptors Are Involved in Electroacupuncture-Induced Antinociception at Different Frequencies on ZuSanLi (ST 36) Acupoint, Chi-Chung Kuo, Huei-Yann Tsai, Jaung-Geng Lin, Hong-Lin Su, and Yuh-Fung Chen
Volume 2013, Article ID 291972, 10 pages

The Possible Neuronal Mechanism of Acupuncture: Morphological Evidence of the Neuronal Connection between Groin A-Shi Point and Uterus, Chun-Yen Chen, Rey-Shyong Chern, Ming-Huei Liao, Yung-Hsien Chang, Jung-Yu C. Hsu, and Chi-Hsien Chien
Volume 2013, Article ID 429186, 13 pages

Hindawi Publishing Corporation
Evidence-Based Complementary and Alternative Medicine
Volume 2013, Article ID 652457, 2 pages
http://dx.doi.org/10.1155/2013/652457

Editorial

Neurobiological Mechanisms of Acupuncture

Lijun Bai,[1] Richard E. Harris,[2] Jian Kong,[3] Lixing Lao,[4] Vitaly Napadow,[5] and Baixiao Zhao[6]

[1] *The Key Laboratory of Biomedical Information Engineering, Ministry of Education, Department of Biomedical Engineering, School of Life Science and Technology, Xi'an Jiaotong University, Xi'an 710049, China*
[2] *Department of Anesthesiology, University of Michigan, Ann Arbor, MI 48109, USA*
[3] *Department of Psychiatry, Massachusetts General Hospital (MGH), Harvard Medical School, Boston, MA 02129, USA*
[4] *School of Chinese Medicine, The University of Hong Kong, 10 Sassoon Road, Pokfulam, Hong Kong*
[5] *MGH/HMS/MIT Martinos Center for Biomedical Imaging, Massachusetts General Hospital, Harvard Medical School, Boston, MA 02129, USA*
[6] *School of Acupuncture-Moxibustion and Tuina, Beijing University of Chinese Medicine, Beijing 100029, China*

Correspondence should be addressed to Lijun Bai; bailj4152615@gmail.com

Received 24 November 2013; Accepted 24 November 2013

Acupuncture, an age-old healing art, has been accepted to effectively treat various diseases, particularly chronic pain and neurodegenerative diseases. Since its public acceptance and good efficacy, increasing attention has been now paid to exploring the physiological and biochemical mechanisms underlying acupuncture, particularly the brain mechanisms. Basic and clinical acupuncture studies on neurobiological mechanisms of acupuncture are crucial for the development of acupuncture. This issue compiles 32 exciting papers, most of which are very novel and excellent investigations in this field.

The neural mechanism underlying acupuncture analgesia was addressed in four articles. J. Wang et al. established a postincisional pain model of rats and investigated electroacupuncture effect on the brain oscillations involving postoperative pain. B.-S. Lim et al., using interesting bee venom acupuncture, explored whether it can relieve oxaliplatin-induced cold allodynia and which endogenous analgesic system is implicated. The paper by Y. Maeda et al. aimed to evaluate this linkage between brain response to acupuncture and subsequent analgesia in chronic pain patients with carpal tunnel syndrome. Since many articles aimed to assess the effect of electroacupuncture induced analgesia, W. Kim et al. systemically conducted a review to assess the efficacy and clarify its mechanism on neuropathic pain. In addition, as a great challenge in acupuncture analgesia and treatment evaluations, D. Zhu et al. outlined the advantages and disadvantages of kinds of acupuncture controls and highlighted how the differences among placebo devices can be used to isolate distinct components of acupuncture treatment.

Five papers deal with potential neural mechanism underlying acupuncture treatments on the stroke, hypertension, and mild cognitive impairments. The paper by L. Liu and R. T. F. Cheung aimed to investigate whether the combination of melatonin and electroacupuncture therapies could be beneficial against transient focal cerebral ischemia in a rat model of transient middle cerebral artery occlusion. W. Qin et al. accompanied by L. Liu and R. T. F. Cheung's paper explored the importance of anti-inflammatory acupuncture treatment for the focal cerebral ischemia/reperfusion by inhibiting the NF-κB signaling pathway. Another two papers mainly focused on the acupuncture modulation of neural mechanism for hypertension regulation with long-term as well as short-term treatments. The paper by G.-H. Tian et al. addressed the long-term electroacupuncture on cerebral microvessels and neurons in CA1 region of hippocampus in spontaneously hypertensive rats. H. Chen et al. aimed to explore the hypothalamus-anchored resting brain network underlying primary hypertension patients after short-term acupuncture treatments. Moreover, for mild cognitive impairments, S. Chen et al. have pointed out that acupuncture

at KI3 at different cognitive states and with varying needling depths may induce distinct reorganizations of effective connectivity of brain networks.

The neuroendocrine system involving acupuncture has been addressed by the following three papers. Z. Yu et al. has suggested that TRPV1 receptor is partially involved in the electroacupuncture-mediated modulation of gastric motility. The paper by C.-C. Kuo et al. explored the mechanism of electroacupuncture (EAc) induced antinociception involved opioid receptors and the serotonergic system. Q.-Q. Li et al. conducted a systemic review about the central mechanism of acupuncture in modulating various autonomic responses. Moreover, other papers focused on the relatively acupoint specificity from wide aspects. One of the studies by L. Li et al. suggested that both the size and function of the acupoints comply with the functionality of the internal organs; thus the sensitive degree of acupoints changed according to malfunction of internal organs. C.-Y. Chen et al. implied that somatoparasympathetic neuronal connection (groin-spinal dorsal horn-NTS/DMX-uterus) and a somatosympathetic neuronal connection (groin-spinal dorsal horn-NTS-PVN-uterus) could be the prerequisites to the neuronal basis of the somatovisceral reflex and also the neuronal mechanism of acupuncture. Z. Wang et al. advanced that the modulatory effects of different needling sensations induced by relatively different acupoints contribute to acupuncture modulations of limbic-paralimbic-neocortical network. Although the acupoints were spatially adjacent, there was also relatively functional specificity inflected by brain networks.

By gathering these papers, we hope to enrich our readers and researchers with respect to the underlying neurological mechanism of acupuncture, and we look forward to an increasing number of both clinical trials and experimental studies to further promote the development of understanding the neurological mechanism involving acupuncture.

Lijun Bai
Richard E. Harris
Jian Kong
Lixing Lao
Vitaly Napadow
Baixiao Zhao

Hindawi Publishing Corporation
Evidence-Based Complementary and Alternative Medicine
Volume 2013, Article ID 953162, 12 pages
http://dx.doi.org/10.1155/2013/953162

Research Article

Effects of Pretreatment with a Combination of Melatonin and Electroacupuncture in a Rat Model of Transient Focal Cerebral Ischemia

Lingguang Liu and R. T. F. Cheung

Department of Medicine, Li Ka Shing Faculty of Medicine, University of Hong Kong, Hong Kong

Correspondence should be addressed to R. T. F. Cheung; rtcheung@hku.hk

Received 22 February 2013; Revised 1 July 2013; Accepted 5 August 2013

Academic Editor: Richard E. Harris

Both melatonin and electroacupuncture (EA) have been suggested to be effective treatments against stroke. However, it is unknown whether a combination of these two therapies could be beneficial against transient focal cerebral ischemia. The present study investigated the effects of pretreatment of a combination of melatonin and EA in a rat model of transient middle cerebral artery occlusion (MCAO). After pretreatment of melatonin plus EA (MEA), transient MCAO was induced for 90 minutes in male Sprague-Dawley (SD) rats. The neurological deficit score, brain infarct volume, cerebral edema ratio, neuronal inflammation, and apoptosis were evaluated 24 hours after transient MCAO. The expression of related inflammatory and apoptotic mediators in the brain was also investigated. The results showed that MEA improved neurological outcome, reduced brain infarct volume, and inhibited neuronal inflammation as well as apoptosis 24 hours after transient MCAO. The beneficial effects may derive from downregulation of proinflammatory and proapoptotic mediators and upregulation of antiapoptotic mediators. Thus, these results suggest a preventive effect of pretreatment of MEA on transient focal cerebral ischemia.

1. Introduction

Stroke is a serious cerebral vascular event with increasing prevalence worldwide especially in the society with aging of the population, and ischemic stroke is the most common type. Intravenous thrombolysis using recombinant tissue plasminogen activator (rtPA) is the only approved treatment [1]. Many neuroprotectants have been investigated; they were effective in animals but not in stroke patients [2–4]. Owing to the narrow therapeutic time window [5, 6] and a substantial risk of hemorrhagic complications, clinical use of rtPA is limited to a small number of stroke patients [7]. Thus, broader attention to integrated therapeutics has been advocated repeatedly for treating ischemic stroke to increase the chance of success [4, 8, 9]. Moreover, most of the current therapies are focused on posttreatment after cerebral ischemia. However, accumulating lines of evidence have demonstrated the efficacy of pretreatment therapies which could induce neuroprotection against cerebral ischemic injury.

Melatonin is a potent antioxidant and free radical scavenger with few toxicological effects in animals and humans [10]. An adequate amount of evidence indicates its effective protection against stroke in different models and animal species [11–16]. Although the beneficial effect of melatonin as well as its related mechanisms can be further investigated, some clinical scientists have suggested that melatonin, combined with other neuroprotectants or proven therapies, may enhance the treatment effects or extend the therapeutic time window. Moreover, it is worthy of conducting phase II or III clinical trials of melatonin in stroke patients [11].

Acupuncture has been widely applied to stroke patients in East Asia for centuries. It is easy to manipulate, economical and safe. EA is a combination of traditional acupuncture (manual acupuncture) and electrical stimulation. It is believed to enhance the efficacy of acupuncture and is currently used to treat various kinds of illnesses [17, 18]. Though the research in this field using western scientific methods is still in the very beginning, increasing clinical and

experimental publications have provided physiological rather than metaphysical evidence to confirm and explain both the phenomena and mechanisms of acupuncture [18–22]. Nevertheless, the beneficial effects of acupuncture on stroke recovery remain controversial. This may be due to poor experimental design, inappropriate controls, and small sample size [23].

In traditional Chinese medical theory, acupuncturing at the acupoints along the meridian of Yangming (stomach meridian) is especially efficient for the treatment of flaccid paralysis. Zusanli (ST 36) is the classical acupoint recorded in the ancient Chinese medical literature for thousands of years and has been frequently investigated in scientific study for treating stroke. Moreover, the literature review shows that ST 36 and xiajuxu (ST 39) are the mostly investigated acupoints including animal and clinical studies [24, 25]. Their beneficial effects on ischemic stroke have also been elucidated and reported. In the present study, both ST 36 and ST 39 were chosen for EA treatment.

Evidence from animal research in acute cerebral ischemia shows that combinations of neuroprotectants might be more efficacious than the single agent given alone. Both melatonin and EA have been suggested to be effective treatments against cerebral ischemia. However, it is unknown whether a combination of these two therapies could be beneficial against focal cerebral ischemia.

There are increasing lines of evidence that pretreatment of neuroprotectants effectively improves neurological outcome and interferes with mechanisms of brain injury [26, 27]. In the present study, pretreatment of MEA was conducted to examine whether MEA could exert neuroprotection against transient cerebral ischemia and which mechanisms are behind it.

2. Materials and Methods

2.1. Animals and Surgical Procedures. Adult male SD rats, weighing between 250 and 280 g, were obtained from the Laboratory Animal Unit, The University of Hong Kong, and kept under 12 hours light/12 hours dark conditions. The experiments were performed according to the institutional regulation and guidelines approved by the Committee on the Use of Live Animals in Teaching and Research (CULATR), The University of Hong Kong.

Transient focal cerebral ischemia was induced using right-sided transient endovascular MCAO [28–30] with reperfusion. In brief, the right common carotid artery (CCA), right external carotid artery (ECA), and right internal carotid artery (ICA) were exposed through a midline cervical incision. With the right ECA dissected free and its distal branches coagulated (Bipolar Electric Coagulation, GN60, Aesculap AG and Co., Tuttlingen, Germany), a 5-o silk suture was loosely tied around the ECA stump, and microclips were temporarily placed at both the right CCA and right ICA. A piece of silicone coated 4-o (5 mm coating length with 0.35–0.37 mm diameter) nylon suture (Doccol Corporation, Redlands, CA; Cat no. 4037) was inserted into the lumen of right ECA stump, and the 5-o silk suture was gently tightened to prevent bleeding. Next the nylon suture was gently advanced through right ICA into the right anterior cerebral artery (ACA) to occlude the right middle cerebral artery (MCA) at its origin. The rats were subjected to 90 minutes of focal cerebral ischemia, and then the silicon coated 4-o nylon suture was carefully withdrawn to permit reperfusion. The wounds were closed using 4-o nylon sutures, and the rats were allowed to fully recover from the anesthesia before returning to their cages.

The focal cerebral ischemia was confirmed by obvious changes of regional cerebral blood flow (rCBF) on laser Doppler flow meter (MBF3D, Moor instruments, Ltd., Devon, UK). A burr hole of 2 mm diameter was made on the right side of skull at 5 mm lateral and 2 mm posterior to the bregma with the aid of a stereotaxic device (SR-6N; Narishige Scientific Instrument Laboratory, Tokyo, Japan). Next the laser probe was glued onto the burr hole. Steady-state baseline values were documented before induction of cerebral ischemia, and all rCBF were normalized and expressed as percentages of baseline values.

2.2. Experimental Groups. Rats were assigned to one of two groups: control group and MEA group.

(1) Control group: the vehicle, normal saline containing 3% dimethyl sulfoxide (DMSO, Sigma-Aldrich, St. Louis, MO, USA), was given via an intraperitoneal (i.p.) injection 30 minutes before transient MCAO. Sham EA treatment was given once per day and started 6 days before transient MCAO. During the sham EA treatment, rats were anesthetized with an i.p. injection of sodium pentobarbital at a dose of 40 mg/kg without real EA stimulation.

(2) MEA group: a single dose of melatonin (10 mg/kg) was given via an i.p. injection 30 minutes before transient MCAO. Whilst under anesthesia, EA treatment was given once per day and started 6 days before transient MCAO. Melatonin (Sigma-Aldrich) was dissolved in 1 mL of normal saline containing 3% DMSO.

A schematic overview of the experimental procedures was summarized (Figure 1). All the rats were sacrificed 24 hours after transient MCAO for determination of brain infarct volume, cerebral edema ratio, and tissue processing. Neurological outcome of rats was evaluated before sacrifice.

2.3. Manipulation of EA Treatment. A thirty-minute real or sham EA treatment was applied each time at different time points (daily administration during the 6 days before transient MCAO) with a Han's acupoint nerve stimulator (HANS-200, Jisheng Medical Science and Technology Co., Ltd., Nanjing, China). The stimulation intensity was 0.5 mA, and the stimulation frequency was 2 Hz. Four stainless steel acupuncture needles (0.25 mm in diameter, 25 mm in length; Huatuo, Suzhou Medical Instruments Factory, Suzhou, China) were inserted bilaterally with a 4 mm depth into two acupoints, ST 36 and ST 39. A Han's acupoint stimulator was connected to the inserted acupuncture needles. The location of these two acupoints was based on the transpositional acupoint system

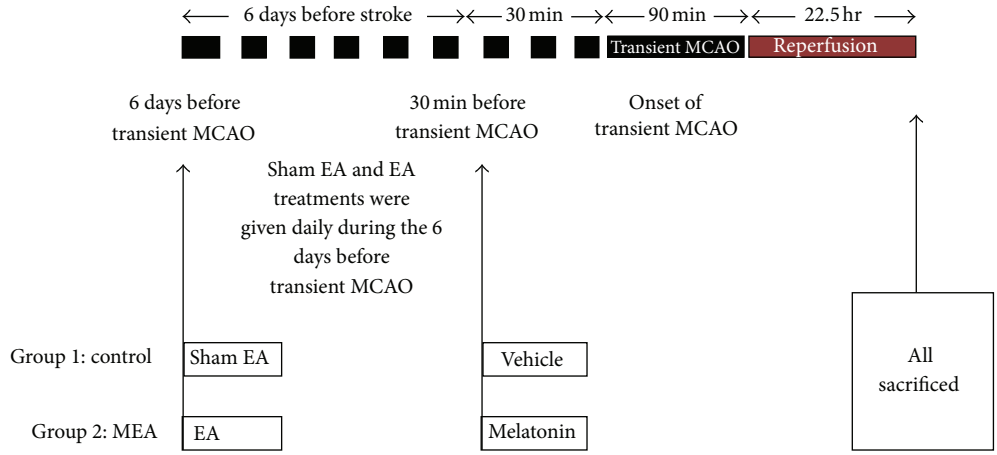

Figure 1: Schematic overview of the experimental procedures in a rat model of transient MCAO. Two groups are included in the experiment. The horizontal line represents time. A single i.p. injection of the vehicle and melatonin was given 30 minutes before transient MCAO in control and MEA groups, respectively. Whilst the rats were under anesthesia, sham and real EA were given daily 6 days before transient MCAO in the sham EA group and EA group, respectively. All the rats were killed 24 hours after transient MCAO for determination of brain infarct volume, cerebral edema ration and tissue processing.

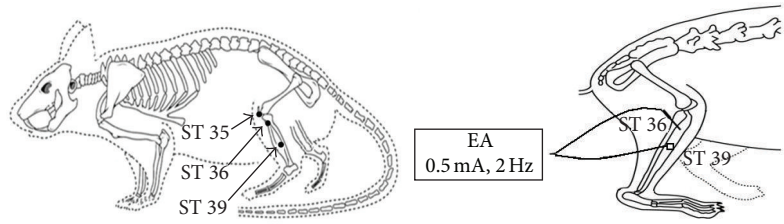

Figure 2: Diagram of the acupoints location and acupuncture manipulation in the rat. ST 35, dubi, is located at the depression lateral to the patella ligament; ST 36, zusanli, is located at proximal one-fifth point on the line from ST 35 to the anterior side of ankle crease; ST 39, xiajuxu, is located at proximal 3 fifths point on the line from ST 35 to the anterior side of ankle crease.

in a rat model [29], which was modified from a former animal transpositional acupoint system [30]. ST 36 is located on the line from dubi (ST 35) to the ankle crease of hind limb and is at proximal one-fifth point of the line. ST 39 is at proximal three-fifths point of the line between ST 35 and the ankle crease. ST 35 is located at the depression on the lateral side of the patella ligament of the hind leg (Figure 2).

2.4. Neurological Behavior Assessment. Neurological deficit scoring system (NDSS) test (Table 1) was used to quantify neurological behavior 24 hours after transient MCAO and was done by a blinded observer. NDSS test was adapted from a validated scoring system [31, 32]. The higher the score, the more severe was the injury. All the rats were trained before operation to be familiar with the testing environment.

2.5. Brain Infarct Volume and Cerebral Edema Ratio Measurement. Brain infarct volume of the right cerebral hemisphere was measured 24 hours after transient MCAO. Under deep anesthesia after an i.p. injection of pentobarbital at 100 mg/kg, the brains were removed and cut into coronal slices of 2 mm thick using a rodent brain matrix (World Precision Instruments, Inc., Sarasota, FL). After reaction with 2% 2,3,5-triphenyltetrazolium chloride (TTC; Sigma-Aldrich) for 20 minutes at 37°C, the slices of brain were fixed in 10% formalin (pH 7.4). Both sides of each slice were scanned for measurement of both hemisphere and infarct volume using a computer assisted image analysis system (Image J Ver. 1.36b, NIH, USA). Unstained areas represented the ischemic lesions. A cerebral edema ratio was calculated from the ratio of the volume of the right hemisphere to the left hemisphere. To compensate for the effect of brain swelling, the actual (corrected) infarct volume was calculated via dividing the volume of infarction by the edema ratio. Brain infarct volume was expressed as a percentage of the contralateral hemisphere [31, 32].

2.6. Histological Examination. At 24 hours after transient MCAO, rats were deeply anesthetized with an i.p. injection of pentobarbital at 100 mg/kg and transcardially perfused with 0.9% normal saline first and then with ice-cold 4% paraformaldehyde (Sigma-Aldrich) in 0.1 M phosphate buffer (PB; pH 7.5). Coronal brain sections at a thickness of 4 μm were made from 2 mm anterior and 1 mm posterior to the

Table 1: Neurological deficit scoring system (NDSS) test.

		Points
Motor tests	*Spontaneous activity*	
	Approaches at least three sides of cage	0
	Approaches at least one rim but not all sides of cage	1
	Slight movement	2
	No movement	3
	Floor walking	
	Straight path	0
	Curvilinear path	1
	Walks only in circles	2
	No walking	3
Sensorimotor tests	*Raising rat by the tail*	
	Flexion of forelimb	1
	Flexion of hindlimb	1
	Thorax twisting	1
	Left limbs placing task	
	Forelimb	
	Normal performance	0
	Delayed (less than 2 seconds)	1
	Delayed (at least 5 seconds) and/or incomplete performance	2
	No performance	3
	Hindlimb	
	Normal performance	0
	Delayed (less than 2 seconds)	1
	Delayed (at least 5 seconds) and/or incomplete performance	2
	No performance	3
Beam balance tests	Walks on the beam	0
	Grasps side of beam	1
	Hugs the beam and one limb falls down from the beam	2
	Hugs the beam and two limbs fall down from the beam or spins on beam (>60 s)	3
	Attempts to balance on the beam but falls off (>40 s)	4
	Attempts to balance on the beam but falls off (>20 s)	5
	Falls off: with no attempt to balance or hang on the beam (<20 s)	6

Maximal number of point is 21. Points were awarded for inability of performing the tasks. The higher the score, the more severe is the injury.

bregma and stained with hematoxylin and eosin (HE). Terminal deoxynucleotidyl transferase dUTP nick end labeling (TUNEL) assay was also performed using an in situ cell death detection kit (Roche, Indianapolis, IN). Brain sections near bregma level 0 were chosen for quantification. The number of TUNEL-positive cells from five selected regions within the infarction and penumbra in the right cerebral hemisphere was counted, respectively. The number of positive cells was counted by a blinded investigator and expressed as number per square millimeter. The section slides were analyzed under light microscope (Axio Vision Control, Carl Zeiss, Munich, Germany).

2.7. Western Blot Analysis. Western blot analysis was used to determine the expression of inflammatory and apoptotic mediators. Rats from the two groups were decapitated 24 hours after transient MCAO. The infarct region (between 2 mm anterior and 1 mm posterior to the bregma) of the right cerebral hemisphere was dissected on ice. Samples were placed in radioimmune precipitation assay (RIPA) lysis buffer containing a protease inhibitor cocktail and a phosphatase inhibitor cocktail (Sigma-Aldrich). After sonication for 5 seconds, the lysate was kept on ice for 30 minutes. After 20 minutes centrifugation at 12,000 g, the supernatants were collected. The protein concentration was determined using a Bradford protein assay kit (Bio-Rad, Hercules, CA). Forty μg of total protein was mixed with protein loading buffer and separated using 10–15% sodium dodecyl sulfate polyacrylamide gel electrophoresis (SDS-PAGE). After electrophoresis, the proteins were transferred to polyvinylidene difluoride

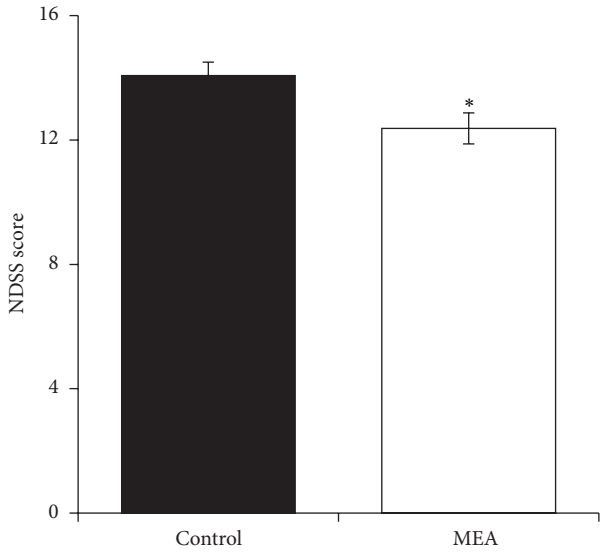

Figure 3: Neurological deficit scoring system (NDSS) score 24 hours after transient MCAO. Data are expressed as mean ± SEM ($n = 14$). $^*P < 0.05$, compared with the control group. The neurological function was significantly improved by MEA pretreatment.

(PVDF) membrane (Bio-Rad) at 4°C. After blocking nonspecific binding sites on the membrane with 5% nonfat milk in Tris-HCL-based buffered saline with 0.1% Tween 20 (TBST; Sigma-Aldrich) at pH 7.4 for 1 hour at room temperature, and the membranes were incubated at 4°C overnight with primary antibodies, including tumor necrosis factor-alpha (TNF-α) (1 : 200 dilution; Santa Cruz Biotechnology, Dallas, TX), cyclooxygenase 2 (COX-2) (1 : 500 dilution; Santa Cruz Biotechnology), B-cell lymphoma 2 (Bcl-2) (1 : 500 dilution; Santa Cruz Biotechnology), Bcl-2-associated X protein (Bax) (1 : 500 dilution; Santa Cruz Biotechnology), and β-actin (1 : 2000 dilution; Santa Cruz Biotechnology). After three washes (15 minutes per time) with TBST, the membranes were incubated with a horseradish peroxidase-conjugated goat secondary antibody (anti-mouse, 1 : 7000 dilution; Santa Cruz Biotechnology; or anti-rabbit, 1 : 7000 dilution; Santa Cruz Biotechnology) at room temperature for 1 hour. After three washes with TBST, the protein bands were visualized using advanced chemoluminescence (GE Healthcare Life Sciences, Hong Kong), recorded by GelDoc-2000 Imagine System (Bio-Rad), and the relative intensity of protein expression was quantified using Quantity One software (Bio-Rad).

2.8. Data Analysis. All the data were analyzed using SPSS (Window version 13.0; SPSS Inc., Chicago, IL) and expressed as mean ± SEM. One sample t-test was used to detect a significant change in rCBF data from the baseline value at different time points in each group. Data were compared using Student's t-test. $P < 0.05$ was used to infer statistical significance.

3. Results

3.1. Relative rCBF. During transient cerebral ischemia, the normalized rCBF was significantly decreased; there was no statistically significant difference at different time points within the same group. During reperfusion, the normalized rCBF returned towards baseline values; there was no statistically significant difference within the same group. No significant difference was observed between the control and MEA groups at the same time points during ischemia and reperfusion ($P > 0.05$), as shown in Tables 2, 3, and 4.

3.2. Effect of MEA on Neurological Deficit Score. When compared with the control group (14.07 ± 0.43), neurological function was significantly improved by MEA pretreatment (12.37 ± 0.50) 24 hours after transient MCAO ($P < 0.05$), as shown in Figure 3.

3.3. Effect of MEA on Brain Infarct Volume and Cerebral Edema Ratio. Figure 4(a) summarizes the representative brain slices after reaction with TTC 24 hours after transient MCAO. The right cerebral infarct was evident as the whitish region. Figure 4(b) summarizes the computer assisted image analysis data revealing the relative brain infarct volumes in the two groups 24 hours after transient cerebral ischemia. The relative infarct volume was expressed as mean ± SEM. When compared with the control group (36.5 ± 2.6%), MEA pretreatment (27.1 ± 3.7%) significantly decreased the infarct volume by 25.7% ($P < 0.05$). Figure 5 summarizes the data revealing the cerebral edema ratio in the two groups 24 hours after transient cerebral ischemia. There was no significant difference between the two groups ($P > 0.05$).

3.4. Effect of MEA on Histological Changes of Brain Inflammation 24 Hours after Transient MCAO. Brain section near bregma level 0 stained with HE revealed the histological changes 24 hours after transient MCAO (Figure 6). In the control group, many necrotic neurons and infiltrated neutrophils were seen in the infarcted cortex after transient MCAO. In rats pretreated with MEA, neutrophil infiltration within the ischemic cerebral cortex was suppressed.

3.5. Effect of MEA on Histological Changes of Brain Apoptosis 24 Hours after Transient MCAO. Five regions within the cortex and penumbra were respectively selected for cell counting on the right cerebral hemisphere. Many TUNEL-positive cells were seen within the infarct and penumbral areas of the right cerebral hemisphere in the control group 24 hours after transient MCAO. In the MEA pretreatment group, increase in the number of TUNEL-positive cell within the ischemic cerebral cortex and penumbra was significantly reduced (Figures 7 and 8).

3.6. Effect of MEA on Protein Expression of Inflammatory Mediators 24 Hours after Transient MCAO. The expression of inflammatory mediators, including TNF-α (Figure 9) and COX-2 (Figure 10), was investigated using western blot analysis 24 hours after transient MCAO. Immunoblots of these

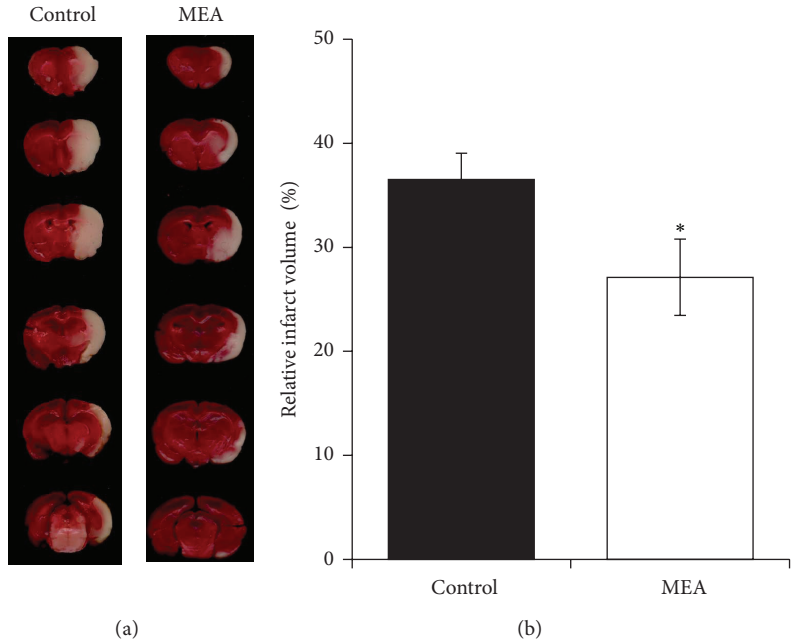

Figure 4: Brain infarct volume measurement 24 hours after transient MCAO. (a) Digital photographs of the 2 mm thick coronal brain slices between the bregma levels +4 mm (anterior) and −6 mm (posterior) in control and MEA groups 24 hours after right-sided endovascular transient MCAO. TTC reaction showed viable brain tissue in red and infarcted brain tissue in white. (b) Quantitative analyses of brain infarct volume 24 hours after transient MCAO. The data are expressed as percentage of the contralateral hemispheric volume (mean ± SEM, in %, $n = 14$). *Indicates the significant difference between the control group and MEA group ($P < 0.05$).

Table 2: Normalized regional cerebral blood flow (rCBF, %) at different time points in relation to the onset of transient MCAO with MEA pretreatment in the study on neurological function and brain infarct volume in rats.

Group (number of rats)	Before MCAO	Onset of MCAO	30 min after MCAO	60 min after MCAO	Onset of reperfusion	30 min after reperfusion
Control (14)	100	23.3 ± 1.7	23.4 ± 1.6	25.2 ± 1.7	87.0 ± 3.3	99.4 ± 4.0
MEA (14)	100	24.8 ± 1.4	25.1 ± 1.8	26.8 ± 2.2	88.4 ± 4.2	94.1 ± 5.1

Data are expressed as mean ± SEM. Normalized rCBF dropped to less than 30% during transient MCAO and returned to more than 70% at the onset of reperfusion. There was no statistically significant difference between the control and MEA groups at the same time points ($P > 0.05$).

Table 3: Normalized regional cerebral blood flow (rCBF, %) at different time points in relation to the onset of transient MCAO with MEA pretreatment in the study on tissue apoptosis in the right cerebral hemisphere of the rats.

Group (number of rats)	Before MCAO	Onset of MCAO	30 min after MCAO	60 min after MCAO	Onset of reperfusion	30 min after reperfusion
Control (5)	100	24.6 ± 1.6	25.5 ± 1.5	27.2 ± 1.7	96.5 ± 6.2	98.0 ± 5.5
MEA (5)	100	23.3 ± 2.1	24.4 ± 1.9	26.2 ± 2.3	104.3 ± 6.8	102.1 ± 10.2

Data are expressed as mean ± SEM. Normalized rCBF dropped to less than 30% during transient MCAO and returned to more than 70% at the onset of reperfusion. There was no statistically significant difference between the control and MEA groups at the same time points ($P > 0.05$).

Table 4: Normalized regional cerebral blood flow (rCBF, %) at different time points in relation to the onset of transient MCAO with MEA pretreatment in the study on western blot in the right cerebral hemisphere of the rats.

Group (number of rats)	Before MCAO	Onset of MCAO	30 min after MCAO	60 min after MCAO	Onset of reperfusion	30 min after reperfusion
Control (3)	100	23.2 ± 2.2	24.8 ± 2.6	26.2 ± 2.0	105.7 ± 6.6	106.4 ± 8.8
MEA (3)	100	25.2 ± 2.6	25.7 ± 2.5	27.6 ± 2.8	107.5 ± 9.1	114.9 ± 11.1

Data are expressed as mean ± SEM. Normalized rCBF dropped to less than 30% during transient MCAO and returned to more than 70% at the onset of reperfusion. There was no statistically significant difference between the control and MEA groups at the same time points ($P > 0.05$).

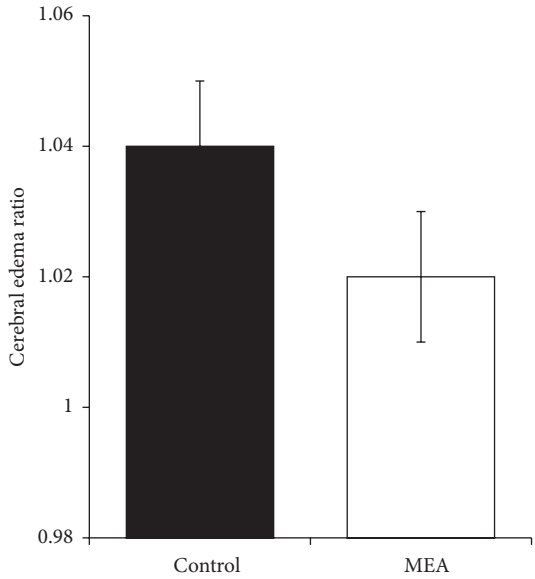

Figure 5: Data of cerebral edema ratio 24 hours after transient MCAO. Data are expressed as mean ± SEM ($n = 14$). Student's t-test reveals no significant difference in cerebral edema ratio 24 hours after transient MCAO between the control and MEA group ($P > 0.05$).

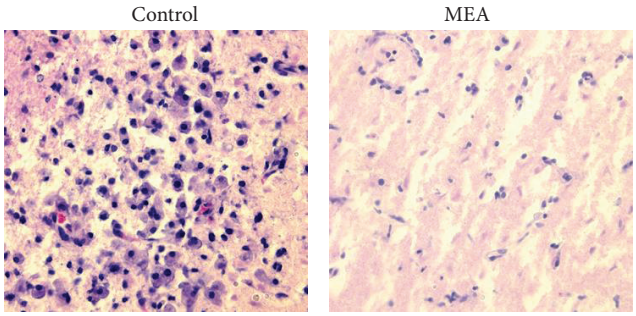

Figure 6: Photomicrographs of HE-stained brain sections near bregma level 0 24 hours after right-sided transient MCAO (magnification: 400x). In the control group, neutrophil infiltration was mainly present in the infarcted cortex. Neutrophil infiltration in the ischemic cerebral cortex was suppressed by the MEA pretreatment group 24 hours after transient MCAO.

inflammatory mediators were obtained from right cerebral hemisphere. When compared with the control group, MEA pretreatment significantly decreased the upregulated protein expression of TNF-α and COX-2 ($P < 0.01$).

3.7. Effect of MEA on Protein Expression of Bcl-2 Family Proteins 24 Hours after Transient MCAO. The expression of Bax and Bcl-2 was investigated using western blot analysis (Figures 11 and 12) 24 hours after transient MCAO. Immunoblots of these proteins were obtained from right cerebral hemisphere. When compared with the control group, the relative protein expression of Bax was significantly decreased by MEA pretreatment ($P < 0.05$). The protein expression of Bcl-2 was significantly increased by MEA when compared with the control group ($P < 0.01$).

4. Discussion

Increasing evidence shows that pretreatment with various kinds of neuroprotectants induces beneficial effects against stroke in animal models; however, many of them have limitations and adverse effects that may prevent the clinical application in patients [33, 34]. Although it is suggested that therapeutics for prevention of first and recurrent stroke, such as blood pressure control and anti-thrombosis, are highly recommended in clinical practice [35, 36], some of these drugs, like antiplatelets and anticoagulants, have a risk of causing hemorrhage. Therefore, it is desirable to develop not only efficient but also safe strategies aiming at preventing cerebral ischemia as well as reducing ischemic injury. A previous study in our lab (unpublished data) has shown that posttreatment of MEA may induce neuroprotective effect in transient MCAO. The present study was performed to explore whether pretreatment of the combined therapy may prevent the brain from cerebral ischemic injury.

Firstly, the effect of MEA pretreatment on NDSS score, brain infarct volume, and cerebral edema ratio was investigated. The data showed that when compared with the control group, pretreatment of MEA significantly improved neurological functions 24 hours after transient MCAO. Meanwhile, MEA reduced the brain infarct volume by 25.7% 24 hours after transient MCAO. No significant changes in the cerebral edema ratio were observed. There were no significant differences in rCBF data during cerebral ischemia and reperfusion.

Secondly, the effect of MEA pretreatment on histological and cellular inflammation after transient ischemic stroke was examined. HE staining of brain sections shows that many necrotic neurons and infiltrated neutrophils were seen in the infarcted cortex after transient MCAO. In rats pretreated with MEA, neutrophil infiltration within the ischemic cerebral cortex was suppressed. In addition, MEA pretreatment reduced the upregulated protein expression of two proinflammatory mediators, TNF-α and COX-2, in the ischemic right cerebral hemisphere 24 hours after transient MCAO. These results indicate the anti-inflammatory effects of MEA pretreatment of against transient MCAO.

Thirdly, the effect of MEA pretreatment on histological and cellular apoptosis after transient ischemic stroke was evaluated. In the present study, TUNEL staining of brain sections shows that there were many TUNEL-positive cells within the ischemic infarction and penumbra of the right cerebral hemisphere in the control group 24 hours after transient MCAO. The number of TUNEL-positive cells was significantly decreased in the same areas by MEA pretreatment 24 hours after transient MCAO.

Moreover, MEA pretreatment decreased the level of proapoptotic protein Bax and increased the level of antiapoptotic protein Bcl-2 24 hours after transient MCAO when compared to the control group. The present data suggest the antiapoptotic effect of MEA pretreatment in transient MCAO.

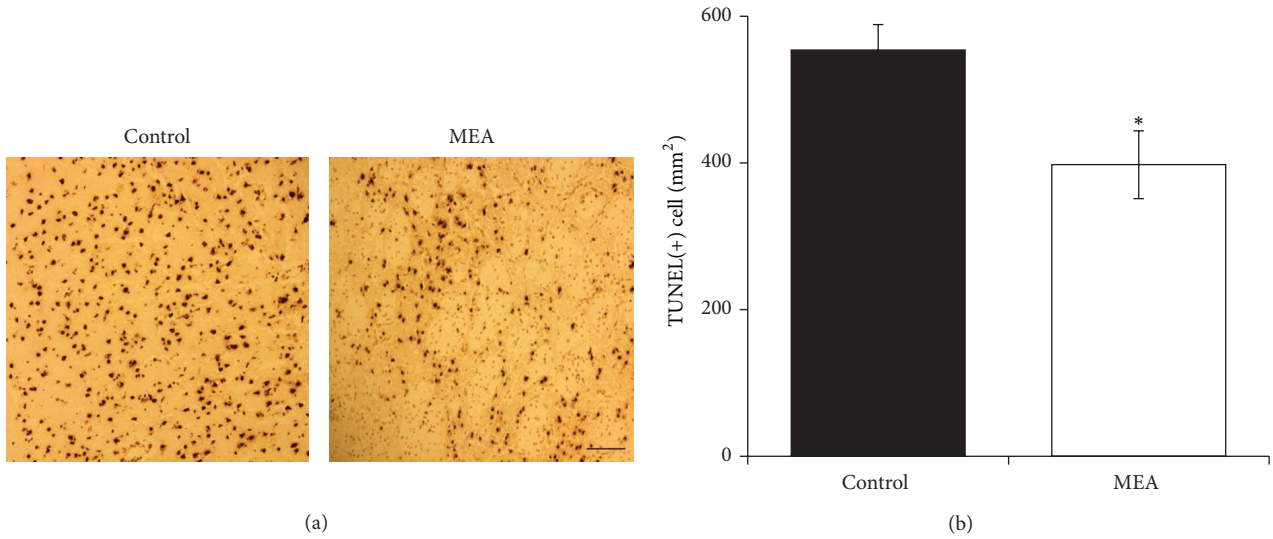

Figure 7: Apoptosis in the infarcted cortex of right ischemic cerebral hemisphere 24 hours after transient MCAO. (a) Representative images of TUNEL staining in the infarcted cortex of right ischemic cerebral hemisphere 24 hours after transient MCAO. The brown staining within the nuclei reveals TUNEL-positive cells. (b) Quantitative analysis of TUNEL-positive cells. Data are expressed as means ± SEM ($n = 5$). $^*P < 0.05$, compared with the control group. The number of TUNEL-positive cells was significantly decreased by MEA pretreatment. Scale bar = 100 μm.

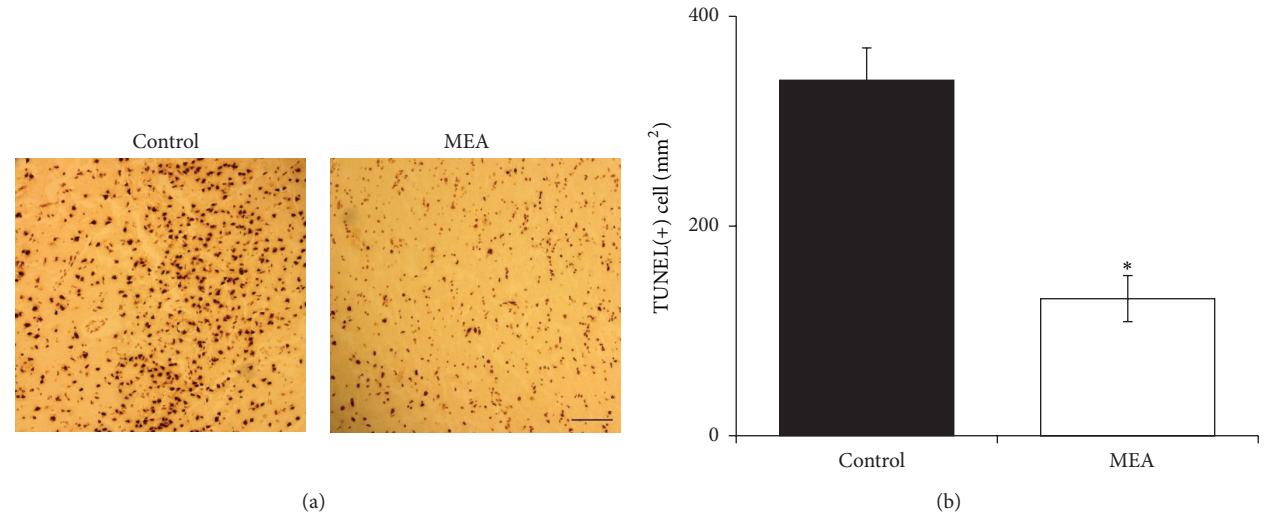

Figure 8: Apoptosis in the penumbra of right ischemic cerebral hemisphere 24 hours after transient MCAO. (a) Representative images of TUNEL staining in the penumbra of right ischemic cerebral hemisphere 24 hours after transient MCAO. The brown staining within the nuclei reveals TUNEL-positive cells. (b) Quantitative analysis of TUNEL-positive cells. Data are expressed as means ± SEM ($n = 5$). $^*P < 0.01$, compared with the control group. The number of TUNEL-positive cells was significantly decreased by MEA pretreatment. Scale bar = 100 μm.

Previous research indicates that inflammatory response is induced in the cerebral infarct and its surrounding areas after cerebral ischemia [37]. Various proinflammatory mediators, such as TNF-α and COX-2, are upregulated after stroke. These mediators play critical roles in the process of neuronal survival following brain injury [38, 39]. Inhibition of TNF-α reduced the brain infarct volume and suppressed the inflammatory responses in a mouse model of transient cerebral ischemia [40]. Overexpression of COX-2 may exacerbate brain damage [41]. According to the present data, the neuroprotection with regard to neurological outcome and brain infarct volume may be partly due to the inhibitory effect of MEA on TNF-α and COX-2.

The damage resulting from cerebral ischemia is constituted by two principal zones: infarct core and ischemic penumbra. After ischemic stroke, neuronal apoptosis occurs mainly in the penumbral area [42]. In particular after transient focal ischemia, apoptosis may be a contributing factor to the final infarct volume [43]. According to the present data, the number of TUNEL-positive cells was significantly

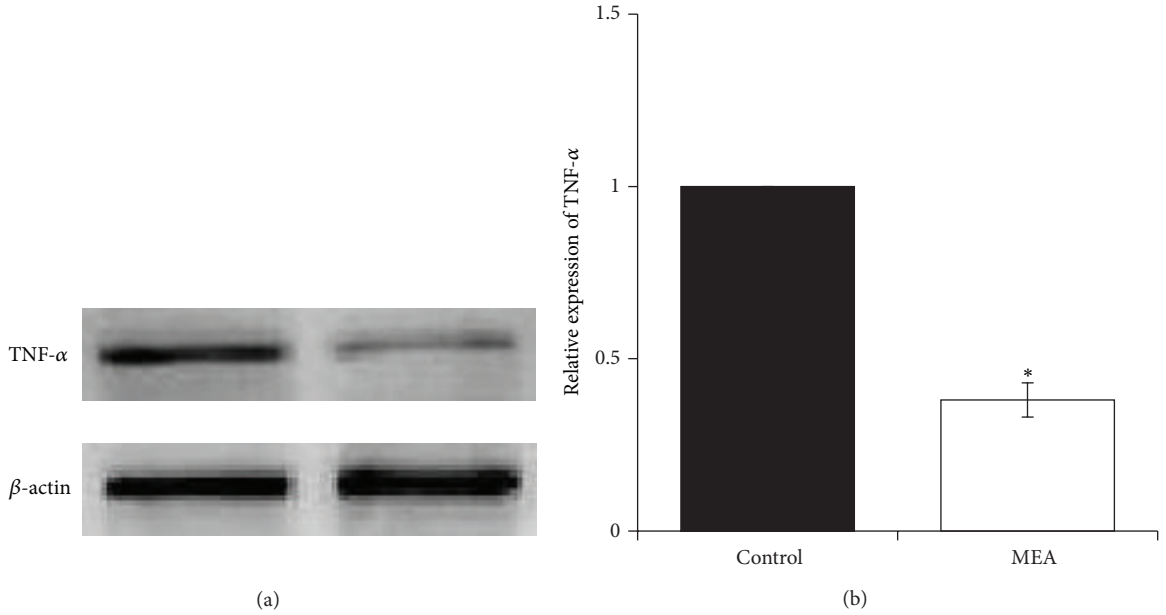

Figure 9: Protein expression of TNF-α 24 hours after transient MCAO in different groups. (a) Representative immunoblots of TNF-α in the right cerebral hemisphere of different groups 24 hours after transient MCAO. (b) Semiquantitative analysis of protein expression of TNF-α. Data are expressed as means ± SEM ($n = 3$). $^*P < 0.01$, compared with the control group. The relative expression of TNF-α was significantly inhibited by MEA pretreatment.

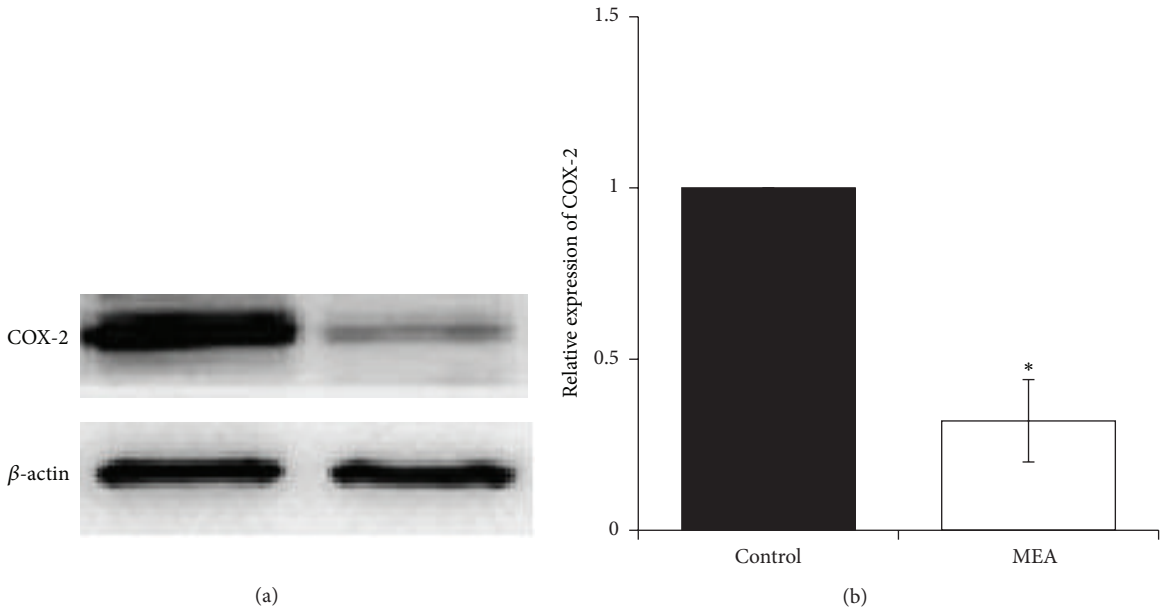

Figure 10: Protein expression of COX-2 24 hours after transient MCAO in different groups. (a) Representative immunoblots of COX-2 in the right cerebral hemisphere of different groups 24 hours after transient MCAO. (b) Semiquantitative analysis of protein expression of COX-2. Data are expressed as means ± SEM ($n = 3$). $^*P < 0.01$, compared with the control group. The relative expression of COX-2 was significantly decreased by MEA pretreatment.

decreased in the penumbral area by MEA pretreatment 24 hours after transient MCAO. This finding may partly explain the result of infarct volume reduction after MEA pretreatment. In addition, Bax and Bcl-2 are suggested to be distinct regulators of apoptosis in the early stages of stroke [44]. Upregulation of Bax and downregulation of Bcl-2 are repeatedly observed in the penumbral area following cerebral ischemia [45]. Bax inhibition results in neuroprotection against stroke [46]. Decreased expression of Bcl-2 leads to increased oxidative stress [46, 47]. The present data

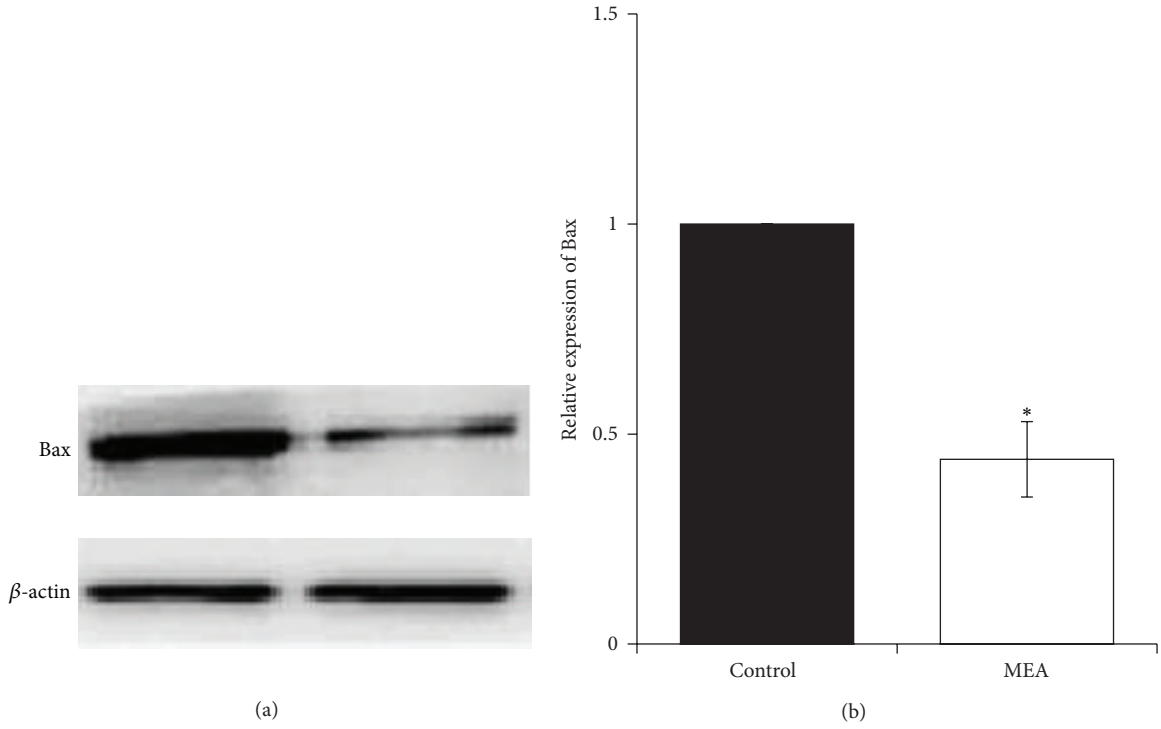

Figure 11: Protein expression of Bax 24 hours after transient MCAO in different groups. (a) Representative immunoblots of Bax in the right cerebral hemisphere of different groups 24 hours after transient MCAO. (b) Semiquantitative analysis of protein expression of Bax. Data are expressed as means ± SEM ($n = 3$). $^*P < 0.05$, compared with the control group. The relative expression of Bax was significantly decreased by MEA pretreatment.

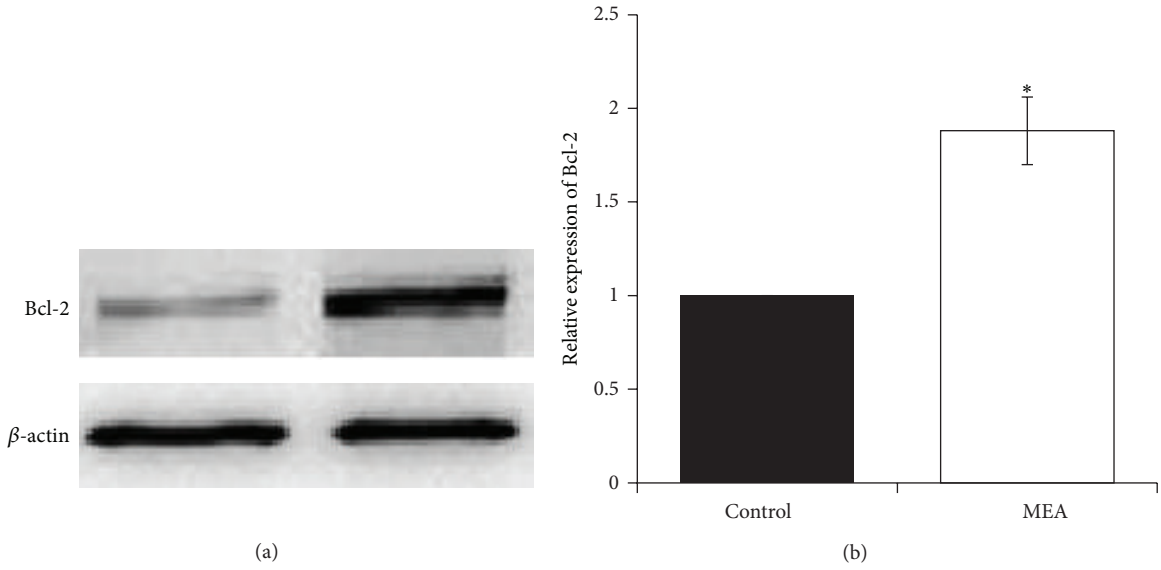

Figure 12: Protein expression of Bcl-2 24 hours after transient MCAO in different groups. (a) Representative immunoblots of Bcl-2 in the right cerebral hemisphere of different groups 24 hours after transient MCAO. (b) Semiquantitative analysis of protein expression of Bcl-2. Data are expressed as means ± SEM ($n = 3$). $^*P < 0.01$, compared with the control group. The relative expression of Bcl-2 was significantly increased by MEA pretreatment.

indicate the antiapoptotic effect of MEA pretreatment via downregulation of Bax and upregulation of Bcl-2.

In conclusion, this study provides some preliminary data with regard to the effect of MEA pretreatment on transient focal cerebral ischemia. The present results indicate that MEA pretreatment may induce a neuroprotection against transient MCAO in terms of improved neurological function and decreased brain infarct volume. The beneficial effects are partly mediated by anti-inflammation and antiapoptosis.

Acknowledgment

This research was supported by the Committee on Research and Conference Grants (200907176032), The University of Hong Kong, Hong Kong.

References

[1] W. Hacke, M. Kaste, E. Bluhmki et al., "Thrombolysis with alteplase 3 to 4.5 hours after acute ischemic stroke," *The New England Journal of Medicine*, vol. 359, no. 13, pp. 1317–1329, 2008.

[2] Y. D. Cheng, L. Al-Khoury, and J. A. Zivin, "Neuroprotection for ischemic stroke: two decades of success and failure," *NeuroRx*, vol. 1, no. 1, pp. 36–45, 2004.

[3] A. I. Faden and B. Stoica, "Neuroprotection: challenges and opportunities," *Archives of Neurology*, vol. 64, no. 6, pp. 794–800, 2007.

[4] L. Zhang, Z. G. Zhang, and M. Chopp, "The neurovascular unit and combination treatment strategies for stroke," *Trends in Pharmacological Sciences*, vol. 33, no. 8, pp. 415–422, 2012.

[5] O. Adeoye, R. Hornung, P. Khatri, and D. Kleindorfer, "Recombinant tissue-type plasminogen activator use for ischemic stroke in the united states: a doubling of treatment rates over the course of 5 years," *Stroke*, vol. 42, no. 7, pp. 1952–1955, 2011.

[6] G. C. Fonarow, E. E. Smith, J. L. Saver et al., "Timeliness of tissue-type plasminogen activator therapy in acute ischemic stroke: patient characteristics, hospital factors, and outcomes associated with door-to-needle times within 60 minutes," *Circulation*, vol. 123, no. 7, pp. 750–758, 2011.

[7] M. Lee, J. L. Saver, J. R. Alger et al., "Blood-brain barrier permeability derangements in posterior circulation ischemic stroke: frequency and relation to hemorrhagic transformation," *Journal of the Neurological Sciences*, vol. 313, no. 1-2, pp. 142–146, 2012.

[8] J. M. Hallenbeck and K. U. Frerichs, "Stroke therapy: it may be time for an integrated approach," *Archives of Neurology*, vol. 50, no. 7, pp. 768–770, 1993.

[9] J. Hart, "Poststroke recovery: emerging complementary therapies," *Alternative and Complementary Therapies*, vol. 16, no. 5, pp. 277–280, 2010.

[10] B. Guardiola-Lemaître, "Toxicology of melatonin," *Journal of Biological Rhythms*, vol. 12, no. 6, pp. 697–706, 1997.

[11] R. T. F. Cheung, "The utility of melatonin in reducing cerebral damage resulting from ischemia and reperfusion," *Journal of Pineal Research*, vol. 34, no. 3, pp. 153–160, 2003.

[12] P. Giusti, M. Gusella, M. Lipartiti et al., "Melatonin protects primary cultures of cerebellar granule neurons from kainate but not from-methyl-d-aspartate excitotoxicity," *Experimental Neurology*, vol. 131, no. 1, pp. 39–46, 1995.

[13] H. Manev, U. Z. Tolga, A. Kharlamov, and J. Joo, "Increased brain damage after stroke or excitotoxic seizures in melatonin-deficient rats," *The FASEB Journal*, vol. 10, no. 13, pp. 1546–1551, 1996.

[14] C. V. Borlongan, M. Yamamoto, N. Takei et al., "Glial cell survival is enhanced during melatonin-induced neuroprotection against cerebral ischemia," *The FASEB Journal*, vol. 14, no. 10, pp. 1307–1317, 2000.

[15] K. Sinha, M. N. Degaonkar, N. R. Jagannathan, and Y. K. Gupta, "Effect of melatonin on ischemia reperfusion injury induced by middle cerebral artery occlusion in rats," *European Journal of Pharmacology*, vol. 428, no. 2, pp. 185–192, 2001.

[16] H. Lin and E.-J. Lee, "Effects of melatonin in experimental stroke models in acute, sub-acute, and chronic stages," *Neuropsychiatric Disease and Treatment*, vol. 5, no. 1, pp. 157–162, 2009.

[17] S. Lee, G. H. Choi, C. H. Lee et al., "Exploration of new electroacupuncture needle material," *Evidence-Based Complementary and Alternative Medicine*, vol. 2012, Article ID 612545, 10 pages, 2012.

[18] G. A. Ulett, S. Han, and J. Han, "Electroacupuncture: mechanisms and clinical application," *Biological Psychiatry*, vol. 44, no. 2, pp. 129–138, 1998.

[19] B. Pomeranz, G. Stux, and C. Han, *Scientific Bases of Acupuncture*, Springer, New York, NY, USA, 1989.

[20] H. M. Langevin, P. M. Wayne, H. MacPherson et al., "Paradoxes in acupuncture research: strategies for moving forward," *Evidence-Based Complementary and Alternative Medicine*, vol. 2011, Article ID 180805, 11 pages, 2011.

[21] J. Park, K. Linde, E. Manheimer et al., "The status and future of acupuncture clinical research," *Journal of Alternative and Complementary Medicine*, vol. 14, no. 7, pp. 871–881, 2008.

[22] H. MacPherson, R. Nahin, C. Paterson, C. M. Cassidy, G. T. Lewith, and R. Hammerschlag, "Developments in acupuncture research: big-picture perspectives from the leading edge," *Journal of Alternative and Complementary Medicine*, vol. 14, no. 7, pp. 883–887, 2008.

[23] H. M. Wu, J. L. Tang, X. P. Lin et al., "Acupuncture for stroke rehabilitation," *The Cochrane Library*, no. 1, pp. 1–25, 2009.

[24] W. Chen, H. Gu, W. Ma et al., "Multicentral randomized controlled study on effects of acupuncture at Zusanli (ST 36) and Xuanzhong (GB 39) on cerebrovascular function in the patient of ischemic stroke," *Zhongguo Zhen Jiu*, vol. 26, no. 12, pp. 851–853, 2006.

[25] W. Gong, T. Zhang, L. Cui, Y. Yang, and X. Sun, "Electroacupuncture at Zusanli (ST 36) to improve lower extremity motor function in sensory disturbance patients with cerebral stroke: a randomized controlled study of 240 cases," *Neural Regeneration Research*, vol. 4, no. 11, pp. 935–940, 2009.

[26] T. Kondoh, Y. Ueta, and K. Torii, "Pre-treatment of adrenomedullin suppresses cerebral edema caused by transient focal cerebral ischemia in rats detected by magnetic resonance imaging," *Brain Research Bulletin*, vol. 84, no. 1, pp. 69–74, 2011.

[27] K. Schmerbach, T. Pfab, Y. Zhao et al., "Effects of aliskiren on stroke in rats expressing human renin and angiotensinogen genes," *PLoS ONE*, vol. 5, no. 11, Article ID e15052, 2010.

[28] L. Belayev, O. F. Alonso, R. Busto, W. Zhao, and M. D. Ginsberg, "Middle cerebral artery occlusion in the rat by intraluminal suture: neurological and pathological evaluation of an improved model," *Stroke*, vol. 27, no. 9, pp. 1616–1623, 1996.

[29] M. Khan, C. Elango, M. A. Ansari, I. Singh, and A. K. Singh, "Caffeic acid phenethyl ester reduces neurovascular inflammation and protects rat brain following transient focal cerebral ischemia," *Journal of Neurochemistry*, vol. 102, no. 2, pp. 365–377, 2007.

[30] E. Z. Longa, P. R. Weinstein, S. Carlson, and R. Cummins, "Reversible middle cerebral artery occlusion without craniectomy in rats," *Stroke*, vol. 20, no. 1, pp. 84–91, 1989.

[31] J. H. Garcia, S. Wagner, K.-F. Liu, X.-J. Hu, and J. P. Mohr, "Neurological deficit and extent of neuronal necrosis attributable to middle cerebral artery occlusion in rats: statistical validation," *Stroke*, vol. 26, no. 4, pp. 627–635, 1995.

[32] D. Reglodi, A. Tamás, and I. Lengvári, "Examination of sensorimotor performance following middle cerebral artery occlusion in rats," *Brain Research Bulletin*, vol. 59, no. 6, pp. 459–466, 2003.

[33] J. Montaner, C. A. Molina, J. Monasterio et al., "Matrix metalloproteinase-9 pretreatment level predicts intracranial hemorrhagic complications after thrombolysis in human stroke," *Circulation*, vol. 107, no. 4, pp. 598–603, 2003.

[34] M. Krikov, C. Thone-Reineke, S. Müller, A. Villringer, and T. Unger, "Candesartan but not ramipril pretreatment improves outcome after stroke and stimulates neurotrophin BNDF/TrkB system in rats," *Journal of Hypertension*, vol. 26, no. 3, pp. 544–552, 2008.

[35] G. Tsivgoulis, M. Saqqur, V. K. Sharma, A. Y. Lao, M. D. Hill, and A. V. Alexandrov, "Association of pretreatment blood pressure with tissue plasminogen activator-induced arterial recanalization in acute ischemic stroke," *Stroke*, vol. 38, no. 3, pp. 961–966, 2007.

[36] P. B. Gorelick, "Stroke prevention therapy beyond antithrombotics: unifying mechanisms in ischemic stroke pathogenesis and implications for therapy: an invited review," *Stroke*, vol. 33, no. 3, pp. 862–875, 2002.

[37] G. Stoll, S. Jander, and M. Schroeter, "Inflammation and glial responses in ischemic brain lesions," *Progress in Neurobiology*, vol. 56, no. 2, pp. 149–171, 1998.

[38] J. M. Hallenbeck, "The many faces of tumor necrosis factor in stroke," *Nature Medicine*, vol. 8, no. 12, pp. 1363–1368, 2002.

[39] S. Nogawa, F. Zhang, M. Elizabeth Ross, and C. Iadecola, "Cyclo-oxygenase-2 gene expression in neurons contributes to ischemic brain damage," *The Journal of Neuroscience*, vol. 17, no. 8, pp. 2746–2755, 1997.

[40] G. Yang, C. Gong, Z. Qin, W. Ye, Y. Mao, and A. L. Bertz, "Inhibition of TNFα attenuates infarct volume and ICAM-1 expression in ischemic mouse brain," *NeuroReport*, vol. 9, no. 9, pp. 2131–2134, 1998.

[41] S. Doré, T. Otsuka, T. Mito et al., "Neuronal overexpression of cyclooxygenase-2 increases cerebral infarction," *Annals of Neurology*, vol. 54, no. 2, pp. 155–162, 2003.

[42] Y. Li, M. Chopp, N. Jiang, F. Yao, and C. Zaloga, "Temporal profile of in situ DNA fragmentation after transient middle cerebral artery occlusion in the rat," *Journal of Cerebral Blood Flow and Metabolism*, vol. 15, no. 3, pp. 389–397, 1995.

[43] C. Y. Hsu, G. An, J. S. Liu, J. J. Xue, Y. Y. He, and T. N. Lin, "Expression of immediate early gene and growth factor mRNAs in a focal cerebral ischemia model in the rat," *Stroke*, vol. 24, supplement 12, pp. I78–I81, 1993.

[44] D. E. Merry and S. J. Korsmeyer, "Bcl-2 gene family in the nervous system," *Annual Review of Neuroscience*, vol. 20, no. 1, pp. 245–267, 1997.

[45] S. Krajewski, J. K. Mai, M. Krajewska, M. Sikorska, M. J. Mossakowski, and J. C. Reed, "Upregulation of bax protein levels in neurons following cerebral ischemia," *The Journal of Neuroscience*, vol. 15, no. 10, pp. 6364–6376, 1995.

[46] C. M. Troy, D. Derossi, A. Prochiantz, L. A. Greene, and M. L. Shelanski, "Downregulation of Cu/Zn superoxide dismutase leads to cell death via the nitric oxide-peroxynitrite pathway," *The Journal of Neuroscience*, vol. 16, no. 1, pp. 253–261, 1996.

[47] A. Hochman, H. Sternin, S. Gorodin et al., "Enhanced oxidative stress and altered antioxidants in brains of Bcl-2-deficient mice," *Journal of Neurochemistry*, vol. 71, no. 2, pp. 741–748, 2002.

Hindawi Publishing Corporation
Evidence-Based Complementary and Alternative Medicine
Volume 2013, Article ID 294789, 6 pages
http://dx.doi.org/10.1155/2013/294789

Research Article

Electroacupuncture Stimulation at CV12 Inhibits Gastric Motility via TRPV1 Receptor

Zhi Yu,[1] Xin Cao,[1,2] Youbing Xia,[1,3] Binbin Ren,[1] Hong Feng,[1] Yali Wang,[1] Jingfeng Jiang,[1] and Bin Xu[1]

[1] *Key Laboratory of Integrated Acupuncture and Drugs Constructed by the Ministry of Education and Jiangsu Province, Nanjing University of Chinese Medicine, Nanjing 210029, China*
[2] *Toho University, Tokyo 143-8540, Japan*
[3] *Nanjing Medical University, Nanjing 210029, China*

Correspondence should be addressed to Bin Xu; xuuuux@sina.com

Received 25 February 2013; Accepted 9 August 2013

Academic Editor: Jian Kong

Gastric dysmotility is one of the major pathophysiological factors in functional gastrointestinal disorders. Acupuncture, as one of the alternative approaches, is efficacious in the treatment of gastrointestinal motility disorders; however, the mechanism underlying its action is unclear. In the present study, we used both capsazepine, a TRPV1 antagonist, and TRPV1 knockout mice. Animals were divided into wild-type group (WT), capsazepine injection group (CZP, 0.5 mg/kg, i.p.), and TRPV1 knockout mice group ($TRPV1^{-/-}$). Each of these three groups was divided into three subgroups, which were subjected to EA stimulation at acupoint Zhongwan (CV12) at a different intensity (1, 2, or 4 mA). We demonstrated that electroacupuncture at Zhongwan (CV12) markedly inhibited gastric motility at 2 and 4 mA in an intensity-dependent manner in wild-type mice. The inhibitory effect was also observed in capsazepine-injected and $TRPV1^{-/-}$ mice but was no longer intensity dependent, indicating that TRPV1 is partially involved in the electroacupuncture-mediated modulation of gastric motility.

1. Introduction

Gastric motility is one of the most critical physiological functions of the human body. Coordinated gastric motility is necessary for the digestion and absorption of dietary nutrients. Impairment of gastric motility results in delayed gastric emptying and symptoms such as nausea, vomiting, and abdominal pain and discomfort [1]. Recent studies have shown that gastric dysmotility is one of the major pathophysiological factors in functional gastrointestinal disorders, which has a public health cost of over 30 billion dollars annually [2, 3], including functional dyspepsia [4] and gastroesophageal reflux disease [5].

Acupuncture has been practiced for thousands of years in Eastern countries and has become very popular worldwide as a complementary and alternative approach. Numerous studies on both humans and animals support the efficacy of acupuncture for treating gastrointestinal symptoms and/or diseases of gastrointestinal secretion [6, 7], sensation [8], and myoelectrical activity [9]. Acupuncture of the abdomen has been used for treating abdominal pain, suggesting that acupuncture of this site may inhibit gastric motility and/or reduce gastrospasm [10]. Recently, many studies have explored the efficacy of electroacupuncture (EA) for the treatment of gastrointestinal motility disorders and concluded that EA can alter gastrointestinal motility and improve gastrointestinal motility disorders [11]. While this therapeutic effect of EA has been proved, little is known about the underlying mechanism(s).

The transient receptor potential vanilloid-1 (TRPV1; transient receptor potential (TRP) cation channel, subfamily V, member 1) is a member of the superfamily of TRP cation channels [12]. TRPV1 plays an important role in the modulation of EA efficacy, owing to its function in heat and mechanical sensations [13–15]. However, research on TRPV1 and EA has mainly been confined to the treatment of pain, such as cancer-related pain or hyperalgesia. Few studies have reported the relationship between EA and TRPV1 in

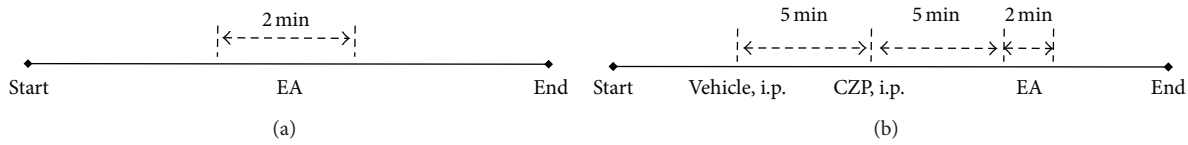

Figure 1: Experimental procedure. (a) Time scale of stimulation in the wild-type and TRPV1$^{-/-}$ groups. (b) Time scale of stimulations in the capsazepine (CZP) injection group.

the regulation of gastrointestinal motility. We previously reported the modulatory effects of EA on gastric motility [16]. Given the emerging role of TRPV1 receptors in mediating sensory and visceral functions, the aim of the present study was to further elucidate the mechanism of EA-mediated gastric motility modulation and to confirm whether TRPV1 was involved in this mechanism.

2. Materials and Methods

2.1. Animals. TRPV1$^{-/-}$ mice (n = 30, male, 22–28 g, B6.129X1-TRPV1$^{tm1Jul/NJU}$, J003770) and their wild-type counterparts (WT, n = 60, male, 22–28 g) were purchased from Model Animal Research Center of Nanjing University (Nanjing, China). Food and water were made available ad libitum, and the animals were housed under controlled environmental conditions (22°C, 40%–60% relative humidity, 12-h alternate light/dark cycles). All experimental manipulations were undertaken in accordance with the National Institutes of Health Guide for the Care and Use of Laboratory Animals and with the approval of the Scientific Investigation Board of the Nanjing University of Traditional Chinese Medicine, Nanjing, China.

2.2. Experimental Groups. Capsazepine injections were used in 30 of the 60 WT mice (CZP group), but not in the remaining 30 WT mice (WT group) or the 30 TRPV1 knockout mice (TRPV1$^{-/-}$ group). Each of these three groups was divided into three subgroups of 10 mice each, and the three subgroups of each group were subjected to EA stimulation at a different intensity (1, 2, or 4 mA).

2.3. Experimental Procedure. The animals were fasted overnight with free access to water and anesthetized with urethane (1.2 g/kg i.p.; U2500, Sigma, USA). The trachea was cannulated to keep the respiratory tract patent, and gastric motility was recorded using a previously described method [17]. A small incision was made in the duodenum about 1-2 cm from the pylorus. A small balloon made of flexible condom rubber was inserted into the pyloric area via incision. The pressure in the balloon was measured with a transducer (YP200; Chengdu Instrument Factory, Chengdu, China) and recorded with a physiological signal-acquisition system (RM6240; Chengdu Instrument Factory) for further analysis. During the experiment, the temperature of the animal was maintained at 37°C ± 0.5°C, using an electric heating board.

The experimental procedure in the WT and TRPV1$^{-/-}$ groups is shown in Figure 1(a). The time scale of each stimulation in the capsazepine injection group is shown in Figure 1(b). Capsazepine (0.5 mg/kg, i.p.; C191, Sigma, USA) was dissolved in a vehicle (1% dimethyl sulfoxide; D8418, Sigma, USA).

2.4. EA Stimulation. A pair of needle electrodes (diameter, 0.3 mm) were inserted approximately 5 mm deep into the Zhongwan point (CV12), which is located at the center of the abdomen, in the midline of the body [17]. The EA intensity was set as 1, 2, or 4 mA, with alternating frequencies of 2 Hz and 15 Hz for 2 min.

2.5. Statistical Analysis. Data were analyzed using SPSS 17.0 software (SPSS, Chicago, USA). Differences before and after treatment were compared using a paired-sample t-test, and those between two groups were compared using an independent-sample t-test. Comparison among groups was performed using analysis of variance. $P < 0.05$ was considered statistically significant. All data were expressed as mean ± SE.

3. Results

3.1. Gastric Motility. In the resting condition (prior to EA), rhythmic gastric contractions at a frequency of 3–6/min were observed in the TRPV1$^{-/-}$ and WT mice, and the contractile amplitude of the rhythmic waves was approximately 0.05–0.3 kPa, when balloon pressure was maintained at about 0.4–0.6 kPa by filling the balloon with 0.1–0.2 mL warm water. Injection of 0.5 mg/kg capsazepine, i.p., caused no change in gastric movement or amplitude.

3.2. Gastric Response to Different Intensities of EA Stimulation at CV12. In WT mice, EA stimulation at CV12 at an intensity of 1 mA (n = 10) produced no significant effect on gastric motility (Figure 2(a)). In contrast, EA stimulation at 2 mA slightly inhibited gastric motility, while stimulation at 4 mA strongly inhibited it. Thus, the inhibition of gastric motility by EA stimulation was intensity dependent.

3.3. TRPV1 Is Involved in Gastric Motility Modulation by EA Stimulation. To determine the mechanism underlying the inhibitory effect of EA stimulation at CV12, we used capsazepine, a specific antagonist of TRPV1. In the WT mice, significant inhibition of gastric motility was obtained after EA stimulation at 2 and 4 mA, but not at 1 mA; moreover, this inhibitory effect was intensity dependent, being greater at 4 mA than at 2 mA (Figure 4(e)). After capsazepine injection, EA stimulation at 1 mA (n = 10) produced no significant inhibition, while that at 2 mA produced mild inhibition (Figure 3(a)); however, the effect of EA stimulation at 4 mA

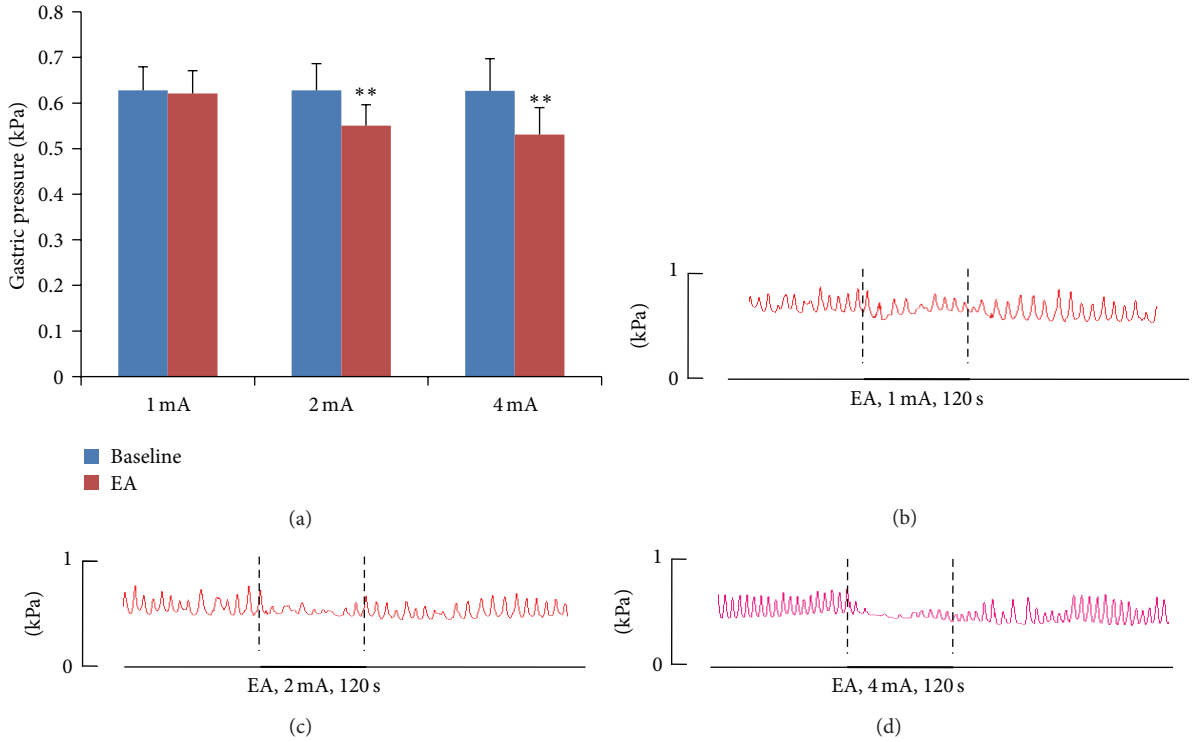

Figure 2: Gastric response to electroacupuncture (EA) stimulation at CV12 in wild-type mice. (a) Significant inhibition of gastric motility was induced by EA stimulation at intensities 2 mA ($n = 10$) and 4 mA ($n = 10$). **: Versus baseline, $P < 0.001$. (b)–(d) Representative examples of EA stimulation at CV12 with different intensities.

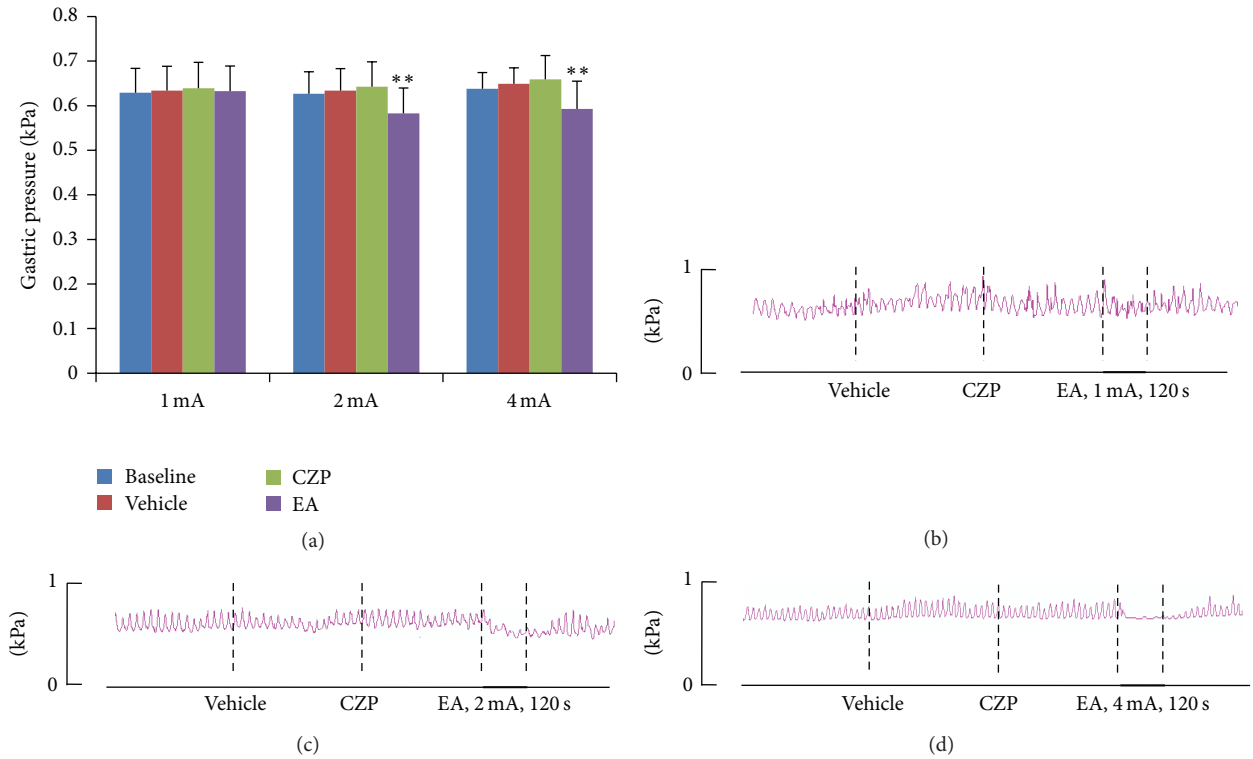

Figure 3: Gastric responses to electroacupuncture (EA) stimulation at CV12 after capsazepine (CZP) injection. (a) Significant inhibition of gastric motility was induced by EA at intensities 2 mA ($n = 10$) and 4 mA ($n = 10$). **: Versus CZP, $P < 0.001$. (b)–(d) Representative examples of EA stimulation at CV12 with different intensities.

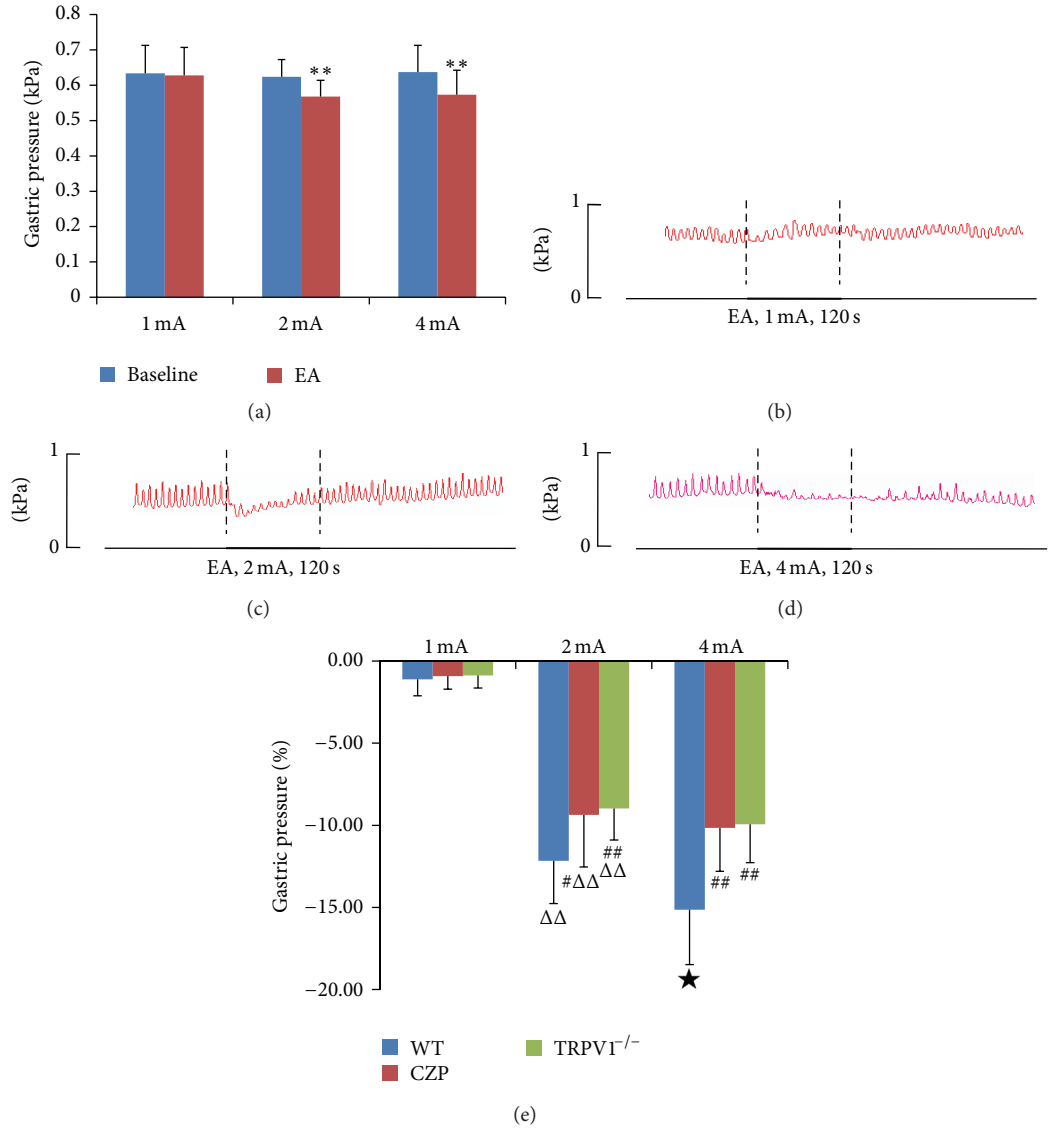

FIGURE 4: Gastric responses to electroacupuncture (EA) stimulation at CV12 in TRPV1$^{-/-}$ mice. (a) Significant inhibition of gastric motility was induced by EA at intensities 2 mA ($n = 10$) and 4 mA ($n = 10$). **: Versus baseline, $P < 0.001$. (b)–(d) Representative examples of EA stimulation at CV12 with different intensities. (e) Percentage inhibition of gastric motility after EA stimulation at CV12 with different intensities in all three experimental groups. #: Versus WT, $P < 0.05$; ##: Versus WT, $P < 0.01$; ΔΔ: Versus 1 mA, $P < 0.001$; ★: Versus 2 mA, $P < 0.05$.

was partially blocked (Figure 4(e)). Thus, the intensity-dependent characteristic of EA stimulation disappeared after TRPV1 channel blockage. Similar results were obtained in the TRPV1$^{-/-}$ mice (Figures 4(a)–4(e)), suggesting an important role of TRPV1 in EA-mediated modulation of gastric motility.

4. Discussion

The reported ameliorating effect of EA on gastric dysrhythmia has been consistent and reproducible, suggesting a robust role of EA in the treatment of gastric motility disorders [11]. The primary mechanism underlying the clinical effects of acupuncture appears to be the activation of afferent nerve fibers that innervate the skin and muscles [18]. In this study, we determined whether TRPV1 was involved in the EA-mediated regulation of gastric motility after stimulation of CV12 with different intensities. For this purpose, we used both capsazepine, which is a TRPV1 antagonist, and TRPV1 knockout mice. Acupuncture stimulation of various segmental areas of the body has been shown to alter gastric motility in anesthetized animals [19, 20]; this alteration has been facilitative or inhibitory, depending on which acupoints are stimulated. Consistent with these reports, our data showed that EA at CV12 significantly inhibited gastric motility, but only at intensities 2 and 4 mA. Moreover, this inhibitory effect was intensity dependent (Figure 4), which was in accordance with previous reports [20]. Somatic afferent nerve fibers are

composed of A-α, A-β, A-δ, and C-fibers. The mean threshold of the action potentials of A-δ fibers is approximately 2 mA [20], while that of unmyelinated fibers is approximately 3 mA [21]. Consistent with this [20], EA stimulation could modulate gastric motility only at an intensity greater than the threshold for the activation of A-δ and/or C-fibers. In other words, the inhibitory effect of EA at 2 mA was mediated by A-δ fibers, while the effect of EA at 4 mA was mediated by unmyelinated fibers.

TRPV1 mediates the transductions of intra- and extracellular signals and modulates organ functions by activating a variety of endogenous and exogenous stimuli such as mechanical stimuli, noxious heat, proteins, and capsaicin [22]. The presence of a class of visceral and somatic afferents of dorsal root origin and their functional significance in pain sensation have been well documented [23]. Recently, TRPV1 was found to be expressed at acupuncture points, indicating that it contributed to the effects of EA stimulation [24]. The above findings suggest the importance of TRPV1 in EA stimulation. To confirm whether TRPV1 was involved in the regulation of gastric motility after CV12 stimulation, we assessed the effects of EA at CV12 on gastric motility in TRPV1-null animals. After TRPV1 blockage or knockout, EA at CV12 continued to inhibit gastric motility, although, interestingly, the intensity-dependent nature of EA-mediated inhibition disappeared, especially at intensities 2 and 4 mA. Caterina et al. [25] reported that in VR1-null mice, none of the C-fibers examined were activated by capsaicin, a specific TRPV1 agonist; whereas 11 of 22 wild-type afferent nerves responded vigorously to this stimulus. Among myelinated nociceptors, only one of 13 wild-type fibers and none of the nine fibers from $VR1^{-/-}$ mice responded to capsaicin. These results indicated that TRPV1 was mainly coexpressed with C-fibers, rather than with myelinated nociceptors [25]. Consistent with this, Koerber et al. [26] reported that TRPV1 was specifically localized in a subpopulation of C-fiber nociceptors that responded to heat (CH-fibers) but not to mechanical or cold stimuli. The majority of C-fibers innervating the skin are C-polymodal afferents that respond to both mechanical and thermal stimuli. The coexpression of TRPV1 and C-fibers combined with the identical thresholds for the elicitation of nerve action potentials and EA responses indicate that TRPV1 is involved in the intensity-dependent regulation of gastric motility by EA stimulation at CV12.

Conflict of Interests

The authors declare they have no conflict of interests.

Acknowledgments

The authors thank Professor X. H. Jing (Institute of Acupuncture and Moxibustion, China Academy of Chinese Medical Sciences) for advise and Y. Wang (Nanjing University of Chinese Medicine) for the assistance during experiment. This work was supported by grants from the National Key Basic Research Program (973 Program, no. 2011CB505206), the National Natural Science Foundation of China (nos. 81202744 and 81373749), the Natural Science Research Project of Higher Education of Jiangsu Province (no. 11KJB360008), and Jiangsu Provincial Qinglan Project Sci-tech Innovation Team.

References

[1] S. Zhao, H. Sha, Z. Y. Li, and C. S. Ren, "Electrical bioimpedance gastric motility measurement based on an electrical-mechanical composite mechanism," *World Journal of Gastroenterology*, vol. 18, no. 25, pp. 3282–3287, 2012.

[2] N. J. Talley, "Functional gastrointestinal disorders as a public health problem," *Neurogastroenterology and Motility*, vol. 20, 1, pp. 121–129, 2008.

[3] B. Cash, S. Sullivan, and V. Barghout, "Total costs of IBS: employer and managed care perspective," *The American Journal of Managed Care*, vol. 11, no. 1, pp. S7–16, 2005.

[4] Y. Matsumoto, M. Ito, D. Kamino, S. Tanaka, K. Haruma, and K. Chayama, "Relation between histologic gastritis and gastric motility in Japanese patients with functional dyspepsia: evaluation by transabdominal ultrasonography," *Journal of Gastroenterology*, vol. 43, no. 5, pp. 332–337, 2008.

[5] M. Nahata, S. Muto, N. Oridate et al., "Impaired ghrelin signaling is associated with gastrointestinal dysmotility in rats with gastroesophageal reflux disease," *American Journal of Physiology Gastrointestinal and Liver Physiology*, vol. 303, no. 1, pp. G42–G53, 2012.

[6] H. S. Hwang, K.-J. Han, Y. H. Ryu et al., "Protective effects of electroacupuncture on acetylsalicylic acid-induced acute gastritis in rats," *World Journal of Gastroenterology*, vol. 15, no. 8, pp. 973–977, 2009.

[7] E. Noguchi, "Acupuncture regulates gut motility and secretion via nerve reflexes," *Autonomic Neuroscience*, vol. 156, no. 1-2, pp. 15–18, 2010.

[8] X. Y. Tian, Z. X. Bian, X. G. Hu, X. J. Zhang, L. Liu, and H. Zhang, "Electro-acupuncture attenuates stress-induced defecation in rats with chronic visceral hypersensitivity via serotonergic pathway," *Brain Research*, vol. 1088, no. 1, pp. 101–108, 2006.

[9] C. M. Witt, K. Meissner, D. Pach et al., "Stimulation of gastric slow waves with manual acupuncture at acupuncture points ST36 and PC6—a randomized single blind controlled trial," *Neurogastroenterology and Motility*, vol. 24, no. 5, pp. 438–445, 2012.

[10] Y.-Q. Li, B. Zhu, P.-J. Rong, H. Ben, and Y.-H. Li, "Effective regularity in modulation on gastric motility induced by different acupoint stimulation," *World Journal of Gastroenterology*, vol. 12, no. 47, pp. 7642–7648, 2006.

[11] J. Yin and J. D. Z. Chen, "Gastrointestinal motility disorders and acupuncture," *Autonomic Neuroscience*, vol. 157, no. 1-2, pp. 31–37, 2010.

[12] R. Rahmati, "The transient receptor potential vanilloid receptor 1, TRPV1 (VR1) inhibits peristalsis in the mouse jejunum," *Archives of Iranian Medicine*, vol. 15, no. 7, pp. 433–438, 2012.

[13] Z. Zhang, C. Wang, G. Gu et al., "The effects of electroacupuncture at the ST36 (Zusanli) acupoint on cancer pain and transient receptor potential vanilloid subfamily 1 expression in walker 256 tumor-bearing rats," *Anesthesia and Analgesia*, vol. 114, no. 4, pp. 879–885, 2012.

[14] S. J. Wang, H. Y. Yang, and G. S. Xu, "Acupuncture alleviates colorectal hypersensitivity and correlates with the regulatory mechanism of trpV1 and p-ERK," *Evidence-Based Complementary and Alternative Medicine*, vol. 2012, Article ID 483123, 10 pages, 2012.

[15] L. Manni, F. Florenzano, and L. Aloe, "Electroacupuncture counteracts the development of thermal hyperalgesia and the alteration of nerve growth factor and sensory neuromodulators induced by streptozotocin in adult rats," *Diabetologia*, vol. 54, no. 7, pp. 1900–1908, 2011.

[16] Z. Yu, Y. B. Xia, M. X. Lu, J. Lin, W. J. Yu, and B. Xu, "Influence of electroacupuncture stimulation of tianshu (ST25), quchi (LI11) and shangjuxu (ST37) and their pairs on gastric motility in the rat," *Acupuncture Research*, vol. 38, no. 1, pp. 40–47, 2013.

[17] X. Y. Wang, H. Shi, H. Y. Shang et al., "Are primo vessels (PVs) on the surface of gastrointestine involved in regulation of gastric motility induced by stimulating acupoints ST36 or CV12?" *Evidence-Based Complementary and Alternative Medicine*, vol. 2012, Article ID 787683, 8 pages, 2012.

[18] F. Kagitani, S. Uchida, and H. Hotta, "Afferent nerve fibers and acupuncture," *Autonomic Neuroscience*, vol. 157, no. 1-2, pp. 2–8, 2010.

[19] A. Sato, Y. Sato, A. Suzuki, and S. Uchida, "Neural mechanisms of the reflex inhibition and excitation of gastric motility elicited by acupuncture-like stimulation in anesthetized rats," *Neuroscience Research*, vol. 18, no. 1, pp. 53–62, 1993.

[20] Y.-Q. Li, B. Zhu, P.-J. Rong, H. Ben, and Y.-H. Li, "Neural mechanism of acupuncture-modulated gastric motility," *World Journal of Gastroenterology*, vol. 13, no. 5, pp. 709–716, 2007.

[21] H. Ohsawa, S. Yamaguchi, H. Ishimaru, M. Shimura, and Y. Sato, "Neural mechanism of pupillary dilation elicited by electro-acupuncture stimulation in anesthetized rats," *Journal of the Autonomic Nervous System*, vol. 64, no. 2-3, pp. 101–106, 1997.

[22] D.-L. Liu, W.-T. Wang, J.-L. Xing, and S.-J. Hu, "Research progress in transient receptor potential vanilloid 1 of sensory nervous system," *Neuroscience Bulletin*, vol. 25, no. 4, pp. 221–227, 2009.

[23] L. M. Patterson, H. Zheng, S. M. Ward, and H.-R. Berthoud, "Vanilloid receptor (VR1) expression in vagal afferent neurons innervating the gastrointestinal tract," *Cell and Tissue Research*, vol. 311, no. 3, pp. 277–287, 2003.

[24] T. S. Abraham, M.-L. Chen, and S.-X. Ma, "TRPV1 expression in acupuncture points: response to electroacupuncture stimulation," *Journal of Chemical Neuroanatomy*, vol. 41, no. 3, pp. 129–136, 2011.

[25] M. J. Caterina, A. Leffler, A. B. Malmberg et al., "Impaired nociception and pain sensation in mice lacking the capsaicin receptor," *Science*, vol. 288, no. 5464, pp. 306–313, 2000.

[26] H. R. Koerber, S. L. McIlwrath, J. J. Lawson et al., "Cutaneous C-polymodal fibers lacking TRPV1 are sensitized to heat following inflammation, but fail to drive heat hyperalgesia in the absence of TPV1 containing C-heat fibers," *Molecular Pain*, vol. 6, no. 58, 2010.

Hindawi Publishing Corporation
Evidence-Based Complementary and Alternative Medicine
Volume 2013, Article ID 483105, 15 pages
http://dx.doi.org/10.1155/2013/483105

Research Article

Neural Encoding of Acupuncture Needling Sensations: Evidence from a fMRI Study

Xiaoling Wang,[1,2] Suk-Tak Chan,[2] Jiliang Fang,[1,2] Erika E. Nixon,[2] Jing Liu,[2] Kenneth K. Kwong,[2] Bruce R. Rosen,[2] and Kathleen K. S. Hui[2]

[1] *Department of Radiology, Guang An Men Hospital, China Academy of Chinese Medical Sciences, Beijing 100053, China*
[2] *Athinoula A. Martinos Center for Biomedical Imaging, Department of Radiology, Massachusetts General Hospital and Harvard Medical School, Charlestown, MA 02129, USA*

Correspondence should be addressed to Suk-Tak Chan; phoebe@nmr.mgh.harvard.edu

Received 22 February 2013; Revised 7 July 2013; Accepted 14 July 2013

Academic Editor: Lijun Bai

Deqi response, a psychophysical response characterized by a spectrum of different needling sensations, is essential for Chinese acupuncture clinical efficacy. Previous neuroimaging research works have investigated the neural correlates of an overall *deqi* response by summating the scores of different needling sensations. However, the roles of individual sensations in brain activity and how they interact with each other remain to be clarified. In this study, we applied fMRI to investigate the neural correlates of individual components of *deqi* during acupuncture on the right LV3 (Taichong) acupoint. We selected a subset of *deqi* responses, namely, pressure, heaviness, fullness, numbness, and tingling. Using the individual components of *deqi* of different subjects as covariates in the analysis of percentage change of bold signal, pressure was found to be a striking sensation, contributing to most of negative activation of a limbic-paralimbic-neocortical network (LPNN). The similar or opposite neural activity in the heavily overlapping regions is found to be responding to different needling sensations, including bilateral LPNN, right orbitofrontal cortex, and bilateral posterior parietal cortex. These findings provide the neuroimaging evidence of how the individual needle sensations interact in the brain, showing that the modulatory effects of different needling sensations contribute to acupuncture modulations of LPNN network.

1. Introduction

The needling sensation of *deqi*, a psychophysical response, is considered by traditional Chinese medicine to play a key role in the clinical efficacy of acupuncture [1–4]. *Deqi* is a composite of a series of needling sensations which include but are not limited to aching, pressure, soreness, heaviness, fullness, temperature change (warmth or coolness), numbness, tingling, and dull pain [2, 3, 5]. It has been demonstrated that the *deqi* sensations during acupuncture stimulation are conveyed by different nerve fiber systems [6]. For example, Aβ fibers convey numbness. Heaviness and fullness are mediated by Aδ fibers [6]. However, the link between the needling sensation and the acupuncture effect on the brain remains an ongoing area of research. Moreover, the different components of *deqi* may attribute to effective treatment in some disorders. It has been demonstrated that numbness and soreness but not stabbing, throbbing, tingling, burning, heaviness, fullness, or aching are correlated with clinical efficacy of analgesia [4]. In this paper we investigated how components of the *deqi* sensation were individually related to the brain responses to acupuncture.

Previous neuroimaging fMRI and PET research has been studying the brain responses to acupuncture in multiple disorders which included pain, stroke, Parkinson's disease, functional dyspepsia, and Alzheimer disease [7–13]. A few acupuncture imaging reports accounted for the needling sensation [8, 9, 14–18]. A number of fMRI studies on healthy subjects including ours have consistently revealed that acupuncture with *deqi* induced extensive negative BOLD signal change (deactivation) of a limbic-paralimbic-neocortical network (LPNN) and positive BOLD signal

change of somatosensory regions of the brain [9, 14–16, 19, 20]. Both commonality and specificity were observed in brain responses to acupuncture at different acupoints [16, 17, 21]. It was reported that the sensation of sharp pain and overall *deqi* were associated with separate patterns of brain activity [9, 14–16, 22]. The previous literatures has reported so far only the relationship between brain responses and overall *deqi* sensation. However, questions on the roles of individual needling sensations of *deqi* in brain activity and how they interact with each other remain to be clarified, especially the correlation with negative or positive brain activations.

In the present study, we attempted to characterize the brain response to a subset of needle sensations relating to *deqi* during the manual acupuncture at right LV3 acupoint (Taichong) on the dorsum of distal foot, with the primary purpose of confirming the hypothesis that each individual needling sensation may correspond with a distinct map of brain responses to acupuncture. The five selected sensations are pressure, numbness, heaviness, fullness, and tingling. The other *deqi* sensations related with pain, including aching, soreness, dull pain, warmth, or coolness were investigated in another separate paper. The differences in the pattern of *deqi*, including frequency and intensity in individual sensation, were used to discriminate between acupuncture and simple tactile stimulation used as control. We hypothesized that the modulatory effects of different needling sensations contribute to acupuncture modulations of LPNN network. To our knowledge, we are the first team to explore the relationship between individual components of *deqi* and brain activity during acupuncture.

2. Materials and Methods

2.1. Subjects. In the present study, we extracted data from a larger project that investigated the brain effect of acupuncture at the Athinoula A. Martinos Center for Biomedical Imaging at Massachusetts General Hospital. This study included 37 acupuncture-naïve and right-handed healthy subjects (30 subjects for acupuncture stimulation, 19–47 years old, mean ± SD 28.6 ± 8.05, 14M/16F; 15 subjects for tactile stimulation, 21–45 years old, mean ± SD, 28 ± 7.74, 4M/11F). Eight subjects had acupuncture stimulation and tactile stimulation in the same session. Six subjects had twice acupuncture stimulations and eight subjects had performed twice tactile stimulations for different objectives, such as the comparison of real acupuncture and sham acupuncture, different acupoints, different acupuncture stimulations. The study was in compliance with the Code of Ethics of the World Medical Association (Declaration of Helsinki) and the standards established by the Institutional Review Board of the hospital and the National Center of Complementary and Alternative Medicine (NCCAM) of the NIH. Subjects were screened to exclude neurological, mental and medical disorders, drug abuse, history of head trauma with loss of consciousness, and contraindications for exposure to high magnetic field. All experimental procedures were explained to the subjects, and signed informed consent was obtained prior to participation in the study.

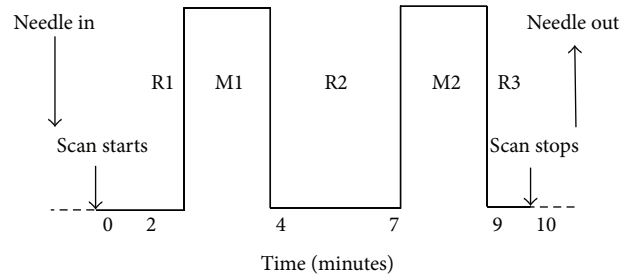

Figure 1: Paradigms: in each fMRI session, two periods of 2-minute acupuncture stimulation were interleaved with 3 periods of rest which lasted 2-3 minutes each. The paradigms were identical in both acupuncture and tactile stimulation.

2.2. Acupuncture and Tactile Stimulations. During a single session, we administered acupuncture to LV3 on the right dorsum of distal foot using sterile, single-use, stainless steel acupuncture needles (0.20 mm diameter) (KINGLI Medical Appliance Co., Wuxi, China). Stimulation was enhanced with manipulation of the needle to elicit *deqi,* the composite of unique sensations related to efficacy according to TCM [2]. To avoid noxious pain, we tested the subject's tolerance to needle manipulation after inserting the needle at the acupoint. During the ten-minute scan, the needle was rotated approximately 180° in each direction, with even motion at the rate of 1 Hz, for two minutes during the two stimulation periods and left in place during the three rest periods (Figure 1). A licensed acupuncturist (JL) with more than 25 years of clinical acupuncture experience administered acupuncture for all subjects.

Tactile stimulation over LV3 on the right foot was used as a control for expectation and superficial sensory evaluation, as reported previously [2, 9, 15]. The skin over the acupoint was tapped gently with a 5.88 von Frey monofilament using the same paradigm as acupuncture.

2.3. Psychophysical Response: Needling Sensation of Deqi. The subjects were told that acupuncture would be performed at point using different techniques; while lying in the supine position in the scanner subjects were not able to see where the acupuncturist was working. At the completion of each scan, the subject was asked to report a full set sensations of aching, soreness, pressure, heaviness, fullness or distension, warmth or coolness, numbness, tingling, dull pain, and sharp pain and to rate each sensation, if it was experienced, on a scale of 1 to 10 [2]. If the subjects did not feel the sensation, it was noted as 0. Psychophysical data from only a subset of selected five sensations, including pressure, numbness, heaviness, fullness, and tingling, were analyzed, and the results were reported here.

2.4. fMRI Acquisitions. fMRI was performed on a 1.5 Tesla scanner (Siemens Sonata, Erlangen, Germany) equipped with a standard quadratic head coil. The subjects lay supine with earplugs to suppress scanner noise and cushions to immobilize the head. We acquired (1) standard high-resolution

Table 1: The variance inflation factors (VIF) by regressing scores of each sensation as a dependent variable on the scores of all the other sensations as independent variables.

	Independent variables				
	Heaviness	Fullness	Numbness	Pressure	Tingling
Dependent variable					
Heaviness	—	1.376	1.463	1.109	1.187
Fullness	1.867	—	1.641	1.424	1.164
Numbness	3.186	2.634	—	1.442	1.162
Pressure	2.823	2.671	1.686	—	1.193
Tingling	3.894	2.813	1.75	1.537	—

sagittal images with a T1-weighted 3D-MPRAGE sequence, and (2) whole-brain BOLD fMRI images encompassing the brain stem with a gradient-echo echo planar imaging (EPI) sequence (TR = 4000 ms, TE = 30 ms, flip angle = 90°, FOV = 200 mm, matrix = 64 × 64, thickness = 3 mm, gap = 0.6 mm), while the subject was administered acupuncture at the LV3 acupoint. Each fMRI run lasted 10 minutes.

2.5. Psychophysical Data Analysis. The chi-Square tests were performed for comparing the frequency of individual needling sensation between acupuncture and tactile stimulation using SPSS 19.0 (Chicago, IL, USA). Mann-Whitney U tests were performed for comparing the intensity of individual sensation between the acupuncture and tactile stimulation using SPSS 19.0 as well.

2.6. fMRI Data Analysis. All fMRI data were analyzed using the Analysis of Functional NeuroImage (AFNI) software package [23]. The first 15 volumes acquired in the first minutes of each functional dataset were discarded to eliminate the drifting of MR signals commonly seen at the beginning of acupuncture fMRI scans. Each functional dataset was motion-corrected, registered onto the subject's anatomical scan, transformed to the standardized space of Talairach and Tournoux [24], spatially smoothed with a Gaussian filter of full-width half-maximum 5 mm, and normalized to its mean intensity value across the time series. Multiple regression analysis was performed to identify brain areas showing change in the MR signal as a result of needle manipulation during acupuncture periods (ACUP), using as reference the needle left in place during the rest periods (REST). The six motion parameters were included as regressors for the removal of residual motion correlated activity.

Brain volumes with percent MR signal change to acupuncture from different subjects were then grouped and analyzed with Analysis of Covariance (ANCOVA), where the scores of 5 individual needling sensations (pressure, numbness, heaviness, fullness, and tingling) were included as covariates. The same group analysis was applied onto the brain volumes with percent MR signal change to tactile stimulation. The statistical parametric maps showing the percent MR signal change to acupuncture/tactile stimulation with respect to individual needling sensations were obtained.

In the group analysis, multicollinearity may happen when one or more of the independent sensation scores are highly correlated with one or more of the other independent sensation scores. To reliably examine the perfect or near-perfect multicollinearity, we used the variance inflation factors (VIF) by regressing scores of each sensation as a dependent variable on the scores of all the other sensations as independent variables. VIF measures the seriousness of the multicollinearity among the regressors and a VIF of 5 or above indicates a multicollinearity problem [25]. The VIF for the sensation scores in this study ranged from 1.16 to 3.894 (Table 1). Although some of the VIF were slightly higher when regressing numbness, pressure, and tingling, their values were below 5 indicating that the multicollinearity may not cause problem.

To protect against type I error, we set an individual voxel probability threshold of $P < 0.02$ to correct the overall significance level to $\alpha < 0.05$ using Monte Carlo simulation [26]. Based on Monte Carlo simulation with 1000 iterations processed with ClusterSim program [27], the overall corrected threshold of the group activation maps for acupuncture and tactile stimulation was $P < 0.05$ with cluster volume of 108 mm^3, and uncorrected $P < 0.02$. The group activation maps were then overlaid on the high-resolution anatomical map of the cohort in the standardized Talairach space [24]. Anatomical localization and masking of the functional data were determined by both Talairach coordinates and direct inspection.

3. Results

3.1. Psychophysical Response. Thirty-six psychophysical datasets during acupuncture stimulation at LV3 and twenty-three psychophysical datasets during tactile stimulation were acquired. During acupuncture, more subjects experienced pressure (58.3% versus 8.7%), tingling (55.6% versus 13.0%), and numbness (38.9% versus 0%) compared with tactile stimulation ($P < 0.05$) (Table 2, Figure 2). No significant difference in the number of subjects experiencing heaviness (19.4% versus 4.3%) and fullness (13.9% versus 4.3%) was found between acupuncture and tactile stimulation ($P > 0.05$).

The intensities of individual sensations in subjects were variant. The scores were not in normal distribution in each group. The Mann-Whitney U tests were used to compare the difference between two groups. The intensity of pressure (2.01±0.40 versus 0.11±0.07), numbness (1.29±0.33 versus 0),

Table 2: The chi-Square tests were performed for comparing the frequency of individual sensation between acupuncture and tactile stimulation.

Deqi	χ^2	P
Pressure	14.537	<0.001
Heaviness	2.729	0.099
Fullness	1.398	0.237
Numbness	11.727	0.001
Tingling	9.475	0.002

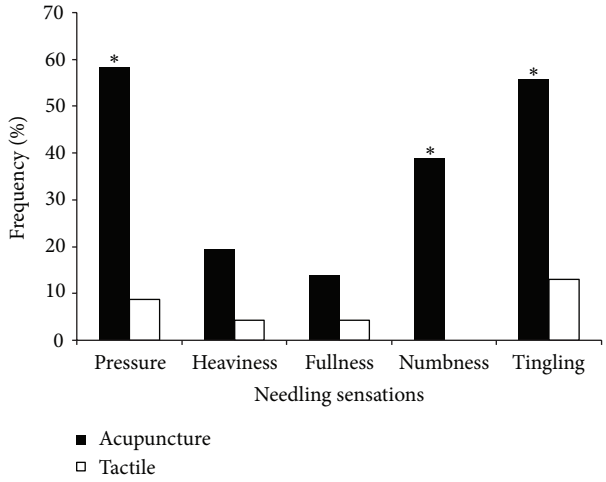

Figure 2: Comparison of the frequency of different sensations between acupuncture and tactile stimulation. In acupuncture, pressure was the most common sensation. The frequency of pressure, numbness, and tingling during acupuncture was more common than that during tactile stimulation. $^*P < 0.05$.

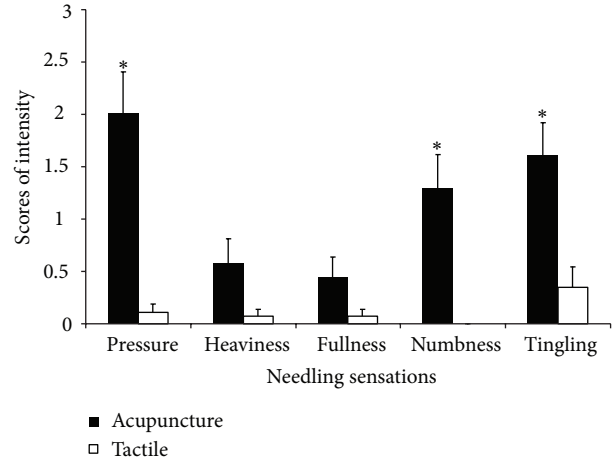

Figure 3: Comparison of the intensity of different sensations between acupuncture ($n = 36$) and tactile stimulation ($n = 23$). The intensity of pressure, numbness, and tingling during acupuncture was greater than that during tactile stimulation. The bar showed standard error of mean of the scores. $^*P < 0.05$.

Table 3: Mann-Whitney U tests were performed for comparing the intensity of individual sensation between the acupuncture and tactile stimulation.

Deqi	Z	P
Pressure	−3.93	<0.001
Heaviness	−1.698	0.09
Fullness	−1.245	0.213
Numbness	−3.358	0.001
Tingling	−3.079	0.002

and tingling (1.61 ± 0.31 versus 0.35 ± 0.19) was found to be greater for acupuncture relative to tactile stimulation ($P < 0.05$) (Table 3, Figure 3). No significant difference in the intensity of heaviness (0.58 ± 0.23 versus 0.07 ± 0.06) and fullness (0.44 ± 0.2 versus 0.07 ± 0.06) was found between acupuncture stimulation and tactile stimulation ($P > 0.05$).

3.2. fMRI Data: Brain Response. Thirty-six fMRI datasets during acupuncture stimulation at LV3 and twenty-three fMRI datasets during tactile stimulation at LV3 were acquired. Psychophysical responses acquired immediately after the fMRI sessions were included as covariates in this analysis.

3.2.1. Mean Effect of Overall Brain Activity during Acupuncture and Tactile Stimulation. Consistent with our previous studies [9, 17], acupuncture stimulation at LV3 elicited extensive deactivation in LPNN, such as anterior cingulate cortex (ACC), medial temporal lobe (temporal pole, amygdala, hippocampus, and parahippocampus gyrus), and precuneus (Figure 4). Most of the deactivations showed bilateral distribution. Sparse positive activations were identified in left splenium of corpus callosum, left thalamus, left anterior, and bilateral superior segments of circular sulcus of the insula, left postcentral sulcus, right superior frontal gyrus, bilateral supramarginal gyrus, and bilateral cerebellar cortex. The summary of the regions showing positive and negative activations elicited by acupuncture stimulation is shown in Table 4.

3.2.2. Brain Activity Associated with Individual Sensation Related to Deqi during Acupuncture Stimulation. Comparing with tactile stimulation, more needlingsensations during acupuncture showed extensive significant association with certain brain regions. In this paper, we focused on the brain responses which were correlated with the five sensations including pressure, fullness, heaviness, numbness, and tingling reported by the subjects (Table 4, Figure 5). The brain regions associated with differential individual sensation are

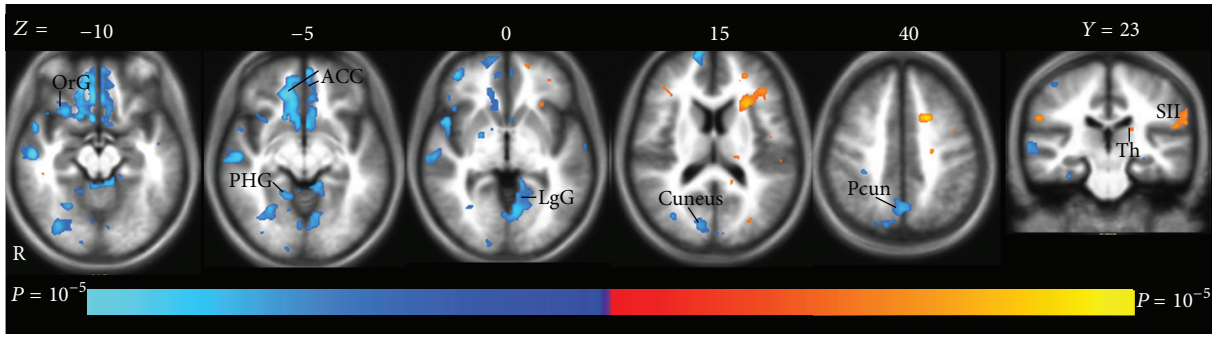

FIGURE 4: The mean brain positive (yellow) and negative (blue) bold responses to acupuncture stimulation. The extensive deactivation showed limbic-paralimbic-neocortical network (LPNN), such as anterior cingulated cortex (ACC), parahippocampal gyrus (PHG), lingual gyrus (LgG), precuneus (Pcun), and cuneus. The orbital gyrus (OrG) also showed deactivation. Left thalamus (Th) and secondary somatosensory cortex (SII) demonstrated activation.

partly overlapped, such as bilateral ACC, right lateral prefrontal cortex, bilateral medial temporal cortex, and bilateral posterior parietal cortex.

The pressure elicited negative activation bilaterally in LPNN network, such as ACC and medial temporal cortex (hippocampus and parahippocampus). Reduced brain activity was also observed unilaterally in left superior frontal gyrus, left straight gyrus, right orbital gyrus and sulcus, right superior temporal gyrus and sulcus, right temporal pole, and right anterior segments of circular sulcus of the insula (Table 4, Figures 5(a), 6(a), 6(b)). Increased brain response was sparsely shown in the left intraparietal sulcus (IPS), left transverse parietal sulci, and right superior segments of circular sulcus of the insula.

While fullness also contributes to the negative activations at the right lateral prefrontal cortex and ACC as in pressure sensation, heaviness demonstrates positive activity at the same areas (Table 4, Figures 5(b), 5(c)). A number of brain regions showing negative activations with the increased intensity in pressure sensation were found to have positive activations with the increased intensity in heaviness sensation (Figures 6(c), 6(d)). These regions include the bilateral ACC, right inferior frontal cortex (orbital gyri and sulcus), left superior frontal gyrus, right anterior segment of circular sulcus of the insula, right superior temporal sulcus, right middle temporal gyrus, and right hippocampus.

On the contrary, the negative activity related to heaviness at the posterior parietal cortex (bilateral IPS and transverse parietal sulci) overlaps with the positive activity related to numbness. Numbness decreased brain activity in the bilateral hippocampus, left parahippocampus, and left thalamus and increased brain activity in the right superior frontal gyrus and bilateral posterior parietal cortex (angular gyrus, superior parietal lobule, supramarginal gyrus, IPS, and transverse parietal sulci) (Table 4, Figure 5(d)).

Tingling sensation was correlated with the brain response mainly in two areas: positive correlation at posterior corpus callosum (posterior midbody, isthmus, and splenium) but negative correlation at posterior parietal cortex (bilateral angular gyrus, bilateral IPS and transverse parietal sulci, right superior parietal lobule, right postcentral gyrus, and left supramarginal gyrus) (Table 4, Figure 5(e)).

Tactile control stimulation elicited deactivation in the aforementioned areas far less than acupuncture stimulation. Positive activations were also found in the left inferior segment of circular sulcus of the insula, left postcentral sulcus, and left supramarginal gyrus, but the extent was much smaller than that in acupuncture stimulation. The summary of the regions showing positive and negative activations elicited by tactile control stimulation is shown in Table 5.

3.2.3. Brain Activity Associated with Individual Sensation Related to Deqi during Tactile Stimulation. For tactile stimulation, the sensation of pressure, tingling, fullness, and heaviness had the sparse impact on the brain activity. The pressure and tingling mainly correlated with positive brain activity, while fullness and heaviness mainly demonstrated negative activity.

Pressure significantly is associated with positive activation in the sensorimotor regions, such as bilateral precentral gyrus, bilateral postcentral gyrus and sulcus, right anterior and superior segments of circular sulcus of the insula, and left inferior segment of circular sulcus of the insula (Table 5, Figure 7(a)).

Heaviness and fullness had the same impact on the brain activity because only one subject had the two sensations with the same intensity score. The two sensations were mainly associated with the negative activity in the bilateral superior temporal gyrus, right precentral gyrus, right central sulcus, left operculum part of the inferior frontal gyrus, left temporal pole, left parahippocampus, and left lingual gyrus (Table 5, Figure 7(b)).

Tingling was mainly associated with sparse positive brain activity in right anterior and superior segments of circular sulcus of the insula, right opercular part of the inferior frontal gyrus, and right hippocampus (Table 5, Figure 7(c)).

4. Discussion

Deqi response [1–4], a psychophysical response characterized by a spectrum of different needling sensations, is essential

Table 4: Summary of anatomic foci showing brain activity of acupuncture stimulation and positive and negative bold responses associated with the intensity of individual needling sensation ($P < 0.05$ corrected).

Atlas structure at the center of maximum difference		Mean fMRI response to acupuncture				Pressure				Heaviness			
		x	y	z	t^*	x	y	z	t^*	x	y	z	t^*
Straight gyrus	L	−2	29	−10	−4.40	−2	59	−1	−3.64				
	R	5	11	−10	−4.65								
Superior frontal gyrus	L					−5	50	27	−3.19	−5	−14	48	2.94
	R	8	32	48	5.01								
	R	8	53	24	−4.19								
Orbital gyri	R	11	44	−13	−4.97	35	29	−7	−3.78	35	29	−7	4.52
Orbital sulci	R	17	41	−10	−3.71	32	29	−7	−3.45	38	32	−4	4.33
Anterior cingulate cortex	L	−8	32	−4	−3.17	−5	32	3	−3.08	−5	41	3	3.70
	R	8	32	−7	−5.01	8	38	3	−3.29	8	44	3	3.84
Subcallosal gyrus	L	−2	11	−7	−3.94	−2	14	3	−2.77				
	R	5	11	−10	−4.65								
Middle-anterior cingulate cortex	R												
Postcentral gyrus	R	44	−20	51	−3.40								
Postcentral sulcus	L	−47	−32	36	3.85								
Superior parietal lobule	L	−11	−65	51	−3.28								
	R	20	−74	39	−3.26								
Intraparietal sulcus	L					−35	−59	39	2.90	−38	−56	39	−4.08
	R									29	−53	42	−4.07
Angular gyrus	L					−53	−59	30	−3.44				
	R	44	−71	30	−3.25	44	−65	33	−2.72				
Supramarginal gyrus	L	−62	−32	33	4.14								
	R	56	−23	24	3.10								
Precuneus	L	−8	−62	48	−3.69					−5	−59	33	2.81
	R	5	−62	42	−3.34								
Ant. insula	L	−26	26	6	2.85								
	R	29	17	−10	−3.73	29	17	−10	−3.34	29	23	−7	3.57
Sup. insula	L	−26	20	15	4.16								
	R	35	26	15	2.82	29	23	12	2.95				
Superior temporal gyrus	R	53	8	−13	−4.92	47	17	−10	−3.23				
Superior temporal sulcus	R	53	−17	−10	−4.94	56	−2	−16	−3.80	50	−2	−10	3.41
Middle temporal gyrus	L	−62	−26	−7	−3.04	−62	−41	3	−4.16				
	R	56	2	−16	−5.19	59	−2	−19	−5.25	62	−17	−13	3.48
Hippocampus	L	−29	−23	−7	−2.72	−23	−41	−1	−3.50				
	R	23	−11	−16	−3.37	32	−35	−4	−4.45	32	−35	−4	2.87
Amygdala	R	26	−8	−16	−3.27								
Parahippocampal gyrus	L	−11	−38	−7	−4.09	−23	5	−19	−4.86				
	R	23	2	−25	−3.98	20	5	−22	−3.46				
Lingual gyrus	L	−8	−62	−1	−4.21	−5	−80	−13	−3.95				
	R	14	−47	−7	−3.65	11	−50	−4	−3.32				
Temporal pole	R	32	17	−28	−5.17	23	5	−28	−3.74				
Cuneus	L	−5	−83	12	−3.64								
	R	5	−86	12	−2.79								
Thalamus proper	L	−17	−20	18	3.09								
	R												
Corpus callosum	L	−12	−42	19	3.09								

Table 4: Continued.

	R												
Cerebellum cortex	L	−35	−68	−25	4.48					−8	−53	−31	2.72
	L	−11	−38	−10	−3.93	−38	−56	−25	−3.01				
	R	29	−44	−43	3.83								
	R	5	−41	−10	−3.48	41	−68	−34	−4.36				
Brain stem		5	−26	−34	−3.00								
Atlas structure at the center of maximum difference		Fullness				Numbness				Tingling			
		x	y	z	t^*	x	y	z	t^*	x	y	z	t^*
Straight gyrus	L									−2	53	−7	−3.54
	R												
Superior frontal gyrus	L	−14	56	27	−2.88					−20	8	60	−3.73
	R					8	−2	57	3.69				
	R									17	44	39	−2.93
Orbital gyri	R	29	26	−10	−3.48					38	50	−1	−3.83
Orbital sulci	R	32	29	−7	−2.99								
Anterior cingulate cortex	L												
	R	11	41	−1	−4.20								
Subcallosal gyrus	L												
	R												
Middle-anterior cingulate cortex	R					5	8	30	3.61				
Postcentral gyrus	R									47	−29	54	−3.46
Postcentral sulcus	L					−56	−23	30	3.10				
Superior parietal lobule	L					−23	−71	36	2.98				
	R	20	−68	42	2.61	20	−68	48	2.96	20	−68	45	−3.38
Intraparietal sulcus	L					−20	−68	39	3.19	−44	−47	39	−3.40
	R	29	−50	39	3.71	32	−56	39	4.47	32	−65	39	−2.79
Angular gyrus	L					−29	−68	36	2.65	−44	−56	42	−3.66
	R	56	−44	27	−2.95	35	−65	39	3.55	38	−65	42	−3.37
Supramarginal gyrus	L					−62	−29	36	3.67	−44	−47	42	−2.96
	R	50	−23	18	3.31	56	−23	30	3.00				
Precuneus	L									−14	−47	57	−2.69
	R												
Ant. insula	L												
	R	29	23	−7	−2.91								
Sup. insula	L												
	R					35	26	15	3.03				
Superior temporal gyrus	R												
Superior temporal sulcus	R	47	−2	−19	−2.62	53	−14	−10	−2.85	44	−71	24	−2.59
Middle temporal gyrus	L									−62	−32	−4	−2.79
	R	62	−17	−16	−3.16	56	2	−16	−4.02				
Hippocampus	L					−20	−32	−7	−3.92	−17	−29	−7	4.69
	R					35	−32	−7	−2.56	35	−26	−7	2.90
Amygdala	R												
Parahippocampal gyrus	L					−14	−38	−7	−3.65	−14	−32	−7	3.87
	R												
Lingual gyrus	L					−11	−86	−7	2.50				
	R												

Table 4: Continued.

Temporal pole	R												
Cuneus	L					−5	−86	12	2.79				
	R												
Thalamus proper	L					−20	−32	−4	−3.90	−8	−32	6	5.48
	R									11	−29	15	3.56
Corpus callosum	L									−17	−35	24	5.17
	R									8	−35	18	4.70
Cerebellum cortex	L	−2	−44	−19	2.50	−47	−56	−28	3.55	−38	−71	−31	3.89
	L					−14	−38	−13	−2.75				
	R	2	−44	−19	3.12					44	−41	−40	4.00
	R					35	−56	−40	3.14				
Brain stem						8	−29	−34	4.02	−14	−23	−7	3.76

t^* is the value taken from the voxel with maximal signal change.
"−" means negative bold responses.
Ant. insula: anterior segment of the circular sulcus of the insula.
Sup. insula: superior segment of the circular sulcus of the insula.

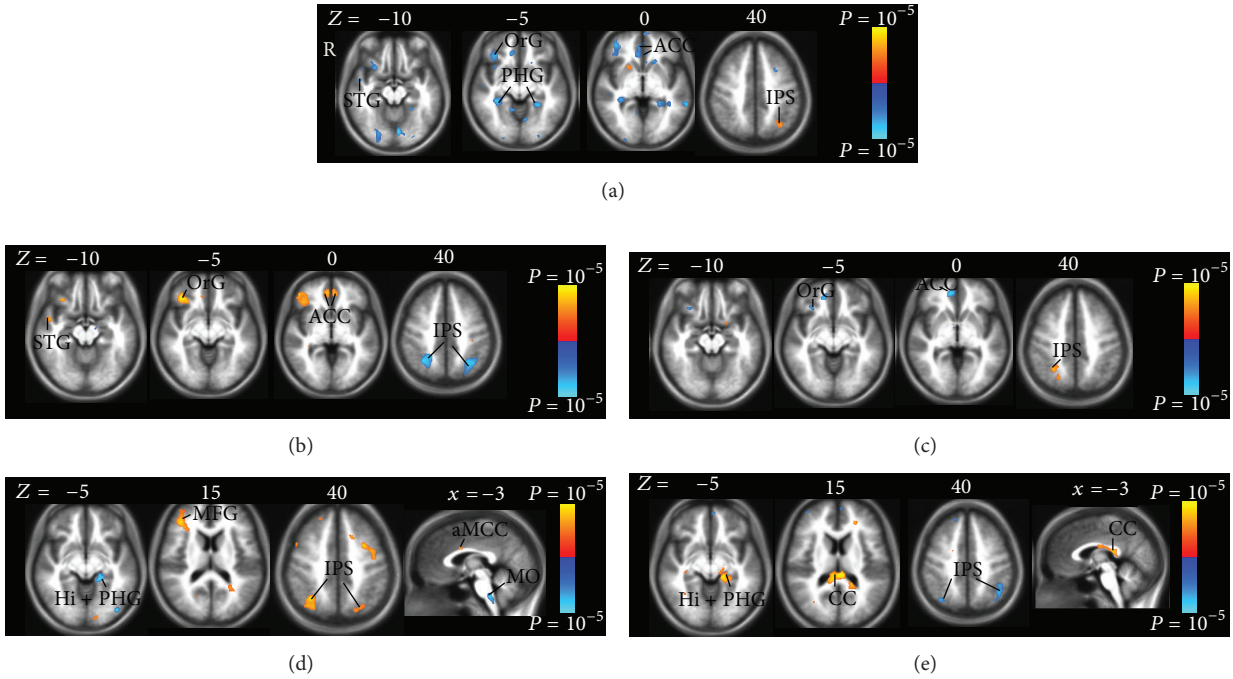

Figure 5: Brain positive (yellow) and negative (blue) bold responses associated with the intensity of individual needling sensation during acupuncture stimulation. The individual sensations are pressure (a), heaviness (b), fullness (c), numbness (d), and tingling (e). The brain regions associated with differential individual sensation are partly overlapped, such as bilateral ACC, right lateral prefrontal cortex (OrG, orbital gyrus), bilateral medial temoral cortex (Hi, hippocampus; PHG, parahippocampal gyrus), and bilateral posterior parietal cortex (IPS, intraparietal sulcus). (a) Pressure contributed to the negative activity in the LPNN network and showed symmetric distributions, such as ACC and PHG. (b) Heaviness showed positive activity in the bilateral ACC, right superior temporal gyrus (STG), and right OrG and negative activity in the bilateral IPS. Heaviness and pressure showed anticorrelated impact on the regions mentioned previously. (c) Fullness was associated with the negative activity in the right ACC and OrG and the positive activity in the right IPS. (d) Numbness showed positive activity in the right middle frontal gyrus (MFG), right anterior middle cingulate cortex (aMCC), and bilateral IPS and negative activity in the left hippocampus (Hi), left PHG, and medulla oblongata (MO). (e) Tingling showed positive activity in the posterior corpus callosum (CC) but negative activity in the posterior parietal cortex (IPS). Tingling and numbness showed anticorrelated impact on bilateral IPS, left Hi, and left PHG.

Table 5: Summary of anatomic foci showing brain activity of tactile stimulation and positive and negative bold responses associated with the intensity of individual needling sensation ($P < 0.05$ corrected).

Atlas structure at the center of maximum difference		Mean fmri response to tactile				Pressure				Heaviness				Fullness				Tingling			
		x	y	z	t^*	x	y	z	t^*	x	y	z	t^*	x	y	z	t^*	x	y	z	t^*
Inferior frontal gyrus	L									−53	14	24	−4.01	−53	14	24	−4.01				
	R					56	−2	12	3.37									41	8	12	3.02
Superior frontal gyrus	L									−11	62	21	−2.91	−11	62	21	−2.91				
	R	20	−2	63	−3.20																
Precentral gyrus	L	−20	−26	63	−2.86	−56	5	24	4.64												
	R	35	−26	48	−2.78	56	−5	24	3.44	35	−26	51	−3.05	35	−26	51	−3.05				
Orbital gyri	R	14	47	−10	−3.29																
Central sulcus	L	−38	−29	57	−3.20																
	R	38	−20	42	−4.55	56	−5	24	3.44	32	−26	51	−3.02	32	−26	51	−3.02				
Postcentral gyrus	L	−38	−29	57	−3.20	−59	−17	30	3.46												
	R	47	−17	45	−3.01	50	−17	48	3.63												
Postcentral sulcus	L	−56	−23	30	3.31	−56	−20	30	4.03												
	R	26	−38	57	−3.30	53	−20	36	3.00												
Supramarginal gyrus	L	−62	−26	24	3.71	−56	−23	30	3.72												
	R					56	−29	27	3.36												
Inf. insula	L	−32	−23	9	3.20	−35	−23	9	3.79												
Ant. insula	R	29	23	6	−3.71	32	26	6	3.08									29	23	6	3.08
Sup. insula	R	35	−14	21	−3.53	35	8	15	3.02									38	11	15	3.55
Superior temporal gyrus	L	−47	8	−19	−3.62	−50	8	−4	3.55	−62	−26	12	−3.19	−62	−26	12	−3.19				
	R	59	−8	−1	−5.02	65	−32	15	3.18	62	−8	6	−3.33	62	−8	6	−3.33				
Superior temporal sulcus	L	−47	5	−19	−3.99					−47	−35	−1	−4.53	−47	−35	−1	−4.53				
	R	59	−11	−1	−4.84																
Middle temporal gyrus	L	−47	8	−22	−3.52																
	R	44	2	−25	−3.68																
Parahippocampal gyrus	L									−20	−29	−16	3.01	−20	−29	−16	3.01	−20	−14	−25	5.48
	L	−32	−17	−22	−2.95					−14	−41	−4	−3.00	−14	−41	−4	−3.00	−32	−11	−31	−4.28
Hippocampus	R	32	−26	−13	−5.38													29	−26	−13	3.86
Lingual gyrus	L	−2	−83	−7	−3.02					−8	−74	6	−3.96	−8	−74	6	−3.96				
Temporal pole	L	−47	5	−28	−3.07					−20	8	−31	−8.18	−20	8	−31	−8.18	−32	−8	−31	−5.31
	R	47	11	−25	−3.06	41	−2	−34	2.77												
Cerebellum cortex	L									−8	−77	−31	3.38	−8	−77	−31	3.38				
	L	−2	−53	−31	−3.08					−32	−47	−52	−3.95	−32	−47	−52	−3.95				
	R	2	−50	−31	−3.26	35	−53	−52	4.07												
Brain stem						−5	−29	−22	3.28												

t^* is the value taken from the voxel with maximal signal change.
"−" means negative bold responses.
Inf. insula: inferior segment of the circular sulcus of the insula.
Ant. insula: anterior segment of the circular sulcus of the insula.
Sup. insula: superior segment of the circular sulcus of the insula.

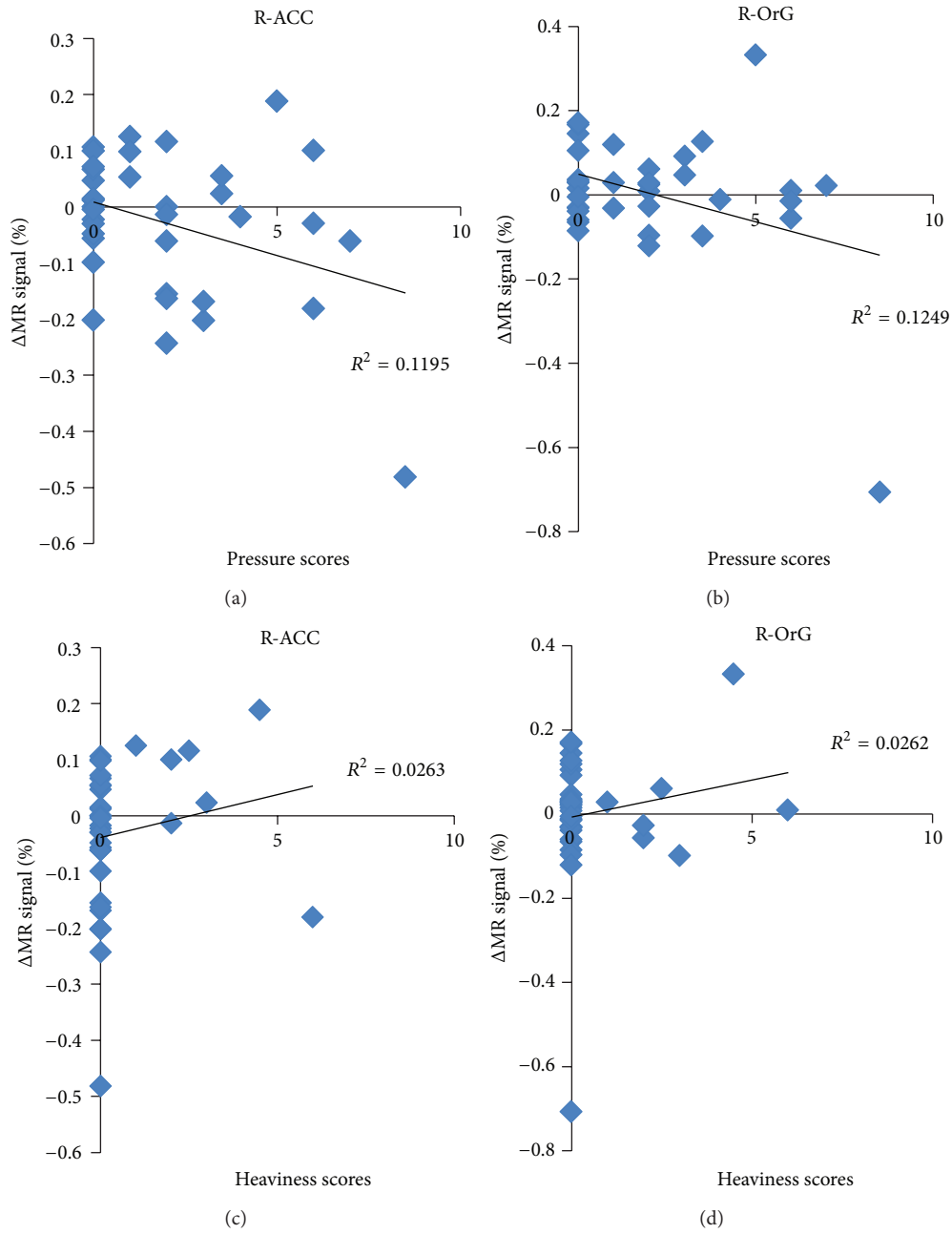

Figure 6: Variance in activity is accounted for by scores of intensity of pressure and heaviness during acupuncture. The negative correlation between the score of pressure and mean MR signal percentage change was shown in the (a) right ACC (anterior cingulate cortex) and (b) right OrG (orbital gyrus). The positive correlation between the score of heaviness and mean MR signal percentage change was shown in the (c) right ACC and (d) right OrG.

for Chinese acupuncture clinical efficacy. A number of fMRI studies including ours have revealed brain activity to acupuncture stimulation [9, 14–16, 19, 20]. However, it has not been reported the impact of these individual sensations of *deqi* on the brain activity during acupuncture stimulation. In this part of the study, we applied fMRI to investigate the neural correlates of five individual sensations including pressure, heaviness, numbness, fullness, and tingling, of *deqi* response during acupuncture at LV3 acupoint. The major findings in the present study included that (1) the pressure sensation was associated with the extensive deactivation of LPNN network during acupuncture; (2) partial overlapping of the positive or negative activity at some of the brain regions associated with the five individual sensations. They included bilateral LPNN, the right lateral orbitofrontal cortex and bilateral posterior parietal cortex. Some needling sensations showed anticorrelated association within the same brain regions; (3) the tingling sensation showed positive correlation

with the brain activity in the bilateral posterior corpus callosum. These findings provide the neuroimaging evidence showing how the different individual needle sensations of *deqi* could both interact differently with the brain and share common interaction with the brain.

4.1. The Pressure Sensation on the Brain Activity of LPNN and Default Mode Network. According to the psychophysical responses, pressure stood out as the most important needling sensation of acupuncture in this study. In addition to the highest frequency (Figure 2) and intensity (Figure 3) among all the related sensations of *deqi* response, pressure also contributed significantly to the extensive deactivation of LPNN, by which acupuncture may mediate its antipain, antianxiety, and other diverse modulatory effect [16].

The salient brain regions that correlate with pressure included bilateral ACC, right inferior frontal cortex, bilateral hippocampus and parahippocampus, bilateral lingual gyrus, right temporal pole, and right insula (Table 4, Figure 5(a)). Many of these brain regions associated with pressure have been shown to be overlapped with those in the default mode network [9, 18, 28]; the integrity of default mode network has been postulated to be central to the balance of global neurological function and the maintenance of health [29].

On the contrary, the increase in the intensity of pressure sensation during tactile stimulation increased brain activity in the sensorimotor regions, such as precentral cortex, postcentral cortex, and insula (Table 5, Figure 7). Such an extreme difference is likely due to the stimulation on the nerves at the cutaneous level during tactile stimulation compared to deep nerve stimulation during manual acupuncture. The LV3 acupoint is located on the dorsum of the foot in the fossa distal to the junction of the first and second metatarsal bones 2 *cuns* (the proportional unit of accurate location of the acupuncture points) above the web of the toe. In tactile stimulation, the mechanoreceptors in the superficial layers transmit pressure sensation to sensorimotor regions by Aδ and Aβ fibers [30]. In acupuncture stimulation, the needle passage includes skin, subcutaneous tissue, the lateral side of the extensor hallucis brevis muscle, deep peroneal nerve, first dorsal metatarsal artery and vein, and first dorsal interosseous muscle [31]. With the deep stimulation at LV3, gentle and repetitive manipulation producing mechanical pressure and tissue distortions activates more mechanoreceptors and nociceptors that are innervated by thin myelinated Aδ and C fibers [32]. Both frequency and intensity of pressure in the acupuncture were therefore higher than those in the tactile stimulation, which was also shown in our analysis of psychophysical data (Figures 2, 3). This is also supported by an earlier human acupuncture study at LI4 (Hegu) on hand, which has the similar tissue composition as LV3 on foot. Chiang et al. found that acupuncture analgesia was completely abolished by blockade of deep nerve branches innervating muscle fibers but not cutaneous nerve fibers [33]. Moreover, the studies on pressure sensation elicited by nonacupuncture mechanical stimulation in deep and superficial tissue had the similar findings [34, 35]. Graven-Nielsen et al. [34] found that the nonpainful pressure sensation can be evoked mechanically from human muscle tissue with complete cutaneous anesthesia. They concluded that the nonpainful pressure sensation is mediated by Aδ and C afferents involving low-threshold mechanoreceptors in the deep tissues. The pressure sensation induced by the temporal summation of mechanical stimulation in deep tissue was shown to be more potent than that in the pure skin stimulation, suggesting that Aδ and C muscle afferent fibers mediate the deep tissue pressure sensation [35].

In addition to the Aδ and Aβ fibers located in superficial layers, our findings indicated that pressure sensation elicited by acupuncture stimulation mainly involved Aδ and C afferent fibers in deep tissues. The studies using EEG [36] and MEG [37, 38] showed that selective stimulation of C-fibers induced the ultra-late evoked brain potentials at the ACC [36, 38], posterior parietal cortex [37], insula, and somatosensory cortex [37, 38]. An recent fMRI study showed that increased activity in the right frontal operculum, inferior frontal cortex and anterior insula to C-fiber alone stimulation as compared to Aδ-fiber alone stimulation. The simulation of Aδ-fiber or C-fiber were both associated with activation in ACC, SMA and thalamus [39]. These brain regions associated with C-fiber/Aδ-fiber in the experimental studies are consistent with our findings in a majority, such as ACC, inferior frontal cortex, and insula. Moreover, a co-stimulation of C- and A-fiber input as produced by usual large-area laser stimulations prevents the recording of ultralate evoked brain potentials (ULEPs), potentials that can be recorded in response to selective stimulation of C-fibers [36]. The negative activity associated with pressure sensation may be the results of the costimulation of C- and Aδ-fiber input, leading to a repression of the central processing of the C-fiber input [39].

4.2. Interplay of the Sensations Pressure, Heaviness, Fullness, Tingling, and Numbness to the Overlapped Brain Regions. The richness of sensory experience is obviously conveyed not by a single receptor or sensory axon but by populations of nerve fibers [30]. It is well accepted that a wide spectrum of myelinated and unmyelinated nerve fibers in cutaneous and/or muscular layers are involved during acupuncture stimulation [6, 40–43]. In a human acupuncture study by means of analyzing power spectrum of the unit discharges with FFT, Wang and colleagues found the relationship between heaviness and fullness and Aδ nerve fibers [6]. In our study, we found that pressure, heaviness, and fullness were associated with heavily overlapping neural activity in ACC, inferior frontal cortex, and insula (Table 4, Figures 5(a), 5(b)). It is consistent with brain response to the stimulation of Aδ and C fiber discussed previously. Compared with pressure, heaviness demonstrated anticorrelated positive activity, while fullness showed similar negative activity in these brain regions. It is possible that fullness also is involved in C-fiber.

All the five sensations demonstrated the associations with brain activity in the posterior parietal cortex including the superior parietal lobule, the inferior parietal lobule, and IPS (Table 4, Figure 5). The posterior parietal cortex receives somatosensory and/or visual input. IPS is crucial for integrating these sensory information related to the body, which through motor signals controls movement of limb

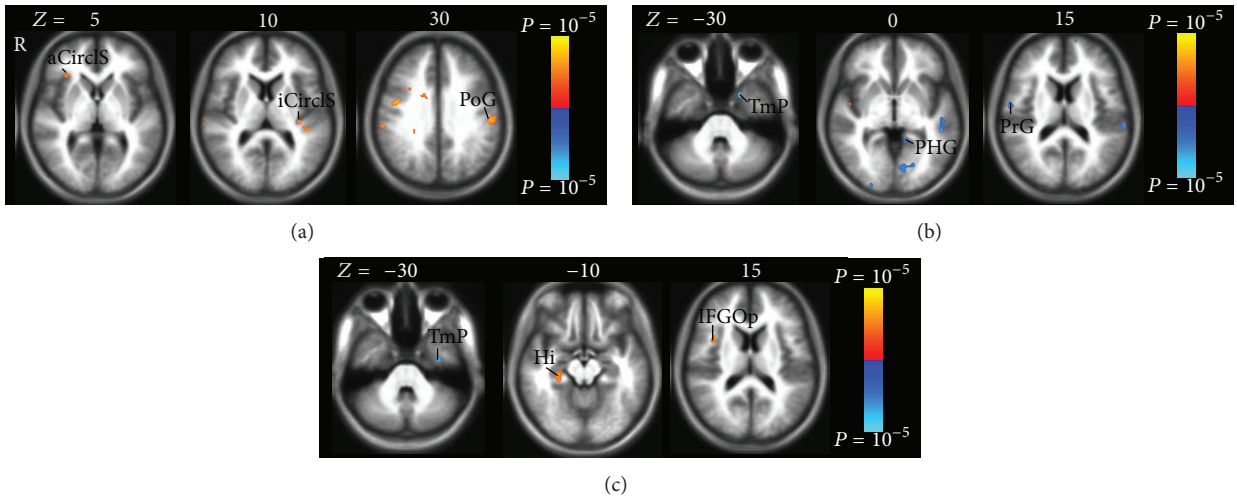

Figure 7: Brain positive (yellow) and negative (blue) bold responses associated with the intensity of individual sensation during tactile stimulation. The individual sensations are pressure (a), heaviness/fullness (b), and tingling (c). (a) Pressure associated with positive activation in the sensorimotor regions, such as right anterior segment of the circular sulcus of the insula (aCirclS), left inferior segment of the circular sulcus of the insula (iCirclS), and left postcentral gyrus (PoG). (b) Heaviness and fullness had the same impact on the negative activation in the right precentral gyrus (PrG), left parahippocampal gyrus (PHG), and left temporal pole (TmP). (c) Tingling was associated with sparse positive brain activity in right opercular part of the inferior frontal gyrus (IFGOp) and right hippocampus (Hi) and negative brain activity in left Tmp.

and eye movement [44]. The study using MEG showed that both selective stimulation of Aδ-fiber or C-fibers induced the ultra-late evoked brain potentials at posterior parietal cortex [37], which supported our findings in the sensations of pressure, heaviness, and fullness involving Aδ-fiber and/or C-fibers. On the other hand, the relationship between the sensations of numbness and tingling and posterior parietal cortex also can be supported by tingling and numbness of limbs commonly found in patients with parietal lobe epilepsy [45, 46].

A number of studies have shown that acupuncture elicits clinical effects via the activation of afferent nerve fibers innervating the skin and muscles [41–43, 47, 48]. The somatic afferent information of nerve fibers has various effects on body function, including analgesia, somatic, autonomic and hormonal response [41, 42, 47, 48]. For example, in a human study on the characteristics of afferent fiber innervation on ST36 (zusanli), which has a significant suppressive effect on jaw movement response (JMR) and electromyogram of digastric muscle induced by acupuncture stimulation, Lu found that these effects were weakened or abolished by sectioning the peroneal nerve and blocking Aβ and some Aδ-fiber. They had a conclusion that the predominance of large afferent fibers was thought to be one of the fundamental characteristics of the acupoint [43].

In line with these studies, these brain regions associated with needling sensation play a role in a wide variety of emotional regulation, cognition, memory, and pain modulation [49–54].The present results in the humans clearly show how these nerve fibers impact on the central nervous system.

4.3. White Matter (Corpus Callosum) Activity during Acupuncture Stimulation. We found that tingling sensation demonstrated significant positive correlation at posterior corpus callosum (posterior midbody, isthmus, and splenium) (Figure 5(e)), which is the principal white matter fiber bundle connecting neocortical areas of the two hemispheres. As the white matter, the corpus callosum is seldom reported in the acupuncture fMRI studies, though a growing number of studies are reporting the fMRI activation in white matter, specifically corpus callosum [55–59]. Our findings can be supported by that the lesions of splenial corpus callosum are responsible for numbness and tingling sensations of unilateral limb or face in patients [60, 61], where the corpus callosum is structurally connected to the functional network of gray matter regions that are involved in the interhemispheric transfer task [57]. Human and monkey studies have shown that the posterior corpus callosum contains connections between the parietal and occipital cortices and plays a role in transferring sensory information [62–66]. Consistent with these results, all the five needling sensations in the present study were associated with posterior parietal cortex as mentioned previously, especially tingling and numbness, supporting that the activation in corpus callosum is the important hemodynamic response of acupuncture stimulation instead of artifact. We further postulate that the corpus callosum may be an important component of acupuncture convey pathway.

4.4. Differences in Brain Activity: Mean Effect versus Individual Needling Sensations Effect of Acupuncture Stimulation. The overlapped regions of the effect of individual needling sensations of acupuncture stimulation provide the details in the modulatory effect of the mean effect. On the other hand, some important brain regions, which are salient in the individual needling sensations effect, might show small or no significant

activity in the mean effect (Figures 4, 5). For example, the posterior corpus callosum demonstrated bilateral extensive activation associated with tingling, while the unilateral small activation shown in the mean effect may be missed as a small artifact [59]. Similarly, for the region of IPS, being crucial for integrating the sensory information related to the body [44], it was extensively associated with all the five individual needling sensations. However, no significant activity was shown in the mean effect. That is why it is insufficient to study the mean effect alone for acupuncture effects.

5. Limitations

In the present study, we extracted data from a larger project that investigated the brain effect of acupuncture. Some of the subjects had more than once acupuncture experiments for different objectives, such as the comparison of real acupuncture and sham acupuncture, different acupoints, and different acupuncture stimulations. However, the data are qualified for the purpose of this study to evaluate the correlation between behavior response and brain response during acupuncture. Considering of the variability of needling sensation during acupuncture stimulation, the further investigation on larger sample size is warranted.

6. Conclusions

The similar or opposite neural activity in the heavily overlapping regions of LPNN and DMN are found responding to different sensations of *deqi* elicited by acupuncture stimulation. The posterior corpus callosum is involved in acupuncture sensation convey pathway. Our data provide the neuroimaging evidence of how the individual needle sensations of *deqi* interact in the brain during acupuncture, and the messages of individual sensation are integrated as the signals converge on processing centers in the central nervous system. It is confirmed that the different psychophysical responses are correlated with the distinct hemodynamic activities.

Acknowledgments

This work was supported by funding from the National Institutes of Health, National Center for Complementary and Alternative Medicine (R21 AT00978, 1-PO1-002048-01, and F05 AT003022), the National Center for Research Resources (P41 RR14075, U54 EB005149, and 424 RR021382), the Human Brain Project Grant (NS34189), the Mental Illness and Neuroscience Discovery Institute (MIND), and the National Natural Science Foundation of China (2013–2016) (Grant no. 81273674). There is no conflict of interests for any author.

References

[1] W. Takeda and J. Wessel, "Acupuncture for the treatment of pain of osteoarthritic knees," *Arthritis Care and Research*, vol. 7, no. 3, pp. 118–122, 1994.

[2] K. K. S. Hui, E. E. Nixon, M. G. Vangel et al., "Characterization of the "deqi" response in acupuncture," *BMC Complementary and Alternative Medicine*, vol. 7, article 33, 2007.

[3] J. Kong, R. Gollub, T. Huang et al., "Acupuncture deqi, from qualitative history to quantitative measurement," *Journal of Alternative and Complementary Medicine*, vol. 13, no. 10, pp. 1059–1070, 2007.

[4] J. Kong, D. T. Fufa, A. J. Gerber et al., "Psychophysical outcomes from a randomized pilot study of manual, electro, and sham acupuncture treatment on experimentally induced thermal pain," *Journal of Pain*, vol. 6, no. 1, pp. 55–64, 2005.

[5] X. Cheng, *Chinese Acupuncture and Moxibustion*, Foreign Language Press, Beijing, China, 1987.

[6] K. M. Wang, S. M. Yao, Y. L. Xian, and Z. L. Hou, "A study on the receptive field of acupoints and the relationship between characteristics of needling sensation and groups of afferent fibres," *Scientia Sinica B*, vol. 28, no. 9, pp. 963–971, 1985.

[7] G. Li and E. S. Yang, "An fMRI study of acupuncture-induced brain activation of aphasia stroke patients," *Complementary Therapies in Medicine*, vol. 19, supplement 1, pp. S49–S59, 2011.

[8] V. Napadow, R. P. Dhond, J. Kim et al., "Brain encoding of acupuncture sensation: coupling on-line rating with fMRI," *NeuroImage*, vol. 47, no. 3, pp. 1055–1065, 2009.

[9] K. K. S. Hui, O. Marina, J. D. Claunch et al., "Acupuncture mobilizes the brain's default mode and its anti-correlated network in healthy subjects," *Brain Research*, vol. 1287, pp. 84–103, 2009.

[10] J. Yang, F. Zeng, Y. Feng et al., "A PET-CT study on the specificity of acupoints through acupuncture treatment in migraine patients," *BMC Complementary and Alternative Medicine*, vol. 12, article 123, no. 1, 2012.

[11] Y. Huang, X. Jiang, Y. Zhuo, A. Tang, and G. Wik, "Complementary acupuncture treatment increases cerebral metabolism in patients with parkinson's disease," *International Journal of Neuroscience*, vol. 119, no. 8, pp. 1190–1197, 2009.

[12] F. Zeng, W.-Z. Song, X.-G. Liu et al., "Brain areas involved in acupuncture treatment on functional dyspepsia patients: a PET-CT study," *Neuroscience Letters*, vol. 456, no. 1, pp. 6–10, 2009.

[13] S. Yeo, S. Lim, I. H. Choe et al., "Acupuncture stimulation on GB34 activates neural responses associated with Parkinson's disease," *CNS Neuroscience and Therapeutics*, vol. 18, no. 9, pp. 781–790, 2012.

[14] K. K. Hui, J. Liu, N. Makris et al., "Acupuncture modulates the limbic system and subcortical gray structures of the human brain: evidence from fMRI studies in normal subjects," *Human Brain Mapping*, vol. 9, no. 1, pp. 13–25, 2000.

[15] K. K. S. Hui, J. Liu, O. Marina et al., "The integrated response of the human cerebro-cerebellar and limbic systems to acupuncture stimulation at ST 36 as evidenced by fMRI," *NeuroImage*, vol. 27, no. 3, pp. 479–496, 2005.

[16] J. Fang, Z. Jin, Y. Wang et al., "The salient characteristics of the central effects of acupuncture needling: limbic-paralimbic-neocortical network modulation," *Human Brain Mapping*, vol. 30, no. 4, pp. 1196–1206, 2009.

[17] J. D. Claunch, S. T. Chan, E. E. Nixon et al., "Commonality and specificity of acupuncture action at three acupoints as evidenced by FMRI," *The American Journal of Chinese Medicine*, vol. 40, no. 4, pp. 695–712, 2012.

[18] R. P. Dhond, C. Yeh, K. Park, N. Kettner, and V. Napadow, "Acupuncture modulates resting state connectivity in default and sensorimotor brain networks," *Pain*, vol. 136, no. 3, pp. 407–418, 2008.

[19] V. Napadow, N. Makris, J. Liu, N. W. Kettner, K. K. Kwong, and K. K. S. Hui, "Effects of electroacupuncture versus manual acupuncture on the human brain as measured by fMRI," *Human Brain Mapping*, vol. 24, no. 3, pp. 193–205, 2005.

[20] K. K. S. Hui, O. Marina, J. Liu, B. R. Rosen, and K. K. Kwong, "Acupuncture, the limbic system, and the anticorrelated networks of the brain," *Autonomic Neuroscience*, vol. 157, no. 1-2, pp. 81–90, 2010.

[21] J. Kong, T. J. Kaptchuk, J. M. Webb et al., "Functional neuroanatomical investigation of vision-related acupuncture point specificity: a multisession fMRI study," *Human Brain Mapping*, vol. 30, no. 1, pp. 38–46, 2009.

[22] A. U. Asghar, G. Green, M. F. Lythgoe, G. Lewith, and H. MacPherson, "Acupuncture needling sensation: the neural correlates of deqi using fMRI," *Brain Research*, vol. 1315, pp. 111–118, 2010.

[23] R. W. Cox, "AFNI: software for analysis and visualization of functional magnetic resonance neuroimages," *Computers and Biomedical Research*, vol. 29, no. 3, pp. 162–173, 1996.

[24] J. Talairach and P. Tournoux, *Co-Planar Stereotaxic Atlas of the Human Brain*, Thieme Medical, New York, NY, USA, 1988.

[25] R. M. O'Brien, "A caution regarding rules of thumb for variance inflation factors," *Quality and Quantity*, vol. 41, no. 5, pp. 673–690, 2007.

[26] S. Gold, B. Christian, S. Arndt et al., "Functional MRI statistical software packages: a comparative analysis," *Human Brain Mapping*, vol. 6, no. 2, pp. 73–84, 1998.

[27] L. L. Wald, *Simultaneous Inference For FMRI Data*, Biophysics Research Institute, Medical College of Wisconsin, 1997.

[28] J. Fang, X. Wang, H. Liu et al., "The limbic-prefrontal network modulated by electroacupuncture at CV4 and CV12," *Evidence-Based Complementary and Alternative Medicine*, vol. 2012, Article ID 515893, 11 pages, 2012.

[29] R. L. Buckner, J. R. Andrews-Hanna, and D. L. Schacter, "The brain's default network: anatomy, function, and relevance to disease," *Annals of the New York Academy of Sciences*, vol. 1124, pp. 1–38, 2008.

[30] R. K. Eric, H. S. James, and M. J. T, *Principles of Neural Science*, McGraw-Hill, 4th edition, 2000.

[31] E. Chen, *Cross-Section Anatomy of Acupoints*, Churchill Livingstone, 1995.

[32] Z.-J. Zhang, X.-M. Wang, and G. M. McAlonan, "Neural acupuncture unit: a new concept for interpreting effects and mechanisms of acupuncture," *Evidence-Based Complementary and Alternative Medicine*, vol. 2012, Article ID 429412, 23 pages, 2012.

[33] C. Y. Chiang, C. T. Chang, H. C. Chu, and L. F. Yang, "Peripheral afferent pathway for acupuncture anlgesia," *Scientia Sinica*, vol. 16, pp. 210–217, 1973.

[34] T. Graven-Nielsen, S. Mense, and L. Arendt-Nielsen, "Painful and non-painful pressure sensations from human skeletal muscle," *Experimental Brain Research*, vol. 159, no. 3, pp. 273–283, 2004.

[35] H. Nie, L. Arendt-Nielsen, H. Andersen, and T. Graven-Nielsen, "Temporal summation of pain evoked by mechanical stimulation in deep and superficial tissue," *Journal of Pain*, vol. 6, no. 6, pp. 348–355, 2005.

[36] E. Opsommer, T. Weiss, L. Plaghki, and W. H. R. Miltner, "Dipole analysis of ultralate (C-fibres) evoked potentials after laser stimulation of tiny cutaneous surface areas in humans," *Neuroscience Letters*, vol. 298, no. 1, pp. 41–44, 2001.

[37] N. Forss, T. T. Raij, M. Seppä, and R. Hari, "Common cortical network for first and second pain," *NeuroImage*, vol. 24, no. 1, pp. 132–142, 2005.

[38] M. Ploner, J. Gross, L. Timmermann, and A. Schnitzler, "Cortical representation of first and second pain sensation in humans," *Proceedings of the National Academy of Sciences of the United States of America*, vol. 99, no. 19, pp. 12444–12448, 2002.

[39] T. Weiss, T. Straube, J. Boettcher, H. Hecht, D. Spohn, and W. H. R. Miltner, "Brain activation upon selective stimulation of cutaneous C- and Aδ-fibers," *NeuroImage*, vol. 41, no. 4, pp. 1372–1381, 2008.

[40] R. Radhakrishnan and K. A. Sluka, "Deep tissue afferents, but not cutaneous afferents, mediate transcutaneous electrical nerve stimulation-induced antihyperalgesia," *Journal of Pain*, vol. 6, no. 10, pp. 673–680, 2005.

[41] F. Kagitani, S. Uchida, H. Hotta, and Y. Aikawa, "Manual acupuncture needle stimulation of the rat hindlimb activates groups I, II, III and IV single afferent nerve fibers in the dorsal spinal roots," *Japanese Journal of Physiology*, vol. 55, no. 3, pp. 149–155, 2005.

[42] F. Kagitani, S. Uchida, and H. Hotta, "Afferent nerve fibers and acupuncture," *Autonomic Neuroscience*, vol. 157, no. 1-2, pp. 2–8, 2010.

[43] G. W. Lu, "Characteristics of afferent fiber innervation on acupuncture points zusanli," *The American Journal of Physiology*, vol. 245, no. 4, pp. R606–612, 1983.

[44] C. Grefkes and G. R. Fink, "The functional organization of the intraparietal sulcus in humans and monkeys," *Journal of Anatomy*, vol. 207, no. 1, pp. 3–17, 2005.

[45] M. A. Rahal, G. M. de Araújo Filho, L. O. S. F. Caboclo et al., "Somatosensory aura in mesial temporal lobe epilepsy: semiologic characteristics, MRI findings and differential diagnosis with parietal lobe epilepsy," *Journal of Epilepsy and Clinical Neurophysiology*, vol. 12, no. 3, pp. 155–160, 2006.

[46] J. Yamamoto, A. Ikeda, M. Matsuhashi et al., "Seizures arising from the inferior parietal lobule can show ictal semiology of the second sensory seizure (SII seizure)," *Journal of Neurology Neurosurgery and Psychiatry*, vol. 74, no. 3, pp. 367–369, 2003.

[47] A. Kimura and A. Sato, "Somatic regulation of autonomic functions in anesthetized animals: neural mechanisms of physical therapy including acupuncture," *Japanese Journal of Veterinary Research*, vol. 45, no. 3, pp. 137–145, 1997.

[48] H. Ohsawa, S. Yamaguchi, H. Ishimaru, M. Shimura, and Y. Sato, "Neural mechanism of pupillary dilation elicited by electro-acupuncture stimulation in anesthetized rats," *Journal of the Autonomic Nervous System*, vol. 64, no. 2-3, pp. 101–106, 1997.

[49] J. R. Andrews-Hanna, J. S. Reidler, J. Sepulcre, R. Poulin, and R. L. Buckner, "Functional-anatomic fractionation of the brain's default network," *Neuron*, vol. 65, no. 4, pp. 550–562, 2010.

[50] A. R. Aron, T. W. Robbins, and R. A. Poldrack, "Inhibition and the right inferior frontal cortex," *Trends in Cognitive Sciences*, vol. 8, no. 4, pp. 170–177, 2004.

[51] Z.-Q. Zhao, "Neural mechanism underlying acupuncture analgesia," *Progress in Neurobiology*, vol. 85, no. 4, pp. 355–375, 2008.

[52] L.-G. Lei, Y.-Q. Zhang, and Z.-Q. Zhao, "Pain-related aversion and Fos expression in the central nervous system in rats," *NeuroReport*, vol. 15, no. 1, pp. 67–71, 2004.

[53] Y.-J. Gao, W.-H. Ren, Y.-Q. Zhang, and Z.-Q. Zhao, "Contributions of the anterior cingulate cortex and amygdala to pain- and fear-conditioned place avoidance in rats," *Pain*, vol. 110, no. 1-2, pp. 343–353, 2004.

[54] D. D. Price, "Psychological and neural mechanisms of the affective dimension of pain," *Science*, vol. 288, no. 5472, pp. 1769–1772, 2000.

[55] J. R. Gawryluk, R. C. N. D'Arcy, E. L. Mazerolle, K. D. Brewer, and S. D. Beyea, "Functional mapping in the corpus callosum: a 4T fMRI study of white matter," *NeuroImage*, vol. 54, no. 1, pp. 10–15, 2011.

[56] J. R. Gawryluk, K. D. Brewer, S. D. Beyea, and R. C. N. D'Arcy, "Optimizing the detection of white matter fMRI using asymmetric spin echo spiral," *NeuroImage*, vol. 45, no. 1, pp. 83–88, 2009.

[57] E. L. Mazerolle, S. D. Beyea, J. R. Gawryluk, K. D. Brewer, C. V. Bowen, and R. C. N. D'Arcy, "Confirming white matter fMRI activation in the corpus callosum: co-localization with DTI tractography," *NeuroImage*, vol. 50, no. 2, pp. 616–621, 2010.

[58] E. L. Mazerolle, R. C. N. D'Arcy, and S. D. Beyea, "Detecting functional magnetic resonance imaging activation in white matter: interhemispheric transfer across the corpus callosum," *BMC neuroscience*, vol. 9, article 84, 2008.

[59] L. M. Fraser, M. T. Stevens, S. D. Beyea, and R. C. D'Arcy, "White versus gray matter: fMRI hemodynamic responses show similar characteristics, but differ in peak amplitude," *BMC Neuroscience*, vol. 13, article 91, 2012.

[60] T.-P. Chang and C.-F. Huang, "Unilateral paresthesia after isolated infarct of the splenium: case report," *Acta Neurologica Taiwanica*, vol. 19, no. 2, pp. 116–119, 2010.

[61] N. Bulakbasi, M. Kocaoglu, C. Tayfun, and T. Ucoz, "Transient splenial lesion of the corpus callosum in clinically mild influenza-associated encephalitis/encephalopathy," *The American Journal of Neuroradiology*, vol. 27, no. 9, pp. 1983–1986, 2006.

[62] M. Zarei, H. Johansen-Berg, S. Smith, O. Ciccarelli, A. J. Thompson, and P. M. Matthews, "Functional anatomy of interhemispheric cortical connections in the human brain," *Journal of Anatomy*, vol. 209, no. 3, pp. 311–320, 2006.

[63] S. F. Witelson, "Hand and sex differences in the isthmus and genu of the human corpus callosum. A postmortem morphological study," *Brain*, vol. 112, no. 3, pp. 799–835, 1989.

[64] M. C. de Lacoste, J. B. Kirkpatrick, and E. D. Ross, "Topography of the human corpus callosum," *Journal of Neuropathology and Experimental Neurology*, vol. 44, no. 6, pp. 578–591, 1985.

[65] D. N. Pandya, E. A. Karol, and D. Heilbronn, "The topographical distribution of interhemispheric projections in the corpus callosum of the rhesus monkey," *Brain Research*, vol. 32, no. 1, pp. 31–43, 1971.

[66] M. G. Funnell, P. M. Corballis, and M. S. Gazzaniga, "Insights into the functional specificity of the human corpus callosum," *Brain*, vol. 123, no. 5, pp. 920–926, 2000.

Hindawi Publishing Corporation
Evidence-Based Complementary and Alternative Medicine
Volume 2013, Article ID 369324, 8 pages
http://dx.doi.org/10.1155/2013/369324

Research Article

Effect of Bee Venom Acupuncture on Oxaliplatin-Induced Cold Allodynia in Rats

Bong-Soo Lim,[1] Hak Jin Moon,[1] Dong Xing Li,[2] Munsoo Gil,[1] Joon Ki Min,[1] Giseog Lee,[1,2] Hyunsu Bae,[2] Sun Kwang Kim,[2] and Byung-Il Min[1,3]

[1] *Department of East-West Medicine, Graduate School, Kyung Hee University, Seoul 130-701, Republic of Korea*
[2] *Department of Physiology, College of Korean Medicine, Kyung Hee University, Seoul 130-701, Republic of Korea*
[3] *Department of Physiology, College of Medicine, Kyung Hee University, Seoul 130-701, Republic of Korea*

Correspondence should be addressed to Sun Kwang Kim; skkim77@khu.ac.kr and Byung-Il Min; mbi@khu.ac.kr

Received 19 February 2013; Accepted 18 July 2013

Academic Editor: Jian Kong

Oxaliplatin, a chemotherapy drug, often leads to neuropathic cold allodynia after a single administration. Bee venom acupuncture (BVA) has been used in Korea to relieve various pain symptoms and is shown to have a potent antiallodynic effect in nerve-injured rats. We examined whether BVA relieves oxaliplatin-induced cold allodynia and which endogenous analgesic system is implicated. The cold allodynia induced by an oxaliplatin injection (6 mg/kg, i.p.) was evaluated by immersing the rat's tail into cold water (4°C) and measuring the withdrawal latency. BVA (1.0 mg/kg, s.c.) at Yaoyangguan (GV3), Quchi (LI11), or Zusanli (ST36) acupoints significantly reduced cold allodynia with the longest effect being shown in the GV3 group. Conversely, a high dose of BVA (2.5 mg/kg) at GV3 did not show a significant antiallodynic effect. Phentolamine (α-adrenergic antagonist, 2 mg/kg, i.p.) partially blocked the relieving effect of BVA on allodynia, whereas naloxone (opioid antagonist, 2 mg/kg, i.p.) did not. We further confirmed that an intrathecal administration of idazoxan (α_2-adrenergic antagonist, 50 μg) blocked the BVA-induced anti-allodynic effect. These results indicate that BVA alleviates oxaliplatin-induced cold allodynia in rats, at least partly, through activation of the noradrenergic system. Thus, BVA might be a potential therapeutic option in oxaliplatin-induced neuropathy.

1. Introduction

Colorectal cancer (CRC) was the third most common cancer in both men and women, and it caused about 608,000 deaths in 2008 worldwide, making it the fourth most common cause of death from cancer [1]. Oxaliplatin is an important chemotherapy drug for the treatment of patients with metastatic CRC [2, 3]. Because of its platinum-based molecular structure, it causes a neurotoxic side effect, characterized by the rapid onset of spontaneous severe pain and cold allodynia in the hands, feet, perioral area, or throat, even from a single administration [4, 5]. It is the only major dose-limiting toxicity associated with oxaliplatin use [6]. Since the mechanism is still unclear, an effective treatment of established neuropathic allodynia has yet to be found [7]. Therefore, it would be highly important to find the potential therapeutic options to manage oxaliplatin-induced neuropathic pain.

Bee venom acupuncture (BVA), a treatment method of injecting bee venom (BV) into one or more acupoints, has been used traditionally in East Asia, especially Korea, to relieve pain and treat various diseases, such as arthritis, rheumatism, back pain, sprain, and herniation of nucleus pulposus [8–12]. It is well known that the analgesic effects of acupuncture or electroacupuncture (EA) are mediated by the endogenous opioid and/or noradrenergic system [13–18]. In contrast, the antinociceptive actions of BVA were reported to be mediated by the noradrenergic system, not by the opioids [19–21]. In peripheral nerve-injured rats, Lee and his colleagues have demonstrated that BVA attenuated mechanical allodynia, heat hyperalgesia, and cold allodynia, mainly through the activation of the central noradrenergic system [22–24]. However, the effect of BVA on oxaliplatin-induced neuropathic pain and its mechanism has not been studied.

In the present study, we investigated whether BVA relieves oxaliplatin-induced cold allodynia, and if so, which endogenous analgesic system is implicated. We report here that BVA has a potent antiallodynic effect on oxaliplatin-induced peripheral neuropathy in rats, which is acupoint- and dose-related, and that it involves the noradrenergic system partially, but not the endogenous opioid system.

2. Materials and Methods

2.1. Animals. Adult male Sprague-Dawley rats (210–250 g, 8 weeks old) (Daehan Biolink, Chungbuk, Korea) were housed in cages (3-4 rats per cage) with water and food available *ad libitum*. The room was maintained with a 12 h-light/dark cycle (a light cycle; 08:00–20:00, a dark cycle; 20:00–08:00) and kept at 23 ± 2°C. All animals were acclimated in their cages for 1 week prior to any experiments. All procedures involving animals were approved by the Institutional Animal Care and Use Committee of Kyung Hee University (KHUASP(SE)-12-044) and were conducted in accordance with the guidelines of the International Association for the Study of Pain [25].

2.2. Oxaliplatin Injection. As described previously [5, 26], oxaliplatin (Sigma Chemical Co., USA) was dissolved in a 5% glucose (Sigma, USA) solution at a concentration of 2 mg/mL and was intraperitoneally administered at 6 mg/kg. The same volume of 5% glucose solution was injected in the vehicle control group.

2.3. Behavioral Tests. To estimate whether cold allodynia was induced, cold immersion test was carried out as described previously [27, 28]. Briefly, each animal was lightly immobilized in a plastic holder and its tail was drooped for proper application of cold water stimuli. The rats were adapted to the holder for 2 days before starting behavioral tests. The tail was immersed in 4°C water, and then the tail withdrawal latency (TWL) was measured with a cut-off time of 15 seconds. The cold immersion test was repeated five times at 5 min intervals. When calculating the average latency, the cut-off time was assigned to the normal responses. The average latency was taken as a measure for the severity of cold allodynia; a shorter TWL was interpreted as more severe allodynia.

Because our previous study showed that a significant allodynic behavior is induced from 3 days after a single oxaliplatin (6 mg/kg, i.p.) injection and lasted up to 1 week after an injection (unpublished data), we tested whether and how BVA relieves oxaliplatin-induced cold allodynia from 3 to 7 days after an oxaliplatin administration.

2.4. BVA Treatment. To determine the optimal acupoint of BVA, oxaliplatin-injected rats were divided randomly into three groups: Quchi (LI11), Zusanli (ST36), and Yaoyangguan (GV3) groups (n = 4/group). After baseline cold sensitivity was measured, BV (1.0 mg/kg) dissolved in normal saline (N/S, 0.05 cc) was injected subcutaneously at GV3, right LI11, or right ST36 acupoints, respectively (Figure 1). The cold immersion test was performed again at 1 hour and 2 hours after BVA. LI11 is located at the depression medial to the extensor carpi radialis, at the lateral end of cubital crease [29]. ST36 is located in the anterior tibial muscle, 5 mm lateral and distal from the anterior tubercle of the tibia [30]. GV3 acupoint is located between the spinous processes of the fourth and the fifth lumbar vertebrae [29].

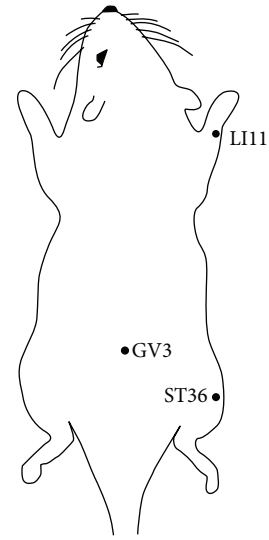

Figure 1: Schematic representation of acupoints used in this study: Quchi (LI11), Zusanli (ST36), and Yaoyangguan (GV3).

In order to find the effective dose of BVA, the rats with cold allodynia were divided randomly into four groups BV2.5, BV1.0, BV0.25, and CON groups (n = 4/group). BV (2.5 mg/kg, 1.0 mg/kg or 0.25 mg/kg) dissolved in N/S was injected subcutaneously at GV3 acupoint. To the control group (CON), only 0.05 cc of N/S was injected subcutaneously at the same acupoint.

2.5. Drug Treatment. To investigate the mechanism of BVA, oxaliplatin-injected rats were divided randomly into three groups: N/S + BV, Naloxone + BV, and Phentolamine + BV (n = 6/group). After baseline, cold sensitivity was checked; Naloxone + BV and Phentolamine + BV groups were treated intraperitoneally with naloxone and phentolamine (2 mg/kg, dissolved in normal saline to a concentration of 1 mg/mL), respectively. N/S + BV group was treated intraperitoneally with normal saline. Twenty minutes later, all groups were treated subcutaneously with 0.25 mg/kg of BV at GV3 acupoint. To further confirm the noradrenergic mechanism of BVA-induced antiallodynia, an idazoxan (α_2-adrenergic receptor antagonist, 50 μg dissolved in 50 μL N/S) or N/S, was administered intrathecally under isoflurane anesthesia as described previously [31]. The cold immersion test was performed again 30 min after BVA. All drugs were obtained from Sigma-Aldrich (St. Louis, MO, USA).

2.6. Statistical Analysis. All the data are presented as mean ± SEM. Statistical analysis and graphic works were done with Prism 5.0 (Graph Pad Software, USA). Paired t-test or repeated measures analysis of variance (ANOVA) followed by Dunnett's post hoc test was used for statistical analysis. In all cases, $P < 0.05$ was considered significant.

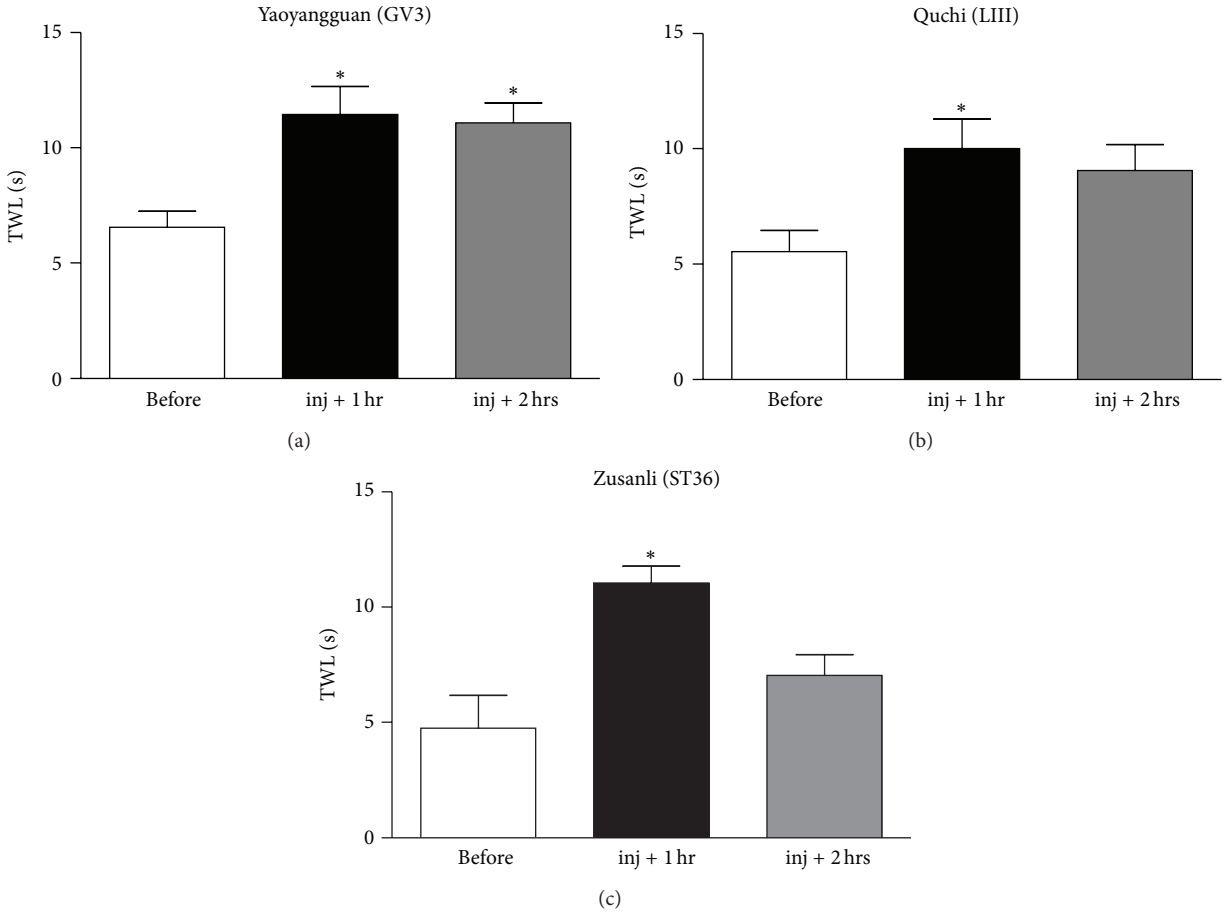

Figure 2: Effects of BVA at different acupoints on oxaliplatin-induced cold allodynia. The behavioral tests for cold allodynia were performed before and after BVA (1.0 mg/kg) at GV3, (a), right LI11 (b), or right ST36 (c) acupoints ($n = 4$/group). In all groups, the tail withdrawal latency (TWL) 1 hr after BVA increased significantly as compared with the TWL before injection. Only GV3 group showed a significant increase in the TWL 2 hr after BVA. Data are presented as mean ± SEM. $^*P < 0.05$ by repeated measures one-way ANOVA followed by Dunnett's post hoc test.

3. Results

3.1. Effects of BVA on Oxaliplatin-Induced Cold Allodynia: Acupoints and Doses. The anti-allodynic effects of BVA at different acupoints (GV3, LI11, or ST36) in oxaliplatin-injected rats are shown in Figure 2. In all groups, BVA treatments (1.0 mg/kg, s.c.) significantly increased TWL at 1 hr after BVA as compared with the baseline TWL ($P < 0.05$). Such anti-allodynic effect of BVA at GV3 lasted up to 2 hr after the treatment ($P < 0.05$), whereas the well-known analgesic acupoints, LI11 and ST36 BVA treatments, showed no significant effects at 2 hr after BVA ($P > 0.05$). In control experiments, no significant difference in TWLs before and after a light immobilization without BVA (data not shown) or N/S injection at GV3 ($P > 0.05$, Figure 3(d)) was observed. These results suggest that BVA treatments has potent analgesic actions, of which efficacy is dependent on acupoint.

Figure 3 shows the effects of BVA with different doses on oxaliplatin-induced cold allodynia. A high dose of BVA (2.5 mg/kg) or N/S injection at GV3 did not show a significant anti-allodynic effect ($P > 0.05$), whereas low doses of BVA (0.25 mg/kg and 1.0 mg/kg) at GV3 markedly increased TWLs 1 hr after injection as compared with the TWL before injection ($P < 0.01$ and $P < 0.05$, resp.). BVA at ST36 or LI11 with the highest (2.5 mg/kg) or lowest (0.25 mg/kg) dose showed no significant anti-allodynic effects (TWLs before versus after BVA: 3.13 ± 1.10 versus 7.35 ± 2.09 (2.5 mg/kg BVA at ST36); 4.65 ± 1.16 versus 8.61 ± 1.25 (2.5 mg/kg BVA at LI11); 4.90 ± 0.75 versus 9.04 ± 2.00 (0.25 mg/kg BVA at ST36); 3.87 ± 0.60 versus. 6.49 ± 2.41 (0.25 mg/kg BVA at LI11); $n = 4$/group, $P > 0.05$ by paired t-test).

3.2. Effects of Opioid and Adrenergic Receptor Antagonists on BVA-Induced Antiallodynia. Since 0.25 mg/kg of BVA was slightly more effective than 1.0 mg/kg BVA (Figures 3(b)-3(c)), 0.25 mg/kg of BVA at GV3 was used to see which endogenous analgesic system mediates BVA-induced anti-allodynic action. As shown in Figure 4, phentolamine-(α-adrenergic receptor antagonist, 2 mg/kg, i.p.) pretreated group exhibited no significant difference in TWL before and after BVA ($P > 0.05$), suggesting that the noradrenergic system plays a role in mediating the suppressive effect of BVA

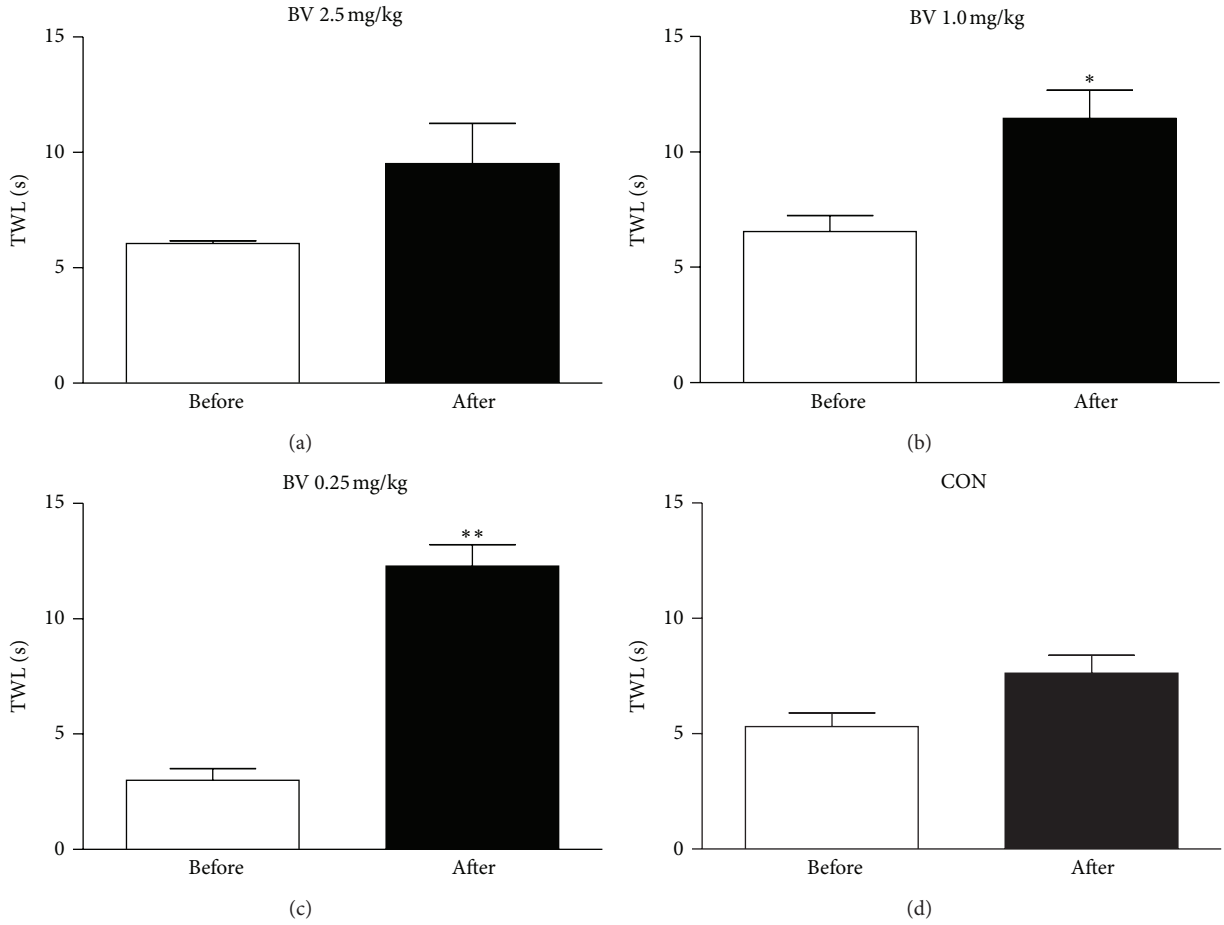

Figure 3: Effects of BVA in different doses of BV on oxaliplatin-induced cold allodynia. The behavioral tests for cold allodynia were performed before and after 2.5 mg/kg (a), 1.0 mg/kg (b), or 0.25 mg/kg (c) BVA treatment at GV3 acupoint (n = 4/group). In the control group (CON), only 0.05 cc of normal saline was injected (d). In BV1.0 and BV0.25 groups, the TWL after BVA significantly increased as compared with TWL before BVA. No significant difference between TWLs before and after injection was observed in BV2.5 and CON groups. Data are presented as mean ± SEM. $^{*}P < 0.05$, $^{**}P < 0.01$ by paired t-test.

on oxaliplatin-induced cold allodynia. We further confirmed that an intrathecal (i.t.) injection of idazoxan (α_2-adrenergic receptor antagonist, 50 μg), but not N/S, blocked the BVA-induced anti-allodynic effect (Figures 4(d)-4(e). In contrast, naloxone (opioid antagonist, 2 mg/kg, i.p.) and N/S showed significant increase in TWL after BVA treatment ($P < 0.01$ and $P < 0.05$, resp.), indicating that the endogenous opioid system is not involved in BVA-induced anti-allodynia.

4. Discussion

Oxaliplatin is a platinum-based third-generation chemotherapy drug to treat patients with metastatic CRC [2, 3]. Thus, it is structurally similar to cisplatin and carboplatin and has a neurotoxic side effect, but no nephrotoxicity and hematotoxicity have been observed [2, 4]. This acute oxaliplatin-induced neurotoxicity is developed even through a single oxaliplatin administration [5, 26]. There were only a few reports showing the effective treatment or prevention of oxaliplatin-induced neuropathic pain symptoms. Although the intravenous calcium and magnesium therapy could attenuate the development of oxaliplatin-induced neuropathy [32, 33], it was not complete yet in the treatment of the established allodynia [7, 34]. Therefore, it is now required to find the potential therapeutic options to manage oxaliplatin-induced neuropathic pain.

This study clearly shows that BVA has a potent anti-allodynic effect in oxaliplatin-injected rats (Figures 2 and 3). To see acupoint-dependent effect, we examined which acupoint has the most relieving effect on oxaliplatin-induced cold allodynia. Although BVA at LI11, ST36, and GV3 acupoints all had significant analgesic effects, BVA at GV3 acupoint had a longer lasting effect than the other acupoints (Figure 2). This duration of anti-allodynic action of BVA at GV3 (lasting for ~2 hr) is clinically important because morphine (1, 2, and 4 mg/kg, i.p.) showed no significant analgesic effect at 2 hr after its administration [26]. It also should be noted that GV3 acupoint is closer to the tail, where cold immersion test was performed, than the other acupoints. Interestingly, we found that EA stimulation at a point on

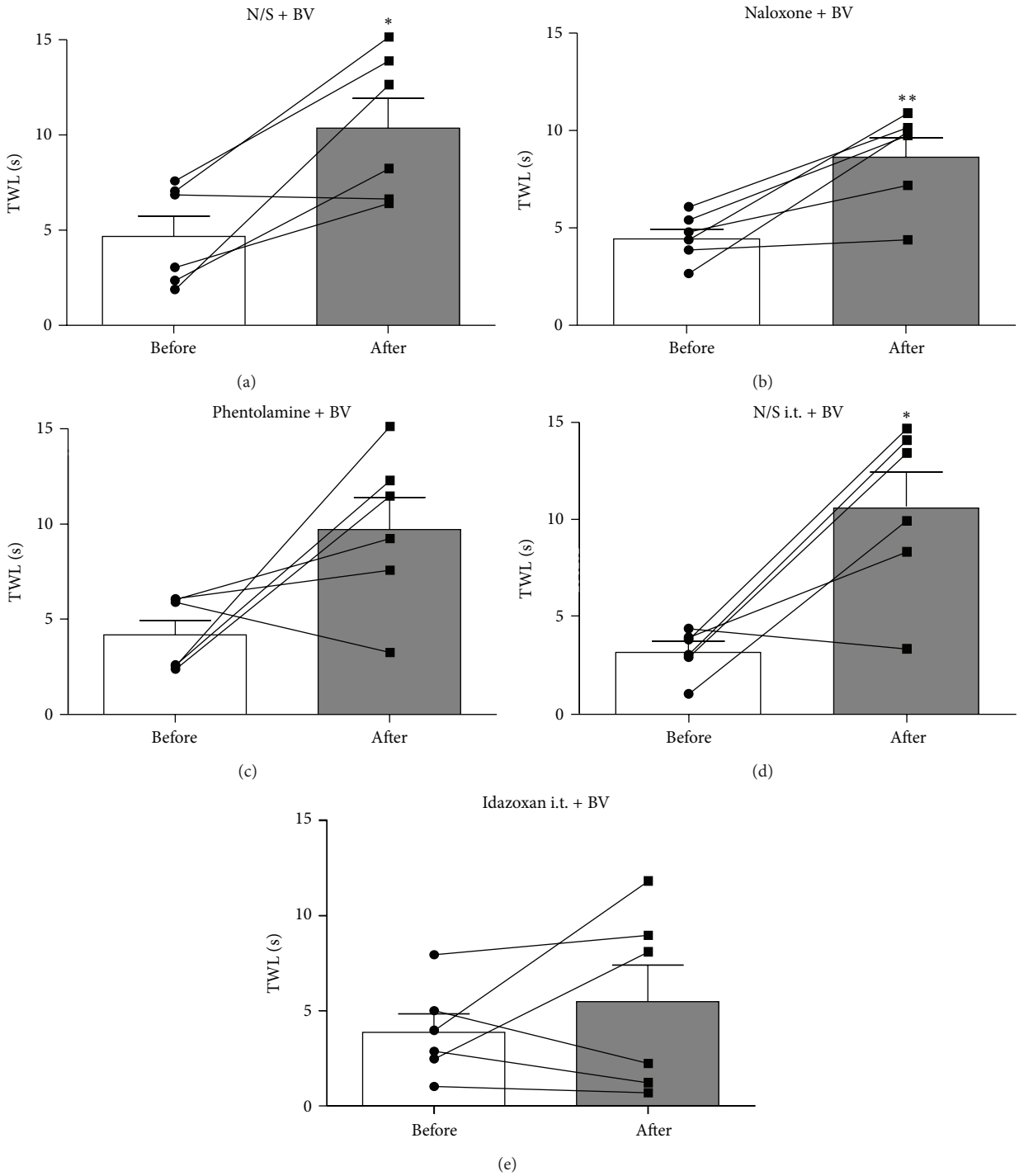

Figure 4: Effects of opioid and adrenergic receptor antagonists on BVA-induced anti-allodynic action. The behavioral tests for cold allodynia were performed before pretreatment of antagonists and after BVA (0.25 mg/kg) treatment at GV3 acupoint. (a) N/S + BV (normal saline (i.p.) pretreatment + BVA, $n = 6$). (b) Naloxone + BV (naloxone (2 mg/kg, i.p.) pretreatment + BVA, $n = 6$). (c) Phentolamine + BV (phentolamine (2 mg/kg, i.p.) pretreatment + BVA, $n = 6$). In N/S + BV and Naloxone + BV groups, TWLs after BVA significantly increased as compared with baseline TWL. In contrast, Phentolamine + BV group showed no significant increase in TWL after BVA. Note that TWL of three subjects of Phentolamine + BV group substantially increased after BVA, whereas TWL of the other three subjects did not. (d) N/S i.t. + BV (normal saline (i.t.) pretreatment + BVA, $n = 6$). (e) Idazoxan i.t. + BV (idazoxan pretreatment (50 μg, i.t.) + BVA, $n = 6$). Data are presented as mean ± SEM. Dots and lines represent the TWL change of individual subject. $^{*}P < 0.05$, $^{**}P < 0.01$ by paired t-test.

the hind limb had a greater anti-allodynic effect than EA at a point that is close to the tested tail (unpublished data). These results might suggest that proximal acupoint stimulation is more effective in BVA treatment on oxaliplatin-induced neuropathic pain, whereas distal acupoint stimulation is more effective in EA treatment.

In regard to the effective dose of BVA, we demonstrate that a low dose of BVA (1.0 or 0.25 mg/kg) has a significant anti-allodynic effect in oxaliplatin-injected rats while a high dose of BVA (2.5 mg/kg) has no significant effect (Figure 3). Such result is different from the results in a previous study by Kang et al. [23] showing that a low dose (0.25 mg/kg) of BVA did not produce significant anti-allodynic effect, while a high dose of BVA (2.5 mg/kg) significantly reduced cold allodynia in a rat model of sciatic nerve chronic constriction injury (CCI). This discrepancy might be due to the differences in pain model (sciatic nerve CCI versus oxaliplatin), the region of the cold allodynia test (hind paw versus tail), and acupoints used (ST36 versus GV3). In the present study, however, one of the rats treated with a high dose (2.5 mg/kg) of BVA showed a gradual decrease in TWL (before BVA = 6.40 sec; 1 hour after BVA = 4.89 sec; 2 hours after BVA = 3.85 sec), suggesting more severe pain. BV is also called a "double-edged sword" having nociceptive and antinociceptive effects together [35]. Therefore, it might be of high importance to find a proper concentration of BVA through disease-by-disease approaches. In ongoing studies, the optimal dose of BVA in various disease models is to be investigated.

Acupuncture has been used for thousands of years in East Asia including Korea, China, and Japan to treat various diseases generating few side effects. In recent years, it has received attention as an alternative method of medicine in Western countries [36, 37]. For decades ago, it has been demonstrated in many clinical and animal studies that acupuncture or EA analgesia is mediated by the endogenous analgesic systems, especially opioid [13, 16, 18, 38] and noradrenergic inhibitory systems [14, 15, 17, 39, 40]. Our previous studies using a rat model of peripheral nerve injury suggested that both of the opioid and noradrenergic systems equally contributed to the anti-allodynic effects of EA [41–43]. On the other hand, BVA has been reported to attenuate neuropathic pain symptoms induced by CCI through activation of α_2-adrenergic receptors, but not opioid receptors, in the rat spinal cord [22–24]. Similarly, the present results (Figure 4) suggest that the relieving effect of BVA on oxaliplatin-induced cold allodynia involves the noradrenergic, but not opioid, system. Thus, BVA and EA might have different mechanisms of anti-allodynic action in oxaliplatin-induced neuropathy. However, the anti-allodynic effect of BVA in this study was just partially blocked by phentolamine pretreatment ($P = 0.065$). The TWL of three subjects of Phentolamine + BV group substantially increased after BVA as compared with baseline TWL, whereas the TWL of the other three subjects did not. This might be due to individual differences in response to phentolamine, as previously shown in nerve injury models [44]. Alternatively, the other descending inhibitory systems like serotonergic, GABA, and/or cholinergic systems might be involved [19, 30, 43]. Further studies on this issue may increase our understanding of the neurological mechanisms of BVA analgesia.

5. Conclusions

In conclusion, our findings in the present study suggest that BVA has a potent relieving effect on oxaliplatin-induced cold allodynia and that GV3 acupoint and low dose of BV have an optimal effect. Such anti-allodynic effect of BVA is partially mediated by the noradrenergic, but not opioid, system. Thus, we propose that BVA treatment can be a potential therapeutic option in oxaliplatin-induced neuropathic pain.

Conflict of Interests

The authors declare that they have no conflict of interests.

Acknowledgments

This work was supported by the National Research Foundation of Korea (NRF) grant funded by Korea Government (MEST) (no. 2012-0005755). The authors thank Ji-Hwan Lee and Hyunseong Kim for excellent technical support and discussions on the paper.

References

[1] J. Ferlay, H.-R. Shin, F. Bray, D. Forman, C. Mathers, and D. M. Parkin, "Estimates of worldwide burden of cancer in 2008: GLOBOCAN 2008," *International Journal of Cancer*, vol. 127, no. 12, pp. 2893–2917, 2010.

[2] D. Screnci, M. J. McKeage, P. Galettis, T. W. Hambley, B. D. Palmer, and B. C. Baguley, "Relationships between hydrophobicity, reactivity, accumulation and peripheral nerve toxicity of a series of platinum drugs," *British Journal of Cancer*, vol. 82, no. 4, pp. 966–972, 2000.

[3] D. E. Baker, "Oxaliplatin: a new drug for the treatment of metastatic carcinoma of the colon or rectum," *Reviews in Gastroenterological Disorders*, vol. 3, no. 1, pp. 31–38, 2003.

[4] D. Screnci and M. J. McKeage, "Platinum neurotoxicity: clinical profiles, experimental models and neuroprotective approaches," *Journal of Inorganic Biochemistry*, vol. 77, no. 1-2, pp. 105–110, 1999.

[5] B. Ling, M.-A. Coudoré-Civiale, D. Balayssac, A. Eschalier, F. Coudoré, and N. Authier, "Behavioral and immunohistological assessment of painful neuropathy induced by a single oxaliplatin injection in the rat," *Toxicology*, vol. 234, no. 3, pp. 176–184, 2007.

[6] J. M. Extra, M. Espie, F. Calvo, C. Ferme, L. Mignot, and M. Marty, "Phase I study of oxaliplatin in patients with advanced cancer," *Cancer Chemotherapy and Pharmacology*, vol. 25, no. 4, pp. 299–303, 1990.

[7] S. Wolf, D. Barton, L. Kottschade, A. Grothey, and C. Loprinzi, "Chemotherapy-induced peripheral neuropathy: prevention and treatment strategies," *European Journal of Cancer*, vol. 44, no. 11, pp. 1507–1515, 2008.

[8] J.-D. Lee, S.-Y. Kim, T.-W. Kim et al., "Anti-inflammatory effect of bee venom on type II collagen-induced arthritis," *American Journal of Chinese Medicine*, vol. 32, no. 3, pp. 361–367, 2004.

[9] J.-D. Lee, H.-J. Park, Y. Chae, and S. Lim, "An overview of bee venom acupuncture in the treatment of arthritis," *Evidence-Based Complementary and Alternative Medicine*, vol. 2, no. 1, pp. 79–84, 2005.

[10] H.-S. Jang, H.-S. Chung, E. Ko et al., "Microarray analysis of gene expression profiles in response to treatment with bee venom in lipopolysaccharide activated RAW 264.7 cells," *Journal of Ethnopharmacology*, vol. 121, no. 2, pp. 213–220, 2009.

[11] E. S. Chung, H. Kim, G. Lee, S. Park, and H. Bae, "Neuro-protective effects of bee venom by suppression of neuroinflammatory responses in a mouse model of Parkinson's disease: role of regulatory T cells," *Brain, Behavior, and Immunity*, vol. 26, pp. 1322–1330, 2012.

[12] M. S. Choi, S. Park, T. Choi et al., "Bee venom ameliorates ovalbumin induced allergic asthma via modulating $CD4^{+}CD25^{+}$ regulatory T cells in mice," *Cytokine*, vol. 61, no. 1, pp. 256–265, 2013.

[13] D. J. Mayer, D. D. Price, and A. Rafii, "Antagonism of acupuncture analgesia in man by the narcotic antagonist naloxone," *Brain Research*, vol. 121, no. 2, pp. 368–372, 1977.

[14] L. V. Laitinen, "Inhibition of cutaneous nociception by deep musculoskeletal pain. A clinical observation," *Pain*, vol. 13, no. 4, pp. 373–377, 1982.

[15] S. T. Koo, Y. I. Park, K. S. Lim, K. Chung, and J. M. Chung, "Acupuncture analgesia in a new rat model of ankle sprain pain," *Pain*, vol. 99, no. 3, pp. 423–431, 2002.

[16] J.-S. Han, "Acupuncture: neuropeptide release produced by electrical stimulation of different frequencies," *Trends in Neurosciences*, vol. 26, no. 1, pp. 17–22, 2003.

[17] S. T. Koo, K. S. Lim, K. Chung, H. Ju, and J. M. Chung, "Electroacupuncture-induced analgesia in a rat model of ankle sprain pain is mediated by spinal α-adrenoceptors," *Pain*, vol. 135, no. 1-2, pp. 11–19, 2008.

[18] H. Y. Kim, J. Wang, I. Lee, H. K. Kim, K. Chung, and J. M. Chung, "Electroacupuncture suppresses capsaicin-induced secondary hyperalgesia through an endogenous spinal opioid mechanism," *Pain*, vol. 145, no. 3, pp. 332–340, 2009.

[19] H. W. Kim, Y. B. Kwon, H. J. Han, I. S. Yang, A. J. Beitz, and J. H. Lee, "Antinociceptive mechanisms associated with diluted bee venom acupuncture (apipuncture) in the rat formalin test: involvement of descending adrenergic and serotonergic pathways," *Pharmacological Research*, vol. 51, no. 2, pp. 183–188, 2005.

[20] Y. H. Baek, J. E. Huh, J. D. Lee, D. Y. Choi, and D. S. Park, "Antinociceptive effect and the mechanism of bee venom acupuncture (Apipuncture) on inflammatory pain in the rat model of collagen-induced arthritis: mediation by α2-adrenoceptors," *Brain Research*, vol. 1073-1074, no. 1, pp. 305–310, 2006.

[21] S.-Y. Kang, C.-Y. Kim, D.-H. Roh et al., "Chemical stimulation of the ST36 acupoint reduces both formalin-induced nociceptive behaviors and spinal astrocyte activation via spinal alpha-2 adrenoceptors," *Brain Research Bulletin*, vol. 86, no. 5-6, pp. 412–421, 2011.

[22] D.-H. Roh, Y.-B. Kwon, H.-W. Kim et al., "Acupoint stimulation with diluted bee venom (apipuncture) alleviates thermal hyperalgesia in a rodent neuropathic pain model: involvement of spinal alpha2-adrenoceptors," *The Journal of Pain*, vol. 5, no. 6, pp. 297–303, 2004.

[23] S. Y. Kang, D. H. Roh, J. H. Park, H. J. Lee, and J. H. Lee, "Activation of spinal α2-adrenoceptors using diluted bee venom stimulation reduces cold allodynia in neuropathic pain rats," *Evidence-Based Complementary and Alternative Medicine*, vol. 2012, Article ID 784713, 8 pages, 2012.

[24] S.-Y. Kang, D.-H. Roh, S.-Y. Yoon et al., "Repetitive treatment with diluted bee venom reduces neuropathic pain via potentiation of locus coeruleus noradrenergic neuronal activity and modulation of spinal NR1 phosphorylation in rats," *Journal of Pain*, vol. 13, no. 2, pp. 155–166, 2012.

[25] M. Zimmermann, "Ethical guidelines for investigations of experimental pain in conscious animals," *Pain*, vol. 16, no. 2, pp. 109–110, 1983.

[26] B. Ling, F. Coudoré, L. Decalonne, A. Eschalier, and N. Authier, "Comparative antiallodynic activity of morphine, pregabalin and lidocaine in a rat model of neuropathic pain produced by one oxaliplatin injection," *Neuropharmacology*, vol. 55, no. 5, pp. 724–728, 2008.

[27] H. S. Na, J. S. Han, K. H. Ko, and S. K. Hong, "A behavioral model for peripheral neuropathy produced in rat's tail by inferior caudal trunk injury," *Neuroscience Letters*, vol. 177, no. 1-2, pp. 50–52, 1994.

[28] Y. I. Kim, H. S. Na, Y. W. Yoon, H. C. Han, K. H. Ko, and S. K. Hong, "NMDA receptors are important for both mechanical and thermal allodynia from peripheral nerve injury in rats," *NeuroReport*, vol. 8, no. 9-10, pp. 2149–2153, 1997.

[29] C. S. Yin, H.-S. Jeong, H.-J. Park et al., "A proposed transpositional acupoint system in a mouse and rat model," *Research in Veterinary Science*, vol. 84, no. 2, pp. 159–165, 2008.

[30] J. H. Park, S. K. Kim, H. N. Kim et al., "Spinal cholinergic mechanism of the relieving effects of electroacupuncture on cold and warm allodynia in a rat model of neuropathic pain," *The Journal of Physiological Sciences*, vol. 59, no. 4, pp. 291–298, 2009.

[31] J. L. de la Calle and C. L. Paíno, "A procedure for direct lumbar puncture in rats," *Brain Research Bulletin*, vol. 59, no. 3, pp. 245–250, 2002.

[32] E. Gamelin, L. Gamelin, L. Bossi, and S. Quasthoff, "Clinical aspects and molecular basis of oxaliplatin neurotoxicity: current management and development of preventive measures," *Seminars in Oncology*, vol. 29, no. 5, pp. 21–33, 2002.

[33] L. Gamelin, M. Boisdron-Celle, R. Delva et al., "Prevention of oxaliplatin-related neurotoxicity by calcium and magnesium infusions: a retrospective study of 161 patients receiving oxaliplatin combined with 5-fluorouracil and leucovorin for advanced colorectal cancer," *Clinical Cancer Research*, vol. 10, no. 12, pp. 4055–4061, 2004.

[34] S. Ushio, N. Egashira, H. Sada et al., "Goshajinkigan reduces oxaliplatin-induced peripheral neuropathy without affecting anti-tumour efficacy in rodents," *European Journal of Cancer*, vol. 48, pp. 1407–1413, 2012.

[35] J. Chen and W. R. Lariviere, "The nociceptive and anti-nociceptive effects of bee venom injection and therapy: a double-edged sword," *Progress in Neurobiology*, vol. 92, no. 2, pp. 151–183, 2010.

[36] T. J. Kaptchuk, "Acupuncture: theory, efficacy, and practice," *Annals of Internal Medicine*, vol. 136, no. 5, pp. 374–383, 2002.

[37] D. C. Cherkin, K. J. Sherman, R. A. Deyo, and P. G. Shekelle, "A review of the evidence for the effectiveness, safety, and cost of acupuncture, massage therapy, and spinal manipulation for back pain," *Annals of Internal Medicine*, vol. 138, no. 11, pp. 898–906, 2003.

[38] R.-X. Zhang, L. Lao, L. Wang et al., "Involvement of opioid receptors in electroacupuncture-produced anti-hyperalgesia in

rats with peripheral inflammation," *Brain Research*, vol. 1020, no. 1-2, pp. 12–17, 2004.

[39] S. P. Zhang, J. S. Zhang, K. K. L. Yung, and H. Q. Zhang, "Non-opioid-dependent anti-inflammatory effects of low frequency electroacupuncture," *Brain Research Bulletin*, vol. 62, no. 4, pp. 327–334, 2004.

[40] J. H. Kim, H. Y. Kim, K. Chung, and J. M. Chung, "Electroacupuncture reduces the evoked responses of the spinal dorsal horn neurons in ankle-sprained rats," *Journal of Neurophysiology*, vol. 105, no. 5, pp. 2050–2057, 2011.

[41] B. G. Hwang, B.-I. Min, J. H. Kim, H. S. Na, and D. S. Park, "Effects of electroacupuncture on the mechanical allodynia in the rat model of neuropathic pain," *Neuroscience Letters*, vol. 320, no. 1-2, pp. 49–52, 2002.

[42] J. H. Kim, B.-I. Min, H. S. Na, and D. S. Park, "Relieving effects of electroacupuncture on mechanical allodynia in neuropathic pain model of inferior caudal trunk injury in rat: mediation by spinal opioid receptors," *Brain Research*, vol. 998, no. 2, pp. 230–236, 2004.

[43] S. K. Kim, J. H. Park, S. J. Bae et al., "Effects of electroacupuncture on cold allodynia in a rat model of neuropathic pain: mediation by spinal adrenergic and serotonergic receptors," *Experimental Neurology*, vol. 195, no. 2, pp. 430–436, 2005.

[44] S. K. Kim, B. I. Min, J. H. Kim et al., "Individual differences in the sensitivity of cold allodynia to phentolamine in neuropathic rats," *European Journal of Pharmacology*, vol. 523, no. 1-3, pp. 64–66, 2005.

Hindawi Publishing Corporation
Evidence-Based Complementary and Alternative Medicine
Volume 2013, Article ID 127271, 12 pages
http://dx.doi.org/10.1155/2013/127271

Research Article

Multivariate Granger Causality Analysis of Acupuncture Effects in Mild Cognitive Impairment Patients: An fMRI Study

Shangjie Chen,[1] Lijun Bai,[2] Maosheng Xu,[1] Fang Wang,[1] Liang Yin,[1] Xuming Peng,[3] Xinghua Chen,[3] and Xuemin Shi[4]

[1] *Baoan Hospital, Southern Medical University, Shenzhen 518101, China*
[2] *The Key Laboratory of Biomedical Information Engineering of Ministry of Education, Department of Biomedical Engineering, School of Life Science and Technology, Xi'an Jiaotong University, Xi'an 710049, China*
[3] *The First Affiliated Hospital, Guangzhou University of Traditional Chinese Medicine, Guangzhou 510405, China*
[4] *The First Affiliated Hospital, Tianjin University of Traditional Chinese Medicine, Tianjin 300193, China*

Correspondence should be addressed to Lijun Bai; bailj4152615@gmail.com and Xuemin Shi; sxmtjtcm@gmail.com

Received 21 February 2013; Revised 11 April 2013; Accepted 2 June 2013

Academic Editor: Baixiao Zhao

Evidence from clinical reports has indicated that acupuncture has a promising effect on mild cognitive impairment (MCI). However, it is still unknown that by what way acupuncture can modulate brain networks involving the MCI. In the current study, multivariate Granger causality analysis (mGCA) was adopted to compare the interregional effective connectivity of brain networks by varying needling depths (deep acupuncture, DA; superficial acupuncture, SA) and at different cognitive states, which were the MCI and healthy control (HC). Results from DA at KI3 in MCI showed that the dorsolateral prefrontal cortex and hippocampus emerged as central hubs and had significant causal influences with each other, but significant in HC for DA. Moreover, only several brain regions had remarkable causal interactions following SA in MCI and even few brain regions following SA in HC. Our results indicated that acupuncture at KI3 at different cognitive states and with varying needling depths may induce distinct reorganizations of effective connectivities of brain networks, and DA at KI3 in MCI can induce the strongest and more extensive effective connectivities related to the therapeutic effect of acupuncture in MCI. The study demonstrated the relatively functional specificity of acupuncture at KI3 in MCI, and needling depths play an important role in acupuncture treatments.

1. Introduction

Mild cognitive impairment (MCI) is the key and hot point in cognitive-brain study. Incidence of dementia is widely acknowledged to increase greatly with advancing age. Sousa and coworkers report that dementia made the largest contribution to disability in China, Cuba, Dominican Republic, Mexico, Peru, and urban India [1]. Dementia is a leading cause of death in the United States but is underrecognized as a terminal illness. The median survival was 478 days, and the probability of death within 6 months was 24.7% [2]. Multivariable analyses show that dementia and cognitive impairment are by far the most strongly and independently associated chronic health disorders [3]. Increasing evidence shows that subtle losses in cognitive function may be a symptomatic transition to early AD [4]. MCI is an intermediate state between normal aging and Alzheimer's disease (AD) which is the world's most common dementia [5, 6]. MCI represents a significant risk factor for the development of dementia [4] and is an appropriate condition for investigation [4, 7]. Further research is needed on treatments of delaying the conversion from MCI to AD [4]. However, there is no sufficient evidence that drug can delay long-term progression and conversion to dementia [1, 6]. Feasible complementary and alternative therapies with low side effects, such as acupuncture and exercise, have shown some benefits [8, 9]. The use of acupuncture as a complementary therapeutic way to treat a variety of neurologic diseases, including MCI and AD, is popular in certain parts of the world [10]. In spite of its public acceptance and promising effect, the underlying neural mechanism is still elusive.

Since the late 1990s, functional magnetic resonance imaging (fMRI) has been used to investigate the underlying

mechanisms of acupuncture [11], especially the relative functional specificity of acupoints. Neuroimaging studies have indicated that the primary acupuncture effects are mediated by the central nervous system [12–20], and acupuncture can activate certain cognitive-related regions in AD and MCI patients [9]. KI3 is one of the most frequently used acupoint in treatment of cognitive impairment [21]. Our previous studies have also indicated that acupuncture at KI3 can activate certain cognitive-related regions [22–25].

However, there are several problems in fMRI studies of acupuncture. Firstly, most of these studies have been performed on healthy subjects [12–20]. However, acupoint selection often has a very wide range of therapeutic actions related to functional state of the human body based on theory of the traditional chinese medicine (TCM). It is generally accepted that acupuncture plays a homeostatic role and thus may have a greater effect on patients with a pathological imbalance compared with healthy controls (HC) [7, 26, 27]. Therefore, exploring brain function evoked by acupuncture in patients may further help to elucidate its mechanism. In addition, most fMRI studies focus on comparison of brain activity patterns induced by acute effects of acupuncture at acupoint and nonacupoint, or different acupoints. However, few studies have evaluated the modulated effects in the poststimulus resting state networks (RSN) induced by varied needling depth (DA, deep acupuncture; SA, superficial acupuncture) though the depth of needling is also the key of specificity of acupuncture according to the theory of TCM. A primary interest in this area is therefore whether these different depths of needling elicit similar or different responses. Deep acupuncture may better overlap with its proximity to ascending nerve tracks than to the density of cutaneous afferents [28]. In addition, SA has been assumed to minimize the therapeutic effect while triggering most of the nonspecific effects of needling [29]. Therefore, comparing connectivity patterns of brain regions modulated by DA with that of the effects modulated by SA may provide precise and specific modulatory patterns related to the therapeutic effect of acupuncture.

Moreover, many studies generally adopted the block-designed fMRI paradigm conform to the "on-off" specifications. But, function responses induced by acupuncture have time-varying characteristics [15–18]. In recent years, some studies started to pay attention to the sustained effect of the acupuncture and its influence on the postacupuncture RSN with the functional connectivity analysis, which was a kind of undirected graph analysis of temporal correlations between different brain regions [7, 14, 16]. However, little was known about the direction and strength of the information flow between these brain regions modulated by acupuncture. Further investigation of the interregional causal interactions may be helpful to explain the neurophysiological action underlying acupuncture [20, 23]. Recently, a newly multivariate Granger causality analysis (mGCA) has been introduced as an effective connectivity method to analyze direct causal interactions among multiple brain areas from fMRI data [20, 23, 30–33]. By exploring this approach to analyze the causal influences of the activated regions evoked by acupuncture, we can account for its modulatory effects on multiple relevant regions simultaneously.

Based on the previous study, we employed the mGCA to evaluate the effective connectivity patterns among multiple brain regions following acupuncture at KI3 in MCI patients and HC for DA and SA condition. By examining the directionality and strength of causal influence between multiple brain regions following acupuncture at KI3 in MCI patients and HC for DA and SA condition, we can find whether there is relatively specific modulatory effect at different cognitive states (MCI and HC) and with varying different depths of needling (DA and SA). By detecting the functional specificity of acupuncture for different cognitive states and varied depths of needling during the postresting acupuncture period, we can provide further evidence to explore the relative functional specificity of acupuncture effects.

2. Materials and Methods

2.1. Subjects. A total of 24 subjects were recruited in the study. 12 MCI patients (1 males and 11 females; ages 59.3 ± 3.3 years; MMSE 26.4 ± 0.9; 7 middle school education and 5 college degree) and 12 age-matched HC subjects (4 males and 8 females; ages 60.6 ± 5.8 years; MMSE 29.8 ± 0.4; 9 middle school education and 3 college degree) were included. All subjects were right handed with normal or corrected-to-normal vision and acupuncture naive according to the edinburgh handedness inventory [34]. MCI patients were diagnosed by using the criteria for amnestic MCI [35], with Mini-Mental State Examination (MMSE) scores >25 [36] and Clinical Dementia Rating (CDR) scale scores of 0.5 [37]. Subjects were excluded if they had serious medical, neurological, or psychiatric illness, or if they were taking medication or other substances known to influence cerebral function, or if they have any contraindications to exposure to a high magnetic field. After being fully explained of the study, all subjects signed the informed consent. All protocols were approved by a local subcommittee on human studies and were conducted in accordance with the Declaration of Helsinki.

2.2. Experimental Procedures. For each subject, functional runs lasting for 15 min of the experiment consisted of four phases (Figure 1(b)). In the first phase, a resting state (REST) scan was first conducted for 6 min without any stimulation for a baseline control. In the second phase, an acupuncture needle was then inserted in acupoint KI3 (Taixi, located in a depression between the medial malleolus and heel tendon, Figure 1(a)) on the right leg, and retained for 1 min. In the third phase, the needle was manipulated for 2 min by rotating the needle at a rate of 120 times per min in frequency and at 60° in angle. In the end, another REST scan was conducted for 6 min without any stimulation again. All participants were asked to remain relaxed without engaging in any mental tasks. To facilitate blinding, they were also instructed to keep their eyes closed during fMRI scan to prevent them from actually observing the procedures. According to participants' reports after the scanning, they were affirmed keeping awake during the whole process. Standard acupuncture needles, which are made of ferromagnetic steel, however, are problematic in fMRI studies for several reasons, such as attraction by the scanner's magnetic field, significant image distortions,

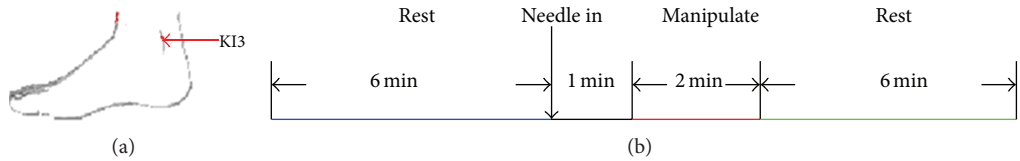

Figure 1: (a) Anatomical locations of the acupuncture stimulation points of KI3. (b) Experimental paradigm. Functional run lasting for 15 min consisted of four phases: 6-minute REST scanning was done before and after acupuncture, inserted in and retained for 1 min and manipulated for 2 min.

and signal dropouts, when positioned close to the head or even heating due to absorption of radio frequency (RF). Nonferromagnetic metal needles seem to be the best choice for acupoints outside of the transmitter coil [38]. Therefore, acupuncture stimulation was delivered by a silver needle with 0.35 mm in diameter and 25 mm in length (silver content above 85%, Acupuncture Supplies Company in Suzhou, China) in this study. The acupuncture procedure was conducted by the same experienced and licensed acupuncturist on all subjects.

We employed two functional runs (DA and SA) for each subject, but only one single stimulation period was given during each of these two runs. The needle was inserted vertically to a depth of 1-2 cm in DA, but of 1-2 mm in SA. Instead of inserting depth, other manipulation methods were all identical in the DA and SA groups. The presentation sequence of two runs was randomized and balanced throughout the population, and every participant performed only one run each week in order to eliminate potential long-lasting effect following acupuncture administration. All participants were not informed of the order in which these runs would be performed.

At the end of each acupuncture scan, the subjects were questioned about aching, pressure, soreness, heaviness, fullness, warmth, coolness, numbness, tingling, dull or sharp pain, and any other sensations they felt during the stimulation [15, 20, 39]. A 10-point visual analogue scale (VAS), which was scaled at 0 = no sensation, 1–3 = mild, 4–6 = moderate, 7-8 = strong, 9 = severe, and 10 = unbearable sensation, was adopted to self-rate the intensities about the deqi sensations [15, 39, 40]. To quantitatively summarize the full multivariate breadth and depth of the De-qi sensations for each subject, the VAS index was calculated [15, 20, 39].

2.3. fMRI-Scanning Procedure. Magnetic resonance imaging data were collected from a 3T MR scanner. A standard birdcage head coil was used, along with restraining foam pads to minimize head motion and to diminish scanner noise. For each subject, functional scans of acupuncture stimulation were taken after the anatomical scans. The scan covered the entire brain including the cerebellum and brainstem. Thirty axial slices were obtained using a $T2^*$-weighted single-shot, gradient-recalled echo planar imaging (EPI) sequence (TR = 2000 ms, TE = 30 ms, FOV = 220 mm × 220 mm, matrix = 64 × 64, thickness = 4 mm, Slice Space = 1 mm, flip angle = 77°). High-resolution structural information on each subject was also acquired using three-dimensional (3D) MRI sequences with a voxel size of 1 mm^3 for anatomical localization (TR = 2.1 s, TE = 4.6 ms, FOV = 230 mm × 230 mm, matrix = 256 × 256, slice thickness = 1 mm, flip angle = 8°).

2.4. fMRI Data Analysis. Preprocessing was performed using the Statistical Parametric Mapping software (SPM5, http://www.fil.ion.ucl.ac.uk/spm/). Initially, the first five time points were discarded in order to avoid the instability of the initial MRI signal [40]. The image data underwent slice-timing correction and realignment for head motions using least-squares minimization. None of the subjects had head movements exceeding 1 mm on any axis and head rotation greater than one degree. A mean image created from the realigned volumes was co-registered with the subject's individual structural T1-weighted volume image [20]. Then, the images were normalized to the standard EPI template and re-sampled to a voxel size of 2 mm × 2 mm × 2 mm [41]. Subsequently, these data were filtered by using a bandpass filter (0.01–0.08 Hz) to reduce the effect of low-frequency drift and high-frequency noise [42, 43]. Finally, the images were smoothed spatially by using a 6 mm full-width-at-half maximum (FWHM) isotropic Gaussian kernel.

Taking into account of the sustained effects of acupuncture, the resting period before acupuncture was taken as the baseline. For each subject, the difference in the BOLD response was estimated at every voxel across the whole brain by using the general linear model (GLM) in SPM5. The obtained t-maps at individual levels were then entered into the "random effect" group analysis framework by the one-sample t-test summary statistic ($P < 0.005$, uncorrected). The statistical maps indicated the brain activation in response to acute effects of acupuncture, thereby functionally defining ROI. Each peak voxel with its nearest 10 neighbors was defined as a group ROI. Considering the anatomical variance across subjects, subject-specific peak voxels and subject-specific ROIs were defined on individual t-maps as follows. The given group ROI was used as a mask and then, based on individual t-maps, and the voxel with the largest t-value within this mask served as the subject-specific peak voxel. ROIs were selected based on the acupuncture-stimulation results. Firstly, the time series from the poststimulus resting period of BOLD signal intensities from these selected ROIs were selected. Then, the time series were averaged across voxels within each ROI and normalized across subjects separately for each group to form a single vector per ROI [20].

In order to describe the effective connectivity during the postacupuncture resting period [30], the mGCA was

used to detect causal interactions between brain regions by computing directed transfer function (DTF) from a multivariate autoregressive model of the time course of selected ROIs [20, 23]. Based on the principle of Granger causality, the DTF was rendered in a multivariate formulation [44]. Therefore, the DTF can effectively model the inherently multivariate nature of neuronal networks. The algorithm was coded in MATLAB7 (The MathWorks, Inc.) [20]. Effective connectivity graphs were constructed using the thickness of connecting lines and arrows to indicate the strength and direction of the causal influences. Only links that showed significant effective connectivity were presented in the network ($P < 0.05$). Graphs were visualized using Pajek software (http://vlado.fmf.uni-lj.si/pub/networks/pajek/).

3. Results

3.1. Psychophysical Response. The prevalence of deqi sensations was expressed as the percentage of the individuals in the group that reported the sensations (Figure 2(a)). Differences did exist with respect to the type of sensations. Both in the MCI and HC group, the soreness, numbness, fullness, warmth, and heaviness were found to be more frequent for DA than that of SA. Whether for the DA or SA, warmth and tingling were found to be more frequent in the MCI group than HC group.

The intensity of sensations was expressed as the average score ± S.E. (Figure 2(b)). Differences did also exist with respect to the type of sensations. In both MCI and HC groups, the sensations of soreness, numbness, fullness, and warmth were found to be stronger for DA than SA. For both conditions, a statistical analysis found no significant difference between the MCI and HC groups with regard to the intensity of these sensations.

3.2. mGCA Result of Resting Brain Networks Modulated by Acupuncture. In this study, we explored the causal interactions within and among the resting brain networks modulated by acupuncture at KI3 in MCI and HC, for DA and SA. The effective connectivity patterns of resting brain networks were described as directed graphs. The thickness of connecting lines and the directions of arrows indicated strength and directions of the causal influences (green line in Figure 3). Only significant effective connectivity ($P < 0.05$) was presented in the graphs.

Following acupuncture at KI3 in MCI-Deep, the mGCA result showed that the dorsolateral prefrontal cortex (DLPFC) and hippocampus (Hipp) emerged as central hubs. The DLPFC received causal inflows from most nodes in the brain network, including the Thalamus, Insula, middle temporal gyrus (MTG), and primary motor cortex (M1). The Hipp received causal inflows from the DLPFC, anterior cingulate cortex (ACC), orbitofrontal cortex (OFC), and Caudate. In addition, Insula received causal inflows from Thalamus. The precuneus (PreCN) received causal inflows from ACC and fusiform gyrus (FG). The secondary somatosensory cortex (SII) received causal inflows from Insula and DLPFC. Declive received causal inflows from Caudate, DLPFC, M1, and Uvula. There were strong causal inflows from Thalamus to Insula and DLPFC, from Insula to SII and DLPFC, from Caudate to Declive, from OFC to Hipp, and from ACC to PreCN and Hipp. Of interests, we found that the DLPFC and Hipp were not only central hubs but also had significant causal influence on each other. The path weights of mGCA result for MCI-Deep were tabulated in Table 1 with significant connections shown in blue color.

Notably, several of these brain regions (the Hipp and DLPFC) mentioned above also have remarkably causal interactions following acupuncture at KI3 in HC-Deep, but they were more noncohesive than in MCI-Deep. Following acupuncture at KI3 in HC-Deep, the mGCA result showed that the Hipp, OFC, DLPFC, and Uvula emerged as central hubs. There were strong causal inflows from ACC and OFC to Hipp, from DLPFC and Declive to Uvula, from MTG to OFC, from Cuneus to PreCN, from Insula to DLPFC and Putamen, from Hipp to Caudate and DLPFC, and from Thalamus to OFC and Insula. The path weights of mGCA result for HC-Deep were tabulated in Table 2 with significant connections shown in blue color.

Only several of brain regions had remarkably causal interactions following acupuncture at KI3 in MCI-Shallow. Following acupuncture at KI3 in MCI-Shallow, the mGCA result showed that there were causal inflows from pMCC and Cuneus to PreCN, from MPFC to Cuneus, from Putamen to FG, from M1 to primary somatosensory cortex (SI), and from Insula to Thalamus. The path weights of mGCA result for MCI-shallow were tabulated in Table 3 with significant connections shown in blue color. It is also notable that a few brain regions had remarkably causal interactions following acupuncture at KI3 in HC-Shallow.

4. Discussion

KI3 is one of the most frequently used acupoints and prove to have various efficacies in the treatment of dementia [15]. Our previous studies have indicated that acupuncture at KI3 can activate certain cognitive-related regions [22–25]. In this study, we have further investigation on effective connectivity of postacupuncture resting brain networks at KI3 in different cognitive states and with varying acupuncture depths.

Previous functional connectivity analysis primarily focused on the correlation patterns, and this method was limited to assess brain regions functionally connected to the initially selected seed and was unable to directly characterize interactions between multiple brain regions [20]. Few studies paid attention to the direction and strength of the information flow between these brain regions modulated by acupuncture. Effective connectivity in the poststimulus resting brain may underlie the neural mechanism of acupuncture for the treatment of MCI, but very few studies have yet investigated it. By visualizing the effective connectivity, we can obtain both the direction and strength of the information flow between multiple brain regions in the resting state network following acupuncture. In this study, a newly mGCA was employed to explore the specific effective connectivity poststimulus resting period following acupuncture at KI3. Our results demonstrated that acupuncture at KI3 in different cognitive states and with varying acupuncture depths

Table 1: Path weights from multivariate Granger causality analyses under the MCI-Deep ($P < 0.01$).

	ACC	FG	OFC	Hypo	Caudate	DLPFC	MTG	PreCN	Declive	MPFC	Cuneus	SMA	M1	IPL	Insula	Uvula	MCC	Hipp	SII	SI	Thalamus
ACC	—	×	×	×	×	×	×	**2.03**	×	×	×	×	×	×	×	×	×	**1.56**	×	×	×
FG	×	—	×	×	×	×	×	**0.79**	×	×	×	×	×	×	×	×	×	×	×	×	×
OFC	×	×	—	×	×	×	×	×	×	×	×	×	×	×	×	×	×	**2.15**	×	×	×
Hypo	×	×	×	—	×	×	×	×	×	×	×	×	×	×	×	×	×	×	×	×	×
Caudate	×	×	×	×	—	×	×	×	**1.97**	×	×	×	×	×	×	×	×	**0.78**	×	×	×
DLPFC	×	×	×	×	×	—	×	×	**1.1**	×	×	×	×	×	×	×	×	**0.98**	**0.43**	×	×
MTG	×	×	×	×	×	**1.1**	—	×	×	×	×	×	×	×	×	×	×	×	×	×	×
PreCN	×	×	×	×	×	×	×	—	×	×	×	×	×	×	×	×	×	×	×	×	×
Declive	×	×	×	×	×	×	×	×	—	×	×	×	×	×	×	×	×	×	×	×	×
MPFC	×	×	×	×	×	×	×	×	×	—	×	×	×	×	×	×	×	×	×	×	×
Cuneus	×	×	×	×	×	×	×	×	×	×	—	×	×	×	×	×	×	×	×	×	×
SMA	×	×	×	×	×	×	×	×	×	×	×	—	×	×	×	×	×	×	×	×	×
M1	×	×	×	×	×	**0.57**	×	×	**0.67**	×	×	×	—	×	×	×	×	×	×	×	×
IPL	×	×	×	×	×	×	×	×	×	×	×	×	×	—	×	×	×	×	×	×	×
Insula	×	×	×	×	×	**1.56**	×	×	×	×	×	×	×	×	—	×	×	×	**3.2**	×	×
Uvula	×	×	×	×	×	×	×	×	**0.43**	×	×	×	×	×	×	—	×	×	×	×	×
MCC	×	×	×	×	×	×	×	×	×	×	×	×	×	×	×	×	—	×	×	×	×
Hipp	×	×	×	×	×	×	×	×	×	×	×	×	×	×	×	×		—	×	×	×
SII	×	×	×	×	×	×	×	×	×	×	×	×	×	×	×	×	×	×	—	×	×
SI	×	×	×	×	×	×	×	×	×	×	×	×	×	×	×	×	×	×	×	—	×
Thalamus	×	×	×	×	×	**2.34**	×	×	×	×	×	×	×	×	**3.45**	×	×	×	×	×	—

Only the significant paths are listed. Influences are from column ROI to row ROI. × indicates the weights below the significance. Abbreviations: ACC: anterior cingulate cortex; FG: fusiform gyrus; OFC: orbitofrontal cortex; HYPO: hypothalamus; DLPFC: dorsolateral prefrontal cortex; MTG: middle temporal gyrus; PreCN: precuneus; MPFC: medial prefrontal cortex; SMA: supplementary motor area; M1: primary motor cortex; IPL: inferior parietal lobule; MCC: middle cingulate cortex; HIPP: hippocampus; SII: secondary somatosensory cortex; SI: primary somatosensory cortex.

Table 2: Path weights from multivariate Granger causality analyses under the HC-Deep ($P < 0.01$).

	ACC	FG	OFC	SI	Caudate	DLPFC	MTG	PreCN	Declive	MPFC	Cuneus	SMA	M1	IPL	Insula	Uvula	MCC	Hipp	Putamen	Thalamus
ACC	—	**0.66**	×	×	×	×	×	×	×	×	×	×	×	×	×	×	×	**1.92**	×	×
FG	×	—	×	×	×	×	×	×	×	×	×	×	×	×	×	×	×	×	×	×
OFC	×	×	—	×	×	×	×	×	×	×	×	×	×	×	×	×	×	**3.45**	×	×
SI	×	×	×	—	×	×	×	×	×	×	×	×	×	**0.4**	×	×	×	×	×	×
Caudate	×	×	×	×	—	×	×	×	×	×	×	×	×	×	×	**0.46**	×	×	×	×
DLPFC	×	×	×	×	×	—	**0.4**	×	×	×	×	×	×	×	×	**2.1**	×	×	×	×
MTG	×	×	**2.04**		×	×	—	×	×	×	×	×	×	×	×	×	×	×	×	×
PreCN	×	×	×	×	×	×	×	—	×	×	×	×	×	×	×	×	×	×	×	×
Declive	×	×	×	×	×	×	×	**0.94**	—	×	×	×	×	×	×	**2.08**	×	×	×	×
MPFC	×	×	×	×	×	×	×	×	×	—	×	×	×	×	×	×	×	×	×	×
Cuneus	×	×	×	×	×	×	×	**1.29**	×	×	—	×	×	×	×	×	×	×	×	×
SMA	×	**0.26**	×	×	×	×	×	×	×	×	×	—	**0.3**	×	×	×	×	×	×	×
M1	×	×	×	×	×	×	×	×	×	×	×	×	—	×	×	**0.87**	×	×	×	×
IPL	×	×	×	×	×	×	×	×	×	×	×	×	×	—	×	×	×	×	×	×
Insula	×	×	×	×	×	**1.12**	×	**0.48**	×	×	×	×	×	×	—	×	×	×	**2.2**	×
Uvula	×	×	×	×	×	×	×	×	×	×	×	×	×	×	×	—	×	×	×	×
MCC	×	×	×	×	×	×	×	×	×	×	×	×	×	×	×	×	—	×	×	×
Hipp	×	×	×	×	**3.78**	**1.56**	×	×	×	×	×	×	×	×	×	×	×	—	×	×
Putamen	×	×	×	×	×	×	×	×	**0.83**	×	×	×	×	×	×	×	×	×	—	×
Thalamus	×	×	**2.34**	×	×	×	×	×	×	×	×	×	×	×	**1.45**	×	×	×	×	—

Only the significant paths are listed. Influences are from column ROI to row ROI. × indicates the weights below the significance. Abbreviations: ACC: anterior cingulate cortex; FG: fusiform gyrus; OFC: orbitofrontal cortex; SI: primary somatosensory cortex; DLPFC: dorsolateral prefrontal cortex; MTG: middle temporal gyrus; PreCN: precuneus; MPFC: medial prefrontal cortex; SMA: supplementary motor area; M1: primary motor cortex; IPL: inferior parietal lobule; MCC: middle cingulate cortex; HIPP: hippocampus.

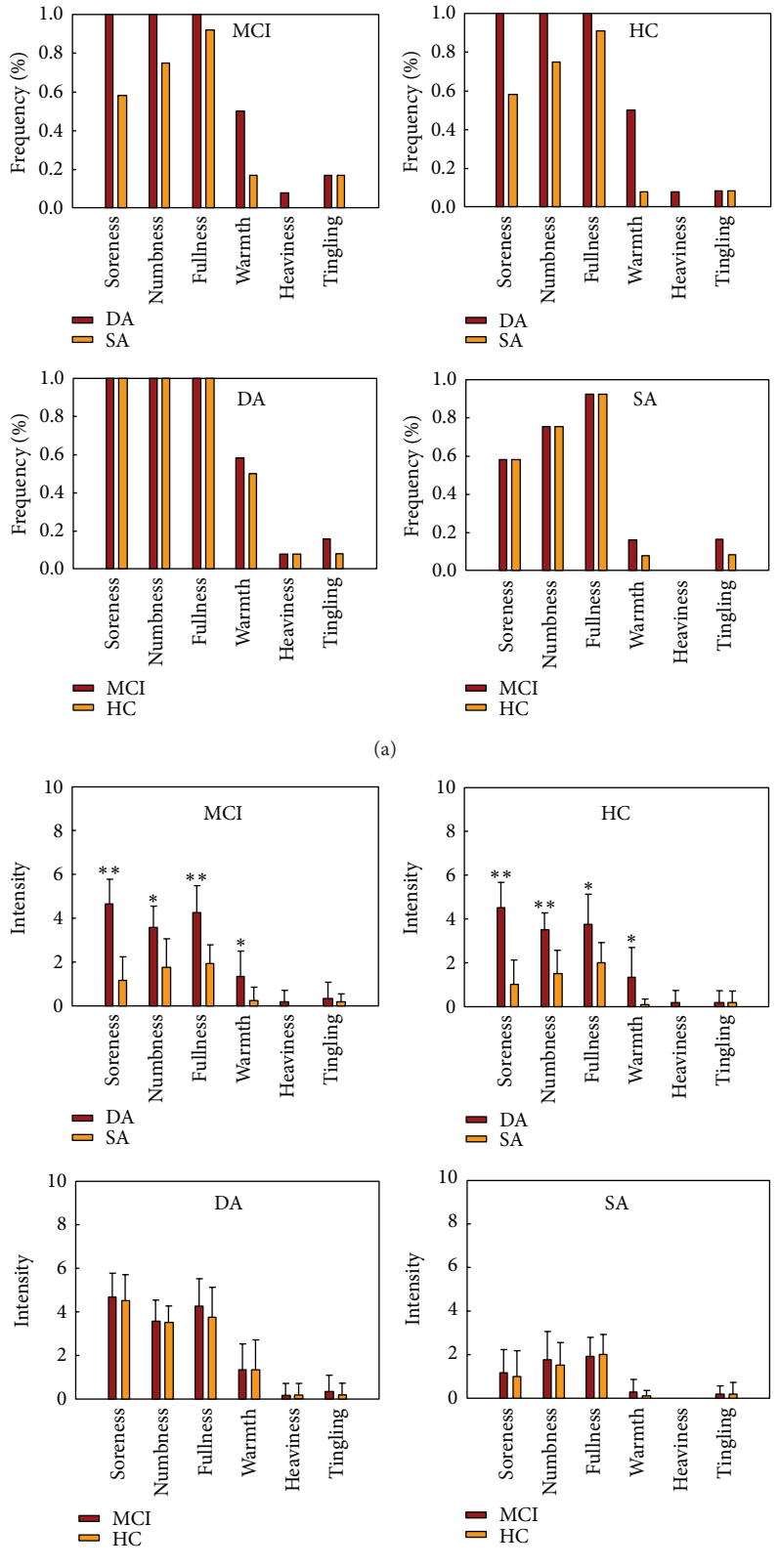

Figure 2: (a) The prevalence of deqi sensations. It was expressed as the percentage of the individuals in the group that reported the sensation (at least one subject experienced the seven sensations listed). (b) The intensity of sensations. It was expressed as the average score ± S.E by measuring on a scale from 0 denoting no sensation to 10 denoting an unbearable sensation. The intensity of numbness, fullness, and soreness was found to be greater for the DA than the SA under Fisher's Exact Test ($^{*}P < 0.01$; $^{**}P < 0.001$).

Table 3: Path weights from multivariate Granger causality analyses under the MCI-Shallow ($P < 0.01$).

	pMCC	FG	MPFC	Putamen	STG	PreCN	Culmen	Cuneus	M1	IPL	Insula	aMCC	SI	Thalamus
pMCC	—	×	×	×	×	**0.98**	×	×	×	×	×	×	×	×
FG	×	—	×	×	×	×	×	×	×	×	×	×	×	×
MPFC	×	×	—	×	×	×	×	**0.63**	×	×	×	×	×	×
Putamen	×	**0.78**	×	—	×	×	×	×	×	×	×	×	×	×
STG	×	×	×	×	—	×	×	×	×	×	×	×	×	×
PreCN	×	×	×	×	×	—	×	×	×	×	×	×	×	×
Culmen	×	×	×	×	×	×	—		×	×	×	×	×	×
Cuneus	×	×	×	×	×	**0.56**	×	—	×	×	×	×	×	×
M1	×	×	×	×	×	×	×	×	—	×	×	×	**1.34**	×
IPL	×	×	×	×	×	×	×	×	×	—	×	×	×	×
Insula	×	×	×	×	×	×	×	×	×	×	—	×	×	**0.32**
aMCC	×	×	×	×	×	×	×	×	×	×	×	—	×	×
SI	×	×	×	×	×	×	×	×	×	×	×	×	—	×
Thalamus	×	×	×	×	×	×	×	×	×	×	×	×	×	—

Only the significant paths are listed. Influences are from column ROI to row ROI. × indicates the weights below the significance. Abbreviations: pMCC: posterior middle cingulate cortex; FG: fusiform gyrus; MPFC: medial prefrontal cortex; STG: superior temporal gyrus; PreCN: precuneus; M1: primary motor cortex; IPL: inferior parietal lobule; aMCC: anterior middle cingulate cortex; SI: primary somatosensory cortex.

may exert heterogeneous modulatory effects on the causal interactions of brain areas during the poststimulus resting state. These different effective connectivity patterns may be related to the special effects of acupuncture in clinical settings [20, 23]. Our findings may be helpful to understand the basic neurophysiological mechanisms underlying the specificity of acupuncture.

According to the mGCA results following acupuncture at KI3 in MCI-Deep, we identified that brain regions have extensive causal interactions, mainly locating at the DLPFC, Hipp, Thalamus, Insula, Declive, MTG, ACC, OFC, and Caudate. The results from mGCA showed that the DLPFC and Hipp emerged as central hubs and had significant causal influence on each other. The DLPFC received causal inflows from most nodes in the brain network, including the Thalamus, Insula, MTG, and M1. One study showed that the DLPFC disconnections may be the substrates of cognitive impairments in MCI patients [45]. The DLPFC plays a role in sustaining attention and working memory [46, 47]. Lesions in the DLPFC can impair the short-term memory and cause difficulties in inhibiting responses [46]. In addition, the DLPFC has recently been found to be involved in exhibiting self-control [47]. The inhibition of the right DLPFC could modulate the excitability of a network of brain regions, in the ipsilateral as well as in the contralateral hemisphere, to enhance function in HC or restore an adaptive equilibrium in the MCI [48]. In addition, the Hipp received causal inflows from the DLPFC, ACC, OFC, and Caudate. In addition, the Insula received strong causal inflows from the Thalamus. One study showed abnormalities in the connectivity associated with the hippocampus in MCI [49]. Functional results indicated that the hippocampus reduced cortical activation in the DMN for MCI patients, compared with age- and education-matched healthy elderly controls [50]. The hippocampus plays a key role in a distributed network supporting memory encoding and retrieval [51]. The meta-analyses of 1,768 functional neuroimaging experiments revealed four functionally distinct regions on the human insula, which map to the social-emotional, the sensorimotor, the olfactory-gustatory, and the cognitive network of the brain [52]. Abnormal insula functional network is associated with episodic memory decline in amnestic mild cognitive impairment [53]. The thalamus is functionally connected to the hippocampus as part of the extended hippocampal system [54]. The literature seems to support the hypothesis that specialization of cortical areas in the MTL, as for their involvement in recollection and familiarity processes, may also extend to discrete regions of the thalamus [55]. Functional connectivity between the left thalamus and a set of regions was decreased in MCI, increased functional connectivity between the left thalamus and the right thalamus in MCI [56]. The DLPFC connectivity with the IPL and thalamus significantly correlated with the cognitive performance of patients measured by minimental state examination, clock drawing test, and California verbal learning test scores [57]. Therefore, the causal interactions related with these cognitive-related regions following DA may relate to the therapeutic effect of acupuncture for the treatment of MCI.

In addition, we also found that the hippocampus and DLPFC related with cognitive-related regions mentioned above also have remarkably causal interactions following acupuncture at KI3 in HC-Deep. Compared with that in MCI, causal interactions were significant noncohesive in HC. Many studies showed that there were specific functional changes of brain in the MCI patients compared with age- and education-matched healthy elderly controls [45, 50]. Acupuncture plays a homeostatic role and thus may have a greater effect on patients with a pathological imbalance compared to HC [7, 26, 27]. For HC, effect of acupuncture is weak. Our results demonstrated that there were different effective connectivities of postacupuncture at KI3 in different cognitive states,

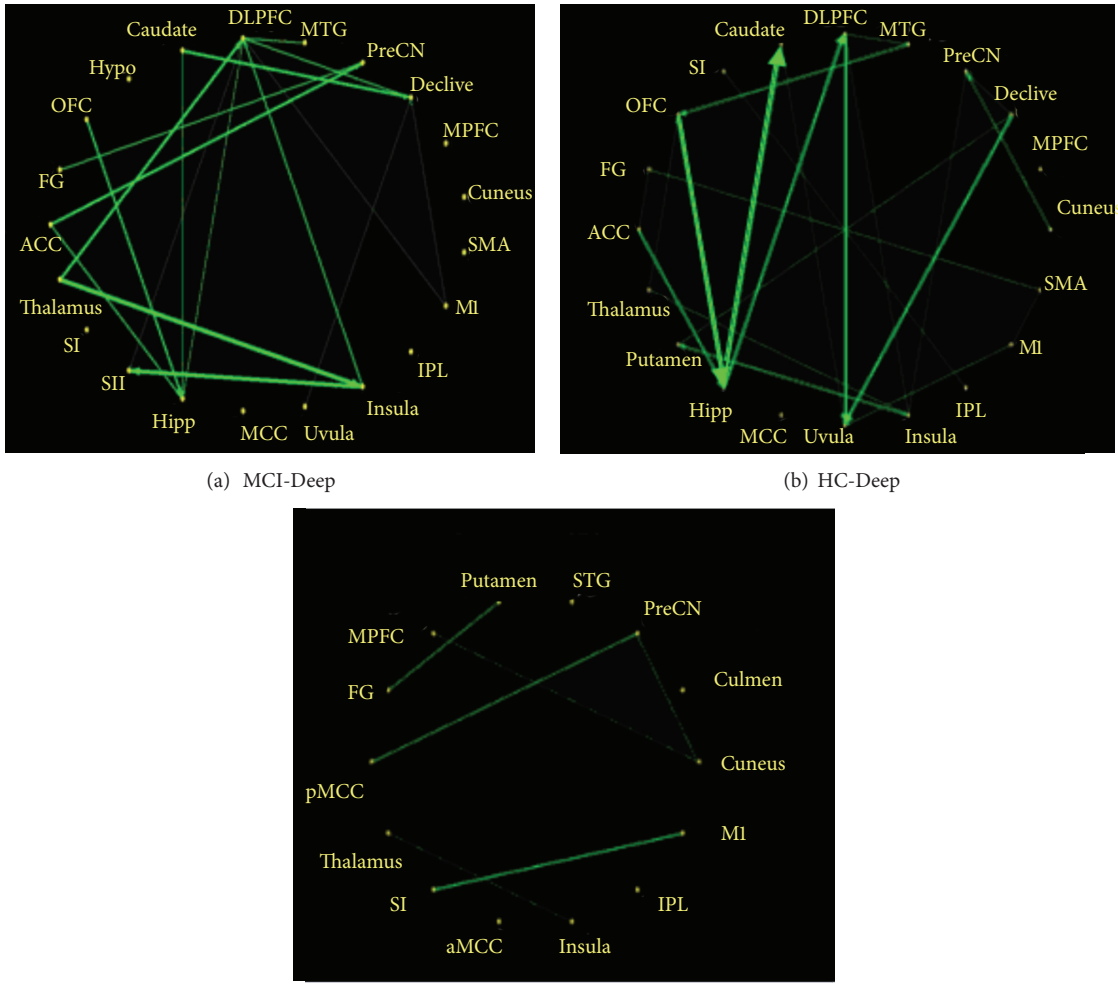

(a) MCI-Deep

(b) HC-Deep

(c) MCI-Shallow

Figure 3: Multivariate Granger causality relationships. There were remarkably causal interactions ($P < 0.05$) following acupuncture at KI3 in MCI-Deep, HC-Deep, and MCI-Shallow, but no causal interactions following acupuncture at KI3 in HC-Shallow. Relative strength of path weights (in arbitrary units) was indicated by the width of the arrows. Abbreviations: ACC, anterior cingulate cortex; FG, fusiform gyrus; OFC, orbitofrontal cortex; HYPO, hypothalamus; DLPFC, dorsolateral prefrontal cortex; MTG, middle temporal gyrus; PreCN, precuneus; MPFC, medial prefrontal cortex; SMA, supplementary motor area; M1, primary motor cortex; IPL, inferior parietal lobule; MCC, middle cingulate cortex; HIPP, hippocampus; SII, secondary somatosensory cortex; SI, primary somatosensory cortex; pMCC, middle part of the posterior cingulate cortex; STG, superior temporal gyrus; aMCC, middle part of the anterior cingulate cortex.

and effect of acupuncture was stronger in MCI compared with that in HC.

Moreover, only several of brain regions had remarkably causal interactions following acupuncture at MCI-Shallow. Most interestingly, no brain regions had remarkably causal interactions following acupuncture at HC-Shallow. The mGCA results demonstrated that effective connectivity of postacupuncture at KI3 in shallow of needling was very weak. Furthermore, the effect of postacupuncture at KI3 in HC-Shallow of needling was too weak to evoke causal interactions. Deep insertion of the needle affects several structures including the skin, muscle fascia, and muscle, and acupoints may better overlap with their proximity to ascending nerve tracks than to the density of cutaneous afferents [28]. The muscular afferents affect greater number of receptors to achieve a special clinical effect than the cutaneous afferents from shallow insertion of the needle. Therefore, the stronger effective connectivity associated with the cognitive-related regions following DA may suggest that deep muscle acupuncture has a better therapeutic effect for the treatment of MCI. The heterogeneous effective connectivity patterns between DA and SA may suggest the importance of the muscular afferents in acupuncture. The results of psychophysical response showed that there were different prevalence and intensity of sensations for both conditions. Soreness, numbness, fullness, and warmth were found to be more frequent and stronger for DA than SA. Effect of acupuncture is better if sensation is stronger based on TCM. But, one study suggested that acupuncture needle stimulation at two different depths of needling, superficial, and deep did not elicit significantly different BOLD responses [58]. This result may be related to the mistaken design of block design and acupuncture in HC.

Moreover, the author also pointed out that the participants in that study were healthy individuals, and it is possible that superficial and deep acupuncture could potentially have different effects when being used to treat people with pathology. Our results demonstrated that there was different effective connectivity of postacupuncture at KI3 in different depths of needling, and effect of acupuncture was stronger for DA compared with that for SA.

In conclusion, results indicated that acupuncture at acupoint KI3 in different cognitive state and different acupuncture depth may induce distinct reorganization of the effective connectivity across different neural subsystems, and acupuncture at KI3 in MCI-Deep can induce the strongest and more extensive effective connectivity related to the therapeutic effect of acupuncture for the treatment of MCI.

5. Conclusions

The current study demonstrated that the significantly enhanced correlations in the cognitive-related brain regions following acupuncture may be related to the therapeutic effects of acupuncture for the treatment of MCI. Our results also revealed that there existed more tightly effective connectivity patterns during the poststimulus resting state following acupuncture at acupoint KI3 in MCI patients compared to HC, stronger effective connectivity patterns for DA compared to SA, and acupuncture effects could last for a long period even though the needling process was terminated. We suggested that the distinct modulation patterns of the resting brain networks attributed to the specific effects which was evoked by acupuncture in different cognitive states and different needling depths. The study demonstrated that acupoint can play a better role in the suitable depth of needle and disease state. This preliminary finding may provide a new clue to decipher the relatively functional specificity of acupuncture effects. Our findings may help to understand the neurophysiological mechanism underlying acupuncture specificity and to employ KI3 for the treatment of MCI in the clinical practice.

Conflict of Interests

The authors declare no conflict of interests.

Acknowledgments

This study was supported by the National Natural Science Foundation of China under Grant nos. 81173354 and 81071217, the Fundamental Research Funds for the Central University, the Beijing Nova program (Grant no. Z111101054511116), the Beijing Natural Science Foundation (Grant no. 4122082), the National Key Basic Research and Development Program (973) under Grant no. 2010CB530506, the Natural Science Foundation of Guangdong Province under Grant nos. 10451810101005862 and 8451040701000553, and the Administration of Traditional Chinese Medicine of Guangdong Province under Grant no. 20111032.

References

[1] S. R. Sabat, "Dementia in developing countries: a tidal wave on the horizon," *The Lancet*, vol. 374, no. 9704, pp. 1805–1806, 2009.

[2] A. Hsu and H. Kao, "The clinical course of advanced dementia," *New England Journal of Medicine*, vol. 362, no. 4, pp. 363–365, 2010.

[3] R. M. Sousa, C. P. Ferri, D. Acosta et al., "Contribution of chronic diseases to disability in elderly people in countries with low and middle incomes: a 10/66 Dementia Research Group population-based survey," *The Lancet*, vol. 374, no. 9704, pp. 1821–1830, 2009.

[4] A. Levey, J. Lah, F. Goldstein, K. Steenland, and D. Bliwise, "Mild cognitive impairment: an opportunity to identify patients at high risk for progression to Alzheimer's disease," *Clinical Therapeutics*, vol. 28, no. 7, pp. 991–1001, 2006.

[5] R. C. Petersen, G. E. Smith, S. C. Waring, R. J. Ivnik, E. G. Tangalos, and E. Kokmen, "Mild cognitive impairment: clinical characterization and outcome," *Archives of Neurology*, vol. 56, no. 3, pp. 303–308, 1999.

[6] M. R. Farlow, "Treatment of mild cognitive impairment (MCI)," *Current Alzheimer Research*, vol. 6, no. 4, pp. 362–367, 2009.

[7] Y. Feng, L. Bai, Y. Ren et al., "FMRI connectivity analysis of acupuncture effects on the whole brain network in mild cognitive impairment patients," *Magnetic Resonance Imaging*, vol. 30, no. 5, pp. 672–682, 2012.

[8] H. Cheng, J. Yu, Z. Jiang et al., "Acupuncture improves cognitive deficits and regulates the brain cell proliferation of SAMP8 mice," *Neuroscience Letters*, vol. 432, no. 2, pp. 111–116, 2008.

[9] Z. Wang, B. Nie, D. Li et al., "Effect of acupuncture in mild cognitive impairment and Alzheimer disease: a functional MRI study," *PLoS One*, vol. 7, no. 8, Article ID e42730, 2012.

[10] NIH, "NIH consensus conference statement acupuncture," *Journal of the American Medical Association*, vol. 280, no. 17, pp. 1518–1524, 1998.

[11] F. Beissner and C. Henke, "Methodological problems in fMRI studies on acupuncture: a critical review with special emphasis on visual and auditory cortex activations," *Evidence-Based Complementary and Alternative Medicine*, vol. 2011, Article ID 607637, 7 pages, 2011.

[12] K. K. S. Hui, J. Liu, N. Makris et al., "Acupuncture modulates the limbic system and subcortical gray structures of the human brain: evidence from fMRI studies in normal subjects," *Human Brain Mapping*, vol. 9, no. 1, pp. 13–25, 2000.

[13] S. Yoo, E. Teh, R. A. Blinder, and F. A. Jolesz, "Modulation of cerebellar activities by acupuncture stimulation: evidence from fMRI study," *NeuroImage*, vol. 22, no. 2, pp. 932–940, 2004.

[14] R. P. Dhond, C. Yeh, K. Park, N. Kettner, and V. Napadow, "Acupuncture modulates resting state connectivity in default and sensorimotor brain networks," *Pain*, vol. 136, no. 3, pp. 407–418, 2008.

[15] L. Bai, W. Qin, J. Tian et al., "Time-varied characteristics of acupuncture effects in fMRI studies," *Human Brain Mapping*, vol. 30, no. 11, pp. 3445–3460, 2009.

[16] L. Bai, W. Qin, J. Tian et al., "Acupuncture modulates spontaneous activities in the anticorrelated resting brain networks," *Brain Research*, vol. 1279, pp. 37–49, 2009.

[17] J. Fang, Z. Jin, Y. Wang et al., "The salient characteristics of the central effects of acupuncture needling: limbic-paralimbic-neocortical network modulation," *Human Brain Mapping*, vol. 30, no. 4, pp. 1196–1206, 2009.

[18] L. Bai, H. Yan, N. Li et al., "Neural specificity of acupuncture stimulation at pericardium 6: evidence from an fMRI study," *Journal of Magnetic Resonance Imaging*, vol. 31, no. 1, pp. 71–77, 2010.

[19] L. Bai, J. Tian, C. Zhong et al., "Acupuncture modulates temporal neural responses in wide brain networks: evidence from fMRI study," *Molecular Pain*, vol. 6, p. 73, 2010.

[20] Y. Feng, L. Bai, W. Zhang et al., "Investigation of acupoint specificity by multivariate granger causality analysis from functional MRI data," *Journal of Magnetic Resonance Imaging*, vol. 34, no. 1, pp. 31–42, 2011.

[21] Y. Zhou and J. Jia, "Effect of acupuncture given at the HT 7, ST 36, ST 40 and KI 3 acupoints on various parts of the brains of Alzheimer's disease patients," *Acupuncture and Electro-Therapeutics Research*, vol. 33, no. 1-2, pp. 9–17, 2008.

[22] W. Q. Qiu, J. Claunch, J. Kong et al., "The effects of acupuncture on the brain networks for emotion and cognition: an observation of gender differences," *Brain Research*, vol. 1362, pp. 56–67, 2010.

[23] C. Zhong, L. Bai, R. Dai et al., "Modulatory effects of acupuncture on resting-state networks: a functional MRI study combining independent component analysis and multivariate granger causality analysis," *Journal of Magnetic Resonance Imaging*, vol. 35, no. 3, pp. 572–581, 2012.

[24] T. Xue, L. Bai, S. Chen et al., "Neural specificity of acupuncture stimulation from support vector machine classification analysis," *Magnetic Resonance Imaging*, vol. 29, no. 7, pp. 943–950, 2011.

[25] S. Chen, L. Meng, H. Yan et al., "Functional organization of complex brain networks modulated by acupuncture at different acupoints belonging to the same anatomic segment," *Chinese Medical Journal*, vol. 125, no. 15, pp. 2694–2700, 2012.

[26] J. P. Plummer, "Acupuncture and homeostasis: physiological, physical (postural) and psychological," *American Journal of Chinese Medicine*, vol. 9, no. 1, pp. 1–14, 1981.

[27] T. Kaptchuk, "Acupuncture: theory, efficacy, and practice," *Annals of Internal Medicine*, vol. 136, no. 5, pp. 374–383, 2002.

[28] N. Goldman, M. Chen, T. Fujita et al., "Adenosine A1 receptors mediate local anti-nociceptive effects of acupuncture," *Nature Neuroscience*, vol. 13, no. 7, pp. 883–888, 2010.

[29] C. Vincent and G. Lewith, "Placebo controls for acupuncture studies," *Journal of the Royal Society of Medicine*, vol. 88, no. 4, pp. 199–202, 1995.

[30] Z. Liu, Y. Zhang, L. Bai et al., "Investigation of the effective connectivity of resting state networks in Alzheimer's disease: a functional MRI study combining independent components analysis and multivariate Granger causality analysis," *NMR in Biomedicine*, vol. 25, no. 12, pp. 1311–1320, 2012.

[31] G. Deshpande, S. LaConte, G. A. James, S. Peltier, and X. Hu, "Multivariate granger causality analysis of fMRI data," *Human Brain Mapping*, vol. 30, no. 4, pp. 1361–1373, 2009.

[32] W. Liao, J. Ding, D. Marinazzo et al., "Small-world directed networks in the human brain: multivariate Granger causality analysis of resting-state fMRI," *NeuroImage*, vol. 54, no. 4, pp. 2683–2694, 2011.

[33] F. Krueger, S. Landgraf, E. Van Der Meer, G. Deshpande, and X. Hu, "Effective connectivity of the multiplication network: a functional MRI and multivariate granger causality mapping study," *Human Brain Mapping*, vol. 32, no. 9, pp. 1419–1431, 2011.

[34] R. Oldfield, "The assessment and analysis of handedness: the Edinburgh inventory," *Neuropsychologia*, vol. 9, no. 1, pp. 97–113, 1971.

[35] R. Petersen, R. Doody, A. Kurz et al., "Current concepts in mild cognitive impairment," *Archives of Neurology*, vol. 58, no. 12, pp. 1985–1992, 2001.

[36] S. D. Forman, J. D. Cohen, M. Fitzgerald, W. F. Eddy, M. A. Mintun, and D. C. Noll, "Improved assessment of significant activation in functional magnetic resonance imaging (fMRI): use of a cluster-size threshold," *Magnetic Resonance in Medicine*, vol. 33, no. 5, pp. 636–647, 1995.

[37] J. Morris, "The clinical dementia rating (CDR): current version and scoring rules," *Neurology*, vol. 43, no. 11, pp. 2412–2414, 1993.

[38] F. Beissner, U. Nöth, and T. Schockert, "The problem of metal needles in acupuncture-fMRI studies," *Evidence-based Complementary and Alternative Medicine*, vol. 2011, Article ID 808203, 5 pages, 2011.

[39] J. Kong, R. Gollub, T. Huang et al., "Acupuncture De Qi, from qualitative history to quantitative measurement," *Journal of Alternative and Complementary Medicine*, vol. 13, no. 10, pp. 1059–1070, 2007.

[40] J. Sun, W. Qin, L. Jin et al., "Impact of global normalization in fMRI acupuncture studies," *Evidence-Based Complementary and Alternative Medicine*, vol. 2012, Article ID 467061, 22 pages, 2012.

[41] O. Demirci, M. C. Stevens, N. C. Andreasen et al., "Investigation of relationships between fMRI brain networks in the spectral domain using ICA and Granger causality reveals distinct differences between schizophrenia patients and healthy controls," *NeuroImage*, vol. 46, no. 2, pp. 419–431, 2009.

[42] M. D. Greicius, B. Krasnow, A. L. Reiss, and V. Menon, "Functional connectivity in the resting brain: a network analysis of the default mode hypothesis," *Proceedings of the National Academy of Sciences of the United States of America*, vol. 100, no. 1, pp. 253–258, 2003.

[43] Q. Jiao, G. Lu, Z. Zhang et al., "Granger causal influence predicts BOLD activity levels in the default mode network," *Human Brain Mapping*, vol. 32, no. 1, pp. 154–161, 2011.

[44] K. J. Blinowska, R. Kuś, and M. Kamiński, "Granger causality and information flow in multivariate processes," *Physical Review E*, vol. 70, no. 5, Article ID 050902, pp. 50902–50606, 2004.

[45] P. Liang, Z. Wang, Y. Yang, X. Jia, and K. Li, "Functional disconnection and compensation in mild cognitive impairment: evidence from DLPFC connectivity using resting-state fMRI," *PLoS ONE*, vol. 6, no. 7, Article ID e22153, 2011.

[46] M. Petrides, "Dorsolateral prefrontal cortex: comparative cytoarchitectonic analysis in the human and the macaque brain and corticocortical connection patterns," *European Journal of Neuroscience*, vol. 11, no. 3, pp. 1011–1036, 1999.

[47] T. A. Hare, C. F. Camerer, and A. Rangel, "Self-control in decision-making involves modulation of the vmPFC valuation system," *Science*, vol. 324, no. 5927, pp. 646–648, 2009.

[48] P. Turriziani, D. Smirni, G. Zappalà, G. R. Mangano, M. Oliveri, and L. Cipolotti, "Enhancing memory performance with rTMS in healthy subjects and individuals with mild cognitive impairment: the role of the right dorsolateral prefrontal cortex," *Frontiers in Human Neuroscience*, vol. 6, p. 62, 2012.

[49] F. Bai, Z. Zhang, D. R. Watson et al., "Abnormal functional connectivity of hippocampus during episodic memory retrieval processing network in amnestic mild cognitive impairment," *Biological Psychiatry*, vol. 65, no. 11, pp. 951–958, 2009.

[50] F. D. Vogelaere, P. Santens, E. Achten, P. Boon, and G. Vingerhoets, "Altered default-mode network activation in mild cognitive impairment compared with healthy aging," *Neuroradiology*, vol. 54, no. 11, pp. 1195–1206, 2012.

[51] M. Moser and E. I. Moser, "Distributed encoding and retrieval of spatial memory in the hippocampus," *Journal of Neuroscience*, vol. 18, no. 18, pp. 7535–7542, 1998.

[52] F. Kurth, K. Zilles, P. T. Fox, A. R. Laird, and S. B. Eickhoff, "A link between the systems: functional differentiation and integration within the human insula revealed by meta-analysis," *Brain structure & Function*, vol. 214, no. 5-6, pp. 519–534, 2010.

[53] C. Xie, F. Bai, H. Yu et al., "Abnormal insula functional network is associated with episodic memory decline in amnestic mild cognitive impairment," *Neuroimage*, vol. 63, no. 1, pp. 320–327, 2012.

[54] T. Stein, C. Moritz, M. Quigley, D. Cordes, V. Haughton, and E. Meyerand, "Functional connectivity in the thalamus and hippocampus studied with functional MR imaging," *American Journal of Neuroradiology*, vol. 21, no. 8, pp. 1397–1401, 2000.

[55] G. A. Carlesimo, M. G. Lombardi, and C. Caltagirone, "Vascular thalamic amnesia: a reappraisal," *Neuropsychologia*, vol. 49, no. 5, pp. 777–789, 2011.

[56] Z. Wang, X. Jia, P. Liang et al., "Changes in thalamus connectivity in mild cognitive impairment: evidence from resting state fMRI," *European Journal of Radiology*, vol. 81, no. 2, pp. 277–285, 2012.

[57] P. Liang, Z. Wang, Y. Yang, X. Jia, and K. Li, "Functional disconnection and compensation in mild cognitive impairment: evidence from DLPFC connectivity using resting-state fMRI," *PLoS ONE*, vol. 6, no. 7, Article ID e22153, 2011.

[58] H. MacPherson, G. Green, A. Nevado et al., "Brain imaging of acupuncture: comparing superficial with deep needling," *Neuroscience Letters*, vol. 434, no. 1, pp. 144–149, 2008.

Hindawi Publishing Corporation
Evidence-Based Complementary and Alternative Medicine
Volume 2013, Article ID 436913, 11 pages
http://dx.doi.org/10.1155/2013/436913

Review Article

Mechanisms of Electroacupuncture-Induced Analgesia on Neuropathic Pain in Animal Model

Woojin Kim,[1] Sun Kwang Kim,[2] and Byung-Il Min[1,3]

[1] *Department of East-West Medicine, Graduate School, Kyung Hee University, Seoul 130-701, Republic of Korea*
[2] *Department of Physiology, College of Korean Medicine, Kyung Hee University, Seoul 130-701, Republic of Korea*
[3] *Department of Physiology, College of Medicine, Kyung Hee University, Seoul 130-701, Republic of Korea*

Correspondence should be addressed to Byung-Il Min; mbi@khu.ac.kr

Received 20 February 2013; Revised 23 June 2013; Accepted 11 July 2013

Academic Editor: Lixing Lao

Neuropathic pain remains as one of the most difficult clinical pain syndromes to treat. Electroacupuncture (EA), involving endogenous opioids and neurotransmitters in the central nervous system (CNS), is reported to be clinically efficacious in various fields of pain. Although multiple experimental articles were conducted to assess the effect of EA-induced analgesia, no review has been published to assess the efficacy and clarify the mechanism of EA on neuropathic pain. To this aim, this study was firstly designed to evaluate the EA-induced analgesic effect on neuropathic pain and secondly to guide and help future efforts to advance the neuropathic pain treatment. For this purpose, articles referring to the analgesic effect of acupuncture on neuropathic pain and particularly the work performed in our own laboratory were analyzed. Based on the articles reviewed, the role of spinal opioidergic, adrenergic, serotonergic, cholinergic, and GABAergic receptors in the mechanism of EA-induced analgesia was studied. The results of this research demonstrate that μ and δ opioid receptors, α_2-adrenoreceptors, 5-HT_{1A} and 5-HT_3 serotonergic receptors, M_1 muscarinic receptors, and $GABA_A$ and $GABA_B$ GABAergic receptors are involved in the mechanisms of EA-induced analgesia on neuropathic pain.

1. Introduction

Acupuncture has been a widely used method in traditional medicine in East Asia for thousands of years. Since its introduction to western countries in the 1970s, the global interest in acupuncture has increased, and significant evidence supports acupuncture as a useful tool for treating a diverse spectrum of diseases. In fact, more than 40 disorders have been endorsed by the World Health Organization (WHO) as conditions that can benefit from acupuncture treatment [1]. Among these disorders, pain is known to be particularly sensitive to acupuncture and has been a compelling field for research. In a total of 3,975 acupuncture research articles published from 1991 to 2009, 1647 (41%) focus on pain and analgesia [2].

Multiple theories of pain control mechanisms such as gate-control theory [3], spinal segmental mechanism [4], endogenous opioid system [5], descending noradrenergic and serotonergic systems [6], and diffuse noxious inhibitory control [7] have been investigated over the last several decades to clarify the mechanism of acupuncture and EA. Acupuncture is now proven to be clinically efficacious in various fields of pain, such as, lower back pain [8], chronic knee pain [9], and chronic headache [10], and a recent meta-analysis also demonstrates the effect of acupuncture on different types of chronic pain [11]. EA is a modified acupuncture technique that, as its name implies, utilizes electrical stimulation, and its analgesic effect on different types of acute pains and persistent inflammatory pains has appeared in both rodents and humans [12–14].

According to the NeuPSIG (Special Interest Group on Neuropathic Pain), neuropathic pain is defined as "pain arising as a direct consequence of a lesion or disease affecting the somatosensory system" [15]. It is often reported as having a lancinating or continuous burning character and is frequently associated with the appearance of abnormal sensory signs such as allodynia (pain as a result of a stimulus which normally does not provoke pain) or hyperalgesia

(an increased response to a stimulus which is normally painful) [16]. The underlying mechanisms are complex and appear to involve both peripheral and central components of the nervous system [17].

The spectrum of neuropathic pain covers a variety of disease states and presents itself in the clinic through a variety of symptoms, namely, lumbar radiculopathy (lower back pain caused by disk compression or herniation), spinal cord injury, phantom pain, diabetic neuropathy, postherpetic neuralgia, and in some patients, fibromyalgia, and cancer-related pain [18].

It is estimated that neuropathic pain affects over 26 million patients worldwide, resulting in a worldwide healthcare cost of over $3 billion per year, with a significant portion of this money paid to drug therapies that originally were developed for other medical conditions [19].

Current pharmacological treatment for neuropathic pain typically will include some combination of agents from several of the following drug classes: opioids, tricyclic antidepressants, anticonvulsant agents, or nonsteroidal anti-inflammatory drugs (NSAIDs)/analgesics. Ironically, even with such an impressive arsenal of powerful drugs, these approaches only provide an approximate 30–50% reduction of pain in about 50% of patients. In addition, there are various side effects associated with these drugs [20, 21].

These results underscore the importance of considering a complementary and alternative neuropathic pain treatment. Previously, several clinical studies have shown the effectiveness of EA on various neuropathic pain diseases such as neuropathic pain of malignancy [22], diabetic neuropathy [23, 24], phantom limb pain [25, 26], and below-level central neuropathic pain [27]. However, although multiple reviews exist on the analgesic mechanisms of EA, no previous review has been published on the effect of EA in neuropathic pain, and still the mechanism that lies behind it remains unclear.

For many years, and since the publishing of the first article of Hwang et al. [28] on neuropathic pain published from our laboratory, our research has focused on clarifying the mechanisms of EA on neuropathic pain, and different experimental designs were used to understand the analgesic effect of EA in neuropathic pain rats. So far, the mechanisms of EA on spinal endogenous opioidergic [28–31] adrenergic and serotonergic [32], cholinergic [33, 34], and GABAergic [35] systems have been clarified as a result of these studies, and efforts to clarify further mechanisms are on their way [36].

To guide future efforts in the advancement of neuropathic pain treatment, we believed that a timely review was important. In this review, based on the articles published in our laboratory, we will proceed to expand on clarification of the effect of EA on neuropathic pain and quantify its mechanism.

2. Endogenous Opioids and Descending Inhibitory System

Since 1970, the mechanism of acupuncture analgesia has been broadly investigated, and numerous pieces of evidence demonstrated that acupuncture analgesia is mediated via neuronal mechanisms correlated with the central nervous system (CNS) [6, 37, 38]. The most recognized mechanisms are endogenous opiates mechanisms [5, 39] and descending inhibitory mechanisms [6]. Endogenous opioids are known to be mediated through its μ, δ, κ receptors and descending inhibitory pathway through its monoaminergic neurotransmitters and their receptors. In this review, to clarify the mechanism of EA in neuropathic pain, we have focused on the neurotransmitters receptors present in the CNS, especially in the spinal level.

2.1. Opioidergic Receptors. Ever since the publication of the article by Arner and Meyerson in 1988 titled "lack of an effect of opioids on neuropathic and idiopathic forms of pain" [40], multiple studies have been published supporting the efficacy of opioids for neuropathic pain, and it is now known that opioids can clearly provide effective analgesia for neuropathic pain [41, 42]. Endogenous opioids are involved in both ascending and descending parts of the inhibition pathway. In the ascending portion, all three receptors (μ, δ, κ) play a part, but only μ and δ receptors are responsible in the descending portion [43].

The involvement of opioid receptors in mediating acupuncture analgesia is demonstrated in several articles. Han reported that EA analgesia is mediated by enkephalin, β-endorphin, endomorphin, and dynorphin released in the CNS and that μ, δ, κ opioid receptors are involved in the mechanisms [39, 44]. David Mayer clarified the role of endogenous opioid in the mechanisms proving that the analgesic effect of acupuncture was prevented or reversed by the opioid receptors blocker naloxone [45, 46].

To determine whether the EA analgesic effect is mediated by endogenous opioid in the rat model of neuropathic pain, Hwang et al. conducted an experiment by injecting opioid antagonist naloxone intraperitoneally 20 min before the EA in rat specimens [28]. The EA was applied at Houxi acupoint (SI3), and mechanical allodynia was assessed by a normally innocuous stimulation of the tail with the Von Frey Hair. An abrupt tail movement of more than 0.5 cm was considered to be an abnormal response attributed to mechanical allodynia. The results show that the antiallodynic effect of EA was reversed by intraperitoneal injected naloxone but not through normal saline. Further experimentation with intraperitoneal morphine also demonstrates that mechanical allodynia was relieved in a dose-dependent manner. The result reports that a higher dose (1.5 mg/kg) of morphine relieves more effectively the signs of mechanical allodynia than a lower dose (0.5 mg/kg) and that EA with 1.5 mg/kg of morphine induced a slightly more antiallodynic effect. These results are consistent with the previous results of Mayer and Omana [46, 47].

In addition, through cDNA microarray analysis and dot-blot analysis, Ko et al. identified the opioid signaling events involved in neuropathic pain [31]. This data suggest that the opioid receptor probably plays an important role in the development of neuropathic pain and the analgesic effects of EA.

Furthermore, Kim et al. [29] conducted an experiment to clarify which opioidergic receptors are involved in

the relieving effect of EA on mechanical allodynia in the spinal cord. Selective μ (β-FNA), δ (naltrindole), and κ (nor-BNI) antagonists were administered intrathecally separated by 10 min in cumulative doses to examine whether the effect of EA was blocked by these antagonists. The EA was also applied into Zusanli (ST36). Results show that relieving effects on mechanical allodynia are blocked by μ and δ selective opioid antagonists but not by κ selective opioid antagonists. The fact that κ selective opioid antagonist did not work might be due to the low frequency (2 Hz) used in the experiment. Chen and Han [48] and Wu et al. [49] reported that 2 Hz EA-induced analgesia is mediated by met-enkephalin via μ, δ receptors; however, the antinociception effect induced by high-frequency (100 Hz) EA is mediated by dynorphin via κ receptors in the spinal cord of rats. This report is consistent with the review of Han [39].

Kim et al. [30] also reported that the increased expression level of CCK-A receptors, the site of action for the antiopioid peptide cholecystokinin (CCK) in the hypothalamus, might decrease the sensitivity of EA and result in the decrease of the analgesic effect and antiallodynic effect on neuropathic pain model rats. This result is supported by other studies of Lee et al. [50, 51] reporting that the presence of CCK-A receptor might decrease the analgesic effect of EA.

2.2. Adrenergic Receptors. Noradrenalin (NE) is known to be one of the main transmitters involved in the descending inhibitory system with serotonin and opioids [43]. It was previously reported that noradrenergic inputs in the spinal cord originate from the locus coeruleus (LC) and adjacent noradrenergic nuclei in the brainstem [52]. Unlike the serotonergic axons descending from nucleus raphe magnus (NRM) and operating through enkephalinergic interneurons in the spinal cord, noradrenergic fibers are known to bring about direct inhibition on the many types of spinal cell with which they make synaptic contacts [53]. Supraspinal descending pathways are known to be the only source of NE in the spinal dorsal horn [54].

There are two major groups of adrenoreceptors, α and β, with several subtypes. Among these receptors, α_1- and α_2-adrenoreceptors are shown to be largely involved in pain modulation [54], and results from recent studies indicate that both the α_1- and α_2-adrenoreceptors are involved in neuropathic pain [55]. Some articles report that NE enhances the spinal GABAergic and cholinergic transmission by activating α_1- [56] and α_2- [57] adrenoreceptors. An analgesic effect in the rat, caused by intrathecal administered NE, has been shown to be blocked by phentolamine, a nonselective α-adrenoreceptors antagonist [43]. Also, epidural injection of the α_2-adrenoreceptors, clonidine, has been reported to result in pain relief in cancer patients with neuropathic pain [58].

To examine the role of α_1- and α_2-adrenoreceptors in the mechanisms of EA, Kim et al. conducted a research administering one dose of α_1- and α_2-adrenoreceptors antagonists (prazosin or yohimbine, resp.) intrathecally with EA. Needles were inserted into Zusanli (ST36), and 30 μg of prazosin and yohimbine were injected to neuropathic pain rats [32]. The relieving effects of EA on cold allodynia were blocked by the α_2-adrenoreceptors antagonist yohimbine but not by the α_1-adrenoreceptors antagonist prazosin. This result shows that the effect of an EA analgesic might be mediated by the spinal α_2-adrenoreceptors but not by the α_1-adrenoreceptors. This data is consistent with Kim's et al. [59] previous study conducted with only α_1- and α_2-adrenoreceptor antagonists, prazosin, and yohimbine intraperitoneally administrated without the EA insertion. Jiang et al. and several other studies [60–63] also reported that intrathecal administration of the α_2-adrenoreceptors agonist in a neuropathic pain model rats significantly attenuated hyperalgesia and tactile allodynia.

Contrary to the role of α_2-adrenoreceptors, a lot of evidence and results from these experiments suggest that not only are spinal α_1-adrenoreceptors not involved in pain inhibition [64, 65] but also they play an important role in the prenociception of animals and humans [66, 67]. These results are in agreement with other previous studies [54, 68, 69] which show how in the nervous system α_1-adrenoreceptors and α_2-adrenoreceptors antagonist yohimbine work as an excitatory although α_2-adrenoreceptors and α_1-adrenoreceptors antagonist prazosin works as an inhibitory and demonstrate that spinal α_2-adrenoreceptors are involved in the relieving effects of EA on cold allodynia.

2.3. Serotonergic Receptors. Serotonin is known to have antinociceptive effect spinally, depending on the receptor type activated and dosage use [70, 71]. The role of serotonin in the descending inhibitory pathway of the CNS was also demonstrated [72, 73]. The involvement of serotonin in the analgesic effect of EA was mentioned in an early study of Cheng and Pomeranz [74]. They previously hypothesized that two distinct pain relieving mechanisms are involved in the effects of EA, including endogenous endorphin and nonendorphin systems. They further reported that nonendorphinergic actions may be mediated by monoaminergic neurons such as serotonin and NE [13]. The analgesic effect of serotonin is reported to be mediated from periaqueductal grey (PAG), NRM, and serotonergic receptors present in the spinal dorsal horn [75]. The spinal release of opioid may be driven by a serotonergic descending pathway [76–78] and is at least in part elicited by activation of 5-HT_3 receptors [79]. The electrolytic lesion of the NRM, a procedure known to decrease the release of 5-HT in the spinal cord [80], attenuates EA-induced analgesia [81]. Research from a number of studies has demonstrated that analgesia by peripheral stimulation is mediated by the serotonergic pathway in the descending inhibitory system [82–84], and the involvement of serotonin receptors in the analgesic mechanism of acupuncture in a neuropathic pain model rat was shown in the study of Zhao [85]. Seven subtypes (5-HT_{1-7}) of serotonin receptors have been identified. 5-HT_1 5-HT_2 or 5-HT_3 are known to be the most commonly implicated in the spinal analgesic effect induced by peripheral stimulation [86–88].

However, conflicting results have been reported regarding the involvement of these three 5-HT receptors. Horiuchi et al. [89] reported that intrathecal administration of 5-HT_{1A} and 5-HT_3 but not 5-HT_{2A} receptor agonists inhibited thermal hyperalgesia induced by spinal cord injury. Chang et al. [13] are in agreement with Horiuchi et al. and showed that

intracerebroventricular administration of 5-HT_{1A} and 5-HT_3 but not 5-HT_{2A} receptor antagonists blocked the analgesic effect induced by EA. Baek et al. [12] also demonstrated that in the rat model of collagen-induced arthritis the analgesic effect of EA was blocked by intraperitoneal pretreatment of 5-HT_{1A} receptor antagonist and 5-HT_3 receptor antagonist but not by 5-HT_2 receptor antagonist. These results suggest that the EA analgesic effect can be mediated by 5-HT_{1A} and 5-HT_3 receptors but not by a 5-HT_{2A} receptor.

Conversely, Radhakrishnan et al. [88] by administrating different 5-HT subtype antagonist intrathecally showed that spinal 5-HT_{2A} and 5-HT_3 but not 5-HT_{1A} receptors mediate transcutaneous electrical nerve stimulation (TENS) and induced antihyperalgesia in inflammatory pain model rats. Takagi and Yonehara [90] also reported that intravenously injected 5-HT_1, except 5-HT_{1A}, 5-HT_2, except 5-HT_{2A}, and 5-HT_3 receptors are involved in EA-induced analgesia.

Thus, to clarify which serotonin receptor is involved in the spinal mechanisms of EA analgesia on neuropathic pain in rats, Kim et al. conducted a further study [32]. Serotonin receptor antagonists of 5-HT_{1A} (NAN-190, 15 μg), 5-HT_{2A} (ketanserin, 30 μg), and 5-HT_3 (MDL-72222, 12 μg) were injected intrathecally and needles were inserted into Zusanli (ST36). The relieving effect of EA on cold allodynia was blocked by the 5-HT_{1A} antagonist (NAN-190) and by the 5-HT_3 antagonist (MDL-72222) significantly, but not by the 5-HT_1 antagonist (ketanserin). This result is consistent with previous studies showing that 5-HT_{1A} receptors [91–93] and 5-HT_3 receptors [94–96] have antinociceptive roles.

Also, evidence suggests that 5-HT_{1A} receptors inhibit the nociceptive sign in the second-order spinothalamic tract [97], and 5-HT_3 involves GABAergic, ENKergic (enkephalinergic), and other classes of spinal intrinsic neurons at the spinal level [82, 98–101].

The discordance with the previous result of Radhakrishnan et al. and Takagi and Yonehara might be due to a difference in experiment design, as Radhakrishnan investigated on the inflammation of the knee joint and used TENS but not EA. And Yonehara investigated in the trigeminal nucleus caudalis in rabbits.

2.4. Cholinergic Receptors. Cholinergic receptors are known to have both excitatory and inhibitory actions. They mediate acetylcholine (ACh) and induce an analgesic effect by the activation of spinal nicotinic or muscarinic acetylcholine receptors. Both the nicotinic and muscarinic receptors are located in the superficial and deep dorsal horn of the spinal cord where nociceptive information is transmitted and modulated [54, 57, 102]. Cholinergic innervations of the dorsal spinal cord are known to be primarily intrinsic [57], but evidence for cholinergic fibers descending from the brainstem to the spinal cord has also appeared as a result of several studies [103, 104].

The role of nicotinic and muscarinic receptors in the mechanisms of analgesia is known to be different. A large majority of studies indicate that antinociceptive and antiallodynic effects of cholinergic drugs are mediated mainly by the muscarinic receptors but not by the nicotinic receptors [57, 105–107]. Also, previous studies reported that systemic administration of atropine (nonselective muscarinic antagonist) prevented the analgesic effects of EA [12, 108].

To investigate whether spinal nicotinic or muscarinic receptors are involved in the relieving effects of EA on cold and warm allodynia, Park et al. conducted research with intrathecally administered atropine (nonselective muscarinic antagonist) and mecamylamine (nonselective nicotinic antagonist) on neuropathic pain model rats [34]. The relieving effects of EA on both cold allodynia and warm allodynia were completely blocked by atropine but not by mecamylamine. This outcome showed that the antiallodynic effect of EA in neuropathic pain rats is mediated mainly by the muscarinic receptor.

A further study was conducted by Park et al. [34], to determine which muscarine receptor subtype is involved in the antiallodynic action of EA. Currently, five classes of muscarinic receptor have been identified (i.e., M_{1-5}). However, the subtypes implicated in the spinal nociceptive transmission and modulations are known to be consisting of M_1, M_2, and M_3 [106, 107, 109]. Pirenzepine (M_1 muscarinic receptor antagonist), methoctramine (M_2 muscarinic antagonist), and 4-DAMP (M_3 muscarinic antagonist) were injected intrathecally on rats, and acupuncture needles were inserted into "Zusanli" (ST36). Among these three antagonists, only pirenzepine (M_1 muscarinic receptor antagonist) completely blocked the relieving effect of EA on cold allodynia and warm allodynia, whereas methoctramine and 4-DAMP did not.

Kim et al. [33], with intrathecally administered cholinesterase inhibitor neostigmine, showed that EA has an effect that is equivalent to 0.1 μg of neostigmine on neuropathic pain rats. Neostigmine is known to induce analgesia by mediating spinal muscarinic system and especially at the M_1 receptor subtype. On the other hand, neostigmine is also known to produce dose-dependent side effects such tremor, writhing action, or urination at doses of 0.3, 1 and 3 μg, in some rats [110, 111]. However, the combination of intrathecal neostigmine (0.1 μg) and EA stimulation produced a synergetic effect lasting more than 80 min., becoming maximal at 20 min., the same as a dose of 0.3 μg of neostigmine, but without side effects. In summary, these results demonstrate that EA stimulation activates spinal M_1 muscarinic receptors to relieve cold and warm allodynia signs in neuropathic pain rats. This conclusion is in agreement with previous studies showing that M_1 receptor subtype mediates spinal antinociception and antiallodynia [105, 107, 112–114].

2.5. GABAergic Receptors. One of the major inhibitory neuropeptides, GABA is known to be contained in the PAG and plays an important role in the descending pain control pathway of the CNS [115–118]. It is also reported to be involved in multiple physiological and pathological functions. In the spinal cord, GABA exerts tonic modulation of nociceptive neurotransmission between primary afferents and second-order spinothalamic tract neurons [119, 120]. Intrathecally injected baclofen ($GABA_B$ receptor agonist) has been demonstrated to produce analgesia in animal models of acute and neuropathic pain [121]. Three GABA receptor subtypes have been identified: $GABA_A$, $GABA_B$, and $GABA_C$ [120], but it has been known that $GABA_A$ and

$GABA_B$ receptors, present in the spinal cord [122], mainly contribute to modulation of pain [54, 123]. Also, $GABA_A$ and $GABA_B$ receptor agonists have been demonstrated to have antinociceptive effects in a variety of rodent models [124]. The role of GABA and its receptors, in the acupuncture analgesia, has been demonstrated by several studies. Han et al. [125] reported that the microinjecting of muscimol, a $GABA_A$ receptor agonist, or 3-MP, a GABA synthesis inhibitor, into the PAG remarkably potentiated or suppressed acupuncture analgesia, respectively. And Fusumada et al. [126] proved that by inserting EA at "Zusanli" (ST36), EA could induce analgesic effect along with the increasing expression of GABA in PAG. Also, Fu and Longhurst [127] and Tjen-A-Looi et al. [128] studies reported that EA decreases the release of GABA in ventrolateral PAG, by modulating the sympathoexcitatory reflex responses through endocannabinoids. These results are in line with the study of Fusumada as the decrease of GABA release may result in the increase of GABA in PAG.

First, Park et al. conducted research to investigate whether spinal GABAergic receptors are involved in the relieving effects of EA on cold allodynia in a rat tail model of neuropathic pain [35]. EA stimulation was applied to "Zusanli" (ST36) and rats were intrathecally injected with gabazine ($GABA_A$ receptor antagonist, 0.0003, 0.001, or 0.003 μg) or saclofen ($GABA_B$ receptor antagonist, 3, 10, or 30 μg). The relieving effect of EA on cold allodynia on neuropathic pained rats was blocked by gabazine at a dose of 0.001 or 0.003 μg. Saclofen also blocked the effect of EA-induced analgesic effect at a dose of 10 or 30 μg. The results show that both the $GABA_A$ and $GABA_B$ receptor antagonists dose dependently blocked the relieving effects of EA on cold allodynia. Also, these findings are consistent with the previous studies of Zhu et al. [129, 130], in which intrathecal administration of $GABA_A$ and $GABA_B$ receptor antagonists partially blocked the acupuncture analgesia. In brief, this evidence supports EA-induced antiallodynia as partially mediated by the activation of spinal inhibitory receptors including GABA receptors. Therefore, it is possible that EA treatment could enhance the analgesic effects of the GABAergic drugs, such as GABA agonists, on neuropathic pain in clinics and vice versa.

3. Summary and Discussion

Neuropathic pain is a complex phenomenon, involving several independent pathophysiological mechanisms in both peripheral and CNS. The accurate mechanisms of neuropathic pain and the relationships between its mechanisms, signs, and symptoms are not fully understood, and no consensus on the optimal management of neuropathic pain has been established yet. Although acupuncture's mechanisms of antinociception have not been fully explained, due to the overwhelming amount of research investigated in the last several decades, its analgesic effects are gradually being understood.

In this review, based on published reports from several research laboratories around the world and particularly the work performed in our laboratory, we demonstrated that spinal opioidergic, adrenergic, serotonergic, cholinergic, and GABAergic systems mediate the analgesic effects of EA in neuropathic pain rats. Data from our experiments show that spinal μ and δ opioid receptors, α_2-adrenoreceptors, 5-HT_{1A} and 5-HT_3 serotonergic receptors, M_1 muscarinic receptors, and $GABA_A$ and $GABA_B$ GABAergic receptors are involved in the analgesic effect of EA on neuropathic pain, mediated by the descending inhibitory system in the CNS (Figure 1).

The descending inhibitory pathway consisted of hypothalamus-PAG-rostal ventromedial medulla (RVM)-dorsal horn and mediates the release of serotonin in the PAG and NE in LC. NE, via α_2-adrenoreceptors in the dorsal horn, enhances the spinal cholinergic and GABAergic intrinsic neurons, involves a reduction in the release of pronociceptive transmitters in the primary afferents fibers, and inhibits the transmission of pain signals to the supraspinal level in the secondary afferents fibers [131]. Serotonin activates enkephalin (ENK) and GABA spinal intrinsic neurons through 5-HT_3 serotonergic receptors and inhibits secondary afferents fiber via 5-HT_{1A} serotonergic receptors [54]. Spinal cholinergic, ENKergic, GABAergic neurons, through its M_1 muscarinic receptors, μ, δ opioid receptors, and $GABA_{A/B}$ receptors control nociceptive inputs from the periphery to higher areas in the CNS [54, 57]. The EA stimulation is carried up from marginal (M) cells tract to the brain via spinothalamic tract, where the signal is transmitted to the cortex and becomes conscious, and also to intrinsic dorsal neurons where it involves cholinergic, ENKergic, and GABAergic neurons [53, 121, 132].

Also, the role of glial activation on EA-induced analgesia should be considered alongside the mechanisms of neurons, as microglial activation has been reported to contribute to the initiation of pathological pain responses and astrocytic activation to pain maintenance in a rat model of neuropathic pain [133, 134]. The involvement of glial activation in the analgesic effect of EA is demonstrated in the article of Wang et al. [135], and Gim et al. [36] reported recently that repeated EA attenuates mechanical and warm allodynia by suppressing microglial and astrocyte activation inhibiting the release of proinflammatory cytokine such as TNF-α, IL-6, and IL-1β.

Most of the articles included in this review used mechanical allodynia and thermal allodynia (warm or cold) to assess the effect of EA. However, they are reported to be mediated differently. Shir and Seltzer [136] demonstrated in his work that mechanical allodynia is mediated by A-fibers and thermal allodynia by C-fibers. Among the works included in this review, Hwang et al. [28] and Kim et al. [29] used mechanical allodynia, while Kim et al. [32, 59], Park et al. [34, 35], and Kim et al. [33] used thermal allodynia to assess the effect of EA on neuropathic pain model rat. On mechanical allodynia the effect of EA marked significant increase up to 20 min after 30 min of EA administration [28], while on thermal allodynia, the EA group showed statistically significant increases in response to latency for up to 50 min after 30 min of EA insertion [32]. These results suggest that the analgesic effect of EA may be more efficacious on thermal allodynia than on mechanical allodynia.

This review is based on articles with animal experience and does not include any controlled clinical trial. Some controlled clinical trials have been published previously to assess the effectiveness of EA on neuropathic pain; however, the data

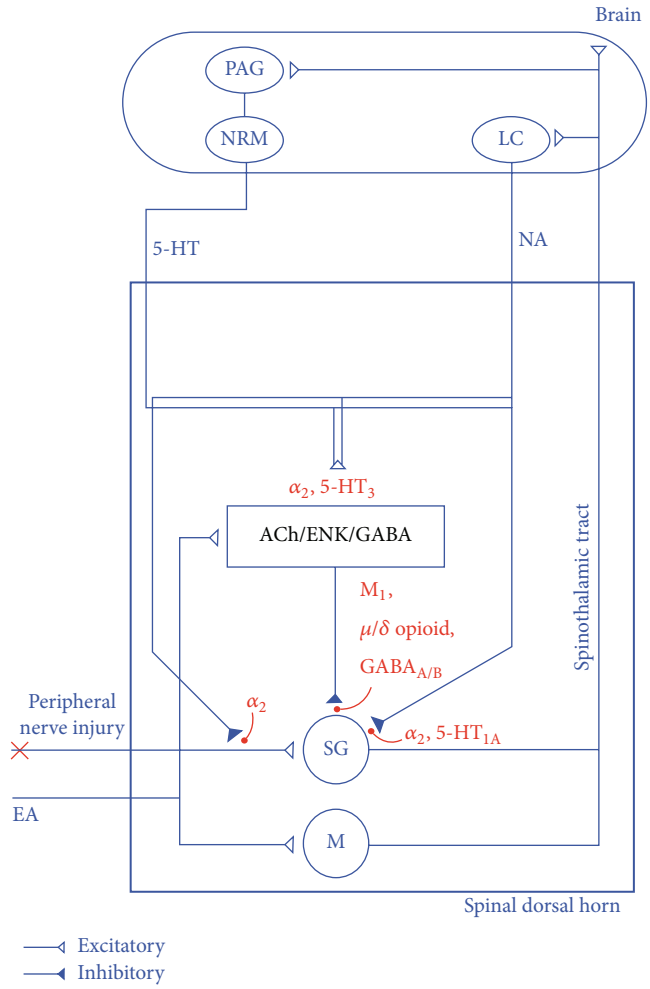

Figure 1: Schematic diagram of EA-induced analgesia in neuropathic pain in the CNS. The peripheral injury information is first transmitted to substantia gelatinosa (SG) cells by primary afferent fibers. EA stimulation is carried up from marginal (M) cells tract to the brain via spinothalamic tract, where the signal is transmitted to the cortex and becomes conscious and also to intrinsic dorsal neurons where it involves cholinergic, ENKergic, and GABAergic neurons. The PAG in the midbrain projects down to the NRM in the middle of the medulla oblongata, and this in turn sends 5-HT fibers to the dorsal horn. LC sends NE fibers to the dorsal horn. NE, via α_2-adrenoreceptors, enhances the spinal cholinergic and GABAergic neurons, involves a reduction in the release of pronociceptive transmitters in the primary afferents fibers, and inhibits the transmission of pain signals to the supraspinal level in the secondary afferents fibers. Serotonin activates enkephalin (ENK) and GABA intrinsic neurons through 5-HT$_3$ serotonergic receptors and inhibits secondary afferents fibers via 5-HT$_{1A}$ serotonergic receptors. Cholinergic, ENKergic, GABAergic neurons, through its M$_1$ muscarinic receptors, μ, δ opioid receptors, and GABA$_A$ and GABA$_B$ receptors control nociceptive inputs from the periphery to higher areas in the CNS. Abbreviations are as follows: SG: substantia gelatinosa; M: marginal cells; PAG: periaqueductal grey; NRM: nucleus raphe magnus; LC: locus coeruleus; 5-HT: serotonin; NE: noradrenalin; Ach: acetylcholine; and ENK: enkephalin.

are still controversial, and the number of controlled clinical trials is insufficient to determine its role in the clinic [137, 138]. Although, there are still no randomized clinical trials to support the analgesic effect of EA on neuropathic pain in clinic, we believe that various experimental models and results reported from the work included in our review could guide future efforts to publish a well-designed randomized clinical trial on neuropathic pain.

4. Conclusion

In conclusion, based on results from our study, we can conclude that both endogenous opioid system and descending inhibitory system mediate the antiallodynic mechanism of EA, and that spinal opioidergic, adrenergic, serotonergic, cholinergic and GABAergic systems are involved in the mechanisms. Also, these results suggest that EA can be an efficacious complementary and alternative treatment to relieve the neuropathic pain.

Furthermore, since a functional interrelationship exists among the opioidergic, noradrenergic, serotonergic, cholinergic and GABAergic systems in the spinal dorsal horn and supraspinal level [54, 57], further studies should investigate how those receptors interact and to what degree each receptor system contributes independently to EA induced analgesia.

References

[1] G. Stux, B. Berman, and B. Pomeranz, *Basics of Acupuncture*, Springer, 2003.

[2] M. K. Lee, S. R. Han, M. K. Park, M. J. Kim, Y. C. Bae, S. K. Kim et al., "Behavioral evidence for the differential regulation of p-p38 MAPK and p-NF-kappaB in rats with trigeminal neuropathic pain," *Molecular Pain*, vol. 7, p. 57, 2011.

[3] R. Melzack and P. D. Wall, "Pain mechanisms: a new theory," *Science*, vol. 150, no. 3699, pp. 971–979, 1965.

[4] Z. Bing, L. Villanueva, and D. Le Bars, "Acupuncture-evoked responses of subnucleus reticularis dorsalis neurons in the rat medulla," *Neuroscience*, vol. 44, no. 3, pp. 693–703, 1991.

[5] B. Pomeranz and D. Chiu, "Naloxone blockade of acupuncture analgesia: endorphin implicated," *Life Sciences*, vol. 19, no. 11, pp. 1757–1762, 1976.

[6] C. Takeshige, T. Sato, T. Mera, T. Hisamitsu, and J. Fang, "Descending pain inhibitory system involved in acupuncture analgesia," *Brain Research Bulletin*, vol. 29, no. 5, pp. 617–634, 1992.

[7] D. Le Bars, A. H. Dickenson, and J. M. Besson, "Diffuse noxious inhibitory controls (DNIC). I. Effects on dorsal horn convergent neurones in the rat," *Pain*, vol. 6, no. 3, pp. 283–304, 1979.

[8] C. P. O. Carlsson and B. H. Sjölund, "Acupuncture for chronic low back pain: a randomized placebo-controlled study with long-term follow-up," *Clinical Journal of Pain*, vol. 17, no. 4, pp. 296–305, 2001.

[9] A. White, N. E. Foster, M. Cummings, and P. Barlas, "Acupuncture treatment for chronic knee pain: a systematic review," *Rheumatology*, vol. 46, no. 3, pp. 384–390, 2007.

[10] A. J. Vickers, R. W. Rees, C. E. Zollman et al., "Acupuncture for chronic headache in primary care: large, pragmatic, randomised trial," *British Medical Journal*, vol. 328, no. 7442, pp. 744–747, 2004.

[11] A. J. Vickers, A. M. Cronin, A. C. Maschino, G. Lewith, H. MacPherson, N. E. Foster et al., "Acupuncture for chronic pain: individual patient data meta-analysis," *Archives of Internal Medicine*, vol. 172, no. 19, pp. 1444–1453, 2012.

[12] Y. H. Baek, Y. C. Do, I. Y. Hyung, and D. S. Park, "Analgesic effect of electroacupuncture on inflammatory pain in the rat model of collagen-induced arthritis: mediation by cholinergic and serotonergic receptors," *Brain Research*, vol. 1057, no. 1-2, pp. 181–185, 2005.

[13] F.-C. Chang, H.-Y. Tsai, M.-C. Yu, P.-L. Yi, and J.-G. Lin, "The central serotonergic system mediates the analgesic effect of electroacupuncture on zusanli (ST36) acupoints," *Journal of Biomedical Science*, vol. 11, no. 2, pp. 179–185, 2004.

[14] A. Li, Y. Wang, J. Xin et al., "Electroacupuncture suppresses hyperalgesia and spinal Fos expression by activating the descending inhibitory system," *Brain Research*, vol. 1186, no. 1, pp. 171–179, 2007.

[15] R.-D. Treede, T. S. Jensen, J. N. Campbell et al., "Neuropathic pain: redefinition and a grading system for clinical and research purposes," *Neurology*, vol. 70, no. 18, pp. 1630–1635, 2008.

[16] D. Bridges, S. W. N. Thompson, and A. S. C. Rice, "Mechanisms of neuropathic pain," *British Journal of Anaesthesia*, vol. 87, no. 1, pp. 12–26, 2001.

[17] C. J. Woolf and R. J. Mannion, "Neuropathic pain: aetiology, symptoms, mechanisms, and management," *Lancet*, vol. 353, no. 9168, pp. 1959–1964, 1999.

[18] J. W. Scadding and M. Koltzenburg, "Painful peripheral neuropathies," in *Wall and Melzack's Textbook of Pain*, S. B. McMahon and M. Koltzenburg, Eds., pp. 973–999, Elsevier, 2006.

[19] N. Pain, J. A. Butera, and M. R. Brandt, "section I. central nervous system diseases," *Annual Reports in Medicinal Chemistry*, vol. 38, p. 1, 2003.

[20] J. A. Butera, "Current and emerging targets to treat neuropathic pain," *Journal of Medicinal Chemistry*, vol. 50, no. 11, pp. 2543–2546, 2007.

[21] V. L. Tawfik, N. Nutile-McMenemy, M. L. LaCroix-Fralish, and J. A. DeLeo, "Efficacy of propentofylline, a glial modulating agent, on existing mechanical allodynia following peripheral nerve injury," *Brain, Behavior, and Immunity*, vol. 21, no. 2, pp. 238–246, 2007.

[22] J. Filshie, "The non-drug treatment of neuralgic and neuropathic pain of malignancy," *Cancer Surveys*, vol. 7, no. 1, pp. 161–193, 1988.

[23] B. B. Abuaisha, J. B. Costanzi, and A. J. M. Boulton, "Acupuncture for the treatment of chronic painful peripheral diabetic neuropathy: a long-term study," *Diabetes Research and Clinical Practice*, vol. 39, no. 2, pp. 115–121, 1998.

[24] P. J. Goodnick, K. Breakstone, X.-L. Wen, and A. Kumar, "Acupuncture and neuropathy," *American Journal of Psychiatry*, vol. 157, no. 8, pp. 1342–1343, 2000.

[25] R. A. Carabelli and W. C. Kellerman, "Phantom limb pain: relief by application of TENS to contralateral extremity," *Archives of Physical Medicine and Rehabilitation*, vol. 66, no. 7, pp. 466–467, 1985.

[26] V. Finsen, L. Persen, M. Lovlien et al., "Transcutaneous electrical nerve stimulation after major amputation," *Journal of Bone and Joint Surgery B*, vol. 70, no. 1, pp. 109–112, 1988.

[27] L. M. Rapson, N. Wells, J. Pepper, N. Majid, and H. Boon, "Acupuncture as a promising treatment for below-level central neuropathic pain: a retrospective study," *Journal of Spinal Cord Medicine*, vol. 26, no. 1, pp. 21–26, 2003.

[28] B. G. Hwang, B.-I. Min, J. H. Kim, H. S. Na, and D. S. Park, "Effects of electroacupuncture on the mechanical allodynia in the rat model of neuropathic pain," *Neuroscience Letters*, vol. 320, no. 1-2, pp. 49–52, 2002.

[29] J. H. Kim, B.-I. Min, H. S. Na, and D. S. Park, "Relieving effects of electroacupuncture on mechanical allodynia in neuropathic pain model of inferior caudal trunk injury in rat: mediation by spinal opioid receptors," *Brain Research*, vol. 998, no. 2, pp. 230–236, 2004.

[30] S. K. Kim, H. J. Moon, J. H. Park et al., "The maintenance of individual differences in the sensitivity of acute and neuropathic pain behaviors to electroacupuncture in rats," *Brain Research Bulletin*, vol. 74, no. 5, pp. 357–360, 2007.

[31] J. Ko, S. N. Doe, H. L. Young et al., "cDNA microarray analysis of the differential gene expression in the neuropathic pain and electroacupuncture treatment models," *Journal of Biochemistry and Molecular Biology*, vol. 35, no. 4, pp. 420–427, 2002.

[32] S. K. Kim, J. H. Park, S. J. Bae et al., "Effects of electroacupuncture on cold allodynia in a rat model of neuropathic pain: mediation by spinal adrenergic and serotonergic receptors," *Experimental Neurology*, vol. 195, no. 2, pp. 430–436, 2005.

[33] H. N. Kim, J. H. Park, S. K. Kim et al., "Electroacupuncture potentiates the antiallodynic effect of intrathecal neostigmine in a rat model of neuropathic pain," *Journal of Physiological Sciences*, vol. 58, no. 5, pp. 357–360, 2008.

[34] J. H. Park, S. K. Kim, H. N. Kim et al., "Spinal cholinergic mechanism of the relieving effects of electroacupuncture on cold and warm allodynia in a rat model of neuropathic pain," *Journal of Physiological Sciences*, vol. 59, no. 4, pp. 291–298, 2009.

[35] J.-H. Park, J.-B. Han, S.-K. Kim et al., "Spinal GABA receptors mediate the suppressive effect of electroacupuncture on cold allodynia in rats," *Brain Research*, vol. 1322, pp. 24–29, 2010.

[36] G.-T. Gim, J.-H. Lee, E. Park et al., "Electroacupuncture attenuates mechanical and warm allodynia through suppression of spinal glial activation in a rat model of neuropathic pain," *Brain Research Bulletin*, vol. 86, no. 5-6, pp. 403–411, 2011.

[37] J. Filshie and A. White, *Medical Acupuncture: A Western Scientific Approach*, Churchill livingstone, Edinburgh, UK, 1998.

[38] J. S. Han, *The Neurochemical Basis of Pain Relief by Acupuncture*, Chinese Medical Science and Technology Press, Beijing, China, 1987.

[39] J. S. Han, "Acupuncture and endorphins," *Neuroscience Letters*, vol. 361, no. 1–3, pp. 258–261, 2004.

[40] S. Arner and B. A. Meyerson, "Lack of analgesic effect of opioids on neuropathic and idiopathic forms of pain," *Pain*, vol. 33, no. 1, pp. 11–23, 1988.

[41] E. Eisenberg, E. D. McNicol, and D. B. Carr, "Efficacy and safety of opioid agonists in the treatment of neuropathic pain of nonmalignant origin: systematic review and meta-analysis of randomized controlled trials," *Journal of the American Medical Association*, vol. 293, no. 24, pp. 3043–3052, 2005.

[42] H. S. Smith, "Opioids and neuropathic pain," *Pain Physician*, vol. 15, no. 3, supplement, pp. ES93–ES110, 2012.

[43] J. A. Stamford, "Descending control of pain," *British Journal of Anaesthesia*, vol. 75, no. 2, pp. 217–227, 1995.

[44] J.-S. Han, "Acupuncture: neuropeptide release produced by electrical stimulation of different frequencies," *Trends in Neurosciences*, vol. 26, no. 1, pp. 17–22, 2003.

[45] D. J. Mayer, "Acupuncture: an evidence-based review of the clinical literature," *Annual Review of Medicine*, vol. 51, pp. 49–63, 2000.

[46] D. J. Mayer, D. D. Price, and A. Rafii, "Antagonism of acupuncture analgesia in man by the narcotic antagonist naloxone," *Brain Research*, vol. 121, no. 2, pp. 368–372, 1977.

[47] I. Omana, V. Olvera, P. Santos, and J. L. Calderon, "Naloxone prevents reduction of pain responses evoked by acupuncture in neuropathic rats," *Proceedings of the Western Pharmacology Society*, vol. 37, pp. 135–136, 1994.

[48] X.-H. Chen and J.-S. Han, "All three types of opioid receptors in the spinal cord are important for 2/15 Hz electroacupuncture analgesia," *European Journal of Pharmacology*, vol. 211, no. 2, pp. 203–210, 1992.

[49] L.-Z. Wu, C.-L. Cui, J.-B. Tian, D. Ji, and J.-S. Han, "Suppression of morphine withdrawal by electroacupuncture in rats: dynorphin and κ-opioid receptor implicated," *Brain Research*, vol. 851, no. 1-2, pp. 290–296, 1999.

[50] G. Lee, S. Rho, M. Shin, M. Hong, B.-I. Min, and H. Bae, "The association of cholecystokinin-A receptor expression with the responsiveness of electroacupuncture analgesic effects in rat," *Neuroscience Letters*, vol. 325, no. 1, pp. 17–20, 2002.

[51] G. S. Lee, J. B. Han, M. K. Shin, M. C. Hong, S. W. Kim, B. I. Min et al., "Enhancement of electroacupuncture-induced analgesic effect in cholecystokinin-a receptor deficient rats," *Brain Research Bulletin*, vol. 62, no. 2, pp. 161–164, 2003.

[52] W. Ma and J. C. Eisenach, "Chronic constriction injury of sciatic nerve induces the up-regulation of descending inhibitory noradrenergic innervation to the lumbar dorsal horn of mice," *Brain Research*, vol. 970, no. 1-2, pp. 110–118, 2003.

[53] D. Bowsher, *Mechanisms of Acupuncture. Western Acupuncture: A Western Scientific Approach Edinburgh, UK*, Churchill Livingstone, 1998.

[54] M. J. Millan, "Descending control of pain," *Progress in Neurobiology*, vol. 66, no. 6, pp. 355–474, 2002.

[55] A. H. Hord, D. D. Denson, B. Stowe, and R. M. Haygood, "α-1 and α-2 adrenergic antagonists relieve thermal hyperalgesia in experimental mononeuropathy from chronic constriction injury," *Anesthesia and Analgesia*, vol. 92, no. 6, pp. 1558–1562, 2001.

[56] H. Baba, K. Shimoji, and M. Yoshimura, "Norepinephrine facilitates inhibitory transmission in substantia gelatinosa of adult rat spinal cord (Part 1): effects of axon terminals of GABAergic and glycinergic neurons," *Anesthesiology*, vol. 92, no. 2, pp. 473–484, 2000.

[57] J. C. Eisenach, "Muscarinic-mediated analgesia," *Life Sciences*, vol. 64, no. 6-7, pp. 549–554, 1999.

[58] J. C. Eisenach, S. DuPen, M. Dubois, R. Miguel, and D. Allin, "Epidural clonidine analgesia for intractable cancer pain," *Pain*, vol. 61, no. 3, pp. 391–399, 1995.

[59] S. K. Kim, B.-I. Min, J. H. Kim et al., "Effects of α_1- and α_2-adrenoreceptor antagonists on cold allodynia in a rat tail model of neuropathic pain," *Brain Research*, vol. 1039, no. 1-2, pp. 207–210, 2005.

[60] J.-X. Hao, W. Yu, X.-J. Xu, and Z. Wiesenfeld-Hallin, "Effects of intrathecal vs. systemic clonidine in treating chronic allodynia-like response in spinally injured rats," *Brain Research*, vol. 736, no. 1-2, pp. 28–34, 1996.

[61] L.-Y. Jiang, S.-R. Li, F.-Y. Zhao, D. Spanswick, and M.-T. Lin, "Norepinephrine can act via α_2-adrenoceptors to reduce the hyper-excitability of spinal dorsal horn neurons following chronic nerve injury," *Journal of the Formosan Medical Association*, vol. 109, no. 6, pp. 438–445, 2010.

[62] T. J. Martin and J. C. Eisenach, "Pharmacology of opioid and nonopioid analgesics in chronic pain states," *Journal of Pharmacology and Experimental Therapeutics*, vol. 299, no. 3, pp. 811–817, 2001.

[63] M. Namaka, C. Leong, A. Grossberndt et al., "A treatment algorithm for neuropathic pain: an update," *Consultant Pharmacist*, vol. 24, no. 12, pp. 885–902, 2009.

[64] R. M. Danzebrink and G. F. Gebhart, "Antinociceptive effects of intrathecal adrenoceptor agonists in a rat model of visceral nociception," *Journal of Pharmacology and Experimental Therapeutics*, vol. 253, no. 2, pp. 698–705, 1990.

[65] J. F. Miller and H. K. Proudfit, "Antagonism of stimulation-produced antinociception from ventrolateral pontine sites by intrathecal administration of α-adrenergic antagonists and naloxone," *Brain Research*, vol. 530, no. 1, pp. 20–34, 1990.

[66] P. D. Drummond, S. Skipworth, and P. M. Finch, "α_1-Adrenoceptors in normal and hyperalgesic human skin," *Clinical Science*, vol. 91, no. 1, pp. 73–77, 1996.

[67] A. K. Ouseph and J. D. Levine, "α_1-Adrenoceptor-mediated sympathetically dependent mechanical hyperalgesia in the rat," *European Journal of Pharmacology*, vol. 273, no. 1-2, pp. 107–112, 1995.

[68] T. Akasu, J. P. Gallagher, and T. Nakamura, "Noradrenaline hyperpolatization and depolarization in cat vesical parasympathetic neurones," *Journal of Physiology*, vol. 361, pp. 165–184, 1985.

[69] D. A. Brown and M. P. Caulfield, "Hyperpolarizing "alpha 2"-adrenoceptors in rat sympathetic ganglia," *British Journal of Pharmacology*, vol. 65, no. 3, pp. 435–445, 1979.

[70] C. Schmauss, D. L. Hammond, J. W. Ochi, and T. L. Yaksh, "Pharmacological antagonism of the antinociceptive effects of serotonin in the rat spinal cord," *European Journal of Pharmacology*, vol. 90, no. 4, pp. 349–357, 1983.

[71] T. L. Yaksh and P. R. Wilson, "Spinal serotonin terminal system mediates antinociception," *Journal of Pharmacology and Experimental Therapeutics*, vol. 208, no. 3, pp. 446–453, 1979.

[72] L. He, M. Wang, M. Gao, and J. Zhou, "Expression of C-fos protein in serotonergic neurons of rat brainstem following electroacupuncture," *Acupuncture and Electro-Therapeutics Research*, vol. 17, no. 4, pp. 243–248, 1992.

[73] Q. P. Ma, Y. Zhou, Y. X. Yu, and J. S. Han, "Electroacupuncture accelerated the expression of c-fos protooncogene in serotonergic neurons of nucleus raphe dorsalis," *International Journal of Neuroscience*, vol. 67, no. 1-4, pp. 111–117, 1992.

[74] R. S. S. Cheng and B. Pomeranz, "Electroacupuncture analgesia could be mediated by at least two pain-relieving mechanisms; Endorphin and non-endorphin systems," *Life Sciences*, vol. 25, no. 23, pp. 1957–1962, 1979.

[75] L. D. Aimone, S. L. Jones, and G. F. Gebhart, "Stimulation-produced descending inhibition from the periaqueductal gray and nucleus raphe magnus in the rat: mediation by spinal monoamines but not opioids," *Pain*, vol. 31, no. 1, pp. 123–136, 1987.

[76] T. S. Jensen and T. L. Yaksh, "Spinal monoamine and opiate systems partly mediate the antinociceptive effects produced by glutamate at brainstem sites," *Brain Research*, vol. 321, no. 2, pp. 287–297, 1984.

[77] M. M. Morgan, M. S. Gold, J. C. Liebeskind, and C. Stein, "Periaqueductal gray stimulation produces a spinally mediated, opioid antinociception for the inflamed hindpaw of the rat," *Brain Research*, vol. 545, no. 1-2, pp. 17–23, 1991.

[78] G. Zorman, G. Belcher, J. E. Adams, and H. L. Fields, "Lumbar intrathecal naloxone blocks analgesia produced by microstimulation of the ventromedial medulla in the rat," *Brain Research*, vol. 236, no. 1, pp. 77–84, 1982.

[79] M. Tsuchiya, H. Yamazaki, and Y. Hori, "Enkephalinergic neurons express 5-HT_3 receptors in the spinal cord dorsal horn: single cell RT-PCR analysis," *NeuroReport*, vol. 10, no. 13, pp. 2749–2753, 1999.

[80] H. K. Proudfit, "Effects of raphe magnus and raphe pallidus lesions on morphine-induced analgesia and spinal cord monoamines," *Pharmacology Biochemistry and Behavior*, vol. 13, no. 5, pp. 705–714, 1980.

[81] J. S. Han and L. Terenius, "Neurochemical basis of acupuncture analgesia," *Annual Review of Pharmacology and Toxicology*, vol. 22, pp. 193–220, 1982.

[82] L. Bardin, M. Bardin, J. Lavarenne, and A. Eschalier, "Effect of intrathecal serotonin on nociception in rats: influence of the pain test used," *Experimental Brain Research*, vol. 113, no. 1, pp. 81–87, 1997.

[83] E. J. A. Scherder and A. Bouma, "Possible role of the Nucleus Raphe Dorsalis in analgesia by peripheral stimulation: theoretical considerations," *Acupuncture and Electro-Therapeutics Research*, vol. 18, no. 3-4, pp. 195–205, 1993.

[84] T. Shimizu, "Effects of peripheral electric stimulation on the central 5-hydroxytryptamine in mice: relation to the peripheral stimulation-produced analgesia," *Folia Pharmacologica Japonica*, vol. 77, no. 4, pp. 347–360, 1981.

[85] Z.-Q. Zhao, "Neural mechanism underlying acupuncture analgesia," *Progress in Neurobiology*, vol. 85, no. 4, pp. 355–375, 2008.

[86] A. A. Alhaider, S. Z. Lei, and G. L. Wilcox, "Spinal 5-HT_3 receptor-mediated antinociception: possible release of GABA," *Journal of Neuroscience*, vol. 11, no. 7, pp. 1881–1888, 1991.

[87] T. Crisp, J. L. Stafinsky, L. J. Spanos, M. Uram, V. C. Perni, and H. B. Donepudi, "Analgesic effects of serotonin and receptor-selective serotonin agonists in the rat spinal cord," *General Pharmacology*, vol. 22, no. 2, pp. 247–251, 1991.

[88] R. Radhakrishnan, E. W. King, J. K. Dickman, C. A. Herold, N. F. Johnston, M. L. Spurgin et al., "Spinal 5-HT_2 and 5-HT_3 receptors mediate low, but not high, frequency TENS-induced antihyperalgesia in rats," *Pain*, vol. 105, no. 1-2, pp. 205–213, 2003.

[89] H. Horiuchi, T. Ogata, T. Morino, J. Takeba, and H. Yamamoto, "Serotonergic signaling inhibits hyperalgesia induced by spinal cord damage," *Brain Research*, vol. 963, no. 1-2, pp. 312–320, 2003.

[90] J. Takagi and N. Yonehara, "Serotonin receptor subtypes involved in modulation of electrical acupuncture," *Japanese Journal of Pharmacology*, vol. 78, no. 4, pp. 511–514, 1998.

[91] P. K. Eide and K. Hole, "Different role of 5-HT_{1A} and 5-HT_2 receptors in spinal cord in the control of nociceptive responsiveness," *Neuropharmacology*, vol. 30, no. 7, pp. 727–731, 1991.

[92] T. Oyama, M. Ueda, Y. Kuraishi, A. Akaike, and M. Satoh, "Dual effect of serotonin on formalin-induced nociception in the rat spinal cord," *Neuroscience Research*, vol. 25, no. 2, pp. 129–135, 1996.

[93] W. Xu, X. C. Qiu, and J. S. Han, "Serotonin receptor subtypes in spinal antinociception in the rat," *Journal of Pharmacology and Experimental Therapeutics*, vol. 269, no. 3, pp. 1182–1189, 1994.

[94] S. R. Glaum, H. K. Proudfit, and E. G. Anderson, "5-HT_3 receptors modulate spinal nociceptive reflexes," *Brain Research*, vol. 510, no. 1, pp. 12–16, 1990.

[95] D. Paul, D. Yao, P. Zhu, L. D. Minor, and M. M. Garcia, "5-Hydroxytryptamine3 (5-HT_3) receptors mediate spinal 5-HT antinociception: an antisense approach," *Journal of Pharmacology and Experimental Therapeutics*, vol. 298, no. 2, pp. 674–678, 2001.

[96] Y. B. Peng, Q. Lin, and W. D. Willis, "The role of 5-HT_3 receptors in periaqueductal gray-induced inhibition of nociceptive dorsal horn neurons in rats," *Journal of Pharmacology and Experimental Therapeutics*, vol. 276, no. 1, pp. 116–124, 1996.

[97] Q. Lin, Y. B. Peng, and W. D. Willis, "Antinociception and inhibition from the periaqueductal gray are mediated in part by spinal 5-hydroxytryptamine(1A) receptors," *The Journal of Pharmacology and Experimental Therapeutics*, vol. 276, no. 3, pp. 958–967, 1996.

[98] L. Bardin, J. Schmidt, A. Alloui, and A. Eschalier, "Effect of intrathecal administration of serotonin in chronic pain models in rats," *European Journal of Pharmacology*, vol. 409, no. 1, pp. 37–43, 2000.

[99] S. M. Garraway and S. Hochman, "Pharmacological characterization of serotonin receptor subtypes modulating primary afferent input to deep dorsal horn neurons in the neonatal rat," *British Journal of Pharmacology*, vol. 132, no. 8, pp. 1789–1798, 2001.

[100] S. M. Garraway and S. Hochman, "Serotonin increases the incidence of primary afferent-evoked long-term depression in rat deep dorsal horn neurons," *Journal of Neurophysiology*, vol. 85, no. 5, pp. 1864–1872, 2001.

[101] M. J. Millan, S. Girardon, and K. Bervoets, "8-OH-DPAT-induced spontaneous tail-flicks in the rat are facilitated by the selective serotonin (5-HT)$_{2C}$ agonist, RO 60-0175: blockade of its actions by the novel 5-HT_{2C} receptor antagonist SE 206,553," *Neuropharmacology*, vol. 36, no. 4-5, pp. 743–745, 1997.

[102] R. E. Coggeshall and S. M. Carlton, "Receptor localization in the mammalian dorsal horn and primary afferent neurons," *Brain Research Reviews*, vol. 24, no. 1, pp. 28–66, 1997.

[103] C.-Y. Chiang and M. Zhuo, "Evidence for the involvement of a descending cholinergic pathway in systemic morphine analgesia," *Brain Research*, vol. 478, no. 2, pp. 293–300, 1989.

[104] B. E. Jones, M. Pare, and A. Beaudet, "Retrograde labeling of neurons in the brain stem following injections of [3H]choline into the rat spinal cord," *Neuroscience*, vol. 18, no. 4, pp. 901–916, 1986.

[105] J.-H. Hwang, K.-S. Hwang, J.-K. Leem, P.-H. Park, S.-M. Han, and D.-M. Lee, "The antiallodynic effects of intrathecal cholinesterase inhibitors in a rat model of neuropathic pain," *Anesthesiology*, vol. 90, no. 2, pp. 492–499, 1999.

[106] E. T. Iwamoto and L. Marion, "Characterization of the antinociception produced by intrathecally administered muscarinic agonists in rats," *Journal of Pharmacology and Experimental Therapeutics*, vol. 266, no. 1, pp. 329–338, 1993.

[107] M. Naguib and T. L. Yaksh, "Antinociceptive effects of spinal cholinesterase inhibition and isobolographic analysis of the interaction with μ and α_2 receptor systems," *Anesthesiology*, vol. 80, no. 6, pp. 1338–1348, 1994.

[108] Y. Wang, S. Wang, and J. Wu, "Effects of atropine on the changes of pain threshold and contents of leucine-enkephalin and catecholamines of the brain in rats induced by EA," *Journal of Traditional Chinese Medicine*, vol. 12, no. 2, pp. 137–141, 1992.

[109] M. Zhuo and G. F. Gebhart, "Tonic cholinergic inhibition of spinal mechanical transmission," *Pain*, vol. 46, no. 2, pp. 211–222, 1991.

[110] G. R. Lauretti and I. C. P. R. Lima, "The effects of intrathecal neostigmine on somatic and visceral pain: improvement by association with a peripheral anticholinergic," *Anesthesia and Analgesia*, vol. 82, no. 3, pp. 617–620, 1996.

[111] G. R. Lauretti, M. P. Reis, W. A. Prado, and J. G. Klamt, "Dose-response study of intrathecal morphine versus intrathecal neostigmine, their combination, or placebo for postoperative analgesia in patients undergoing anterior and posterior vaginoplasty," *Anesthesia and Analgesia*, vol. 82, no. 6, pp. 1182–1187, 1996.

[112] C. Ghelardini, N. Galeotti, and A. Bartolini, "Loss of muscarinic antinociception by antisense inhibition of M1 receptors," *British Journal of Pharmacology*, vol. 129, no. 8, pp. 1633–1640, 2000.

[113] K. Honda, K. Koga, T. Moriyama, M. Koguchi, Y. Takano, and H.-O. Kamiya, "Intrathecal α_2 adrenoceptor agonist clonidine inhibits mechanical transmission in mouse spinal cord via activation of muscarinic M1 receptors," *Neuroscience Letters*, vol. 322, no. 3, pp. 161–164, 2002.

[114] K. Koga, K. Honda, S. Ando, I. Harasawa, H.-O. Kamiya, and Y. Takano, "Intrathecal clonidine inhibits mechanical allodynia via activation of the spinal muscarinic M1 receptor in streptozotocin-induced diabetic mice," *European Journal of Pharmacology*, vol. 505, no. 1–3, pp. 75–82, 2004.

[115] M. F. Belin, M. Aguera, and M. Tappaz, "GABA-accumulating neurons in the nucleus raphe dorsalis and periaqueductal gray in the rat: a biochemical and radioautographic study," *Brain Research*, vol. 170, no. 2, pp. 279–297, 1979.

[116] D. B. Reichling and A. I. Basbaum, "Contribution of brainstem GABAergic circuitry to descending antinociceptive controls: II. Electron microscopic immunocytochemical evidence of GABAergic control over the projection from the periaqueductal gray to the nucleus raphe magnus in the rat," *Journal of Comparative Neurology*, vol. 302, no. 2, pp. 378–393, 1990.

[117] D. B. Reichling and A. I. Basbaum, "Contribution of brainstem GABAergic circuitry to descending antinociceptive controls: I. GABA-immunoreactive projection neurons in the periaqueductal gray and nucleus raphe magnus," *Journal of Comparative Neurology*, vol. 302, no. 2, pp. 370–377, 1990.

[118] J. Sandkuhler, E. Willmann, and Q.-G. Fu, "Blockade of GABA(A) receptors in the midbrain periaqueductal grey abolishes nociceptive spinal dorsal horn neuronal activity," *European Journal of Pharmacology*, vol. 160, no. 1, pp. 163–166, 1989.

[119] Q. Lin, Y. B. Peng, and W. D. Willis, "Role of GABA receptor subtypes in inhibition of primate spinothalamic tract neurons: difference between spinal and periaqueductal gray inhibition," *Journal of Neurophysiology*, vol. 75, no. 1, pp. 109–123, 1996.

[120] M. Malcangio and N. G. Bowery, "GABA and its receptors in the spinal cord," *Trends in Pharmacological Sciences*, vol. 17, no. 12, pp. 457–462, 1996.

[121] J. R. T. Silva, M. L. Silva, and W. A. Prado, "Analgesia induced by 2- or 100-Hz electroacupuncture in the rat tail-flick test depends on the activation of different descending pain inhibitory mechanisms," *Journal of Pain*, vol. 12, no. 1, pp. 51–60, 2011.

[122] G. W. Price, G. P. Wilkin, M. J. Turnbull, and N. G. Bowery, "Are baclofen-sensitive GABA(B) receptors present on primary afferent terminals of the spinal cord?" *Nature*, vol. 307, no. 5946, pp. 71–74, 1984.

[123] M. J. Millan, "The induction of pain: an integrative review," *Progress in Neurobiology*, vol. 57, no. 1, pp. 1–164, 1999.

[124] J. Sawynok, "GABAergic mechanisms of analgesia: an update," *Pharmacology Biochemistry and Behavior*, vol. 26, no. 2, pp. 463–474, 1987.

[125] J. S. Han, J. Tang, and M. F. Ren, "Central neurotransmitters and acupuncture analgesia," *American Journal of Chinese Medicine*, vol. 8, no. 4, pp. 331–348, 1980.

[126] K. Fusumada, T. Yokoyama, T. Miki et al., "C-Fos expression in the periaqueductal gray is induced by electroacupuncture in the rat, with possible reference to GABAergic neurons," *Okajimas Folia Anatomica Japonica*, vol. 84, no. 1, pp. 1–10, 2007.

[127] L.-W. Fu and J. C. Longhurst, "Electroacupuncture modulates vlPAG release of GABA through presynaptic cannabinoid CB1 receptors," *Journal of Applied Physiology*, vol. 106, no. 6, pp. 1800–1809, 2009.

[128] S. C. Tjen-A-Looi, P. Li, and J. C. Longhurst, "Processing cardiovascular information in the vlPAG during electroacupuncture in rats: roles of endocannabinoids and GABA," *Journal of Applied Physiology*, vol. 106, no. 6, pp. 1793–1799, 2009.

[129] L. Zhu, C. Li, B. Yang, C. Ji, and W. Li, "The effect of neonatal capsaicin on acupuncture analgesia–to evaluate the role of C fibers in acupuncture analgesia," *Acupuncture Research*, vol. 15, no. 4, pp. 285–291, 1990.

[130] L. X. Zhu, C. Y. Li, C. F. Ji, and Q. Yu, "Involvement of GABA in acupuncture analgesia," *Acupuncture research*, vol. 11, no. 2, pp. 126–131, 1986.

[131] M. J. Millan, "The role of descending noradrenergic and serotoninergic pathways in the modulation of nociception: focus on receptor multiplicity," in *The Pharmacology of Pain, Handbook of Experimental Pharmacology*, A. Dickenson and J. M. Besson, Eds., vol. 130, pp. 385–446, Springer, Berlin, Germany, 1997.

[132] Z. Bing, F. Cesselin, S. Bourgoin, A. M. Clot, M. Hamon, and D. Le Bars, "Acupuncture-like stimulation induces a heterosegmental release of Met-enkephalin-like material in the rat spinal cord," *Pain*, vol. 47, no. 1, pp. 71–77, 1991.

[133] J. A. DeLeo and R. P. Yezierski, "The role of neuroinflammation and neuroimmune activation in persistent pain," *Pain*, vol. 90, no. 1-2, pp. 1–6, 2001.

[134] V. Raghavendra, F. Tanga, and J. A. Deleo, "Inhibition of microglial activation attenuates the development but not existing hypersensitivity in a rat model of neuropathy," *Journal of Pharmacology and Experimental Therapeutics*, vol. 306, no. 2, pp. 624–630, 2003.

[135] J. Wang, H. Zhao, Q.-L. Mao-Ying, X.-D. Cao, Y.-Q. Wang, and G.-C. Wu, "Electroacupuncture downregulates TLR2/4 and pro-inflammatory cytokine expression after surgical trauma stress without adrenal glands involvement," *Brain Research Bulletin*, vol. 80, no. 1-2, pp. 89–94, 2009.

[136] Y. Shir and Z. Seltzer, "A-fibers mediate mechanical hyperesthesia and allodynia and C-fibers mediate thermal hyperalgesia in a new model of causalgiform pain disorders in rats," *Neuroscience Letters*, vol. 115, no. 1, pp. 62–67, 1990.

[137] P. Penza, M. Bricchi, A. Scola, A. Campanella, and G. Lauria, "Electroacupuncture is not effective in chronic painful neuropathies," *Pain Medicine*, vol. 12, no. 12, pp. 1819–1823, 2011.

[138] Y. Tong, H. Guo, and B. Han, "Fifteen-day acupuncture treatment relieves diabetic peripheral neuropathy," *JAMS Journal of Acupuncture and Meridian Studies*, vol. 3, no. 2, pp. 95–103, 2010.

Hindawi Publishing Corporation
Evidence-Based Complementary and Alternative Medicine
Volume 2013, Article ID 924541, 15 pages
http://dx.doi.org/10.1155/2013/924541

Research Article

Electroacupuncture Could Regulate the NF-κB Signaling Pathway to Ameliorate the Inflammatory Injury in Focal Cerebral Ischemia/Reperfusion Model Rats

Wen-yi Qin,[1,2] Yong Luo,[1,2] Ling Chen,[1,2] Tao Tao,[3] Yang Li,[1,2] Yan-li Cai,[1,2] and Ya-hui Li[2,4]

[1] *Department of Neurology, The First Affiliated Hospital of Chongqing Medical University, Chongqing 400016, China*
[2] *Chongqing Key Laboratory of Neurology, 1 Youyi Road, Yuzhong District, Chongqing 400016, China*
[3] *Department of Neurology, Affiliated Hospital of Luzhou Medical College, Luzhou, Sichuan Province 64600, China*
[4] *Department of Oncology, The First Affiliated Hospital of Chongqing Medical University, Chongqing 400016, China*

Correspondence should be addressed to Yong Luo; luoyong19871987@163.com

Received 23 January 2013; Revised 10 June 2013; Accepted 18 June 2013

Academic Editor: Lijun Bai

The activated nuclear factor-KappaB signaling pathway plays a critical role in inducing inflammatory injury. It has been reported that electroacupuncture could be an effective anti-inflammatory treatment. We aimed to explore the complex mechanism by which EA inhibits the activation of the NF-κB signal pathway and ameliorate inflammatory injury in the short term; the effects of NEMO Binding Domain peptide for this purpose were compared. Focal cerebral I/R was induced by middle cerebral artery occlusion for 2 hrs. Total 380 male Sprague-Dawley rats are in the study. The neurobehavioral scores, infarction volumes, and the levels of IL-1β and IL-13 were detected. NF-κB p65, IκBα, IKKα, and IKKβ were analyzed and the ability of NF-κB binding DNA was investigated. The EA treatment and the NBD peptide treatment both reduced infarct size, improved neurological scores, and regulated the levels of IL-1β and IL-13. The treatment reduced the expression of IKKα and IKKβ and altered the expression of NF-κB p65 and IκBα in the cytoplasm and nucleus; the activity of NF-κB was effectively reduced. We conclude that EA treatment might interfere with the process of NF-κB nuclear translocation. And it also could suppress the activity of NF-κB signaling pathway to ameliorate the inflammatory injury after focal cerebral ischemia/reperfusion.

1. Introduction

The pathological mechanism of focal cerebral ischemia/reperfusion is very complex and involves a myriad of distinct molecular signaling and cytokines pathways [1]. As an important and crucial pathological process following focal cerebral ischemia/reperfusion [2, 3], the excessive activation of inflammation could induce the more serious damage, even the fatal injury than ischemic injury itself [4]. Inflammation is a pathological process that occurs via an amplification cascade, the NF-κB signaling pathway [5], and the complex cytokine network is critical for the occurrence of inflammatory responses [6, 7]. Furthermore, more sophisticated approaches are required for the treatment of focal cerebral ischemia/reperfusion because of the narrow therapeutic time window and complex pathological features of this disease [8]. In Asia, especially in China, electroacupuncture (EA) is a general method for the treatment of cerebrovascular diseases. Many reports of basic research and clinical studies have discussed the efficacy of EA in regulating inflammatory injury [9–12]. However, the exact mechanism and functional targets of EA treatment need to be elucidated. Significantly, the mechanism by which EA suppresses the activity of NF-κB signaling pathway at an early stage of cerebral ischemia/reperfusion needs to be discussed.

The NF-κB family of transcription factors consists of five members, p50, p52, p65 (Rel A), c-Rel, and Rel B. NF-κB prototype is a heterodimer composed of the RelA (p65) and NF-κB1 (p50) subunits. This variant is the most potent gene transactivator among the NF-κB family and is the major NF-κB protein found in the nucleus [13, 14]. The inhibitory protein IκBα, which masks the nuclear localization signals

(NLS) of NF-κB p65 protein and keeps them sequestered in an inactive state in the cytoplasm, leads to constant shuttling of NF-κB/IκBα complexes between the nucleus and the cytoplasm [15, 16]. Degradation of IκBs (especially IκBα) is a rapidly induced signaling event that is initiated upon specific phosphorylation of the molecules by activated IKK [16, 17]. The IKK complex mainly contains IKKα, IKKβ, and a regulatory subunit NEMO (NF-κB essential modulator/IKKγ). IKKγ is not functional in the absence of its interactions with IKKα and IKKβ [18]. Thus, NF-κB p65/IκBα, IKKα, and IKKβ are considered to be some of the most important factors involved in activation of the NF-κB signaling pathway during the early stages of focal cerebral I/R. Consequently, we will observe the change of those important factors in order to explore the mechanism of EA treatment for the inflammatory injury after focal cerebral I/R.

The NF-κB specific inhibitor (wild-type) NBD peptide that disrupts the interaction of NEMO (IKKγ) with the IKKβ has some advantages including the following: (1) does not affect basal NF-κB activity, (2) has well-defined molecular sites of action, (3) is specific for the classical NF-κB activation pathway and does not affect the NF-κB alternative pathway, and (4) does not target the active domain of the kinase and is therefore unlikely to affect other essential kinases [19]. The Pharmacology characteristic of NBD peptide prompts a clear understanding about the mechanism of NBD peptide to inhibit excessive NF-κB activation [20]. On the contrary, the mechanism by which EA inhibits the NF-κB signaling pathway activation is not clear. Therefore, we used NBD peptide as a positive intervention method control for IKKs function research in order to investigate the EA mechanism for inhibition of excessive activation of NF-κB after focal cerebral ischemia/reperfusion. Furthermore, the effects of EA and NBD peptide treatment in this process were compared in order to further elucidate the underlying mechanism and targets of EA treatment.

According to the traditional theory of Traditional Chinese Medicine and the basic acupuncture research principle, the "Baihui" (GV 20) and "Siguan" acupoints were chose in this study. The "Siguan" acupoint is composed of the two "Hegu" (LI 4) and two "Taichong" (LR 3) acupoints. Our aim was to define the effective targets and mechanism of EA treatment that influenced the NF-κB signaling pathway and its function in alleviating inflammatory injury after focal cerebral ischemia/reperfusion during the early stages.

2. Materials and Methods

2.1. Animals. The experimental protocol used in our study was approved by the Ethics Committee for Animal Experimentation of the First Affiliated Hospital of Chongqing Medical University and all procedures were conducted in accordance with the National Institutes of Health Guidelines for Animal Research (Guide for the Care and Use of Laboratory Animals). Male SD rats (280–300 g) were provided by the Experimental Animal Center of the Chongqing Medical University and housed under controlled conditions with a 12-hour light/dark cycle, a temperature at 22 ± 2°C, and humidity at 60% to 70% for at least one week before operation and treatment. The animals were allowed free access to standard rodent diet and tap water. Total 380 rats were randomly divided to four groups: a sham group (n = 95), an I/R group (MCAO for 2 h, n = 95), an EA group (n = 95), and the NBD group (n = 95). These groups were assessed from 6 h to 48 h after reperfusion.

2.2. Induction of Focal Cerebral Ischemia/Reperfusion. Transient focal cerebral ischemia was induced by MCAO in rats as previously described [21, 22]. Briefly, SD rats were fasted for 12 h but were allowed free access to water before surgery. Anesthetization was induced with 3.5% chloral hydrate (1 mL/100 g) by intraperitoneal injection. The right common carotid artery and the right external carotid artery were exposed through a ventral midline neck incision and were ligated proximally and temporarily. A 2.0 monofilament nylon suture (Ethicon Nylon Suture; Ethicon Inc., Osaka, Japan) with its tip rounded by heating in a flame was inserted through an arteriectomy in the common carotid artery just below the carotid bifurcation and then advanced into the internal carotid artery approximately 18 mm to 20 mm distal to the carotid bifurcation until a mild resistance indicated occlusion of the origin of the anterior cerebral artery and the middle cerebral artery. Reperfusion was accomplished by withdrawing the suture after 2 h of ischemia. The incision was sutured and sterilized. The animals were maintained on the 37°C thermostatic table. The sham surgery was conducted in the ischemia/reperfusion (I/R) surgery groups by insertion of the nylon monofilament suture to 10 mm into the internal carotid artery; do not insert into the middle cerebral artery.

Body temperature was monitored in all animals. The rectal temperature was maintained at 38°C ± 0.5°C throughout all portions of the experiment by means of a rectal thermistor probe and a thermostatically regulated heating lamp placed above the body of the animal. Intrastriatal temperature was monitored and was adjusted by manipulating the height of a small high-intensity lamp placed above the head. Prior to the ischemic insult, intrastriatal temperature was held at 36.5°C ± 0.5°C in all groups during ischemia [23, 24].

2.3. Electroacupuncture Treatment. In the EA groups, the total SD rats (n = 95) were anesthetized with 3.5% chloral hydrate (1 mL/100 g) by intraperitoneal injection. According to the Experimental Animals Meridians Mapping, the "Baihui" (GV 20)/"Siguan" acupoints were selected, which were located at the intersection of the sagittal midline and the line linking the ears, the second metacarpal midpoint of radial side, and the second toe tibial collateral in the rear of phalanx. These acupoints were stimulated at an intensity of 1 mA and frequency of 2/20 Hz for 30 min using the G6805-2 EA Instrument (Model no. 227033; Beijing Xinsheng Ltd., China). The SD rats were maintained on the 37°C thermostatic table. The EA treatment was given at once each day (from 6 h to 48 h after reperfusion). After ischemia for 2 h, began the first EA treatment when the nylon monofilament was withdrawn. From 6 h to 48 h, the EA treatment is twice, 3 times, 4 times, and 5 times orderly.

2.4. Drug Intervention Methods. NBD peptide (ENZO Life Sciences Inc., no. BML-P607-0500, soluble in 50 μL DMSO, final concentration 10 μg/μL) was first time injected intracerebroventricularly 2 h before surgery as previously described [25]. Briefly, the total 72 rats were anesthetized and attached to a stereotaxic instrument (Stoelting, USA). According to stereotactic mapping combined with rat size, we determined the right lateral ventricle position and drilled a cranial window (cross-stitch centered, right shift 1.3 mm, backward 1.5 mm, downward 3.8 mm) for injection of 5 μL NBD peptide once each day, until 48 h after reperfusion. The NBD peptide injection times from 6 h to 48 h are twice, 3 times, 4 times, and 5 times.

2.5. Neurobehavioral Evaluation. Neurobehavioral evaluation was carried out in the I/R group, EA groups, and NBD peptide group. After focal cerebral ischemia/reperfusion at different time points, the neurologic deficit scores of model SD rats were assessed by an investigator who was unaware of animal grouping. A modified neurologic deficit score described by Longa et al. was used for neurologic assessment. 0: no deficit; 1: failure to extend left forepaw fully; 2: circling to the left; 3: falling to the left; 4: no spontaneous walking with a depressed level of consciousness. Animals scoring 2 to 3 were included in experiments. Neurobehavioral scores were determined according to the methods described by Garcia et al. [26] and Bederson et al. [27].

2.6. Infarct Volume Assessment. The animals ($n = 5$ for each group) were decapitated and 2 mm thick coronal sections from throughout the brain were stained with 2% 2,3,5-triphenyltetrazolium chloride (Sigma-Aldrich) to evaluate the infarct volume, as described by Wang et al. [28].

2.7. Immunohistochemistry Analysis. Immunohistochemistry was performed using the avidin-biotin-peroxidase complex method. Briefly, brains were fixed in 4% phosphate-buffered paraformaldehyde (PFA) and immersed into 20% sucrose for 3 h. A 4 mm thick coronal brain slice was cut, beginning 8 mm away from the anterior tip of the frontal lobe. Then a longitudinal cut (from top to bottom) was made approximately 2 mm from the midline through the ischemic hemisphere to remove medial parts. Paraffin-embedded tissues were sectioned and dewaxed for antigens retrieval by immersing slides in 0.01 mol/L citrate buffer, pH 6.0, followed by heating in a microwave oven (temperature 92–98°C) for 20 min. Sections were cooled to room temperature and washed with PBS for 5 min and endogenous peroxides were blocked in 3% H_2O_2 for 15 min. Sections were then incubated for 30 min with 5% normal goat blood serum to block nonspecific binding. The primary antibody, NF-κB p65 (C22B4) rabbit mAb (Cell Signaling Technology, 1 : 50), was added and sections incubated at 4°C overnight. The immunostain SP Kit was used. For negative sham group, the primary antibodies were replaced with PBS. A slide image of ischemic penumbra area from each section was scanned and acquired using an OLYMPUS PM20 automatic microscope (Olympus, Tokyo, Japan) and a TCFY-2050 (Yuancheng Inc., Beijing, China) pathology system. The visual fields in each section image (five sections in each brain) were analyzed using the Motic Med 6.0 CMIAS pathology image analysis system (Beihang Motic Inc., Beijing, China).

2.8. Double-Immunofluorescence Labeling. Brain tissue was fixed and frozen, and the 10 μm thick coronal brain slices were cut beginning 8 mm from the anterior tip of the frontal lobe. Frozen sections were air dried at 50°C for 30 min. Sections were treated with ten mol/L sodium citrate buffer (pH 6.0) and heated in a microwave oven for 20 min at 92–98°C. Tissues were permeated with 1% Triton X-100, and sections were incubated in 5% goat serum for 1 h at 37°C. Incubations with primary antibodies were carried out at 4°C overnight. The primary antibodies were NF-κB p65 (C22B4) rabbit mAb (Cell Signaling Technology, 1 : 50), IκBα (L35A5) mouse mAb (Cell Signaling Technology, 1 : 50), IKKα (M-110) (Santa Cruz, no. sc-7183, 1 : 25), and IKKβ (P-20) (Santa Cruz, no. sc-34673, 1 : 25). After washing, slides were incubated with fluorescent isothiocyanate-conjugated anti-rabbit (1 : 50), anti-mouse (1 : 50), and anti-goat (1 : 100) antibodies for 2 h at 37°C. Finally, sections of ischemic penumbra area were examined by laser-scanning confocal microscopy on an Olympus IX70 inverted microscope (Olympus, Tokyo, Japan) equipped with Fluoview FVX confocal scan head (Leica Microsystems Heidelberg GmbH, Wetzlar, Germany).

2.9. Fluorescent Quantitative PCR. Total cellular RNA was isolated with Trizol (Invitrogen, Paisley, UK). cDNA was synthesized with Superscript Reverse Transcriptase (Invitrogen). The polymerase chain reaction was performed with the iQ5 Gradient Real-Time PCR Detection System (Bio-Rad) using primers (Takarad) for NF-κB p65, IκBα, IKKα, and IKKβ (Table 1). Data were individually normalized to the mean of the relative expression of GAPDH. Quantitative PCR (Q-PCR) was performed using the Hot Start Fluorescent PCR Core Reagent Kits (SYBR Green I). Each reaction mixture consisted of first-strand cDNA template, 1.25 μL of primer-probe, and 12.5 μL of SYBR Green in a total volume of 25 μL. The following cycling conditions were used: 95°C for 10 min, followed by 40 cycles of 95°C for 5 s and 60°C for 30 s. Subsequently, each sample underwent dissociation curve analysis to examine primer-target specificity as previously described [29].

2.10. Western Blot Analysis. Rats were anesthetized with 3.5% chloral hydrate (1 mL/100 g) by intraperitoneal injection. The cortex of the ischemic area was homogenized in RIPA lysis buffer (Beyotime, no. P0013B). Total protein and cytoplasmic/nuclear proteins were extracted on ice using Nuclear and Cytoplasmic Protein Extraction Kits (Beyotime, no. P0027). Western blot analysis was performed with 45 μg protein extract separated by 10% SDS-PAGE, which were then transferred to a polyvinylidene fluoride (PVDF) membrane (Millipore Corporation). Nonspecific epitopes were blocked with 5% skim milk/Tween-20-Tris-buffered saline. The following primary antibodies which were used in double-immunofluorescence labeling analysis: appropriate horseradish peroxidase conjugated antibodies (anti-rabbit (1 : 4000), anti-mouse (1 : 4000), and anti-goat (1 : 1000))

Table 1: Primer sequences and annealing temperatures employed for Q-PCR.

Primer name	Sequence	Annealing temperature
NF-κB p65	F 5′-ATCGTGGAGCACTTGGTGACT-3′ R 5′-GCCCTGGTAGGTTACTCTGTTGA-3′	55.2°C
IκBα	F 5′-GTTTCCCCTCATCTTTCCCTCA-3′ R 5′-GGGTGCGTCTTAGTGGTATCTGT-3′	56.7°C
IKKα	F 5′-GTCAGGAGAAGTTCGGTTTGA-3′ R 5′-ATTCCAGTTTCACGCTCATGGAT-3	54.2°C
IKKβ	F 5′-GTCTTGTTGATGGTTCCTGACT-3′ R 5′-AAGACAAACGAGGGCCTCACAT-3′	56.0°C
GAPDH	F 5′-CTTAGCACCCCTGGCCAAG-3′ R 5′-GATGTTCTGGAGAGCCCCG-3′	54.0°C

secondary detection antibodies were incubated for 2 h. Bio-Rad apparatus (Bio-Rad Laboratories, Richmond, CA) and Quantity One software version 4.6.2 (Bio-Rad Laboratories) were used to scan immune blots and for analysis.

2.11. Electrophoretic Mobility Shift Assay (EMSA). Nuclear extracts were prepared as previously described. The NF-κB double-stranded oligonucleotide corresponding to the NF-κB consensus sequence (5′-AGTTGAGGGGACTTT-CCCAGGC-3′) was obtained from Santa Cruz and was end-labeled with Terminal Deoxynucleotidyl Transferase (TdT) using Biotin-11-dUTP (Pierce). Nuclear extracts (8 μg) were incubated at room temperature for 20 min with 1 μL EMSA/Gel-Shift buffer. For competition studies, samples were also incubated with either 100-fold excess of unlabeled (cold) oligonucleotide or unlabeled mutant oligonucleotide. DNA-protein complexes were resolved on a 5% nondenaturing polyacrylamide gel with 20 mA for 3 h in 0.5× Tris-Borate EDTA. After UV cross linking, samples were blocked and incubated with streptavidin-HRP conjugate (15 mL). Hybridized samples were developed and analyzed using a Hybridization Incubator (WD-9403E, Beijing).

2.12. Enzyme-Linked Immunosorbent Assay (ELISA). The levels of IL-1β and IL-13 in cytosolic brain fractions and in serum were analyzed by enzyme-linked immunosorbent assay (Bender, no. 81-BMS630/96T; Abcam, no. ab100766/96T).

3. Statistical Analysis

The software SPSS 16.0 for Windows (SPSS Inc, Chicago, IL) was used to conduct statistical analysis. All values are expressed as mean ± SD (standard deviation). Data were analyzed by a one-way ANOVA, and intergroup differences were detected by multivariate analysis, followed by LSD tests. The neurological deficit scores were expressed as median (range) and were analyzed with Kruskal-Wallis test, followed by the Mann-Whitney U test with Bonferroni correction. Values of $P < 0.05$ were considered as statistically significant.

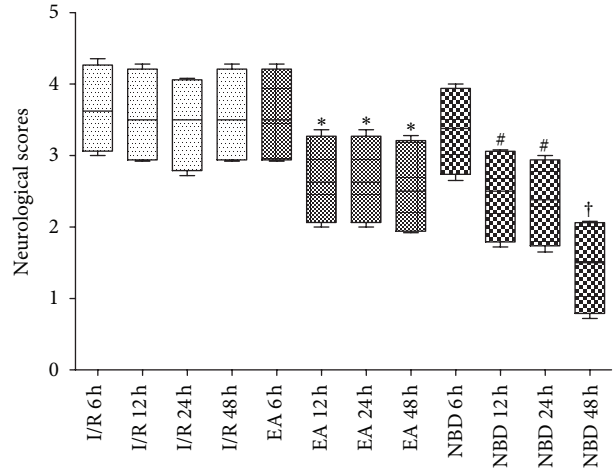

Figure 1: Neurological behavior scores from 6 h to 48 h after reperfusion in the rats with 2 h of MCAO. The neurological behavior scores in I/R group were worse from 6 h to 48 h. The treatment with EA and NBD peptide significantly improved the neurological scores, $^{*}P < 0.05$, $^{\#}P < 0.05$ versus I/R group. There was more significant improvement in NBD peptide group than in EA group, $^{\dagger}P < 0.05$.

4. Results

4.1. EA and NBD Peptide Treatment Significantly Declined the Ischemia/Reperfusion Damage after Focal Cerebral Ischemia/Reperfusion

4.1.1. Neurobehavioral Evaluation. After focal cerebral I/R, the rats showed neurological deficit behavior at every time point (Figure 1). From 6 h to 48 h after reperfusion, compared with the I/R group, the neurobehavioral scores of EA group and NBD group were improved ($P < 0.05$) (Figure 1). The effect in NBD group was more remarkable than that in EA group ($P < 0.05$) (Figure 1). These results suggested that EA treatment and NBD treatment both ameliorated the neurologic deficit symptoms caused by I/R and promoted the movement recovery degree. It showed that EA could alleviate the ischemic lesion in the super early stage of focal cerebral I/R.

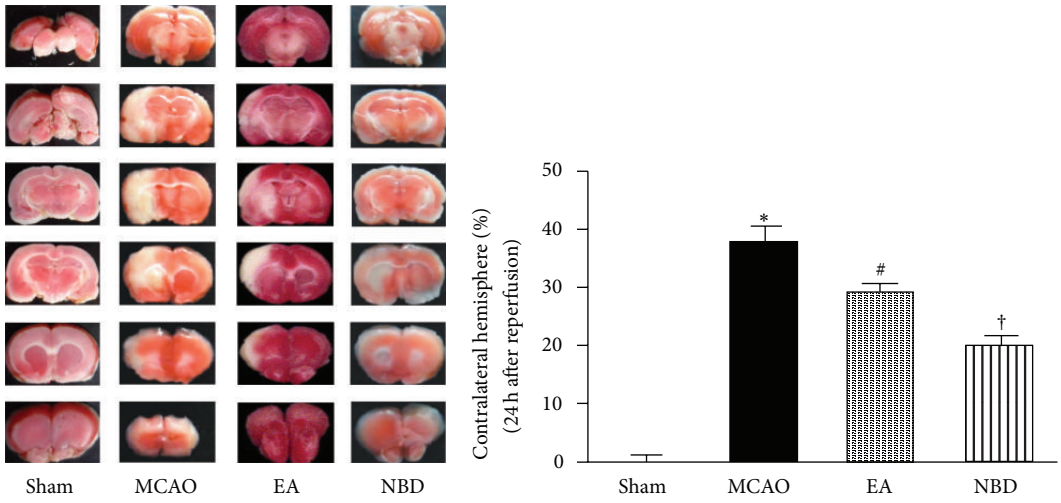

Figure 2: Infarct sizes at 24 h after reperfusion in the rats with 2 h of MCAO (5 rats in each group, total 20 rats). (a) Representative 2,3,5-triphenyltetrazolium chloride staining of the cerebral infarct in comparable sections of rat brain from 4 groups at 24 h after reperfusion. (b) Quantification of infarct volume at 24 h after reperfusion. The EA and NBD peptide treatment significantly reduced the infarct volume, $^{*}P < 0.05$, $^{\#}P < 0.05$ versus I/R group. And the effect of NBD peptide was remarkable than EA group, $^{\dagger}P < 0.05$.

4.1.2. The Infarct Volumes Value after MCAO/R. The infarct volume in EA group showed a smaller brain infarct volume compared with the I/R group ($P < 0.05$) (Figure 2). The brain infarct volume of NBD group was much more significantly reduced than that in EA group and I/R group ($P < 0.05$) (Figure 2). The data suggested EA and NBD peptide treatment could remarkably reduce the infarct size. Moreover, the effect of NBD peptide is more significant than EA treatment.

4.2. After EA and NBD Peptide Treatment, the Level of IL-1β Was Decreased and the Level of IL-13 Was Increased in Focal Cerebral Ischemia/Reperfusion Rats. After focal cerebral I/R, the levels of IL-1β increased significantly from 6 h to 48 h both in the brain (Figures 3(a) and 3(b)) and in serum (Figures 3(c) and 3(d)). However, in EA group and NBD group, IL-1β levels decreased significantly and were lower than that in I/R group ($P < 0.05$) (Figures 3(a) and 3(b)). The IL-13 levels were increased in the I/R group, especially at 48 h in brain and at 24 h in serum. In the EA group and NBD group in the brain and serum, the IL-13 levels were both increased which were significantly higher than those in I/R group at the same time points ($P < 0.05$) (Figures 3(c) and 3(d)). The IL-13 levels in the EA group peaked at 24 h in the brain and at 48 h in serum and peaked at 12 h and 24 h in NBD group (Figures 3(c) and 3(d)). These data suggested that EA and NBD peptide treatment effectively reduced IL-1β levels and increased IL-13 levels in brain and serum. Therefore, the EA and NBD peptide treatment effectively reduce the quantity of IL-1β and restrain the damage caused by inflammatory factor during the early stage. But the peak time points of NBD peptide and EA treatment are not the same.

4.3. EA and NBD Peptide Treatment Probably Inhibits NF-κB Signaling Pathway Activation through Regulating the NF-κB Nuclear Translocation. Immunohistochemical analysis of NF-κB p65 protein expression was conducted after focal cerebral I/R. In sham group, the NF-κB p65 protein was predominantly expressed in the cytoplasm (Figures 4(a) and 4(b)). However, after focal cerebral I/R, expression was observed both in the cytoplasm and nucleus of the neurons in the ischemic penumbra area, although higher expression of NF-κB p65 protein was detected in the nucleus than that in the cytoplasm ($P < 0.05$) (Figures 4(a) and 4(b)). Significant changes of NF-κB p65 protein expression were observed in the EA group and NBD group, which were predominantly detected in the cytoplasm rather than in the nucleus ($P < 0.05$) (Figures 4(a) and 4(b)). These observations demonstrated that the differential localization of the NF-κB p65 protein in the cytoplasm and nucleus was altered after EA and NBD peptide treatment, thus indicating that EA and NBD peptide may effectively inhibit the process of NF-κB nuclear translocation.

4.4. EA and NBD Peptide Treatment Regulated the NF-κB p65/IκBα Feedback Loop to Inhibit the NF-κB Nuclear Translocation. The protein expression and localization of NF-κB p65 (green) and IκBα (red) in the ischemic penumbra area were examined by double-immunofluorescence staining. As shown in Figure 5, in sham group, low levels of NF-κB p65 and IκBα protein expression were observed throughout the hemisphere. After focal cerebral I/R, NF-κB p65 protein expression was observed both in the nucleus and cytoplasm, meanwhile there was a little expression of IκBα protein in the nucleus (Figure 5). In contrast, NF-κB p65 protein expression was remarkably reduced in the nucleus in EA group and NBD group; the IκBα protein expression in the cytoplasm and nucleus was significantly increased (Figure 5). Double-immunofluorescence analysis of NF-κB p65 and IκBα protein expression demonstrated that NF-κB p65 protein was mainly localized in the cytoplasm, while IκBα

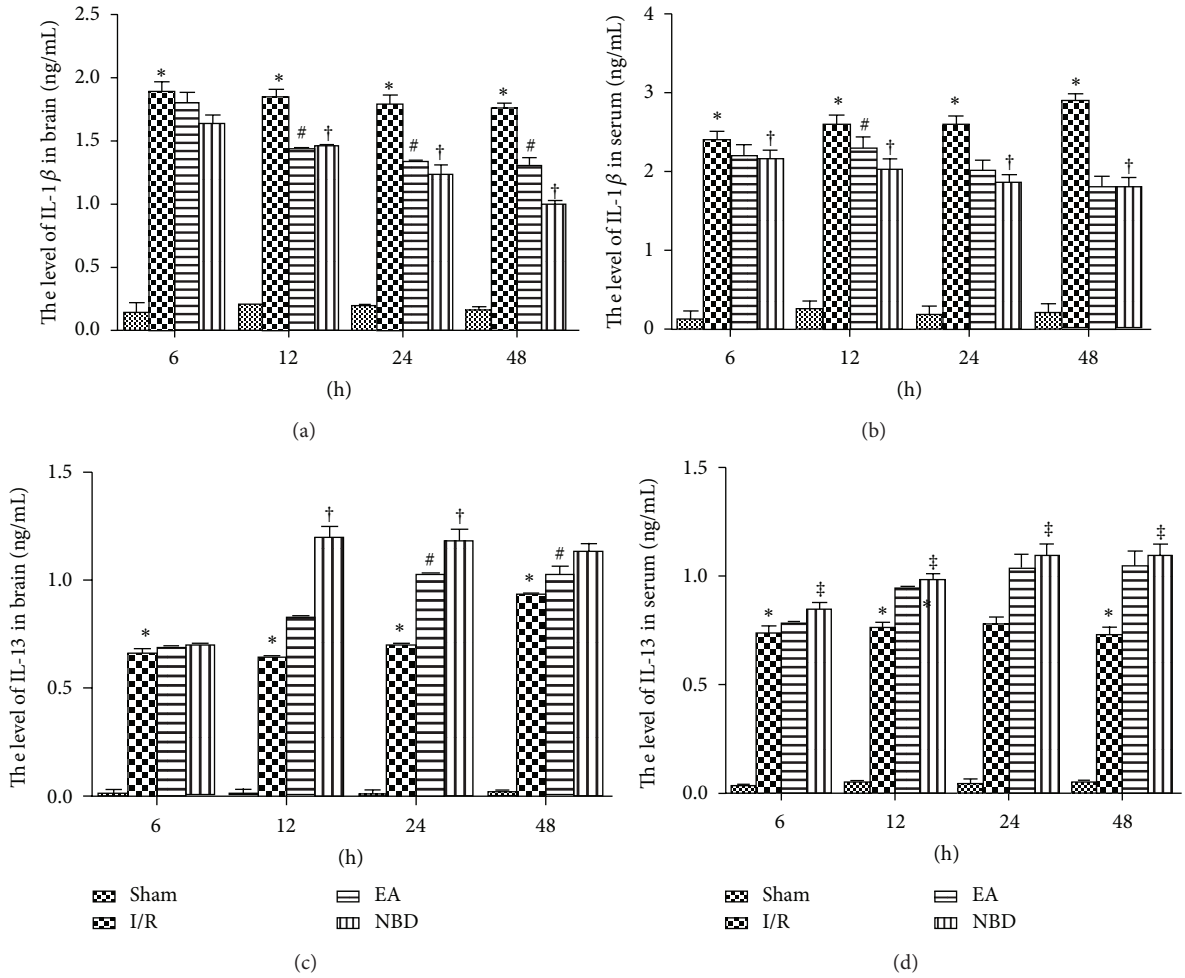

FIGURE 3: Levels of IL-1β and IL-13 in focal ischemic brain tissue and serum of rats among sham, I/R group, EA group, and NBD peptide group at different timepoints (5 rats in each group per time point, total 80 rats). (a) IL-1β levels in the brain of the I/R group increased significantly from 6 h to 48 h which were higher than those in EA group and NBD group, $^{*}P < 0.05$. IL-1β levels in the EA group and NBD peptide group decreased gradually, $^{\#}P < 0.05$, $^{\dagger}P < 0.05$. (b) In serum, IL-1β levels peaked at 48 h in the I/R group and was significantly higher than those in the EA group and NBD group, $^{*}P < 0.05$. $^{\dagger}P < 0.05$. IL-1β levels in the EA group decreased gradually even at 12 h, $^{\#}P < 0.05$. (c) In the brain, IL-13 peaked in the I/R group at 48 h, although these levels were lower than those in the EA group and NBD group, $^{*}P < 0.05$. IL-13 levels peaked in the EA group at 24 h and in the NBD group at 12 h, and 24 h were significantly higher, $^{\#}P < 0.05$, $^{\dagger}P < 0.05$ versus I/R group. (d) There were no significant changes in the serum IL-13 levels in the I/R group at any of the timepoints, and these levels were significantly lower than those in the EA group and NBD group, $^{*}P < 0.05$. The levels in NBD group were higher, $^{\ddagger}P < 0.05$ versus EA group‡.

was highly expressed in nucleus and cytoplasm after EA and NBD peptide treatment.

The fluorescent quantitation-PCR analysis showed that the expression of NF-κB p65 mRNA in I/R group was significantly increased at 24 h and 48 h which were higher than those in EA group and NBD group ($P < 0.05$) (Figure 6(a)). Expression of IκBα mRNA in the EA group and NBD group was obviously increased and was higher than that in I/R group ($P < 0.05$) (Figure 6(b)).

The expression of NF-κB p65 and IκBα proteins were analysed by Western blot among the sham group, I/R group, EA group, and NBD group. In the I/R group, the expression of NF-κB p65 protein in the cytoplasm decreased gradually, meanwhile low levels of IκBα protein were detected. Compared with the I/R group, the expression of NF-κB p65 and IκBα protein in the EA group and NBD group was increased ($P < 0.05$) (Figures 7(a), 7(c), and 7(e)). In contrast in the nucleus, the expression of NF-κB p65 protein was significantly increased in the I/R group and obviously decreased in the EA group and NBD group ($P < 0.05$) (Figures 7(b) and 7(d)). The expression of IκBα protein was obviously increased in the EA group and NBD group, which were higher than that in the I/R group ($P < 0.05$) (Figures 7(b) and 7(f)). These data showed that EA and NBD peptide treatment effectively altered the expression of NF-κB p65 and IκBα proteins in both cytoplasm and nucleus after focal cerebral I/R. They decreased NF-κB p65 protein expression in the nucleus and maintained it in the cytoplasm, while IκBα protein expression was increased in the nucleus and cytoplasm. Therefore, these data indicated

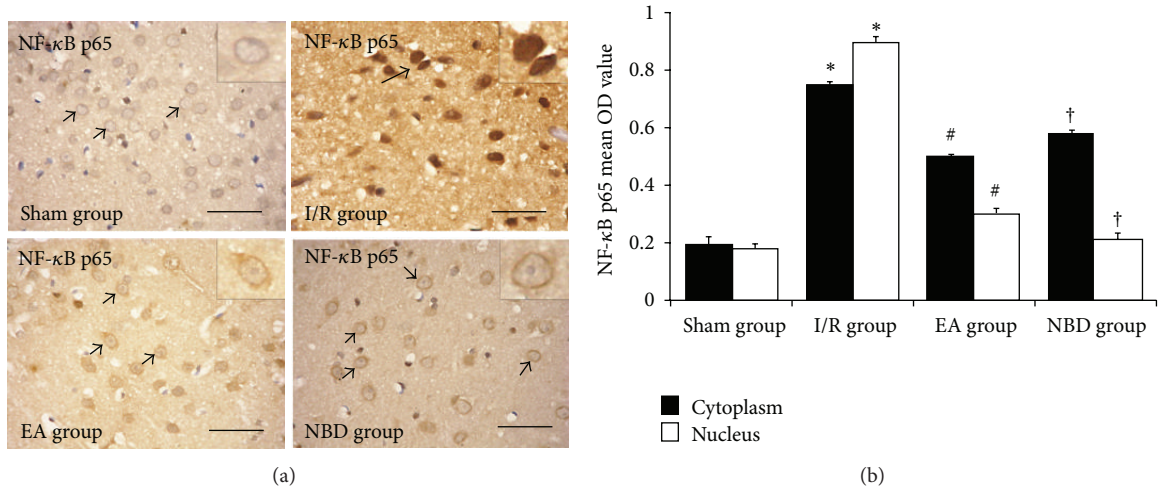

Figure 4: Immunohistochemical analysis of the nuclear translocation of NF-κB p65 in the sham, I/R group, EA group, and NBD group (5 rats in each group, total 20 rats). In the temporal neocortex of sham group, the immunoreactive staining occurred less in the cytoplasm and nucleus. In the I/R group, strong immunoreactive staining occurred in the cytoplasm and nucleus, especially in the nucleus, $^{*}P < 0.05$. In the EA group, immunoreactive staining was predominantly detected in the cytoplasm rather than in the nucleus, $^{\#}P < 0.05$. In the NBD group, immunoreactive staining was also maintained in the cytoplasm, $^{\dagger}P < 0.05$. Comparison of the mean OD value showed that NF-κB p65 was mainly expressed in the nucleus after focal ischemia/reperfusion, and expression of NF-κB p65 protein in the nucleus in the EA group and NBD group was significantly reduced, $^{\#}P < 0.05$, $^{\dagger}P < 0.05$.

that the mechanism by which EA and NBD peptide treatment regulated NF-κB nuclear translocation was related to the high expression of IκBα in the cytoplasm and nucleus.

4.5. EA and NBD Peptide Treatment Regulated the Expression of IKKα and IKKβ mRNA and Protein after Focal Cerebral Ischemia/Reperfusion. The expression of IKKα (green) and IKKβ (red) protein was examined by double-immunofluorescence staining in the sham group, I/R group, EA group, and NBD peptide group. As shown in Figure 8, little expression of IKKα and IKKβ proteins was observed in the sham group (Figure 8), and they were increased significantly after focal cerebral I/R (Figure 8) but were obviously decreased in the EA group and NBD group, especially decreased the IKKβ expression (Figure 8).

The fluorescent quantitation-PCR (Q-PCR) analysis showed that the expression of IKKα and IKKβ mRNA in the I/R group was significantly increased ($P < 0.05$) (Figures 9(a) and 9(b)). The IKKα mRNA expression in the EA group was remarkably reduced, which was lower than that in I/R group ($P < 0.05$) (Figure 9(a)). The peak expression in the NBD group was higher than that in the EA group ($P < 0.05$) (Figure 9(a)). Compared with the I/R group, the expression of IKKβ mRNA in the EA group was obviously decreased ($P < 0.05$) (Figure 9(b)). In the NBD group, IKKβ mRNA expression was negligible from 6 h to 48 h (Figure 9(b)).

The protein expression of IKKα and IKKβ was analysed by Western blot. In the I/R group, IKKα protein expression was persistently increased from 6 h to 48 h (Figures 10(a) and 10(c)). The expression of IKKα protein was decreased in the EA group, which was lower than that in the I/R group ($P < 0.05$) (Figures 10(a) and 10(c)). In the NBD group, expression was also reduced but was still much higher than that in the EA group, especially at 12 h ($P < 0.05$) (Figures 10(b) and 10(d)). Expression of IKKβ protein in the I/R group was significantly increased, especially at 24 h and 48 h ($P < 0.05$) (Figures 10(a) and 10(d)). Compared with the I/R group, expression was remarkably decreased in the EA group ($P < 0.05$) (Figures 10(a) and 10(d)). Furthermore, in the NBD group, IKKβ protein expression was persistently low from 6 h to 48 h ($P < 0.01$) (Figures 10(b) and 10(d)). These data demonstrated that EA and NBD peptide treatment could effectively reduce the high levels of IKKβ expression after focal cerebral I/R, especially at 24 h and 48 h. Compared with the NBD peptide group, EA treatment could else reduce IKKα protein expression.

4.6. EA and NBD Peptide Treatment Effectively Regulated the DNA Binding Capacity of NF-κB. Electrophoretic mobility shift assays (EMSA) were used to further investigate theactivity of NF-κB after focal cerebral I/R and the change in activity mediated by EA treatment and NBD peptide intervention. The activity of NF-κB was increased after I/R, especially at 24 h and 48 h, indicating that the DNA binding capacity of NF-κB was high in the I/R group ($P < 0.05$) (Figures 11(a) and 11(b)). In the EA group and NBD group, the activity of NF-κB was reduced significantly ($P < 0.05$), and there were no remarkable differences between those ($P > 0.05$) (Figures 11(a) and 11(b)). The results suggest that EA and NBD peptide treatment effectively reduces the activity of NF-κB.

5. Discussion

In the present study, we investigated the anti-inflammation effect and probable mechanism of EA on the NF-κB signaling pathway after focal cerebral ischemia/reperfusion. First of all,

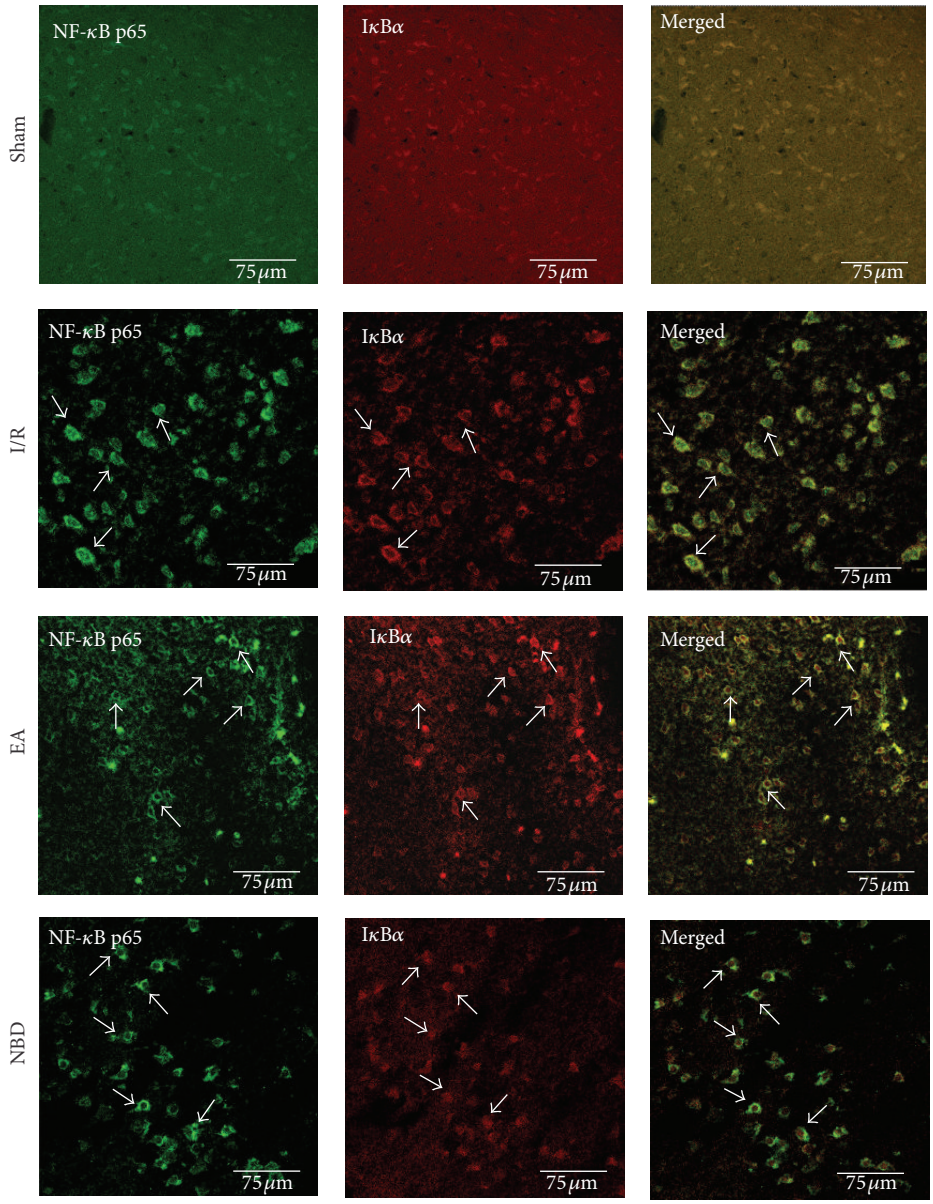

Figure 5: Double-immunofluorescent labeling the NF-κB p65 (green) and IκBα (red) in the cells in the ischemic cortex (5 rats in each group, total 20 rats). It showed that NF-κB p65 and IκBα were both poorly expressed in the sham group. In the I/R group, the NF-κB p65 protein was expressed in cytoplasm and nucleus, especially highly in the nucleus; IκBα protein was poorly expressed in cytoplasm and nucleus. In the EA group and NBD group, the NF-κB p65 protein was mainly expressed in the cytoplasm than in the nucleus, and the IκBα protein was expressed highly in the cytoplasm and nucleus.

we found that EA treatment effectively reduced the cerebral infarct volume and improved the neurobehavioral scores, it seemed able to alleviate the ischemic damage. Secondly, the EA treatment also regulated the levels of interleukin (IL-1β and IL-13) in brain and serum after focal cerebral I/R. More importantly than all of that, we observed that EA treatment reduced the expression of IKKα and IKKβ protein, perhaps decline the function of IKKα and IKKβ, and then regulated the NF-κB p65/IκBα feedback loop for the activation of NF-κB signaling pathway effectively during very early stage of focal cerebral I/R, which demonstrated that EA has obviously protective and anti-inflammatory effect during the focal cerebral I/R injury, via a mechanism related to the suppression of the activation of the NF-κB signaling pathway at a very early phase. Moreover, the effects on the IKKα and IKKβ were remarkably different between EA treatment and NBD peptide.

The inflammatory reaction is an important pathological step in the process of focal cerebral I/R, which causes rapid neuronal death and aggravates the ischemic injury and body burden [30]. Therefore, effectively restraining the occurrence and development of the inflammation is considered to be an important target and direction of the treatment for focal cerebral I/R. The cytokines that cause the inflammatory

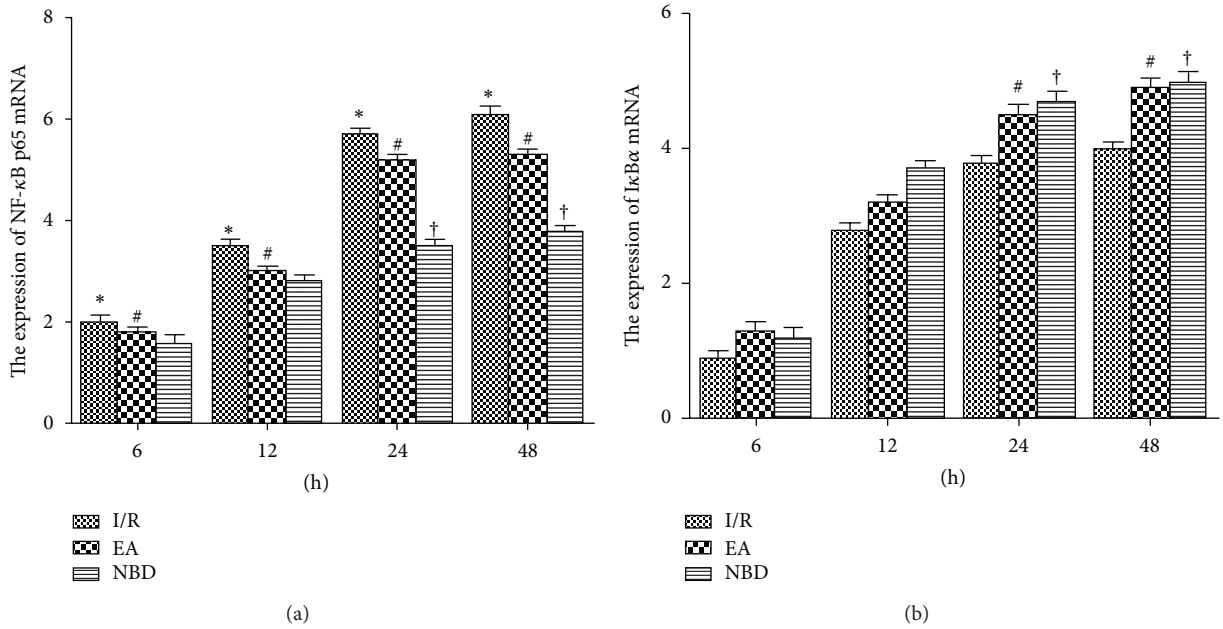

Figure 6: Fluorescent Quantitative-PCR analysis of the NF-κB p65 and IκBα mRNA expression of the sham group, I/R group, EA group, and NBD group in the ischemic brain tissue (5 rats in each group per time point, total 80 rats). (a) The expression of NF-κB p65 mRNA was significantly increased in the I/R group compared with that in the EA and NBD groups, $^{*}P < 0.05$. At 24 h and 48 h, the NF-κB p65 mRNA in the EA group was higher, $^{\#}P < 0.05$, $^{\dagger}P < 0.05$ versus NBD group. (b) The IκBα mRNA expression in EA group and NBD group was higher, $^{\#}P < 0.05$, $^{\dagger}P < 0.05$ versus I/R group.

response include TNF-α, IL-1β, cox-2, iNOS, and many other types of factors [31]. IL-1β is a nerve toxin and a major stimulus factor of the inflammatory reaction. Reducing the level of IL-1β can significantly ameliorate the ischemia infarction volume and the occurrence of inflammation [32]. On the contrary, the cytokines such as IL-10 and IL-13 exert better anti-inflammatory effect. Inflammatory reaction induced by IL-1β stimulation is significantly inhibited by IL-13 [33]. Focused on the inflammatory cytokines in the ischemic brain and serum, we observed that the level and the timing of the peak expression of IL-1β and IL-13 were regulated by EA and NBD peptide treatment. All of these data demonstrated that EA treatment could exert remarkable anti-inflammatory effect during the early stage of focal cerebral I/R which resembles the function of NBD peptide. However, the effect of NBD peptide is more remarkable on the regulation of cytokines.

In order to regulate the inflammatory injury occurred during the early stages after reperfusion, it is necessary to inhibit the activation of NF-κB signaling pathway which is induced by focal cerebral I/R. During the activation process of NF-κB signaling pathway, the interaction of p65 and IκBα on nuclear translocation is the key step [34, 35]. In the present study, we observed that NF-κB p65 expressed both in cytoplasm and nucleus, the NF-κB p65 predominantly expressed in nucleus after focal cerebral I/R. It showed that the ischemia and anoxic pathological factors in the brain stimulated the p65 mainly expressed in the nucleus and promoted the NF-κB nuclear translocation process. We observed that EA and NBD peptide treatment mainly maintained high cytosolic level of p65 and significantly reduced it in nucleus. The discovery demonstrated that EA effectively inhibited p65 nuclear translocation and maintained it in the cytoplasm, which we also found after NBD peptide treatment. According to the general understanding of the NF-κB signal pathway, nuclear NF-κB drives IκBα expression generating a negative feedback loop [36, 37]. In the present study, we found that EA treatment significantly increased IκBα expression in the cytoplasm and nucleus, especially expressed in the nucleus, and altered the NF-κB p65 and IκBα protein expression in nucleus. The results showed that EA treatment could regulate NF-κB/IκBα feedback loop in the nucleus and cytoplasm. Above all, it reveals that EA promotes the inactive heterotrimer generated in nucleus through increasing IκBα expression in the NF-κB/IκBα feedback loop and then maintains the high cytosolic level of p65. It can be speculated that inhibition of NF-κB nuclear translocation is likely to be one of the most important mechanisms by which EA inhibits NF-κB activation.

The function of IκBα is regulated by the IκB kinases (IKKs) in the NF-κB signal pathway, and NF-κB activation depends on the IKK phosphorylation process [38]. Both IKKα and IKKβ phosphorylate IκBα at Ser 32 and Ser 36, although IKKα is less efficient and consequently cannot complement IKKβ knockout cells [18, 38]. In this study, we observed that the expression of IKKα and IKKβ was significantly increased after focal cerebral I/R, which demonstrated that the massive expression of IKKα and IKKβ could be required for NF-κB activation. However, EA treatment remarkably reduced the expression of IKKα and IKKβ, especially for the IKKβ. The results of the EA group

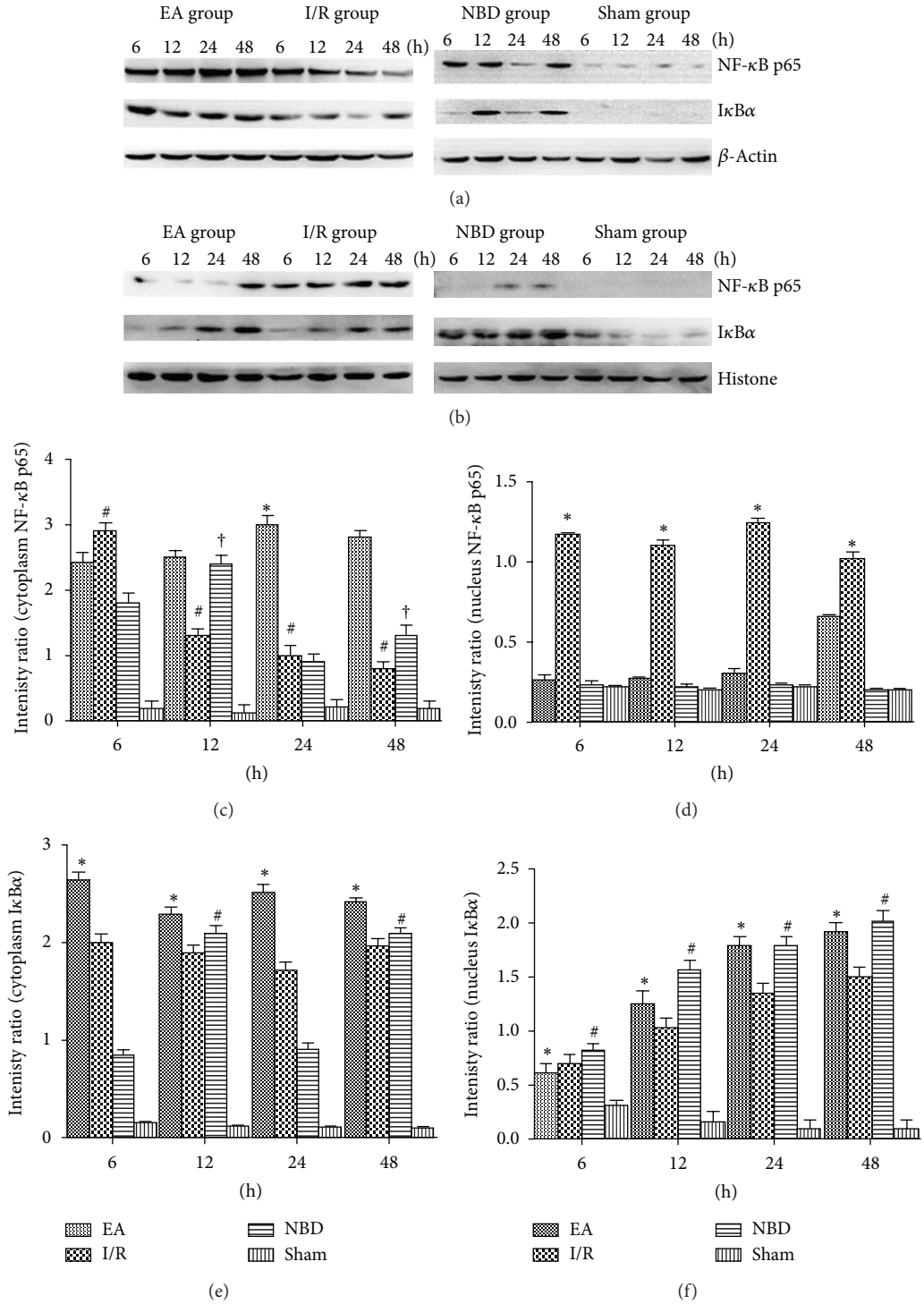

Figure 7: Western blot analysis of the NF-κB p65 and IκBα protein expression in the sham group, I/R group, EA group, and NBD group in ischemic brain tissue (5 rats in each group per time point, total 80 rats). (a)-(b) Representative Western blot images showing bands of NF-κB p65 and IκBα proteins in the cytoplasm and nucleus at 6 h, 12 h, 24 h, and 48 h. (c)–(f) Comparison of the mean intensity ratio of immunoblotting in these groups at each timepoint. (a), (c), (e) The NF-κB p65 and IκBα protein expression in cytoplasm. (b), (d), (f) The NF-κB p65 and IκBα protein expression in the nucleus.

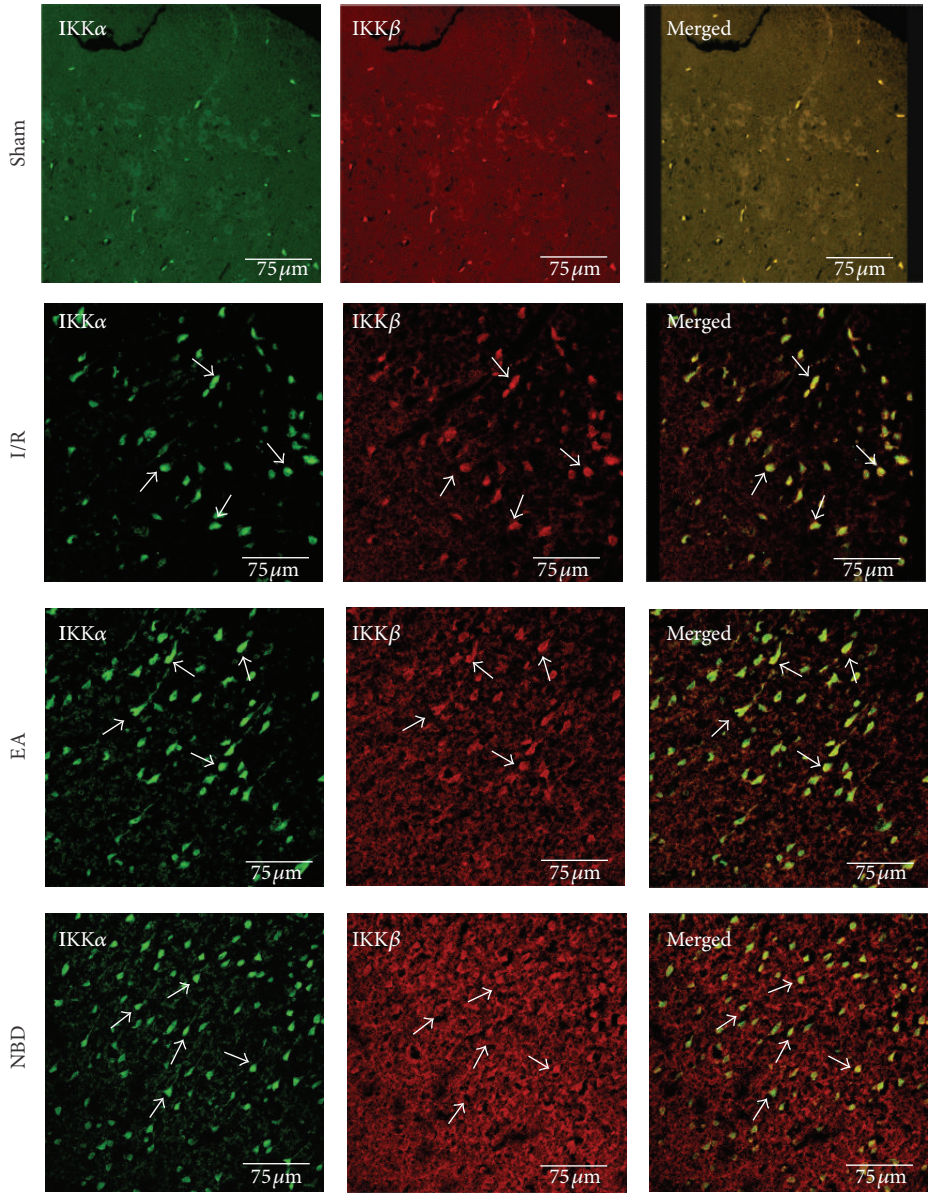

Figure 8: Double-immunofluorescent labeling the IKKα (green) and IKKβ (red) protein in sham group, I/R group, EA group, and NBD group (with the same samples from Figure 5). It showed that IKKα and IKKβ were strongly expressed in cytoplasm in the I/R group. The expression of IKKβ was lowly expressed in EA group and NBD group compared with the I/R group, especially in the NBD group.

were obviously different from the NBD peptide effect which focuses solely on the decreased expression of IKKβ rather than IKKα. The results of the NBD peptide group were consistent with the characteristics of NBD peptide. Thus, we have demonstrated the effect of EA on the IKKα and IKKβ for the first time in the focal cerebral I/R rats.

Furthermore, the different effect and mechanism between EA treatment and NBD peptide on IKKα and IKKβ were also prompted.

Besides, the key step in this process is nuclear translocation; binding of the p65/p50 dimers to the κB sequence on DNA is another important step in the activation of NF-κB signaling pathway [39]. We found that the DNA binding ability of NF-κB was increased after focal cerebral ischemia/reperfusion and was significantly reduced by EA treatment and NBD peptide intervention. This demonstrates that EA treatment and NBD peptide inhibit the NF-κB signaling pathway through inhibiting the ability of NF-κB binding DNA.

In summary, EA effectively inhibits the activation of NF-κB signaling pathway perhaps through reducing the expression of IKKα and IKKβ, which is highly expressed after focal cerebral ischemia/reperfusion. The function of IKKα and IKKβ in the NF-κB pathway maybe inhibited, which probably attenuates IκBα phosphorylation, resulting in increased IκBα expression in the NF-κB/IκBα feedback loop in the nucleus, which may block the nuclear translocation of NF-κB. Furthermore, EA reduced the DNA binding ability

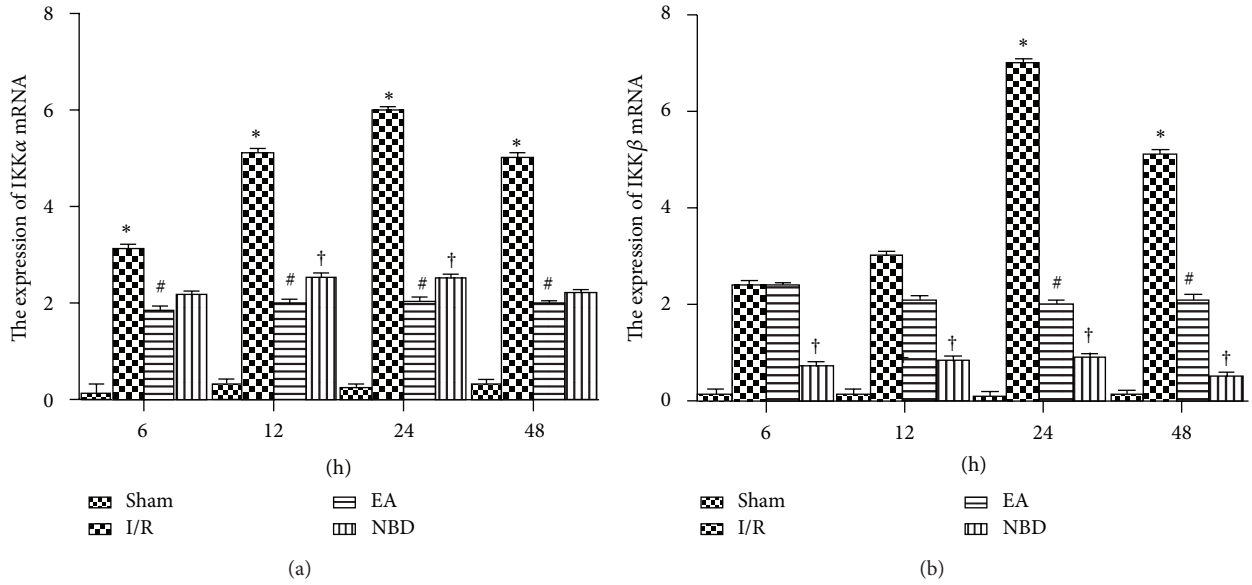

Figure 9: Fluorescent Quantitative-PCR analysis of the IKKα and IKKβ mRNA expression of the sham group, I/R group, EA group, and NBD group in the ischemic brain tissue (with the same samples from Figure 6). (a) The expression of IKKα mRNA was significantly increased in the I/R group compared with that in the EA and NBD group, $^{*}P < 0.05$. The IKKα mRNA expressed lowly in EA group, $^{\#}P < 0.05$ versus I/R group and NBD group. (b) The IKKβ mRNA expression in I/R group was high at 24 h and 48 h, $^{*}P < 0.05$ versus EA group and NBD group. It was lower in NBD group from 6 h to 48 h, $^{\dagger}P < 0.05$ versus EA group.

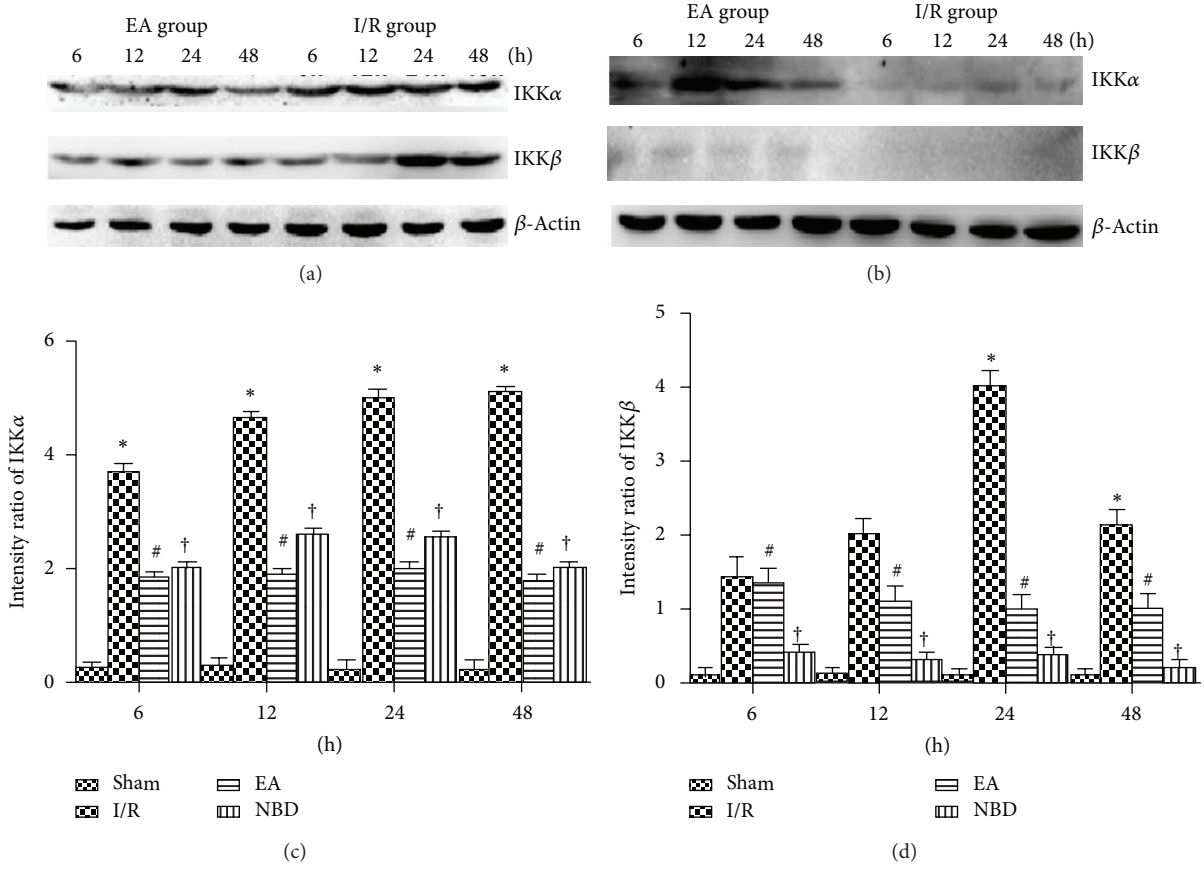

Figure 10: Western blot analysis of the IKKα and IKKβ protein expression in the sham group, I/R group, EA group, and NBD group in ischemic brain tissue (with the same samples from Figure 7). (a)-(b) Representative Western blot images showing bands of IKKα and IKKβ proteins at 6 h, 12 h, 24 h, and 48 h. Comparison of the mean intensity ratio of immunoblotting in these groups at each timepoint. (a), (b), (c) The IKKα protein in I/R group was highly expressed, $^{*}P < 0.05$ versus EA and NBD group. The expression in EA group was lower, $^{\#}P < 0.05$ versus NBD group. (a), (b), (d) The IKKβ protein was highly expressed at 24 h and 48 h, $^{*}P < 0.05$ versus EA and NBD group. The IKKβ protein scarcely expressed in NBD group, $^{\dagger}P < 0.05$ versus EA group.

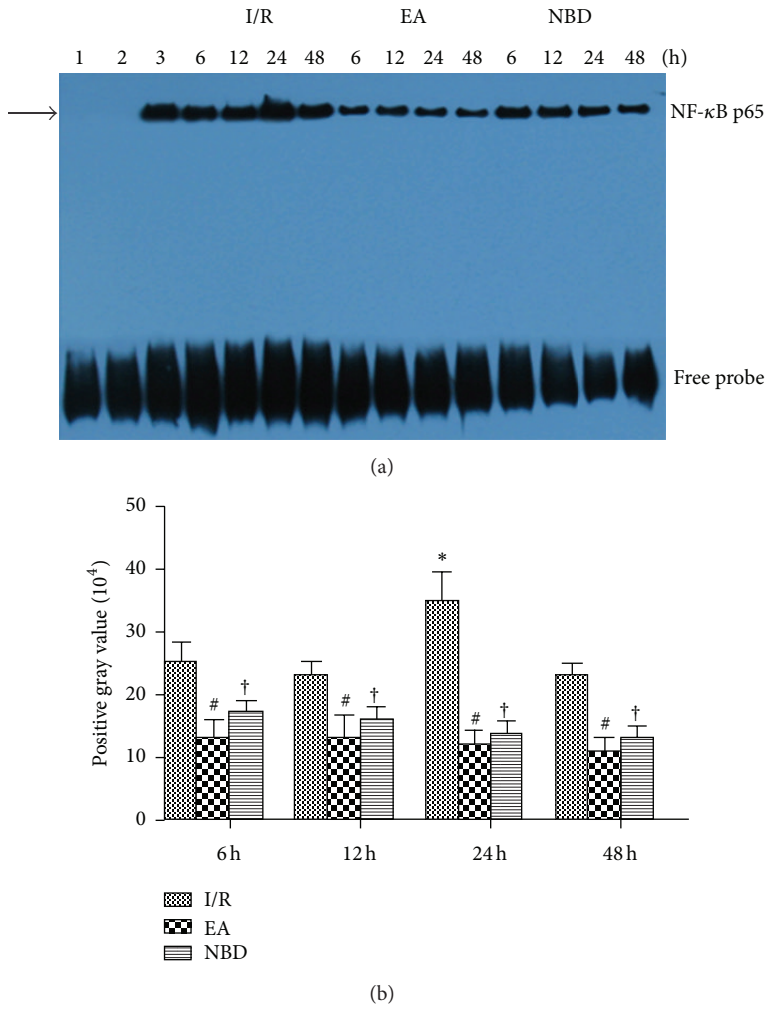

Figure 11: Electrophoretic mobility shift assay detection of NF-κB activity in the I/R, EA, and NBD groups in focal ischemia/reperfusion cortex in rats (5 rats in each group per time point, total 80 rats). (a) lane 1: negative probe, lane 2: cold competition probe, lane 3: positive probe. (b) The highest activity of NF-κB was at 24 h in the I/R group, which was significantly higher than that in the EA group and NBD group, $^{*}P < 0.05$. The NF-κB activity in EA group and NBD group shows no remarkable differences, $^{\#}P > 0.05$.

of NF-κB and thus effectively reduced activation of the NF-κB pathway. Compared with the NBD peptide, EA treatment mediated a reduction in the expression of IKKα. It can be speculated that the differences in these observations reflect the different mechanism of EA treatment and NBD peptide. Unfortunately, we have concentrated only on the canonical pathway. Moreover, because the effect of IKKα serves an anti-inflammatory function by phosphorylating Rel A and c-Rel at sites that accelerate their nuclear turnover [40], the effect and mechanism of EA on IKKα in the noncanonical pathway and the phosphorylation process of IKKs will be investigated in future studies. And the effect of EA on other signaling pathways during the inflammation also is considered to be our next research targets.

In short, we infer that inhibition of the NF-κB signaling pathway activation is involved in the mechanism by which EA treatment ameliorates the inflammatory injury occurred during the early stages of focal cerebral ischemia/reperfusion.

6. Conclusions

In conclusion, the mechanism by which EA inhibits activation of the NF-κB signaling pathway and declines the inflammatory injury involves multiple targets and links. EA treatment could reduce the expression of IKKα and IKKβ and may restrain the function of those to regulate the activation of the NF-κB signaling pathway and ameliorate the inflammation in the early stages of focal cerebral ischemia/reperfusion.

Abbreviations

EA:	Electroacupuncture
NF-κB:	Nuclear factor-κappaB
NBD peptide:	NEMO Binding Domain peptide
I/R:	Ischemia/reperfusion
SD:	Sprague-Dawley
PFA:	Paraformaldehyde

PBS: Phosphate buffer saline
PVDF: Polyvinylidene fluoride
EMSA: Electrophoretic mobility shift assay
RHD: Rel-homology domain
NES: Nuclear export sequences.

Acknowledgments

The research was supported by The National Natural Science Fund for Scientific Research (no. 30470606) and the Program of the Traditional Chinese Medicine Research of Chongqing Municipal Health Bureau (no. 2012-2-128).

References

[1] R. Macrez, C. Ali, O. Toutirais et al., "Stroke and the immune system: from pathophysiology to new therapeutic strategies," *The Lancet Neurology*, vol. 10, no. 5, pp. 471–480, 2011.

[2] C. Iadecola and J. Anrather, "The immunology of stroke: from mechanisms to translation," *Nature Medicine*, vol. 17, no. 7, pp. 796–808, 2011.

[3] P. J. Lindsberg and A. J. Grau, "Inflammation and infections as risk factors for ischemic stroke," *Stroke*, vol. 34, no. 10, pp. 2518–2532, 2003.

[4] L. L. Kate, B. Knut, and F. Bente, "Inflammatory cytokines in experimental and human stroke," *Journal of Cerebral Blood Flow & Metabolism*, vol. 27, pp. 1–22, 2012.

[5] D. A. Ridder and M. Schwaninger, "NF-κB signaling in cerebral ischemia," *Neuroscience*, vol. 158, no. 3, pp. 995–1006, 2009.

[6] A. Kumar, Y. Takada, A. M. Boriek, and B. B. Aggarwal, "Nuclear factor-κB: its role in health and disease," *Journal of Molecular Medicine*, vol. 82, no. 7, pp. 434–448, 2004.

[7] R. G. Baker, M. S. Hayden, and S. Ghosh, "NF-κB, inflammation, and metabolic disease," *Cell Metabolism*, vol. 13, no. 1, pp. 11–22, 2011.

[8] G. A. Donnan, M. Fisher, M. Macleod, and S. M. Davis, "Stroke," *The Lancet*, vol. 371, no. 9624, pp. 1612–1623, 2008.

[9] B. Kavoussi and B. E. Ross, "The neuroimmune basis of anti-inflammatory acupuncture," *Integrative Cancer Therapies*, vol. 6, no. 3, pp. 251–257, 2007.

[10] D. C. Choi, J. Y. Lee, E. J. Lim, H. H. Baik, T. H. Oh, and T. Y. Yune, "Inhibition of ROS-induced p38MAPK and ERK activation in microglia by acupuncture relieves neuropathic pain after spinal cord injury in rats," *Experimental Neurology*, vol. 236, pp. 268–228, 2012.

[11] X. Fu, Y.-Q. Wang, J. Wang, J. Yu, and G.-C. Wu, "Changes in expression of nociceptin/orphanin FQ and its receptor in spinal dorsal horn during electroacupuncture treatment for peripheral inflammatory pain in rats," *Peptides*, vol. 28, no. 6, pp. 1220–1228, 2007.

[12] F. J. Zijlstra, I. Van Den Berg-De Lange, F. J. P. M. Huygen, and J. Klein, "Anti-inflammatory actions of acupuncture," *Mediators of Inflammation*, vol. 12, no. 2, pp. 59–69, 2003.

[13] M. Pizzi, F. Goffi, F. Boroni et al., "Opposing roles for NF-κB/Rel factors p65 and c-Rel in the modulation of neuron survival elicited by glutamate and interleukin-1β," *Journal of Biological Chemistry*, vol. 277, no. 23, pp. 20717–20723, 2002.

[14] A. Schneider, A. Martin-Villalba, F. Weih, J. Vogel, T. Wirth, and M. Schwaninger, "NF-κB is activated and promotes cell death in focal, cerebral ischemia," *Nature Medicine*, vol. 5, no. 5, pp. 554–559, 1999.

[15] S. Ghosh and M. Karin, "Missing pieces in the NF-κB puzzle," *Cell*, vol. 109, no. 2, pp. S81–S96, 2002.

[16] M. S. Hayden and S. Ghosh, "Shared principles in NF-κB signaling," *Cell*, vol. 132, no. 3, pp. 344–362, 2008.

[17] L.-W. Chen, L. Egan, Z.-W. Li, F. R. Greten, M. F. Kagnoff, and M. Karin, "The two faces of IKK and NF-κB inhibition: prevention of systemic inflammation but increased local injury following intestinal ischemia-reperfusion," *Nature Medicine*, vol. 9, no. 5, pp. 575–581, 2003.

[18] H. Häcker and M. Karin, "Regulation and function of IKK and IKK-related kinases," *Science's STKE*, vol. 2006, no. 357, p. re13, 2006.

[19] I. Strickland and S. Ghosh, "Use of cell permeable NBD peptides for suppression of inflammation," *Annals of the Rheumatic Diseases*, vol. 65, no. 3, pp. 75–82, 2006.

[20] S. Dai, T. Hirayama, S. Abbas, and Y. Abu-Amer, "The IκB kinase (IKK) inhibitor, NEMO-binding domain peptide, blocks osteoclastogenesis and bone erosion in inflammatory arthritis," *Journal of Biological Chemistry*, vol. 279, no. 36, pp. 37219–37222, 2004.

[21] E. Z. Longa, P. R. Weinstein, S. Carlson, and R. Cummins, "Reversible middle cerebral artery occlusion without craniectomy in rats," *Stroke*, vol. 20, no. 1, pp. 84–91, 1989.

[22] Q. Wang, L. Xiong, S. Chen, Y. Liu, and X. Zhu, "Rapid tolerance to focal cerebral ischemia in rats is induced by preconditioning with electroacupuncture: window of protection and the role of adenosine," *Neuroscience Letters*, vol. 381, no. 1-2, pp. 158–162, 2005.

[23] A. Buchan and W. A. Pulsinelli, "Hypothermia but not the N-methyl-D-aspartate antagonist, MK-801, attenuates neuronal damage in gerbils subjected to transient global ischemia," *Journal of Neuroscience*, vol. 10, no. 1, pp. 311–316, 1990.

[24] R. Busto, W. D. Dietrich, M. Globus y.t., I. Valdes, P. Scheinberg, and M. D. Ginsberg, "Small differences in intraischemic brain temperature critically determine the extent of ischemic neuronal injury," *Journal of Cerebral Blood Flow and Metabolism*, vol. 7, no. 6, pp. 729–738, 1987.

[25] J. C. Clohisy, Y. Yamanaka, R. Faccio, and Y. Abu-Amer, "Inhibition of IKK activation, through sequestering NEMO, blocks PMMA-induced osteoclastogenesis and calvarial inflammatory osteolysis," *Journal of Orthopaedic Research*, vol. 24, no. 7, pp. 1358–1365, 2006.

[26] J. H. Garcia, S. Wagner, K.-F. Liu, X.-J. Hu, and J. P. Mohr, "Neurological deficit and extent of neuronal necrosis attributable to middle cerebral artery occlusion in rats: statistical validation," *Stroke*, vol. 26, no. 4, pp. 627–635, 1995.

[27] J. B. Bederson, L. H. Pitts, and S. M. Germano, "Evaluation of 2,3,5-triphenyltetrazolium chloride as a stain for detection and quantification of experimental cerebral infarction in rats," *Stroke*, vol. 17, no. 6, pp. 1304–1308, 1986.

[28] Q. Wang, Y. Peng, S. Chen et al., "Pretreatment with electroacupuncture induces rapid tolerance to focal cerebral ischemia through regulation of endocannabinoid system," *Stroke*, vol. 40, no. 6, pp. 2157–2164, 2009.

[29] K. M. Kolodziejska, M. H. Noyan-Ashraf, A. Nagy et al., "c-Myb-dependent smooth muscle cell differentiation," *Circulation Research*, vol. 102, no. 5, pp. 554–561, 2008.

[30] R. B. Borgens and P. Liu-Snyder, "Understanding secondary injury," *Quarterly Review of Biology*, vol. 87, pp. 89–127, 2012.

[31] S. Takashi, S. Ryota, S. Mayu, and Y. Akihiko, "Post-ischemic inflammation in the brain," *Frontiers in Immunology*, vol. 3, pp. 1–7, 2012.

[32] H. Boutin, R. A. LeFeuvre, R. Horai, M. Asano, Y. Iwakura, and N. J. Rothwell, "Role of IL-1α and IL-1β in ischemic brain damage," *Journal of Neuroscience*, vol. 21, no. 15, pp. 5528–5534, 2001.

[33] A. Minty, P. Chalon, J.-M. Derocq et al., "Interleukin-13 is a new human lymphokine regulating inflammatory and immune responses," *Nature*, vol. 362, no. 6417, pp. 248–250, 1993.

[34] C. Jobin and R. Balfour Sartor, "The IκB/NF-κB system: a key determinant of mucosal inflammation and protection," *American Journal of Physiology*, vol. 278, no. 3, pp. C451–C462, 2000.

[35] J. L. Pomerantz and D. Baltimore, "Two pathways to NF-κB," *Molecular Cell*, vol. 10, no. 4, pp. 693–695, 2002.

[36] S. Gerondakis, R. Grumont, R. Gugasyan et al., "Unravelling the complexities of the NF-κB signalling pathway using mouse knockout and transgenic models," *Oncogene*, vol. 25, no. 51, pp. 6781–6799, 2006.

[37] M. Pasparakis, T. Luedde, and M. Schmidt-Supprian, "Dissection of the NF-κB signalling cascade in transgenic and knockout mice," *Cell Death and Differentiation*, vol. 13, no. 5, pp. 861–872, 2006.

[38] M. S. Hayden and S. Ghosh, "Signaling to NF-κB," *Genes and Development*, vol. 18, no. 18, pp. 2195–2224, 2004.

[39] F. Wan and M. J. Lenardo, "Specification of DNA binding activity of NF-kappaB proteins," *Cold Spring Harbor Perspectives in Biology*, vol. 1, no. 4, Article ID a000067, 2009.

[40] T. Lawrence and M. Bebien, "IKKα in the regulation of inflammation and adaptive immunity," *Biochemical Society Transactions*, vol. 35, no. 2, pp. 270–272, 2007.

Hindawi Publishing Corporation
Evidence-Based Complementary and Alternative Medicine
Volume 2013, Article ID 795906, 13 pages
http://dx.doi.org/10.1155/2013/795906

Research Article

Acupuncture-Evoked Response in Somatosensory and Prefrontal Cortices Predicts Immediate Pain Reduction in Carpal Tunnel Syndrome

Yumi Maeda,[1,2] Norman Kettner,[2] Jeungchan Lee,[3] Jieun Kim,[1] Stephen Cina,[1] Cristina Malatesta,[4] Jessica Gerber,[1] Claire McManus,[4] Jaehyun Im,[1] Alexandra Libby,[1] Pia Mezzacappa,[1] Leslie R. Morse,[5] Kyungmo Park,[3] Joseph Audette,[6] and Vitaly Napadow[1,2]

[1] *Athinoula A. Martinos Center for Biomedical Imaging, Department of Radiology, Massachusetts General Hospital, No. 2301 149 Thirteenth Street, Charlestown, MA 02129, USA*
[2] *Department of Radiology, Logan College of Chiropractic/University Programs, Chesterfield, MO 63017, USA*
[3] *Department of Biomedical Engineering, Kyung Hee University, Yongin, Gyeonggido 446-701, Republic of Korea*
[4] *Department of Physical Medicine and Rehabilitation, Spaulding Rehabilitation Hospital, Medford, MA 02155, USA*
[5] *Department of Physical Medicine and Rehabilitation, Harvard Medical School, Spaulding Rehabilitation Hospital, Boston, MA 02114, USA*
[6] *Department of Pain Medicine, Harvard Vanguard Medical Associates, Atrium Health, Boston, MA 02215, USA*

Correspondence should be addressed to Yumi Maeda; ymaeda@nmr.mgh.harvard.edu

Received 23 February 2013; Revised 7 May 2013; Accepted 15 May 2013

Academic Editor: Richard E. Harris

The linkage between brain response to acupuncture and subsequent analgesia remains poorly understood. Our aim was to evaluate this linkage in chronic pain patients with carpal tunnel syndrome (CTS). Brain response to electroacupuncture (EA) was evaluated with functional MRI. Subjects were randomized to 3 groups: (1) EA applied at local acupoints on the affected wrist (PC-7 to TW-5), (2) EA at distal acupoints (contralateral ankle, SP-6 to LV-4), and (3) sham EA at nonacupoint locations on the affected wrist. Symptom ratings were evaluated prior to and following the scan. Subjects in the local and distal groups reported reduced pain. Verum EA produced greater reduction of paresthesia compared to sham. Compared to sham EA, local EA produced greater activation in insula and S2 and greater deactivation in ipsilateral S1, while distal EA produced greater activation in S2 and deactivation in posterior cingulate cortex. Brain response to distal EA in prefrontal cortex (PFC) and brain response to verum EA in S1, SMA, and PFC were correlated with pain reduction following stimulation. Thus, while greater activation to verum acupuncture in these regions may predict subsequent analgesia, PFC activation may specifically mediate reduced pain when stimulating distal acupoints.

1. Introduction

Acupuncture, a component of traditional Chinese medicine, has been commonly applied to alleviate symptoms of patients with chronic pain [1]. Carpal tunnel syndrome (CTS) is mainly driven by partial deafferentation secondary to compression of the median nerve within the carpal tunnel [2]. CTS clinically manifests as slowing of median nerve conduction velocity, local pain, and paresthesia. Recent randomized controlled trials (RCT) for CTS have shown that acupuncture produced significant improvement in symptoms, with effects similar to steroid treatment [3] and night splinting [4]. A recent RCT demonstrated that acupuncture also reduced CTS symptoms significantly greater than placebo [5].

Noninvasive brain imaging techniques, such as functional MRI (fMRI), have offered an unprecedented window into how the human brain responds to acupuncture needle stimulation [6, 7]. However, very few of these studies have been

performed in chronic patient populations, and even fewer have evaluated how brain response to acupuncture relates to the alleviation of clinical symptoms or even evoked-pain ratings. Zhang et al. demonstrated that fMRI response to transcutaneous electrical acupoint stimulation in brain areas such as secondary somatosensory cortex (S2), insula, and primary motor cortex (M1) was associated with reduced heat pain ratings in healthy adults [8]. More recently, Yang et al. found that acupuncture increased metabolism in regions including the prefrontal cortex (PFC), insula, and cingulate, while also decreasing pain levels in acute migraine patients in a positron emission tomography (PET) study [9]. Harris et al. used PET with ^{11}C-carfentanil in fibromyalgia patients and found that long-term increases in resting mu-opioid receptor binding in regions including insula, cingulate, and basal ganglia following 4 weeks of acupuncture correlated with decreased clinical pain levels over this same time period [10]. In CTS patients, compared to healthy adults, manual acupuncture needling has been found to produce more robust fMRI response in several brain areas including insula, cingulate, S1, and PFC, when controlling for the effects of sham (noninserted cutaneous tactile) acupuncture [11]. Enhanced processing in S1 and PFC was particularly interesting, given the fact that these patients demonstrated altered somatosensory-stimulation-evoked brain response in these areas [12] and that S1 activity was specifically modulated by five weeks of acupuncture treatment [13]. Unfortunately, changes in clinical pain were not evaluated in this study. Thus, the association between the brain circuitry processing acupuncture stimulation and postacupuncture clinical outcomes such as pain reduction is currently unknown.

In this cross-sectional study, CTS subjects were randomized to 3 groups: (1) EA applied at local acupoints on the affected wrist (PC-7 to TW-5), (2) EA at distal acupoints (contralateral ankle, SP-6 to LV-4), and (3) sham EA at nonacupoint locations on the affected wrist. In addition to fMRI data acquired during EA, we also evaluated changes in clinical symptoms following acupuncture and correlated fMRI response to EA with changes in symptoms. We hypothesized that both local and distal EA would produce greater symptom reduction compared to sham acupuncture. Furthermore, we hypothesized that the magnitude of symptom reduction would correlate with activation in brain regions previously associated with somatosensory, affective, and cognitive processing of pain and paresthesia in CTS subjects.

2. Methods

2.1. Subjects. Subjects, aged 20 to 60, with a 3-month or greater history of pain and/or paresthesia in median-nerve-innervated areas were enrolled. All subjects were examined for eligibility by a physiatrist at Spaulding Rehabilitation Hospital, which included a physical exam for Phalen's maneuver [14] and Durkan's sign [15] and testing of median and ulnar sensory nerve conduction (NCS: Cadwell Sierra EMG/NCS Device, Kennewick, WA). NCS inclusion criteria consisted of median nerve sensory latency greater than 3.7 ms or median nerve sensory latency greater than 0.5 ms compared to ulnar nerve. Exclusion criteria consisted of contraindications to MRI, history of diabetes mellitus, cardiovascular, respiratory, or neurological illnesses, rheumatoid arthritis, wrist fracture with direct trauma to median nerve, current usage of prescriptive opioid medication, thenar atrophy, previous acupuncture treatment (manual, EA, and TENS) for CTS, nerve entrapment other than median nerve, cervical radiculopathy or myelopathy, generalized peripheral neuropathy, blood dyscrasia or coagulopathy or current use of anticoagulation therapy. History of axis I psychiatric diagnosis (substance use disorder, psychotic disorder, or bipolar disorder), and use of psychotropic medications were also exclusions for this study. Chronic symptomatology for all eligible subjects was evaluated using the Boston Carpal Tunnel Syndrome Questionnaire (BCTSQ) [16].

A total of 59 CTS subjects (49.1 ± 9.8 years old, mean ± SD, 49 Female) were enrolled in this study. For the subjects who had diagnosed bilateral CTS, the more affected hand was determined as the test hand. CTS subjects were randomized to one of the three study arms: (1) local verum EA (n = 22, 17F, 14 right hand affected), (2) distal verum EA (n = 18, 14F, 13R), and (3) sham EA (n = 19, 18F, 11R). All study protocols were approved by the Massachusetts General Hospital and Partners Human Research Committee. Written informed consent was obtained from all subjects.

2.2. Acupuncture Procedure. For local verum EA, MRI-compatible titanium needles (0.2 mm in diameter, 35–50 mm in length, DongBang Acupuncture Inc. Boryeong, Korea) were inserted and *deqi* sensation elicited at acupoints PC7 (pericardium 7, 1st wrist crease) and TW5 (triple-warmer 5, dorsal aspect of forearm), local to the more affected hand (Figure 1(a)). PC-7 was chosen because it is close to the CTS lesion, and this set of points was found to reduce pain and paresthesia in our previous study [13].

For distal verum EA, MRI-compatible titanium needles were inserted and *deqi* sensation elicited at acupoints SP6 (spleen 6, medial aspect of lower leg) and LV4 (liver 4, anterior aspect of the ankle) at the ankle on the contralateral side to the more affected hand (Figure 1(b)). Distal acupoints LV4 and SP6 were chosen based on mirror point methods common in acupuncture practice, where acupoints on the leg/ankle can be used to treat symptoms on the opposite arm/wrist [17].

For sham EA, MRI-compatible blunt-tipped acupuncture needles were placed with a single tap but not inserted percutaneously, over sham points, SH1 (2 cun, or roughly 2-3 cm, distal and slightly volar to acupoint SI-7, which is 5 cun proximal to ulnar edge of the transverse wrist crease, ulnar forearm) and SH2 (1 cun distal and slightly volar to SI-7), on the more affected hand (Figure 1(a)).

For all 3 groups, needles were connected to a constant current electroacupuncture (EA) device (HANS LH202H, Neuroscience Research Center, Peking University, Beijing, China). A licensed acupuncturist trained to place and stimulate acupuncture needles in the scanner performed these procedures. For verum EA, current stimulation frequency

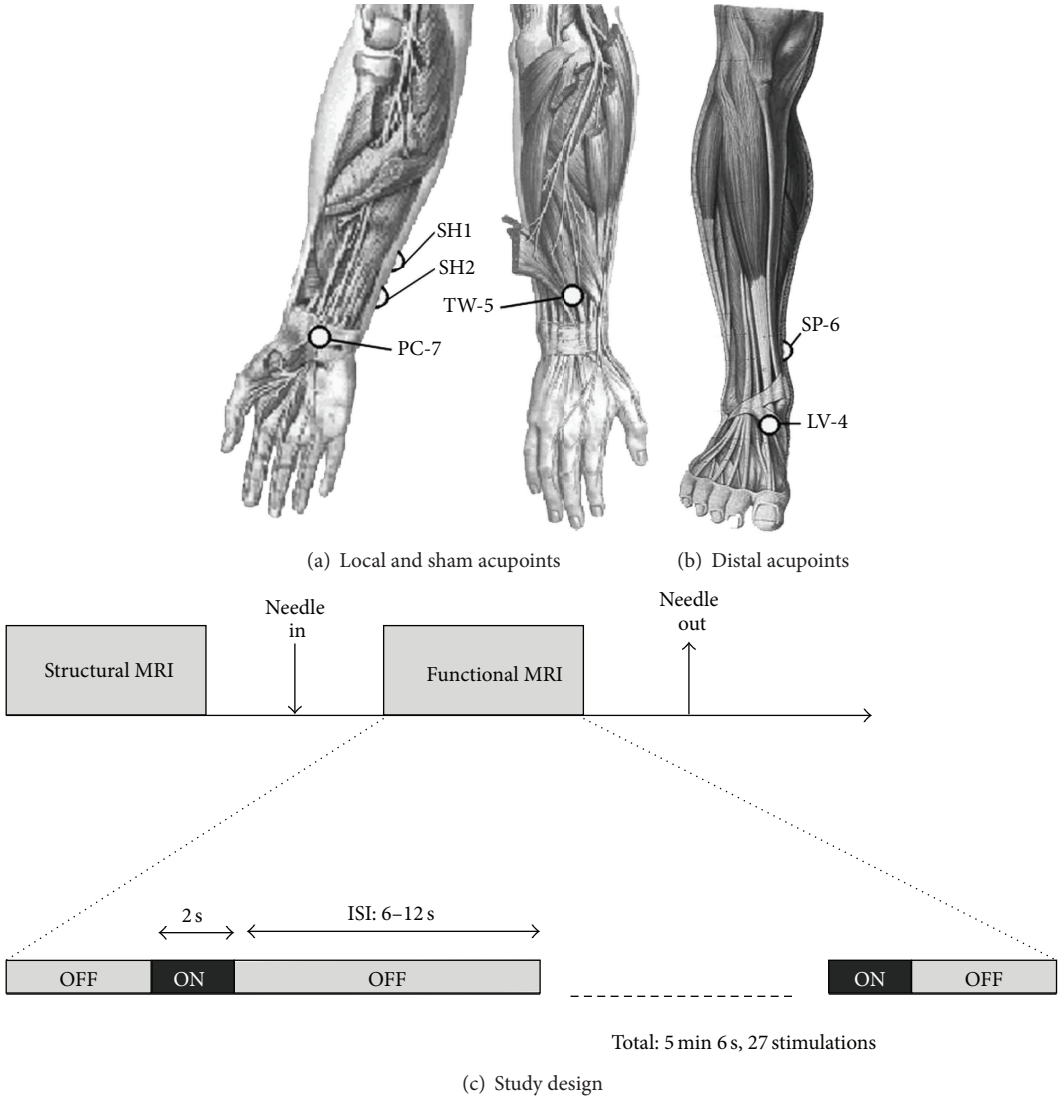

Figure 1: Acupoints and schematic scan session. Verum EA was performed at both (a) local (PC7 to TW5) and (b) distal (SP6 to LV4) acupoints. Sham EA used noninsertive needles placed over sham points, SH1 and SH2. (c) Our fMRI event-related study design for acupuncture stimulation.

was set to 2 Hz, while the current intensity was set just prior to the functional scan. The acupuncturist gradually increased the current intensity until the subject felt a moderately strong but not painful sensation. For sham EA, electrodes were attached to the needles, but no electrical current was passed. Subjects were instructed that the current intensity was set to a predetermined level and that they may or may not feel any sensation at the needle sites. All subjects were instructed to close their eyes and focus on the acupuncture stimulation while remaining as still as possible.

2.3. Data Acquisition. All imaging data were acquired on a 3.0T Siemens Trio (Siemens Medical, Erlangen, Germany) equipped with 32-channel head coil. Structural imaging data were acquired with a multiecho MPRAGE T1-weighted pulse sequence (TR = 2530 ms, TE1/TE2 = 1.64/30.0 ms, TI = 1200 ms, flip angle = 7°, FOV = 256 × 256, slices = 176, sagittal acquisition, spatial resolution = $1 \times 1 \times 1\ mm^3$).

Functional imaging (fMRI) data were acquired using a gradient echo BOLD $T2^*$-weighted pulse sequence (TR/TE = 2000/30 ms, FOV = 200 × 200 mm, 32 axial slices parallel to anterior/posterior commissural plane, voxel size = 3.125 × 3.125 × 3.6 mm, flip angle = 90°). Subjects lay supine in the scanner with earplugs to attenuate acoustic gradient switching noise. For verum EA, stimulation was performed using an event-related design similar to our previously published approach for manual acupuncture [18] (2-second stimulation events with randomized ISI, 6–12 seconds, and total scan time 5 minutes and 6 seconds, Figure 1(c)). For sham EA, procedures were identical, but no electricity was passed through the needles.

Symptoms were assessed using a 0–10 VAS scale for both pain and paresthesia (tingling) at the hand/wrist. The

scale ranged from none (0) to unbearable (10) and was administered at the beginning and the end of the MRI session. In addition, subjects were asked to rate the intensity of acupuncture-evoked sensations after the scan session using the MGH Acupuncture Sensation Scale (MASS) instrument [19].

2.4. Data Analysis. Statistical analyses for behavioral and clinical data were performed with SPSS (SPSS version 10.0.7, Chicago, Il). Median sensory nerve velocities and motor nerve latencies were compared with those of the ulnar nerve in all CTS subjects using a Student's t-test, significant at $P < 0.05$.

Changes in VAS scores for pain and paresthesia were compared between groups using a mixed model ANOVA with interaction of Group (local, distal, and sham) × Time (pre and post). Student's t-test was used to compare change in VAS scores between verum (combined local and distal) and sham groups. EA current intensities were compared between local and distal acupoint groups using a Student's t-test significant at $P < 0.05$. A one-way ANOVA was performed in order to compare evoked acupuncture sensations, as well as the MASS Index (a composite metric of *deqi* sensation) between groups. Post hoc testing was performed with the Tukey test.

FMRI data were preprocessed using the FMRIB software Library (FSL v.4.1), Freesurfer (v.5.1.), and AFNI (v.2.). FMRI data were coregistered with each subject's structural MRI data using boundary-based registration (BB registration, Freesurfer [20]). Preprocessing included slice timing correction, motion correction, high pass filtering with a cut-off period of 50 sec, and spatial smoothing with Gaussian kernel at FWHM = 5 mm (Feat, FSL). Preprocessed fMRI data were then analyzed using a general linear model for all subjects (Feat, FSL), with the explanatory variable set by the event-related design. The resultant parameter estimates and variances from all subjects were transformed to standard MNI space (FNIRT, FSL) in order to perform nonflipped (compare with below) group analyses. Registration was ensured by visualization (AFNI, afni).

In order to better assess brain response for structures known to be lateralized relative to somatosensory input (i.e., S1 and M1, and thalamus), parameter estimates and variances of subjects whose more affected hand was the left hand (and thus experienced local EA on the left hand or distal EA on the right ankle) also had their fMRI parameter estimates flipped across the midsagittal plane before passing them up to the flipped group analysis. Therefore, a total of 21 fMRI datasets (local: 8, distal: 5, sham: 8) were analyzed by flipping across the midsagittal plane.

Group maps were calculated using a mixed effects statistical model (FLAME, Feat, FSL). Difference maps were calculated with an ANOVA using a mixed effect model (FLAME, Feat, FSL). As we found no differences in brain response between local and distal groups, a combined group map for "verum EA" was also calculated in order to increase statistical power and for future testing. Whole brain regression analysis was performed for local, distal, and sham groups, as well as the combined verum group in order to identify brain regions associated with symptom reduction. For the regression analysis with symptom reduction, changes in VAS pain and paresthesia scores (post and pre) were demeaned and added as explanatory variable to the model. All statistical maps were thresholded with cluster forming threshold at $z = 2.3$ (voxel wise threshold $P < 0.01$), and cluster corrected for multiple comparisons at $P < 0.05$ [21].

3. Results

3.1. Demographic and Clinical Features. Bilateral CTS was diagnosed in 44/59 (75%) subjects, while unilateral CTS was diagnosed in 15/59 (25%) subjects. The more affected hand was the right hand in 38/59 (64.4%) subjects and the left hand in 21/59 (35.6%) subjects. Pain was the more severe symptom in 11/59 (18.3%) subjects; paresthesia was more severe in 37/59 (63.3%) subjects, and pain and paresthesia were observed with equal severity in 11/59 (18.3%) subjects. BCTSQ assessment of symptoms on the scale 1 to 5 demonstrated that pain and paresthesia were moderate (2.6 ± 0.9, 2.9 ± 0.8, mean ± S.D., resp.). Pain and paresthesia ratings were positively correlated ($r = 0.68$, $P < 0.001$); that is, those subjects with greater pain also reported greater paresthesia. Self-reported symptom duration was 9.0 ± 8.8 years (mean ± S.D.) and was positively correlated with subjects' age ($r = 0.39$, $P < 0.01$). A significant correlation was found between VAS pain and paresthesia scores before acupuncture (pre; $r = 0.68$, $P < 0.001$). In addition, VAS pain scores at baseline were significantly correlated with the BCTSQ pain score ($r = 0.60$, $P < 0.001$). However, VAS paresthesia scores were not significantly correlated with BCTSQ paresthesia scores ($r = 0.25$, $P = 0.053$).

Phalen's test was positive on the right hand in 39/59 (66.1%) subjects and on the left hand in 34/59 (57.6%) subjects. Durkan's test was positive on the right hand in 26/59 (44.0%) subjects and on the left hand in 24/59 (40.7%) subjects. For the study hand, Phalen's test was positive in 51/59 (86.4%) subjects, while Durkan's test was positive in 38/59 (64.4%) subjects. Median nerve sensory velocities were significantly slower compared to ulnar nerve sensory velocities (median: 37.9 ± 6.9 m/s, ulnar: 55.6 ± 6.7, mean ± SD, $P < 0.0001$). Furthermore, median nerve motor latencies were significantly longer compared to ulnar nerve motor latencies (median: 5.0 ± 1.3 ms, ulnar: 2.9 ± 0.3, mean ± S.D., $P < 0.0001$).

The regular usage of night splints was reported in 33/59 (56.7%) subjects. Subjects' occupational status could be described as "full-time work" in 38/59 (64.4%) subjects and part-time in 8/59 (13.6%) subjects. Mean body mass index (BMI) was 29.0 ± 5.1 (mean ± SD).

3.2. Symptom Change following EA. We found a significant main effect of Time (pre versus post) for VAS score in pain and paresthesia ($F_{1,56} = 19.3$, $P < 0.0001$, $F_{1,56} = 5.2$, $P < 0.03$, resp., Figure 2). There was neither a significant main effect of Group ($P > 0.7$, $P > 0.9$, resp.) nor interaction of Time × Group for either pain or paresthesia ($P > 0.4$,

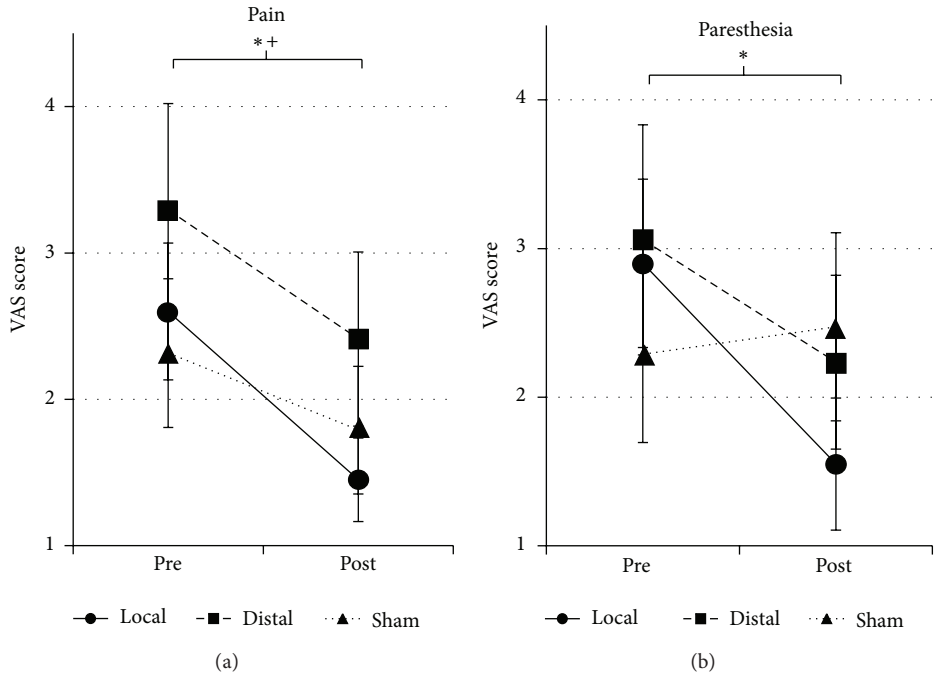

Figure 2: Symptom rating before and after acupuncture. A significant main effect of Time (pre versus post) was found for pain and paresthesia VAS score ($F_{1,56} = 19.3$, $P < 0.0001$; $F_{1,56} = 5.2$, $P < 0.03$, resp.), indicating reduced pain and paresthesia after acupuncture. Post hoc testing found that local EA reduced pain and paresthesia ($^{*}P < 0.01$) while distal EA reduced pain ($^{+}P < 0.05$). Error bars indicate standard error of the mean.

$P > 0.1$, resp.). Post hoc testing revealed that VAS scores for pain showed significant reductions for local and distal groups but not for the sham group (local: -1.2 ± 1.5, $P < 0.005$; distal: -1.2 ± 2.2, $P < 0.05$; sham: -0.5 ± 1.4, $P = 0.12$; mean ± SD). VAS scores for paresthesia showed significant reductions for the local group but not for the distal or sham groups (local: -1.3 ± 1.6, $P < 0.001$; distal: -1.1 ± 2.1, $P = 0.055$; sham: 0.2 ± 3.5, $P = 0.82$; mean ± SD). Also, the combined verum (local and distal) group produced a greater reduction in VAS scores for paresthesia compared to the sham group (verum: -1.2 ± 1.8, sham: 0.2 ± 3.5, mean ± S.D., $P < 0.05$). A statistically significant reduction for verum compared to sham acupuncture was not seen in VAS scores for pain (verum: -1.2 ± 1.8, sham: -0.5 ± 1.4, mean ± SD, $P > 0.1$).

We also found that change in VAS pain scores correlated with change in VAS paresthesia scores for both the local ($r = 0.44$, $P < 0.04$) and sham groups ($r = 0.77$, $P < 0.001$) but not for the distal group ($r = 0.35$, $P = 0.14$).

3.3. Electroacupuncture Current Intensity and EA-Evoked Sensations. EA current intensity did not differ between local and distal groups (local: 1.6 ± 1.0 mA, distal: 2.0 ± 0.9, mean ± S.D., $P > 0.3$). For acupuncture-evoked sensation, an ANOVA demonstrated a significant main effect of Group for Mass index (MI, $F_{2,56} = 6.5$, $P < 0.003$, Figure 3). Post hoc testing revealed that the local group produced greater MI scores compared to the sham group ($P < 0.02$, local: 4.6 ± 2.1, distal: 3.4 ± 1.8, sham: 2.3 ± 2.0, mean ± S.D.). In regard to individual MASS sensations, a significant main effect of

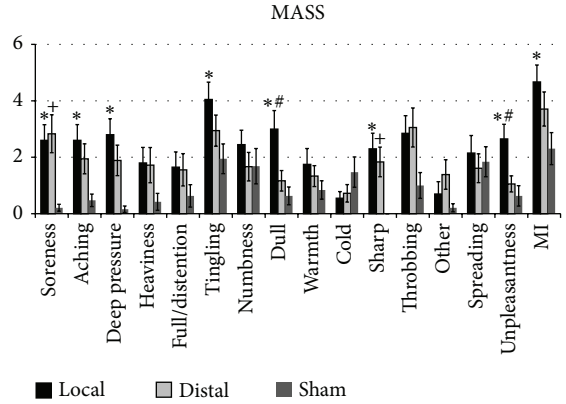

Figure 3: Acupuncture sensations. A significant difference between local and sham EA was found for soreness, aching, deep pressure, tingling, sharp pain, unpleasantness, and MI ($^{*}P < 0.05$). A significant difference between distal and sham EA was found for soreness and sharp pain ($^{+}P < 0.05$). A significant difference between local and distal EA was found for dull pain and unpleasantness ($^{\#}P < 0.05$). Error bars indicate standard error of the mean.

Group was also detected for soreness ($F_{2,56} = 8.1$, $P = 0.001$), aching ($F_{2,56} = 5.5$, $P = 0.006$), deep pressure ($F_{2,56} = 8.7$, $P = 0.001$), tingling ($F_{2,56} = 3.8$, $P = 0.03$), dull pain ($F_{2,56} = 6.9$, $P = 0.002$), sharp pain ($F_{2,56} = 7.6$, $P = 0.001$), and unpleasantness ($F_{2,56} = 6.9$, $P = 0.003$) (Figure 3). Post hoc testing revealed that the local group produced greater sensation compared to the sham group for soreness,

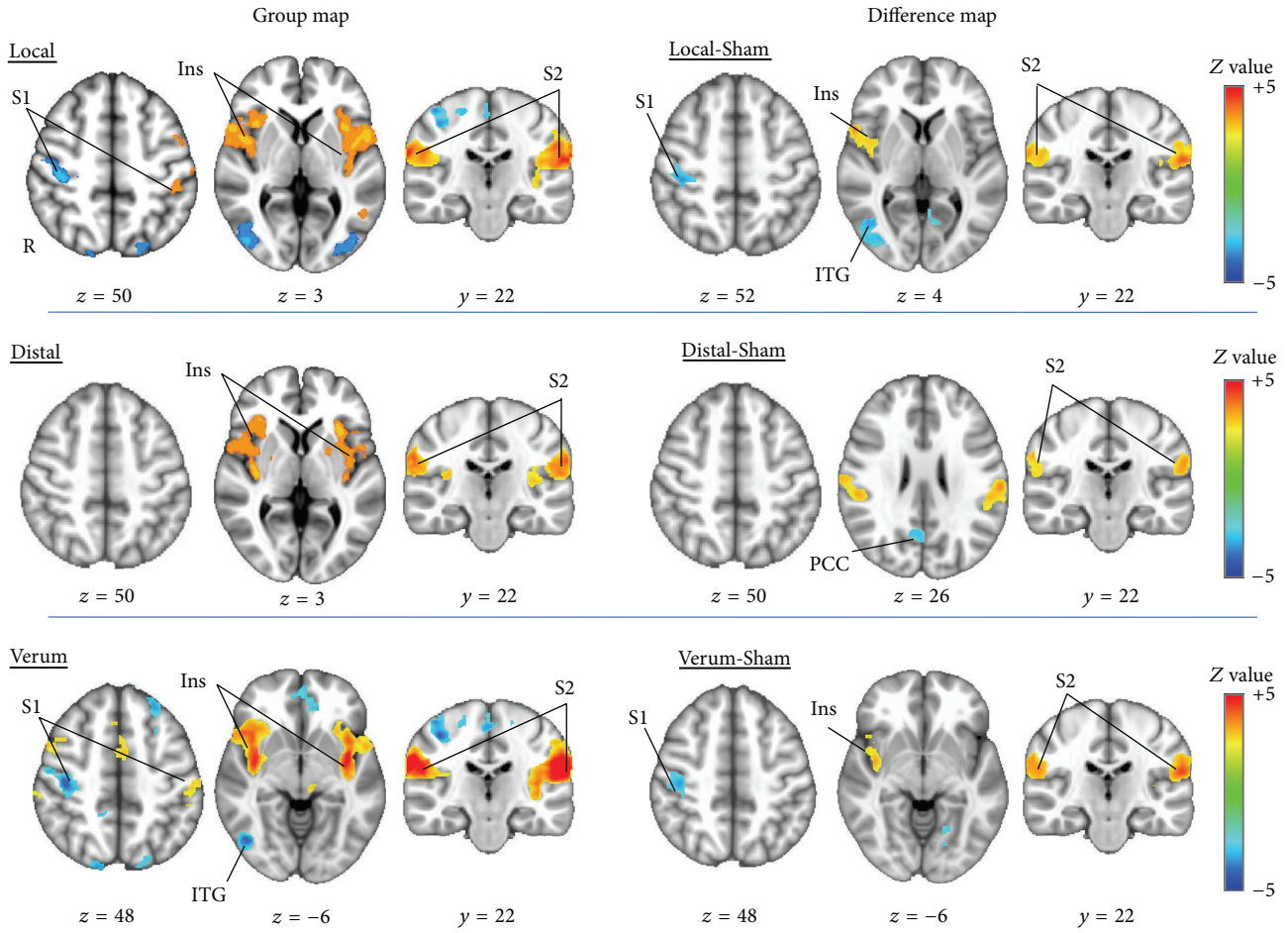

FIGURE 4: Group and difference maps of brain response during acupuncture. Local EA produced activation in contralateral primary somatosensory cortex (S1) and bilateral insulae and secondary somatosensory cortex (S2) and deactivation in ipsilateral S1. Distal EA produced activation in bilateral insula and S2. Verum EA (combined local and distal) produced activation in left S1 and bilateral insulae and secondary somatosensory cortex (S2) and deactivation in the medial prefrontal cortex (PFC) and right S1. Compared to sham EA, local EA produced greater activation in right insula and bilateral S2 and while greater deactivation in ipsilateral S1 and inferior temporal gyrus (ITG). Distal EA produced greater activation in bilateral S2 and greater deactivation in PCC. Verum EA produced greater activation in right insula and bilateral S2 and greater deactivation in right S1. Note: S1 was analyzed using a midsagittal plane flipped analysis (as S1 is known to be lateralized in activity relative to the stimulated side), while other regions were analyzed using a more conventional nonflipped analysis. All coordinates are in MNI space.

aching, deep pressure, tingling, sharp pain, spreading, and unpleasantness ($P < 0.05$). Also, the distal group produced greater sensation compared to sham acupuncture for soreness and sharp pain ($P < 0.05$), while the local group produced greater sensation compared to the distal group for dull pain and unpleasantness ($P < 0.05$, Figure 3). EA current intensity was correlated with numbness for the local group ($r = 0.52$, $P = 0.013$). EA current intensity was correlated with soreness ($r = 0.47$, $P = 0.048$) and cold ($r = 0.50$, $P = 0.035$) for the distal group. In addition, Mass index was not correlated with pain reduction (local: $r = -0.09$, distal: $r = 0.18$, sham: $r = 0.29$) or paresthesia reduction (local: $r = 0.29$, distal: $r = -0.32$, sham: $r = 0.44$) in any group ($P > 0.05$). EA current intensity was not correlated with pain reduction (local: $r = -0.35$, distal: $r = 0.04$) or paresthesia reduction (local: $r = 0.04$, distal: $r = 0.25$) in either the local or distal group ($P > 0.05$).

3.4. fMRI during Acupuncture. Local EA produced activation in bilateral insulae, secondary somatosensory cortex (S2), superior temporal gyrus (STG), and contralateral postcentral gyrus (S1), with deactivation in cuneus and ipsilateral S1 (Table 1, Figure 4). Distal EA produced activation in bilateral insulae, S2, and premotor cortex (PMC), while no deactivation was found (Figure 4). Sham EA showed no significant fMRI response (Table 1). There were no significant differences in brain response between local and distal groups (Table 1); hence we also calculated a combined verum (local and distal) EA group map, which showed activation in bilateral S2, premotor (PMC), supramarginal (SMG), and superior temporal (STG) gyri, as well as anterior and posterior insulae (a.Ins, p.Ins) and thalamus. Activation was also noted in right presupplementary motor area (pSMA) and middle and inferior frontal gyri (MFG, IFG) (Table 1, Figure 4). Verum EA also produced deactivation in bilateral occipital gyrus,

Table 1: Brain response to electroacupuncture.

Region	Side	Cluster size	P value	max_z	MNI (mm)		
					X	Y	Z
Nonflipped analysis							
Local							
S2	R	4813	$3.48E-15$	5.2	66	−20	26
a.Ins	R			3.5	36	16	4
p.Ins	R			3.58	44	−16	19
IPL	R			4.79	58	−28	28
STG	R			4.31	56	12	4
MTG	R			3.18	56	−50	3
S2	L	4750	$4.83E-15$	4.64	−62	−22	20
S1	L			2.74	−54	−22	44
a.Ins	L			4.02	−40	−2	−4
S1	R	1671	$6.56E-07$	−3.78	36	−26	52
cuneus	L	3603	$2.55E-12$	−4.05	−16	−90	30
Distal							
p.Ins	R	2639	$2.6E-10$	4.02	34	−18	16
a.Ins	R			4	31	25	−1
IFG	R			2.96	45	13	26
S2	R	1394	$2.5E-6$	4.47	50	−26	26
STG	R			3.07	57	−37	17
S2	L	3653	$4.31E-13$	4.41	−58	−26	22
MFG	L			3.0	−50	2	15
SMG	L			3.23	−55	−37	41
IPL	L			4.18	−53	−34	27
a.Ins	L			3.63	−32	20	2
p.Ins	L			3.69	−36	−20	12
Sham							
None							
Verum							
S2	R	7869	$2.57E-20$	6.53	62	−24	28
SMG	R			4	60	−29	38
STG	R			4.6	60	−38	18
a.Ins	R			4.8	38	22	−2
p.Ins	R			5.3	40	−6	−4
PMC	R			4.8	50	8	40
ITG	R	2633	$3.18E-09$	−4	44	−70	−6
OCG	R			−3.9	18	−94	28
S1	R	2233	$5.96E-08$	−4.33	42	−22	50
S1	R			−3.8	22	−28	66
pSMA	R	602	$9.15E-03$	3.74	4	8	60
SFG	R			3.1	4	24	46
MFG	R			3.95	42	40	12
IFG	R			5.6	56	12	4
MPFC	R	945	$4.07E-04$	−3.56	4	58	10
Thalamus	R	563	0.0135	3.96	10	−14	8
Thalamus	L			3.79	−10	−18	10
S2	L	7029	$9.15E-19$	6.34	−62	−28	24
PMC	L			4.4	−55	3	3
SMG	L			5.3	−54	−43	28
STG	L			6.3	−62	−28	24
a.Ins	L			4.83	−34	14	4

Table 1: Continued.

Region	Side	Cluster size	P value	max_z	MNI (mm)		
					X	Y	Z
p.Ins	L			5.4	−40	0	−4
OCG	L	924	$4.87E-04$	−3.74	−22	−86	32
Flipped analysis							
Local							
S1	R	1885	$1.19E-07$	−3.84	38	−26	50
S1	L	5566	$5.89E-17$	3.79	−54	20	43
Distal							
M1	L	3798	$1.49E-13$	2.51	−52	−6	39
Sham							
None							
Verum							
S1	R	2419	$1.02E-08$	−4.32	40	−22	48
S1	L	7502	$8.89E-20$	7.05	−62	−20	22
Thalamus	R	588	0.01	4.77	10	−16	8
Thalamus	L			3.65	−14	−14	8

Note: PMC: premotor cortex, MPFC: medial prefrontal cortex, S1: primary somatosensory cortex, S2: secondary somatosensory cortex, SMG: supramarginal gyrus, SFG: superior frontal gyrus, MFG: middle frontal gyrus, IFG: inferior frontal gyrus, pSMA: presupplementary motor area, STG: superior temporal gyrus, MTG: middle temporal gyrus, ITG: inferior temporal gyrus, a.Ins: anterior insula, p.Ins: posterior insula, OCG: occipital gyrus, IPL: inferior parietal lobe. Nonflipped analysis: group map with the original orientation of the data as acquired from the scanner. Flipped analysis: subjects with left-sided lesions had their fMRI data flipped across the midsagittal plane to evaluate brain regions known to be lateralized relative to somatosensory stimulation (i.e., S1, M1, thalamus). Cluster size represents the number of voxels in the cluster. "P value" represents the cluster probability. "max_z" represents normalized probability. "x, y, z" represent the MNI coordinates of the region's peak voxel from the cluster.

right medial prefrontal cortex (PFC), inferior temporal gyrus (ITG), and S1 (Table 1, Figure 4).

In comparison to fMRI response for the sham group, local EA produced greater activation in bilateral S2 and right frontal insular cortex (FIC), while greater deactivation was found in right inferior temporal gyrus (ITG) (Table 2, Figure 4). Distal EA produced greater activation in bilateral S2 and deactivation in posterior cingulate cortex (PCC). Combined (local and distal) verum EA produced greater activation in bilateral S2 and insula and deactivation in PCC, precuneus, and right S1.

Whole brain regression analysis for change in VAS pain score in the distal group revealed a significant correlation in right prefrontal cortex (PFC). Thus, greater activation in PFC was associated with greater pain reduction following distal EA (Table 3, Figure 5). No significant correlations were found for either local or sham groups. For the combined verum EA group, a significant negative correlation was found between changes in VAS pain scores and brain activity in right S1 and bilateral supplemental motor area (SMA) and prefrontal cortex (PFC) (Table 3, Figure 6). Thus, greater activation in S1, SMA, and PFC was associated with greater pain reduction following verum EA.

4. Discussion

This study investigated how brain response to EA was associated with symptom reduction following stimulation in CTS subjects. Our main finding was that pain was reduced following verum (both local and distal) EA and that greater brain activation in PFC, SMA, and S1 in response to verum EA was associated with more pronounced pain reduction. Thus, greater activation in these regions may be a biomarker for immediate analgesia following EA.

Brain response to verum EA produced activation in several regions including dorsolateral prefrontal cortex (dlPFC), pre-SMA (pSMA), S1, bilateral S2, and insula, with the latter two regions also showing greater activation compared to sham EA. Deactivation was noted in ipsilateral S1 and default mode network areas such as the medial prefrontal cortex and lateral temporal cortex, also with evidence of greater deactivation compared to sham EA. These findings are consistent with multiple previous acupuncture fMRI studies [6, 7], which support the veracity of the event-related fMRI data used to correlate with clinical outcomes in this study.

Similar to our findings, linking dorsolateral PFC (dlPFC) activation with pain reduction following EA, Yang et al. used FDG PET and found that acupuncture produced increased brain metabolism in the middle frontal gyrus (a subregion of the dlPFC) and concomitant pain reduction in acute migraine patients [9]. The prefrontal cortex is known to modulate pain [22]. Chronic pain patients demonstrated reduced dlPFC gray matter volume [23], while transcranial magnetic stimulation to this region reduced placebo analgesia [24]. Moreover, recent studies have suggested that PFC dopamine levels mediate pain sensitivity [25]. As EA has been shown to modulate fMRI activity in dopaminergic source regions (i.e., substantia nigra) in a time-dependent manner [26], analgesia related with PFC response to EA in CTS subjects may prove to be mediated by this neuromodulatory catecholamine.

Table 2: Difference map of brain response to electro-acupuncture.

Region	Side	Cluster size	P value	max_z	MNI (mm)		
					X	Y	Z
Nonflipped analysis							
Local-Sham							
ITG	R	1434	$3.0E-5$	−3.55	44	−70	−2
IFG	R	574	0.0207	3.63	56	14	4
S2	L	1111	$2.61E-4$	4.23	−62	−22	20
p.Ins	L		0.0155	2.42	−38	−16	10
S2	R	826	0.00237	4.05	66	−20	26
FIC	R		0.0033	2.94	46	0	6
IPL	R		0.0017	3.13	58	−28	28
STG	R		0.0004	3.56	56	12	4
Distal-sham							
PCC	R	653	0.0102	−3.3	10	−60	18
S2	L	544	0.0273	3.77	−58	−24	18
IPL	L		0.0026	3.01	−52	−34	26
S2	R	489	0.0457	3.46	58	−18	14
IPL	R		0.0065	2.72	52	−34	28
Local-distal							
None							
Verum-sham							
PCC	R	516	0.0354	−3.45	12	−58	14
PCC/precuneus	L	507	0.0385	−3.3	−10	−70	20
Insula	R	879	0.00154	3.38	40	−4	−6
S2	L	1187	$1.49E-4$	4.43	−60	−22	20
SMG	L		0.0016	3.15	−54	−34	30
STG	L		0.0001	3.98	−62	−28	24
p.Ins	L		0.0083	2.64	−38	−20	8
S2	R	897	0.00134	4.27	62	−18	20
a.Ins	R		0.0045	2.84	30	22	8
Flipped analysis							
Local-sham							
S1	R	763	0.00401	−3.46	40	−28	52
Distal-sham							
None							
Local-distal							
None							
Verum-sham							
S1	R	698	0.00698	−3.45	42	−22	48

Note: PCC: posterior cingulate cortex, IFG: inferior frontal gyrus, S1: primary somatosensory cortex, S2: secondary somatosensory cortex, IFG: inferior frontal gyrus, ITG: inferior temporal gyrus, FIC: frontal insula cortex, STG: superior temporal gyrus, MTG: middle temporal gyrus, a.Ins: anterior insula, p.Ins: posterior insula, IPL: inferior parietal lobe. Nonflipped analysis: difference map with the original orientation of the data as acquired from the scanner. Flipped analysis: subjects with left-sided lesions had their fMRI data flipped across the midsagittal plane to evaluate brain regions known to be lateralized relative to somatosensory stimulation (i.e., S1, M1, thalamus). Cluster size represents the number of voxels in the cluster. "P value" represents the cluster probability. "max_z" represents normalized probability. "x, y, z" represent the MNI coordinates of the region's peak voxel from the cluster.

PFC response may also differentiate the underlying analgesic mechanisms for local versus distal EA. Both local and distal EA reduced pain, and we found no differences in brain response between these groups. However, this result does not necessarily suggest that there is no acupoint specificity for brain-linked mediators of acupuncture analgesia in CTS. For instance, greater PFC activation to distal, but not local EA, was associated with greater pain reduction. The tissue at local acupoints (i.e., PC-7) is adjacent to the carpal tunnel, which is known to be perturbed by the increased pressure, fibrosis, swelling, and various biochemical changes within the carpal tunnel [27], while the tissue at distal acupoints is not. Thus, the mechanism by which local EA reduces pain may involve changes in local signaling from the wrist

Table 3: Cortical region significantly correlated with change of pain.

Region	Side	Cluster size	*P* value	max_*z*	MNI (mm)		
					X	*Y*	*Z*
Nonflipped analysis							
Distal							
PFC	R	640	0.00313	−3.36	28	38	20
Verum (local + distal)							
SMA	R/L	788	0.00186	−3.79	0	−30	62
PFC	R	987	0.000342	−3.44	32	48	18
PFC	L	625	0.00826	−3.48	−32	26	38
Flipped analysis							
Verum (local + distal)							
S1	R	198	0.0012	−3.46	32	−26	60

Note: S1: primary somatosensory cortex, SMA: supplementary motor area, PFC: prefrontal cortex. Nonflipped analysis: group map with the original orientation of the data as acquired from the scanner. Flipped analysis: subjects with left-sided lesions had their fMRI data flipped across the midsagittal plane to evaluate brain regions known to be lateralized relative to somatosensory stimulation (i.e., S1, M1, thalamus). Cluster size represents the number of voxels in the cluster. "*P* value" represents the cluster probability. "max_*z*" represents normalized probability. "*x*, *y*, *z*" represent the MNI coordinates of the region's peak voxel from the cluster.

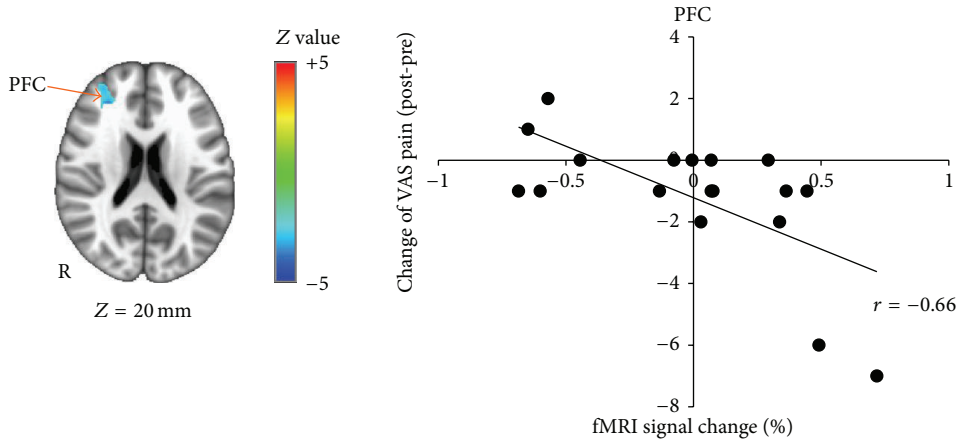

Figure 5: Brain response in right prefrontal cortex correlated with pain reduction in distal group. Brain response in right prefrontal cortex (PFC) was negatively correlated with change in VAS pain score (post-pre) in distal group. Percent signal change in rPFC was extracted from the peak voxel and plotted with change of VAS pain score (post-pre).

lesion (bottom, up), while the mechanism by which distal EA reduces pain may instead involve changes in brain processing (top, down), particularly in the PFC. Interestingly, multiple previous studies have found that PFC activity supports placebo [24, 28] and expectation-mediated analgesia [29]. Future studies should further explore how PFC activity relates to analgesia for different forms of acupuncture and how this is similar to or differs from contextually-mediated analgesic phenomena.

Brain response to verum EA in right S1 was also correlated with pain reduction. We found that greater activation in this region was associated with reduced pain, while more pronounced deactivation was associated with worsening pain following verum EA. The somatotopy of this cluster is consistent with the hand area, which would be ipsilateral for the local group and contralateral (but well outside the leg area) for the distal group. In general, S1 regions outside of the contralateral somatotopic representation for somatosensory stimulated body areas are deactivated [30], and this is clear in the scatterplot for our data as well deactivation is noted in this right S1 cluster for most subjects. Interhemispheric communication modulates subcortical relay of sensory information [31]. Therefore, the balance of left and right S1 activity may modulate the amount of sensory input, which might serve to diminish the spontaneous afferent signal (e.g., pain, paresthesia) from the affected hands in our study.

SMA activation was also correlated with pain reduction following verum EA. SMA is a cortical region that modulates communication between the somatosensory and motor systems and has been shown to be activated by painful stimulation in fMRI [32] and involved in pain control [33]. Greater activation following verum EA may reflect greater transfer of EA-induced somatosensory inputs to the motor system [34], fostering a more normalized sensorimotor communication, compared to the sporadic afference coming from diffuse paresthesia. Thus, EA (whether local or distal) may

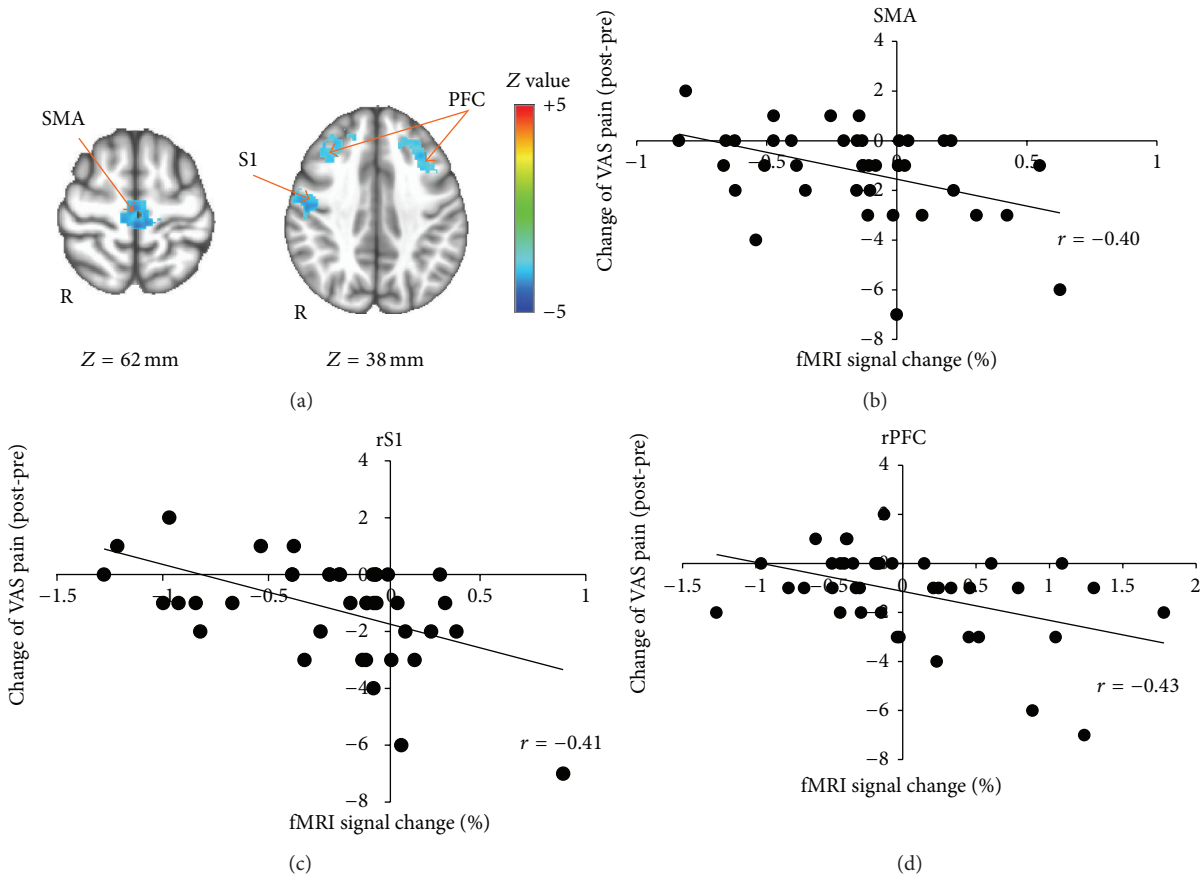

FIGURE 6: Brain response in bilateral SMA, PFC, and right S1 correlated with pain reduction in verum group. Brain response in bilateral SMA, PFC, and right S1 were negatively correlated with changes in VAS pain score (post-pre). fMRI percent signal change in SMA, PFC, and right S1 were extracted from the peak voxel and plotted with change of VAS pain score.

also reduce pain by supplying regulated somatosensory input to the brain.

While verum acupuncture was found to reduce paresthesia significantly more than sham acupuncture, the same was not true for pain. Firstly, these results suggest that compared to pain, paresthesia may be less susceptible to modulation by sham acupuncture. In fact, paresthesia is a hallmark of CTS and other peripheral neuropathic pain disorders stemming from compression of the nerve trunk, and may be more dependent on peripheral factors such as hand positioning and temperature. Our data suggest that reduction of paresthesia is dependent on therapies with significant somatosensory afference, such as verum EA, regardless of whether this afference comes from the site of the lesion. Perception of paresthesia in CTS may be less centralized compared to pain and may thus be less amenable to placebo effects. However, we should also note that controversy regarding the use of sham acupuncture as a control for verum acupuncture exists, as sham procedures are not physiologically inert [35, 36]. In fact, sham acupuncture has been shown to reduce aversive symptom more readily than a placebo pill [37]. Interestingly, while analgesic outcomes may be similar between verum and sham EA, the brain mechanisms supporting this analgesia may differ substantially. In our study, brain response was more profound for verum compared to sham acupuncture, and activity in specific regions in response to verum EA was correlated with pain reductions. These results further support the growing evidence [10] that brain response may serve as an objective marker that differentiates verum and sham acupuncture more readily than subjective pain report does.

Several limitations to our study should be noted. Although brain response to verum or distal EA showed significant correlation with short-term pain reduction, we did not have enough statistical power to show significant correlations between brain response to local or sham EA alone and short-term pain reduction. In addition, our study examined brain response to EA stimulation associated with short-term clinical outcomes, and future studies should extend our analysis to longer-term outcomes. Future studies also should apply alternative fMRI approaches, such as functional connectivity [38], to evaluate how brain connectivity response to both verum and sham acupuncture mediates analgesia in CTS.

In conclusion, EA stimulation at both local and distal acupoints reduced pain, and greater brain activation in PFC, SMA, and S1 was associated with more pronounced pain reduction. Thus, greater PFC, SMA, and S1 activation may support acupuncture analgesia. Brain response in PFC, SMA,

and S1 could serve as predictive biomarkers to identify patients more likely to benefit from acupuncture therapy.

Acknowledgment

This work was supported by NCCAM, National Institutes of Health (R01-AT004714, R01-AT004714-02S1, P01-AT002048).

References

[1] A. J. Vickers, A. M. Cronin, A. C. Maschino et al., "Acupuncture for chronic pain: individual patient data meta-analysis," *Archives of Internal Medicine*, vol. 172, no. 19, pp. 1444–1453, 2012.

[2] M. C. Kiernan, I. Mogyoros, and D. Burke, "Conduction block in carpal tunnel syndrome," *Brain*, vol. 122, no. 5, pp. 933–941, 1999.

[3] C. Yang, C. Hsieh, N. Wang et al., "Acupuncture in patients with carpal tunnel syndrome a randomized controlled trial," *Clinical Journal of Pain*, vol. 25, no. 4, pp. 327–333, 2009.

[4] W. Kumnerddee and A. Kaewtong, "Efficacy of acupuncture versus night splinting for carpal tunnel syndrome: a randomized clinical trial," *Journal of the Medical Association of Thailand*, vol. 93, no. 12, pp. 1463–1469, 2010.

[5] E. Yao, P. K. Gerritz, E. Henricson et al., "Randomized controlled trial comparing acupuncture with placebo acupuncture for the treatment of carpal tunnel syndrome," *PM and R*, vol. 4, no. 5, pp. 367–373, 2012.

[6] W. Huang, D. Pach, V. Napadow et al., "Characterizing acupuncture stimuli using brain imaging with fMRI—a systematic review and meta-analysis of the literature," *PLoS One*, vol. 7, no. 4, Article ID e32960, 2012.

[7] R. P. Dhond, N. Kettner, and V. Napadow, "Neuroimaging acupuncture effects in the human brain," *Journal of Alternative and Complementary Medicine*, vol. 13, no. 6, pp. 603–616, 2007.

[8] W. Zhang, Z. Jin, G. Cui et al., "Relations between brain network activation and analgesic effect induced by low vs. high frequency electrical acupoint stimulation in different subjects: a functional magnetic resonance imaging study," *Brain Research*, vol. 982, no. 2, pp. 168–178, 2003.

[9] J. Yang, F. Zeng, Y. Feng et al., "A PET-CT study on the specificity of acupoints through acupuncture treatment in migraine patients," *BMC Complementary and Alternative Medicine*, vol. 12, article 123, 2012.

[10] R. E. Harris, J. Zubieta, D. J. Scott, V. Napadow, R. H. Gracely, and D. J. Clauw, "Traditional Chinese acupuncture and placebo (sham) acupuncture are differentiated by their effects on μ-opioid receptors (MORs)," *NeuroImage*, vol. 47, no. 3, pp. 1077–1085, 2009.

[11] V. Napadow, N. Kettner, J. Liu et al., "Hypothalamus and amygdala response to acupuncture stimuli in carpal tunnel syndrome," *Pain*, vol. 130, no. 3, pp. 254–266, 2007.

[12] V. Napadow, N. Kettner, A. Ryan, K. K. Kwong, J. Audette, and K. K. S. Hui, "Somatosensory cortical plasticity in carpal tunnel syndrome-a cross-sectional fMRI evaluation," *NeuroImage*, vol. 31, no. 2, pp. 520–530, 2006.

[13] V. Napadow, J. Liu, M. Li et al., "Somatosensory cortical plasticity in carpal tunnel syndrome treated by acupuncture," *Human Brain Mapping*, vol. 28, no. 3, pp. 159–171, 2007.

[14] G. S. Phalen, "The carpal-tunnel syndrome. Seventeen years' experience in diagnosis and treatment of six hundred fifty-four hands," *Journal of Bone and Joint Surgery. American*, vol. 48, no. 2, pp. 211–228, 1966.

[15] J. A. Durkan, "A new diagnostic test for carpal tunnel syndrome," *Journal of Bone and Joint Surgery. American*, vol. 73, no. 4, pp. 535–538, 1991.

[16] D. W. Levine, B. P. Simmons, M. J. Koris et al., "A self-administered questionnaire for the assessment of severity of symptoms and functional status in carpal tunnel syndrome," *Journal of Bone and Joint Surgery. American*, vol. 75, no. 11, pp. 1585–1592, 1993.

[17] R. T. F. Tan, *Acupuncture 1, 2, 3*, Self-Published, San Diego, Calif, USA, 2007.

[18] V. Napadow, J. Lee, J. Kim et al., "Brain correlates of phasic autonomic response to acupuncture stimulation: an event-related fMRI study," *Human Brain Mapping*, 2012.

[19] J. Kong, R. Gollub, T. Huang et al., "Acupuncture De Qi, from qualitative history to quantitative measurement," *Journal of Alternative and Complementary Medicine*, vol. 13, no. 10, pp. 1059–1070, 2007.

[20] D. N. Greve and B. Fischl, "Accurate and robust brain image alignment using boundary-based registration," *NeuroImage*, vol. 48, no. 1, pp. 63–72, 2009.

[21] S. Hayasaka and T. E. Nichols, "Validating cluster size inference: random field and permutation methods," *NeuroImage*, vol. 20, no. 4, pp. 2343–2356, 2003.

[22] J. Lorenz, S. Minoshima, and K. L. Casey, "Keeping pain out of mind: the role of the dorsolateral prefrontal cortex in pain modulation," *Brain*, vol. 126, part 5, pp. 1079–1091, 2003.

[23] A. V. Apkarian, Y. Sosa, S. Sonty et al., "Chronic back pain is associated with decreased prefrontal and thalamic gray matter density," *Journal of Neuroscience*, vol. 24, no. 46, pp. 10410–10415, 2004.

[24] B. Fierro, M. de Tommaso, F. Giglia, G. Giglia, A. Palermo, and F. Brighina, "Repetitive transcranial magnetic stimulation (rTMS) of the dorsolateral prefrontal cortex (DLPFC) during capsaicin-induced pain: modulatory effects on motor cortex excitability," *Experimental Brain Research*, vol. 203, no. 1, pp. 31–38, 2010.

[25] M. F. Dent and D. B. Neill, "Dose-dependent effects of prefrontal dopamine on behavioral state in rats," *Behavioral Neuroscience*, vol. 126, no. 5, pp. 620–639, 2012.

[26] V. Napadow, R. Dhond, K. Park et al., "Time-variant fMRI activity in the brainstem and higher structures in response to acupuncture," *NeuroImage*, vol. 47, no. 1, pp. 289–301, 2009.

[27] R. H. Gelberman, P. T. Hergenroeder, A. R. Hargens, G. N. Lundborg, and W. H. Akeson, "The carpal tunnel syndrome. A study of carpal canal pressures," *Journal of Bone and Joint Surgery. American*, vol. 63, no. 3, pp. 380–383, 1981.

[28] I. Tracey, "Getting the pain you expect: mechanisms of placebo, nocebo and reappraisal effects in humans," *Nature Medicine*, vol. 16, no. 11, pp. 1277–1283, 2010.

[29] T. Koyama, J. G. McHaffie, P. J. Laurienti, and R. C. Coghill, "The subjective experience of pain: where expectations become reality," *Proceedings of the National Academy of Sciences of the United States of America*, vol. 102, no. 36, pp. 12950–12955, 2005.

[30] Y. Hlushchuk and R. Hari, "Transient suppression of ipsilateral primary somatosensory cortex during tactile finger stimulation," *Journal of Neuroscience*, vol. 26, no. 21, pp. 5819–5824, 2006.

[31] L. Li and F. F. Ebner, "Balancing bilateral sensory activity: callosal processing modulates sensory transmission through

the contralateral thalamus by altering the response threshold," *Experimental Brain Research*, vol. 172, no. 3, pp. 397–415, 2006.

[32] R. C. Coghill, C. N. Sang, J. M. Maisog, and M. J. Iadarola, "Pain intensity processing within the human brain: a bilateral, distributed mechanism," *Journal of Neurophysiology*, vol. 82, no. 4, pp. 1934–1943, 1999.

[33] R. Peyron, B. Laurent, and L. García-Larrea, "Functional imaging of brain responses to pain. A review and meta-analysis (2000)," *Neurophysiologie Clinique*, vol. 30, no. 5, pp. 263–288, 2000.

[34] N. Shinoura, Y. Suzuki, R. Yamada, T. Kodama, M. Takahashi, and K. Yagi, "Fibers connecting the primary motor and sensory areas play a role in grasp stability of the hand," *NeuroImage*, vol. 25, no. 3, pp. 936–941, 2005.

[35] I. Lund and T. Lundeberg, "Are minimal, superficial or sham acupuncture procedures acceptable as inert placebo controls?" *Acupuncture in Medicine*, vol. 24, no. 1, pp. 13–15, 2006.

[36] K. Linde, K. Niemann, A. Schneider, and K. Meissner, "How large are the nonspecific effects of acupuncture? A meta-analysis of randomized controlled trials," *BMC Medicine*, vol. 8, article 75, 2010.

[37] T. J. Kaptchuk, W. B. Stason, R. B. Davis et al., "Sham device versus inert pill: randomised controlled trial of two placebo treatments," *British Medical Journal*, vol. 332, no. 7538, pp. 391–394, 2006.

[38] R. P. Dhond, C. Yeh, K. Park, N. Kettner, and V. Napadow, "Acupuncture modulates resting state connectivity in default and sensorimotor brain networks," *Pain*, vol. 136, no. 3, pp. 407–418, 2008.

Hindawi Publishing Corporation
Evidence-Based Complementary and Alternative Medicine
Volume 2013, Article ID 628907, 9 pages
http://dx.doi.org/10.1155/2013/628907

Review Article

Placebo Acupuncture Devices: Considerations for Acupuncture Research

Dan Zhu,[1,2] Ying Gao,[1] Jingling Chang,[1] and Jian Kong[2]

[1] *Department of Neurology, Dongzhimen Hospital, Beijing University of Chinese Medicine, No. 5 Haiyuncang, Dongcheng District, Beijing 100700, China*
[2] *Department of Psychiatry, Massachusetts General Hospital, Harvard Medical School, Boston, MA 02129, USA*

Correspondence should be addressed to Ying Gao; gaoying973@126.com

Received 8 March 2013; Accepted 24 May 2013

Academic Editor: Lijun Bai

Determining an appropriate control for use in acupuncture research remains one of the largest methodological challenges acupuncture researchers face. In general, acupuncture controls fall under one of two categories: (1) sham acupuncture, in which the skin is punctured with real acupuncture needles either fully at nonacupoint locations or shallowly at acupoint locations or both and (2) placebo acupuncture, which utilizes nonpenetrating acupuncture devices. In this study, we will focus on non-penetrating placebo acupuncture devices (blunted-needle and nonneedle devices) that are currently available in acupuncture research. We will describe each device and discuss each device's validation and application in previous studies. In addition, we will outline the advantages and disadvantages of these devices and highlight how the differences among placebo devices can be used to isolate distinct components of acupuncture treatment and investigate their effects. We would like to emphasize that there is no single placebo device that can serve as the best control for all acupuncture studies; the choice of an acupuncture control should be determined by the specific aim of the study.

1. Introduction

Over the past decades, acupuncture treatment has gained popularity in the Western world due to its therapeutic effect. However, studies have achieved contradictory results when using control treatments to test the true efficacy of acupuncture. Studies consistently show that both real and placebo acupuncture treatments confer significant benefits over no-treatment control conditions [1, 2], and while some studies have suggested that real acupuncture is significantly more effective than placebo acupuncture [3–5], others have failed to demonstrate the benefit of real acupuncture over placebo acupuncture [6–9]. Although the reasons for such contradictory results remain unclear, these results call for further investigation of sham/placebo controls in acupuncture research.

Placebo research has revealed several important variables related to acupuncture treatment that can be either modulated or held constant between verum (real) and placebo (control) conditions in order to test the effects of specific and nonspecific components of acupuncture. In general, acupuncture involves the insertion of needles into the body; thus, one of the components of verum acupuncture is skin penetration. While this particular component is not held constant between verum and non-penetrating acupuncture controls, there are several other variables that can be either held constant or modulated, which include sensory stimulation, dose (number of needles), acupoint location, practitioner-patient interaction, and treatment setting.

In acupuncture research, double-blinded randomized clinical trials (RCTs) serve as the gold standard when comparing the effects of a specific treatment to the effects of a placebo control. In acupuncture RCTs, it is ideal for the control treatment to be both physiologically inert and indistinguishable from the real treatment. Thus, an effective inert treatment in the control condition is essential in order for a double-blinded RCT to achieve a high level of scientific validity. Determining the proper inert control for an RCT designed to evaluate the efficacy of acupuncture is methodologically challenging for three main reasons.

(1) It is difficult to create an inert control device that mimics both the visual appearance of the acupuncture treatment device and the method of needle insertion involved in acupuncture treatment.

(2) It is challenging to develop an inert acupuncture device that can control for all nonspecific factors involved in an acupuncture treatment. The therapeutic effect of acupuncture relies on several nonspecific factors, including the ritual procedure of acupuncture administration, the patient-practitioner interaction, the nature of the illness, the treatment, and the treatment setting [10]. The microtrauma resulting from piercing the skin also induces a variety of nonspecific physiological responses involving the microcirculation, local immune function, and neurally mediated analgesic effects [11, 12].

(3) It is challenging to make the acupuncturist who is directly administrating the acupuncture blind to treatment condition.

As a result, over the years, investigators have used a variety of controls in their studies to account for these challenges in terms of their own specific study aims. In acupuncture research, placebo controls for acupuncture studies fall under one of two categories: (1) sham acupuncture, in which the skin is punctured with real acupuncture needles either fully at nonacupoint locations or shallowly at acupoint locations, or both and (2) placebo acupuncture, which utilizes non-penetrating acupuncture devices. In this review, we will focus only on non-penetrating placebo acupuncture devices, including blunted needle and nonneedle devices that are currently available for use in acupuncture research.

2. Placebo Acupuncture Devices

2.1. Blunted Needle Acupuncture Devices

2.1.1. The Streitberger Device

Description. In 1998, Streitberger and Kleinhenz [13] designed a blunted-needle placebo device, comprised of a copper handle and a stainless steel needle with a blunt tip designed to retract inside the handle (Figure 1). When the blunt tip is pressed against the skin, the patient feels a slight pricking sensation, which mimics the sensation elicited by a verum needle but does not actually puncture the skin. As the blunt tip is pressed onto the skin, the needle retracts into the handle, creating the appearance of penetration. This device is anchored in a plastic ring on the skin surface and held in place with surgical tape or plaster.

Validation/Application. The results from the first validation study of the Streitberger device [13] indicate that subjects in this study could not differentiate between verum acupuncture and the Streitberger device. In this crossover study, 60 healthy subjects, blinded to treatment condition, were asked to evaluate subjective ratings of acupuncture sensations using a visual analog scale (VAS) after both the placebo and verum acupuncture treatment.

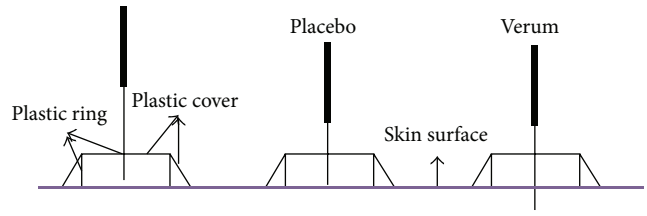

Figure 1: *The Streitberger device*. The Streitberger placebo device uses a short blunt needle within a thin handle. A plastic ring covered with a plastic sheath is used to keep the needle in place.

Subsequently, the Streitberger device has been used as a control in acupuncture research [14–21] and clinical trials covering a range of indications [22, 23], resulting in a variety of findings. After the initial crossover experiment, Streitberger and colleagues conducted several trials in other clinical populations, the results of which indicated that the true efficacy of acupuncture may be specific to certain ailments [24]. For example, the investigators found verum acupuncture to be slightly more effective ($P = .07$) than placebo acupuncture in relieving postoperative nausea and vomiting prophylaxis in patients undergoing gynecological surgery but not for those undergoing breast surgery ($P = .86$) [24]. Results from another RCT conducted by Schneider and colleagues [25] suggest that the efficacy of acupuncture treatment for irritable bowel syndrome is primarily a placebo response. In one randomized trial [26], 52 males with rotator cuff tendinitis underwent 4 weeks of treatment, either with penetrating (verum) or non-penetrating (the Streitberger device) acupuncture, and were asked to rate their pain using the modified Constant-Murley shoulder outcomes scale (including pain, function, range of motion, and strength). The verum acupuncture group showed significantly more improvement in subjective pain ratings compared to the placebo acupuncture control.

2.1.2. Park Device

Description. Park and colleagues [27] invented a placebo device intended to stabilize the needle (either penetrating or blunted) in position with an additional plastic tube (Figure 2). The Park device consists of two tubes. The guide tube holds the needle perpendicular to the skin and is fitted within the Park tube, a larger tube fixed to the ring base, so that the standard guide tube slides freely within the Park tube. A silicon base rests under the ring base and adheres to the skin with double-sided tape. The acupuncturist positions the needle perpendicular to the skin and taps the handle of the needle in a precise imitation of the insertion of a real acupuncture needle. When a verum needle is used within the Park device, the needle is long enough to penetrate the skin. A placebo needle, in contrast, is too short to penetrate the skin through the Park device. After positioning the needle it may then be manipulated by lifting, thrusting, or rotating.

Unlike the Streitberger device, the Park device includes a Park tube that holds the placebo needle more firmly in

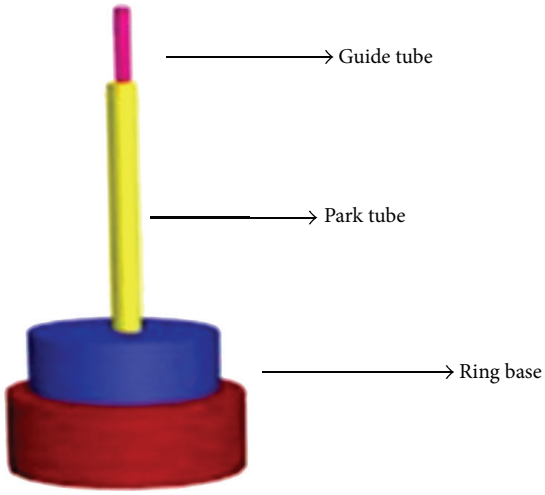

Figure 2: *The Park device*. The Park device is a placebo device that employs an oversize guide tube. The device adheres to the skin with double-sided tape. A second guide tube provides more stability, sliding to fit within the Park tube.

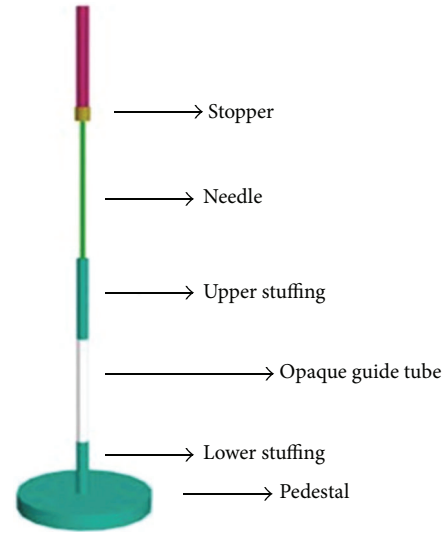

Figure 3: *The Japanese device*. The Japanese device is comprised of an opaque guide tube and an upper stuffing. The stopper prevents the needle handle from advancing further. In addition, the placebo contains stuffing at the bottom to provide a sensation similar to that of skin puncture and tissue penetration.

place and facilitates lifting and thrusting, a common manual stimulation technique in acupuncture. Due to the fact that the guide tube is fixed to the skin, the Park device cannot be used to insert the needle at certain angles or depths. This limitation is problematic when using acupoints requiring shallow or horizontal insertion.

Validation/Application. The Park device was validated in two separate studies by Park and colleagues in 2002 [28]. The first study involved 58 acute stroke patients and the second involved 63 healthy acupuncture-naive volunteers. The purpose of these validation studies was to test the Park device in both a patient population and in healthy volunteers (aged 16 years and older) in order to assess whether the device was indistinguishable from verum acupuncture (study 1) and whether the device was "active" (i.e., whether it elicited sensations (deqi) specific to the needling action) when applied at the Hegu (LI4) point (study 2). The results of this RCT suggested that the Park device was both "indistinguishable" and "inactive" when employed. But there are some problems when using the Park device. For example, it may be more difficult to maintain participant blinding when using the Park device on traditional acupoints compared to nontraditional acupuncture points [29], or on the upper limb (i.e., Triple Energizer Meridian) acupoints compared to the lower limb acupoints (i.e., Bladder Meridian) [30].

Since the original validation studies, the Park device has been used in several acupuncture RCTs as a placebo acupuncture control [31–34]. For instance, in one RCT [35], the authors compared the efficacy of verum acupuncture (56 stroke patients) and the Park device (60 stroke patients) and they found that verum acupuncture was not superior to placebo treatment in terms of improvements in health-related quality of life after suffering a stroke.

2.1.3. Japanese Device

Description. The Japanese device, which employs a non-penetrating placebo needle (Figure 3), was designed by Takakura and Yajima for use in double-blind trials [36]. Like the needle of the Park and Streitberger devices, the tip of the placebo needle in the Japanese device makes non-penetrating contact with the skin. The Japanese device can be used with both verum and placebo needles and blinding of both patients and acupuncturists can be maintained. To our knowledge, the Japanese device is the only needle device that can maintain both patient's and acupuncturist's blinding. The verum and placebo needles used in the Japanese device differ in length. When a placebo needle is employed, the presence of the lower stuffing provides a substrate into which the needle can be inserted. When the verum needle is used, the sharp tip penetrates the skin. Inserting the needle into the lower stuffing of the placebo device produces a sensation similar to the sensation of skin being punctured for the patient and the sensation of tissue penetration for the acupuncturist, which allows both patient and acupuncturist to remain blinded to treatment condition. Both needles have a stopper that prevents the needle handle from advancing beyond the specified position of the penetrating needle or the non-penetrating needle. Due to fixed needle length and stuffing position, the Japanese device, like the Park device, is restricted in its ability to simulate traditional needle manipulation methods and various angles of insertion. This device requires custom manufacturing. Currently, it is only available for use by the inventor-investigators and awaits validation by other clinical trials.

Validation/Application. Investigations of the validity of the Japanese device suggest that it is quite indistinguishable from

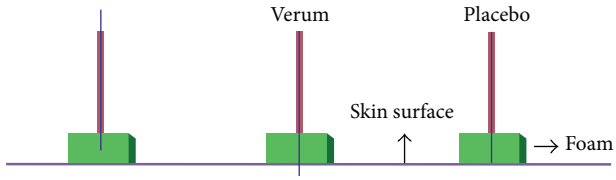

Figure 4: *Foam device*. The foam placebo (one example shown here) device uses a blunted needle inserted through a piece of elastic foam.

a verum device. In one study, the authors found that both experienced acupuncturists and acupuncture-experienced subjects made statistically equal numbers of correct and incorrect judgments of needle type (verum or Japanese device) after administration of treatments [37]. In another study, practitioners made more incorrect judgments than correct judgments [38] suggesting that this device was effective at maintaining practitioner's blinding.

2.1.4. Foam Device

Description. There are several versions of the foam device used for placebo acupuncture treatment (see Figure 4 for one example). This device involves the use of a blunted needle and a cube of elastic foam for needle positioning. The acupuncturist must first fix the foam on a specified acupoint. In contrast to the verum acupuncture device, in which the sharp needle is inserted into skin through the foam, the placebo device holds the blunted needle within the foam. Compared with other devices, the foam device is simple and inexpensive. There are many variations of this device, so the specific design of the device must be taken into consideration. The Goddard device [39], for example, has no needle stopper, so it is the acupuncturist's responsibility to stop pushing the needle when s/he perceives that the placebo needle has touched the skin. Similarly, other foam devices require the acupuncturist to be careful during needle rotation not to advance the needle too far, in order to avoid skin contact entirely [40]. For all of the foam devices, the foam pad visually conceals the needle's point of entry, so that the subject cannot discern which technique is being used; it also helps to hold the needle in place so that it appears identical to real acupuncture needle positioning.

Validation/Application. In one randomized single-blind validation study, 49 healthy subjects were divided into two treatment groups: acupuncture group and placebo group. Goddard and colleagues [39] demonstrated that subjects were not able to differentiate between verum and placebo acupuncture. Placebo acupuncture was conducted by lightly pricking the skin with a shortened, blunted acupuncture needle through a foam pad, without penetrating the skin.

In a study of 36 rheumatoid arthritis patients conducted by Tam and colleagues [40], investigators adhered a standard cube of foam material (2 cm × 2 cm × 2 cm) to the skin around the acupoint visible to patients. The recipient could not see the depth of the needle since the cube of foam hid the tip of the needles.

In another validation study using a crossover design [41], 32 healthy volunteers were randomly first assigned to either a verum acupuncture group or a placebo acupuncture group. After 30 minutes, the subjects received another modality of treatment. The main outcome measurement was a self-report questionnaire of deqi sensations. In this study, an adhesive patch made of two pieces of high-density foam, 13 mm in length, 5 mm in height, and 12.7 mm in width was perforated in order to hold a needle guidance tube. The guide tube sufficiently masked the needle from view such that subjects were not able to determine whether they were receiving real or placebo acupuncture when the patch was placed on the skin. In this study, a shortened needle with a blunted tip was used in order to avoid pricking the skin after tapping the needle. In this crossover study, there were no significant differences in ability to differentiate between the real and placebo needles before or after subjects received their second acupuncture condition. These results suggest that this method is credible for the subjects and constitutes a simple, inexpensive technique in use as a control in clinical research with a population of acupuncture-naive subjects.

2.1.5. Other Nonpenetrating Needle Devices

Description. Multiple investigators have designed their own noninvasive needle-delivering apparatuses using blunted needles, toothpicks, or plastic guide tubes. These devices are simple, easy to manipulate, and do not require extra equipment. These control devices are designed to be as effective, inert, and indistinguishable as the devices that have preceded them; however, they do not mimic the appearance of the verum acupuncture devices with regard to needle insertion and therefore must be kept outside of the subject's visual range. They can be applied to the neck, back, and any other body region that the subject cannot see. If visible acupoints must be targeted, subjects' eyes must be covered to prevent unblinding.

Application. The blunted needle device employs a needle, with the tip removed. The blunt tip of this specialized needle prevents the needle from penetrating the skin. The cut ends are manually smoothed with sandpaper under sterile conditions. The acupuncturist mimics needle insertion by applying the sparrow pecking technique (i.e., rapid stimulation of a single acupoint with the blunt tip of the needle) [4, 42].

Plastic guide tubes are also used as placebo devices, as they provide the sensation of acupuncture stimulation but do not penetrate the skin [43]. The plastic guide tube can also be combined with a blunted needle or toothpick to further provide the sensation of acupuncture stimulation [3, 7, 44–47].

Trials involving these devices are difficult to replicate because the devices are not standardized. Since the majority of these trials have not been precisely replicated (i.e., the devices are slightly different), the validity of the results of RCTs that use these devices remains to be tested.

2.2. Nonneedle Acupuncture Devices

2.2.1. Transcutaneous Electrical Nervous Stimulation (TENS)

Description. Transcutaneous electrical nerve stimulation (TENS) is the application of a mild electrical current to the cutaneous nerve fibers using surface electrodes. It is characterized by current, pulse width, and frequency. The amplitude of the current is usually adjusted to just above or below sensory threshold. The duration of stimulation varies from a short period of time (e.g., 20 minutes) to continuous stimulation (e.g., 60 minutes or even longer). The placebo TENS device uses a nonfunctional TENS apparatus with no electrical stimulation. While the efficacy of verum TENS remains unknown, the placebo TENS device is an example of a double-blind placebo device that can act as a control to estimate the efficacy of the verum device because it is visually indistinguishable from the verum device. TENS differs entirely from needle acupuncture and thus the placebo TENS device may best serve as a control for verum TENS trials.

A new variation of TENS device worth noting is a special electrode designed for ear stimulation. It consists of two pair carbon-impregnated silicone electrodes fixed to one ear clamp; only one pair of the electrodes is connected to the electrical wire. Given that the electrode wiring is imbedded in the clamp, this design allows for subject and practitioner blinding [48].

Validation/Application. In an early double-blinded validation study on TENS-naive chronic low back pain patients, real TENS was compared to sham TENS. The results showed that every patient in the real TENS group believed the unit was functioning correctly with varying degrees of certainty. In the sham TENS group, 84% patients believed they have a functioning unit, with significant lower certainty level [49].

Several subsequent clinical trials have employed placebo TENS to investigate the efficacy of verum TENS. In a study of chronic back pain, a 2 × 2 factorial design was used to compare TENS, placebo TENS, exercise, and no exercise. No superior benefit was found for verum TENS over placebo TENS using a VAS of pain ratings and other clinical outcome measures [50].

In another study, verum TENS versus placebo TENS was studied in patients with multiple sclerosis and chronic low back pain. After correcting for multiple comparisons, there were no significant differences on pain visual analog scale and other self-evaluation scales between the verum and placebo TENS groups [51].

In one study, investigators studied the efficacy of TENS compared to placebo TENS and a control no-treatment group in a population of patients with chronic low back pain. Average pain ratings collected immediately before and after each treatment demonstrated a significant reduction in pain in both the verum and placebo TENS groups. Pain intensity was reduced significantly more for those in the TENS group compared to the placebo TENS group. Additionally, investigators studied the additive effects of 10-week treatment (administered twice weekly) and found that TENS but not placebo TENS demonstrated a reduction in pain intensity over the first 16 treatments. Similarly, verum TENS was more effective than placebo TENS in maintaining pain reduction one week after the last treatment. The benefit in pain reduction continued for 3 and 6 months after completion of the study regardless of whether subjects received verum or placebo TENS treatment. The no-treatment control condition, in contrast, demonstrated no natural improvement in pain over the same course of time [52].

2.2.2. Laser Acupuncture

Description. Laser acupuncture is defined as the stimulation of traditional acupuncture points with low-intensity, nonthermal laser irradiation. Verum laser acupuncture produces a wavelength of infrared laser light. Both verum and placebo laser acupuncture are manufactured with visual red light and acoustic signal.

Validation/Application. In 2001, Irnich and colleagues [53] were the first investigators to adopt the placebo laser acupuncture device. They used placebo laser acupuncture as the inert control in a study that compared conventional massage with acupuncture (verum needle and placebo laser acupunctures) for the treatment of chronic neck pain. The placebo laser acupuncture was performed with an inactive laser pen, which produced a red light with no infrared properties. The results from this study suggest that needle acupuncture is significantly more effective than massage and equally as effective as a short-term treatment for patients with chronic neck pain, indicating that placebo laser acupuncture might share some of the same nonspecific effects with needle acupuncture.

The validity of the placebo laser acupuncture as a general acupuncture control was thoroughly discussed in an article written by Irnich et al. [54]. In another study they also investigated the validity of the placebo laser acupuncture device as a laser acupuncture control. The results of this randomized, double-blind crossover study suggested that placebo laser acupuncture produces the same nonspecific effects as laser acupuncture. Additionally, there were no significant differences between the efficacy ratings of acupuncture-experienced and acupuncture-naive subjects in this study. Neither the subject nor the treating acupuncturists were able to distinguish between the real and placebo laser devices. Over the years, this device has been applied in several trials to treat diseases such as acute tonsillitis, and pharyngitis, vasomotor rhinitis and whiplash injuries [55–58].

3. Discussion

Finding a proper control remains a primary methodological concern in acupuncture research. Traditionally, two main categories of acupuncture control have existed: (1) sham acupuncture, which involves the use of real needles that puncture the skin and (2) placebo acupuncture, which is nonpenetrating. Sham acupuncture utilizes penetrating needles that are either applied fully to nonacupoints or shallowly to acupoints or both [8]. But the problem is that it can

Table 1: Considerations for use of placebo devices in acupuncture research.

Types of device	Considerations									
	Visually indistinguishable	Somato-sensation	Constraint of needle insertion	Commercial availability	Self-made	Modality specific	Price	Reusable	Appropriate for double-blind study design	Appropriate for crossover study design
Blunted needles devices										
The Steitberger device	√			√		√	\$6.3 per needle			
The Park device	√		√	√		√	\$2.9 per needle			
The Japanese device	√		√			√	NA		√	
Foam device	√		√		√		NA	√		
Others	√				√		NA	√		
Nonneedle devices										
Placebo TENS	√		NA	√		√	\$59 to \$260 per unit	√	√	√
Placebo laser acupuncture	√	√	NA	√		√	\$hundred to thousand per unit	√	√	√

Prices according to Google Shopping. The actual prices may vary across vendors.

be difficult to find a noninfluential site on the skin that is not near other acupoint, and shallow needling can resemble some traditional Chinese acupuncture techniques. Several studies, however, have indicated that sham acupuncture can also produce a therapeutic response and elicit neurobiological responses at various levels in the central nervous system [59].

Thus, a placebo acupuncture device may be a more appropriate control for verum acupuncture because it minimizes the physiologic response and is relatively inert. In this paper, we have described a range of placebo acupuncture devices currently used in acupuncture research. Table 1 lists the relative advantages and disadvantages of the devices, as well as the common and unique aspects of the devices as discussed below. With this table, we seek to highlight some of the considerations investigators should take when designing their placebo-controlled acupuncture studies.

Placebo acupuncture is generally noninvasive. The blunted needles used in these devices are relatively inert and indistinguishable from real acupuncture needles. The Streitberger, Park, and Japanese devices are three of the most commonly used placebo needle devices in acupuncture research. The Japanese device is the only needling device that can be employed in double-blinded trials. All three of these devices are used in a similar manner; a blunted needle is inserted, touches the skin, and is retracted. These three devices, while standardized and validated, are not widely available for researchers worldwide since they are custom fabricated. Aside from the Streitberger device, all other placebo devices have physical limitations with regard to their ability to facilitate a range of manipulation methods, such as shallow or horizontal insertion. They are also not effective for all acupoint types and acupuncture positions. The foam device, simple toothpick, and blunted needle device are not standardized and thus cannot be validated. Since these devices have not been validated, the quality of the results from RCTs using these devices remains unconfirmed.

All placebo needle devices involve contact with the skin. Physical contact with the surface of the skin may provide sensory stimulation, indicating that even blunted needle devices are not entirely inert and may elicit a therapeutic effect of their own. For instance, Han and Lund et al. noted that the sensation produced by a needle tip "touch" was substantial [60] and it may activate parts of the peripheral nervous system [61]. Thus, using blunted needle devices on nonacupoints in acupuncture studies might make the placebo acupuncture relatively inert.

The response to placebo acupuncture treatment is due to a variety of factors, including the presence or absence of deqi sensations. The deqi phenomenon is a complex set of physiological sensations associated with acupuncture treatment [14, 62]. Those who have experienced acupuncture deqi sensations prior to treatment are often cognizant of the absence of deqi when they receive placebo acupuncture treatment. For instance, in one single-blind randomized, crossover pilot study [63] that involved patients with chronic pain receiving both verum and placebo acupuncture treatment, subjects who received the placebo treatment first thought that they were receiving verum treatment after one single treatment. However, after the second treatment, nearly 40% of those

same subjects were able to detect a difference between the two needles. Thus, it is also important to measure the deqi sensation in acupuncture clinical trials even when sham devices are applied. In light of this finding, some investigators [46] choose to exclude patients with previous acupuncture experience.

Similar to other longitudinal treatment studies involving placebo treatments, maintaining patient's blinding throughout a treatment study involving multiple acupuncture treatments can be difficult. All blunted needle placebo acupuncture devices can be useful in short-term, acute intervention trials. However, in conditions requiring long-term treatment, maintaining patient's blinding may be difficult due to the subjects' natural curiosity and/or motivation to learn more about the type of treatment they have been receiving, which can lead to unblinding (e.g., patients may talk to each other, read about acupuncture, or go to another acupuncturist). It is important for investigators to assess whether or not the subject blinding can be maintained through the end of the study.

Unlike verum acupuncture, some placebo devices require tape or foam for successful application of the placebo treatment. Devices that require tape or foam may induce allergic reactions and thus may not be tolerated by all subjects. In addition, there is risk of infection if the needle were to be inserted through the tape and thus it is necessary to use sterile techniques. Additionally, these devices may not be suitable for all acupoints, such as points on the scalp, fingers, and toes that cannot provide a flat surface for tape or foam.

"Nonneedle" placebo acupuncture devices (TENS and laser acupuncture) have their own set of common considerations. Neither placebo TENS nor laser acupuncture provide repeated needle stimulation of the skin and thus are relatively physiologically inert. Nonneedle placebo devices are also effective for both acupuncture-experienced and acupuncture-naive subjects. The major disadvantage of nonneedle devices like TENS and laser acupuncture is that they differ from verum needle acupuncture in design and concept, as well as in context and culture. Therefore, placebo TENS and placebo laser acupuncture may only be considered to serve as valid placebo controls in TENS and laser acupuncture studies, respectively.

Finally, we would like to emphasize that this paper is developed to aid investigators in designing studies that test and explore the efficacy and mechanism of acupuncture and to facilitate the selection of appropriate acupuncture placebo devices. The most appropriate placebo acupuncture devices are those that are the most indistinguishable and inert in consideration of the specific design on the study.

Acknowledgments

The authors thank the valuable suggestions, comments, and English editing form Sonya Freeman, Rosa Spaeth, and Lisette Roman in the Department of Psychiatry, Massachusetts General Hospital. This work was supported by the National Science Foundation of China (Grant no. 81072768), New Century Excellent Talents in University of Ministry of Education of China (Grant no. NCET-11-0603), Chinese Medicine Clinical Evaluation Research Team in Brain Disease of Beijing University of Chinese Medicine (Grant no. 2011-CXTD-22), R01AT006364, R21AT004497, and R03AT218317 to Jian Kong, and P01AT006663 to Bruce Rosen.

References

[1] S. Ballegaard, T. Muteki, H. Harada et al., "Modulatory effect of acupuncture on the cardiovascular system: a cross-over study," *Acupuncture and Electro-Therapeutics Research*, vol. 18, no. 2, pp. 103–115, 1993.

[2] R. M. Coan, G. Wong, and S. Liang Ku, "The acupuncture treatment of low back pain: a randomized controlled study," *American Journal of Chinese Medicine*, vol. 8, no. 1-2, pp. 181–189, 1980.

[3] B. M. Berman, L. Lao, P. Langenberg, W. L. Lee, A. M. K. Gilpin, and M. C. Hochberg, "Effectiveness of acupuncture as adjunctive therapy in osteoarthritis of the knee. A randomized, controlled trial," *Annals of Internal Medicine*, vol. 141, no. 12, pp. 901–910, 2004.

[4] K. Itoh, Y. Katsumi, S. Hirota, and H. Kitakoji, "Effects of trigger point acupuncture on chronic low back pain in elderly patients—a sham-controlled randomised trial," *Acupuncture in Medicine*, vol. 24, no. 1, pp. 5–12, 2006.

[5] A. J. Vickers, A. M. Cronin, A. C. Maschino et al., "Acupuncture for chronic pain: individual patient data meta-analysis," *Archives of Internal Medicine*, vol. 172, no. 19, pp. 1444–1453, 2012.

[6] A. R. White, K.-L. Resch, J. C. K. Chan et al., "Acupuncture for episodic tension-type headache: a multicentre randomized controlled trial," *Cephalalgia*, vol. 20, no. 7, pp. 632–637, 2000.

[7] N. P. Assefi, K. J. Sherman, C. Jacobsen, J. Goldberg, W. R. Smith, and D. Buchwald, "A randomized clinical trial of acupuncture compared with sham acupuncture in fibromyalgia," *Annals of Internal Medicine*, vol. 143, no. 1, pp. 10–19, 2005.

[8] M. Haake, H. Müller, C. Schade-Brittinger et al., "German Acupuncture Trials (GERAC) for chronic low back pain: randomized, multicenter, blinded, parallel-group trial with 3 groups," *Archives of Internal Medicine*, vol. 167, no. 17, pp. 1892–1898, 2007.

[9] D. C. Cherkin, K. J. Sherman, A. L. Avins et al., "A randomized trial comparing acupuncture, simulated acupuncture, and usual care for chronic low back pain," *Archives of Internal Medicine*, vol. 169, no. 9, pp. 858–866, 2009.

[10] T. J. Kaptchuk, "The placebo effect in alternative medicine: can the performance of a healing ritual have clinical significance?" *Annals of Internal Medicine*, vol. 136, no. 11, pp. 817–825, 2002.

[11] D. E. Kendall, "A scientific model for acupuncture," *American Journal of Acupuncture*, vol. 7, no. 3, pp. 251–268, 1989.

[12] D. B. Le, L. Villaneuva, J. Willer et al., "Diffuse noxious inhibitory control (DNIC) in man and animals," *Acupuncture in Medicine*, no. 9, pp. 47–57, 1991.

[13] K. Streitberger and J. Kleinhenz, "Introducing a placebo needle into acupuncture research," *The Lancet*, vol. 352, no. 9125, pp. 364–365, 1998.

[14] J. Kong, D. T. Fufa, A. J. Gerber et al., "Psychophysical outcomes from a randomized pilot study of manual, electro, and sham acupuncture treatment on experimentally induced thermal pain," *Journal of Pain*, vol. 6, no. 1, pp. 55–64, 2005.

[15] C. A. McManus, R. N. Schnyer, J. Kong et al., "Sham acupuncture devices—practical advice for researchers," *Acupuncture in Medicine*, vol. 25, no. 1-2, pp. 36–40, 2007.

[16] J. Kong, T. J. Kaptchuk, G. Polich et al., "Expectancy and treatment interactions: a dissociation between acupuncture analgesia and expectancy evoked placebo analgesia," *NeuroImage*, vol. 45, no. 3, pp. 940–949, 2009.

[17] J. Kong, R. L. Gollub, I. S. Rosman et al., "Brain activity associated with expectancy-enhanced placebo analgesia as measured by functional magnetic resonance imaging," *The Journal of Neuroscience*, vol. 26, no. 2, pp. 381–388, 2006.

[18] D. D. Dougherty, J. Kong, M. Webb, A. A. Bonab, A. J. Fischman, and R. L. Gollub, "A combined [11C]diprenorphine PET study and fMRI study of acupuncture analgesia," *Behavioural Brain Research*, vol. 193, no. 1, pp. 63–68, 2008.

[19] J. Kong, T. J. Kaptchuk, G. Polich et al., "An fMRI study on the interaction and dissociation between expectation of pain relief and acupuncture treatment," *NeuroImage*, vol. 47, no. 3, pp. 1066–1076, 2009.

[20] J. Kong, R. L. Gollub, G. Polich et al., "A functional magnetic resonance imaging study on the neural mechanisms of hyperalgesic nocebo effect," *The Journal of Neuroscience*, vol. 28, no. 49, pp. 13354–13362, 2008.

[21] C. E. Zyloney, K. Jensen, G. Polich et al., "Imaging the functional connectivity of the Periaqueductal Gray during genuine and sham electroacupuncture treatment," *Molecular Pain*, vol. 6, article 80, 2010.

[22] A. D. Wasan, J. Kong, L. Pham, T. J. Kaptchuk, R. Edwards, and R. L. Gollub, "The impact of placebo, psychopathology, and expectations on the response to acupuncture needling in patients with chronic low back pain," *Journal of Pain*, vol. 11, no. 6, pp. 555–563, 2010.

[23] T. J. Kaptchuk, J. M. Kelley, L. A. Conboy et al., "Components of placebo effect: randomised controlled trial in patients with irritable bowel syndrome," *British Medical Journal*, vol. 336, no. 7651, pp. 999–1003, 2008.

[24] K. Streitberger, M. Diefenbacher, A. Bauer et al., "Acupuncture compared to placebo-acupuncture for postoperative nausea and vomiting prophylaxis: a randomised placebo-controlled patient and observer blind trial," *Anaesthesia*, vol. 59, no. 2, pp. 142–149, 2004.

[25] A. Schneider, P. Enck, K. Streitberger et al., "Acupuncture treatment in irritable bowel syndrome," *Gut*, vol. 55, no. 5, pp. 649–654, 2006.

[26] J. Kleinhenz, K. Streitberger, J. Windeler, A. Gußbacher, G. Mavridis, and E. Martin, "Randomised clinical trial comparing the effects of acupuncture and a newly designed placebo needle in rotator cuff tendinitis," *Pain*, vol. 83, no. 2, pp. 235–241, 1999.

[27] J. Park, A. White, H. Lee, and E. Ernst, "Development of a new sham needle," *Acupuncture in Medicine*, vol. 17, no. 2, pp. 110–112, 1999.

[28] J. Park, A. White, C. Stevinson, E. Ernst, and M. James, "Validating a new non-penetrating sham acupuncture device: two randomised controlled trials," *Acupuncture in Medicine*, vol. 20, no. 4, pp. 168–174, 2002.

[29] C. Tan, L. Christie, V. St-Georges, and N. Telford, "Discrimination of real and sham acupuncture needles using the park sham device: a preliminary study," *Archives of Physical Medicine and Rehabilitation*, vol. 90, no. 12, pp. 2141–2145, 2009.

[30] C. Tan, P. Sheehan, and D. Santos, "Discrimination accuracy between real and sham needles using the Park sham device in the upper and lower limbs," *Acupuncture in Medicine*, vol. 29, no. 3, pp. 208–214, 2011.

[31] L. M. Pastore, C. D. Williams, J. Jenkins, and J. T. Patrie, "True and sham acupuncture produced similar frequency of ovulation and improved LH to FSH ratios in women with polycystic ovary syndrome," *Journal of Clinical Endocrinology and Metabolism*, vol. 96, no. 10, pp. 3143–3150, 2011.

[32] P. Smith, D. Mosscrop, S. Davies, P. Sloan, and Z. Al-Ani, "The efficacy of acupuncture in the treatment of temporomandibular joint myofascial pain: a randomised controlled trial," *Journal of Dentistry*, vol. 35, no. 3, pp. 259–267, 2007.

[33] C. A. Whale, S. J. A. MacLaran, C. I. Whale, and M. Barnett, "Pilot study to assess the credibility of acupuncture in acute exacerbations of chronic obstructive pulmonary disease," *Acupuncture in Medicine*, vol. 27, no. 1, pp. 13–15, 2009.

[34] Y. Chae, H. Lee, H. Kim, H. Sohn, J. Park, and H. Park, "The neural substrates of verum acupuncture compared to non-penetrating placebo needle: an fMRI study," *Neuroscience Letters*, vol. 450, no. 2, pp. 80–84, 2009.

[35] J. Park, A. R. White, M. A. James et al., "Acupuncture for subacute stroke rehabilitation: a sham-controlled, subject- and assessor-blind, randomized trial," *Archives of Internal Medicine*, vol. 165, no. 17, pp. 2026–2031, 2005.

[36] N. Takakura and H. Yajima, "A double-blind placebo needle for acupuncture research," *BMC Complementary and Alternative Medicine*, vol. 7, article 31, 2007.

[37] N. Takakura and H. Yajima, "A placebo acupuncture needle with potential for double blinding—a validation study," *Acupuncture in Medicine*, vol. 26, no. 4, pp. 224–230, 2008.

[38] N. Takakura, M. Takayama, A. Kawase, T. J. Kaptchuk, and H. Yajima, "Double blinding with a new placebo needle: a further validation study," *Acupuncture in Medicine*, vol. 28, no. 3, pp. 144–148, 2010.

[39] G. Goddard, Y. Shen, B. Steele, and N. Springer, "A controlled trial of placebo versus real acupuncture," *Journal of Pain*, vol. 6, no. 4, pp. 237–242, 2005.

[40] L. Tam, P. Leung, T. K. Li, L. Zhang, and E. K. Li, "Acupuncture in the treatment of rheumatoid arthritis: a double-blind controlled pilot study," *BMC Complementary and Alternative Medicine*, vol. 7, article 35, 2007.

[41] M. Kreiner, A. Zaffaroni, R. Alvarez, and G. Clark, "Validation of a simplified sham acupuncture technique for its use in clinical research: a randomised, single blind, crossover study," *Acupuncture in Medicine*, vol. 28, no. 1, pp. 33–36, 2010.

[42] T. Nabeta and K. Kawakita, "Relief of chronic neck and shoulder pain by manual acupuncture to tender points—a sham-controlled randomized trial," *Complementary Therapies in Medicine*, vol. 10, no. 4, pp. 217–222, 2002.

[43] M. Inoue, H. Kitakoji, N. Ishizaki et al., "Relief of low back pain immediately after acupuncture treatment—a randomised, placebo controlled trial," *Acupuncture in Medicine*, vol. 24, no. 3, pp. 103–108, 2006.

[44] E. A. Tough, A. R. White, S. H. Richards, B. Lord, and J. L. Campbell, "Developing and validating a sham acupuncture needle," *Acupuncture in Medicine*, vol. 27, no. 3, pp. 118–122, 2009.

[45] K. J. Sherman, C. J. Hogeboom, D. C. Cherkin, and R. A. Deyo, "Description and validation of a noninvasive placebo acupuncture procedure," *Journal of Alternative and Complementary Medicine*, vol. 8, no. 1, pp. 11–19, 2002.

[46] L. Lao, S. Bergman, G. R. Hamilton, P. Langenberg, and B. Berman, "Evaluation of acupuncture for pain control after oral surgery: a placebo-controlled trial," *Archives of Otolaryngology*, vol. 125, no. 5, pp. 567–572, 1999.

[47] L. Lao, S. Bergman, P. Langenberg, R. H. Wong, and B. Berman, "Efficacy of Chinese acupuncture on postoperative oral surgery pain," *Oral Surgery, Oral Medicine, Oral Pathology, Oral Radiology and*, vol. 79, no. 4, pp. 423–428, 1995.

[48] P. Rong, J. Fang, J. Kong et al., "Trancutanous vagus nerve stimulation for the treatment of depression: a study protocol for a double blinded randomized clinical trails," *BMC Complementary and Alternative Medicine*, vol. 12, no. 1, article 255, 2012.

[49] R. A. Deyo, N. E. Walsh, L. S. Schoenfeld, and S. Ramamurthy, "Can trials of physical treatments be blinded? The example of transcutaneous electrical nerve stimulation for chronic pain," *American Journal of Physical Medicine and Rehabilitation*, vol. 69, no. 1, pp. 6–10, 1990.

[50] R. A. Deyo, N. E. Walsh, D. C. Martin, L. S. Schoenfeld, and S. Ramamurthy, "A controlled trial of transcutaneous electrical nerve stimulation (TENS) and exercise for chronic low back pain," *The New England Journal of Medicine*, vol. 322, no. 23, pp. 1627–1634, 1990.

[51] J. Al-Smadi, K. Warke, I. Wilson et al., "A pilot investigation of the hypoalgesic effects of transcutaneous electrical nerve stimulation upon low back pain in people with multiple sclerosis," *Clinical Rehabilitation*, vol. 17, no. 7, pp. 742–749, 2003.

[52] S. Marchand, J. Charest, J. Li, J.-R. Chenard, B. Lavignolle, and L. Laurencelle, "Is TENS purely a placebo effect? A controlled study on chronic low back pain," *Pain*, vol. 54, no. 1, pp. 99–106, 1993.

[53] D. Irnich, N. Behrens, H. Molzen et al., "Randomised trial of acupuncture compared with conventional massage and "sham" laser acupuncture for treatment of chronic neck pain," *British Medical Journal*, vol. 322, no. 7302, pp. 1574–1578, 2001.

[54] D. Irnich, N. Salih, M. Offenbacher et al., "Is sham laser a valid control for acupuncture trials?" *Evidence-Based Complementary and Alternative Medicine*, vol. 2011, Article ID 485945, 8 pages, 2011.

[55] J. Fleckenstein, C. Lill, R. Lüdtke, J. Gleditsch, G. Rasp, and D. Irnich, "A single point acupuncture treatment at large intestine meridian a randomized controlled trial in acute tonsillitis and pharyngitis," *Clinical Journal of Pain*, vol. 25, no. 7, pp. 624–631, 2009.

[56] J. Fleckenstein, C. Raab, J. Gleditsch et al., "Impact of acupuncture on vasomotor rhinitis: a randomized placebo-controlled pilot study," *Journal of Alternative and Complementary Medicine*, vol. 15, no. 4, pp. 391–398, 2009.

[57] N. Aigner, C. Fialka, C. Radda, and V. Vecsei, "Adjuvant laser acupuncture in the treatment of whiplash injuries: a prospective, randomized placebo-controlled trial," *Wiener Klinische Wochenschrift*, vol. 118, no. 3-4, pp. 95–99, 2006.

[58] X. Shen, L. Zhao, G. Ding et al., "Effect of combined laser acupuncture on knee osteoarthritis: a pilot study," *Lasers in Medical Science*, vol. 24, no. 2, pp. 129–136, 2009.

[59] J. Zhang and X. Cao, "Neuronal specificity of needling acupoints at same meridian: a control functional magnetic resonance imaging study with electroacupuncture," *Acupuncture and Electro-Therapeutics Research*, vol. 32, no. 3-4, pp. 179–193, 2007.

[60] J. Han, "Acupuncture analgesia: areas of consensus and controversy," *Pain*, vol. 152, supplement 3, pp. S41–S48, 2011.

[61] I. Lund, J. Näslund, and T. Lundeberg, "Minimal acupuncture is not a valid placebo control in randomised controlled trials of acupuncture: a physiologist's perspective," *Chinese Medicine*, vol. 4, article 1, 2009.

[62] J. Kong, R. Gollub, T. Huang et al., "Acupuncture De Qi, from qualitative history to quantitative measurement," *Journal of Alternative and Complementary Medicine*, vol. 13, no. 10, pp. 1059–1070, 2007.

[63] P. White, G. Lewith, V. Hopwood, and P. Prescott, "The placebo needle, is it a valid and convincing placebo for use in acupuncture trials? A randomised, single-blind, cross-over pilot trial," *Pain*, vol. 106, no. 3, pp. 401–409, 2003.

Hindawi Publishing Corporation
Evidence-Based Complementary and Alternative Medicine
Volume 2013, Article ID 808971, 9 pages
http://dx.doi.org/10.1155/2013/808971

Research Article

Hypothalamus-Related Resting Brain Network Underlying Short-Term Acupuncture Treatment in Primary Hypertension

Hongyan Chen,[1] Jianping Dai,[1,2] Xiaozhe Zhang,[3] Kai Wang,[1] Shuhua Huang,[4] Qingtian Cao,[4] Hong Wang,[5] Yuhong Liang,[5] Chuanying Shi,[6] Mengyuan Li,[1] Tingting Ha,[1] Lin Ai,[1,2] Shaowu Li,[1,2] Jun Ma,[1] Wenjuan Wei,[7] Youbo You,[7] Zhenyu Liu,[7] Jie Tian,[7] and Lijun Bai[8]

[1] *Department of Radiology, Beijing Tiantan Hospital Affiliated to Capital Medical University, Tiantan Xili No. 6, Beijing 100050, China*
[2] *Beijing Neurosurgery Institute, Tiantan Xili No. 6, Beijing 100050, China*
[3] *Department of Pain, Beijing Tiantan Hospital Affiliated to Capital Medical University, Tiantan Xili No. 6, Beijing 100050, China*
[4] *Department of Medicine, China North Vehicle Research Institute Worker's Hospital, Huaishuling No. 4, Fengtai District, Beijing 100072, China*
[5] *Tiantan Community Health Service Center, Fenchang Hutong No. 57, Dongcheng District, Beijing 100061, China*
[6] *Ultrasonic Center, Beijing Tiantan Hospital Affiliated to Capital Medical University, Tiantan Xili No. 6, Beijing 100050, China*
[7] *Institute of Automation, Chinese Academy of Sciences, Beijing 100190, China*
[8] *The Key Laboratory of Biomedical Information Engineering of Ministry of Education, Department of Biomedical Engineering, School of Life Science and Technology, Xi'an Jiaotong University, Xi'an 710049, China*

Correspondence should be addressed to Jianping Dai; jpdai2008@yahoo.cn and Lijun Bai; bailj4152615@gmail.com

Received 22 February 2013; Revised 31 March 2013; Accepted 11 April 2013

Academic Editor: Baixiao Zhao

The present study attempted to explore modulated hypothalamus-seeded resting brain network underlying the cardiovascular system in primary hypertensive patients after short-term acupuncture treatment. Thirty right-handed patients (14 male) were divided randomly into acupuncture and control groups. The acupuncture group received a continuous five-day acupuncture treatment and undertook three resting-state fMRI scans and 24-hour ambulatory blood pressure monitoring (ABPM) as well as SF-36 questionnaires before, after, and one month after acupuncture treatment. The control group undertook fMRI scans and 24-hour ABPM. For verum acupuncture, average blood pressure (BP) and heart rate (HR) decreased after treatment but showed no statistical differences. There were no significant differences in BP and HR between the acupuncture and control groups. Notably, SF-36 indicated that bodily pain ($P = 0.005$) decreased and vitality ($P = 0.036$) increased after acupuncture compared to the baseline. The hypothalamus-related brain network showed increased functional connectivity with the medulla, brainstem, cerebellum, limbic system, thalamus, and frontal lobes. In conclusion, short-term acupuncture did not decrease BP significantly but appeared to improve body pain and vitality. Acupuncture may regulate the cardiovascular system through a complicated brain network from the cortical level, the hypothalamus, and the brainstem.

1. Introduction

Hypertension is a common chronic disease affecting one-third of all adults worldwide and causing 51% of stroke deaths and 45% of coronary heart disease deaths in 2012 [1]. Investigating hypertension relief has therefore gained increasing attention and interest.

Acupuncture has emerged as a common alternative or complementary therapeutic intervention in western medicine. Reports have stated that acupuncture has certain curative effects for high BP and cardiac pain, with few side effects observed [2]. Despite its public acceptance, unequivocal scientific explanations regarding the mechanism underlying

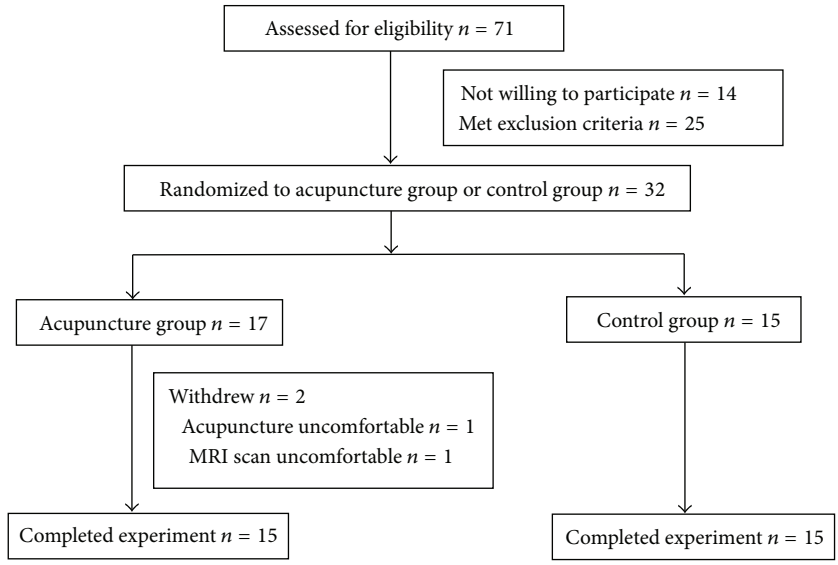

Figure 1: Participants flowchart diagram.

acupuncture in high BP treatment has not been attained and awaits further investigation.

In the recent years, the therapeutic effect of acupuncture in lowering BP has been investigated and discussed in many case reports and small-scale clinical trials [3–7], as well as several large-scale clinical trials on hypertension with acupuncture treatments [8–10]. However, these studies have only focused on the efficacy of acupuncture, and the mechanism of acupuncture in hypertension relief remains unknown.

In the past two decades, converging evidence from fMRI studies has demonstrated that acupuncture stimulation can modulate neural activities in a wide cortical-subcortical network, particularly the limbic system [11–19]. In practice, the well-identified physical effects of acupuncture and its purported clinical efficacy also suggest that it helps maintain a homeostatic balance of the internal state within and across multiple brain systems. Evidence from animal studies has demonstrated that acupuncture stimulation can facilitate the release of certain neuropeptides in the central nervous system (CNS), eliciting profound physiological effects and even activating self-healing mechanisms [20, 21]. Electroacupuncture studies in rats revealed that both low-frequency and high-frequency stimulation induced analgesia, but differential effects existed in low- and high-frequency acupuncture on the types of endorphins released [20]. Peripheral acupuncture stimulation in deeper areas also activated various brain structures, such as the limbic, hypothalamic, and brainstem neural nuclei [21].

The present study attempted to investigate short-term acupuncture treatment in hypertension relief using resting state fMRI combined with a 24-hour ABPM. The aim was to (i) observe if short-term acupuncture decreased BP of hypertensive patients and improved quality of life and (ii) determine the possible mechanism of short-term acupuncture for treating hypertension in the hypothalamus-related brain network.

2. Materials and Methods

2.1. Participants. We recruited hypertensive participants from the Beijing Dongcheng District Tiantan community health service center and Fengtai District 201 community hospital. The eligibility criteria included (1) clinical diagnosis in line with WHO diagnostic criteria of essential hypertension: systolic blood pressure (SBP) ≥140 mmHg and diastolic blood pressure (DBP) ≥90 mmHg without antihypertensive drugs, two or more repeated measurements, normal BP now with the use of antihypertensive drugs but with a clear history of hypertension, and species and dose of antihypertensive medicine not changed or suspended or not taking antihypertensive drugs during the study period [8, 9]; (2) 30–75 years old; (3) without cerebral infarction history and without cerebral infarction by MRI preliminary screening; (4) without nervous system disease, mental disease, diabetes, or other serious illness; (5) no drug addiction history; (6) no MRI contraindication and acupuncture contraindication; (7) no acupuncture experience over the past year; (8) right-handed by Edinburgh handedness questionnaire [19]; (9) provision of informed consent. The exclusion criteria included (1) could not receive acupuncture; (2) any unsuitable situation in the study. The drop-off criteria are as follows: (1) hypertensive crisis or other emergency; (2) could not adhere to acupuncture treatment. The present study was according to the principles of the Declaration of Helsinki (Version Edinburgh 2000).

Of the 71 participants recruited, only 30 (14 male, 35–74 years, mean age of 56.73 ± 9.29 years) met the eligibility criteria and finished the experiment (Figure 1). All subjects

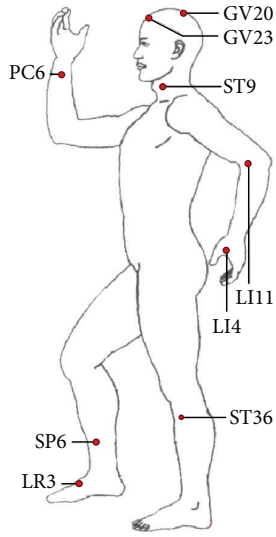

Figure 2

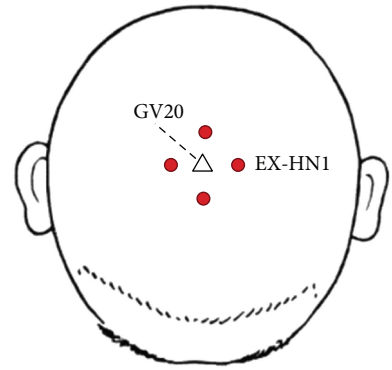

Figure 3

were randomly divided into the acupuncture group and the control group, with 15 participants in each.

2.2. Acupuncture Interventions. Participants underwent five acupuncture treatments over five consecutive days, with each session lasting about 30 minutes. During each treatment, seven acupoints used to treat hypertension in clinical settings were selected and needled bilaterally (except single points like GV20 (baihui), GV23 (shangxing), and four points EX-HN1 (sishencong)), including ST9 (renying), LI11 (quchi), PC6 (neiguan), LI4 (hegu), ST36 (zusanli), SP6 (sanyinjiao), and LR3 (taichong) [10, 22] (Figures 2 and 3). After local skin disinfection, sterile acupuncture needles (0.2 mm in diameter, 40 mm long, Hua tuo acupuncture needles, Suzhou, China) were inserted into the skin to a depth of 15–50 mm according to different acupoints and were gently twisted in a mild reinforcing-reducing method 4–6 times till a *deqi* response was obtained. Control group participants did not receive acupuncture treatment and took medicine according to their original treatment programs. The acupuncture procedure was performed by the same experienced and licensed acupuncturist (15 years of experience) on all subjects.

Figures 2 and 3 show needling acupoints for hypertension treatment. GV20 (baihui) is located in the center of the head; EX-HN1 (sishencong) includes four acupoints located around GV20, each about 3 cm to GV20; ST9 (renying) is located in the neck, beside the Adam's apple, in the midpoint of the leading edge of the sternocleidomastoid; LI11 (quchi) is located in the outer end of the elbow stripes; LI4 (hegu) is located in the back of the hand, between the first and second metacarpal, radial side of the midpoint of the second metacarpal; PC6 (neiguan) is located in the volar forearm, about 6 cm above the wrist stripes between tendon and radial measured wrist flexor tendon; ST36 (zusanli) is located in the anterolateral leg, between the tibialis anterior muscle and extensor digitorum longus, about 10 cm below the knee, about 1.5 cm from the tibia leading edge; SP6 (sanyinjiao) is located in the medial leg, about 10 cm above the medial condyle tip; LR3 (taichong) is located in the dorsal foot and the first metatarsal gap rear depression.

2.3. Data Acquisition. The participants were scanned in a 3.0 Tesla Siemens Trio MR whole body scanner. A foam pillow and a band across the forehead were used to fix the head. Resting state functional images were acquired with a single-shot gradient recalled echo planar imaging sequence. The sequence covered the whole brain, axial view, parallel to the AC-PC line, TR = 2000 ms, TE = 30 ms, measurement = 240, resolution = 64 × 64, field of view (FOV) = 240 mm × 240 mm, flip angle = 90°, slice thickness = 5 mm without gap, 32 slices, and scan time = 8,06 minutes. A set of T1-weighted high-resolution structural images were collected using a 3D MPRAGE sequence for anatomical localization. TR = 1900 ms, TE = 2.39 ms, field of view (FOV) = 256 mm × 256 mm, flip angle = 7°, in-plane resolution = 1 mm × 1 mm, slice thickness: 1 mm without gap, 32 slices, and scan time = 8,26 minutes.

2.4. Experiment Workflow. The experiment workflow is shown in Figure 3. The first MRI scan adopted the T2WI sequence to exclude participants with cerebral infarction. Participants who met the inclusion criteria underwent resting state fMRI and 3D T1WI structure sequences. The second and third MRI scans were only performed in the resting state fMRI sequence. The BP and heart rate (HR) of the participants were measured three times before and after every MRI scan, with the average taken for the three measurements. Participants sat quietly for 5 minutes before each measurement. We used a MOBIL GRAPH sphygmomanometer (Germany) to monitor 24-hour ambulatory blood pressure (ABMP). The BP and HR of the participants were also tested three times before and after every acupuncture treatment, with the average taken for the three recordings.

The acupuncture group received 24-hour ABMP and an MRI scan at multiple time points (before acupuncture, after acupuncture, and one month later). The control group only received 24-hour ABMP and one MRI scan. During the study period, participants maintained their original treatments, and drug type and dosage were not modified except for

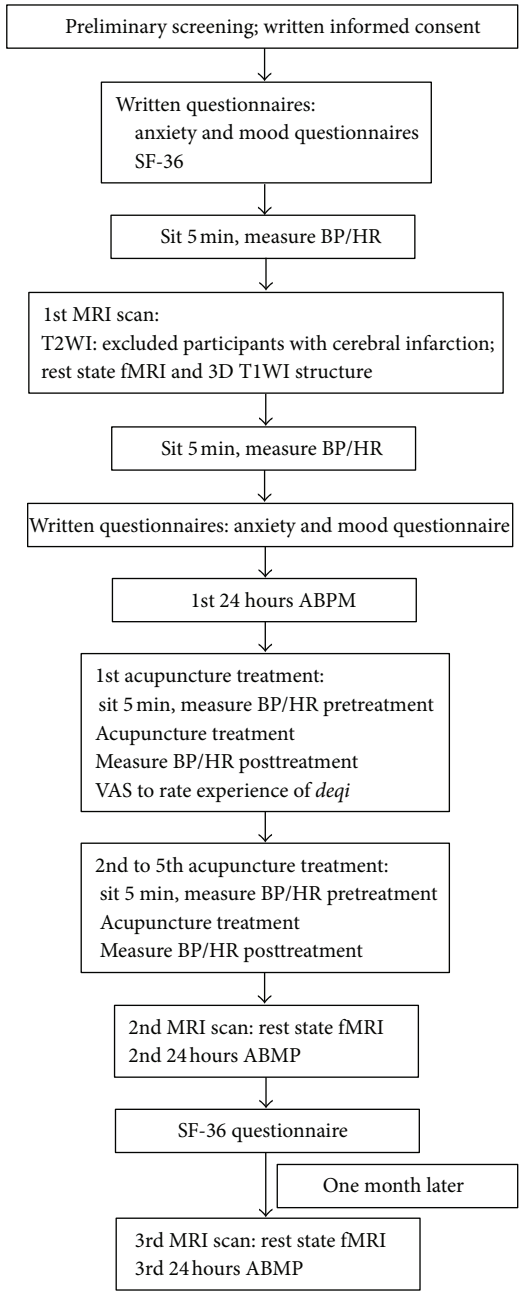

Figure 4: Experimental workflow.

emergency situations (SBP ≥ 180 mmHg, DBP ≥ 110 mmHg, or other emergency situations). In case of emergency, the participants were moved into the drop-off group.

At the end of the first acupuncture treatment, the participants completed a questionnaire using a 10-point visual analog scale (VAS) to rate the experience of *deqi* during intervention. The questionnaire included aching, pressure, heaviness, coolness, soreness, fullness, numbness, warmth, tingling, dull pain, and sharp pain. The VAS was defined as 0 = no sensation, 1–3 = mild, 4–6 = moderate, 7-8 = strong, 9 = severe, and 10 = unbeatable sensation.

Considering that BP and HR can be easily affected by psychological factors, such as affective states and anxiety, participants filled out questionnaires for assessments of anxiety (State Trait Anxiety Inventory (STAI)) [23] and affective state (BFS mood survey) [24]. To evaluate quality of life (QoL), subjects also completed questionnaires on MOS item short from health survey (SF-36) [25] before and after acupuncture treatment in the acupuncture group. The control group participants also completed the SF-36 (see Figure 4).

2.5. Statistical Analysis

2.5.1. Physiological Data. Since 24-hour ABMP is affected by movement and other factors, the data collected from each participate was not exactly the same. Therefore, we selected independent sample t-tests to compare the physiological data and paired t-tests to analyze the SF-36 survey. We used SPSS 13.0 for statistical analyses, with $P < 0.05$ indicating statistical difference and $P < 0.01$ indicating significant statistical difference.

2.5.2. Image Preprocessing. All preprocessing steps were carried out using statistical parametric mapping (SPM5, http://www.fil.ion.ucl.ac.uk/spm/). Functional images were preprocessed using sinc interpolation for slice scan time correction, trilinear sinc interpolation for alignment (motion correction) of functional volumes, and high-pass temporal filtering to 1 Hz to remove slow drifts in the data. The image data were further processed with spatial normalization based on the MNI space and resampled at 2 mm × 2 mm × 2 mm. Poststimuli resting data were also filtered using a band pass filter (0.01~0.08 Hz) to reduce low-frequency drift and high-frequency noise. Finally, the functional images were spatially smoothed with a 6 mm full width at half maximum (FWHM) Gaussian kernel. All resting state functional images were preprocessed using Statistical Parametric Mapping 5 (SPM5) and included motion correction, normalization, and smoothing.

2.5.3. Functional Connectivity Analysis. For each subject, the "seeding" time courses of the hypothalamus were, respectively, cross-correlated with all low-pass filtered voxels to generate functional connectivity maps within each of the three conditions. This approach was termed within-condition interregional covariance analysis (WICA). The resulting correlation coefficient r-maps were normalized and corrected to roughly standard normal distributions using methods previously described. The normality of the distribution was then tested using Kurtosis tests ($P < 0.001$). The three z-maps of each individual were entered into one-sample t-tests, respectively, to determine whether group data was significantly different from zero. For visualization, all connectivity results were transformed into the Talairach stereotactic space and overlaid on MRIcro (http://www.mccauslandcenter.sc.edu/CRNL/) for presentation purposes. All resulting t-maps were then cluster-filtered to remove correlations involving less than three contiguous voxels and then superimposed on high-resolution anatomical images using a $P < 0.001$ cutoff threshold (uncorrected).

Table 1: Physiological data of acupuncture and control groups.

	SBP (mmHg)	SD	DBP (mmHg)	SD	HR (bpm)	SD
ACU						
B	127.13	5.52	81.71	8.40	71.50	8.67
A	126.74	7.93	80.86	13.36	69.83	9.53
L	123.22	9.47	81.11	16.23	69.98	9.60
CON	133.40	18.58	80.93	11.49	72.71	6.43

ACU: acupuncture group; CON: control group; B: before acupuncture; A: after acupuncture; L: one month later.

The above image processing programs were coded in MATLAB7 (MathWorks, Inc.).

3. Results

3.1. Physiological Data. Average BP at different time points for the acupuncture and control groups are shown in Table 1. Two independent sample t-tests were used to compare the BP and HR between the two groups, $t = -1.529$, $P = 0.127$, with no statistical differences observed in physiological data, indicating comparable balance in the two groups.

Comparison between acupuncture treatment before and after showed that the average SBP, DBP, and HR tended to decrease after acupuncture, although no statistical differences were observed (Table 2). Comparison between the acupuncture and control group showed that average SBP, DBP, and HR demonstrated no statistical differences between the two groups (Table 3).

In the SF-36 survey for QoL, participants in the acupuncture group reported increased scores of bodily pain (baseline: mean ± SD, 79.4 ± 12.3 versus after acupuncture: mean ± SD, 87.0 ± 10.6, $P = 0.005$) and vitality (80.0 ± 15.9 versus 83.2 ± 11.9, $P = 0.036$). Changes in physical functioning (92.7 ± 11.9 versus 92.7 ± 11.9), role physical (76.7 ± 38.3 versus 78.3 ± 35.2, $P = 0.582$), general health (67.0 ± 15.2 versus 68.7±13.9, $P = 0.334$), social functioning (96.7± 23.36 versus 98.3 ± 19.4, $P = 0.334$), role emotional (91.1 ± 26.6 versus 93.3 ± 25.8, $P = 0.334$), and mental health (70.4 ± 12.9 versus 71.2 ± 12.5, $P = 0.082$) did not differ among participants.

3.2. Connectivity Mapping. At the baseline, the hypothalamus showed prominently spontaneous activations associated with limbic, cortical, and subcortical regions ($P < 0.001$), including the bilateral cerebellum, middle brain, bilateral insula, thalamus, and most of the frontal lobes. These results demonstrated a hypothalamus-anchored resting brain network under baseline conditions. Conversely, spontaneous deactivation was mainly located in the left cerebella vermis, as well as the left superior and right inferior frontal gyrus.

After acupuncture treatment, these spontaneous activation and deactivation networks anchored by the hypothalamus remained relatively stable (Figure 5, $P < 0.001$). In comparison with baseline conditions, however, we also identified significant changes (both in spatial distributions and response magnitudes) after acupuncture treatment. There were prominently increased spontaneous activations in the bilateral cerebellum, brainstem, limbic system (bilateral insula, hippocampus, amygdala, and cingulate cortex), bilateral thalamus, and bilateral frontal lobes. Enhanced deactivations were located in the bilateral cerebellum, bilateral frontal lobes, and right parietal gyrus.

Results from after and before acupuncture showed a wide range activation of brain regions (Figure 5). Notably, the most modulated changes were exhibited in the cerebellum, brainstem, insula, and frontal lobe. Increased positive correlations were primarily located in the cerebellum, limbic system (insula, parahippocampal gyrus, and cingulate cortex), bilateral thalamus, and frontal lobes. It is also worth noting that enhanced deactivation was only identified in the temporal lobe, left posterior cingulum, and right parietal lobe. Results from the acupuncture and control groups also showed significant differences in the cerebellum, amygdala, brain stem, and insula, and frontal lobes (see Figure 6).

4. Discussion

The present short-term acupuncture intervention study used common acupoints to clinically treat hypertension once a day over five consecutive days. After acupuncture, no statistical differences were found in SBP, DBP, and HR between the before acupuncture and control groups. However, average SBP, DBP, and HR did decrease after acupuncture treatment. The SF-36 survey from the acupuncture group showed statistical differences in body pain and vitality after acupuncture compared to the baseline. Our results did not indicate any differential benefit of short-term acupuncture for controlling BP and HR, but it may improve quality of life for patients in relation to body pain and vitality. This is the first study to investigate the hypothalamus-anchored brain network involving acupuncture treatments for hypertension.

Several large scale hypertension studies have investigated and discussed the therapeutic effects of acupuncture treatment. Flachskampf et al. [8] randomized 160 hypertensive participants in a single-blind 6-week trial using active or sham acupuncture and found significant ($P < 0.001$) differences in posttreatment BP between the two groups. Yin et al. [9] recruited 41 hypertensive or prehypertensive patients and designed a randomized, double-blind, placebo-controlled trial. All subjects were randomly assigned into real or sham acupuncture groups, and after 8 weeks of intervention, the mean BP of the acupunctured group was

Table 2: Physiological data comparison of acupuncture group (independent t-test).

	SBP				DBP				HR			
	t value	P value	95% CI		t value	P value	95% CI		t value	P value	95% CI	
B-A	0.453	0.658	−5.090	3.327	1.194	0.254	−2.967	0.855	1.647	0.124	−0.493	3.657
B-L	1.278	0.242	−3.321	11.138	0.008	0.994	−5.871	5.910	1.021	0.341	−1.996	5.029
A-L	0.935	0.361	0.609	6.992	−0.802	0.449	−16.831	8.307	−0.119	0.908	−3.227	2.917

B: before acupuncture; A: after acupuncture; L: one month later.

Table 3: Physiological data comparisons between acupuncture and control group (independent t-test).

	SBP				DBP				HR			
	t value	P value	95% CI		t value	P value	95% CI		t value	P value	95% CI	
B-C	−1.900	0.076	−19.976	1.118	0.207	0.838	−7.031	8.602	−0.074	0.941	−6.144	5.715
A-C	−1.646	0.117	−19.451	2.360	0.453	0.655	−6.521	10.205	−0.656	0.517	−7.422	3.830
L-C	−1.774	0.091	−26.264	2.126	0.030	0.976	−12.157	12.511	−0.802	0.432	−9.837	4.376

B: before acupuncture; A: after acupuncture; L: one month later; C: control group.

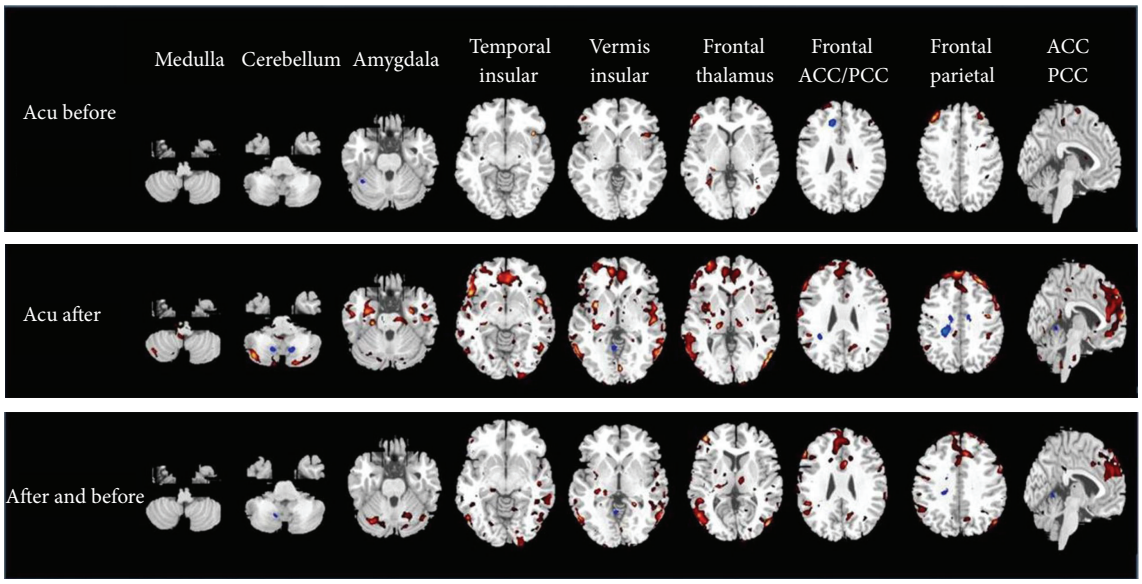

Figure 5: Functional connectivity anchored with the hypothalamus after and before acupuncture treatment.

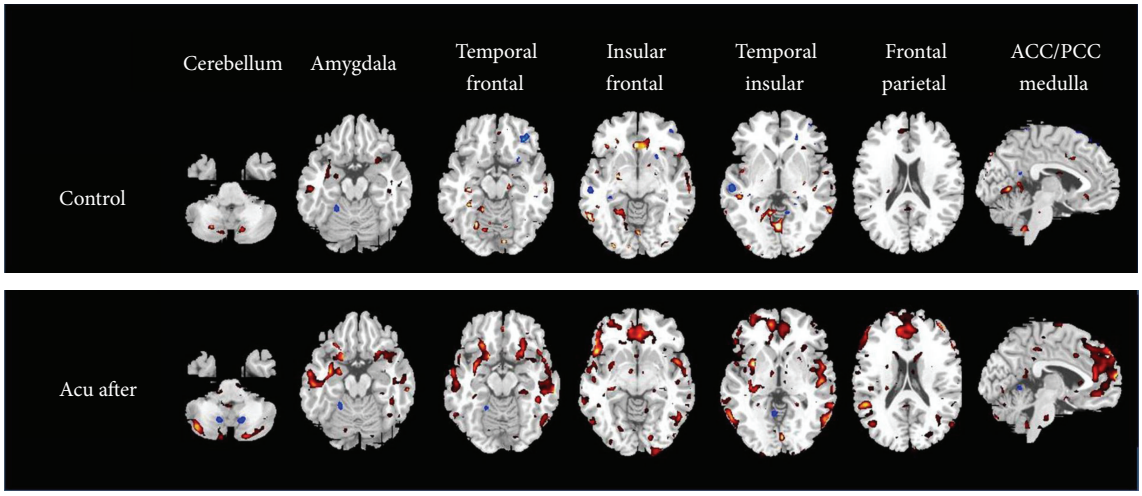

Figure 6: Functional connectivity anchored with the hypothalamus resulting from acupuncture control.

significantly decreased ($P < 0.01$). The Stop Hypertension with Acupuncture Research Program (SHARP) [10] showed there were no significant differences in BP decrease in the individualized traditional Chinese acupuncture group (IND), standardized acupuncture group (STD), and invasive sham acupuncture group (CNTL). Despite there being no statistically significant differences, mean decreases in BP after 10 weeks of treatment were observed between active (IND and STD) and sham acupuncture in comparison to the baseline in the SHARP study. The trials of Flachskampf et al. [8] and Yin et al. [9] showed a decrease in BP after acupuncture, but SHARP [10] only showed a downtrend without statistical differences. In previous studies, we found that the Flachskampf's and Yin's studies were long term with intensive frequency of acupuncture treatment, while the SHARP study was long term with infrequent acupuncture treatment. Acupuncture in our study was short term and intensive, which resulted in no significant differences between acupuncture and control group. Considering that acupuncture has sustained and cumulative effects, short term use may lead to inconsistent results. We therefore speculated that the efficacy of frequent, long-term acupuncture would be better than long interval use or short-term treatment in hypertensive patients.

The cardiovascular center is mainly located in the medulla oblongata and hypothalamus, and these areas are not in the default brain network [26]. Many electrophysiological studies [27–31] have shown that the hypothalamus may be a key hub in the CNS in relation to cardiovascular regulation. Thus, we selected the hypothalamus as the seed point region to explore modulated brain network changes underlying acupuncture hypertension treatment. Our results suggested that increased functional connectivity existed between the hypothalamus and other regions after acupuncture. The functional connection with the hypothalamus was enhanced in some areas, mainly in the bilateral frontal lobe (vmPFC, dlPFC), limbic system (bilateral insula, amygdala, hippocampus, anterior cingulate cortex, and posterior cingulate cortex), bilateral cerebellum, and medulla oblongata. The central regulatory region of the cardiovascular system is very wide from brainstem to cortex, and includes the medulla oblongata, pons (locus coeruleus), midbrain (periaqueductal gray, substantia nigra), and limbic system (hypothalamus, the amygdaloid, subfornical organ, and insula), which together make up a complete network [27]. The medulla oblongata is the basic center, which includes the rostral ventrolateral medulla (vasoconstriction), ventrolateral part of the medulla oblongata (vasodilation), ambiguous nucleus and dorsal nucleus of the vagus nerve (restrains heart function), and tractus solitarius medulla oblongata (afferent nerve terminal) [28]. Past research has indicated that the medulla oblongata regulates the cardiovascular system through neurotransmitters such as glutamate, P substance and γ-aminobutyric acid [29–31].

Previous studies on electrophysiology have shown that the periaqueductal gray (PAG), hypothalamus, and other parts of the limbic system were important parts of the cardiovascular center [32–40] through different neurotransmitters, adjusting the sympathovagal balance to regulate the cardiovascular system. Many projection fibers are found between the ventrolateral medulla, PAG, and hypothalamus arcuate nucleus for their closely interconnected, and adjusted the cardiovascular system in common [32–34]. The limbic system also plays an important part in BP regulation in the CNS. Some parts are involved in step-up regulation, such as the paraventricular nucleus, lateral hypothalamus/perifornical area, dorsomedial nucleus, ventromedial nucleus, posterior hypothalamic nucleus, lateral septum ventrolateral part/habenular body, subfornical organ, and the central amygdala and insula, while the anteroventral third ventricle area (AV3V area) and the arcuate nucleus participate in decompression regulator, with interactions occurring between these regions [28, 29, 35–40]. Although the role of the cerebellum in cardiovascular regulation is unclear, animal experiments suggest that the neuronal excitability of the fastigial nucleus has the effect of decreasing BP [41–43]. Electrical stimulation of the fastigial nucleus can increase arterial BP and HR, which relieve neuron injury through chronic cerebral ischemia, and was helpful for damaged arterial baroreflex function recovery [41–43]. Normal adults can also present transient changes in physiological indicators after fastigial nucleus electrical stimulation, which suggests a decrease in peripheral vascular flow and an increase in peripheral resistance and a slight increase in heart rate [44]. In addition, the vermiform process of the cerebellum may be important in cerebellum cycle control [45]. Idiaquez et al. [46] reported on vermis and right cerebellar hemisphere resection from cerebellar hemorrhage, where the patient appeared transient orthostatic hypotensive, suggesting that the cerebellum was involved in cardiovascular regulation. We found a negative correlation to the hypothalamus in the fastigial nucleus, which may play a part in the therapeutic action of acupuncture.

Beissner et al. [47] combined cardiac-gated brainstem-sensitive fMRI to investigate the mechanism of acupuncture. They found that, from the cortical level, the fMRI group showed significant increases activation in dorsolateral prefrontal gyrus (dlPFC), anterior mid cingulated cortex (ACC), insula, and frontal lobe cortex. Deactivations were found in the ventromedial prefrontal and orbitofrontal cortices (vmPFC/pgACC). They supposed that these areas were involved in acupuncture-induced heart rate changes. Further, as these areas are typical cortical and brainstem centers of pain and autonomic processing, they hypothesized that acupuncture may be a low-intensity deep pain stimulus that can activate autonomic concomitants and exert nonanalgesic effects with therapeutic potential. Our results also indicated a positive correlation with the hypothalamus in vmPFC, ACC, insula, and dlPFC, and these areas may participate in cardiovascular regulation in acupuncture treatment of hypertension and relieve patient pain.

The present study was limited by the small sample size. During our research, patients were found to have different reactions to acupuncture, with some being sensitive to acupuncture and some not. A larger sample size would be necessary to draw more definitive conclusions. Secondly, clinical experience and comparison with large trials indicated that long-term, frequent acupuncture may have good efficacy. The present study indicated that short-term acupuncture

did not improve the BP of primary hypertensive patients. Finally, nonbrainstem sensitive fMRI sequences were used here. Because the main cardiovascular center is located in the brainstem, a more brainstem sensitive sequence is needed to investigate the mechanism of acupuncture for treating hypertension.

5. Conclusions

According to our results, short-term acupuncture did not decrease BP significantly but may have improved body pain and vitality. Acupuncture may also regulate the cardiovascular system through a complicated brain network from the cortical level, the hypothalamus, and the brainstem. However, the mechanism remains unclear and needs further investigation.

Conflict of Interests

The authors declare that they do not have conflict of interests.

Acknowledgments

This study was supported by the National Natural Science Foundation of China under Grant nos. 81071137, 81071217, 61171002, 81071139, and 30770617, the Beijing Nova Program (Grant no. Z111101054511116), Beijing Natural Science Foundation (Grant no. 4122082), open program of the CAS Institute of Automation, and the Technology Development Program of Beijing Municipal Commission of Education (Grant no. KZ201010025025). The authors thank Hui Hu, Ling Pan, and Peng Chen for developing the acupuncture program, as well as Wei You and Jing Wang for acupuncture manipulations. The authors also thank Xiaojuan Ru and Dongling Sun for their statistical assistance.

References

[1] World Health Organization, *World Health Statistics 2012*, World Health Organization, 2012.

[2] "NIH Consensus Conference, Acupuncture," *Journal of the American Medical Association*, vol. 280, pp. 1518–1529, 1998.

[3] H. Huang and S. Liang, "Acupuncture at otoacupoint heart for treatment of vascular hypertension," *Journal of Traditional Chinese Medicine*, vol. 12, no. 2, pp. 133–136, 1992.

[4] Y. J. Chiu, A. Chi, and I. A. Reid, "Cardiovascular and endocrine effects of acupuncture in hypertensive patients," *Clinical and Experimental Hypertension*, vol. 19, no. 7, pp. 1047–1063, 1997.

[5] K. C. Tam and H. H. Yiu, "The effect of acupuncture on essential hypertension," *American Journal of Chinese Medicine*, vol. 3, no. 4, pp. 369–375, 1975.

[6] W. Guo and G. Ni, "The effects of acupuncture on blood pressure in different patients," *Journal of Traditional Chinese Medicine*, vol. 23, no. 1, pp. 49–50, 2003.

[7] J. D. Pandian, G. Toor, R. Arora et al., "Complementary and alternative medicine treatments among stroke patients in India," *Topics in Stroke Rehabilitation*, vol. 19, no. 5, pp. 384–394, 2012.

[8] F. A. Flachskampf, J. Gallasch, O. Gefeller et al., "Randomized trial of acupuncture to lower blood pressure," *Circulation*, vol. 115, no. 24, pp. 3121–3129, 2007.

[9] C. Yin, B. Seo, H. J. Park et al., "Acupuncture, a promising adjunctive therapy for essential hypertension: a double-blind, randomized, controlled trial," *Neurological Research*, vol. 29, supplement 1, pp. S98–S103, 2007.

[10] E. A. Macklin, P. M. Wayne, L. A. Kalish et al., "Stop Hypertension with the Acupuncture Research Program (SHARP): results of a randomized, controlled clinical trial," *Hypertension*, vol. 48, no. 5, pp. 838–845, 2006.

[11] Z. H. Cho, S. C. Chung, J. P. Jones et al., "New findings of the correlation between acupoints and corresponding brain cortices using functional MRI," *Proceedings of the National Academy of Sciences of the United States of America*, vol. 95, no. 5, pp. 2670–2673, 1998.

[12] K. K. S. Hui, J. Liu, O. Marina et al., "The integrated response of the human cerebro-cerebellar and limbic systems to acupuncture stimulation at ST 36 as evidenced by fMRI," *NeuroImage*, vol. 27, no. 3, pp. 479–496, 2005.

[13] W. Qin, J. Tian, L. J. Bai et al., "FMRI connectivity analysis of acupuncture effects on an amygdale-associated brain network," *Molecular Pain*, vol. 4, article 55, 2008.

[14] L. Bai, H. Yan, N. Li et al., "Neural specificity of acupuncture stimulation at pericardium 6: evidence from an fMRI study," *Journal of Magnetic Resonance Imaging*, vol. 31, no. 1, pp. 71–77, 2010.

[15] L. Bai, W. Qin, J. Tian et al., "Acupuncture modulates spontaneous activities in the anticorrelated resting brain networks," *Brain Research*, vol. 1279, no. C, pp. 37–49, 2009.

[16] L. Bai, W. Qin, J. Tian, J. Dai, and W. Yang, "Detection of dynamic brain networks modulated by acupuncture using a graph theory model," *Progress in Natural Science*, vol. 19, no. 7, pp. 827–835, 2009.

[17] L. Bai, J. Tian, C. Zhong et al., "Acupuncture modulates temporal neural responses in wide brain networks: evidence from fMRI study," *Molecular Pain*, vol. 6, article 73, 2010.

[18] L. Bai, W. Qin, J. Tian et al., "Time-varied characteristics of acupuncture effects in fMRI studies," *Human Brain Mapping*, vol. 30, no. 11, pp. 3445–3460, 2009.

[19] Y. B. You, L. J. Bai, R. W. Dai et al., "Acupuncture induces divergent alterations of functional connectivity within conventional frequency bands: evidence from MEG recordings," *Plos One*, vol. 7, no. 11, Article ID e49250, 2012.

[20] J. S. Han, "Acupuncture: neuropeptide release produced by electrical stimulation of different frequencies," *Trends in Neurosciences*, vol. 26, no. 1, pp. 17–22, 2003.

[21] G. G. Xing, F. Y. Liu, X. X. Qu et al., "Long-term synaptic plasticity in the spinal dorsal horn and its modulation by electroacupuncture in rats with neuropathic pain," *Journal of Pharmacology and Experimental Therapeutics*, vol. 321, pp. 1046–1053, 2007.

[22] X. Y. Shen, *Meridians and Acupoints*, China Press of Traditional Chinese Medicine, Beijing, China, 2nd edition, 2002.

[23] L. Laux, P. Glanzmann, P. Schaffner et al., *Das State-Trait-Angstinventar, Theotetische Grundlagen und Handanweisung*, Beltz, Weinheim, Germany, 1981.

[24] B. A. Abele and W. Brehm, "The conceptualization and measurement of mood: the development of the "Mood Survey"," *Diagnostica*, vol. 32, pp. 209–228, 1986.

[25] J. E. Ware and C. D. Sherbourne, "The MOS 36-item short-form health survey (SF-36). I. Conceptual framework and item selection," *Medical Care*, vol. 30, no. 6, pp. 473–483, 1992.

[26] S. Ji, X. Sun, W. Zhang, Q. Gu, and R. He, "Mechanisms underlying blood pressure control of cardiovascular centers," *Journal of Biomedical Engineering*, vol. 26, no. 1, pp. 216–220, 2009.

[27] Y. H. Gu, "Mechanisms underlying effects of pressor and depressor areas in limbic forebrain," *Journal of Progress in Physiology*, vol. 25, no. 4, pp. 205–211, 1994.

[28] Y. Z. Chang and Y. H. Gu, "Functional connections among pressor areas of nucleus hypothalamicus posterior, locus coeruleus and rostral ventrolateral," *Journal of Peking University*, vol. 24, no. 1, p. 27, 1992.

[29] B. C. Ding and P. Wang, "Role of ventrolateral medullary areas in depressor reflex," *Progress in Physiology*, vol. 29, no. 3, pp. 271–274, 1998.

[30] A. Kantzides, N. C. Owens, R. De Matteo, and E. Badoer, "Right atrial stretch activates neurons in autonomic brain regions that project to the rostral ventrolateral medulla in the rat," *Neuroscience*, vol. 133, no. 3, pp. 775–786, 2005.

[31] S. N. Yang and S. Wang, "The functional connection of rat habenular nucleus and lateral hypothalamic area in the regulation of cardiovascular activities," *Acta Physiologica Sinica*, vol. 42, no. 1, pp. 82–88, 1990.

[32] P. Li, S. C. Tjen-A-Looi, and J. C. Longhurst, "Excitatory projections from arcuate nucleus to ventrolateral periaqueductal gray in electroacupuncture inhibition of cardiovascular reflexes," *American Journal of Physiology*, vol. 290, no. 6, pp. H2535–H2542, 2006.

[33] S. C. Tjen-A-Looi, P. Li, and J. C. Longhurst, "Midbrain vlPAG inhibits rVLM cardiovascular sympathoexcitatory responses during electroacupuncture," *American Journal of Physiology*, vol. 290, no. 6, pp. H2543–H2553, 2006.

[34] P. Li, S. C. Tjen-A-Looi, Z. L. Guo, L. W. Fu, and J. C. Longhurst, "Long-loop pathways in cardiovascular electroacupuncture responses," *Journal of Applied Physiology*, vol. 106, no. 2, pp. 620–630, 2009.

[35] Y. Wang, Y. Gu, Y. Lu, L. Li, and L. Tan, "Role of substance P in pressor response of lateral hypothamus-perifornical region to glutamate," *Chinese Journal of Applied Physiology*, vol. 13, no. 4, pp. 337–341, 1997.

[36] X. Ding, J. S. Wu, and Y. H. Gu et at, "Mechanisms underlying pressor response of nucleus dorsomedialis hypothalami to glutamate," *Journal of Beijing Medical University*, vol. 31, pp. 124–126, 1999.

[37] Y. Liang, Y. H. Gu, and Y. C. Lv, "Nucleus paraventricularis and sympathetic nervous system mediate pressor response of nucleus amygdaloideus centralis," *Journal of Beijing Medical University*, vol. 27, no. 3, pp. 165–167, 1995.

[38] J. S. Wu, Y. H. Gu, L. S. Li et al., "Mechanism underlying pressor response of nucleus ventromedialis is involved in pressor response of central amygdaloid nucleus," *Journal of Beijing Medical University*, vol. 31, no. 5, pp. 422–425, 1999.

[39] Y. Z. Chang and Y. H. Gu, "Role of brain angiotensin II system in subfornical organ-pressor responses," *Acta Physiologica Sinica*, vol. 51, no. 1, pp. 38–44, 1999.

[40] W. K. Xu and Y. H. Gu, "Rostral ventrolateral medulla-sympathetic vasoconstrictor nerve system mediated insular cortex-pressor response," *Acta Physiologica Sinica*, vol. 46, no. 6, pp. 591–596, 1994.

[41] Z. X. Qian, W. M. Dai, S. G. Fu et al., "Effects of cerebellar fastigial stimulation on the arterial blood pressure and respiratory activities in rabbits," *Natural Science Journal of Hainan University*, vol. 13, no. 1, pp. 60–64, 1995.

[42] M. Nakai, C. Iadecola, and D. J. Reis, "Global cerebral vasodilation by stimulation of rat fastigial cerebellar nucleus," *The American Journal of Physiology*, vol. 243, no. 2, pp. H226–235, 1982.

[43] R. F. Zhang, L. R. Gao, N. K. Zhang et al., "Effects of fastigial nucleus electro-stimulation on mortality and arterial baroreflex sensitivity in rats after myocardial infarction," *Journal of Shanxi Medical University*, vol. 41, no. 7, pp. 588–590, 2010.

[44] J. Wang, X. L. Tian, X. Zhang et al., "Effects of fastigial nucleus stimulation on crucial cardiovascular physiological parameters," *Chinese Journal of Applied Physiology*, vol. 26, no. 4, pp. 507–509, 2010.

[45] M. J. Holmes, L. A. Cotter, H. E. Arendt, S. P. Cass, and B. J. Yates, "Effects of lesions of the caudal cerebellar vermis on cardiovascular regulation in awake cats," *Brain Research*, vol. 938, no. 1-2, pp. 62–72, 2002.

[46] J. Idiaquez, R. Fadic R, and C. J. Mathias, "Transient orthostatic hypertension after partial cerebellar resection," *Clinical Autonomic Research*, vol. 21, no. 1, pp. 57–59, 2011.

[47] F. Beissner, R. Deichmann, C. Henke et al., "Acupuncture-deep pain with an autonomic dimension?" *NeuroImage*, vol. 60, pp. 653–660, 2012.

Hindawi Publishing Corporation
Evidence-Based Complementary and Alternative Medicine
Volume 2013, Article ID 267959, 6 pages
http://dx.doi.org/10.1155/2013/267959

Review Article

Acupuncture Effect and Central Autonomic Regulation

Qian-Qian Li, Guang-Xia Shi, Qian Xu, Jing Wang, Cun-Zhi Liu, and Lin-Peng Wang

Acupuncture and Moxibustion Department, Beijing Hospital of Traditional Chinese Medicine affiliated to Capital Medical University, 23 Meishuguanhou Street, Dongcheng District, Beijing 100010, China

Correspondence should be addressed to Cun-Zhi Liu; lcz623780@126.com

Received 7 February 2013; Revised 3 April 2013; Accepted 3 April 2013

Academic Editor: Lijun Bai

Acupuncture is a therapeutic technique and part of traditional Chinese medicine (TCM). Acupuncture has clinical efficacy on various autonomic nerve-related disorders, such as cardiovascular diseases, epilepsy, anxiety and nervousness, circadian rhythm disorders, polycystic ovary syndrome (PCOS) and subfertility. An increasing number of studies have demonstrated that acupuncture can control autonomic nerve system (ANS) functions including blood pressure, pupil size, skin conductance, skin temperature, muscle sympathetic nerve activities, heart rate and/or pulse rate, and heart rate variability. Emerging evidence indicates that acupuncture treatment not only activates distinct brain regions in different kinds of diseases caused by imbalance between the sympathetic and parasympathetic activities, but also modulates adaptive neurotransmitter in related brain regions to alleviate autonomic response. This review focused on the central mechanism of acupuncture in modulating various autonomic responses, which might provide neurobiological foundations for acupuncture effects.

1. Introduction

Acupuncture has been practiced for over 3000 years with beneficial clinical effects on many disorders [1]. There is sufficient evidence of the value of acupuncture to expand its application into conventional medicine and to encourage further studies of its physiological and clinical values [2]. According to traditional Chinese medicine (TCM), "acupuncture is believed to restore the balance between *Yin* and *Yang*." This can be translated into the Western medicine terminology as "acupuncture modulates the imbalance between the parasympathetic and sympathetic activity [3]." Acupuncture has been effectively used in various autonomic nerve-related disorders, such as cardiovascular diseases, epilepsy, anxiety and nervousness, circadian rhythm disorders, polycystic ovary syndrome (PCOS), and subfertility [4–8]. It could influence some known indicators of autonomic activities, such as blood pressure [9–11], pupil size [12], skin conductance [13], skin temperature [14], muscle sympathetic nerve activities [15], heart rate and/or pulse rate [16], and heart rate variability [17, 18]. Acupuncture has been proposed to treat autonomic nerve-related diseases through modulating the imbalance between the sympathetic and parasympathetic activities [19]. Previous study has shown that changes in parasympathetic nervous activity are correlated with the amount of *De-Qi* (i.e., arrival of *Qi*) sensations during acupuncture manipulation [20]. On the other hand, the affecting degree of acupuncture on the autonomic nerve is still unknown because part of the acupuncture effects is dependent on the *De-Qi* sensation [21].

A literature review was conducted using PubMed, EBSCOhost, and the China National Knowledge Infrastructure (CNKI). Keywords used in the searching were "acupuncture," "brain" or "cerebrum" and "sympathetic," "vagus," "autonomic," or "parasympathetic." Articles were collected from December 2007 to present in each database. The identified 44 publications in this search were related to acupuncture basic study and central autonomic regulation. Among these 44 articles which met the criteria, 35 articles are in English and 9 articles are in Chinese. In this review, the underlying central mechanism of acupuncture-induced autonomic modulation is discussed based on basic studies that have been published in the past 5 years. We will, in particular, focus on two aspects as follows: (1) the brain region which plays an important role in initiating autonomic responses during acupuncture; (2) neurohumoral autonomic modulation of acupuncture in the central autonomic nerve system (ANS).

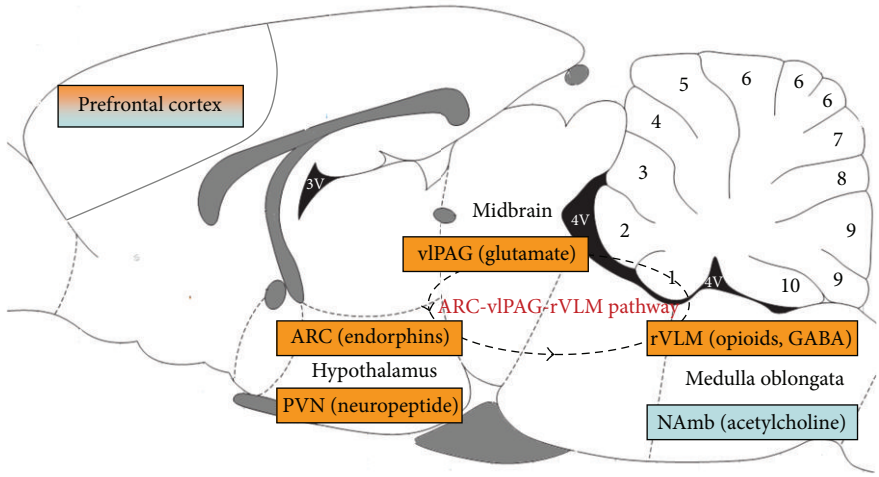

Figure 1: Acupuncture autonomic regulation mechanism. Blue indicates the area involved in acupuncture parasympathetic regulation. Orange indicates the area involved in acupuncture sympathetic regulation.

2. Acupuncture Effect and Central Autonomic Structures

Several studies have demonstrated that the autonomic dimension of the acupuncture stimulation was mediated by a mesencephalic and brainstem network [22, 23] (Figure 1), which is comprised of the hypothalamus, medulla oblongata, ventrolateral periaqueductal gray, and the dorsomedial prefrontal cortex. All of these areas are involved in the autonomic regulation [24–26].

2.1. Hypothalamus. Hypothalamus is the most important brain center that controls the ANS [27]. As the site of autonomic regulation, hypothalamus has been proved to be involved in the pathway of electroacupuncture (EA) attenuating sympathetic activity. Impulses generated in sensory fibres in the skin connect with interneurons to modulate activities of the motoneurons hypothalamus to change autonomic functions [28]. Increased sympathetic activity in hypertension may act as a stimulus for nitric oxide (NO) release in the hypothalamus. EA application on ST36 could effectively modulate the activity and expression of neuronal nitric oxide synthase (nNOS) in the hypothalamus of spontaneously hypertensive rats (SHR). The effect may through its connections to sympathetic and parasympathetic nervous system and also through its control of endocrine organs [29]. However, which part of the hypothalamus that participates in the mechanism of action is still remained unclear. Effects on decreased neuropeptide Y (NPY) production due to stimulation on the paraventricular nucleus (PVN) of hypothalamus [30] is one of the several hypotheses which have been proposed in the literature regarding the action mechanism. The PVN of hypothalamus is a cell group that plays an important role in the regulation of sympathetic vasomotor tone and autonomic stress responses [31, 32]. Acupuncture could decrease NPY [33] and corticotropin-releasing hormone [34] expressions in the PVN and produce some specific effects on suppressing the sympathetic outflow in response to chronic stressors [35].

Arcuate (ARC) nucleus projects to other brain regions that regulate the sympathetic outflow include the dorsomedial hypothalamus, midbrain periaqueductal grey, rostral ventrolateral medulla (rVLM), and the nucleus of the solitary tract [36]. Neurons in the ARC nucleus projecting to the rVLM potentially participate in EA inhibition of reflex cardiovascular sympathoexcitation [37]. Ventrolateral periaqueductal gray (vlPAG) projections from the ARC are required for EA regulation of sympathoexcitatory presympathetic rVLM activity and the cardiovascular excitatory reflex responses, while a direct pathway between the ARC and rVLM might serve as a source of endorphins for EA cardiovascular modulation.

2.2. Medulla Oblongata. Specific regions of the medulla oblongata mediate central control of autonomic function. In the central nervous system (CNS), the rVLM is an important part of the sympathetic efferent limb of cardiovascular reflex activity and, as such, it is important in the maintenance of arterial blood pressure [38]. It projects to the intermediolateral columns of the thoracic spinal cord, which is the origin of sympathetic preganglionic neurons [39]. Inhibition of neuronal function in this nucleus results in large decreasing of blood pressure [40]. EA could inhibit cardiovascular autonomic responses through modulating rVLM neurons [41, 42]. Moreover, opioids and gamma-aminobutyric acid (GABA) participate in the long-term EA-related inhibition of sympathoexcitatory cardiovascular responses in the rVLM [43]. Activation of the nucleus raphe pallidus (NRP) attenuates sympathoexcitatory cardiovascular reflexes through a mechanism involving serotonergic neurons and 5-HT1A receptors in the rVLM during EA. Serotonergic projections from the NRP to the rVLM contribute to the EA-cardiovascular responses [44].

The nucleus ambiguus (NAmb), located in the ventrolateral division of the hindbrain, is considered to be an

important site of origin of preganglionic parasympathetic vagal motor neurons that ultimately regulate autonomic function through the releasing of acetylcholine [45]. The recent study of that neurons colabeled with c-Fos and choline acetyltransferase (ChAT) were activated in the EA-treated animals instead of sham EA group indicates that some NAmb neurons activated by EA are preganglionic vagal neurons [18]. It is suggested that stimulation on a special acupoint is crucial to achieve modulate effect on autonomic function by activating NAmb neurons. It is consistent with TCM theory that genuine acupoints treatment is more effective than nonacupoints treatment based on specific physiological effects related to meridians and collections of meridian *Qi*.

2.3. Midbrain. Ventrolateral periaqueductal gray (vlPAG) is an essential midbrain nuclei that process information from somatic afferents during EA [46]. Caudal vlPAG is a significant region in the long-loop arcuate-rVLM pathway for the EA-cardiovascular response, while the rostral vlPAG plays a major role in the reciprocal arcuate-vlPAG pathway that helps to prolong EA-cardiovascular modulation [47]. Excitation of vlPAG neurons enhances the arcuate response to splanchnic stimulation, while blockade of vlPAG neurons limits excitation of arcuate neurons by EA. These observations indicate that EA-induced excitation of arcuate neurons requires input from the vlPAG, and the reciprocal reinforcement between the midbrain and the ventral hypothalamus serves to prolong the influence of EA on the baseline blood pressure [48].

2.4. Dorsomedial Prefrontal Cortex (DMPFC). The prefrontal cortex (PFC) is vital for mediating behavioral and somatic responses to stress in the autonomic centers via projections [49]. A near-infrared spectroscopy (NIRS) study found that the right PFC activity predominantly modulated sympathetic effects during a mental stress task [50]. Acupuncture stimulation might decrease sympathetic activity and increase parasympathetic activity through its inhibitory effects on dorsomedial PFC activity [51]. This might be beneficial to treat chronic pain induced by hyperactivity of the sympathetic nervous system. However, Sakatani et al. found no significant correlation between the PFC activity and ANS function during acupuncture. One of the possible explanations of the poor correlations might be that the PFC activity induced by acupuncture is not closely linked with ANS function [52].

3. Acupuncture Effect and Neurohumoral Modulation

Some neurotransmitters, including serotonin, opioid peptides, catecholamines, and amino acids in the brain appear to be participated in the modulation mechanism of acupuncture for certain ANS [53, 54].

3.1. Endogenous Opioids. EA was able to restore the impaired gastric motility and dysrhythmic slow waves by enhancing vagal activity, which was mediated via the opioid pathway [55, 56]. Ameliorating effects of EA at ST-36 on gastric motility might activate the central opioids that, in turn, inhibit sympathetic outflow [57]. Although acupuncture produced significant heart rate decreases in pentobarbital-anesthetized rats, this response is related to the activation of GABAergic neurons instead of opioid [58]. This opinion is proved by another study, which indicates that an opioid receptor-mediated transmission is not responsible for the present bradycardiac response induced by acupuncture-like stimulation [59]. These views suggest that acupuncture treatment on different diseases may be mediated by different neurotransmitters, which is in accordance with holistic view of acupuncture treatment in TCM theory.

EA activates enkephalinergic neurons in several brain areas that regulate sympathetic outflow, including the arcuate nucleus, rostral ventrolateral medulla, raphé nuclei, among others [60, 61]. Consistent with this, Li et al. [62] found that EA at P5-P6 transiently stimulates the production of enkephalin in a region of the brain, which regulates sympathetic outflow. It is suggested that a single brief acupuncture treatment can increase the expression of this modulatory neuropeptide. The β-endorphin is a key mediator of changes in autonomic functions [63]. Acupuncture may hypothetically affect the hypothalamic-pituitary-adrenal (HPA) axis by decreasing cortisol concentrations and the hypothalamic-pituitary-gonadal (HPG) axis by modulating central β-endorphin production and secretion [64]. Some reports have also shown that a negative perception of acupuncture might produce enhanced sympathetic activation to the acupuncture stimulus [65], which may be mediated through endorphin pathway [66]. It is conceivable that a specific neuroendocrine-immune network is crucial to the produce of acupuncture therapeutic effect. Further studies are required to reveal involved molecules and underlying mechanisms.

3.2. Amino Acids. Amino acid sensors could regulate the activity of vagal afferent fibers [67]. Amino acids are directly involved in signaling the vagus pathway in the ARC [68]. Recent studies have shown that vesicular glutamate transporter 3 (VGLUT3) in the ARC neurons [69, 70] and vlPAG [60, 71] were activated by EA at the P5-P6 acupoints. Glutamate only partially but significantly contributes to the activation of ARC-vlPAG reciprocal pathways during EA stimulation of somatic afferents [47]. In addition, reduction of GABA release disinhibits vlPAG cells, which, in turn, modulates the activity of rVLM neurons to attenuate the sympathoexcitatory reflex responses [46]. EA modulates the sympathoexcitatory reflex responses by decreasing the release of GABA in the vlPAG [43], most likely through a presynaptic CB1 receptor mechanism [72]. Studies conducted so far on amino acids suggest that glutamate and GABA are involved in the mechanism of acupuncture for autonomic alteration. This response is closely related to vlPAG.

3.3. Nerve Growth Factor (NGF). The NGF is a neurotrophin, which regulates the function and survival of peripheral sensory, sympathetic, and forebrain cholinergic neurons. It could modulate sensory and autonomic activity as a mediator of acupuncture effects in the CNS [73]. The therapeutic potential of EA could modulate the activity of the ANS by a long-lasting depression of the sympathetic branch,

which is associated with a peripheral downregulation of NGF in organs. Manneråas et al. [74] found that EA could effectively improve PCOS-related metabolic disorders, alter sympathetic markers [75], and normalize the DHT-induced increase of $mRNA^{NGF}$. The data on EA/NGF interaction in PCOS models further suggested that the decrease of NGF expression in peripheral organs could benefit EA to modulate the activity of the ANS [76]. Although NGF in organs has been proved to be associated with the acupuncture effect on ANS, there is a lack of sufficient evidence to demonstrate the relationship between acupuncture effect and NGF in central autonomic nerve system.

4. Conclusion

Emerging evidence indicates that acupuncture treatment not only activates distinct brain regions in different kinds of diseases caused by imbalance between the sympathetic and parasympathetic activities, but also modulates adaptive neurotransmitter in related brain regions to alleviate autonomic response. However, it is not clear whether different pathway is activated by specific acupoint, such as local points and distant points, or the autonomic regulation effect of acupoints from different meridians. Further rigorous RCTs are required for the study of this topic. It enables us to understand the importance of acupuncture therapy in the autonomic regulation. Then, acupuncture can be used in the treatment of various autonomic disorders as a novel alternative therapy.

Acknowledgments

The study was funded by the New Century Excellent Talents in University (NCET-09-0007) and the Technology New Star Program of Beijing (2009B46).

References

[1] W. Huang, N. Kutner, and D. L. Bliwise, "Autonomic activation in insomnia: the case for acupuncture," *Journal of Clinical Sleep Medicine*, vol. 7, no. 1, pp. 95–102, 2011.

[2] NIH Consensus Conference, "Acupuncture," *The Journal of the American Medical Association*, vol. 280, no. 17, pp. 1518–1524, 1998.

[3] T. Takahashi, "Mechanism of acupuncture on neuromodulation in the gut—a review," *Neuromodulation*, vol. 14, no. 1, pp. 8–12, 2011.

[4] J. L. Zhang, S. P. Zhang, and H. Q. Zhang, "Antiepileptic effect of electroacupuncture versus vagus nerve stimulation in the rat thalamus," *Neuroscience Letters*, vol. 441, no. 2, pp. 183–187, 2008.

[5] E. Stener-Victorin, E. Jedel, P. O. Janson, and Y. B. Sverrisdottir, "Low-frequency electroacupuncture and physical exercise decrease high muscle sympathetic nerve activity in polycystic ovary syndrome," *The American Journal of Physiology*, vol. 297, no. 2, pp. R387–R395, 2009.

[6] V. Vickland, C. Rogers, A. Craig, and Y. Tran, "Anxiety as a factor influencing physiological effects of acupuncture," *Complementary Therapies in Clinical Practice*, vol. 15, no. 3, pp. 124–128, 2009.

[7] J. H. Wu, H. Y. Chen, Y. J. Chang et al., "Study of autonomic nervous activity of night shift workers treated with laser acupuncture," *Photomedicine and Laser Surgery*, vol. 27, no. 2, pp. 273–279, 2009.

[8] K. Imai, H. Ariga, and T. Takahashi, "Electroacupuncture improves imbalance of autonomic function under restraint stress in conscious rats," *The American Journal of Chinese Medicine*, vol. 37, no. 1, pp. 45–55, 2009.

[9] M. Bäcker, F. Schaefer, N. Siegler et al., "Impact of stimulation dose and personality on autonomic and psychological effects induced by acupuncture," *Autonomic Neuroscience*, vol. 170, no. 1-2, pp. 48–55, 2012.

[10] K. Tachibana, N. Ueki, T. Uchida, and H. Koga, "Randomized comparison of the therapeutic effect of acupuncture, massage, and Tachibana-style-method on stiff shoulders by measuring muscle firmness, VAS, pulse, and blood pressure," *Evidence-Based Complementary and Alternative Medicine*, vol. 2012, Article ID 989705, 7 pages, 2012.

[11] A. Y. M. Jones, Y. L. Kwan, N. T. F. Leung, R. P. W. Yu, C. M. Y. Wu, and D. E. R. Warburton, "Electrical stimulation of acupuncture points and blood pressure responses to postural changes: a pilot study," *The American Journal of Critical Care*, vol. 20, no. 3, pp. e67–e74, 2011.

[12] H. Ohsawa, S. Yamaguchi, H. Ishimaru, M. Shimura, and Y. Sato, "Neural mechanism of pupillary dilation elicited by electro-acupuncture stimulation in anesthetized rats," *Journal of the Autonomic Nervous System*, vol. 64, no. 2-3, pp. 101–106, 1997.

[13] C. C. Hsu, C. S. Weng, T. S. Liu, Y. S. Tsai, and Y. H. Chang, "Effects of electrical acupuncture on acupoint BL15 evaluated in terms of heart rate variability, pulse rate variability and skin conductance response," *The American Journal of Chinese Medicine*, vol. 34, no. 1, pp. 23–36, 2006.

[14] K. Agarwal-Kozlowski, A. C. Lange, and H. Beck, "Contact-free infrared thermography for assessing effects during acupuncture: a randomized, single-blinded, placebo-controlled crossover clinical trial," *Anesthesiology*, vol. 111, no. 3, pp. 632–639, 2009.

[15] E. Haker, H. Egekvist, and P. Bjerring, "Effect of sensory stimulation (acupuncture) on sympathetic and parasympathetic activities in healthy subjects," *Journal of the Autonomic Nervous System*, vol. 79, no. 1, pp. 52–59, 2000.

[16] C. L. Hsieh, J. G. Lin, T. C. Li, and Q. Y. Chang, "Changes of pulse rate and skin temperature evoked by electroacupuncture stimulation with different frequency on both *Zusanli* acupoints in humans," *The American Journal of Chinese Medicine*, vol. 27, no. 1, pp. 11–18, 1999.

[17] G. Litscher, L. P. Wang, L. Wang, C. Z. Liu, and X. M. Wang, "Sino-European transcontinental basic and clinical high-tech acupuncture studies-part 4: "fire of life" analysis of heart rate variability during acupuncture in clinical studies.," *Evidence-Based Complementary and Alternative Medicine*, vol. 2012, Article ID 153480, 8 pages, 2012.

[18] Z. L. Guo, M. Li, and J. C. Longhurst, "Nucleus ambiguus cholinergic neurons activated by acupuncture: relation to enkephalin," *Brain Research*, vol. 1442, pp. 25–35, 2012.

[19] E. H. Y. Ng, W. S. So, J. Gao, Y. Y. Wong, and P. C. Ho, "The role of acupuncture in the management of subfertility," *Fertility and Sterility*, vol. 90, no. 1, pp. 1–13, 2008.

[20] E. Hori, K. Takamoto, S. Urakawa, T. Ono, and H. Nishijo, "Effects of acupuncture on the brain hemodynamics," *Autonomic Neuroscience*, vol. 157, no. 1-2, pp. 74–80, 2010.

[21] Y. Kurono, M. Minagawa, T. Ishigami, A. Yamada, T. Kakamu, and J. Hayano, "Acupuncture to Danzhong but not to Zhongting increases the cardiac vagal component of heart rate variability," *Autonomic Neuroscience*, vol. 161, no. 1-2, pp. 116–120, 2011.

[22] F. Beissner, R. Deichmann, C. Henke, and K. J. Bär, "Acupuncture—deep pain with an autonomic dimension?" *NeuroImage*, vol. 60, no. 1, pp. 653–660, 2012.

[23] E. Noguchi, "Acupuncture regulates gut motility and secretion via nerve reflexes," *Autonomic Neuroscience*, vol. 156, no. 1-2, pp. 15–18, 2010.

[24] V. G. Macefield and L. A. Henderson, "Real-time imaging of the medullary circuitry involved in the generation of spontaneous muscle sympathetic nerve activity in awake subjects," *Human Brain Mapping*, vol. 31, no. 4, pp. 539–549, 2010.

[25] V. Napadow, R. Dhond, G. Conti, N. Makris, E. N. Brown, and R. Barbieri, "Brain correlates of autonomic modulation: combining heart rate variability with fMRI," *NeuroImage*, vol. 42, no. 1, pp. 169–177, 2008.

[26] J. F. Thayer, A. L. Hansen, E. Saus-Rose, and B. H. Johnsen, "Heart rate variability, prefrontal neural function, and cognitive performance: the neurovisceral integration perspective on self-regulation, adaptation, and health," *Annals of Behavioral Medicine*, vol. 37, no. 2, pp. 141–153, 2009.

[27] F. M. Abboud, S. C. Harwani, and M. W. Chapleau, "Autonomic neural regulation of the immune system: implications for hypertension and cardiovascular disease," *Hypertension*, vol. 59, no. 4, pp. 755–762, 2012.

[28] G. Burnstock, "Acupuncture: a novel hypothesis for the involvement of purinergic signalling," *Medical Hypotheses*, vol. 73, no. 4, pp. 470–472, 2009.

[29] J. I. Kim, Y. S. Kim, S. K. Kang et al., "Electroacupuncture decreases nitric oxide synthesis in the hypothalamus of spontaneously hypertensive rats," *Neuroscience Letters*, vol. 446, no. 2-3, pp. 78–82, 2008.

[30] J. J. Bonavera, M. G. Dube, P. S. Kalra, and S. P. Kalra, "Anorectic effects of estrogen may be mediated by decreased neuropeptide-Y release in the hypothalamic paraventricular nucleus," *Endocrinology*, vol. 134, no. 6, pp. 2367–2370, 1994.

[31] K. A. Frahm, M. J. Schow, and S. A. Tobet, "The vasculature within the paraventricular nucleus of the hypothalamus in mice varies as a function of development, subnuclear location, and GABA signaling," *Hormone and Metabolic Research*, vol. 44, no. 8, pp. 619–624, 2012.

[32] N. Nunn, M. Womack, C. Dart, and R. Barrett-Jolley, "Function and pharmacology of spinally-projecting sympathetic preautonomic neurones in the paraventricular nucleus of the hypothalamus," *Current Neuropharmacology*, vol. 9, no. 2, pp. 262–277, 2011.

[33] E. H. Kim, Y. Kim, M. H. Jang et al., "Auricular acupuncture decreases neuropeptide Y expression in the hypothalamus of food-deprived Sprague-Dawley rats," *Neuroscience Letters*, vol. 307, no. 2, pp. 113–116, 2001.

[34] L. Eshkevari, E. Permaul, and S. E. Mulroney, "Acupuncture blocks cold stress-induced increases in the hypothalamus-pituitary-adrenal axis in the rat," *Journal of Endocrinology*, vol. 217, no. 1, pp. 95–104, 2013.

[35] L. Eshkevari, R. Egan, D. Phillips et al., "Acupuncture at ST36 prevents chronic stress-induced increases in neuropeptide Y in rat," *Experimental Biology and Medicine*, vol. 237, no. 1, pp. 18–23, 2012.

[36] R. A. L. Dampney, "Arcuate nucleus—a gateway for insulin's action on sympathetic activity," *Journal of Physiology*, vol. 589, no. 9, pp. 2109–2110, 2011.

[37] P. Li, S. C. Tjen-A-Looi, Z. L. Guo, L. W. Fu, and J. C. Longhurst, "Long-loop pathways in cardiovascular electroacupuncture responses," *Journal of Applied Physiology*, vol. 106, no. 2, pp. 620–630, 2009.

[38] E. B. de Oliveira-Sales, E. E. Nishi, M. A. Boim, M. S. Dolnikoff, C. T. Bergamaschi, and R. R. Campos, "Upregulation of At1R and iNOS in the rostral ventrolateral medulla (RVLM) is essential for the sympathetic hyperactivity and hypertension in the 2K-1C wistar rat model," *American Journal of Hypertension*, vol. 23, no. 7, pp. 708–715, 2010.

[39] S. C. Tjen-A-Looi, P. Li, and J. C. Longhurst, "Medullary substrate and differential cardiovascular responses during stimulation of specific acupoints," *The American Journal of Physiology*, vol. 287, no. 4, pp. R852–R862, 2004.

[40] P. G. Guertzenstein and A. Silver, "Fall in blood pressure produced from discrete regions of the ventral surface of the medulla by glycine and lesions," *Journal of Physiology*, vol. 242, no. 2, pp. 489–503, 1974.

[41] P. Li, S. C. Tjen-A-Looi, and J. C. Longhurst, "Nucleus raphé pallidus participates in midbrain-medullary cardiovascular sympathoinhibition during electroacupuncture," *The American Journal of Physiology*, vol. 299, no. 5, pp. R1369–R1376, 2010.

[42] S. C. Tjen-A-Looi, P. Li, and J. C. Longhurst, "Midbrain vlPAG inhibits rVLM cardiovascular sympathoexcitatory responses during electroacupuncture," *The American Journal of Physiology*, vol. 290, no. 6, pp. H2543–H2553, 2006.

[43] S. C. Tjen-A-Looi, P. Li, and J. C. Longhurst, "Role of medullary GABA, opioids, and nociceptin in prolonged inhibition of cardiovascular sympathoexcitatory reflexes during electroacupuncture in cats," *The American Journal of Physiology*, vol. 293, no. 6, pp. H3627–H3635, 2007.

[44] A. Moazzami, S. C. Tjen-A-Looi, Z. L. Guo, and J. C. Longhurst, "Serotonergic projection from nucleus raphe pallidus to rostral ventrolateral medulla modulates cardiovascular reflex responses during acupuncture," *Journal of Applied Physiology*, vol. 108, no. 5, pp. 1336–1346, 2010.

[45] J. Wang, M. Irnaten, R. A. Neff et al., "Synaptic and neurotransmitter activation of cardiac vagal neurons in the nucleus ambiguus," *Annals of the New York Academy of Sciences*, vol. 940, pp. 237–246, 2001.

[46] S. C. Tjen-A-Looi, P. Li, and J. C. Longhurst, "Processing cardiovascular information in the vlPAG during electroacupuncture in rats: roles of endocannabinoids and GABA," *Journal of Applied Physiology*, vol. 106, no. 6, pp. 1793–1799, 2009.

[47] Z. L. Guo and J. C. Longhurst, "Activation of reciprocal pathways between arcuate nucleus and ventrolateral periaqueductal gray during electroacupuncture: involvement of VGLUT3," *Brain Research*, vol. 1360, pp. 77–88, 2010.

[48] P. Li, S. C. Tjen-A-Looi, Z. L. Guo, and J. C. Longhurst, "An arcuate-ventrolateral periaqueductal gray reciprocal circuit participates in electroacupuncture cardiovascular inhibition," *Autonomic Neuroscience*, vol. 158, no. 1-2, pp. 13–23, 2010.

[49] R. M. Buijs and C. G. van Eden, "The integration of stress by the hypothalamus, amygdala and prefrontal cortex: balance between the autonomic nervous system and the neuroendocrine system," *Progress in Brain Research*, vol. 126, pp. 117–132, 2000.

[50] M. Tanida, M. Katsuyama, and K. Sakatani, "Effects of fragrance administration on stress-induced prefrontal cortex activity and

sebum secretion in the facial skin," *Neuroscience Letters*, vol. 432, no. 2, pp. 157–161, 2008.

[51] M. Passatore and S. Roatta, "Influence of sympathetic nervous system on sensorimotor function: whiplash associated disorders (WAD) as a model," *European Journal of Applied Physiology*, vol. 98, no. 5, pp. 423–449, 2006.

[52] K. Sakatani, T. Kitagawa, N. Aoyama, and M. Sasaki, "Effects of acupuncture on autonomic nervous function and prefrontal cortex activity," *Advances in Experimental Medicine and Biology*, vol. 662, pp. 455–460, 2010.

[53] P. Li and J. C. Longhurst, "Neural mechanism of electroacupuncture's hypotensive effects," *Autonomic Neuroscience*, vol. 157, no. 1-2, pp. 24–30, 2010.

[54] W. Zhou and J. C. Longhurst, "Neuroendocrine mechanisms of acupuncture in the treatment of hypertension," *Evidence-Based Complementary and Alternative Medicine*, vol. 2012, Article ID 878673, 9 pages, 2012.

[55] J. Chen, G. Q. Song, J. Yin, T. Koothan, and J. D. Z. Chen, "Electroacupuncture improves impaired gastric motility and slow waves induced by rectal distension in dogs," *The American Journal of Physiology*, vol. 295, no. 3, pp. G614–G620, 2008.

[56] H. Ouyang, J. Xing, and J. Chen, "Electroacupuncture restores impaired gastric accommodation in vagotomized dogs," *Digestive Diseases and Sciences*, vol. 49, no. 9, pp. 1418–1424, 2004.

[57] J. Yin, J. Chen, and J. D. Z. Chen, "Ameliorating effects and mechanisms of electroacupuncture on gastric dysrhythmia, delayed emptying, and impaired accommodation in diabetic rats," *The American Journal of Physiology*, vol. 298, no. 4, pp. G563–G570, 2010.

[58] S. Uchida, F. Kagitani, and H. Hotta, "Mechanism of the reflex inhibition of heart rate elicited by acupuncture-like stimulation in anesthetized rats," *Autonomic Neuroscience*, vol. 143, no. 1-2, pp. 12–19, 2008.

[59] S. Uchida, F. Kagitani, and H. Hotta, "Neural mechanisms of reflex inhibition of heart rate elicited by acupuncture-like stimulation in anesthetized rats," *Autonomic Neuroscience*, vol. 157, no. 1-2, pp. 18–23, 2010.

[60] Z. L. Guo and J. C. Longhurst, "Expression of c-Fos in arcuate nucleus induced by electroacupuncture: relations to neurons containing opioids and glutamate," *Brain Research*, vol. 1166, no. 1, pp. 65–76, 2007.

[61] Z. L. Guo, A. R. Moazzami, S. Tjen-A-Looi, and J. C. Longhurst, "Responses of opioid and serotonin containing medullary raphe neurons to electroacupuncture," *Brain Research*, vol. 1229, pp. 125–136, 2008.

[62] M. Li, S. C. Tjen-A-Looi, and J. C. Longhurst, "Electroacupuncture enhances preproenkephalin mRNA expression in rostral ventrolateral medulla of rats," *Neuroscience Letters*, vol. 477, no. 2, pp. 61–65, 2010.

[63] N. Boyadjieva, J. P. Advis, and D. K. Sarkar, "Role of β-endorphin, corticotropin-releasing hormone, and autonomic nervous system in mediation of the effect of chronic ethanol on natural killer cell cytolytic activity," *Alcoholism: Clinical and Experimental Research*, vol. 30, no. 10, pp. 1761–1767, 2006.

[64] H. Harbach, B. Moll, R. H. Boedeker et al., "Minimal immunoreactive plasma β-endorphin and decrease of cortisol at standard analgesia or different acupuncture techniques," *European Journal of Anaesthesiology*, vol. 24, no. 4, pp. 370–376, 2007.

[65] Y. Chae, S. Y. Kim, H. S. Park, H. Lee, and H. J. Park, "Experimentally manipulating perceptions regarding acupuncture elicits different responses to the identical acupuncture stimulation," *Physiology and Behavior*, vol. 95, no. 3, pp. 515–520, 2008.

[66] M. Amanzio and F. Benedetti, "Neuropharmacological dissection of placebo analgesia: expectation-activated opioid systems versus conditioning-activated specific subsystems," *Journal of Neuroscience*, vol. 19, no. 1, pp. 484–494, 1999.

[67] T. Tsurugizawa, T. Kondoh, and K. Torii, "Forebrain activation induced by postoral nutritive substances in rats," *NeuroReport*, vol. 19, no. 11, pp. 1111–1115, 2008.

[68] D. Tomé, J. Schwarz, N. Darcel, and G. Fromentin, "Protein, amino acids, vagus nerve signaling, and the brain," *The American Journal of Clinical Nutrition*, vol. 90, no. 3, pp. 838S–843S, 2009.

[69] J. Noh, R. P. Seal, J. A. Garver, R. H. Edwards, and K. Kandler, "Glutamate co-release at GABA/glycinergic synapses is crucial for the refinement of an inhibitory map," *Nature Neuroscience*, vol. 13, no. 2, pp. 232–238, 2010.

[70] R. P. Seal, X. Wang, Y. Guan et al., "Injury-induced mechanical hypersensitivity requires C-low threshold mechanoreceptors," *Nature*, vol. 462, no. 7273, pp. 651–655, 2009.

[71] T. Ishide, A. Amer, T. J. Maher, and A. Ally, "Nitric oxide within periaqueductal gray modulates glutamatergic neurotransmission and cardiovascular responses during mechanical and thermal stimuli," *Neuroscience Research*, vol. 51, no. 1, pp. 93–103, 2005.

[72] L. W. Fu and J. C. Longhurst, "Electroacupuncture modulates vlPAG release of GABA through presynaptic cannabinoid CB1 receptors," *Journal of Applied Physiology*, vol. 106, no. 6, pp. 1800–1809, 2009.

[73] L. Manni, M. Albanesi, M. Guaragna, S. B. Paparo, and L. Aloe, "Neurotrophins and acupuncture," *Autonomic Neuroscience*, vol. 157, no. 1-2, pp. 9–17, 2010.

[74] L. Mannerås, I. H. Jonsdottir, A. Holmäng, M. Lönn, and E. Stener-Victorin, "Low-frequency electro-acupuncture and physical exercise improve metabolic disturbances and modulate gene expression in adipose tissue in rats with dihydrotestosterone-induced polycystic ovary syndrome," *Endocrinology*, vol. 149, no. 7, pp. 3559–3568, 2008.

[75] L. Mannerås, S. Cajander, M. Lönn, and E. Stener-Victorin, "Acupuncture and exercise restore adipose tissue expression of sympathetic markers and improve ovarian morphology in rats with dihydrotestosterone-induced PCOS," *The American Journal of Physiology*, vol. 296, no. 4, pp. R1124–R1131, 2009.

[76] L. Mani, M. L. Roco, S. B. Paparo, and M. Guaragna, "Electroacupucture and nerve growth factor: potential clinical applications," *Archives Italiennes de Biologie*, vol. 149, no. 2, pp. 247–255, 2011.

Hindawi Publishing Corporation
Evidence-Based Complementary and Alternative Medicine
Volume 2013, Article ID 932581, 5 pages
http://dx.doi.org/10.1155/2013/932581

Research Article

fMRI Evidence of Acupoints Specificity in Two Adjacent Acupoints

Hua Liu,[1,2] Jian-Yang Xu,[3] Lin Li,[1,2] Bao-Ci Shan,[1,2] Bin-Bin Nie,[1,2] and Jing-quan Xue[1,2]

[1] *Key Laboratory of Nuclear Analysis Techniques, Institute of High Energy Physics, Chinese Academy of Sciences, Beijing 100049, China*
[2] *Beijing Engineering Research Center of Radiographic Techniques and Equipment, Beijing 100049, China*
[3] *General Hospital of Chinese People's Armed Police Forces, Beijing 100039, China*

Correspondence should be addressed to Bao-Ci Shan; shanbc@ihep.ac.cn

Received 21 February 2013; Accepted 28 March 2013

Academic Editor: Lijun Bai

Objectives. Acupoint specificity is the foundation of acupuncture treatment. The aim of this study is to investigate whether the acupoint specificity exists in two adjacent acupoints. *Design and Setting*. Two adjacent real acupoints, LR3 (Taichong) and ST44 (Neiting), and a nearby nonacupoint were selected. Thirty-three health volunteers were divided into three groups in random order, and each group only received acupuncture at one of the three points. While they received acupuncture, fMRI scan was performed. *Results*. The common cerebral activated areas responding to LR3 and ST44 included the contralateral primary somatosensory area (SI) and ipsilateral cerebellum. Acupuncture at LR3 specifically activated contralateral middle occipital gyrus, ipsilateral medial frontal gyrus, superior parietal lobe, middle temporal gyrus, rostral anterior cingulate cortex (rACC), lentiform nucleus, insula, and contralateral thalamus. Stimulation at ST44 selectively activated ipsilateral secondary somatosensory area (SII), contralateral middle frontal gyrus, inferior frontal gyrus, lingual gyrus, lentiform nucleus, and bilateral posterior cingulate cortex (PCC). *Conclusions*. Acupuncture at adjacent acupoints elicits distinct cerebral activation patterns, and those specific patterns might be involved in the mechanism of the specific therapeutic effects of different acupoints.

1. Introduction

Acupuncture, originated in ancient China, has been used as a treatment method in Asia for thousands of years. Nowadays, the therapeutic effect of acupuncture is gradually recognized in the western world. The National Institutes for Health of the United States have recommended acupuncture as an alternative and complementary treatment for many health conditions [1]. According to the traditional Chinese acupuncture theory as well as clinical practices, performance in specific acupoints can treat specific disorders. However, the exact physiological mechanism of acupuncture therapy is still unclear.

In the past decades, many studies of acupuncture on experimental animals have shown that acupuncture elicits therapeutic effect through modulating the neuroendocrine system [2]. Since 1990s, owing to the development of non-invasive brain imaging techniques such as functional MRI (fMRI) and positron emission tomography (PET), people have begun to address acupuncture investigation in human beings using functional imaging methods [3–6]. Siedentopf et al. reported that acupuncture at vision-related acupoints in the foot activated the visual association cortex with fMRI imaging [7]. Acupuncture at acupoints with strong analgesic effect, such as LI4 (Hegu), ST36 (Zusanli), and GB36 (Waiqiu), can modulate the hypothalamus and limbic system which are pain-related neuromatrix [8–12]. These results imply that the modulation effect of acupuncture might be related to the central nervous system. Moreover, acupuncture at specific acupoints could induce cerebral specific activation patterns. Our former work also shows there are specific cerebral patterns responding to different acupoints [13].

In the former studies on the acupoints specificity, the selected acupoints were generally far-between each other on the human body. In the current study, we chose two different and adjacently located acupoints to minimize the effect of general neural stimulation. If similar cerebral responses are derived from two real acupoints, the acupoints specificity

needs to be further discussed. Otherwise, if significantly different activated areas are found, the theory of acupoint specificity will be supported.

2. Design and Setting

2.1. Subjects. This study comprised 33 healthy right-handed volunteers (17 males and 16 females), aged 25.3 ± 2.8 (mean ± S.D.), without any history of psychiatric, neurological disorders, and substance abuse. All subjects had no acupuncture therapy experience. Each subject had provided informed consent with the adequate understanding of the procedure and purpose of this study. All subjects were free to withdraw from the experiment at any time. The protocol was approved by the local Ethics Committee.

2.2. Stimuli. Since manual acupoint stimulation is classical acupuncture, we adopted this acupuncture mode in this experiment. The silver needle is 0.30 mm in diameter and 25 mm in length. All acupuncture manipulations were performed by the same skilled acupuncturist. Two real acupoints and one nearby nonacupoint were selected in this experiment. The acupoint LR3 (Taichong) is located in the dorsum of the foot, in the depression anterior to the junction of the first and second metatarsals. The acupoint ST44 (Neiting) is located on the dorsum of the foot, proximal to the web margin between the second and third toes. Their nearby nonacupoint is located on the dorsum between the first and second metatarsals, approximately 10 mm anterolateral to LR3 and posteromedial to ST44 (Figure 1). The skilled acupuncturist identified that it was not located in any meridians.

All volunteers were divided into three groups in random order, and each group only received acupuncture at one of the three points. They were informed that they would receive acupuncture on the foot without being told the nature of the stimulation point. All the acupoints in this experiment were on right foot and anatomically innervated by the L5 spinal nerve.

2.3. Scanning Procedure. The experiments were performed on a 1.5 Tesla whole body scanner (Sonata, Siemens, Germany), with a standard head coil. The images covered whole brain and paralleled to the AC-PC line. Initially, the T_1-weighted spin-echo images were obtained for anatomical reference. For the fMRI images, we employed a blood oxygenation level-dependent (BOLD) T_2^*-weighted gradient-echo EPI sequence with TR 3000 ms, TE 50 ms, flip angle 90°, field of view 220 mm × 220 mm, matrix 64 × 64, 6 mm slice thickness and 1.2 mm gap.

Given the fact that the therapeutic effect of acupuncture will last several minutes to several hours, which is called post effect, we adopted a single block design to avoid the influence of unknown duration of post effect [6, 13]. During scanning, subjects lay supinely on the scanner bed, keeping relaxed and calm. Their eyes were covered with blinders (Aearo Co., USA) and ears were plugged with earplugs (Aearo Co., USA). The lights in the scanning room were dimmed, and there were no sounds except scanner noise. When 62 baseline scans were finished, a sterile silver needle was inserted and twirled for 60 scans. Then the needle was withdrawn. While the scan continued, till total 402 scans were acquired. The needle was twirled manually clockwise and anticlockwise at about 1 Hz frequency with "even reinforcing and reducing" manipulation. The depth of needle insertion was approximately 15 mm for the real acupoint as well as the nonacupoint.

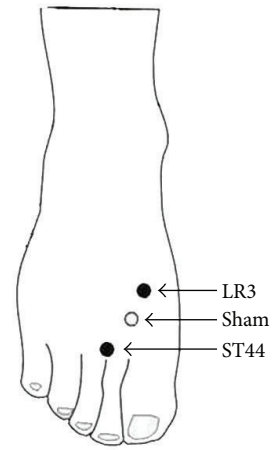

Figure 1: Anatomical location of the stimulation points: LR3, Taichong; ST44, Neiting; and their nearby nonacupoint.

2.4. Data Analysis. The fMRI data were analyzed with statistical parametric mapping software (SPM2, Welcome Department of Imaging Neuroscience, London, United Kingdom, http://www.fil.ion.ucl.ac.uk/spm/). The first two images of each scan were discarded to avoid the nonequilibrium effects of magnetization, so every subject had 400 volumes. All volume images were automatically realigned to the first image of the time series to correct for head movement between scans. After realignment, the images were normalized and transformed into the Montreal Neurological Institute (MNI) space. Then spatial smoothing was done with a 9 mm × 9 mm × 9 mm Gaussian kernel. The smoothed data were processed with two levels. At the first level, each subject's data was, respectively, analyzed using fixed effect analysis based on the general linear model with a box-car reference waveform. The cerebral areas activated during acupuncture at the real acupoint and the nonacupoint relative to baseline were obtained. At the second level, in order to acquire the specific active areas induced by stimulating at the real acupoint compared to the nonacupoint, group analysis was performed using random effects analysis based on the two-sample t-test model with the results of first level (height threshold, $P = 0.01$ corrected, spatial extent threshold, 10 voxels). The coordinates in Talairach space were obtained by applying the Mattew Brett correction (mni2tal: http://imaging.mrc-cbu.cam.ac.uk/imaging/MniTalairach) to the SPM-MNI coordinates.

3. Results

Deqi is a unique sensation of numbness, tingling, fullness, and dull ache that develops at the site of acupuncture and may spread some distance from the acupuncture point during

Table 1: Activated regions of brain induced by acupuncture at real acupoint versus nonacupoint.

Brain areas	Side	LR3 versus nonacupoint Talairach (mm)				ST44 versus nonacupoint Talairach (mm)			
		X	Y	Z	Z_{max}	X	Y	Z	Z_{max}
Primary somatosensory area	R	30	−14	60	2.54				
	L	−38	−14	60	2.45	−30	−13	60	3.09
Secondary somatosensory area	R					59	−9	21	3.03
Middle frontal gyrus	R	14	65	10	3.04				
	L					−8	63	23	2.71
Inferior frontal gyrus	L					−53	33	−5	2.98
superior parietal lobe	R	14	−50	47	3.16				
Middle temporal gyrus	R	61	−16	−14	2.78				
Middle occipital gyrus	R					28	−59	−7	2.68
	L	−18	−62	24	3.09				
Lingual gyrus	R					4	−79	−5	3.26
ACC	R	6	−15	41	2.81				
PCC	B					0	−48	15	3.26
Lentiform nucleus	R	28	−18	−1	3.42	18	0	−2	2.70
Thalamus	L	−12	−25	0	2.60				
Insula	R	32	−19	14	2.65				
Cerebellum	R	42	−56	−38	2.46	42	−52	−31	2.71
	L	−8	−64	−5	2.88	−24	−62	−29	3.55

Abbreviations: B: bilateral; R: right; L: left; ACC: anterior cingulate cortex; PCC: posterior cingulate cortex.

needle manipulation. After scan, subjects were questioned as to the type and intensity of their psychophysical feeling to acupuncture. Based on their answers, all subjects who received stimulation at real acupoint experienced distinct sensation of Deqi. In all subjects who received stimulation at nonacupoint, only one subjects reported sensation of Deqi.

Common areas activated by manual acupuncture on two real acupoints relative to nearby nonacupoint were illustrated in Figure 2, and specific areas activated by stimulation of LR3 or ST44 were showed in Figure 3. All results were summarized in Table 1. Acupuncture at LR3 significantly activated contralateral middle occipital gyrus (BA19), bilateral primary somatosensory area (SI), ipsilateral medial frontal gyrus (BA10), superior parietal lobe (BA7), middle temporal gyrus (BA21), rostral anterior cingulate cortex (rACC, BA24), lentiform nucleus, insula, cerebellum, and contralateral thalamus. Alternatively, acupuncture at ST44 selectively activated contralateral primary somatosensory area (SI), ipsilateral secondary somatosensory area (SII), lingual gyrus, lentiform nucleus, contralateral middle frontal gyrus (BA10), inferior frontal gyrus (BA47), bilateral posterior cingulate cortex (PCC, BA29), and cerebellum.

4. Discussion

In the present study, we applied manual acupuncture at two adjacent real acupoints and their nearby nonacupoint, which are all innervated by the same spinal segment, to further explore the acupoint specificity. The result showed that acupuncture at LR3 and ST44 elicited distinct response patterns, though they shared certain activation areas in common.

The obvious overlapping activated areas of LR3 and ST44 were contralateral primary somatosensory area (SI) and ipsilateral cerebellum. The activations of these areas have also been reported by some previous studies on the acupuncture at other acupoints [12, 13, 15–17]. Nakagoshi et al. have acupunctured 6 acupoints, respectively, and summarized that SI might be partly responsible for acupuncture effect [18]. The same situation happened with cerebellum. Stimulation of acupoints might arouse the modulation effect of cerebellum beyond classical involvement of cerebellum in motor coordination [16].

Stimulation of LR3 selectively activated the middle occipital gyrus (BA19) which is considered as visual cortex. The study of Siedentopf et al. found that electroacupuncture at eye-related acupoints in the foot activated visual cortex [7]. Besides middle occipital gyrus (BA19), stimulation of LR3 also activated the medial frontal gyrus (BA10), superior parietal lobe (BA7), thalamus, and the limbic system. These areas were involved in visceral modulation [19]. It is worth to notice that LR3 were also very effective for visceral pain and body paralysis. The results confirmed the view that therapeutic effects of acupuncture may work through the central nervous system pathway.

Acupuncture at ST44 specifically activated superior frontal gyrus, inferior frontal gyrus and secondary somatosensory area (SII). Frontal areas are known to be related to pain [20], especially for abirritation of visceral pain.

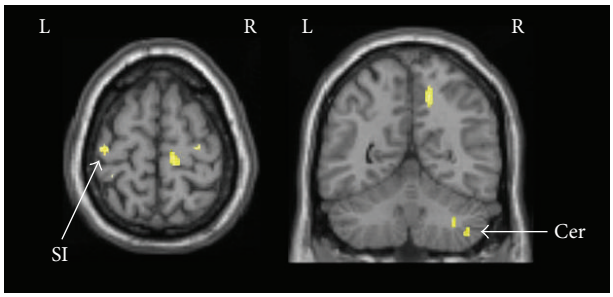

(a)

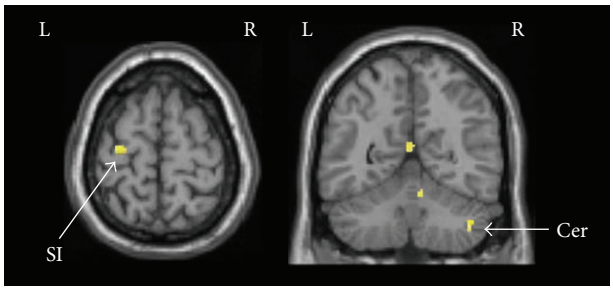

(b)

Figure 2: Common activated areas by acupuncture at LR3 or ST44. (a) Activation areas of LR3 versus nonacupoint. (b) Activation areas of ST44 versus nonacupoint. SI: primary somatosensory area; Cer: cerebellum.

Activation of the SII cortex is thought to be related to the sensory-discriminative aspect of pain processing [21]. These areas have been reported in previous studies of pain treatment by acupuncture [13, 14]. In clinical practice, it is often used to cure toothache, sore throat, stomachache, swelling, and pain of dorsum of foot. This finding implied that acupuncture at ST44 may modulate activities of the frontal areas and SII cortex to inhibit pain.

Compared with previous experiment paradigm, our investigation chose two adjacent acupoints and their nearby nonacupoint to explore the acupoint specificity. Since we adopted two adjacent acupoints, the same nonacupoint could be available. The specific activated areas of two acupoints were acquired by contrasting the real acupoints with the same nonacupoint. Therefore, the effect of neural stimulation might be thoroughly eliminated from acupuncture stimulation. Our results might be more credible than previous studies.

5. Conclusions

In this study, results demonstrated that acupuncture at adjacent acupoints could elicit different fMRI activation patterns in the human brain. It is reasonable to suggest that acupuncture at different acupoints may modulate specific cerebral areas. Our results provide supplementary neuroimaging evidence for the existence of acupoint specificity. It is helpful to interpret the underlying mechanism of acupuncture.

Conflict of Interests

The authors declare that they have no conflict of interests.

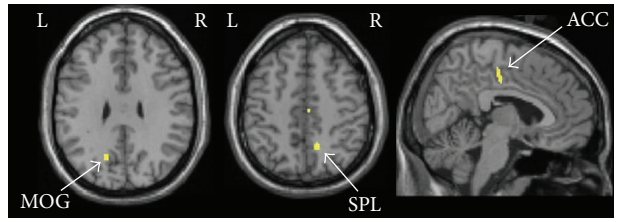

(a)

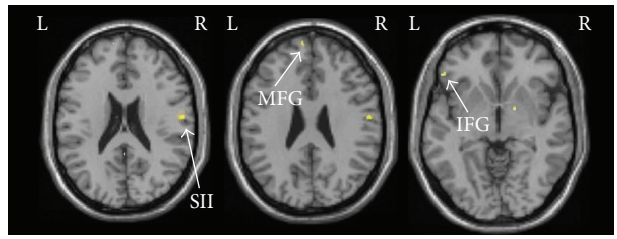

(b)

Figure 3: (a) Specific activated areas of LR3 contrasting to the nearby nonacupoint. (b) Specific activation areas of ST44 contrasting to the nearby nonacupoint. MOG: middle occipital gyrus; SPL: superior parietal lobe; ACC: anterior cingulate cortex; SII: secondary somatosensory area; MFG: middle frontal gyrus; IFG: inferior frontal gyrus.

Acknowledgment

This study was supported by the National Natural Science Foundation of China (Grant no. 91232713) and the National Basic Research Program of China (973 Program) (Grant no. 2013CB835100).

References

[1] "NIH Consensus Conference. Acupuncture," *The Journal of the American Medical Association*, vol. 280, no. 17, pp. 1518–1524, 1998.

[2] J. H. Chiu, H. C. Cheng, C. H. Tai et al., "Electroacupuncture-induced neural activation detected by use of manganese-enhanced functional magnetic resonance imaging in rabbits," *American Journal of Veterinary Research*, vol. 62, no. 2, pp. 178–182, 2001.

[3] Z. H. Cho, T. D. Oleson, D. Alimi, and R. C. Niemtzow, "Acupuncture: the search for biologic evidence with functional magnetic resonance imaging and positron emission tomography techniques," *Journal of Alternative and Complementary Medicine*, vol. 8, no. 4, pp. 399–401, 2002.

[4] J. Kong, L. Ma, R. L. Gollub et al., "A pilot study of functional magnetic resonance imaging of the brain during manual and electroacupuncture stimulation of acupuncture point (LI-4 Hegu) in normal subjects reveals differential brain activation between methods," *Journal of Alternative and Complementary Medicine*, vol. 8, no. 4, pp. 411–419, 2002.

[5] J. L. Fang, T. Krings, J. Weidemann, I. G. Meister, and A. Thron, "Functional MRI in healthy subjects during acupuncture: different effects of needle rotation in real and false acupoints," *Neuroradiology*, vol. 46, no. 5, pp. 359–362, 2004.

[6] K. Li, B. Shan, J. Xu et al., "Changes in fMRI in the human brain related to different durations of manual acupuncture needling,"

Journal of Alternative and Complementary Medicine, vol. 12, no. 7, pp. 615–623, 2006.

[7] C. M. Siedentopf, S. M. Golaszewski, F. M. Mottaghy, C. C. Ruff, S. Felber, and A. Schlager, "Functional magnetic resonance imaging detects activation of the visual association cortex during laser acupuncture of the foot in humans," *Neuroscience Letters*, vol. 327, no. 1, pp. 53–56, 2002.

[8] M. T. Wu, J. C. Hsieh, J. Xiong et al., "Central nervous pathway for acupunture stimulation: localization of processing with functional MR imaging of the brain—preliminary experience," *Radiology*, vol. 212, no. 1, pp. 133–141, 1999.

[9] K. K. Hui, J. Liu, N. Makris et al., "Acupuncture modulates the limbic system and subcortical gray structures of the human brain: evidence from fMRI studies in normal subjects," *Human Brain Mapping*, vol. 9, no. 1, pp. 13–25, 2000.

[10] G. Biella, M. L. Sotgiu, G. Pellegata, E. Paulesu, I. Castiglioni, and F. Fazio, "Acupuncture produces central activations in pain regions," *NeuroImage*, vol. 14, no. 1, part 1, pp. 60–66, 2001.

[11] J. C. Hsieh, C. H. Tu, F. P. Chen et al., "Activation of the hypothalamus characterizes the acupuncture stimulation at the analgesic point in human: a positron emission tomography study," *Neuroscience Letters*, vol. 307, no. 2, pp. 105–108, 2001.

[12] M. T. Wu, J. M. Sheen, K. H. Chuang et al., "Neuronal specificity of acupuncture response: a fMRI study with electroacupuncture," *NeuroImage*, vol. 16, no. 4, pp. 1028–1037, 2002.

[13] B. Yan, K. Li, J. Xu et al., "Acupoint-specific fMRI patterns in human brain," *Neuroscience Letters*, vol. 383, no. 3, pp. 236–240, 2005.

[14] J. Pariente, P. White, R. S. J. Frackowiak, and G. Lewith, "Expectancy and belief modulate the neuronal substrates of pain treated by acupuncture," *NeuroImage*, vol. 25, no. 4, pp. 1161–1167, 2005.

[15] W. T. Zhang, Z. Jin, F. Luo, L. Zhang, Y. W. Zeng, and J. S. Han, "Evidence from brain imaging with fMRI supporting functional specificity of acupoints in humans," *Neuroscience Letters*, vol. 354, no. 1, pp. 50–53, 2004.

[16] S. S. Yoo, E. K. Teh, R. A. Blinder, and F. A. Jolesz, "Modulation of cerebellar activities by acupuncture stimulation: evidence from fMRI study," *NeuroImage*, vol. 22, no. 2, pp. 932–940, 2004.

[17] R. P. Dhond, N. Kettner, and V. Napadow, "Neuroimaging acupuncture effects in the human brain," *Journal of Alternative and Complementary Medicine*, vol. 13, no. 6, pp. 603–616, 2007.

[18] A. Nakagoshi, M. Fukunaga, M. Umeda, Y. Mori, T. Higuchi, and C. Tanaka, "Somatotopic representation of acupoints in human primary somatosensory cortex: an FMRI study," *Magnetic Resonance in Medical Sciences*, vol. 4, no. 4, pp. 187–189, 2005.

[19] A. E. Cavanna and M. R. Trimble, "The precuneus: a review of its functional anatomy and behavioural correlates," *Brain*, vol. 129, part 3, pp. 564–583, 2006.

[20] C. Creac'h, P. Henry, J. M. Caille, and M. Allard, "Functional MR imaging analysis of pain-related brain activation after acute mechanical stimulation," *American Journal of Neuroradiology*, vol. 21, no. 8, pp. 1402–1406, 2000.

[21] R. Peyron, B. Laurent, and L. García-Larrea, "Functional imaging of brain responses to pain. A review and meta-analysis (2000)," *Neurophysiologie Clinique*, vol. 30, no. 5, pp. 263–288, 2000.

Hindawi Publishing Corporation
Evidence-Based Complementary and Alternative Medicine
Volume 2013, Article ID 931283, 7 pages
http://dx.doi.org/10.1155/2013/931283

Research Article

Visceral Nociceptive Afferent Facilitates Reaction of Subnucleus Reticularis Dorsalis to Acupoint Stimulation in Rats

Liang Li,[1] Lingling Yu,[1,2] Peijing Rong,[1] Hui Ben,[1] Xia Li,[1] Bing Zhu,[1] and Rixin Chen[3]

[1] *Institute of Acupuncture and Moxibustion, China Academy of Chinese Medical Sciences, Beijing 100700, China*
[2] *Wuhan Integrated TCM and Western Medicine Hospital, Wuhan 430020, China*
[3] *Jiangxi University of Traditional Chinese Medicine, Nanchang 330004, China*

Correspondence should be addressed to Peijing Rong; drrongpj@163.com and Bing Zhu; zhubing@mail.cintcm.ac.cn

Received 22 February 2013; Revised 18 April 2013; Accepted 23 April 2013

Academic Editor: Lijun Bai

Objective. To explore the area and sensitization variance of acupoint when internal organs are under pathological condition. To observe quantity-effect variance of subnucleus reticularis dorsalis (SRD) to electroacupuncture under both physiological and pathological conditions. To explain medulla oblongata mechanism of acupoint sensitization. *Method*. Mustard oil was imported into colon and rectum of 20 male SD rats in order to observe its influence on acupoint sensitization. SRD neuron activity was recorded. Visceral nociceptive stimulus was generated by colorectal distension (CRD). Quantity-effect variance of neuron activity to electroacupuncture to "Zusanli-Shangjuxu" area both before and after CRD was observed. Paired t-test is used for cross-group comparison; $P < 0.05$ is deemed as of statistical differences. *Result*. Visceral inflammation could facilitate SRD neuron activity to acupoint stimulation. Visceral nociceptive afference could enhance neuron activity to acupoint acupuncture. Wide dynamic range (WDR) neuron activity caused by electroacupuncture increased when visceral nociception increased. *Conclusion*. The size and function of the acupoints comply with the functionality of the internal organs. The sensitive degree of acupoints changed according to malfunction of internal organs.

1. Introduction

The theory ofacupoints has been matured through the development of history. Yet the essence of the acupoint theory remains "selection of the pain point as an acupuncture point" (points with the sense of relief or pain upon pressing), that is, the *ashi* points. Those pain points, in fact, are typical peripheral points that reflect the pathological changes to the correlated organs. It covers the two functions of acupoint as diagnosis (pain upon pressing) and treatment (sense of relief upon pressing) of diseases. Acupoints are windows that reflect specific changes in the internal organs. Points for analgesia contain many features resembling referred pain in western medicine. Referred pain caused by inner organs usually accompanies hyperalgesia of the skin [1] or muscle and often the occurrence of segmental muscle contracture [2, 3]. This kind of acupoint reaction is similar to hyperalgesia and allodynia which appeared due to sickness of inner organs. Hyperalgesia refers to the overreaction of algesia that occurres in our bodies in case of stimulation, which includes pain triggered by subthreshold stimulus that should not cause pain when the body is in its normal condition and severer pain triggered by suprathreshold stimulus that in a normal case would not cause as much pain. Allodynia refers to pain caused by situations which in the normal case should not cause pain. Allodynia is actually a kind of hyperalgesia [4]. For instance, it has been observed that a slight touch on the body surface or hair can trigger pain in the referred pain area [5]. The reason for this kind of "pain upon pressing" actually involves mechanism of hyperalgesia or allodynia in the referred area correlated to certain inner organs.

Pathological changes in the inner organs can be manifested on the surface of the body and cause the sensitization of acupoints with various kinds of pathological reactions mainly led by pain. The reason that pathological changes can achieve the above is that they are the specific reflections of the inner organs manifested through the acupoints. To some degrees, acupoints are capable of reflecting the pathological

conditions of organs and viscera. By examining changes in the feeling, shape and color of acupoints, diagnosis of inner organs can be made. In the meantime, acupuncturing on the points serves the purpose of treating the inner organs by dredging the meridians and regulating *qi* and blood. Therefore, superficial reflection areas where inner organ sicknesses manifest should be the most desirable spots to perform acupuncture so as to regulate the functionality of inner organs thus treating inner organ diseases.

Currently, the neurobiological mechanism of the sensitization of acupoints remains unclear. However, when inner organs are sick, referred pain converges. According to the facilitation theory, the diseased organ and part of the skin where referred pain occurs are both innervated by the afferent fibers from the dorsal spinal nerve, both of which end in the same area in the dorsal horn. As a result, when inner organs are sick, more impulse is sent to the dorsal horn, creating an excitation spot, thus leading to the decreasing of the threshold. Studies on referred pain have preliminarily revealed that body-viscera convergent neurons in the spine and the body of central supraspinal can be sensitized by the stimulation that comes from the inner organs, rendering that convergent neurons react stronger to the input from the body surface [6–8]. This also serves as reliable scientific proof for acupoint sensitization.

Electrophysiologic research reveals that subnucleus reticularis dorsalis (SRD) that locates in the caudal portion of the medulla can be activated by nociceptive mechanical, thermal, and chemical stimulation that comes from different parts of the body [9]. One of the most important features of the SRD neuron is that harmful information that comes from various parts of the body will gather in one neuron. Secondly, what is important is that SRD neurons have spatial summation ability against harmful stimulation: to a certain extent, activation reaction increases with the expansion of stimulating area; once it reaches or exceeds a certain area, the reaction of neurons reach saturation [10], some may even decrease. These data illustrate the occurrence of convergence between the afferent signals of the body and organs.

Discovering the rules and mechanism of the acupoint sensitization with diseased inner organs can provide guidance for clinical acupoint selection and enhance the efficacy of acupuncture in treating inner organs. When organs are sick, superficial acupoints are in different states of "sensitization" and "silence," thus altering the "quality" and "quantity" in the toning or treatment of organs. This research will study on the dynamic variation rules of acupoints from relatively "silence" to "active" state at SRD level. The correlation and other relating mechanism between the sensitization of acupoints and functionality of inner organs are also discussed.

2. Materials and Methods

2.1. Experiment Animals and Method. Experiments were performed on 20 Sprague Dawley rats (between 250 and 300 g). Following an intraperitoneal injection of 100 μg atropine sulfate, the animals were anesthetized with an intraperitoneal injection of urethane ($1.0 \sim 1.2\ \mathrm{g} \cdot \mathrm{kg}^{-1}$). A tracheal cannula was inserted and the animals were paralyzed by intravenous injection of gallamine triethiodide (Flaxedil) and artificially ventilated. Heart rate was continuously monitored and core temperature as maintained at $37 \pm 0.5^{\circ}$C by means of a feedback-controlled homeothermic heating blanket system.

The animals were mounted in a stereotaxic frame with the head fixed in a ventroflexed position by means of a metallic bar cemented to the skull, and the caudal medulla was then exposed by removing the overlying musculature, atlantooccipital membrane, and dura mater.

Unitary extracellular recordings were made with glass micropipettes filled with a mixture of 2% pontamine sky blue and 0.1 M of natrium aceticum (cusp: 5 μm, impedance: 8–12 MΩ).

Single-unit activities were recorded extracellularly and the isolated action potentials were fed into a window discriminator and displayed on an oscilloscope screen. The output of the window discriminator and amplifier were led into a data collection system (PowerLab) and a personal computer data acquisition system (Chart 5.2) to compile histograms or wavemark files.

The micropipettes were inserted on the left side of the medulla, 1.0–2.0 mm caudal to the obex, and 0.5–1.5 mm lateral to the midline. Stability for the recordings was achieved by placing over the surface of the medulla 2% Ringer-agar gel. Nonnoxious and noxious electrical or mechanical search stimuli were used to help isolate unitary activity, and neurons were classified on the basis of their responses to different stimuli applied to their peripheral receptive fields. The neurons that could be activated by noxious stimulation applied to every part of the body, and internal organs were identified as SRD neurons.

For visceral-intrusive inflammatory reaction, catheterization injection was adopted. A conduit was inserted into the rat's colorectum through anus with a depth of 2-3 cm. Then 20 μL of 2.5% mustard oil was injected (Sigma-Aldrich, St. Louis, MO, USA) through the conduit.

Visceral-intrusive stimulation is done by colorectal distension. A condom was used to make a 4–6 cm-long air sac, and it was tied to a 4 mm-diametered rubber tube. The tube was connected to a sphygmomanometer-pressure transducer with a T-tube. During the experiment, the air sac was inserted into the rat's colorectum with a depth of 4 cm. CRD stimulation is carried out by pressure supplied by a 20–80 mm Hg sphygmomanometer for 20 s or longer. Previous research [11, 12] indicated that the pressure bigger than 40 mm Hg is visceral-intrusive stimulation. In order to prevent possible sensitization triggered by over stimulation in the colorectum, the interval between two CRD stimulations should be at least more than 10 minutes.

2.2. Experiment Procedure. (1) First, response of SRD neurons to electroacupuncture at Zusanli (ST36) and Shangjuxu (ST37) in 20 rats before and after the introduction of mustard oil (20 μL) was compared in order to observe if visceral inflammatory reaction can facilitate the response caused by electroacupuncture.

(2) The stimulus intensity of electroacupuncture at Zusanli (ST36) and Shangjuxu (ST37) is 1.5 times stronger than the threshold of Aδ fiber reflection (please refer to

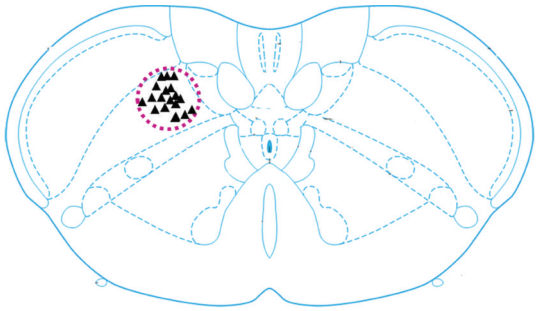

Figure 1: ▲ indicates the pontamine sky blue positioning of SRD neurons.

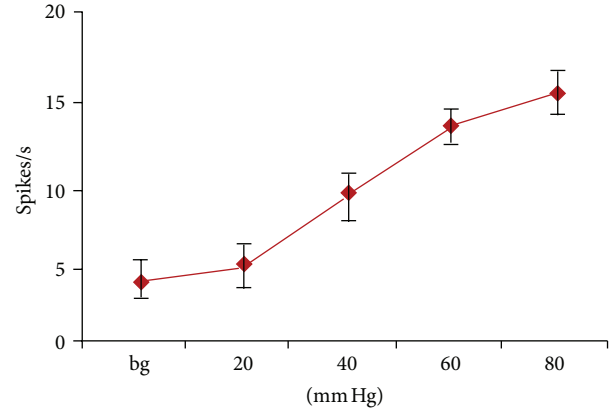

Figure 2: The activation effect of 20–80 mm Hg CRD on SRD neurons.

our previous work for detailed operation [13]. The average intensity of Aδ fiber reflection threshold is 1.77 ± 0.53 mA). The pressure of CRD was 20, 40, 60, and 80 Hg. The dose-effect relationship between visceral-intrusive stimulation and SRD neuron sensitization in various levels; nonintrusive (20 mm Hg), mild (40 mm Hg), moderate (60 mm Hg), and strong (80 mm Hg), was observed.

2.3. Histological Position of the Recorded Sites. After single-unit recording, the location of the recording site was checked by HE coloration. By referring to the brain atlas of the rat (Paxinos and Watson, 2007), the data will be abandoned if the recording site is out of the SRD neurons area.

2.4. Data Collection and Analysis. Neurons discharges per second and the activation/suppression ratio (identify as $\overline{X}$ ± SE%) were calculated with Power-Lab, Chart 5.0, and SPSS13.0. Descriptives were carried out for the average and differences of the pre- and postintervention (identify as $\overline{X}$ ± SE). Paired t-test is used for cross group comparison. $P < 0.05$ is deemed as of statistical differences.

3. Results

3.1. General Features of SRD Neurons. Totally, 65 neurons were recorded in the dorsal medulla in 20 SD male rats, among which 58 were SRD neurons and 7 were neurons from the spinal nucleus of trigeminal nerve. Figure 1 illustrates part of the pontamine sky blue positioning of SRD neurons.

Any suprathreshold electric stimulation at any part of the rat's body is capable of activating SRD neurons. Stimulation at the tale tip or 10 cm from the tip in the basilar area could trigger two peaks in the activation reaction. The latency period of the two peak reactions in the basilar area remains 14~45 ms and 185~260 ms respectively. The latency period of the two reactions in the tale tip area is 22~58 ms and 545~670 ms, respectively. The time difference in the early stage of activation reaction peak between the two areas is 10.5 ± 0.7 ms. Calculations suggest that the conduction velocity of the peripheral fibers is 12.5 ± 1.3 m/s, according with the conduction velocity range of Aδ fibers. The time difference in later period in activation reaction peak between the two basilar areas is 152 ± 14.4 ms. Calculations suggest that the conduction velocity of the peripheral fibers is 0.78 ± 0.13 m/s, in accordance with the conduction velocity range of C fibers. Therefore, an inference can be made that suprathreshold electric stimulation can activate Aδ and C fibers [10].

No SRD neuron reacted to any kind of nonintrusive stimulations (such as sound, light, and proprioceptive stimulus). SRD neurons had significant reactions towards general intrusive mechanical stimulations (e.g., pinching on the skin with toothed forceps) or 48°C water stimulation, and so forth.

3.2. Activation Effect of CRD on SRD Neurons. In the experiment, we examined 9 SRD neurons on their reactions to 20–80 mm Hg CRD stimulations. The degree of activation increased to 4.42 ± 0.68 spikes/s ($P < 0.05$) from 3.55 ± 0.63 spikes/s with 20 mm Hg of CRD; when CRD was set at an intrusive level of 40 mm Hg, the degree of activation of SRD neurons reached 8.80 ± 1.13 spikes/s ($P < 0.001$); when imposed with 60 and 80 mm Hg of CRD, the degree of activation of SRD neurons reached 13.27 ± 2.82 and 15.11 ± 2.63 spikes/s, both of great statistical significance ($P < 0.001$). This indicates that visceral-intrusive damage could activate the activity of SRD neurons in a scale-differentiating manner, and is of significant dose-effect relation (Figure 2).

3.3. The Effect of Acupoint Sensitization by Inserting Mustard Oil into Colorectum on SRD Neurons. Activity of 18 convergent neurons was recorded in 20 rats which could be activated by CRD and stimulation at Zusanli-Shangjuxu area. In normal cases, spontaneous activity was rarely seen among these neurons. After insertion of 20 μL mustard oil through the colorectal conduit, spontaneous activities of the SRD neurons was significantly increased (from 3.42 ± 0.64 spikes/s before insertion and 6.04 ± 1.63 spikes/s after; $P < 0.01$).

By using stimulation of 1.5 times stronger than Aδ fiber reflection threshold at Zusanli (ST36) and Shangjuxu (ST37), activity of 18 SRD neurons were observed before and after the colorectal insertion of the mustard oil. Before the insertion, discharge activity increased from 4.13 ± 0.77 spikes/s to 6.05 ± 1.42 spikes/s. While after injection of mustard oil, electroacupuncture at Zusanli could increase neuron discharge

Table 1: The firing discharges of SRD neurons induced by EA before and after CRD stimulation (spikes/s).

CRD intensity (mmHg)	n	BG (spikes/s)	EA before CRD (spikes/s)	EA after CRD (spikes/s)
20	16	3.25 ± 0.27	5.88 ± 0.72	6.65 ± 0.64
40	16	3.65 ± 0.36	6.31 ± 0.68	8.73 ± 0.47
60	15	3.95 ± 0.44	5.69 ± 0.73	11.18 ± 1.42
80	17	3.77 ± 0.62	5.66 ± 0.54	12.26 ± 1.72

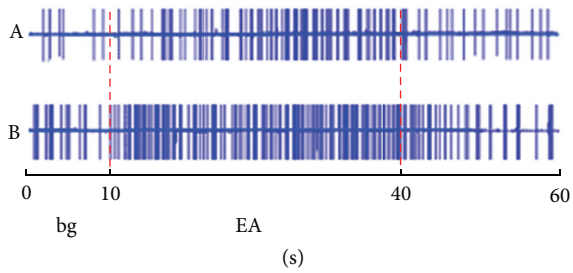

Figure 3: Differences in activation of SRD neurons before (A) and after (B) mustard oil insertion in the colorectum (indicating internal organ inflammatory reaction facilitates afferent from acupoints).

by 46.48 ± 11.45%. This indicates that electroacupuncture could activate SRD neurons with statistical difference ($P < 0.05$). After the insertion of mustard oil, on the other hand, SRD neurons were significantly activated by EA ($P < 0.01$). The activity of SRD neurons increased to 10.47±2.23 spikes/s, which is 70.86 ± 15.48% increasing compared with non-EA. The activation effect of EA stimulation with the same intensity on SRD neurons showed an increase of 73.05 ± 14.22% compared to before the insertion of mustard oil ($P < 0.01$) (Figure 3).

3.4. Effect of Acupuncture on SRD Neurons and Its Relation with CRD. This part of the research is to explore whether continuous nociceptive visceral afferent can trigger sensitization for relating acupoints and the medulla mechanism of acupoint sensitization. 20–80 mm Hg of CRD was carried out on the rat for 30 s to trigger activation of SRD neurons. Then after CRD, changes of SRD neurons activity to electroacupuncture at Zusanli-Shangjuxu area which is 1.5 times stronger than Aδ fiber reflection threshold are observed before and after CRD stimulation respectively.

The activity of SRD neurons increased with CRD pressure increasing in the range of 20–80 mm Hg for 30 s. The activity of SRD neurons increased significantly to EA stimulation after CRD (see Figures 1 and 4). This indicated that acupoint sensitization occurred after continuous nociceptive CRD stimulation was performed on the rat (see Table 1).

Activity of 16 SRD neurons to EA stimulation 1.5 times stronger than Aδ fiber reflection threshold was observed both before and after 20 mm Hg CRD. Figure 4 indicates that before CRD of 20 mm Hg, EA stimulation could significantly activate SRD neurons. Compared to the background, the activation percentage of neurons caused by EA was 80.92 ± 7.84% ($P < 0.001$). After CRD, EA activation to SRD neurons increased 113.10 ± 10.92% compared to its effect before CRD ($P < 0.05$).

Activity of 16 SRD neurons to EA stimulation 1.5 times stronger than Aδ fiber reflection threshold was observed after 40 mm Hg CRD. The intensity of activation caused by EA increased by 38.35 ± 5.12% after CRD, illustrating significant statistical differences ($P < 0.001$). After the intensity of 60 and 80 mm Hg of CRD, the degree of activation of SRD neurons caused by EA increased by 96.49 ± 11.02% and 116.10±12.89% both of which indicating significant statistical significance ($P < 0.001$). From 20 mm Hg to 80 mm Hg, the facilitation effect of CRD to EA activation effect on SRD neurons increases with pressure increasing. There is a linear relation between the two effects (Figure 5).

These results indicate that nociceptive internal organ distention is capable of sensitizing SRD neurons in the medulla which renders its reaction to the EA at acupoints becoming stronger. There is a linear relation between intensity of nociceptive stimulation to internal organ and sensitization of related acupoint. All of the results above demonstrate that SRD participates in the dynamic change of the sensitization of acupoints.

4. Discussion

As we have observed in the experiment, EA is capable of activating the activity of SRD neurons. Yet after CRD was performed, SRD neurons showed stronger reaction to the same intensity of EA at the same acupoint. This reveals that CRD is capable of sensitizing SRD neurons.

Previous studies on the relation of acupoint and organs mostly focus on the acupoints' regulation of the function in healthy state neglecting the fact that the function and area of the acupoints could vary under pathological circumstance. In recent years, we put forward the concept of "dynamics states of acupoints," deeming that the size and function of the points are not in a stable state but a changing and dynamic one. The function and size of acupoints will vary along with the state of the body, especially with the function of internal organ [14]. This experiment reveals the relation of reaction points and acupoints in organ-diseased rats. A morphological study shows that under inflammatory state, sick organs can promote the secretion of Evans blue on the body surface, and those seepage points are related to acupoints on the relating meridians. For rats with ovarian inflammation, their seepage points mainly distribute around "Guanyuan (RN4)"—"Uterus" area, and "Shenshu (BL23)"—"Mingmen (DU4)" follows [15]. For rats with acute gastric mucosa inflammation, the seepage points aligns with nerve segments and are highly related to "Pishu (BL20)," "Shenshu (BL23)," and so forth [16].

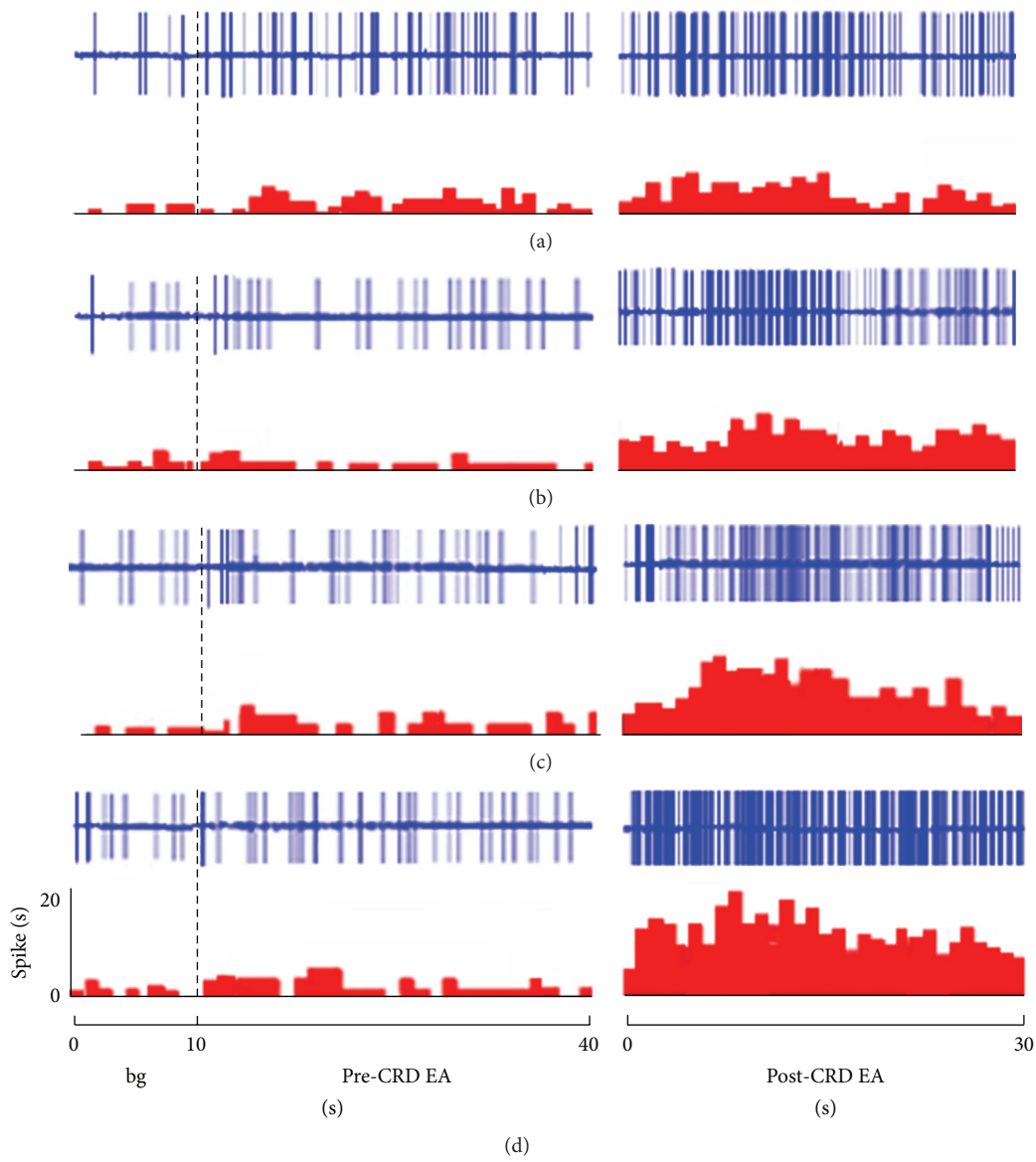

Figure 4: The responses of SRD neurons to EA before and after CRD ((a) 20, (b) 40, (c) 60, and (d) 80 mm Hg, resp.). Note: upper rows showing original unit discharges and lower rows showing histograms.

During our medulla experiment, we discovered that when WDR is activated by intrusive CRD, giving EA in the receptor filed will trigger further activation of WDR neurons. This indicates that peripheral and afferent nerves that derive from the same nerve segments meet at the WDR, thus illustrating concerted reaction. Another part of our experiments shows that after ending long time intrusive CRD stimulation, giving the same intensity of EA in the receptor field causes a stronger activating reaction in WDR and SRD neurons as compared with before the CRD, indicating that CRD has managed to increase the sensitization of neurons.

These studies have shown that along with the changes from healthy to pathological state of the organs, the function of acupoints could alter from silent state into an active or sensitized state becoming rather sensitiveand active.

It is a central mechanismfor acupoints to reflect organ diseases that the primary afferent of the body and organs meet in the nervous centralis. Studies such as Cervero and Connell [17] and Cervero [18] showed that the intercostal nerve and greater splanchnic nerve of the cat convergein the thoracic cord. With light and electron microscope, Jishuo and Binzhi [19] have discovered that visceral primary afferent of the pelvic nerve and corporality primary afferent of the sciatic nerve both project to the sacral dorsal commissural nucleus. He has also found that some of the two afferents converge into the same dendrite of the dorsal commissural nucleus. Alles and Dom [20] injected dual-marking fluorescence indicator into the inner side of the arm and pericardium and found the indicator in the same side of dorsal root ganglion at C_8-T_2. The sensory nerve projection of the rabbit's riyue

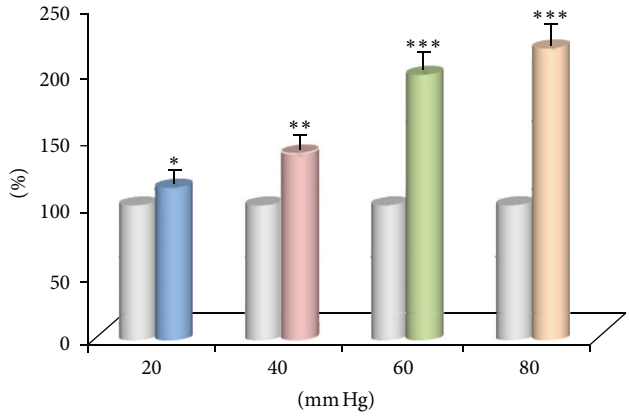

Figure 5: The response of SRD neurons to EA at different CRD levels (Left: before; Right: after). The response of SRD neurons to EA increases with CRD and shows a distinct dose-effect relation ($P < 0.05 \sim 0.001$).

and qimen area shares 5–7 overlapping segments with the sensory nerve in the choledoch ampullary portion [21]. These studies not only prove the convergence of the peripheral and organ afferent but also serve as direct morphological proof inreferred pain in western medicine.

The abnormal hyperalgesia occurance upon pressing acupoints while the internal organs are sick is the result of facilitation and sensitization of the spinal cord and/or supraspinal centrum while pathological changes take place in the organs and is in accordance with the converging sensitization/facilitation mechanism that explains referred pains. Studies have shown [6, 22] that afferent impulse in the organs or deep tissues could sensitize the body-organ convergent neurons in the dorsal horn of the spinal cord, thus rendering that neurons have intensified reaction to the afferents that come from the body surface. After these convergent neurons have experienced sensitization caused by visceral changes (intrusive stimulation), the number of spontaneous discharging cells increases, the frequency of discharging goes up, the threshold of stimulation decreases, and the surface receptor field expands. For instance, for animals with referred muscle hyperalgesia caused by ureteral calculus, the number and frequency of background discharging spinal cord cells exceed that of the normal animals [7]; after chemical stimulation in the bladder, the background discharging of neurons in the dorsal horn of the spinal cord elevates [6]; compared with normal rats, rats with ureteral calculus have a greater number and frequency of background discharging in neurons from the dorsal horn of the spinal cord; the author considers this as referred hyperalgesia [8]. Besides, inflammation in the esophagus [23] and colon [24] may lead to the reduction in reaction threshold. Multiple distending with air sac in the esophagus results in the expansion of the receptor field in dorsal horn neurons in T_{2-4}. By the same token, distending gall bladder with 65–80 mm Hg can lead to the expansion in receptor field for the skin in body-organ convergent neurons in the dorsal horn of the spinal cord. Injecting glutamate in SRD could facilitate the activation reaction of WDR on EA sciatic neurons [25].

5. Conclusions

The convergent sensitization mechanism refers to the reduction of reaction threshold, increasing of background discharging, and the expansion of receptor filed when body-organ convergent neurons experience pathological changes in the organs. This has shown that the size and function of the acupoints comply with the functionality of the internal organs. Those studies have provided scientific proof for acupoints status transforming from silence to activation.

Acknowledgments

This scientific work was supported by National Basic Research Program of China (973 Program, nos. 2011CB505201, 2012CB518503, and 2009CB522902), National Twelfth Five-year Science and Technology Program (no. 2012BAF14B10), and National Natural Science Foundation of China (no. 81102649). All authors approved the paper and there are no conflicting financial interests for this paper.

References

[1] G. N. Verne, M. E. Robinson, L. Vase, and D. D. Price, "Reversal of visceral and cutaneous hyperalgesia by local rectal anesthesia in irritable bowel syndrome (IBS) patients," *Pain*, vol. 105, no. 1-2, pp. 223–230, 2003.

[2] M. A. Giamberardino and L. Vecchiet, "Visceral pain, referred hyperalgesia and outcome: new concepts," *European Journal of Anaesthesiology*, vol. 12, supplement 10, pp. 61–66, 1995.

[3] J. F. B. Morrison, A. Sato, Y. Sato, and T. Yamanisht, "The influence of afferent inputs from skin and viscera on the activity of the bladder and the skeletal muscle surrounding the urethra in the rat," *Neuroscience Research*, vol. 23, no. 2, pp. 195–205, 1995.

[4] E. A. Ziegler, W. Magerl, R. A. Meyer, and R. D. Treede, "Secondary hyperalgesia to punctate mechanical stimuli. Central sensitization to A-fibre nociceptor input," *Brain*, vol. 122, no. 12, pp. 2245–2257, 1999.

[5] M. Koltzenburg, L. E. R. Lundberg, and H. E. Torebjork, "Dynamic and static components of mechanical hyperalgesia in human hairy skin," *Pain*, vol. 51, no. 2, pp. 207–218, 1992.

[6] M. A. Giamberardino, A. Dalal, R. Valente, and L. Vecchiet, "Changes in activity of spinal cells with muscular input in rats with referred muscular hyperalgesia from ureteral calculosis," *Neuroscience Letters*, vol. 203, no. 2, pp. 89–92, 1996.

[7] C. Roza, J. M. A. Laird, and F. Cervero, "Spinal mechanisms underlying persistent pain and referred hyperalgesia in rats with an experimental ureteric stone," *Journal of Neurophysiology*, vol. 79, no. 4, pp. 1603–1612, 1998.

[8] D. W. Garrison, M. J. Chandler, and R. D. Foreman, "Viscerosomatic convergence onto feline spinal neurons from esophagus, heart and somatic fields: effects of inflammation," *Pain*, vol. 49, no. 3, pp. 373–382, 1992.

[9] L. Villanueva, Z. Bing, D. Bouhassira, and D. Le Bars, "Encoding of electrical, thermal, and mechanical noxious stimuli by subnucleus reticularis dorsalis neurons in the rat medulla," *Journal of Neurophysiology*, vol. 61, no. 2, pp. 391–402, 1989.

[10] L. Liang, Y. Jingsheng, R. Peijing et al., "Effect of moxibustion-like thermal stimulation with different temperature and covering different areas of "zhongwan" (CV 12) on discharges of

neurons in medullary subnucleus reticularis dorsalis of rats," *Acupuncture Research*, vol. 36, pp. 313–320, 2011.

[11] T. J. Ness and G. F. Gebhart, "Visceral pain: a review of experimental studies," *Pain*, vol. 41, no. 2, pp. 167–234, 1990.

[12] T. J. Ness, A. M. Metcalf, and G. F. Gebhart, "A psychophysiological study in humans using phasic colonic distension as a noxious visceral stimulus," *Pain*, vol. 43, no. 3, pp. 377–386, 1990.

[13] B. Zhu, W. D. Xu, P. J. Rong, H. Ben, and X. Y. Gao, "A C-fiber reflex inhibition induced by electroacupuncture with different intensities applied at homotopic and heterotopic acupoints in rats selectively destructive effects on myelinated and unmyelinated afferent fibers," *Brain Research*, vol. 1011, no. 2, pp. 228–237, 2004.

[14] Y. Xiaochun, Z. Bing, G. Junhong et al., "Scientific foundation of dynamic process of acupoints," *Journal of Traditional Chinese Medicine*, vol. 48, pp. 971–973, 2007.

[15] S. J. Wang and B. Zhu, "Study on relation of ovary-body surface correlativity with acupoints," *Chinese Acupuncture & Moxibustion*, vol. 27, no. 10, pp. 761–765, 2007.

[16] B. Cheng, H. Shi, C. F. Ji, J. H. Li, S. L. Chen, and X. H. Jing, "Distribution of the activated acupoints after acute gastric mucosal injury in the rat," *Acupuncture Research*, vol. 35, no. 3, pp. 193–197, 2010.

[17] F. Cervero and L. A. Connell, "Distribution of somatic and visceral primary afferent fibres within the thoracic spinal cord of the cat," *Journal of Comparative Neurology*, vol. 230, no. 1, pp. 88–98, 1984.

[18] F. Cervero, "Somatic and visceral inputs to the thoracic spinal cord of the cat: effects of noxious stimulation of the biliary system," *Journal of Physiology*, vol. 337, pp. 51–67, 1983.

[19] L. Jishuo and Q. Binzhi, "Rabbit body (sciatic nerve) and internal organs (bladder) primary afferent neurons to sacral pulp after commissure nucleus of projection—HRP across ganglion tracking observation," *Chinese Journal of Neuroanatomy*, vol. 3, pp. 49–55, 1987.

[20] A. Alles and R. M. Dom, "Peripheral sensory nerve fibers that dichotomize to supply the brachium and the pericardium in the rat: a possible morphological explanation for referred cardiac pain?" *Brain Research*, vol. 342, no. 2, pp. 382–385, 1985.

[21] D. Wei, Q. Li, L. Zhang, C. Li, and X. Zhang, "The correlation of central projection of the acupoints riyue, qimen with correlative viscera, in the rabbit," *Acupuncture Research*, vol. 15, no. 1, pp. 13–17, 1990.

[22] S. B. McMahon, "Neuronal and behavioural consequences of chemical inflammation of rat urinary bladder," *Agents and Actions*, vol. 25, no. 3-4, pp. 231–233, 1988.

[23] E. D. Al-Chaer, K. N. Westlund, and W. D. Willis, "Sensitization of postsynaptic dorsal column neuronal responses by colon inflammation," *NeuroReport*, vol. 8, no. 15, pp. 3267–3273, 1997.

[24] I. Euchner-Wamser, J. N. Sengupta, G. F. Gebhart, and S. T. Meller, "Characterization of responses of T2-T4 spinal cord neurons to esophageal distension in the rat," *Journal of Neurophysiology*, vol. 69, no. 3, pp. 868–883, 1993.

[25] C. Dugast, A. Almeida, and D. Lima, "The medullary dorsal reticular nucleus enhances the responsiveness of spinal nociceptive neurons to peripheral stimulation in the rat," *European Journal of Neuroscience*, vol. 18, no. 3, pp. 580–588, 2003.

Hindawi Publishing Corporation
Evidence-Based Complementary and Alternative Medicine
Volume 2013, Article ID 812568, 9 pages
http://dx.doi.org/10.1155/2013/812568

Review Article

Neurobiological Foundations of Acupuncture: The Relevance and Future Prospect Based on Neuroimaging Evidence

Lijun Bai[1] and Lixing Lao[2]

[1] *The Key Laboratory of Biomedical Information Engineering, Ministry of Education, Department of Biomedical Engineering, School of Life Science and Technology, Xi'an Jiaotong University, Xi'an 710049, China*
[2] *Center for Integrative Medicine, School of Medicine, University of Maryland, 520 W. Lombard Street, Baltimore, MD 21201, USA*

Correspondence should be addressed to Lijun Bai; bailj4152615@gmail.com

Received 21 March 2013; Accepted 17 April 2013

Academic Editor: Baixiao Zhao

Acupuncture is currently gaining popularity as an important modality of alternative and complementary medicine in the western world. Modern neuroimaging techniques such as functional magnetic resonance imaging, positron emission tomography, and magnetoencephalography open a window into the neurobiological foundations of acupuncture. In this review, we have summarized evidence derived from neuroimaging studies and tried to elucidate both neurophysiological correlates and key experimental factors involving acupuncture. Converging evidence focusing on acute effects of acupuncture has revealed significant modulatory activities at widespread cerebrocerebellar brain regions. Given the delayed effect of acupuncture, block-designed analysis may produce bias, and acupuncture shared a common feature that identified voxels that coded the temporal dimension for which multiple levels of their dynamic activities in concert cause the processing of acupuncture. Expectation in acupuncture treatment has a physiological effect on the brain network, which may be heterogeneous from acupuncture mechanism. "Deqi" response, bearing clinical relevance and association with distinct nerve fibers, has the specific neurophysiology foundation reflected by neural responses to acupuncture stimuli. The type of sham treatment chosen is dependent on the research question asked and the type of acupuncture treatment to be tested. Due to the complexities of the therapeutic mechanisms of acupuncture, using multiple controls is an optimal choice.

1. Introduction

Acupuncture is an ancient East Asian healing modality that has been in use for more than 2000 years. Together with herbal medicine, it is regarded as one of the two most pivotal medical skills in East Asian medicines. In the last decades, acupuncture has gained great popularity as an alternative and complementary therapeutic intervention in the western medicine [1]. An estimation of 3 million American adults receive acupuncture treatment each year [2]. Acupuncture is the insertion and stimulation of needles at specific acupoints on the body to facilitate recovery of health. For example, a promising efficacy of acupuncture has been shown in the treatments of postoperative and chemotherapy nausea and vomiting [3]. It has also become a beneficial adjunct for pain management [4, 5]. In spite of its public acceptance, increasing attentions are paid to explore the scientific explanation regarding the physiological mechanism of acupuncture.

Abundant evidence from animal studies has demonstrated that acupuncture stimulation can facilitate the release of certain neuropeptides in the central nervous system (CNS), eliciting profound physiological effects and even activating self-healing mechanisms [6, 7]. Studies of electroacupuncture in rats revealed that both low-frequency and high-frequency stimulation could induce analgesia, but that there are differential effects of low- and high-frequency acupuncture on the types of endorphins released [8]. One recent study demonstrated that peripheral acupuncture stimulation can ease pain by triggering a natural painkilling chemical called adenosine, which typically surges in concentration after any stress or injury. Adenosine works by docking at a protein called the adenosine A1 receptor, which has well-established roles in suppressing pain and is found on neurons that transmit pain signals [9]. Although animal research clearly supports a role for specific neural pathways underlying the action of acupuncture, it is difficult to interpret these studies in

the context of more complex human experience, including the belief states, emotion, and cognition changes. The noninvasive functional magnetic resonance imaging (fMRI) technique has opened a "window" into the brain, allowing us to investigate the central physiological functions involved in acupuncture administration of human beings available. The wide range of physical effects exerted by acupuncture and its purported efficacy for a compendium of clinical pathologies suggest that the brain may be responsible for transmitting the needle stimulus into signals aimed at maintaining homeostatic balance within and across functional subsystems [10–12]. In this review, we have systematically researched and reviewed the literature looking at the neurophysiologic mechanisms of acupuncture on human brain and discussed how these findings contribute to current hypotheses of acupuncture action.

2. Neural Correlates Involving Acupuncture in Human

Converging evidence from fMRI studies on acupuncture at commonly used acupoints have revealed significant modulatory effects at widespread cerebrocerebellar brain regions. These regions process information in circuits that can broadly be assumed to engage endogenous antinociceptive limbic networks as well as higher-order cognitive and affective control centers within the prefrontal cortex and medial temporal lobe [13–20]. Researches from Wu et al. indicated that stimulation at LI4 and ST36 resulted in increases in signal intensity of the hypothalamus and nucleus accumbens, as well as decreases in the rostral part of the anterior cingulated cortex, amygdala, and hippocampus [18]. This evidence supported the hypothesis that acupuncture can activate the structures of descending antinociceptive pathway and deactivate multiple limbic areas subserving affective dimension of pain, largely overlapping with the "neuromatrix" for both pain transmission and perception. These regions process information in circuits that can broadly be assumed to engage: the affective (amygdala, hippocampus), sensory (thalamus, primary (SI) and secondary (SII) somatosensory cortices), cognitive (ACC, anterior insula), and inhibitory (PAG, hypothalamus) processing during the experience of pain. Notably, Hui et al. reported that needle stimulation at ST36 induced a wider range of negative signal changes in the limbic-cerebellum system [14]. This widely decreased limbic-cerebellum network may be one of the central characteristics involved in the action of acupuncture. Collectively, neuroimaging data strongly suggest that acupuncture modulates many distributed cortical and subcortical (i.e., brainstem, limbic, and cerebellum) brain areas. These brain areas may contribute to the therapeutic effect of acupuncture by shifting autonomic nervous system (ANS) balance and altering the affective and cognitive dimensions of pain processing.

Previous neuroimaging studies on acupuncture focus mainly on the spatial distribution of brain activities induced by acupuncture stimuli. Interest in exploring what happens in the human brain when subjects do not perform cognitively demanding tasks has increased in the past few years. Some researchers indicated that even in the task-free state, the brain continuously expends a considerable amount of energy, and external tasks only modestly modulate the effects of such ongoing activity [21–23]. Therefore, as suggested by Raichle and colleagues, in terms of overall brain functions, the ongoing intrinsic activity within various brain systems may be at least as important as the activity evoked by external stimuli [22, 23]. More importantly, a recent study has reported differences in resting-state brain functions of people with chronic pain in contrast with controls, and the authors proposed that this difference in resting-state brain activity might reflect the cognitive and affective complications of chronic pain [24]. Therefore, analysis of resting-state connectivity can not only help us to better understand the long-term effects of pain on brain but also the potential benefits of acupuncture in pain treatments. One pioneer studies using independent component analysis have found that acupuncture, not the sham condition, can enhance interregional functional connectivity within both the default mode network and sensorimotor network [25], including the medial temporal lobe, PAG, and supplementary motor area (SMA). They also reported that connectivity between the hippocampus and DMN saliently correlated with parasympathetic output only following the acupuncture stimulation. This indicated that acupuncture may operate through the regulation of autonomic nervous system, which was consistent with increasing evidence for the involvement of autonomic efferent nerve activity underlying its specific effects [26, 27]. Another study using the spontaneous activity detection approach indicated that acupuncture may not only enhance the dichotomy of the anticorrelated resting networks ("default mode" network and "central-executive" network) but also modulate a larger spatio-temporal extent of spontaneous activities in the salient interoceptive-autonomic network, which may contribute to potential actions in the endogenous pain-modulation circuits and homeostatic control mechanism [28]. This hypothesis needs further investigations in the altered and/or dysfunctional brain networks such as those in patients with chronic pain.

3. Time-Varied Acupuncture Effect and Its Influence on fMRI Study

Abundant clinical reports have indicated that acupuncture can provide relief even beyond the time it is being performed. Psychophysical analysis from Price et al. suggests that the analgesic effects of acupuncture might actually peak long even after the needling session is terminated [29]. Another evidence using pain threshold to potassium iontophoresis also showed the delayed development of acupuncture analgesia [30]. The increase of the pain threshold induced by acupuncture has a peak occurring 20–40 min after needle insertion, and the pain threshold persisted over 30 min after withdrawal of the acupuncture needle. Due to the sustained effect of acupuncture, the temporal aspects of the BOLD response to acupuncture may violate the assumptions of the block-designed GLM estimates (Figure 1) [31].

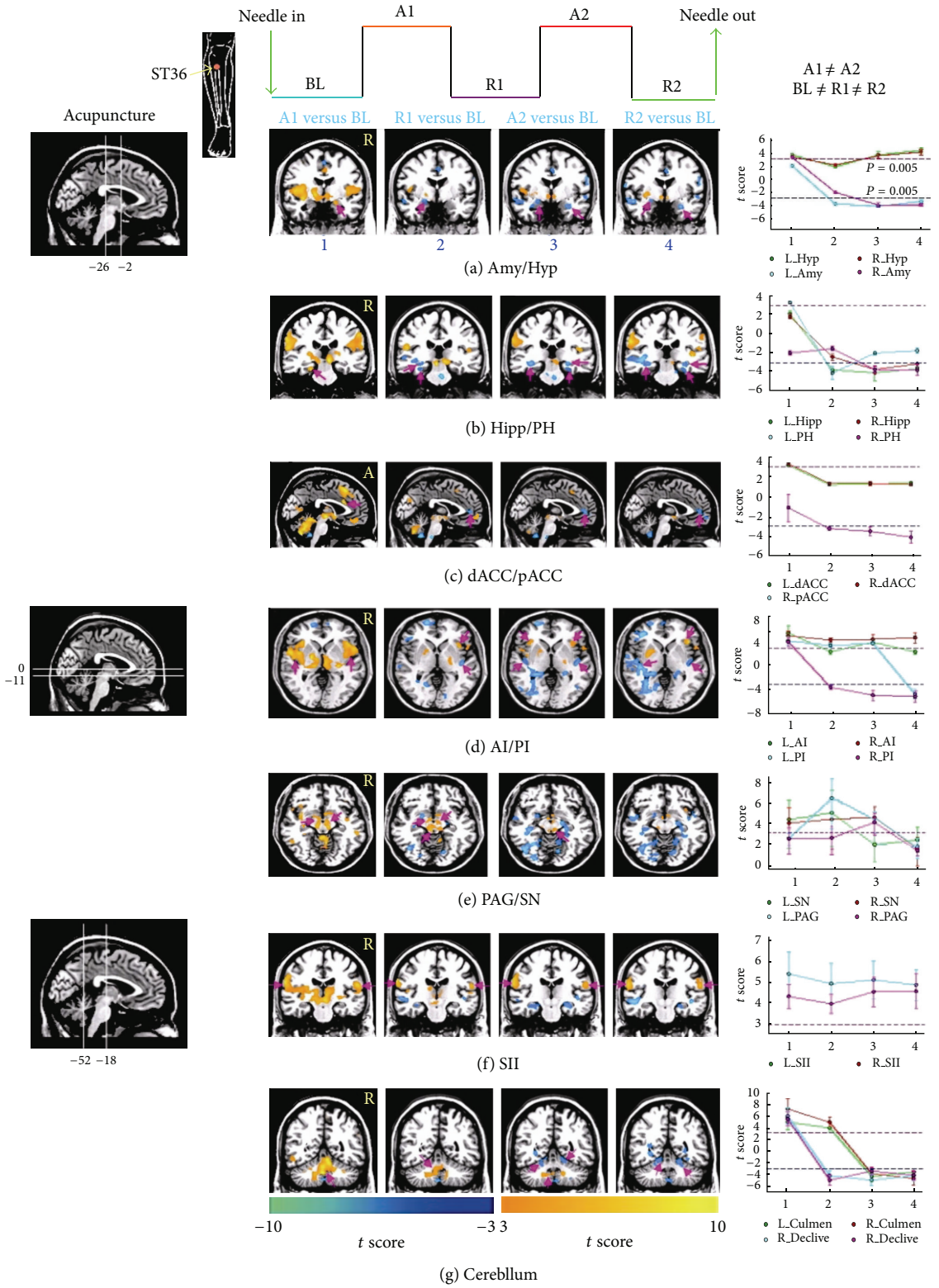

Figure 1: Representative brain areas induced by acupuncture at ST36 for different epochs of multiblock design paradigm ($P < 0.005$, uncorrected). The kinetics of acupuncture was complex and longer acting as a function of time, rather than conforming to simple "on-off" variations predicated by the block-based GLM analysis. Abbreviations: Amy: amygdala; Hipp: hippocampus; PH: parahippocampus; pACC: pregenual anterior cingulate cortex; dACC: dorsal cingulate cortex; AI: anterior insula; PI: posterior insula; SII: secondary somatosensory cortex; Hyp: hypothalamus; PAG: periaqueductal gray; SN: substantia nigra (adapted from [31]).

In the framework of GLM, a specific stimulus sequence (i.e., design matrix) is used to define an ideal hemodynamic response function (HRF), which is convolved with the actual hemodynamic response and produces predictors of the BOLD response. For multiblock design, the temporal changes in the BOLD signal as predicted by the GLM conform to the "on-off" specifications set by the experimenter. Considering that the temporal profile of acupuncture is slow to develop and resolve, the magnitude of BOLD signal in rest period following the initial stimulation is unlikely to have returned to the initial (prestimulus) baseline level. Since fMRI analysis is an inherently contrastive methodology [32], the presence of activity during the baseline condition can seriously compromise the integrity of the sequential results. Due to the slow-acting agent of acupuncture, neural activities during rest periods may reduce, eliminate, or even reverse the sign of activities during stimulation conditions [31]. Therefore, the depiction of dynamic on-going acupuncture effects would be obtained in the absence of any assumption concerning the shape of the hemodynamic response, while the GLM's effectiveness in modeling such state-related activity is limited. In this line, a more flexible model, which captures consistencies in activation magnitude but allows for temporal variations, may be a more optimal choice instead.

Recently, our group has applied data-driven methods, such as the change-point approach with a hierarchical exponentially weighted moving average (HEWMA) analysis to model such slowly varying processes of acupuncture, of which the onset time and durations of underlying psychological activity were uncertain [33]. Our results demonstrated that BOLD signal changes induced by acupuncture shared a common feature that the identified voxels, containing a population of neurons, coded the temporal dimension (Figure 2). Notably, simply needling manipulation can evoke consistently increased signal changes in the wide pain-sensitive regions but more complex and time-varied neural responses during the poststimulus phrase. One possible explanation is that acupuncture manipulation, like kind of painful stimulus, generally involves a needling stimulation in deep tissue with both skin piercing and biochemical reactions to the tissue damage; this predominant experience may be primarily associated with excitatory responses in pain-related areas. As the effect of acupuncture may require a period of time to develop, its complex action on disassemble neural system may occur as time prolonged. For instance, the amygdala and perigenual anterior cingulate cortex (pACC) exhibited increased activities during the needling phrase while decreased gradually to reach significance below the baseline level. The periaqueductal gray (PAG) and hypothalamus presented saliently intermittent activations across the whole session. Relatively persistent activities were also identified in the anterior insula and prefrontal cortices. It is also noteworthy that there were remarkable overlapping brain regions involving acupuncture on both ST36 and nearby nonacupoint, the brain networks were more intrinsically heterogeneous and consisted of subsystems as time prolonged. Specifically, the sham networks consisted of a more time-independent subsystem that mainly included the sensorimotor and association cortices. In contrast, the acupuncture networks were much more extensive and time dependent, involving multiple neural circuitries. Previous investigations, focused on the spatial distribution of neural response to acute effects of acupuncture within a relatively short-term span, have argued that possible neural differences between the verum acupuncture and sham control are too subtle for detection in fMRI. As the effects of acupuncture may require a period of time to develop, the differences may only emerge over time when its delayed effect was being studied. To further test our hypothesis, we also adopted an electrophysiological imaging modality, namely, magnetoencephalography with a more sensitive temporal resolution on the order of milliseconds. Our findings showed that verum acupuncture can increase the connection degree between the temporal cortex (amygdala and hippocampus) and prefrontal cortex within delta (0.5–4 Hz) and beta (13–30 Hz) bands, while such effect occurred only in the delta band for sham control [34].

4. Interactions of Brain Network between Acupuncture and Expectancy

Acupuncture is a procedure in which fine needles are inserted into an individual at discrete points and then manipulated, with the intent of relieving pain. Clinical observations have shown that acupuncture analgesia is very effective in treating chronic pain, helping from 50% to 85% of patients (compared to morphine which helps only 30%). The analgesic effect of acupuncture is not a simple reflection or linear readout of incoming sensory information but can be substantially influenced by variations in individual physiological states. This inference can partially explain why the analgesic effect of acupuncture is generally characterized by tremendous interindividual variability. The existence of psychological factors in acupuncture analgesia when treating a patient's chronic pain is not unexpected, as with many medical treatments. There is still high skepticism whether acupuncture analgesia is predominately attributable to its physiological or just only psychological action. In the majority of randomized controlled trials (RCTs), it is generally concluded that acupuncture relevantly reduces pain but not more than a credible placebo procedure [35–37]. One recent systematic review using individual patient data meta-analyses to identify randomized controlled trials (RCTs) of acupuncture for chronic pain has promising results and indicates that acupuncture is effective for the treatment of chronic pain and is therefore a reasonable referral option. However, the difference of pain relief between acupuncture and placebo only obtain marginal significance. The substantial effect seen in the placebo acupuncture groups presents a significant challenge for both evaluating the efficacy and interpreting the effectiveness of acupuncture.

Distinct from the classical senses, pain is multifaceted and generally involves sensory, affective, and autonomic drive dimensions. The subjective evaluation of one's condition (e.g., "how do you feel?") generally involves several complicated cognitive processes, which can be easily biased by previous

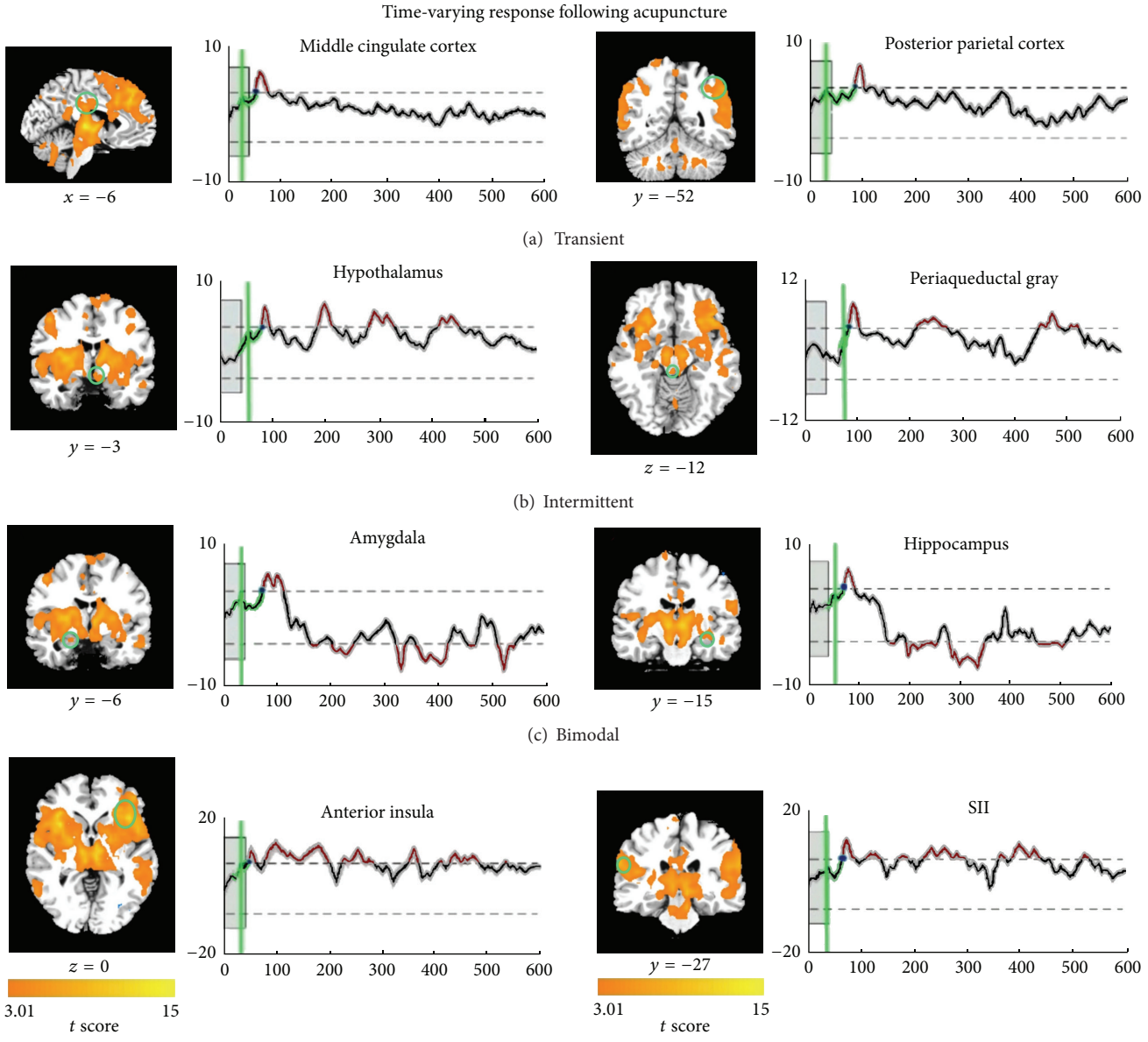

Figure 2: The baseline period was indicated by the shaded gray box, and the EWMA statistic was shown by the thick black line (corrected over time and FDR corrected at $\alpha = 0.05$ over space), with gray shading denoting the standard error across participants. The estimated CP for onset activity was presented in green line. The control limits were shown by dashed lines. Abbreviations: SII: secondary somatosensory cortex (adapted from [33]).

experience and expectation [38]. In this regard, the availability of sophisticated brain imaging methods such as fMRI provides us objective techniques to enhance our understanding of the modulation mechanism of acupuncture. Recent studies have provided neuroimaging evidence to support different mechanisms underlying acupuncture in comparison with placebo/sham [39, 40]. Kong and colleagues examine both the interaction and dissociation between expectancy manipulation and acupuncture and demonstrate that expectancy could significantly influence acupuncture analgesia for the experimental pain, whereas acupuncture might specifically inhibit incoming noxious stimuli in comparison with the expectancy more involving the emotional circuit [39]. Harris et al. also investigate both short- and long-term effects of acupuncture versus sham treatment on in vivo μ-opioid receptor (MOR) binding availability in chronic fibromyalgia pain patients [40]. They suggest that acupuncture therapy could evoke both short-term and long-term increases in MOR binding potential in multiple pain and sensory processing regions associated with reductions in clinical pain, whereas such effect presented absent or even small reduction in the sham group. Another study enrolled fourteen patients with osteoarthritis of the thumb and designed two placebo controls (nonpenetrating Streitberger needle and an overt placebo) to explore both the specific effect of real acupuncture and the nonspecific effect of treatment expectation. The overt

placebo was a nonpenetrating surface skin prick, bearing exactly the same stimulus as the Streitberger needle. However, patients were told in advance that this manipulation had no therapeutic effect. For the specific effect, by comparing the real acupuncture and Streitberger needle, the insula ipsilateral to the site of needling was activated to a greater extent during real acupuncture than during the placebo intervention. For the nonspecific effect, by comparing the Streitberger needle and overt placebo, the only difference was activation in dorsal lateral prefrontal cortex, rostral anterior cingulate cortex, and midbrain, suggesting a possible mechanism for the placebo effect involving acupuncture. The finding demonstrated that expectation in acupuncture treatment has a physiological effect on the brain network which mediates a potential nonspecific clinical response to acupuncture. These lines converge into one notion that divergent neural mechanisms may mediate specific dimensions of acupuncture effects in comparison with the placebo effects.

5. Deqi Sensations and Neural Responses by Acupuncture

In clinical settings, acupuncturists focused on "deqi" feeling during the needling treatment. This sensation was generally experienced by the patients and also by manipulating feeling of the acupuncturist when reaching the level of "qi" in the body. Deqi has recently drawn the attentions of many scientific researchers, and some studies propose that no appreciable therapeutic effect is obtained under a certain stimulation level, which is determined by the appearance of a particular sensation known as deqi [41–44]. One recent report investigated the characteristics of the "deqi" response in acupuncture at different acupoints (ST36, LI4, and LV3) and its association with distinct nerve fibers, compared with the conventional somatosensory or noxious stimuli. They indicated that aching, soreness, and pressure were most common sensations for different acupoints, followed by tingling, numbness, dull pain, heaviness, warmth, fullness, and coolness, and The sharp pain was regarded as inadvertent noxious stimulation. The most specific sensations of deqi were aching, soreness, pressure, and dull pain, in comparison of tactile stimulation control. Such complex composite of deqi sensations indicated involvement of nerve fibers at all levels (myelinated and unmyelinated nerve fibers). Particularly, the deeper muscle layers with its rich supply of slow conducting fibers may play the key role in acupuncture. It is consistent with the findings that deqi sensations are blocked after injection of procaine into the muscle beneath the acupoints. Following lumbar anesthesia, both deqi sensations and electromyography were completely abolished [45]. This phenomenon inferred that acupuncture-induced sensations were mainly generated from muscle, and the activity of polymodal-type receptors in deep tissues may play an important role [46]. This finding partly provides a clue to demonstrate the deqi with modern concepts in neurophysiology and bearing clinical relevance.

Given that deqi plays a pivot role in the therapeutic effect of acupuncture, it is noteworthy to find the relations between the brain activities and acupuncture-induced feelings. One study showed that acupuncture-induced deqi sensations without sharp pain primarily elicited widespread signal decreases in several brain areas, including the frontal pole, VMPF cortex, cingulated cortex, hypothalamus, reticular formation, and the cerebellar vermis, whereas sharp pain elicited signal increases in several areas, including the frontal pole and the anterior, middle and posterior cingulate [14]. They further inferred that acupuncture feeling without sharp pain are related to analgesia and antistress and deactivate the limbic-subcortical regions. By contrast, acupuncture feeling mixed with the sharp pain is associated with needling stimulation in deep tissue with skin piercing and biochemical reaction to tissue damage, and thus, the central effects of pain prevailed, exhibiting an integrated response with predominance of activation over deactivation in the cerebrocerebellar and limbic systems. Another research indicated that individual differences in the deqi scores can modulate the degree to which the right anterior insula was activated only following the verum acupuncture at ST36, compared with sham control [28]. The anterior insula has been widely accepted as a relay station integrating the centrally processed sensory information (visceral and autonomic) for its reciprocal connections with multiple brain regions [47]. This region, particularly the right anterior part, also plays a critical role in the interoceptive awareness of both stimulus-induced and stimulus-independent changes in the homeostatic state [48, 49], which enables us to regulate the organism's current state by initiating appropriate control signals toward the extrapersonal stimuli. This observation may suggest a key role of deqi in characterizing the central expression of acupuncture stimulation at ST36, which is relevant with its clinical efficacy in gastrointestinal analgesia.

6. Sham Control in Acupuncture Studies

Selecting the study design for both clinical and study investigations is prerequisite to answering the research question of interest whether acupuncture really works compared with control group. Thus, the central question is whether a particular acupoint needling manipulation performs better than another prescription, which is generally designed to determine an intervention's effectiveness compared to placebo in clinical trials. However, it is not known which aspects of the acupuncture treatment, such as the mode of stimulation or location of the acupuncture point, are specific to produce these physiological effects. The majority of neuroimaging researchers have suffered from selection of appropriate control challenges in order to address both the specific effect and relative effectiveness of acupuncture. There existed several control modalities. One approach is to apply the retractable nonpenetrating sham needle [50], which gives the impression of skin penetration without piercing the skin. As the needle is pushed against the skin, it causes a pricking sensation; but as increased pressure is applied, the shaft of the needle disappears into the handle, mimicking a "stage dagger." The needle is held in position by a small adhesive plastic ring, which can also be used with the real needles to aid

consistency and credibility. It mainly served as a control for nonspecific cognitive factors (e.g., expectation), whereas it may also lead to the subjects' bias toward the stimulation. To ensure the credibility of this control procedure, the research should enroll and pretest using acupuncture-naïve patients. Another control modality is the sham acupuncture, which is performed on a nearby nonacupoint with needle depth, stimulation intensity, and manipulation method all identical to those used in the real acupuncture. Although it is proved to be far from inactive and does in fact have a physiological effect [51–54], careful design and execution procedures can make it useful to assess the neural specificity of acupuncture with respect to different locations. Other control group included no treatment (or wait-list control), standard care, or combination of treatments. As for wait-list control, the research primarily attempts to factor out the natural history-induced effect. For standard care or another intervention, the study focuses more on the evaluation of the relative merits of different treatment interventions. Considering acupuncture is inherently multifaceted, the decision as to which control should be used will ultimately depend on the particular question that the research model plans to answer. It is thus important for researchers to clearly explain the target questions and select the appropriate control to match the purpose of the study. Using multiple controls at once is an optimal choice.

7. Further Considerations for Acupuncture Neuroimaging

Most of neuroimaging studies generally adopted the GLM analysis to focus on the spatial distribution of acupuncture-induced neural response to the acute effect of acupuncture. In fact, an acupuncture procedure typically involves two administration steps: (1) needling stimulation in deep tissue with skin piercing and biochemical reaction to tissue damage and (2) prolonged effects after the removal of acupuncture needle stimulation [28, 31]. In addition, evidence from both human behavior and animal studies indicates that a striking feature of acupuncture analgesia, in both human and animals, is its longevity—a delayed onset, gradual peaking, and gradual returning [29, 55, 56]. It is also substantiated that the physical needling stimulus, as well as the delayed effect of acupuncture, can similarly activate many areas of the brain [33]. Therefore, it is noteworthy to understand both acute and delayed effects of acupuncture on human brain. In addition, acupuncture, like many complex experiences, emerges from the flow and integration of information between specific brain areas. Great emphasis has been given to understand temporal interactions of these spatially defined brain regions, with consideration for how multiple levels of their dynamic activities in concert cause the processing of acupuncture.

Due to the complexities of the therapeutic mechanisms of acupuncture, research into its neural mechanism has raised a number of difficult methodological issues. Variability in needling technique, deqi sensations, design paradigm, differences in neuroimaging hardware and software, and data postprocessing methods [57], may all account for many of the reported differences in brain response to acupuncture. Therefore, it is urgent to define a standardized reporting system to describe details of acupuncture manipulations [58]. Furthermore, specific selection criteria should also be used to ensure that a truly appropriate treatment is selected for the sham acupuncture treatment. The type of sham treatment chosen is dependent on the research question asked and the type of acupuncture treatment to be tested. For instance, using irrelevant acupoints can help to address the relative functional specificity of acupuncture. While acupuncture on same acupoints but with a different technique for the control condition can answer questions about the specific effects of those techniques, it is not known which aspects of the acupuncture treatment, such as the mode of stimulation or location of the acupuncture point, are specific to produce these physiological effects. In fact, a pilot study is needed to assist in determining if indeed it is an appropriate sham treatment and plays an important role in sample size calculations.

Previous acupuncture studies have generally adopted the multiblock design paradigm with repeated stimuli during a relatively short-term time span. Since acupuncture-related neural responses can be long lasting and not return to the baseline level immediately after the stimuli terminated, the "on-off" specifications set by block design may be violated; further analysis may be susceptible to errors of statistical significance [31]. In block designs, it is also difficult to disentangle the concurrent brain activity related to the needling manipulation from the brain activity associated with its sustained effect resulting from the same stimulation. Therefore, the nonrepeated event-related design paradigm may be more optimal in acupuncture studies. Furthermore, the model-based analysis (GLM) also becomes impractical when the precise timing and duration of acupuncture cannot be specified a priori. In other words, the depiction of dynamic ongoing acupuncture effects would be obtained in the absence of any assumption concerning the shape of the hemodynamic response. For this purpose, the data-driven analysis, free of any hypothesis about the temporal profile of acupuncture-related changes, can be a more optimal choice instead.

Conflict of Interests

There are no conflict of interests for any author.

Acknowledgments

This paper is supported by the National Natural Science Foundation of China under Grant no. 81071217, the Beijing Nova Program (Grant no. Z111101054511116), and the Beijing Natural Science Foundation (Grant no. 4122082).

References

[1] M. A. Bowman, "NIH consensus development panel on acupuncture," *Journal of the American Medical Association*, vol. 280, no. 17, pp. 1518–1529, 1998.

[2] P. M. Barnes, B. Bloom, and R. L. Nahin, "Complementary and alternative medicine use among adults and children: United

States 2007," *National Health Statistics Reports*, vol. 12, pp. 1–23, 2008.

[3] M. Al-Sadi, B. Newman, and S. A. Julious, "Acupuncture in the prevention of postoperative nausea and vomiting," *Anaesthesia*, vol. 52, no. 7, pp. 658–661, 1997.

[4] S. Birch, J. K. Hesselink, F. A. M. Jonkman, T. A. M. Hekker, and A. Bos, "Clinical research on acupuncture: part 1. What have reviews of the efficacy and safety of acupuncture told us so far?" *Journal of Alternative and Complementary Medicine*, vol. 10, no. 3, pp. 468–480, 2004.

[5] Y. D. Kwon, M. H. Pittler, and E. Ernst, "Acupuncture for peripheral joint osteoarthritis: a systematic review and meta-analysis," *Rheumatology*, vol. 45, pp. 1331–1337, 2006.

[6] J. S. Han, "Acupuncture: neuropeptide release produced by electrical stimulation of different frequencies," *Trends in Neurosciences*, vol. 26, no. 1, pp. 17–22, 2003.

[7] G. G. Xing, F. Y. Liu, X. X. Qu, J. S. Han, and Y. Wan, "Long- term synaptic plasticity in the spinal dorsal horn and its modulation by electroacupuncture in rats with neuropathic pain," *Experimental Neurology*, vol. 208, no. 2, pp. 323–332, 2007.

[8] H. F. Guo, J. Tian, X. Wang, Y. Fang, Y. Hou, and J. Han, "Brain substrates activated by electroacupuncture (EA) of different frequencies (II): role of Fos/Jun proteins in EA-induced transcription of preproenkephalin and preprodynorphin genes," *Molecular Brain Research*, vol. 43, no. 1-2, pp. 167–173, 1996.

[9] N. Goldman, M. Chen, T. Fujita et al., "Adenosine A1 receptors mediate local anti-nociceptive effects of acupuncture," *Nature Neuroscience*, vol. 13, no. 7, pp. 883–888, 2010.

[10] T. J. Kaptchuk, "Acupuncture: theory, efficacy, and practice," *Annals of Internal Medicine*, vol. 136, no. 5, pp. 374–383, 2002.

[11] A. White, N. E. Foster, M. Cummings, and P. Barlas, "Acupuncture treatment for chronic knee pain: a systematic review," *Rheumatology*, vol. 46, no. 3, pp. 384–390, 2007.

[12] J. Ezzo, B. Berman, V. A. Hadhazy, A. R. Jadad, L. Lao, and B. B. Singh, "Is acupuncture effective for the treatment of chronic pain? A systematic review," *Pain*, vol. 86, no. 3, pp. 217–225, 2000.

[13] J. Fang, Z. Jin, Y. Wang et al., "The salient characteristics of the central effects of acupuncture needling: limbic-paralimbic-neocortical network modulation," *Human Brain Mapping*, vol. 30, no. 4, pp. 1196–1206, 2009.

[14] K. K. S. Hui, J. Liu, O. Marina et al., "The integrated response of the human cerebro-cerebellar and limbic systems to acupuncture stimulation at ST 36 as evidenced by fMRI," *NeuroImage*, vol. 27, no. 3, pp. 479–496, 2005.

[15] J. Kong, F. Li, R. Li et al., "A pilot study of functional magnetic resonance imaging of the brain during manual and electroacupuncture stimulation of acupuncture point (LI-4 Hegu) in normal subjects reveals differential brain activation between methods," *Journal of Alternative and Complementary Medicine*, vol. 8, no. 4, pp. 411–419, 2002.

[16] V. Napadow, J. Liu, M. Li et al., "Somatosensory cortical plasticity in carpal tunnel syndrome treated by acupuncture," *Human Brain Mapping*, vol. 28, no. 3, pp. 159–171, 2007.

[17] J. Pariente, P. White, R. S. J. Frackowiak, and G. Lewith, "Expectancy and belief modulate the neuronal substrates of pain treated by acupuncture," *NeuroImage*, vol. 25, no. 4, pp. 1161–1167, 2005.

[18] M. T. Wu, J. C. Hsieh, J. Xiong et al., "Central nervous pathway for acupunture stimulation: localization of processing with functional MR imaging of the brain: preliminary experience," *Radiology*, vol. 212, no. 1, pp. 133–141, 1999.

[19] S. S. Yoo, E. K. Teh, R. A. Blinder, and F. A. Jolesz, "Modulation of cerebellar activities by acupuncture stimulation: evidence from fMRI study," *NeuroImage*, vol. 22, no. 2, pp. 932–940, 2004.

[20] W. T. Zhang, Z. Jin, G. H. Cui et al., "Relations between brain network activation and analgesic effect induced by low vs. high frequency electrical acupoint stimulation in different subjects: a functional magnetic resonance imaging study," *Brain Research*, vol. 982, no. 2, pp. 168–178, 2003.

[21] J. N. MacLean, B. O. Watson, G. B. Aaron, and R. Yuste, "Internal dynamics determine the cortical response to thalamic stimulation," *Neuron*, vol. 48, no. 5, pp. 811–823, 2005.

[22] M. E. Raichle and D. A. Gusnard, "Intrinsic brain activity sets the stage for expression of motivated behavior," *Journal of Comparative Neurology*, vol. 493, no. 1, pp. 167–176, 2005.

[23] M. E. Raichle and M. A. Mintun, "Brain work and brain imaging," *Annual Review of Neuroscience*, vol. 29, pp. 449–476, 2006.

[24] M. N. Baliki, P. Y. Geha, A. V. Apkarian, and D. R. Chialvo, "Beyond feeling: chronic pain hurts the brain, disrupting the default-mode network dynamics," *Journal of Neuroscience*, vol. 28, no. 6, pp. 1398–1403, 2008.

[25] R. P. Dhond, C. Yeh, K. Park, N. Kettner, and V. Napadow, "Acupuncture modulates resting state connectivity in default and sensorimotor brain networks," *Pain*, vol. 136, no. 3, pp. 407–418, 2008.

[26] E. Haker, H. Egekvist, and P. Bjerring, "Effect of sensory stimulation (acupuncture) on sympathetic and parasympathetic activities in healthy subjects," *Journal of the Autonomic Nervous System*, vol. 79, no. 1, pp. 52–59, 2000.

[27] S. Sakai, E. Hori, K. Umeno, N. Kitabayashi, T. Ono, and H. Nishijo, "Specific acupuncture sensation correlates with EEGs and autonomic changes in human subjects," *Autonomic Neuroscience*, vol. 133, no. 2, pp. 158–169, 2007.

[28] L. Bai, W. Qin, J. Tian et al., "Acupuncture modulates spontaneous activities in the anticorrelated resting brain networks," *Brain Research*, vol. 1279, pp. 37–49, 2009.

[29] D. D. Price, A. Rafii, L. R. Watkins, and B. Buckingham, "A psychophysical analysis of acupuncture analgesia," *Pain*, vol. 19, no. 1, pp. 27–42, 1984.

[30] J. Han, Z. Zhou, and Y. Xuan, "Acupuncture has an analgesic effect in rabbits," *Pain*, vol. 15, no. 1, pp. 83–91, 1983.

[31] L. Bai, W. Qin, J. Tian et al., "Time-varied characteristics of acupuncture effects in fMRI studies," *Human Brain Mapping*, vol. 30, no. 11, pp. 3445–3460, 2009.

[32] S. Ogawa, T. M. Lee, A. R. Kay, and D. W. Tank, "Brain magnetic resonance imaging with contrast dependent on blood oxygenation," *Proceedings of the National Academy of Sciences of the United States of America*, vol. 87, no. 24, pp. 9868–9872, 1990.

[33] L. Bai, J. Tian, C. Zhong et al., "Acupuncture modulates temporal neural responses in wide brain networks: evidence from fMRI study," *Molecular Pain*, vol. 6, no. 1, pp. 73–84, 2010.

[34] Y. You, L. Bai, R. Dai et al., "Acupuncture induces divergent alterations of functional connectivity within conventional frequency bands: evidence from MEG recordings," *Plos One*, vol. 7, Article ID e49250, 2012.

[35] B. Brinkhaus, C. M. Witt, S. Jena et al., "Acupuncture in patients with chronic low back pain: a randomized controlled trial," *Archives of Internal Medicine*, vol. 166, no. 4, pp. 450–457, 2006.

[36] E. Leibing, U. Leonhardt, G. Köster et al., "Acupuncture treatment of chronic low-back pain: a randomized, blinded, placebo-controlled trial with 9-month follow-up," *Pain*, vol. 96, no. 1-2, pp. 189–196, 2002.

[37] K. Linde, A. Streng, S. Jürgens et al., "Acupuncture for patients with migraine: a randomized controlled trial," *Journal of the American Medical Association*, vol. 293, no. 17, pp. 2118–2125, 2005.

[38] E. K. Miller and J. D. Cohen, "An integrative theory of prefrontal cortex function," *Annual Review of Neuroscience*, vol. 24, pp. 167–202, 2001.

[39] J. Kong, T. J. Kaptchuk, G. Polich et al., "An fMRI study on the interaction and dissociation between expectation of pain relief and acupuncture treatment," *NeuroImage*, vol. 47, no. 3, pp. 1066–1076, 2009.

[40] R. E. Harris, J. K. Zubieta, D. J. Scott, V. Napadow, R. H. Gracely, and D. J. Clauw, "Traditional Chinese acupuncture and placebo (sham) acupuncture are differentiated by their effects on μ-opioid receptors (MORs)," *NeuroImage*, vol. 47, no. 3, pp. 1077–1085, 2009.

[41] E. Haker and T. Lundeberg, "Acupuncture treatment in epicondylalgia: a comparative study of two acupuncture techniques," *Clinical Journal of Pain*, vol. 6, no. 3, pp. 221–226, 1990.

[42] B. Pomeranz, "Acupuncture research related to pain, drug addiction and nerve regeneration," in *Scientific Basis of Acupuncture*, B. Pomeranz and G. Stux, Eds., pp. 45–49, Springer, Berlin, Germany, 1989.

[43] W. Takeda and J. Wessel, "Acupuncture for the treatment of pain of osteoarthritic knees," *Arthritis Care and Research*, vol. 7, no. 3, pp. 118–122, 1994.

[44] C. Witt, B. Brinkhaus, S. Jena et al., "Acupuncture in patients with osteoarthritis of the knee: a randomised trial," *The Lancet*, vol. 366, no. 9480, pp. 136–143, 2005.

[45] E. Shen, W. Y. Wu, H. J. Du, J. Y. Wei, and D. X. Zhu, "Electromyographic activity produced locally by acupuncture manipulation," *Chinese Medical Journal*, vol. 9, pp. 532–535, 1973.

[46] K. Kawakita, K. Itoh, and K. Okada K, "The polymodal receptor hypothesis of acupuncture and moxibustion, and its rational explanation of acupuncture points," *International Congress Series*, vol. 1238, pp. 63–68, 2003.

[47] M. Marsel Mesulam and E. J. Mufson, "Insula of the old world monkey. III: efferent cortical output and comments on function," *Journal of Comparative Neurology*, vol. 212, no. 1, pp. 38–52, 1982.

[48] A. D. Craig, "How do you feel? Interoception: the sense of the physiological condition of the body," *Nature Reviews Neuroscience*, vol. 3, no. 8, pp. 655–666, 2002.

[49] H. D. Critchley, S. Wiens, P. Rotshtein, A. Öhman, and R. J. Dolan, "Neural systems supporting interoceptive awareness," *Nature Neuroscience*, vol. 7, no. 2, pp. 189–195, 2004.

[50] K. Streitberger and J. Kleinhenz, "Introducing a placebo needle into acupuncture research," *The Lancet*, vol. 352, no. 9125, pp. 364–365, 1998.

[51] D. Le Bars, L. Villanueva, J. C. Willer, and D. Bouhassira, "Diffuse noxious inhibitory controls (DNIC) in animals and in man," *Acupuncture in Medicine*, no. 9, pp. 47–65, 1991.

[52] F. E. Staebler, J. Wheeler, J. Young, F. Diebschlag, and R. Blackwell, "Why research into traditional Chinese acupuncture has proved difficult. Strategies of the Council for Acupuncture, UK, to overcome the problem," *Complementary Therapies in Medicine*, vol. 2, no. 2, pp. 86–92, 1994.

[53] E. Ernst and A. R. White, "A review of problems in clinical acupuncture research," *The American Journal of Chinese Medicine*, vol. 25, no. 1, pp. 3–11, 1997.

[54] C. Vincent and G. Lewith, "Placebo controls for acupuncture studies," *Journal of the Royal Society of Medicine*, vol. 88, no. 4, pp. 199–202, 1995.

[55] D. J. Mayer, D. D. Price, and A. Rafii, "Antagonism of acupuncture analgesia in man by the narcotic antagonist naloxone," *Brain Research*, vol. 121, no. 2, pp. 368–372, 1977.

[56] B. Pomeranz and D. Chiu, "Naloxone blockade of acupuncture analgesia: endorphin implicated," *Life Sciences*, vol. 19, no. 11, pp. 1757–1762, 1976.

[57] S. M. Smith, C. F. Beckmann, N. Ramnani et al., "Variability in fMRI: a re-examination of inter-session differences," *Human Brain Mapping*, vol. 24, no. 3, pp. 248–257, 2005.

[58] H. MacPherson, A. White, M. Cummings, K. Jobst, K. Rose, and R. Niemtzow, "Standards for reporting interventions in controlled trials of acupuncture: the STRICTA recommendations," *Complementary Therapies in Medicine*, vol. 9, no. 4, pp. 246–249, 2001.

Hindawi Publishing Corporation
Evidence-Based Complementary and Alternative Medicine
Volume 2013, Article ID 178067, 6 pages
http://dx.doi.org/10.1155/2013/178067

Research Article

Effects of Moxa Smoke on Monoamine Neurotransmitters in SAMP8 Mice

Huanfang Xu,[1,2] Baixiao Zhao,[1] Yingxue Cui,[1] Min Yee Lim,[1,3] Ping Liu,[1] Li Han,[1] Hongzhu Guo,[4] and Lixing Lao[1,5]

[1] *School of Acupuncture-Moxibustion and Tuina, Beijing University of Chinese Medicine, Beijing 100029, China*
[2] *Guang'anmen Hospital, China Academy of Chinese Medical Sciences, Beijing 100053, China*
[3] *China & Nanyang Technological University, 50 Nanyang Avenue, Singapore 639798*
[4] *Beijing Institute for Drug Control, Beijing 100035, China*
[5] *Center For Integrative Medicine, Department of Family and Community Medicine, School of Medicine, University of Maryland, Baltimore, MD 21201, USA*

Correspondence should be addressed to Baixiao Zhao; baixiao100@gmail.com

Received 21 January 2013; Revised 1 April 2013; Accepted 2 April 2013

Academic Editor: Lijun Bai

Objectives. To investigate the anti-aging effects of moxa smoke on SAMP8 mice. *Methods*. Using 2 × 3 factorial design, exposure length (15 or 30 minutes daily), and concentration (low, 5–15 mg/m^3; middle, 25–35 mg/m^3; high, 85–95 mg/m^3), 70 SAMP8 mice were randomly assigned, $n = 10$/group, to a model group or one of six moxa smoke groups: L_1, L_2, M_1, M_2, H_1, or H_2. Ten SAMR1 mice were used as normal control. Mice in moxa smoke groups were exposed to moxa smoke at respective concentrations and exposure lengths; the model and normal control mice were not exposed. Cerebral 5-HT, DA, and NE levels were determined using ELISA. *Results*. Compared to normal control, the model group showed a significant decrease in 5-HT, DA, and NE. Compared to model group, 5-HT and NE were significantly higher in groups L_2, M_1, and M_2 and DA was significantly so in L_2 and M_1. 5-HT, DA, and NE levels were the highest in group M_1 among moxa smoke groups. A marked exposure length × concentration interaction was observed for 5-HT, DA, and NE. *Conclusion*. Moxa smoke increases monoamine neurotransmitter levels, which varies according to concentration and exposure length. Our finding suggests that the middle concentration of moxa smoke for 15 minutes seems the most beneficial.

1. Introduction

Moxibustion, the burning of moxa cones or sticks (made of mugwort, usually *Artemisia vulgaris*) at acupuncture points, is one of the oldest therapies in traditional Chinese medicine (TCM), and it is used for both disease prevention and treatment. During moxibustion, thermal stimulation and moxa smoke are produced simultaneously. The treatment effects of moxa smoke are currently unknown and it is more commonly accepted that thermal stimulation is the key factor for the effects of moxibustion [1]. In fact, it was recorded in the ancient literature that moxa smoke was used to prevent epidemics and it is now used to sterilize the air in hospital wards [2]. Besides, in vitro studies showed that moxa smoke displayed biological activities of tumor-specific cytotoxicity (oral squamous cell carcinoma HSC-2 and HSC-3 and promyelocytic leukemia HL-60) and radical scavenging of O_2^-, $^{\bullet}OH$, $^1O_2$, and ON [3, 4]. All these strongly indicated that moxa smoke probably had some treatment effects, which contributed to the effect of moxibustion. Moxibustion had been reported to be effective for anti-aging through several ways, including enhancing antioxidant ability by increasing SOD activity and suppressing MDA or NO content and NOS activity [5, 6], enhancing immune function by regulation of serum IL-6 level and IL-2 level [7], and improving neuroendocrine function. As part of the normal aging process, neurotransmitters exhibited a marked alteration in different regions of brain [8, 9], such as reduction of serotonin (5-HT) level in cortex, striatum, and hypothalamus, the dopamine (DA) level in the brain cortex and striatum, and

Table 1: 2 × 3 factorial design.

Factor and level	Concentration		
	Low concentration (5~15 mg/m^3)	Middle concentration (25~35 mg/m^3)	High concentration (85~95 mg/m^3)
Time			
15 min	L_1	M_1	H_1
30 min	L_2	M_2	H_2

the norepinephrine (NE) content in brain cortex [9]. Since moxibustion showed a good regulation of 5-HT, NE, and DA [10, 11], we hypothesized that moxa smoke may also regulate age-related alteration of monoamine neurotransmitters. In this study, we used an aging animal model senescence-accelerated prone mouse (SAMP8) to study the influence of moxa smoke on the monoamine neurotransmitters 5-HT, DA, and NE in the aging brain.

2. Material and Methods

2.1. Animals Preparation. The SAMP8 is the commonly used animal model for aging study and senescence-accelerated mouse/resistance (SAMR1) mice were usually used as a normally aging control for SAMP strains. In SAMP8 mice, senescence naturally occurs four to six months after birth; typical symptoms resemble Alzheimer's disease [12, 13], in which cerebral monoamine neurotransmitters greatly decrease. We obtained 70 SAMP8 and 10 SAMR1 male mice of six months of age and weight of 30 ± 2.7 g from the animal center of the First Hospital Affiliated to Tianjin University of TCM (Tianjin, China). Mice were housed in individual cages with free access to food and water. A controlled environment at a temperature of 20~24°C, humidity of 50%~60%, and 12-hour light-dark cycle was maintained throughout the study. All procedures for animal experiments were conducted in accordance with the World Health Organization's International Guiding Principles for Biomedical Research Involving Animals and were approved by the local ethics committee of Beijing University of Chinese Medicine.

After acclimation in the animal room for one week, 10 SAMR1 mice were used as normal control, and the 70 SAMP8 mice were randomly assigned (n = 10/group) to a model group or to one of the six moxa smoke groups. The six moxa smoke groups were divided into L_1, L_2, M_1, M_2, H_1, or H_2 using a 2 × 3 factorial design, length of exposure (15 or 30 minutes daily), and moxa smoke concentration (low, 5~15 mg/m^3; middle, 25~35 mg/m^3; or high, 85~95 mg/m^3) (Table 1). The six moxa smoke groups were exposed to moxa smoke six times a week for four weeks; model and normal control mice were not exposed to moxa smoke.

2.2. Moxa Smoke Intervention. Custom-designed mouse cages that can accommodate a single mouse and in which the mouse can turn around in the cage and make itself comfortable were used during the moxa smoke interventions. Moxa smoke was generated by burning moxa sticks (three-year-old pure moxa, 0.5 cm × 12 cm, Nanyang Hanyi Moxa Co., Ltd., China). The moxa smoke was contained within a custom-designed glass box (80 cm × 80 cm × 60 cm). Its upper cover, with a circular hole 0.6 cm in diameter, can be shifted. A light-scattering digital dust tester (DT, Beijing BINTA Green Technology Co., Ltd) was used to monitor smoke concentration by detecting levels of PM_{10} (particulate matter < 10 μm in diameter).

2.2.1. Intervention for the Six Smoke Groups. Groups receiving the same concentration of moxa smoke were exposed together. The main procedure was as follows. The DT was placed in the middle of the glass box to monitor concentration. Mice were individually put into the custom-designed cages, and groups with the same concentration, such as group L_1 and group L_2, were put into custom-designed cages, and subsequently, groups with the same concentration were placed on opposite sides of the DT. The burning end of a moxa stick was inserted into the glass box from the upper hole while the other end was held in the investigator's hand. When the box filled with the predetermined amount of smoke, which took about 15, 32, and 82 seconds for low, middle, and high concentration, respectively, the stick was withdrawn and the hole was quickly closed. After 15 minutes, the mice that belonging to the 15-minute exposure group were removed, while the 30-minute exposure group continued for another 15 minutes.

To ensure concentrations of moxa smoke in the specified ranges, moxa smoke concentration was monitored dynamically every three minutes by DT. When the concentration exceeded the upper range, the upper cover of the glass box was moved to release some of the smoke and when it fell below the lower range, the burning moxa stick was reinserted to the box for a few seconds.

2.2.2. Intervention for the Two Control Groups. The model and normal groups were not exposed to moxa smoke. Mice in those two groups were caged and put on opposite sides of the glass box for 30 minutes with no exposure to moxa smoke.

2.3. Cerebral Monoamine Neurotransmitter Assessment. Twenty-four hours after the last intervention, the mice were sacrificed, and cerebrum samples were quickly dissected on an ice board. Using enzyme-linked immunosorbent assay kits of 5-HT, DA, and NE (produced by Nanjing Jiancheng Bioengineering Institute, Nanjing, China), values of absorbance were strictly measured by microplate reader (Multiskan MK3, Finland) at 450 nm wavelength. The concentrations of 5-HT, DA, and NE were determined by comparing the O.D. of the samples to the standard curve.

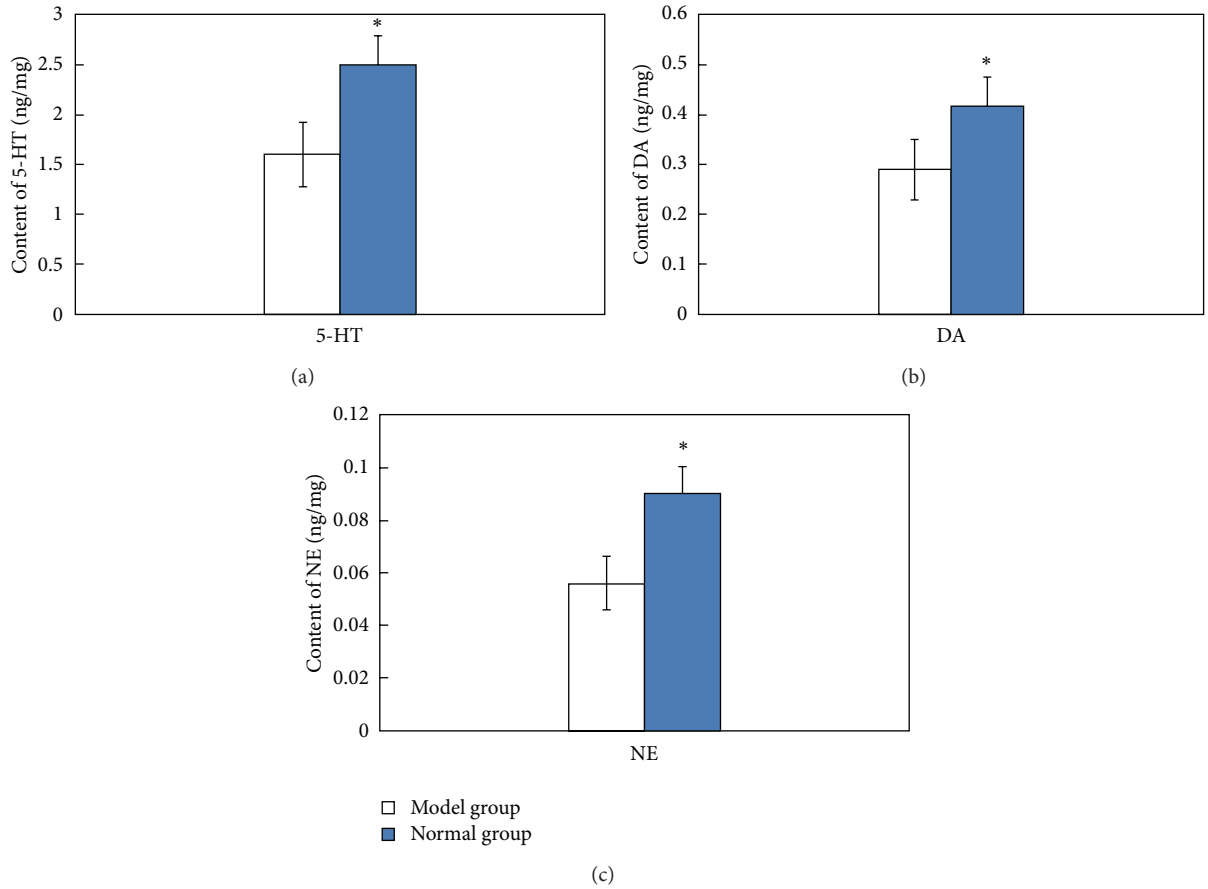

Figure 1: Differences in 5-HT (a), DA (b), and NE (c) levels, normal group (SAMARI mice) versus model group (SAMP8 mice). Note: $^{*}P < 0.05$, versus model group.

2.4. Statistical Analysis. Data were analyzed by analysis of variance (ANOVA), and post hoc analyses were conducted using the Student-Newman-Keuls test. For that of the six smoke groups, ANOVA for factorial data was used. All values were reported as means ± standard error. Analyses were performed with SPSS software version 13.0; $P < 0.05$ was considered to be statistically significant.

3. Results

3.1. Cerebral Monoamine Neurotransmitter in the Normal and Model Groups. Compared to the normal group, the model group showed a remarkable decrease in cerebral 5-HT, DA, and NE levels (Figure 1).

3.2. Effect of Moxa Smoke on Cerebral Monoamine Neurotransmitters in SAMP8 Mice. Moxa smoke groups showed a higher level of monoamine neurotransmitters than model group. Compared to the model group, 5-HT and NE were significantly increased in L_2, M_1, and M_2, while DA was significantly increased in L_2 and M_1 (Figure 2).

3.3. Effects of Concentration and Length of Moxa Smoke Exposure on Cerebral Monoamine Neurotransmitters in SAMP8 Mice. Using ANOVA for factorial data, there was a significant interaction between length of exposure and concentration effects on cerebral monoamine neurotransmitter levels (Figure 3). Levels of 5-HT and NE varied significantly as a function of concentration. No main effect of exposure length on monoamine neurotransmitters was found.

3.4. Optimum Conditions for Interventions with Moxa Smoke. Multiple comparisons showed that moxa smoke intervention for the M_1 group, middle concentration for 15 minutes, manifested the highest effect in increasing cerebral 5-HT, DA, and NE levels among the different combinations between concentration and exposure length (Figure 2).

4. Discussion

In this study, we explored the anti-aging effects of moxa smoke and found that moxa smoke may increase monoamine neurotransmitter levels in SAMP8 mice and the effects were related to exposure length and concentration of moxa smoke. This indicated that moxa smoke may be one of the effective components of moxibustion. 5-HT, DA, and NE were important neurotransmitters in the central nervous system and were closely related to neural functions and aging [14].

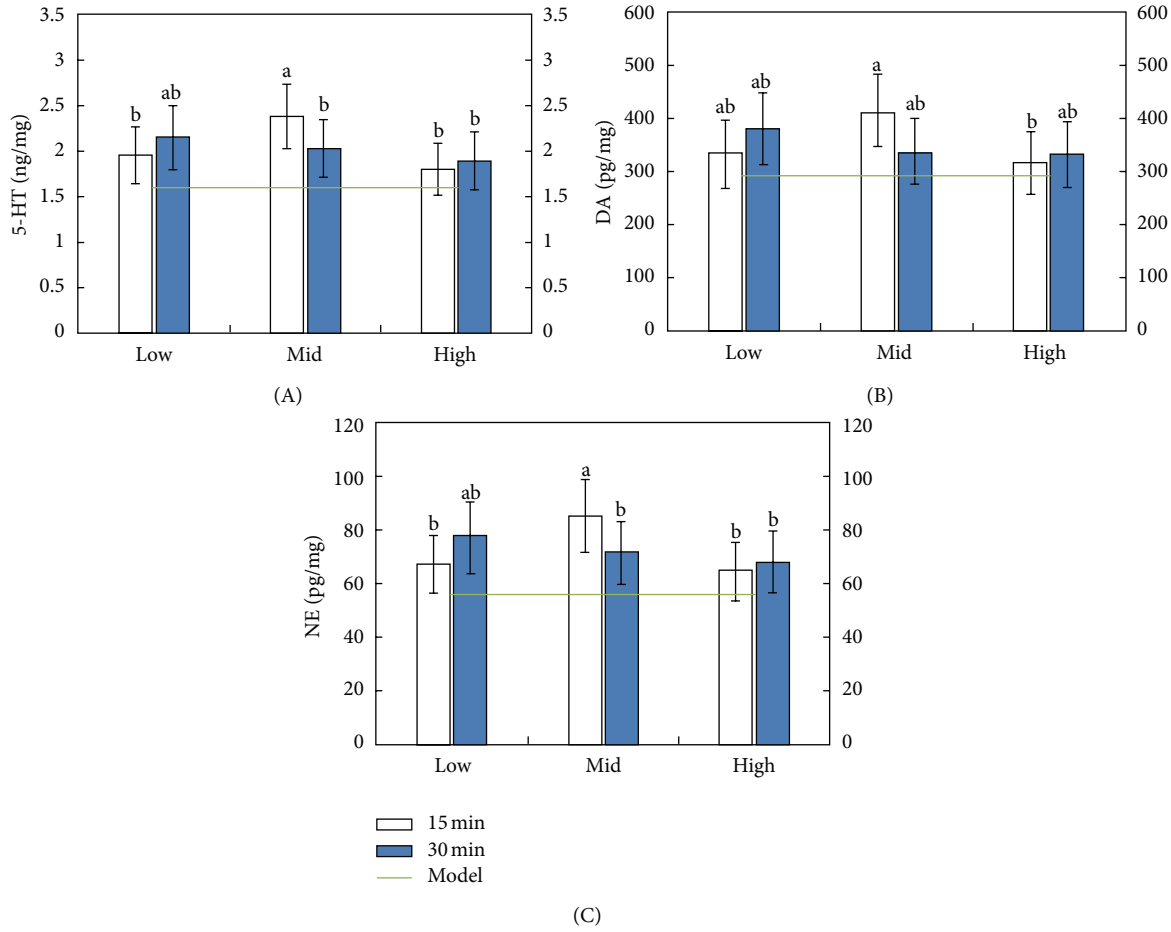

Figure 2: Cerebral levels of 5-HT (A), DA (B), and NE (C) of SAMP8 mice exposed to different concentrations of moxa smoke for various lengths of time. Note: any two groups without a common alphabet (a or b) are significantly different ($P < 0.05$).

More specifically, 5-HT excites the functions of learning and memory [15, 16] and can trigger facilitation, and DA has an excitatory effect on overall behavior and participates in the reappearance of memory trace. NE regulates excitation of the cerebral cortex and influences awakening, sensation, emotions, and advanced cognitive functions; increased excitability of NE improves learning and memory [17]. The SAMP8 mouse is marked by impaired learning and memory. In other studies, six-month-old SAMP8 mice had shown a significant decrease in monoamine and metabolite levels, which was relevant to cognitive impairment, in the cortex and hippocampus [18]. DA levels in the brain had also been shown to decrease with aging, and DA turnover was lower in aged SAMP8 mice than in young ones [19]. Impairment of learning and memory in SAMP8 mice had also been reversed by drugs, and increased cerebral Ach and 5-HT and activation of the PI3 K/AKT pathway were possible mechanisms of this effect [20]. Consistent with those findings, our study showed decreased monoamines in the model SAMP8 mice compared to the SAMR1 mice. Compared to the model mice, SAMP8 mice exposed to moxa smoke showed higher levels of cerebral 5-HT, DA, and NE. This indicated that moxa smoke increased monoamine content, thus postponing senescence.

Moxa floss is made from mugwort leaf (*Artemisia argyi Folium*), and its smoke contains multiple essential oils, suspended particulate matters, and products of chemical oxidation [21]. The chemical ingredients of moxa floss may lay the foundation for the effects of moxa smoke, such as flavones isolated from *Artemisia argyi* inhibiting proliferation of a couple of tumor cell lines [22] and Arteminolides B-D (2-4) isolated from *Artemisia argyi* inhibiting the farnesyl protein transferase [23]. Clinically, moxa floss with good quality has to be specially processed and preserved for a relatively long time. The active ingredients of mugwort leaves mainly lie in their volatile oil, such as caryophyllene and caryophyllene [24], which can be distilled into moxa smoke. Most of these volatile ingredients are nonaromatic essential oils. Widely used in aromatherapy, they have no fragrance in their natural state but disperse their fragrance when burning. An essential oil can exert an effect via absorption through the skin and through inhalation, and it also can act directly on the central nervous system through the olfactory pathway [25]. Considering the similarity of action between essential oils and moxa smoke, we conjecture that moxa smoke and aromatherapy exert their effects similarly. Further studies concerning the active ingredients of moxa smoke

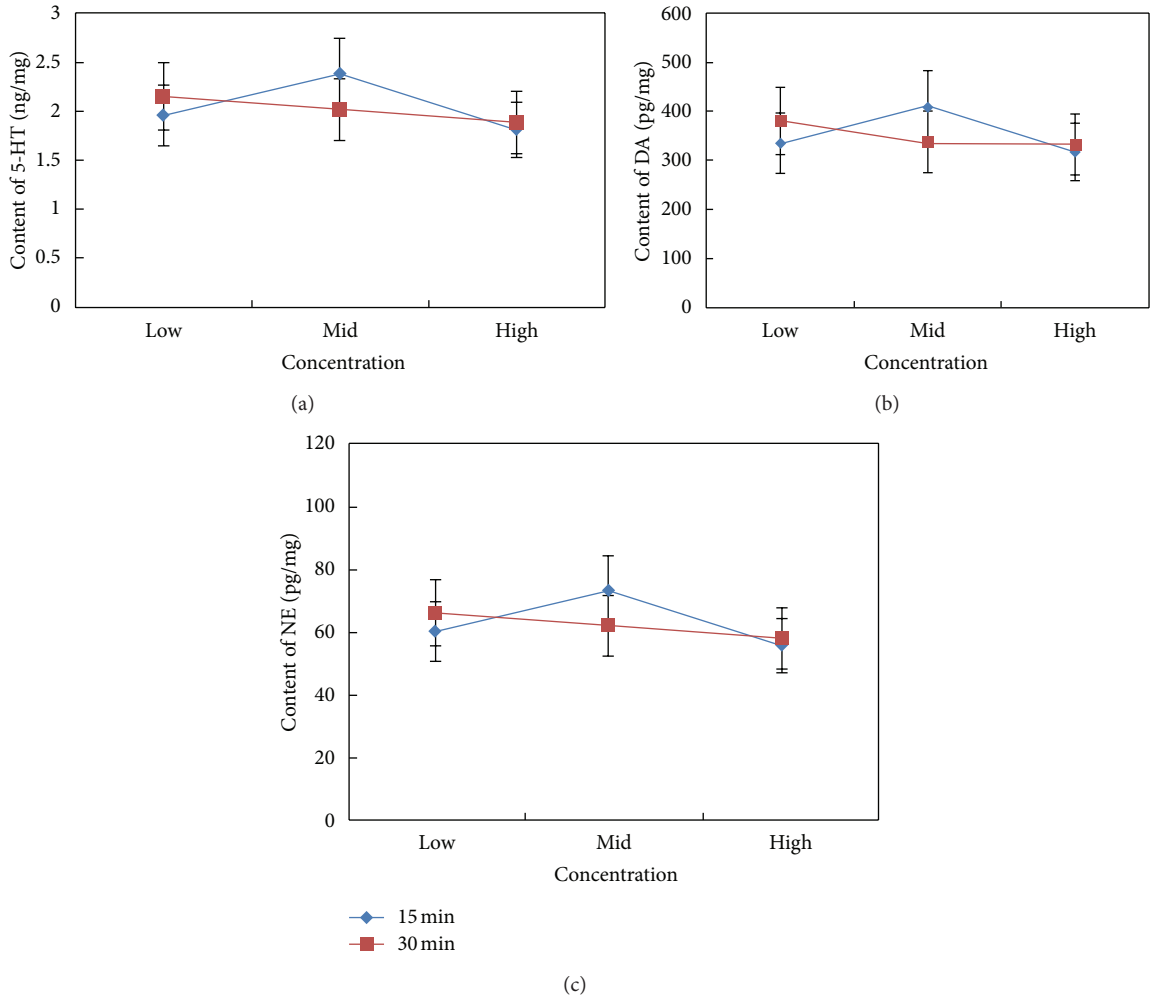

Figure 3: Cerebral levels of 5-HT (a), DA (b), and NE (c) of SAMP8 mice exposed to moxa smoke at different concentrations and for different lengths of time.

are warranted in order to understand the mechanisms of moxa smoke.

In this study, we also find that the anti-aging effect is linked to smoke concentration, and there is an interaction between concentration and length of exposure. According to our results, monoamine neurotransmitter levels were highest in the M_1 group (i.e., middling concentration for 15 minutes), which suggested that these may be the optimum specifications for raising monoamine neurotransmitter levels. There is probably a nonlinear relationship between dose (concentration and exposure length) and effect of moxa smoke based on the present results, however; further study is needed to determine the dose-effect curve.

There exist some limitations in this study. Oxygen concentration was not monitored during the intervention procedure. However, the combustion of moxa stick in the glass box was only for a very short duration from 15 to 82 seconds and the glass box was not completely sealed. Methods to monitor the oxygen supply should be applied in subsequent studies. Secondly, behavioral tests of learning and memory should be recommended for future studies.

In conclusion, our preliminary observation showed that moxa smoke may increase monoamine neurotransmitter in central nerve system and the middle concentration of moxa smoke for 15 minutes seemed most beneficial. However, further investigation to confirm our findings and to explore possible mechanisms of action is warranted.

Conflict of Interests

The authors declare that they have no Conflict of Interests.

Acknowledgments

The authors thank Dr. Lyn Lowry at the Center for Integrative Medicine, University of Maryland School of Medicine, for her English edit. This study was supported by the National Natural Science Foundation of China (no. 81072862) and the National Basic Research Program of China (no. 2009CB522906).

References

[1] X. Shen, G. Ding, J. Wei et al., "An infrared radiation study of the biophysical characteristics of traditional moxibustion," *Complementary Therapies in Medicine*, vol. 14, no. 3, pp. 213–219, 2006.

[2] C. Zhou, X. Feng, J. Wang et al., "Research advance on moxa smoke," *Journal of Acupuncture and Tuina Science*, vol. 9, no. 2, pp. 67–72, 2011.

[3] H. Sakagami, H. Matsumoto, K. Satoh et al., "Cytotoxicity and radical modulating activity of Moxa smoke," *In Vivo*, vol. 19, no. 2, pp. 391–398, 2005.

[4] N. Hitosugi, R. Ohno, J. Hatsukari et al., "Diverse biological activities of Moxa extract and smoke," *In Vivo*, vol. 15, no. 3, pp. 249–254, 2001.

[5] S. Z. Gal and J. Wang, "Clinical observation on drug-separated moxibustion at the navel for anti-aging," *Zhongguo Zhen Jiu*, vol. 27, no. 6, pp. 398–402, 2007.

[6] L. H. Zhao, J. J. Wen, K. Yang, and A. Y. Li, "Effects of moxibustion on cerebral cortical nitric oxide level and nitric oxide synthase activity in aging mice," *Zhen Ci Yan Jiu*, vol. 33, no. 4, pp. 255–261, 2008.

[7] L. H. Li, L. Li, Z. E. Zhao, and Y. Xu, "Effects of moxibustion and Chinese herbs on contents of mitochondrial DNA, serum IL-2 and IL-6 in the aging model rat," *Zhongguo Zhen Jiu*, vol. 28, no. 9, pp. 681–684, 2008.

[8] P. Liu, N. Gupta, Y. Jing, and H. Zhang, "Age-related changes in polyamines in memory-associated brain structures in rats," *Neuroscience*, vol. 155, no. 3, pp. 789–796, 2008.

[9] V. D. Petkov, V. V. Petkov, and S. L. Stancheva, "Age-related changes in brain neurotransmission," *Gerontology*, vol. 34, no. 1-2, pp. 14–21, 1988.

[10] Y. Zhou, "Relationship between the effect of moxibustion on lowering blood pressure in SHR rats and the changes of monoamine neurotransmitter in blood and brain," *Zhen Ci Yan Jiu*, vol. 17, no. 4, pp. 265–267, 1992.

[11] T. Zhaoliang, S. Xiaoge, C. Quanzhu et al., "Experimental study on effects of moxibustion's anti-inflammatory and immunity action on neurotransmitter," *China Journal of Basic Medicine in Traditional Chinese Medicine*, vol. 6, no. 9, pp. 53–55, 2000.

[12] J. E. Morley, "The SAMP8 mouse: a model of Alzheimer disease?" *Biogerontology*, vol. 3, no. 1-2, pp. 57–60, 2002.

[13] K. Tomobe and Y. Nomura, "Neurochemistry, neuropathology, and heredity in samp8: a mouse model of senescence," *Neurochemical Research*, vol. 34, no. 4, pp. 660–669, 2009.

[14] A. J. Nazarali and G. P. Reynolds, "Monoamine neurotransmitters and their metabolites in brain regions in Alzheimer's disease: a postmortem study," *Cellular and Molecular Neurobiology*, vol. 12, no. 6, pp. 581–587, 1992.

[15] J. J. Yan, M. Liu, Y. Hu et al., "Effect and mechanism of dingzhixiao wan on scopolamine-induced learning-memory impairment in mice," *Zhongguo Zhong Yao Za Zhi*, vol. 37, no. 21, pp. 3293–3296, 2012.

[16] A. Meneses and G. Liy-Salmeron, "Serotonin and emotion, learning and memory," *Reviews in the Neurosciences*, vol. 23, no. 5-6, pp. 543–553, 2012.

[17] C. W. Harley, "Norepinephrine and dopamine as learning signals," *Neural Plasticity*, vol. 11, no. 3-4, pp. 191–204, 2004.

[18] X. L. He, W. Q. Zhou, M. G. Bi, and G. H. Du, "Neuroprotective effects of icariin on memory impairment and neurochemical deficits in senescence-accelerated mouse prone 8 (SAMP8) mice," *Brain Research*, vol. 1334, pp. 73–83, 2010.

[19] N. Karasawa, Y. Yamawaki, T. Nagatsu et al., "Age-associated changes in the dopamine synthesis as determined by GTP cyclohydrolase I inhibitor in the brain of senescence-accelerated mouse-prone inbred strains (SAMP8)," *Neuroscience Research*, vol. 35, no. 1, pp. 31–36, 1999.

[20] L. Qiu, L. Zheng, and Y. Zhang, "Effect and mechanism of action of qingkailing on learning and memory capacity of SAMP8 mouse," *Zhongguo Zhong Xi Yi Jie He Za Zhi*, vol. 30, no. 7, pp. 738–742, 2010.

[21] Z. Han-chen, W. Dao-zhi, H. Bao-kang, X. Hai-liang, and Q. Lu-ping, "Advances in ethnobotanic and modern pharmaceutic studies on Folium Artemisiae Argyi," *The Chinese Academic Medical Magazine of Organisms*, vol. 2, pp. 35–39, 2003.

[22] J. M. Seo, H. M. Kang, K. H. Son et al., "Antitumor activity of flavones isolated from Artemisia argyi," *Planta Medica*, vol. 69, no. 3, pp. 218–222, 2003.

[23] S. H. Lee, Y. Seo, H. K. Kim et al., "Arteminolides B, C, and D, new inhibitors of farnesyl protein transferase from Artemisia argyi," *Journal of Organic Chemistry*, vol. 67, no. 22, pp. 7670–7675, 2002.

[24] J. Ran, Z. Baixiao, Y. Mimi et al., "Qualitative analysis on components of moxa combustion products by solid-phase microextraction-gas chromatography-mass spectrography," *Journal of Beijing University of Traditional Chinese Medicine*, vol. 34, no. 9, pp. 632–636, 2011.

[25] C. Dobetsberger and G. Buchbauer, "Actions of essential oils on the central nervous system: an updated review," *Flavour and Fragrance Journal*, no. 26, pp. 300–316, 2011.

Hindawi Publishing Corporation
Evidence-Based Complementary and Alternative Medicine
Volume 2013, Article ID 107380, 12 pages
http://dx.doi.org/10.1155/2013/107380

Research Article

Enhanced Antidepressant-Like Effects of Electroacupuncture Combined with Citalopram in a Rat Model of Depression

Jian Yang,[1] Yu Pei,[1,2] Yan-Li Pan,[1] Jun Jia,[3] Chen Shi,[3] Yan Yu,[3] Jia-Hui Deng,[3] Bo Li,[3] Xiao-Li Gong,[3] Xuan Wang,[3] Xiao-Min Wang,[3] and Xin Ma[1]

[1] *Beijing Anding Hospital, Capital Medical University, 5 Ankang Alley, Beijing 100088, China*
[2] *School of Arts and Law, Beijing University of Chemical Technology, Beijing 100029, China*
[3] *Department of Physiology and Neurobiology, Capital Medical University, Key Laboratory for Neurodegenerative Disease of Education Ministry, 10 You An Men, Beijing 100069, China*

Correspondence should be addressed to Xiao-Min Wang; xmwang@ccmu.edu.cn and Xin Ma; maxinanny@sina.cn

Received 16 February 2013; Revised 13 April 2013; Accepted 22 April 2013

Academic Editor: Vitaly Napadow

Currently, antidepressants are the dominative treatment for depression, but they have limitations in efficacy and may even produce troublesome side effects. Electroacupuncture (EA) has been reported to have therapeutic benefits in the treatment of depressive disorders. The present study was conducted to determine whether EA could enhance the antidepressant efficacy of a low dose of citalopram (an SSRI antidepressant) in the chronic unpredictable stress-induced depression model rats. Here, we show that a combined treatment with 2 Hz EA and 5 mg/kg citalopram for three weeks induces a significant improvement in depressive-like symptoms as detected by sucrose preference test, open field test, and forced swimming test, whereas these effects were not observed with either of the treatments alone. Further investigations revealed that 2 Hz EA plus 5 mg/kg citalopram produced a remarkably increased expression of BDNF and its receptor TrkB in the hippocampus compared with those measured in the vehicle group. Our findings suggest that EA combined with a low dose of citalopram could produce greater therapeutic effects, thereby, predictive of a reduction in drug side effects.

1. Introduction

Depression is a common but serious mental disorder that affects more than 15% of the population during their lifetime [1]. Currently, antidepressants, especially selective serotonin reuptake inhibitors (SSRIs), are the mainstay in the treatment for depression. Unfortunately, many depressed patients do not respond well to presently available antidepressants and suffer from their severe side effects [2–5]. Therefore, it is necessary to seek complementary and alternative strategies with better efficacy of antidepressants and fewer side effects.

Acupuncture is a traditional complementary and alternative medicine approach that involves inserting fine needles into specific points to restore proper energy flow inside the body [6]. Electroacupuncture (EA) is a modification of acupuncture in which the needles inserted are attached with electrodes to deliver a pulsed electrical current. Numerous studies have demonstrated that acupuncture or EA treatment could alleviate depressive symptoms with very few side effects [7–10]. However, some researchers believe that there is a lack of sufficient evidence for supporting a beneficial effect from them [11, 12]. Although their utility in treating depression remains controversial, either of them may be considered as an adjunct to standard therapy [13, 14].

Brain-derived neurotrophic factor (BDNF), a member of the neurotrophin family, plays critical roles in cell differentiation, neuronal survival, migration, and synaptic plasticity [15–17] and has been implicated in the pathophysiology of depression [18–21]. Postmortem studies have shown that hippocampal BDNF levels are decreased in depressed patients and increased in patients receiving antidepressant treatment [22–24]. Animal studies have demonstrated that various types of acute (e.g., immobilization and footshock) and chronic (e.g., chronic unpredictable stress (CUS) and chronic restrain) stress paradigms reduce BDNF expression in the hippocampus, and this reduction can be reversed by chronic

Table 1: Schedule of chronic mild stress procedures.

Day	Stressors	Time
1	10 h crowded cage (5-6 rats per cage)	a.m. to p.m.
2	15 min forced swim (22°C) 15 h wet bedding	p.m.
3	4 h restraint 24 h food deprivation	a.m.
4	5 min cold swim (4°C)	p.m.
5	4 h restraint 24 h water deprivation (including 6 h empty water bottle)	a.m.
6	2 h cold stress (15°C) 4 h restraint	a.m. p.m.
7	4 h restraint 2 min tail pinch	a.m. p.m.

antidepressant treatment [25–28]. Furthermore, several lines of evidence suggest that acupuncture or EA can upregulate hippocampal BDNF expression in normal and depression model rats [29–31].

Considering all of the aforementioned, the present study was designed to determine whether EA intervention combined with citalopram (a widely used SSRI), at a lower dose than what is required for monotherapy, could produce greater therapeutic effects in the CUS rats compared with EA or citalopram treatment alone. Changes in BDNF and its major receptor tropomyosin-related kinase receptor B (TrkB) were also evaluated.

2. Materials and Methods

2.1. Animals. Adult Sprague-Dawley (SD) rats (male, 200–220 g) were obtained from the laboratory animal center, Capital Medical University. Animals were maintained in a standard 12 h light/dark cycle in cages with ad libitum access to food and water and were allowed to acclimate to the environment for 7 days. All experimental procedures were approved by the Ethics Committee on Animal Care and Usage of Capital Medical University. Every effort was made to minimize animal suffering.

2.2. Experimental Design and Animal Groups. Rats in the control group received no CUS during the whole experiment. In the model group, rats were exposed to CUS for 7 weeks. From the beginning of the 5th week, model rats were randomly grouped and subjected to different experiments. In the first experiment, rats were divided into five groups and each group had 8-9 rats. Normal rats were intraperitoneally (i.p.) injected with saline, and model rats were, respectively, injected (i.p.) with saline and 5, 10, and 20 mg/kg citalopram once a day for 3 weeks. In the second experiment, there are four groups and each group had 8 rats. Normal rats received no treatment, while model rats were subjected to EA stimulation for 3 weeks and further divided into three groups: vehicle (received CUS only), 2 Hz EA, and 100 Hz EA. In the third experiment, model rats were administered with combined treatment with EA and citalopram for 3 weeks. In summary, there were five groups and each group had 8-9 rats: (1) vehicle (received CUS only); (2) 2 Hz EA group; (3) Cital 5 group; (4) Cital 5 plus 2 Hz EA group; (5) Cital 10 group. The experimental procedure is shown in Figure 1.

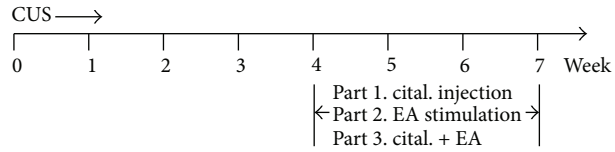

Figure 1: Schematic representation of the experimental procedure.

2.3. CUS Procedure. The CUS protocol was modified from the procedures described by Katz [32] and Willner et al. [33]. It consisted of a variety of sequential stressors applied randomly every day for 7 weeks (Table 1). Rats in the nonstress group were housed in groups of three, unless when they were subjected to sucrose preference test. Those exposed to CUS procedure were housed alone, unless when they were subjected to high-density housing.

2.4. Sucrose Preference Test. The sucrose preference test was performed as previously described with minor modification [34, 35]. This test was carried out before CUS and at the end of each week. Rats were kept individually in separate cages and habituated to two needleless syringes (resp., filled with plain water and 1% sucrose solution) 8 h per day for 2 days. Followed by 12 h period of food and water deprivation, the rats were exposed to the two syringes for 30 min. After an interval of 1 h, the positions of the syringes were exchanged, and the rats were tested for 30 min again. The volume of sucrose solution and water consumption during the total 1 h test was recorded. Sucrose preference was expressed as a ratio of the volume of sucrose solution consumption to the volume of total fluid intake.

2.5. Open Field Test (OFT). Locomotor activity was monitored automatically with infrared beams (each beam space 2.5 cm) in a black chamber before CUS and at the end of 4th and 7th weeks during the CUS procedure (TruScan 2.0 Instruments, Columbus, OH.). Tests were conducted between 9 a.m. and 11 a.m.. Each rat was placed in a corner of the chamber and was allowed to explore freely for 5 min. At the end of each test, the chamber was cleaned with 70% ethanol solution to remove any olfactory cues. Locomotor activity was defined as horizontal (floor plane, FP) and vertical (vertical plane, VP) movement distances and the number of entries into the arena-center (defined as more than 2.5-beam spaces away from the arena walls). Movement distances provide information on general activity. Number of center entries probably reflects anxiety-like behavior, with more "anxious" rats entering fewer times into the arena-center. The data were recorded and analyzed using a DigiScan analyzer and software (TruScan 2.0, Columbus).

2.6. Forced Swimming Test (FST). FST was performed at the end of 4th and 7th weeks during the CUS procedure. This

test consists of a 15 min pretest swim and a 5 min test swim on the following day [36]. Rats were forced to swim in a glass cylinder (diameter 26 cm and height 60 cm) containing 35 cm depth of water at a temperature of 25°C. Water was changed after each test. Behavior was video-recorded using SMART video-tracking system (Panlab, Spain). Three types of behavior were analyzed: immobility, swimming, and climbing [37]. Immobility was defined as floating with no active activity other than those necessary to keep head above the water. Swimming was defined as active movements throughout the cylinder, including crossing into another quadrant. Climbing was defined as upward-directed movements of the forepaws against the cylinder walls.

2.7. Citalopram Treatment. Citalopram hydrobromide (Sigma-Aldrich, MO, USA) was dissolved in 0.9% physiological saline immediately before use and administered intraperitoneally daily from the 5th week to the 7th week during the CUS procedure. Control rats received saline as a vehicle injection.

2.8. EA Treatment. EA stimulation was administered from the 5th week following the CUS procedure. Two stainless steel needles of 0.25 mm in diameter were inserted at a depth of 5 mm into the acupoints of BAIHUI (GV 20, at the midpoint between the auricular apices) and Yintang (EX-HN 3, at the midpoint between the eyebrows). The bidirectional square-wave (0.2 ms) electrical pulse from a medical EA apparatus (HANS LY-257, Beijing) was administered with frequency 2 or 100 Hz for a total of 30 min each day, 6 days per week. The intensity of the stimulation was increased stepwise from 1 to 3 mA. During EA stimulation, the rats were kept under awake and unrestrained conditions in individual cages.

2.9. BDNF Protein Detection. Four to five rats in each group were killed by decapitation one day after behavioral measurements. Hippocampal tissue was dissected for protein assays and trunk blood was collected for the determination of serum BDNF levels. Samples were stored at −80°C until assay. Each frozen hippocampus was homogenized and lysed with RIPA buffer containing protease inhibitor cocktail (Sigma-Aldrich). The total protein concentration was determined using BCA protein assay kit (Pierce, Rockford, IL). For Western blot analysis, equal amounts of proteins were separated by 12% SDS-PAGE and transferred to PVDF (polyvinyldifluoride) membranes (Millipore). After being blocked with 5% nonfat-dried milk for 1 h, the membranes were incubated overnight at 4°C with rabbit polyclonal antibody to BDNF (1 : 300, Santa Cruz), rabbit polyclonal antibody to TrkB (1 : 1000, Millipore), and mouse monoclonal antibody to β-actin (1 : 5000, Sigma-Aldrich). Then the membranes were incubated with IRDye 800 conjugated secondary antibodies (Rockland Immunochemicals). Signals were visualized by the Odyssey infrared double-fluorescence imaging system (American Company LI-COR Biosciences, Lincoln, NE, USA). For enzyme-linked immunoassay (ELISA), hippocampal and serum BDNF levels were analyzed using a Chemokine BDNF ELISA kit according to the manufacturer's protocol (Millipore, Billerica, MA). The optical density was measured at 450 nm using an ELISA reader (Bio-Rad Laboratories Ltd, CA). ELISA results were expressed as ng per mL serum and pg per mg protein. All samples were assayed in duplicate.

2.10. Statistical Analysis. Data were presented as means ± SEM. Statistical significance was assessed with the Student's t-test or one-way analysis of variance (ANOVA) followed by Newman-Keuls as post hoc multiple comparisons test using Prism 5.0 software (GraphPad Software). P value less than 0.05 was considered to be statistically significant.

3. Results

3.1. Chronic Unpredictable Stress Model. Rats subjected to CUS exhibited significantly lower body weight compared with nonstressed controls from the first week after the commencement of CUS procedure (Week 1: control: 272.0 ± 4.028 g, CUS: 259.0 ± 2.152 g; Week 2: control: 290.6 ± 3.461 g, CUS: 261.4 ± 2.824 g; Week 3: control: 307.5 ± 3.090 g, CUS: 261.6 ± 1.946 g; Week 4: control: 331.3 ± 2.916 g, CUS: 266.4 ± 2.386 g.) (Figure 2(a)). Decreased sucrose preference is considered as a symptom resembling anhedonia, which is a core clinical feature of depression in humans [38, 39]. After 4 weeks of CUS, there was a significant decrease in sucrose preference in the model rats as compared with the controls, while the total fluid intake was not affected (Figures 2(b) and 2(c)). In the FST, the model rats demonstrated a significant increase in immobility time, accompanied by remarkably decreased swimming and climbing time (Figure 2(d)). Moreover, when exposed to the OFT, those rats showed significant decreases in the horizontal and vertical movement distances and fewer times into the arena-center (Figures 2(e)–2(g)). Taken together, these results indicate that the 4 weeks of CUS procedure is able to induce depressive-like symptoms (i.e., anhedonia, behavioral despair, and reduced locomotor activity) in the model rats.

3.2. Chronic Administration of Citalopram Ameliorates Depressive-Like Behavior. Model rats were intraperitoneally injected with different doses of citalopram from the 5th week of CUS procedure. After 3 weeks of administration, both 10 and 20 mg/kg citalopram produced significantly increased sucrose preference, without affecting the total fluid intake (Figures 3(a) and 3(b)). In addition, they induced dramatic increases in horizontal and vertical movement distances (Figures 3(d) and 3(e)) and center entries (Figure 3(f)) in the OFT. However, these effects were not detected by treatment with 5 mg/kg citalopram. Moreover, none of these three doses of citalopram exerted any notable effect in the FST (Figure 3(c)). Thus, 5 mg/kg citalopram was considered ineffective and would be chosen to be combined with EA for further investigation.

3.3. EA Treatment Alone Only Improves Locomotor Activity of CUS Rats. To assess whether EA could improve depressive-like behavior, model rats were administered with frequency 2 or 100 Hz EA stimulation from the 5th week of CUS

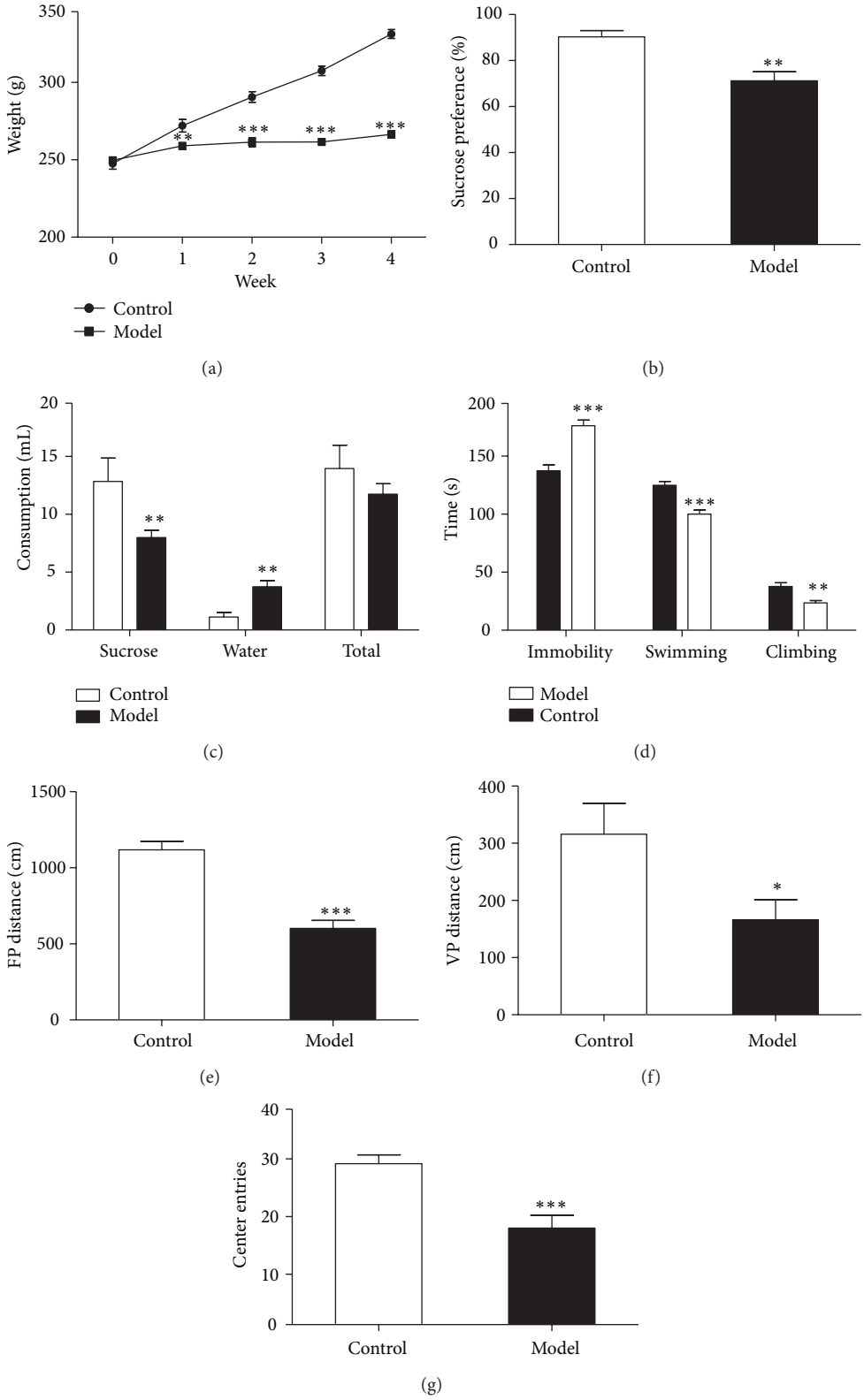

Figure 2: Rats show depressive-like symptoms after 4 weeks of CUS procedure. (a) Body weight. (b) Sucrose preference expressed as a ratio of the volume of sucrose solution consumption to the volume of total fluid intake. (c) The volume of consumption of sucrose solution, water, and total fluid. (d) FST. Data (expressed in seconds) are presented as time spent in immobility, climbing, and swimming. (e)–(g) OFT. Data (expressed in centimeter) are presented as movement distances in the floor plane (FP) (e) and vertical plane (VP) (f) and the number of entries into the arena-center (g). $n = 11$–15 per group. Data represent mean ± SEM, $^{*}P < 0.05$, $^{**}P < 0.01$, and $^{***}P < 0.001$ *versus* the control group.

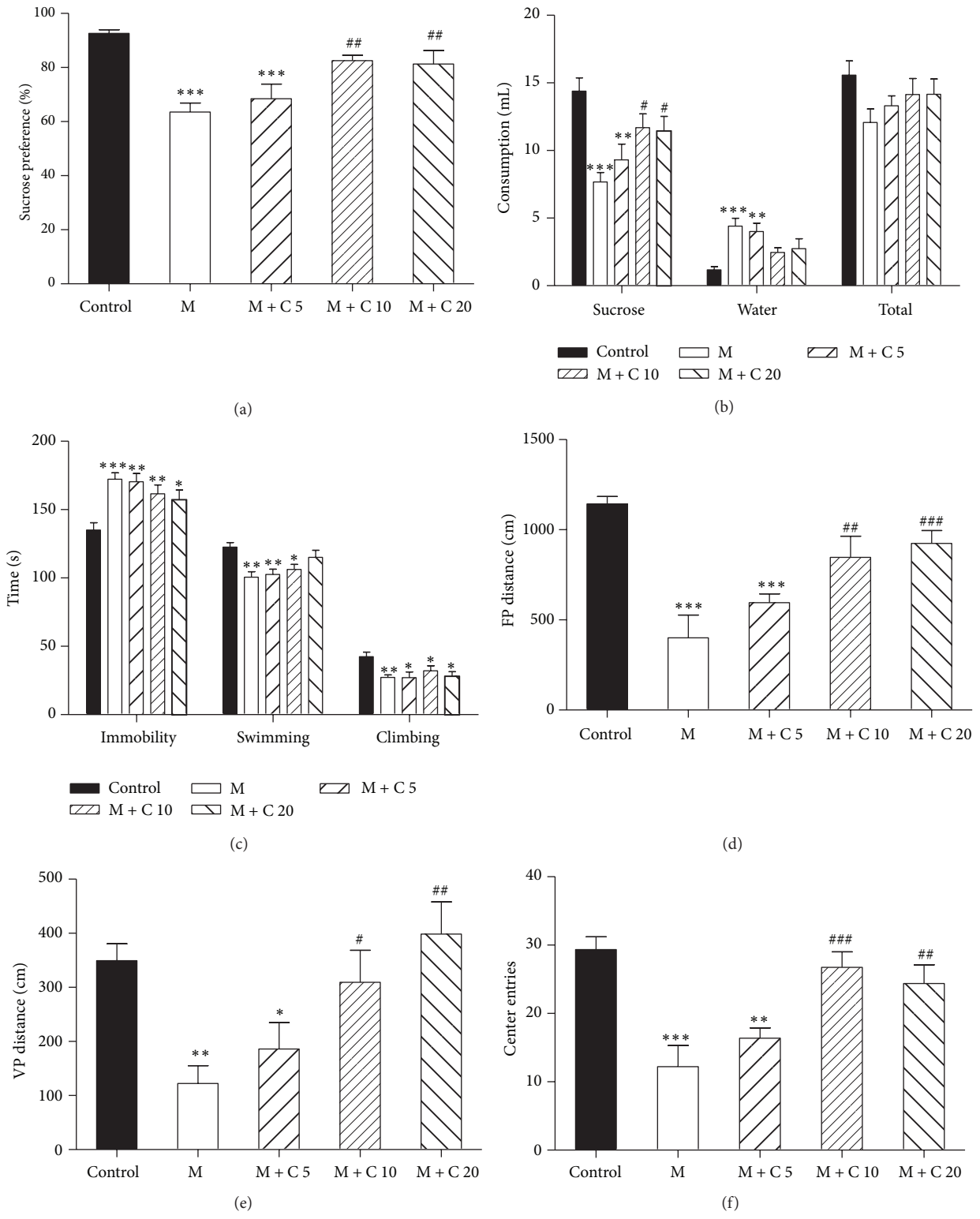

Figure 3: Effects of 3 weeks of treatment with citalopram on CUS-induced depressive-like behavior. (a) Citalopram significantly increased sucrose preference at 10 and 20 mg/kg but not 5 mg/kg. (b) Citalopram remarkably increased sucrose intake without affecting the total fluid intake. (c) Citalopram at different doses (5, 10, and 20 mg/kg) had no effect on immobility, climbing, and swimming in the FST. (d)–(f) In the OFT, citalopram significantly increased horizontal (d) and vertical (e) movement distances and center entries (f) at 10 and 20 mg/kg but not 5 mg/kg. n = 8-9 per group. Data represent mean ± SEM, $^{*}P < 0.05$, and $^{**}P < 0.01$ *versus* the vehicle-treated group.

procedure. After 3 weeks of treatment, neither 2 nor 100 Hz EA stimulation was able to improve anhedonia and behavioral despair as detected by sucrose preference test and FST (Figures 4(a)–4(c)). By contrast, both 2 and 100 Hz EA stimulation significantly increased vertical movement distance and center entries in the OFT, but only 2 Hz EA stimulation demonstrated a significant effect on the horizontal movement distance (Figures 4(d)–4(f)). Thus, we next explored the joint effects of 2 Hz EA and 5 mg/kg citalopram in the subsequent experiment.

3.4. Enhanced Antidepressant Effects of Combined Treatment with EA and Citalopram. To evaluate whether EA combined with citalopram has an additive or synergistic antidepressant effect, combined treatment with 2 Hz EA and a low dose of citalopram was administered from the 5th week of CUS procedure. After 3 weeks, 2 Hz EA plus 5 mg/kg citalopram led to substantial increases in sucrose preference (Figures 5(b) and 5(c)), horizontal/vertical movement distances (Figures 5(e) and 5(f)), and center entries (Figure 5(g)), demonstrating similar effects to 10 mg/kg citalopram. Furthermore, 2 Hz EA plus 5 mg/kg citalopram induced a significant reduction in immobility time, accompanied by an increased climbing time in the FST, whereas these effects were not detected by treatment with 10 mg/kg citalopram (Figure 5(d)). However, there was no remarkable difference in body weight among all the groups (Figure 5(a)). These findings suggest that 2 Hz EA plus 5 mg/kg citalopram could exert better antidepressant effects in comparison with either treatment alone.

3.5. Combined Treatment with EA and Citalopram Induces a Higher Expression of BDNF in the Hippocampus. To explore the possible mechanisms involved in the joint effects of EA and citalopram, the rats were sacrificed one day after behavioral tests. Results from ELISA demonstrated that hippocampal BDNF protein levels were significantly decreased after 4 weeks of CUS procedure (Figure 6(a)). However, 3 weeks of treatment with 2 Hz EA plus 5 mg/kg citalopram, as well as 10 mg/kg citalopram, led to a remarkable increase in BDNF expression in the hippocampus (Figure 6(b)), but not in the prefrontal cortex or serum (data not shown). Western blot analysis also showed that protein levels of both mature BDNF (mBDNF) and BDNF precursor (proBDNF) significantly increased in 2 Hz EA plus 5 mg/kg citalopram group, similar to the observations in 10 mg/kg citalopram group. Moreover, both of these groups revealed a dramatic increase in the expression of TrkB compared with that measured in the vehicle group (Figure 6(c)). These data indicate that EA combined with citalopram could prevent CUS-induced decrease in BDNF signaling in the hippocampus.

4. Discussion

The present study aimed at exploring the therapeutic potentiality of coadministration of EA and an antidepressant by biochemical and behavioral approaches using an animal model predictive of antidepressant-like activity. Here, we demonstrated that the combined treatment with 2 Hz EA and a low dose of citalopram could prevent CUS-induced decrease in hippocampal BDNF signaling and exert better antidepressant effects in the CUS model rats than either treatment alone.

CUS model, which mimics socioenvironmental stressors in everyday life, is one of the most extensively used animal models of depression [40]. Rats subjected to the CUS paradigm for several weeks can exhibit almost all demonstrable depressive symptoms. However, this model is difficult to replicate, because different CUS schedules, including types of stressors, animal strains, and nutritive status, can result in inconsistent findings [39, 41]. It has been reported that chronic restraint stress can induce significant downregulation of BDNF in the hippocampus [27, 42]. Accordingly, restraints were used frequently in our CUS paradigm. Consistent with previous studies, we have demonstrated that rats subjected to CUS for 4 weeks exhibit a significantly decreased sucrose preference, accompanied by other behavioral changes such as increased immobility time and decreased locomotor activity.

FST is widely used as a screening procedure for antidepressants [37, 43]. In this test, animals display "despair" behavior (immobility) and active behaviors (swimming and climbing) (14). It has been demonstrated that different SSRIs may exert different effects on immobility time [44, 45]. In our experiment, citalopram was demonstrated inactive after chronic administration in the FST, consistent with several previous researches [46, 47]. On the contrary, many other studies have shown positive effects of acute administration of citalopram on immobility and swimming time in acute stress models [48–50]. The missing observation of significant changes in our experiment might be attributed to two main causes. One is the rat strain. It has been shown that SD rats respond to various antidepressants not so well as Wistar-Kyoto rats in the FST [44]. The other is the type of stressors. Repeated swimming stress may depress the sensitivity of model rats to FST. Also, it has been reported that food restriction with modest weight reduction can attenuate the behavioral effects of SSRIs [51]. Even so, we demonstrated that high doses (10 and 20 mg/kg) of citalopram were able to result in significantly increased sucrose preference and improved locomotor activity in the model rats as previously reported [52, 53].

Acupuncture has been applied to treat depressive disorders with a long clinical history, but a recent Cochrane review identified that no consistent benefit was noted with any form of acupuncture (manual acupuncture, EA, or laser acupuncture) in depressed patients [6, 14]. In the present study, we found that sucrose preference and immobility time in the model rats were not significantly affected by EA treatment, even though there was a tendency of increase or reduction after 3 weeks of stimulation. These results are in agreement with several previous studies that were also performed on the CUS model rats [54–56]. Liu and his colleagues demonstrated that 3 weeks of EA stimulation produced a significant increase in the number of crossing in the OFT and a nonsignificant increase in the sucrose intake [55]. Another study reported by Yu et al. showed that sucrose preference and immobility time in the depressive rats were not significantly changed by 6 weeks of treatment with EA alone [56]. Because frequency

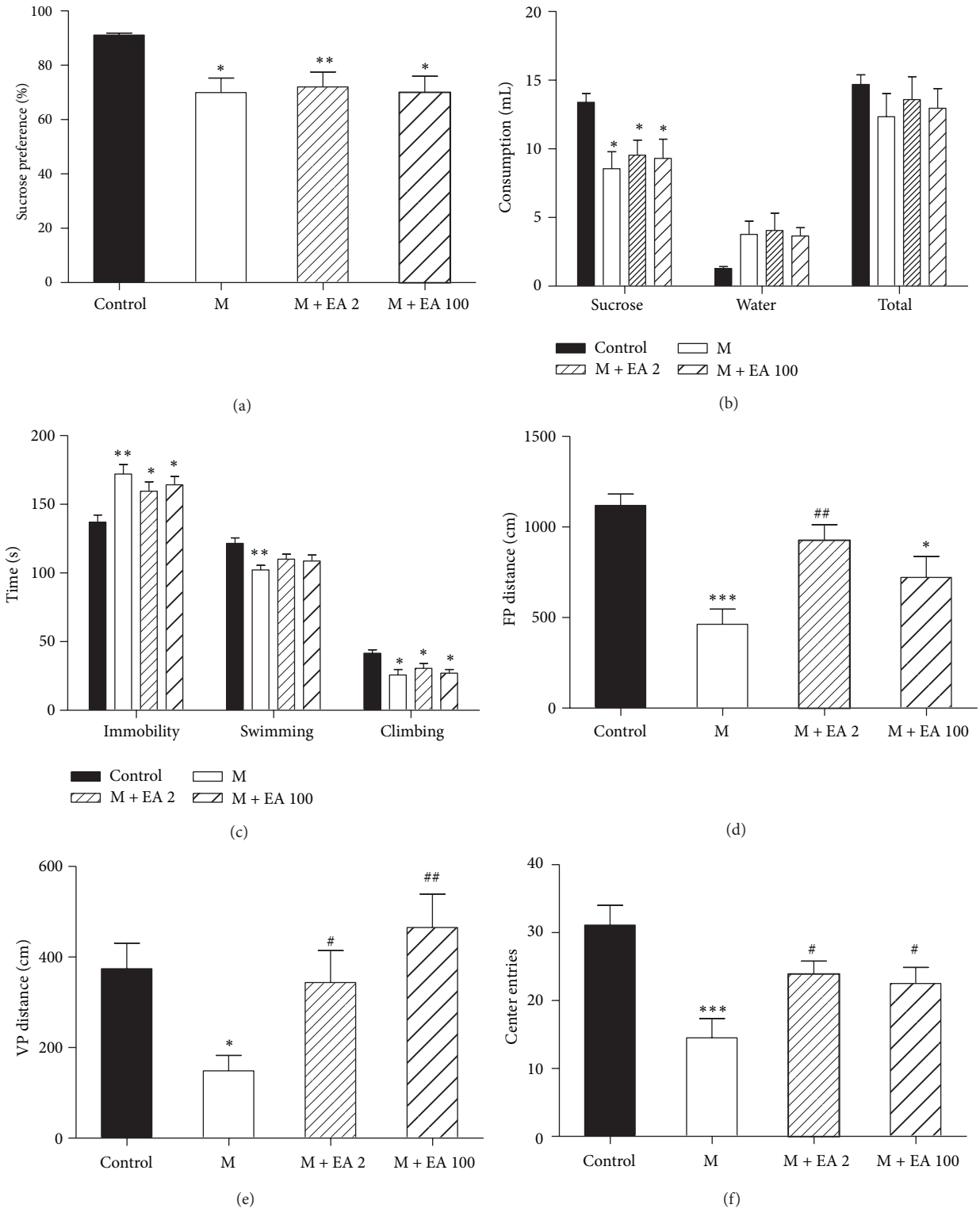

FIGURE 4: Effects of 3 weeks of EA stimulation on CUS-induced depressive-like behavior. (a)-(b) 2 Hz or 100 Hz EA stimulation had no effect on sucrose preference and sucrose intake. (c) Neither 2 Hz nor 100 Hz EA had any effect on immobility, climbing, and swimming in the FST. (d)–(f) In the OFT, 2 Hz EA induced significantly increased horizontal (d) and vertical (e) movement distances and center entries (f), while 100 Hz EA demonstrated no effect on the horizontal movement distance. $n = 8$ per group. Data represent mean ± SEM, $^{*}P < 0.05$, and $^{**}P < 0.01$ *versus* the vehicle-treated group.

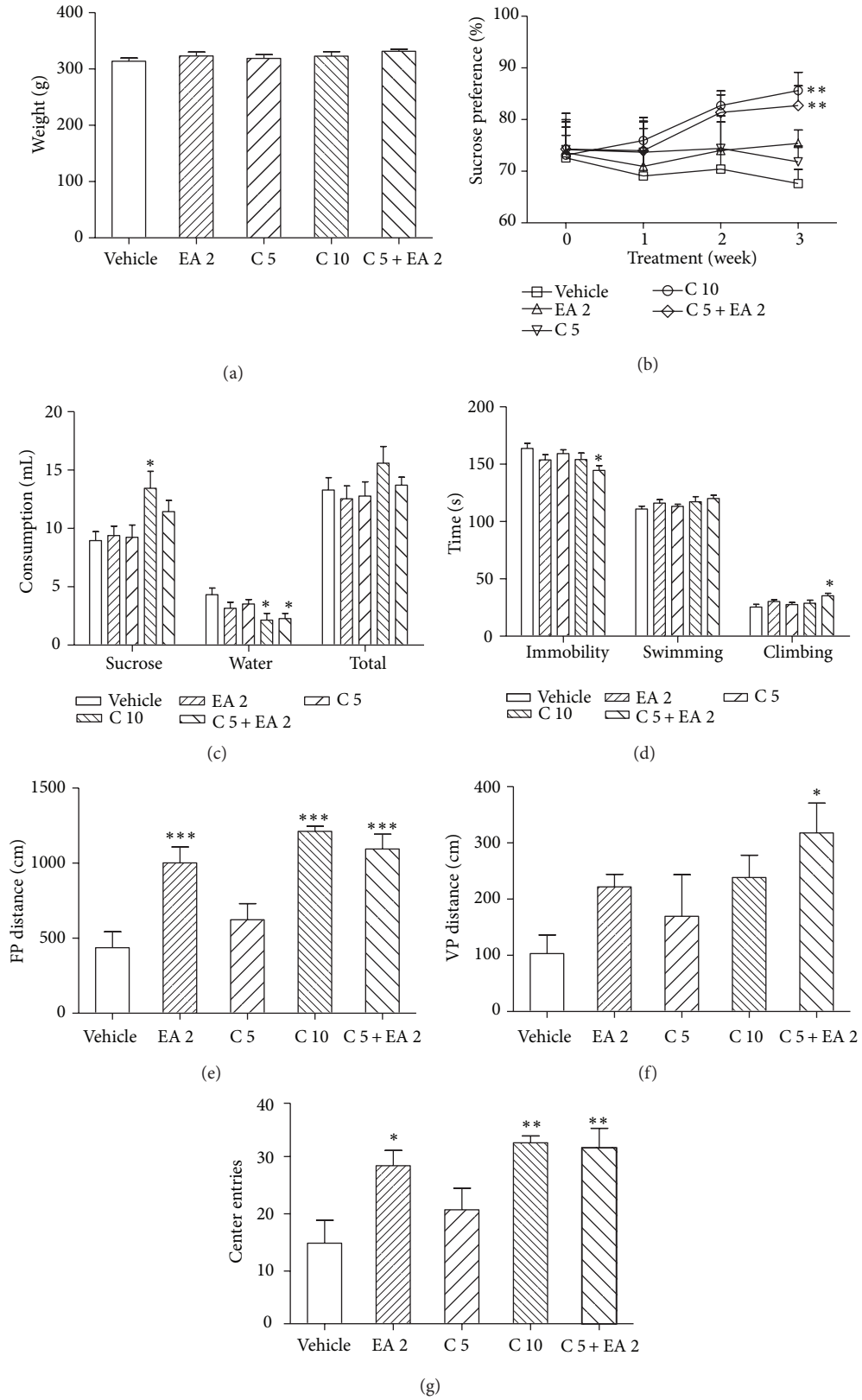

Figure 5: Effects of 3 weeks of combined treatment with EA and citalopram on CUS-induced depressive-like behavior. (a) Body weight. (b)-(c) 2 Hz EA plus 5 mg/kg citalopram as well as 10 mg/kg citalopram produced a substantial increase in sucrose preference without affecting the total fluid intake. (d) 2 Hz EA plus 5 mg/kg citalopram induced significantly decreased immobility time and increased climbing time in the FST. (e)–(g) 2 Hz EA plus 5 mg/kg citalopram led to significantly increased horizontal (e) and vertical (f) movement distances and center entries (g). n = 8-9 per group. Data represent mean ± SEM, $^{*}P < 0.05$, $^{**}P < 0.01$, and $^{***}P < 0.001$ *versus* the vehicle-treated group.

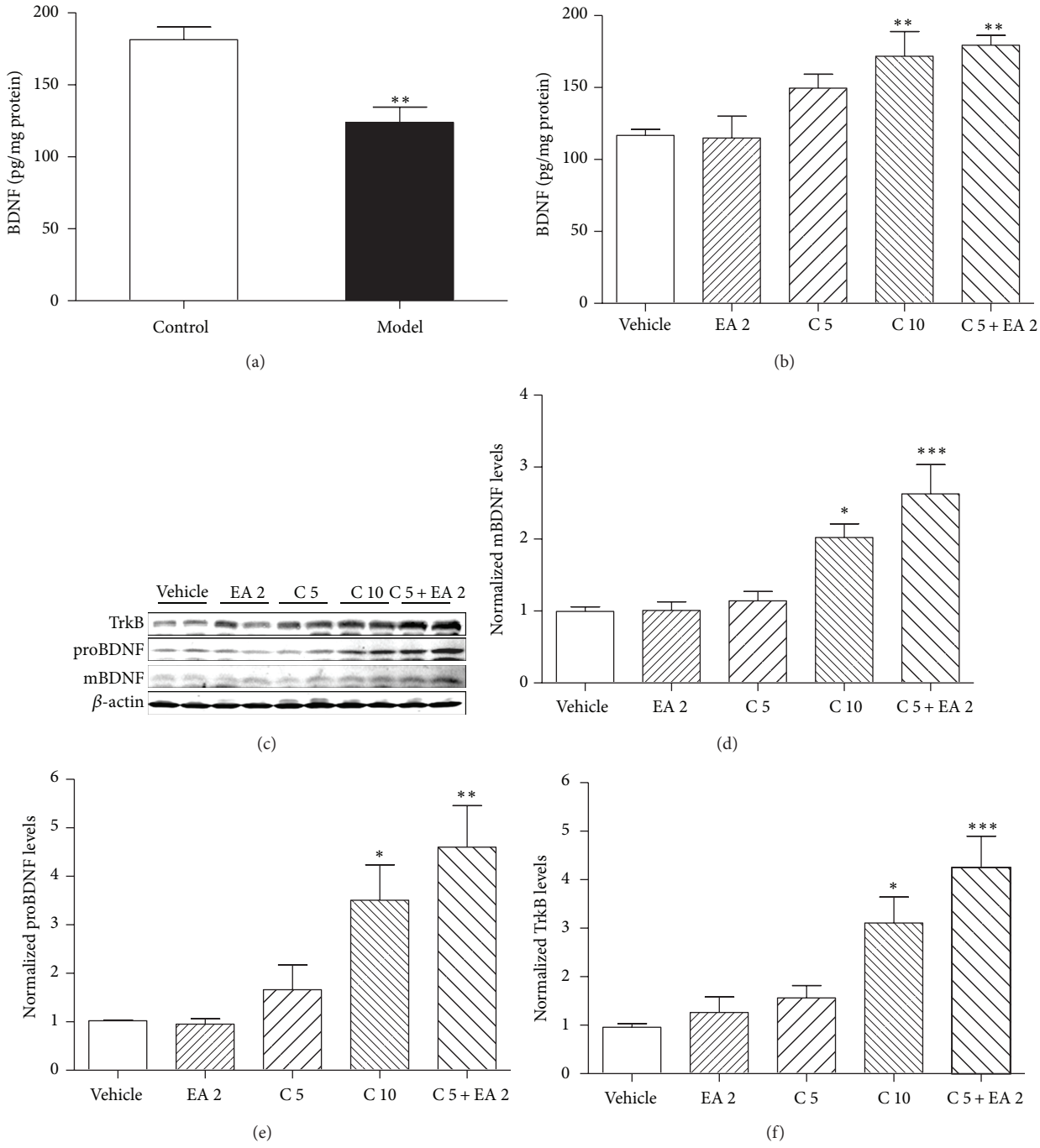

Figure 6: CUS-induced downregulation of BDNF expression was reversed by 3 weeks of combined treatment with EA and citalopram. (a) Hippocampal BDNF protein levels were significantly decreased after 4 weeks of CUS procedure. (b) ELISA results showed that 2 Hz EA plus 5 mg/kg citalopram as well as 10 mg/kg citalopram induced remarkably increased BDNF protein levels in the hippocampus. (c) Western blot analysis of hippocampal mBDNF, proBDNF, and TrkB protein levels. β-actin was used as an internal control. (d)–(f) Quantitative analysis of mBDNF, proBDNF, and TrkB protein levels in (b). n = 4-5 per group. Data represent mean ± SEM, $^{*}P < 0.05$, $^{**}P < 0.01$, and $^{***}P < 0.001$ *versus* the vehicle-treated group.

is an important parameter involved in the efficiency of EA [57], we explored the effects of both high- (100 Hz) and low-frequency (2 Hz) EA in the present study. Although neither of them had a definite antidepressant-like effect, 2 Hz EA exerted a remarkable increase in the horizontal movement distance and a better tendency in sucrose preference and immobility time. Thus, we supposed that 2 Hz EA might be more suitable for combined treatment with a lower dose of citalopram.

As expected, we found that 2 Hz EA combined with a low dose of citalopram led to significant improvement in the sucrose preference test and FST, showing a greater

effect on depressive-like behavior than either treatment alone. Similarly, several previous literatures have shown that EA augmented antidepressant-like effects of a tricyclic antidepressant, clomipramine or mianserin, in depression model rats or patients [54, 56, 58]. It has also been reported that application of acupuncture to low-dose fluoxetine-treated depressed patients is as effective as a recommended dose of fluoxetine treatment. However, the mechanisms underlying these combined effects remain unknown.

The delayed onset of SSRIs suggests that their therapeutic effects are mediated beyond a simple enhancement in serotonergic neurotransmission but may be more related to reorganization of neuronal networks [59]. Numerous studies have identified a key role of BDNF in the development and treatment of depression. BDNF needs binding to high-affinity protein kinase receptor family, TrkB, to exert its biological effects, such as neuronal survival, differentiation, neurotransmitter release, and synaptic plasticity. There is a clear evidence that BDNF-TrkB signaling mediates the actions of antidepressants [60]. For instance, chronic SSRI treatment could increase BDNF expression and TrkB receptor activation in rodent hippocampus [25, 61]. Consistent with these findings, the present study demonstrates that chronic administration of 10 mg/kg citalopram increased both BDNF and TrkB protein levels in rat hippocampus. Moreover, combined treatment with 2 Hz EA and 5 mg/kg citalopram, but not either treatment alone, produced similar effects, corresponding to improved depressive-like behavior. However, the relationship between the change of BDNF-TrkB signaling and the antidepressant-like effect of the combined therapy needs further investigation.

In conclusion, our study points out that the combined treatment with EA and a low dose of citalopram could prevent CUS-induced decrease in hippocampal BDNF signaling and lead to greater antidepressant effects than either treatment alone. These findings could provide a new perspective on clinical therapy for depression.

Authors' Contribution

J. Yang and Y. Pei contributed equally to this work and should be considered co-first authors.

Acknowledgments

This work was supported by the Grants from National Natural Science Foundation of China (81071102 and 81072858), Beijing Postdoctoral Research Foundation (2011ZZ-10), Training Programme Foundation for the Beijing Municipal Excellent Talents (20081D0301100089), and the National Basic Research Program of China (2011CB504100).

References

[1] D. Richards, "Prevalence and clinical course of depression: a review," *Clinical Psychology Review*, vol. 31, no. 7, pp. 1117–1125, 2011.

[2] B. Arroll, S. Macgillivray, S. Ogston et al., "Efficacy and tolerability of tricyclic antidepressants and SSRIs compared with placebo for treatment of depression in primary care: a meta-analysis," *Annals of Family Medicine*, vol. 3, no. 5, pp. 449–456, 2005.

[3] P. Cassano and M. Fava, "Tolerability issues during long-term treatment with antidepressants," *Annals of Clinical Psychiatry*, vol. 16, no. 1, pp. 15–25, 2004.

[4] C. M. Dording, D. Mischoulon, T. J. Petersen et al., "The pharmacologic management of SSRI-induced side effects: a survey of psychiatrists," *Annals of Clinical Psychiatry*, vol. 14, no. 3, pp. 143–147, 2002.

[5] A. Cipriani, T. A. Furukawa, G. Salanti et al., "Comparative efficacy and acceptability of 12 new-generation antidepressants: a multiple-treatments meta-analysis," *The Lancet*, vol. 373, no. 9665, pp. 746–758, 2009.

[6] C. A. Smith, P. P. Hay, and H. Macpherson, "Acupuncture for depression.," *Cochrane Database of Systematic Reviews*, no. 1, p. CD004046, 2010.

[7] J. J. B. Allen, R. N. Schnyer, A. S. Chambers, S. K. Hitt, F. A. Moreno, and R. Manber, "Acupuncture for depression: a randomized controlled trial," *Journal of Clinical Psychiatry*, vol. 67, no. 11, pp. 1665–1673, 2006.

[8] H. Luo, F. Meng, Y. Jia, and X. Zhao, "Clinical research on the therapeutic effect of the electro-acupuncture treatment in patients with depression," *Psychiatry and Clinical Neurosciences*, vol. 52, pp. S338–S340, 1998.

[9] J. Wu, A. S. Yeung, R. Schnyer, Y. Wang, and D. Mischoulon, "Acupuncture for depression: a review of clinical applications," *Canadian Journal of Psychiatry*, vol. 57, no. 7, pp. 397–405, 2012.

[10] Z. J. Zhang, R. Ng, S. C. Man et al., "Dense cranial electroacupuncture stimulation for major depressive disorder—a single-blind, randomized, controlled study," *PLoS One*, vol. 7, no. 1, Article ID e29651, 2012.

[11] Y. Mukaino, J. Park, A. White, and E. Ernst, "The effectiveness of acupuncture for depression—a systematic review of randomised controlled trials," *Acupuncture in Medicine*, vol. 23, no. 2, pp. 70–76, 2005.

[12] A. F. Thachil, R. Mohan, and D. Bhugra, "The evidence base of complementary and alternative therapies in depression," *Journal of Affective Disorders*, vol. 97, no. 1–3, pp. 23–35, 2007.

[13] R. J. Leo and J. S. A. Ligot, "A systematic review of randomized controlled trials of acupuncture in the treatment of depression," *Journal of Affective Disorders*, vol. 97, no. 1–3, pp. 13–22, 2007.

[14] R. Nahas and O. Sheikh, "Complementary and alternative medicine for the treatment of major depressive disorder," *Canadian Family Physician*, vol. 57, no. 6, pp. 659–663, 2011.

[15] M. M. Poo, "Neurotrophins as synaptic modulators," *Nature Reviews Neuroscience*, vol. 2, no. 1, pp. 24–32, 2001.

[16] H. Thoenen, "Neurotrophins and neuronal plasticity," *Science*, vol. 270, no. 5236, pp. 593–598, 1995.

[17] K. Kohara, A. Kitamura, M. Morishima, and T. Tsumoto, "Activity-dependent transfer of brain-derived neurotrophic factor to postsynaptic neurons," *Science*, vol. 291, no. 5512, pp. 2419–2423, 2001.

[18] M. A. H. Rot, S. J. Mathew, and D. S. Charney, "Neurobiological mechanisms in major depressive disorder," *Canadian Medical Association Journal*, vol. 180, no. 3, pp. 305–313, 2009.

[19] E. Castren, "Is mood chemistry?" *Nature Reviews Neuroscience*, vol. 6, no. 3, pp. 241–246, 2005.

[20] E. Castren, V. Voikar, and T. Rantamaki, "Role of neurotrophic factors in depression," *Current Opinion in Pharmacology*, vol. 7, no. 1, pp. 18–21, 2007.

[21] H. Yu and Z. Y. Chen, "The role of BDNF in depression on the basis of its location in the neural circuitry," *Acta Pharmacologica Sinica*, vol. 32, no. 1, pp. 3–11, 2011.

[22] B. Chen, D. Dowlatshahi, G. M. MacQueen, J. F. Wang, and L. T. Young, "Increased hippocampal BDNF immunoreactivity in subjects treated with antidepressant medication," *Biological Psychiatry*, vol. 50, no. 4, pp. 260–265, 2001.

[23] F. Karege, G. Vaudan, M. Schwald, N. Perroud, and R. La Harpe, "Neurotrophin levels in postmortem brains of suicide victims and the effects of antemortem diagnosis and psychotropic drugs," *Molecular Brain Research*, vol. 136, no. 1-2, pp. 29–37, 2005.

[24] Y. Dwivedi, H. S. Rizavi, R. R. Conley, R. C. Roberts, C. A. Tamminga, and G. N. Pandey, "Altered gene expression of brain-derived neurotrophic factor and receptor tyrosine kinase B in postmortem brain of suicide subjects," *Archives of General Psychiatry*, vol. 60, no. 8, pp. 804–815, 2003.

[25] M. Nibuya, S. Morinobu, and R. S. Duman, "Regulation of BDNF and trkB mRNA in rat brain by chronic electroconvulsive seizure and antidepressant drug treatments," *Journal of Neuroscience*, vol. 15, no. 11, pp. 7539–7547, 1995.

[26] A. M. Rasmusson, L. Shi, and R. Duman, "Downregulation of BDNF mRNA in the hippocampal dentate gyrus after re-exposure to cues previously associated with footshock," *Neuropsychopharmacology*, vol. 27, no. 2, pp. 133–142, 2002.

[27] H. Xu, Z. Chen, J. He et al., "Synergetic effects of quetiapine and venlafaxine in preventing the chronic restraint stress-induced decrease in cell proliferation and BDNF expression in rat hippocampus," *Hippocampus*, vol. 16, no. 6, pp. 551–559, 2006.

[28] Y. Zhang, F. Gu, J. Chen, and W. Dong, "Chronic antidepressant administration alleviates frontal and hippocampal BDNF deficits in CUMS rat," *Brain Research*, vol. 1366, no. C, pp. 141–148, 2010.

[29] I. K. Hwang, J. Y. Chung, D. Y. Yoo et al., "Effects of electroacupuncture at zusanli and baihui on brain-derived neurotrophic factor and cyclic AMP response element-binding protein in the hippocampal dentate gyrus," *Journal of Veterinary Medical Science*, vol. 72, no. 11, pp. 1431–1436, 2010.

[30] B. Lee, B. J. Sur, S. Kwon et al., "Acupuncture stimulation alleviates corticosterone-induced impairments of spatial memory and cholinergic neurons in rats," *Evidence-Based Complementary and Alternative Medicine*, vol. 2012, Article ID 670536, 14 pages, 2012.

[31] S. J. Yun, H. J. Park, M. J. Yeom, D. H. Hahm, H. J. Lee, and E. H. Lee, "Effect of electroacupuncture on the stress-induced changes in brain-derived neurotrophic factor expression in rat hippocampus," *Neuroscience Letters*, vol. 318, no. 2, pp. 85–88, 2002.

[32] R. J. Katz, "Animal models and human depressive disorders," *Neuroscience and Biobehavioral Reviews*, vol. 5, no. 2, pp. 231–246, 1981.

[33] P. Willner, A. Towell, D. Sampson, S. Sophokleous, and R. Muscat, "Reduction of sucrose preference by chronic unpredictable mild stress, and its restoration by a tricyclic antidepressant," *Psychopharmacology*, vol. 93, no. 3, pp. 358–364, 1987.

[34] M. Banasr, G. W. Valentine, X. Y. Li, S. L. Gourley, J. R. Taylor, and R. S. Duman, "Chronic unpredictable stress decreases cell proliferation in the cerebral cortex of the adult rat," *Biological Psychiatry*, vol. 62, no. 5, pp. 496–504, 2007.

[35] K. R. Luo, C. J. Hong, Y. J. Liou, S. J. Hou, Y. H. Huang, and S. J. Tsai, "Differential regulation of neurotrophin S100B and BDNF in two rat models of depression," *Progress in Neuro-Psychopharmacology and Biological Psychiatry*, vol. 34, no. 8, pp. 1433–1439, 2010.

[36] R. D. Porsolt, G. Anton, N. Blavet, and M. Jalfre, "Behavioural despair in rats: a new model sensitive to antidepressant treatments," *European Journal of Pharmacology*, vol. 47, no. 4, pp. 379–391, 1978.

[37] Y. Shirayama, A. C. H. Chen, S. Nakagawa, D. S. Russell, and R. S. Duman, "Brain-derived neurotrophic factor produces antidepressant effects in behavioral models of depression," *Journal of Neuroscience*, vol. 22, no. 8, pp. 3251–3261, 2002.

[38] R. J. Katz, "Animal model of depression: pharmacological sensitivity of a hedonic deficit," *Pharmacology Biochemistry and Behavior*, vol. 16, no. 6, pp. 965–968, 1982.

[39] P. Willner, "Chronic mild stress (CMS) revisited: consistency and behavioural- neurobiological concordance in the effects of CMS," *Neuropsychobiology*, vol. 52, no. 2, pp. 90–110, 2005.

[40] P. Willner, "Validity, reliability and utility of the chronic mild stress model of depression: a 10-year review and evaluation," *Psychopharmacology*, vol. 134, no. 4, pp. 319–329, 1997.

[41] X. Y. Lu, C. S. Kim, A. Frazer, and W. Zhang, "Leptin: a potential novel antidepressant," *Proceedings of the National Academy of Sciences of the United States of America*, vol. 103, no. 5, pp. 1593–1598, 2006.

[42] H. Xu, H. Qing, W. Lu et al., "Quetiapine attenuates the immobilization stress-induced decrease of brain-derived neurotrophic factor expression in rat hippocampus," *Neuroscience Letters*, vol. 321, no. 1-2, pp. 65–68, 2002.

[43] S. C. Dulawa, K. A. Holick, B. Gundersen, and R. Hen, "Effects of chronic fluoxetine in animal models of anxiety and depression," *Neuropsychopharmacology*, vol. 29, no. 7, pp. 1321–1330, 2004.

[44] C. López-Rubalcava and I. Lucki, "Strain differences in the behavioral effects of antidepressant drugs in the rat forced swimming test," *Neuropsychopharmacology*, vol. 22, no. 2, pp. 191–199, 2000.

[45] C. Sánchez and E. Meier, "Behavioral profiles of SSRIs in animal models of depression, anxiety and aggression. Are they all alike?" *Psychopharmacology*, vol. 129, no. 3, pp. 197–205, 1997.

[46] G. Wegener, Z. Bandpey, I. L. Heiberg, A. Mørk, and R. Rosenberg, "Increased extracellular serotonin level in rat hippocampus induced by chronic citalopram is augmented by subchronic lithium: neurochemical and behavioural studies in the rat," *Psychopharmacology*, vol. 166, no. 2, pp. 188–194, 2003.

[47] M. Tõnissaar, T. Mällo, M. Eller, R. Häidkind, K. Kõiv, and J. Harro, "Rat behavior after chronic variable stress and partial lesioning of 5-HT-ergic neurotransmission: effects of citalopram," *Progress in Neuro-Psychopharmacology and Biological Psychiatry*, vol. 32, no. 1, pp. 164–177, 2008.

[48] M. Kuźmider, J. Solich, P. Pałach, and M. Dziedzicka-Wasylewska, "Effect of citalopram in the modified forced swim test in rats," *Pharmacological Reports*, vol. 59, no. 6, pp. 785–788, 2007.

[49] E. Takahashi, M. Katayama, K. Niimi, and C. Itakura, "Additive subthreshold dose effects of cannabinoid CB1 receptor antagonist and selective serotonin reuptake inhibitor in antidepressant behavioral tests," *European Journal of Pharmacology*, vol. 589, no. 1–3, pp. 149–156, 2008.

[50] Y. C. Chen, Q. R. Tan, W. Dang et al., "The effect of citalopram on chronic stress-induced depressive-like behavior in rats through GSK3beta/beta-catenin activation in the medial

prefrontal cortex," *Brain Research Bulletin*, vol. 88, no. 4, pp. 338–344, 2012.

[51] C. P. France, J. X. Li, W. A. Owens, W. Koek, G. M. Toney, and L. C. Daws, "Reduced effectiveness of escitalopram in the forced swimming test is associated with increased serotonin clearance rate in food-restricted rats," *International Journal of Neuropsychopharmacology*, vol. 12, no. 6, pp. 731–736, 2009.

[52] R. Rygula, N. Abumaria, G. Flügge et al., "Citalopram counteracts depressive-like symptoms evoked by chronic social stress in rats," *Behavioural Pharmacology*, vol. 17, no. 1, pp. 19–29, 2006.

[53] S. H. Wang, Z. J. Zhang, Y. J. Guo, H. Zhou, G. J. Teng, and B. A. Chen, "Anhedonia and activity deficits in rats: impact of post-stroke depression," *Journal of Psychopharmacology*, vol. 23, no. 3, pp. 295–304, 2009.

[54] J. Yu, Q. Liu, Y. Q. Wang et al., "Electroacupuncture combined with clomipramine enhances antidepressant effect in rodents," *Neuroscience Letters*, vol. 421, no. 1, pp. 5–9, 2007.

[55] J. H. Liu, Z. F. Wu, J. Sun, L. Jiang, S. Jiang, and W. B. Fu, "Role of AC-cAMP-PKA cascade in antidepressant action of electroacupuncture treatment in rats," *Evidence-Based Complementary and Alternative Medicine*, vol. 2012, Article ID 932414, 7 pages, 2012.

[56] J. Yu, X. Y. Li, X. D. Cao, and G. C. Wu, "Sucrose preference is restored by electro-acupuncture combined with chlorimipramine in the depression-model rats," *Acupuncture and Electro-Therapeutics Research*, vol. 31, no. 3-4, pp. 223–232, 2006.

[57] X. B. Liang, Y. Luo, X. Y. Liu et al., "Electro-acupuncture improves behavior and upregulates GDNF mRNA in MFB transected rats," *NeuroReport*, vol. 14, no. 8, pp. 1177–1181, 2003.

[58] J. Röschke, C. Wolf, M. J. Müller et al., "The benefit from whole body acupuncture in major depression," *Journal of Affective Disorders*, vol. 57, no. 1–3, pp. 73–81, 2000.

[59] E. Castrén and T. Rantamäki, "The role of BDNF and its receptors in depression and antidepressant drug action: reactivation of developmental plasticity," *Developmental Neurobiology*, vol. 70, no. 5, pp. 289–297, 2010.

[60] J. H. Krystal, D. F. Tolin, G. Sanacora et al., "Neuroplasticity as a target for the pharmacotherapy of anxiety disorders, mood disorders, and schizophrenia," *Drug Discovery Today*, vol. 14, no. 13-14, pp. 690–697, 2009.

[61] T. Saarelainen, P. Hendolin, G. Lucas et al., "Activation of the TrkB neurotrophin receptor is induced by antidepressant drugs and is required for antidepressant-induced behavioral effects," *Journal of Neuroscience*, vol. 23, no. 1, pp. 349–357, 2003.

Hindawi Publishing Corporation
Evidence-Based Complementary and Alternative Medicine
Volume 2013, Article ID 160357, 11 pages
http://dx.doi.org/10.1155/2013/160357

Research Article

Modulation of Brain Electroencephalography Oscillations by Electroacupuncture in a Rat Model of Postincisional Pain

Jing Wang,[1] Jing Wang,[2] Xuezhu Li,[1] Duan Li,[3] Xiao-Li Li,[2] Ji-Sheng Han,[1,4] and You Wan[1,4]

[1] *Neuroscience Research Institute, Peking University, Beijing 100191, China*
[2] *State Key Lab of Cognitive Neuroscience and Learning, Beijing Normal University, Beijing 100875, China*
[3] *Institute of Electrical Engineering, Yanshan University, Qinhuangdao 066004, China*
[4] *Key Laboratory for Neuroscience, Ministry of Education/Ministry of Health, Beijing 100191, China*

Correspondence should be addressed to You Wan; ywan@hsc.pku.edu.cn

Received 21 January 2013; Revised 1 March 2013; Accepted 21 March 2013

Academic Editor: Lijun Bai

The present study aimed to investigate how ongoing brain rhythmical oscillations changed during the postoperative pain and whether electroacupuncture (EA) regulated these brain oscillations when it relieved pain. We established a postincisional pain model of rats with plantar incision to mimic the clinical pathological pain state, tested the analgesic effects of EA, and recorded electroencephalography (EEG) activities before and after the EA application. By analysis of power spectrum and bicoherence of EEG, we found that in rats with postincisional pain, ongoing activities at the delta-frequency band decreased, while activities at theta-, alpha-, and beta-frequency bands increased. EA treatment on these postincisional pain rats decreased the power at high-frequency bands especially at the beta-frequency band and reversed the enhancement of the cross-frequency coupling strength between the beta band and low-frequency bands. After searching for the PubMed, our study is the first time to describe that brain oscillations are correlated with the processing of spontaneous pain information in postincisional pain model of rats, and EA could regulate these brain rhythmical frequency oscillations, including the power and cross-frequency couplings.

1. Introduction

Brain rhythmical oscillations in the low (delta, theta, and alpha) and high (beta and gamma) frequencies of electroencephalography (EEG) have been demonstrated to be linked to broad varieties of perceptual, sensorimotor, and cognitive operations [1]. Interaction of oscillations at different frequencies, for example, cross-frequency phase synchronization between alpha, beta, and gamma oscillations, could be observed during working memory, perception, and consciousness [2].

Pain, as a perception, is subserved by an extended network of brain areas [3], or different brain networks are involved in the perception of pain [4]. Previous studies on acute pain disclosed that painful stimulation altered the activities of different frequency oscillations [5, 6], including their power and phase couplings.

It is also noticed that most EEG neurophysiological studies on acute pain were based on phasic pain models with experimental pain induced by short-lasting, noninvasive painful stimuli (e.g., laser noxious heat stimulation). When we consider clinical situations, it is obvious that tonic pathological pain models could better mimic clinical pain than phasic pain models [7].

Postoperative incisional pain is common in clinic. In the rat model of incisional pain, persistent pain existed for several days after the hind paw incision with peripheral and central sensitization [8, 9]. On human subjects after the incision, an imaging study observed increased brain activities in the anterior cingulate cortex (ACC), the insular cortex, the thalamus, the frontal cortex, and the somatosensory cortex [10], and it would be useful to know how the brain EEG oscillation changes in tonic pathological pain states like postoperative pain (postincisional pain in the rat model).

Acupuncture has been widely used in clinical settings. Acupuncture or electroacupuncture (EA) has therapeutic effects in various painful conditions, and these effects could last for a long period of time even hours after acupuncture application being terminated [11–13]. Neuroimaging studies revealed that acupuncture or EA application elicited widespread changes in cerebrocerebellar brain regions [14, 15], largely overlapped with the neural networks for both pain transmission and perception. Acupuncture could directly affect EEG activities on healthy volunteers as well as on animals [16, 17]. Experimental and clinical evidence indicated that pain could affect cognitive processes [18], default-mode network dynamics [19] and even decreased the grey matter volume of brain regions [20]. To examine the neural consequences of acupuncture or EA treatment on pain, it would be useful to determine how acupuncture or EA treatment modulates cortical activities under tonic pathological pain conditions.

We established a rat model of plantar incision to mimic the clinic pain and observed the analgesic effects of EA on this model. On this basis, with EEG study, we further investigated changes of spontaneous brain oscillations in the incisional pain and the EA modulation on EEG oscillations.

2. Materials and Methods

All experimental procedures were in accordance with the guideline of the International Association for the Study of Pain [21] and were approved by the Animal Care and Use Committee of our university. The behavioral experimenters were kept blind.

2.1. Animals and Housing. Adult Sprague-Dawley male rats were provided by the Department of Experimental Animal Sciences of our university (30 rats for the behavior test, weighing 180–230 g; and 16 rats for EEG recordings, weighing 300–350 g at the beginning of the experiment). They were housed individually in cage with free access to food and water. The temperature was maintained at about 22°C under natural light/dark cycles. Rats were habituated to the environment and handled daily for one week before the experiment.

2.2. The Plantar Incisional Pain Model of Rats. The rat model of incisional pain employed a 1 cm longitudinal incision with muscle involvement [22]. Briefly, the animal was placed in a sealed glass container with 5% isoflurane mixed with air to induce anesthesia and delivered 1.5–2% isoflurane via a nose cone to maintain the anesthesia during the following surgical operation. The left hind paw of the rat was sterilized with 10% povidone-iodine, and a sterile no. 11 scalpel blade was used to make a 1 cm long incision through the skin and fascia of the plantar hind paw including the underlying muscles, beginning 0.5 cm from the heel. The wound was closed with two mattress sutures of 5–0 nylon, covering with the antibiotic ointment.

2.3. EA Application. Before the incisional surgery, the rat was loosely immobilized by the bandage on a metal mesh floor with the head, hind legs, and the tail protruding and habituated for 3-4 days, at least 20 min a day, in order to minimize the discomfort and the tension during the EA operation and application.

Two hours after the plantar incision, rats were divided into three groups: the restriction (incision) group, which received plantar incision in the left hind paw and was loosely immobilized by the bandage; the sham EA group, which received needling at "acupoints" without electrical stimulation after the incision; and the EA group, which received EA application bilaterally after the incision. EA was applied according to the routine procedure as in our previous reports [23–26]. Stainless-steel needles (0.4 mm in diameter, 4 mm in length) were inserted into the "acupoints" on each hind leg. Two commonly used acupoints, "Zusanli" (ST36, 4 mm lateral to the anterior tubercle of the tibia, which is marked by a notch) and "Sanyinjiao" (SP6, 3 mm proximal to the medial malleolus, at the posterior border of the tibia), were stimulated with square waves of 0.2 ms in pulse width and 2 Hz in frequency from a Han's Acupoint Nerve Stimulator (HANS, LH series, manufactured in our university). The EA intensities were increased in a stepwise manner at 1-2-3 mA, with each intensity lasting for 10 min.

2.4. Assessment of Mechanical Allodynia. Mechanical allodynia was assessed by measuring the 50% paw withdrawal threshold (PWT) as described in our previous reports [26, 27]. The 50% PWT in response to a series of *von* Frey filaments (Semmes-Weinstein Monofilaments, North Coast Medial Inc., San Jose, CA, USA) was determined by the up-down method [28]. The rat was restricted on a metal mesh floor covered with an inverted clear plastic cage (18 × 8 × 8 cm) and allowed a 15–20 min period for habituation. Eight *von* Frey filaments with approximately equal logarithmic incremental (0.224) bending forces were chosen (0.41, 0.70, 1.20, 2.00, 3.63, 5.50, 8.50, and 15.10 g). Each trial started with a *von* Frey force of 2.00 g delivered perpendicularly to the plantar surface of the left hind paw adjacent to the wound near the medial heel. An abrupt withdrawal of the foot during the stimulation or immediately after the removal of the filament was recorded as a positive response. Once a positive or a negative response was evoked, the next weaker or stronger filament was applied, respectively. This procedure was terminated until 6 stimuli after the first change in response occurred. The 50% PWT was calculated using the following formula:

$$50\%\ \mathrm{PWT} = \frac{10^{(X_f + k\delta)}}{10^4}, \tag{1}$$

where X_f is the value of the last *von* Frey filament used (in log unit), k is a value measured from the pattern of positive/negative responses, and $\delta = 0.224$ which is the average interval (in log unit) between the *von* Frey filaments [29]. The mechanical allodynia of the left hind paw was tested at 6 time points, that is, before the incision, after the incision but before the EA application, 10, 20, and 30 min during the EA application, and 30 min after the EA application. The data were analyzed with one-way ANOVA followed by Tukey post

hoc test, and $P < 0.05$ was chosen as statistically significant level.

2.5. Electrode Implantation for EEG Recording. Sixteen male rats were anesthetized with sodium pentobarbital (50 mg/kg, *i.p.*). After removing the scalp of the rat and exposing the skull, 14 stainless steel screws (tip diameter 1 mm, impedance 300–350 Ω) with sockets were implanted bilaterally as epidural electrodes into the skull to record the cortical EEGs. The locations of these electrodes were determined by the method from Shaw et al. [30]: anterior frontal (FL1, FR1), anterior (A) +4.5 mm, lateral (L) ±1.5 mm; centrofrontal (FL2, FR2, PR1, PL1), A ±1.5 mm, L ±4.5 mm; lateral frontal (PL2, PR2), A 0.0 mm, L ±4.5 mm; frontooccipital (LFL, RFR, LPL, RPR), A −4.5 mm, L ±1.5 mm for LFL, RFR, and A −3.0 mm, L ±4.5 mm for LPL, RPR. The reference and the ground electrodes were positioned 2 mm and 4 mm caudal to the lambda, respectively (Figure S1 of the Supplementary Material available at http://dx.doi.org/10.1155/2013/160357). The electrodes were fixed to the skull with dental cement and had no any connections with muscles. Penicillin (6×10^4 U, i.m.) was administrated for 3 consecutive days to prevent possible infection.

2.6. EEG Signals Collection and Analysis. After one week recovery from the surgery, rats were habituated to the restriction for 3-4 days as the above mentioned, then the EEG rats were randomly divided into EA group or control group (restriction only) ($n = 8$ for each group). Rats were loosely immobilized on a metal mesh floor for the convenience of EA application during EEG recordings. EEG signals were collected in awake rats during three sessions, that is, before the plantar incision, 1.5–2 h after the plantar incision, and after the EA application. Each session lasted for 25–30 min.

The ASA-Lab EEG/ERP recording system (ANT Inc., The Netherlands) was used. Data were analyzed offline with Matlab (The Mathworks, Natick, MA, USA) EEGLAB software. The movement artifact or the baseline drift was removed from all channels, and the channels with impedance values above 25 k Ohms were also discarded. The EEG signals were digitized at a sampling rate of 256 Hz, rereferenced to an average of residual channels, and filtered through a 1–45 Hz band pass to avoid the interference of 50 Hz signals.

The wavelet power spectrum was used to obtain the power of the on going EEG activities [31]. The Morlet wavelet transform was employed with the wavelet central angle frequency of 6 ($\omega = 6$). Five spectral bands were examined: 1–4, 4–8, 8–13, 13–30, 30–45 Hz, corresponding to delta, theta, alpha, beta, and gamma bands, respectively [32, 33], with a step of 0.5 Hz.

The bispectral analysis, including the amplitude and the phase information, is used to quantify the degree of quadratic phase coupling (QPC) among different frequency components of a signal [34]. Bicoherence method is the normalized form of the bispectral analysis; it is independent of the amplitude of the signal, therefore; it can be used as an indicator of phase coupling in nonlinear signals. In this study, general harmonic wavelet bicoherence was employed to measure the comodulation of oscillations between two frequency bands [35]. Signals were divided into a series of 2-second epochs, with an overlap of 75%. For each epoch, bicoherence values were computed in all pairs of frequencies from 1 to 45 Hz, with a step of 1 Hz and a bandwidth of 2 Hz. The same epoch as the power analysis in the above was used to calculate the filtered wavelet bicoherence value (FIWBIC).

2.7. Statistical Analysis of EEG Data. For power spectral data, a paired t-test was used to analyze at which frequency ranges the change of the EEG power was significant. In the EA and the restriction groups, the change of power was expressed as the percentage relative to the power value during the session before the incision, which was defined as (After − Before)/Before × 100%, and paired t-tests were used in the interior-group. Unpaired t-tests were further used between the two groups.

For the wavelet bicoherence data, the statistical analysis was focused on their characteristics to determine if a significant difference existed between different recording sessions; so prior to the comparison, the total bicoherence value at the frequency bands ($f_j^L \le f_j \le f_j^U$ and $f_k^L \le f_j \le f_k^U$) was extracted, which was defined as

$$b = \sum \sum b_{xxx}^2 \left(f_j, f_k\right), \tag{2}$$

where b_{xxx} is the bicoherence value (FIWBIC). This value is a measure of the degree of QPC between frequency bands and can be used to measure the phase coupling strength between different waves [35]. Then, a Wilcoxon rank-sum test was conducted to determine significant difference, with P value less than 0.05 as a statistically significant standard.

3. Results

3.1. EA Treatment Attenuates Mechanical Allodynia in the Incisional Pain Model of Rats. We established the plantar incisional pain model of rats and applied 2 Hz EA to "Zusanli" and "Sanyinjiao" acupoints in bilateral sides of the hind paw. A 50% of PWT to calibrated *von* Frey filaments was measured over time. Mechanical allodynia was attenuated significantly during EA application, and this antinociceptive effect could last for at least 30 min after EA application compared to that in the sham EA group or in the restriction group (Figure 1).

3.2. Changes of EEG Oscillations in the Incisional Pain Model of Rats. To examine the ongoing brain activities induced by the plantar incision, we calculated the power of different oscillations for each recording session (Figure 2). Compared with the session before the incision, the relative spontaneous EEG power of delta-frequency oscillation decreased, while the power in theta, alpha, and beta bands increased in rats after plantar incision. In addition, no significant change in gamma power was observed.

Furthermore, we compared the power of each channel at different frequency bands between different sessions. The corresponding topographies were shown in Figure 3(a). The locations where power changed significantly at different frequency bands during the sessions after the plantar incision

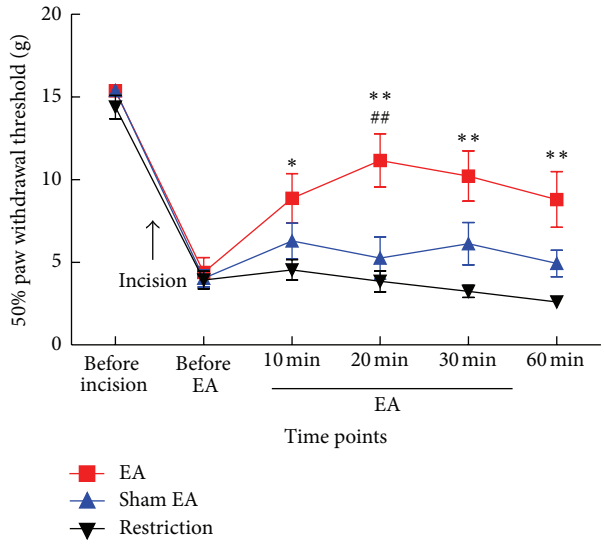

Figure 1: The effect of EA treatment on mechanical allodynia in the postincisional pain model of rats. Mechanical allodynia of the left hind paw was tested before incision, before EA treatment, 10, 20, and 30 min during EA, and 30 min after EA application. A 50% of paw withdrawal threshold (PWT) significantly increased after EA. $^{*}P < 0.05$, $^{**}P < 0.01$ compared with the restriction group; $^{\#\#}P < 0.01$ compared with the sham-treatment group. Data were presented as means ± SEM, $n = 9$-10.

and after EA application were summarized in Figure 3(b), respectively. We found that the changes mainly located at bilateral fronto-parietal lobes in low and medium frequency bands after the plantar incision.

Synchronization of networks is often reflected by cross-frequency interaction, and the power spectrum could not reflect the phase information. In order to measure the degree of phase couplings at different frequency bands, we computed the filtered wavelet bicoherence (FIWBIC) values with general harmonic wavelet bicoherence [35]. As shown in Figure 4, the FIWBIC values were divided into bands from delta to gamma. A statistical analysis of estimated average of synchronization of FIWBIC values at different bifrequency bands was conducted on the 16 samples from sessions before the incision and compared to that from sessions after the incision. The Wilcoxon rank-sum test at $P < 0.05$ was performed. The boxplots showed that the mean of the synchronization values among the beta, the alpha, and the theta increased, that is, the cross-frequency coupling strength between delta and alpha, and between theta and theta/alpha/beta, between alpha and alpha/beta during the session after the incision was significantly strengthened. Meanwhile, the coupling in the delta band before the incision was higher compared to that after the incision.

3.3. EA Treatment-Induced EEG Power Changes in the Incisional Pain Model of Rats. In view of behavior results described above, both the sham EA treatment group and the restriction (without EA) group showed similar pain behaviors, and we chose the restriction group as control. The 16 rats were randomized into two groups: one group received EA application for 30 min from 2 h to 2.5 h after the plantar incision, and the other remained in restriction as control. We compared the power change at different oscillation bands in two groups (Figure 5). Figures 5(a) and 5(b) showed the change rate of averaged absolute power after EA treatment or restriction, separately. Figures 5(c) and 5(d) presented the change rate of relative power during the sessions before and after the EA application relative to the session before the incision in two groups, respectively. Only after EA treatment, the negative change rate relative to the baseline (before the incision) showed significant reduction in high-frequency bands, especially in the beta band. A tendency of reduction was also found in the gamma band. Additionally, the change of power values during the two sessions before EA or restriction was not different between two groups (Figure S2).

Furthermore, after EA application, the change at the beta band mainly located over the electrodes of FR1, FR2, PR2, PL2, RFR, and LFL (Figure 6(b)), corresponding to the right fronto-parietal lobe, the left posterior parietal lobe, and the bilateral temporal lobes; meanwhile, the change at the gamma band located in the bilateral frontal lobes and the left posterior parietal lobe according to the location of electrodes (Figure 6(b)).

Similarly, we computed FIWBIC values in EA treatment group and the restriction group, respectively. The statistical results of Wilcoxon rank-sum tests at $P < 0.05$ at the different frequency bands in two groups are shown in Figure 7 and Figure S3, respectively. From Figure 7, it is shown that after EA treatment, the strength of bifrequency coupling between beta and delta/theta/alpha attenuated significantly, whereas the coupling of beta-gamma bands became greater. In contrast, no significant difference was found in the strength of phase coupling between bands after restriction compared with that after the incision (Figure S3).

4. Discussion

In the incisional pain model of rats, by analysis of power spectrum and bicoherence of EEG, we found that the ongoing activities at the delta band decreased, while the activities at theta, alpha, and beta bands increased in the plantar-incisional pain rats; EA treatment decreased the power in high-frequency bands, especially at the beta band, and reversed the enhancement of the cross-frequency coupling strength between the beta and low-frequency bands.

4.1. Brain EEG Oscillations in Postincisional Pain. With rat EEG, we observed significant changes of the ongoing power spectra in different frequency oscillations ranging from the delta band to the beta band except the gamma band we also noticed the obvious changes of bi-frequency coherence during the postincisional pain. It is well known that pain perception is a multidimensional experience with sensory-discriminative, affective-emotional, and cognitive-evaluative components [3], and different brain areas are

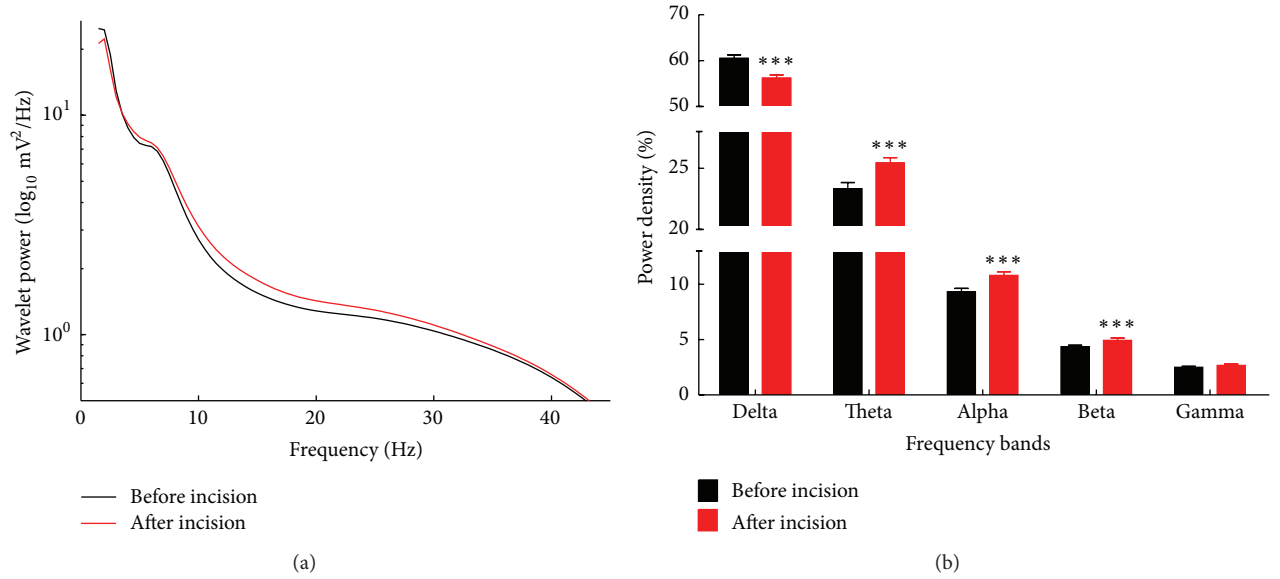

FIGURE 2: Changes of EEG power spectra in the postincisional pain model of rats. (a) The average of absolute EEG power before the incision (black line) and after the incision (red line). The y-axis represented power value, and x-axis represented frequency bands. (b) The relative power (normalized to the overall power) at 5 frequency bands. A significant increase of relative power at theta, alpha, and beta frequencies as well as a decrease at delta frequency was observed after the incision (red columns), compared with the power before the plantar surgery (black columns). $^{**}P < 0.01$, $^{***}P < 0.001$ compared with before incision. All data were expressed as means ± SEM.

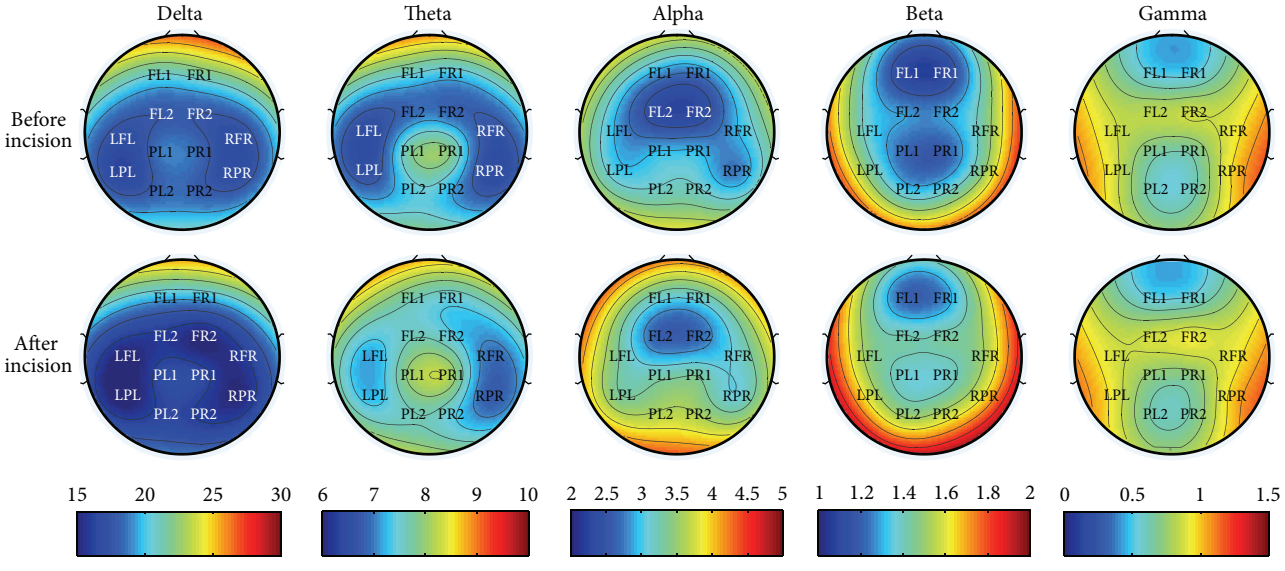

(a)

Delta	Theta	Alpha	Beta	Gamma
FL1 FR1 FR2 PR1 LFL PR2	FL2 FR2	FL1 FR1 PL2 PR1 RFR PR2	FL1 FL2 PL1 PL2 PR1 PR2	

(b)

FIGURE 3: Locations of electrodes with significant EEG power change in the postincisional pain model of rats. (a) Topographic mapping of EEG during two sessions before (upper) and after (lower) the plantar incision. Averaged EEG power densities ranged from delta to gamma bands. Values were color-coded and plotted at the corresponding position on the planar projection of the epidural surface and interpolated between electrodes (dots). (b) Locations of electrodes showing statistically significant difference ($P < 0.05$) of power changes at different bands.

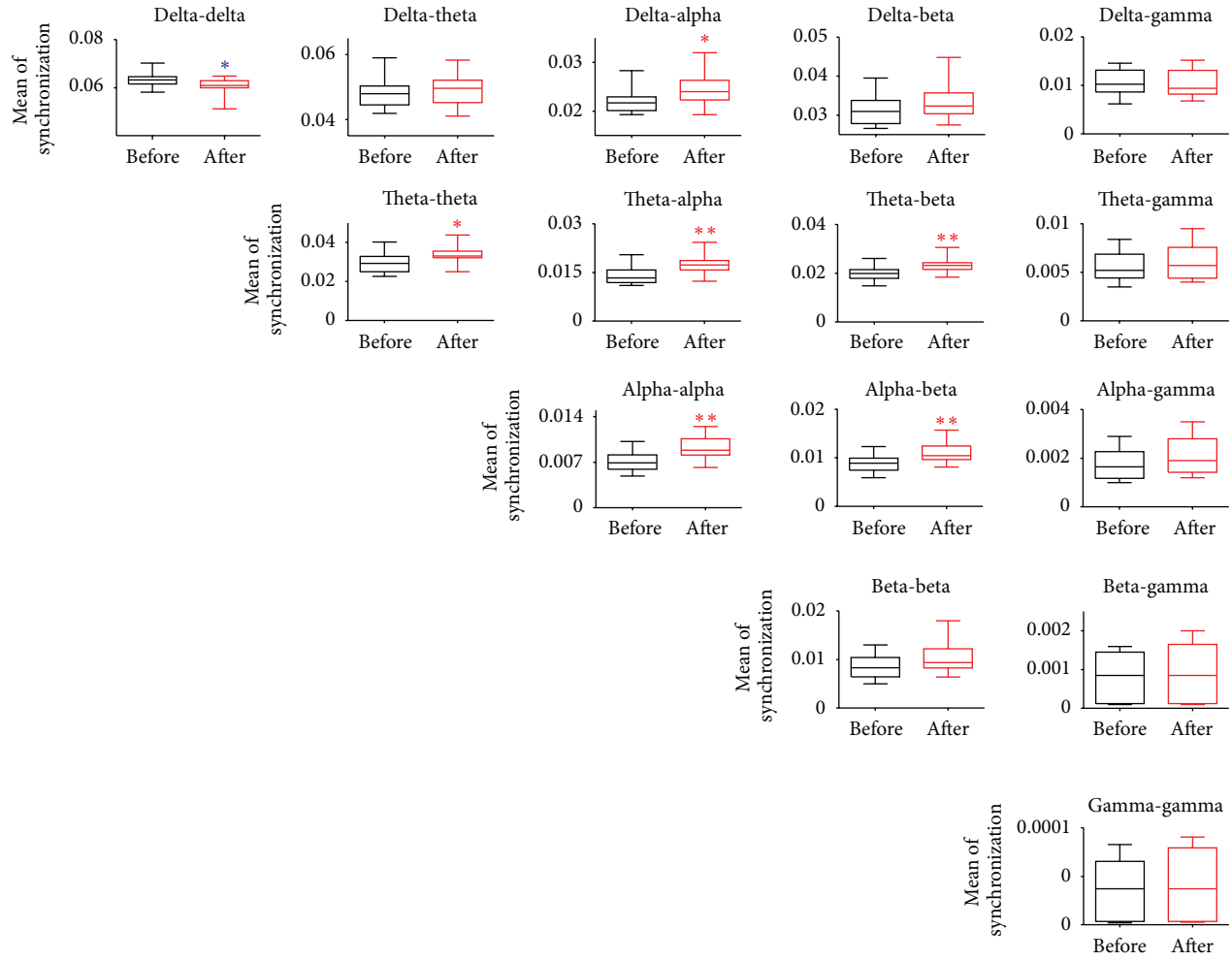

Figure 4: Phase couplings at different frequency bands: statistical analysis of the filtered wavelet bicoherence (FIWBIC) values in the postincisional pain model of rats. Boxplots stand for the phase coupling at local frequency bands, and the y-axis represents the mean of synchronization. The synchronization values increased between delta and alpha, between theta and theta/alpha/beta, between alpha and alpha/beta, whereas the value decreased at delta band after the plantar incision. Wilcoxon rank-sum test was used. $^{*}P < 0.05$, $^{**}P < 0.01$, $^{***}P < 0.001$, $n = 16$.

involved in different dimensions. Moreover, different cognitive systems are related to neuronal networks of different sizes and distribution, networks of different sizes oscillate at different frequencies, and mutual interactions of cross-frequency oscillations could be well positioned to regulate the multinetwork integration [36]. Thus, it might be conceivable that extensive range of neuronal oscillations participated in pathological pain cortical processing; any oscillation itself is not sufficient for integrating all the distributed information required for pain perception.

It has been accepted that delta-band oscillation is associated with compromised neuronal function [37]; theta-band is linked with emotional arousal [38]; beta-band may relate to the maintenance of the current sensorimotor or cognitive state, and its pathological enhancement may result in an abnormal persistence of the status quo and a deterioration of flexible behavior and cognitive control [39]. Thus, in our results, the reduced delta activity, as well as the increased theta and beta activities, might reflect the cortical overactivation induced by different pain dimensions in the resting state. Alpha oscillation is well known to mainly serve as a top-down controlled inhibitory mechanism [38]. One possible explanation for the increased alpha oscillation is that the evaluative component of pain, represented by paw lifting, was weakened by the activation of the descending pain inhibition network. Meanwhile, no significant change in the gamma oscillation was found during the postincisional pain. Owning that the gamma band is well recognized to be linked with feature binding, working memory, attention, or sensory selection [1], whereas our current study focused on the sustained, spontaneous pain in acute stage, it may be speculated that sensory selection or pain memory was not engaged in the pain processing. More importantly, the findings on alterations of phase coupling strength across distinct oscillations might reflect the synchronization of neuronal networks involved in different pain dimensions and

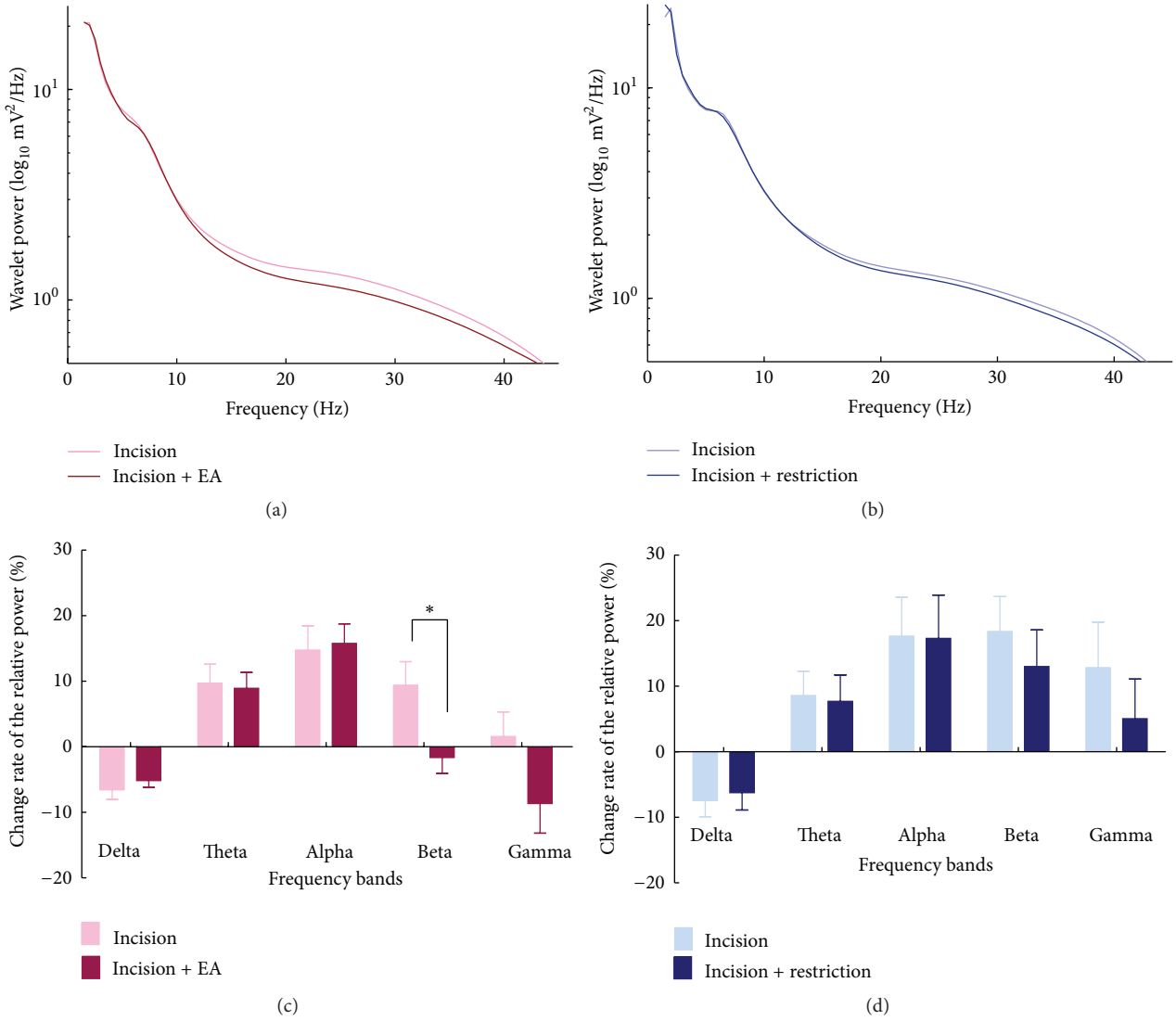

Figure 5: Changes of EEG power spectra after EA treatment in the postincisional pain model of rats. (a) The averaged absolute EEG power after EA treatment (red curve) compared with that before EA treatment (pink curve). The y-axis represented power value, and x-axis represented frequency bands. (b) The averaged absolute EEG power after restriction (dark blue color) compared with that before restriction (light blue curve). The y-axis represents power value, and the x-axis represents the frequency bands. (c) Change of the relative power in the EA group. The relative power value in EA group was normalized as the percentage relative to that before the incision. There was a significant decrease at the beta band after EA (red bar) compared with that after the incision (pink bar). (d) Change of the relative power in the restriction group. No significant changes were observed (light blue bar versus dark blue bar). $^*P < 0.05$ (paired t-test).

the integration of pain inhibition and facilitation networks. It is also in accordance with the idea of neuronal processing with various simultaneous oscillations [36].

Topography findings showed the change of power in different frequency bands mainly located over bilateral frontal and parietal cortices (Figure 3). These are locations of the primary somatosensory cortex and the anterior cingulate cortex in rat. In this study, we selected the recording session from 1.5 to 2 h after the plantar incision. Given anatomical and physiological connections between right and left hemispheres, it was reasonable that the change of power occurred in bilateral cortices via communication and integration of persistent painful information in the whole brain.

4.2. EA Modulation on Incisional Pain-Related Brain Oscillations. In the present study, we investigated the modulation of EA treatment on the incisional pain-related brain oscillations in rats. As a basis, we firstly investigated the analgesic effects of EA treatment in the incisional pain rats. We found that EA treatment on "Zusanli" and "Sanyinjiao" acupoints on bilateral sides in hind paws relieved the mechanical allodynia in rats after the plantar incision. These results, in line with other reports [11–13], suggested that EA was effective in relieving plantar incisional pain and this antinociceptive effect could maintain at least 30 min.

We further explored the neural oscillation mechanism of EA analgesia. From our results, brain oscillations induced

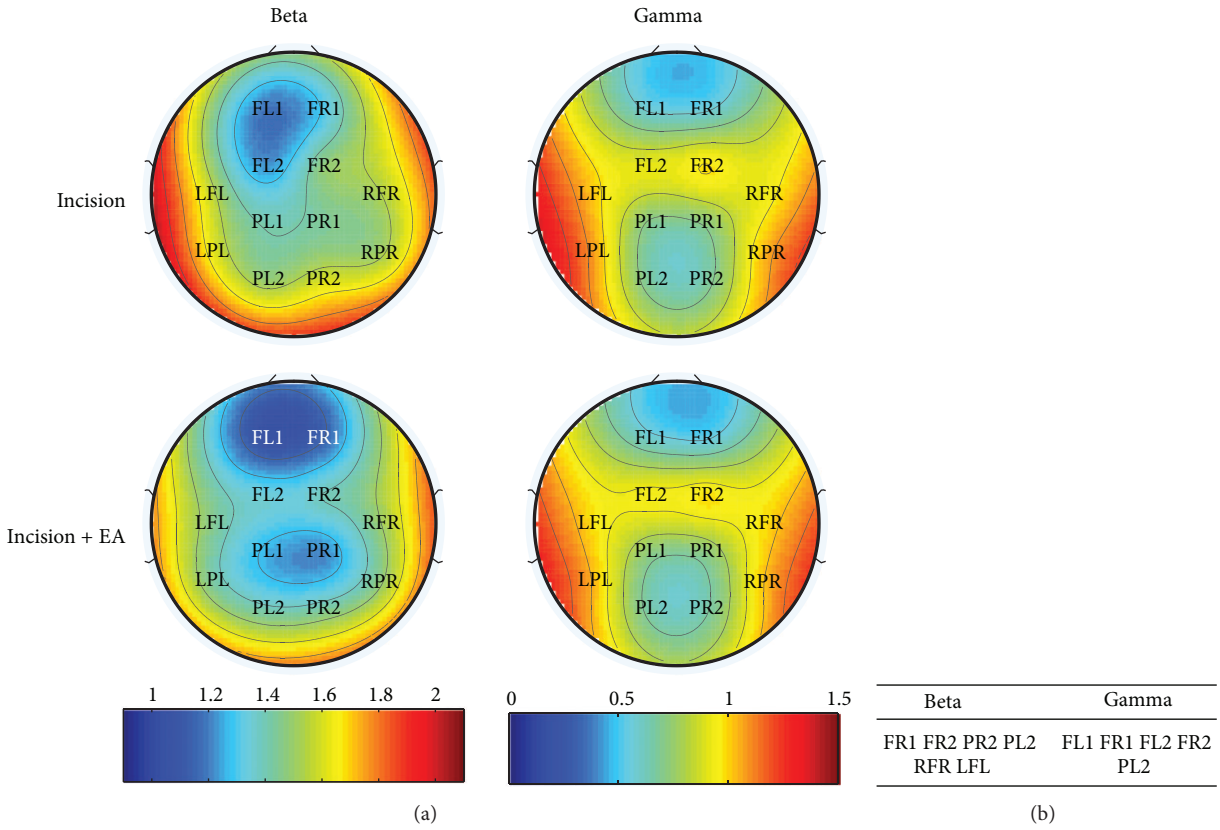

Figure 6: Locations of electrodes with significant EEG power change after EA treatment in incisional pain model of rats. (a) Topographic mapping of EEG power in beta band (left) and gamma band (right) after EA application compared with that before EA application. Averaged EEG power density values were color-coded and plotted at the corresponding position on the planar projection of the epidural surface and interpolated between electrodes (dots). (b) Electrodes with statistically significant difference ($P < 0.05$) of power change in the beta and gamma band.

by EA application and those in nociceptive processing were not identical; the change of power after EA occurred at the beta band. It provides evidence that neuronal networks participated in EA treatment are different from those in pain perception. The networks oscillate at different frequencies, although brain areas activated by both EA treatment and incisional pain itself have large overlap from imaging studies [14, 15, 40], which is also in line with our results of topographic mapping.

As we mentioned before, the enhancement of the beta oscillation might be linked to the deterioration of flexible behavior and cognitive control [39]. Accumulating evidence suggests that EA facilitates the descending pain inhibitory pathway by increasing the release of opioid peptides in the central nervous system. Therefore, in our results, the decrease of activities at the beta band is reasonable, because EA treatment facilitates the descending inhibitory system of pain.

Prior studies indicated that inhibitory GABAergic interneurons network played a key role in the modulation of beta and gamma oscillations. Elevated endogenous GABA levels could cause the elevation of beta power [41, 42]. In the EA antinociceptive effects, GABA agonists showed reverse interaction with opioid receptor agonists [43, 44]. In addition, EA could decrease intracerebral GABA content in the cortex on the lesioned side in the rat model of Parkinson's disease [45]. Taken together, it is conceivable that the decreased power of high-frequency oscillations in our results might reflect the inhibition of GABAergic interneurons induced by EA application in pain situation.

It has been accepted that low-frequency oscillations might be involved in the integration across widely spatially distributed neural assemblies and high-frequency oscillations (beta and gamma bands) distributed over a more limited topographic area. The integration of different local high-frequency oscillations is mediated by the large scale interactions of low-frequency oscillations. By analysis of the cross-frequency couplings, we found that EA treatment reversed the enhancement of the couplings between low-frequency bands and beta band in incisional pain and also strengthened the couplings between beta and gamma band. It may be speculated that EA exerted antinociceptive effect by modulation on power and cross-frequency coupling strength, which disturbed the cortex excitability and the multinetwork integration of nociceptive information in incisional pain.

In conclusion, the present study suggests that broad frequency oscillations ranging from delta-to beta-frequency bands are correlated with the cortical processing of the nociceptive information in the plantar incisional pain rats. EA reverses the increased beta power and the cross-frequency couplings between the beta and low-frequency bands induced

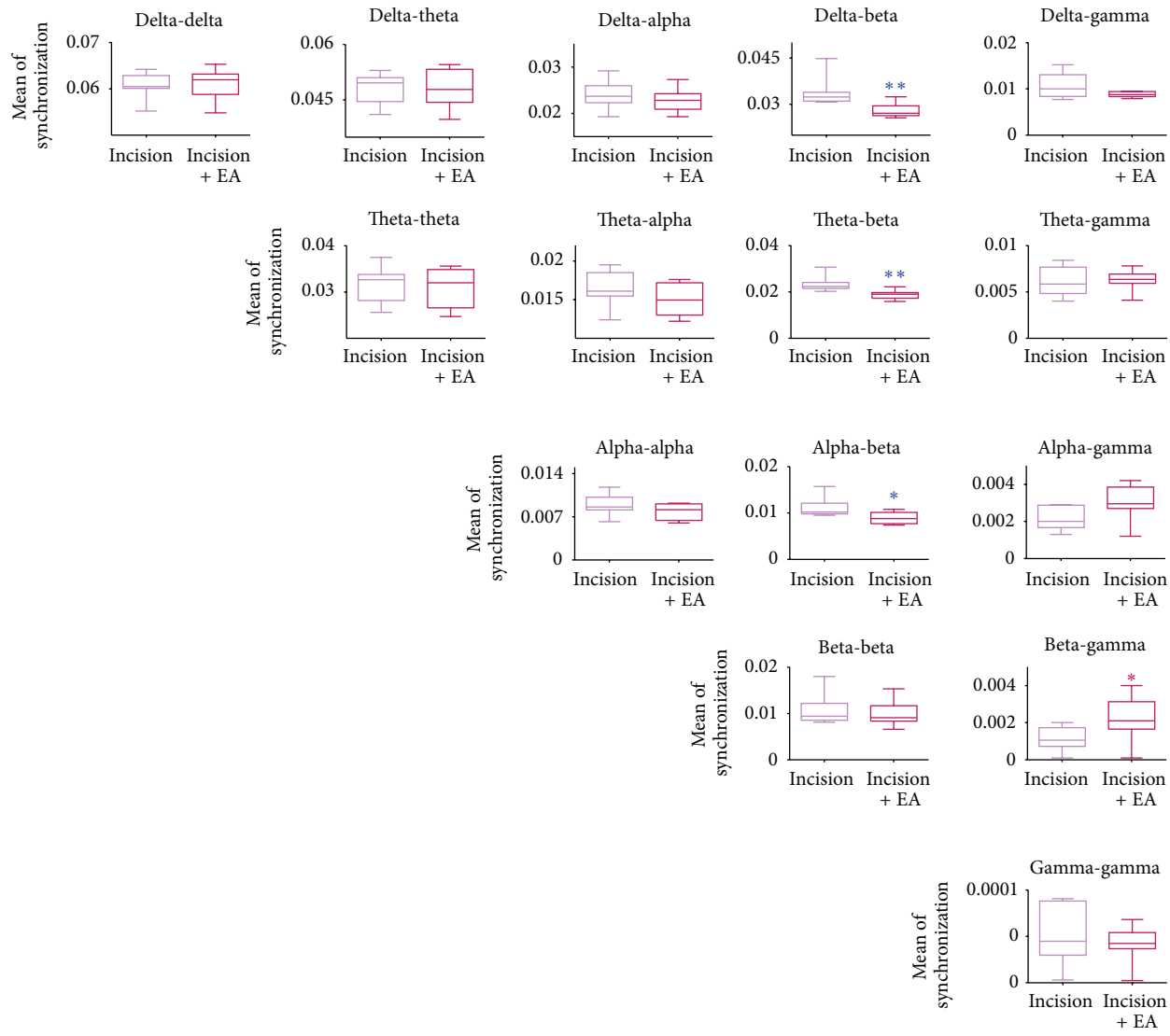

Figure 7: Phase couplings at different frequency bands: statistical analysis of the filtered wavelet bicoherence (FIWBIC) values after EA treatment in the postincisional pain model of rats. Boxplots stand for the phase coupling at local frequency bands, and the y-axis represents the mean of synchronization. After EA application, the synchronization value between beta and delta/theta/alpha decreased, that is, synchronization became weaker; whereas the value between beta and gamma increased, that is, synchronization became stronger. Wilcoxon rank-sum test was used. $^{*}P < 0.05$, $^{**}P < 0.01$, $^{***}P < 0.001$, $n = 8$.

by postincisional pain, suggesting that EA could regulate the neuronal networks involved in the central processing and the integration of spontaneous nociceptive information. These results can deepen our understanding in the central neuromodulatory mechanisms of EA analgesia.

Conflict of Interests

The authors have declared that no conflict of interests exists.

Acknowledgments

This research was supported by Grants from the National Basic Research Program of the Ministry of Science and Technology of China (2013CB531905), Key Project of Ministry of Education of China (109003), and the "111" Project of the Ministry of Education of China (B07001). Authors would like to thank Zifang Zhao for his help in optimization in Matlab computation, Dr. Miguel A. L. Nicolelis, Dr. Miguel Santos Pairs Vieira, Dr. Eric Thomson, and Gary Lehew in Duke University, USA, for their discussion and kind help in editing.

References

[1] C. E. Schroeder and P. Lakatos, "Low-frequency neuronal oscillations as instruments of sensory selection," *Trends in Neurosciences*, vol. 32, no. 1, pp. 9–18, 2009.

[2] S. Palva and J. M. Palva, "New vistas for α-frequency band oscillations," *Trends in Neurosciences*, vol. 30, no. 4, pp. 150–158, 2007.

[3] X. Moisset and D. Bouhassira, "Brain imaging of neuropathic pain," *NeuroImage*, vol. 37, supplement 1, pp. S80–S88, 2007.

[4] A. V. Apkarian, M. C. Bushnell, R. D. Treede, and J. K. Zubieta, "Human brain mechanisms of pain perception and regulation in health and disease," *European Journal of Pain*, vol. 9, no. 4, pp. 463–484, 2005.

[5] C. Babiloni, F. Babiloni, F. Carducci et al., "Human brain oscillatory activity phase-locked to painful electrical stimulations: a multi-channel EEG study," *Human Brain Mapping*, vol. 15, no. 2, pp. 112–123, 2002.

[6] J. Wang, D. Li, X. Li et al., "Phase-amplitude coupling between theta and gamma oscillations during nociception in rat electroencephalography," *Neuroscience Letters*, vol. 499, no. 2, pp. 84–87, 2011.

[7] A. Mouraux and G. D. Iannetti, "Nociceptive laser-evoked brain potentials do not reflect nociceptive-specific neural activity," *Journal of Neurophysiology*, vol. 101, no. 6, pp. 3258–3269, 2009.

[8] M. M. Hämäläinen, G. F. Gebhart, and T. J. Brennan, "Acute effect of an incision on mechanosensitive afferents in the plantar rat hindpaw," *Journal of Neurophysiology*, vol. 87, no. 2, pp. 712–720, 2002.

[9] C. F. Villarreal, V. A. V. Kina, and W. A. Prado, "Participation of brainstem nuclei in the pronociceptive effect of lesion or neural block of the anterior pretectal nucleus in a rat model of incisional pain," *Neuropharmacology*, vol. 47, no. 1, pp. 117–127, 2004.

[10] E. M. Pogatzki-Zahn, C. Wagner, A. Meinhardt-Renner et al., "Coding of incisional pain in the brain: a functional magnetic resonance imaging study in human volunteers," *Anesthesiology*, vol. 112, no. 2, pp. 406–417, 2010.

[11] S. J. Wang, H. Y. Yang, and G. S. Xu, "Acupuncture alleviates colorectal hypersensitivity and correlates with the regulatory mechanism of TrpV1 and p-ERK," *Evidence-Based Complementary and Alternative Medicine*, vol. 2012, Article ID 483123, 10 pages, 2012.

[12] K. H. Chang, R. Won, I. Shim, H. Lee, and B. H. Lee, "Effects of electroacupuncture at BL60 on formalin-induced pain in rats," *Evidence-Based Complementary and Alternative Medicine*, vol. 2012, Article ID 324039, 7 pages, 2012.

[13] A. Li, Y. Zhang, L. Lao et al., "Serotonin receptor 2A/C is involved in electroacupuncture inhibition of pain in an osteoarthritis rat model," *Evidence-based Complementary and Alternative Medicine*, vol. 2011, Article ID 619650, 6 pages, 2011.

[14] G. T. Lewith, P. J. White, and J. Pariente, "Investigating acupuncture using brain imaging techniques: the current state of play," *Evidence-Based Complementary and Alternative Medicine*, vol. 2, no. 3, pp. 315–319, 2005.

[15] J. Fang, X. Wang, H. Liu et al., "The limbic-prefrontal network modulated by electroacupuncture at CV4 and CV12," *Evidence-Based Complementary and Alternative Medicine*, vol. 2012, Article ID 515893, 11 pages, 2012.

[16] S. F. Hsu, C. Y. Chen, M. D. Ke, C. H. Huang, Y. T. Sun, and J. G. Lin, "Variations of brain activities of acupuncture to TE5 of left hand in normal subjects," *American Journal of Chinese Medicine*, vol. 39, no. 4, pp. 673–686, 2011.

[17] G. Litscher, "Ten years evidence-based high-tech acupuncture part 3: a short review of animal experiments," *Evidence-Based Complementary and Alternative Medicine*, vol. 7, no. 2, pp. 151–155, 2010.

[18] D. A. Seminowicz and K. D. Davis, "Pain enhances functional connectivity of a brain network evoked by performance of a cognitive task," *Journal of Neurophysiology*, vol. 97, no. 5, pp. 3651–3659, 2007.

[19] M. N. Baliki, P. Y. Geha, A. V. Apkarian, and D. R. Chialvo, "Beyond feeling: chronic pain hurts the brain, disrupting the default-mode network dynamics," *Journal of Neuroscience*, vol. 28, no. 6, pp. 1398–1403, 2008.

[20] R. Ruscheweyh, M. Deppe, H. Lohmann et al., "Pain is associated with regional grey matter reduction in the general population," *Pain*, vol. 152, no. 4, pp. 904–911, 2011.

[21] M. Zimmermann, "Ethical guidelines for investigations of experimental pain in conscious animals," *Pain*, vol. 16, no. 2, pp. 109–110, 1983.

[22] T. J. Brennan, E. P. Vandermeulen, and G. F. Gebhart, "Characterization of a rat model of incisional pain," *Pain*, vol. 64, no. 3, pp. 493–501, 1996.

[23] Y. Wan, S. G. Wilson, J. S. Han, and J. S. Mogil, "The effect of genotype on sensitivity to electroacupuncture analgesia," *Pain*, vol. 91, no. 1-2, pp. 5–13, 2001.

[24] C. Huang, Z. Q. Huang, Z. P. Hu et al., "Electroacupuncture effects in a rat model of complete Freund's adjuvant-induced inflammatory pain: antinociceptive effects enhanced and tolerance development accelerated," *Neurochemical Research*, vol. 33, no. 10, pp. 2107–2111, 2008.

[25] C. Huang, H. Long, Y. S. Shi, J. S. Han, and Y. Wan, "Ketamine enhances the efficacy to and delays the development of tolerance to electroacupuncture-induced antinociception in rats," *Neuroscience Letters*, vol. 375, no. 2, pp. 138–142, 2005.

[26] G. G. Xing, F. Y. Liu, X. X. Qu, J. S. Han, and Y. Wan, "Long-term synaptic plasticity in the spinal dorsal horn and its modulation by electroacupuncture in rats with neuropathic pain," *Experimental Neurology*, vol. 208, no. 2, pp. 323–332, 2007.

[27] F. Y. Liu, Y. N. Sun, F. T. Wang et al., "Activation of satellite glial cells in lumbar dorsal root ganglia contributes to neuropathic pain after spinal nerve ligation," *Brain Research*, vol. 1427, pp. 65–77, 2012.

[28] S. R. Chaplan, F. W. Bach, J. W. Pogrel, J. M. Chung, and T. L. Yaksh, "Quantitative assessment of tactile allodynia in the rat paw," *Journal of Neuroscience Methods*, vol. 53, no. 1, pp. 55–63, 1994.

[29] W. J. Dixon, "Efficient analysis of experimental observations," *Annual Review of Pharmacology and Toxicology*, vol. 20, pp. 441–462, 1980.

[30] F. Z. Shaw, R. F. Chen, H. W. Tsao, and C. T. Yen, "A multichannel system for recording and analysis of cortical field potentials in freely moving rats," *Journal of Neuroscience Methods*, vol. 88, no. 1, pp. 33–43, 1999.

[31] X. Li, X. Yao, J. Fox, and J. G. Jefferys, "Interaction dynamics of neuronal oscillations analysed using wavelet transforms," *Journal of Neuroscience Methods*, vol. 160, no. 1, pp. 178–185, 2007.

[32] D. Mantini, M. G. Perrucci, C. Del Gratta, G. L. Romani, and M. Corbetta, "Electrophysiological signatures of resting state networks in the human brain," *Proceedings of the National Academy of Sciences of the United States of America*, vol. 104, no. 32, pp. 13170–13175, 2007.

[33] Y. F. Zuo, J. Y. Wang, J. H. Chen et al., "A comparison between spontaneous electroencephalographic activities induced by morphine and morphine-related environment in rats," *Brain Research*, vol. 1136, no. 1, pp. 88–101, 2007.

[34] A. A. Koronovskii and A. E. Khramov, "Wavelet bicoherence analysis as a method for investigating coherent structures in an electron beam with an overcritical current," *Plasma Physics Reports*, vol. 28, no. 8, pp. 666–681, 2002.

[35] X. Li, D. Li, L. J. Voss, and J. W. Sleigh, "The comodulation measure of neuronal oscillations with general harmonic wavelet bicoherence and application to sleep analysis," *NeuroImage*, vol. 48, no. 3, pp. 501–514, 2009.

[36] J. M. Palva, S. Monto, S. Kulashekhar, and S. Palva, "Neuronal synchrony reveals working memory networks and predicts individual memory capacity," *Proceedings of the National Academy of Sciences of the United States of America*, vol. 107, no. 16, pp. 7580–7585, 2010.

[37] M. Steriade, "Grouping of brain rhythms in corticothalamic systems," *Neuroscience*, vol. 137, no. 4, pp. 1087–1106, 2006.

[38] G. G. Knyazev, "Motivation, emotion, and their inhibitory control mirrored in brain oscillations," *Neuroscience and Biobehavioral Reviews*, vol. 31, no. 3, pp. 377–395, 2007.

[39] A. K. Engel and P. Fries, "Beta-band oscillations-signalling the status quo?" *Current Opinion in Neurobiology*, vol. 20, no. 2, pp. 156–165, 2010.

[40] K. K. Hui, J. Liu, N. Makris et al., "Acupuncture modulates the limbic system and subcortical gray structures of the human brain: evidence from fMRI studies in normal subjects," *Human Brain Mapping*, vol. 9, no. 1, pp. 13–25, 2000.

[41] S. D. Hall, I. M. Stanford, N. Yamawaki et al., "The role of GABAergic modulation in motor function related neuronal network activity," *NeuroImage*, vol. 56, no. 3, pp. 1506–1510, 2011.

[42] S. D. Muthukumaraswamy, J. F. Myers, S. J. Wilson et al., "The effects of elevated endogenous GABA levels on movement-related network oscillations," *Neuroimage C*, vol. 66, pp. 36–41, 2012.

[43] G. B. Kaplan, K. A. Leite-Morris, M. Joshi, M. H. Shoeb, and R. J. Carey, "Baclofen inhibits opiate-induced conditioned place preference and associated induction of Fos in cortical and limbic regions," *Brain Research*, vol. 987, no. 1, pp. 122–125, 2003.

[44] T. C. Chen, Y. Y. Cheng, W. Z. Sun, and B. C. Shyu, "Differential regulation of morphine antinociceptive effects by endogenous enkephalinergic system in the forebrain of mice," *Molecular Pain*, vol. 4, article 41, 2008.

[45] J. Du, Z. L. Sun, J. Jia, X. Wang, and X. M. Wang, "High-frequency electro-acupuncture stimulation modulates intracerebral gamma-aminobutyric acid content in rat model of Parkinson's disease," *Sheng Li Xue Bao*, vol. 63, no. 4, pp. 305–310, 2011.

Hindawi Publishing Corporation
Evidence-Based Complementary and Alternative Medicine
Volume 2013, Article ID 482947, 10 pages
http://dx.doi.org/10.1155/2013/482947

Research Article

Long-Term Stimulation with Electroacupuncture at DU20 and ST36 Rescues Hippocampal Neuron through Attenuating Cerebral Blood Flow in Spontaneously Hypertensive Rats

Gui-Hua Tian,[1,2,3] Kai Sun,[3,4] Ping Huang,[3,4] Chang-Man Zhou,[3,5] Hai-Jiang Yao,[1] Ze-Jun Huo,[1] Hui-Feng Hao,[3,4,6] Lei Yang,[5] Chun-Shui Pan,[3,4] Ke He,[3,4,6] Jing-Yu Fan,[3,4] Zhi-Gang Li,[1] and Jing-Yan Han[3,4,6]

[1] *School of Acupuncture and Moxibustion, Beijing University of Chinese Medicine, Beijing 100029, China*
[2] *Dongzhimen Hospital Affiliated to Beijing University of Chinese Medicine, Beijing 101121, China*
[3] *Tasly Microcirculation Research Center, Peking University Health Science Center, Beijing 100191, China*
[4] *Key Laboratory of Microcirculation, State Administration of Traditional Chinese Medicine of the People's Republic of China, Beijing 100191, China*
[5] *Department of Anatomy, School of Basic Medical Sciences, Peking University, Beijing 100191, China*
[6] *Department of Integration of Chinese and Western Medicine, School of Basic Medical Sciences, Peking University, Beijing 100191, China*

Correspondence should be addressed to Zhi-Gang Li; lizhglq620@163.com and Jing-Yan Han; hanjingyan@bjmu.edu.cn

Received 24 January 2013; Revised 10 March 2013; Accepted 14 March 2013

Academic Editor: Lixing Lao

This study was designed to investigate the effect of long-term electroacupuncture at Baihui (DU20) and Zusanli (ST36) on cerebral microvessels and neurons in CA1 region of hippocampus in spontaneously hypertensive rats (SHR). A total of 45 male Wistar rats and 45 SHR were randomly grouped, with or without electroacupuncture (EA) at DU20 and ST36, once every other day for a period of 8 weeks. The mean arterial pressure (MAP) was measured once every 2 weeks. Cerebral blood flow (CBF) and the number of open microvessels in hippocampal CA1 region were detected by Laser Doppler and immunohistochemistry, respectively. Nissl staining and Western blotting were performed, respectively, to determine hippocampus morphology and proteins that were implicated in the concerning signaling pathways. The results showed that the MAP in SHR increased linearly over the observation period and was significantly reduced following electroacupuncture as compared with sham control SHR rats, while no difference was observed in Wistar rats between EA and sham control. The CBF, learning and memory capacity, and capillary rarefaction of SHR were improved by EA. The upregulation of angiotensin II type I receptor (AT1R), endothelin receptor (ETAR), and endothelin-1 (ET-1) in SHR rats was attenuated by electroacupuncture, suggesting an implication of AT1R, ETAR, and ET-1 pathway in the effect of EA.

1. Introduction

The incidence of hypertension is up to about 30% in the world [1]. Severe, long-term hypertension is accompanied by continuous vasoconstriction that has influence on end blood supply and can eventually lead to vital target organ damage such as heart failure, cerebral disease, and renal failure, the diseases known to be related to the microcirculatory alterations [2].

Cognitive impairment is one of the principal cerebrovascular diseases evoked by hypertension. Several epidemiologic studies have indicated a correlation between blood pressure level and cognitive decline or vascular dementia [3–5]. It has been well accepted that a reduction in the number of small

arterioles and capillaries per volume of tissue (rarefaction) plays a major role in the elevation of vascular resistance and, consequently, of blood pressure. On the other hand, impairment of cerebral perfusion resulting from rarefaction contributes to hypoperfusion of the brain, leading to neuronal dysfunction and progressive cognitive failure [6, 7]. Therefore, besides lowering of blood pressure, attenuation of rarefaction and resultant hypoperfusion in cerebral tissue is reasoned as an essential goal for the treatment of cognitive dysfunction following hypertension.

Baihui (DU20), an acupoint in humans located on the top of the head at the intersection of middle sagittal line and the connection of two ear apexes, is extensively used in Chinese medicine for management of palpitations, forgetfulness, dementia and insomnia, and so forth [8]. Zusanli (ST36) is located 3 cm below Dubi (ST35) and one finger-breadth before the anterior crest of the tibia, and is known as an acupoint for its role in reducing blood pressure [9]. A recently published study showed that acupuncture at DU20 can upregulate brain derived neurotrophic factor (BDNF) expression and facilitate the support of BDNF for neurons, thus ameliorate learning and memory in early dementia rats [10]. In clinic, long-term electroacupuncture stimulation at acupoints DU20 and ST36 has an obvious effect on both reducing blood pressure and protection of forgetfulness. However, it is so far unclear whether or not electroacupuncture at both acupoints DU20 and ST36 can reverse cerebral rarefaction and further ameliorate neuronal dysfunction and, if yes, what are the underlying mechanisms. In this study, using spontaneously hypertensive rats (SHR), we demonstrated the recovery effects of long-term electroacupuncture at DU20 and ST36 on cerebral blood flow (CBF) in cortex, and density of small arterioles and capillaries in hippocampal CA1 region, as well as learning and memory capacity, which can be attributed to the suppression of angiotensin II type 1 receptor (AT1R), endothelin-1 (ET-1), and endothelin receptor (ETAR) in brain tissues.

2. Materials and Methods

2.1. Animals. Male Wistar rats and SHR (8 weeks) were obtained from the Animal Center of Peking University Health Science Center (Beijing, certificate no. SCXK 2006-0008). SHR are a genetic model of hypertension that is widely accepted in medical research because of the features they share with idiopathic hypertension in humans. This model was developed by Okamoto and Aoki in Kyoto School of Medicine, 1963, from outbred Wistar Kyoto male with marked elevation of blood pressure mated to female with slightly elevated blood pressure [11]. The animals were housed in cages at 22 ± 2°C and humidity of 40 ± 5% under a 12-hour light/dark cycle and received standard diet and water ad libitum. The experimental procedures were in accordance with the European commission guidelines (2010/63/EU). All animals were handled according to the guidelines of the Peking University Animal Research Committee. The protocols were approved by the Committee on the Ethics of Animal Experiments of the Health Science Center of Peking University (LA2011-38).

2.2. Electroacupuncture Treatment and Animal Grouping. A total of 45 Wistar rats and 45 SHR were randomly divided into 6 groups: Wistar group ($n = 15$), Wistar + Sham group (Wistar rats with stimulation at nonacupoints, $n = 15$), Wistar + EA group (Wistar rats with stimulation at acupoints, $n = 15$), SHR group ($n = 15$), SHR + Sham group (SHR with stimulation at nonacupoints, $n = 15$), and SHR + EA group (SHR with stimulation at acupoints, $n = 15$). The animals in Wistar + EA group and SHR + EA group were subjected to stimulation by electroacupuncture at acupoint DU20 (located at the midmost point of parietal bone) and ST36 (5 mm below head of right fibula under knee joint, and 2 mm lateral to the anterior tubercle of the tibia). Sterilized disposable stainless steel needles (0.3 mm × 40 mm, Global brand, Suzhou, China) were inserted 2 mm deep at DU20 with a slope of 30 degrees. Perpendicular needling was performed with the depth of 5 mm at ST36. Both needles were connected to Han's Acupoint Nerve Stimulator (Model LH 202H, Huawei Ltd, Beijing, China). To keep animals quiet during electrostimulation, the rats were fastened to an animal plate and adapted for 10 min before electroacupuncture stimulation. Electric stimulation proceeded for 20 minutes each time, once every other day, for a period of 8 weeks, and the stimulation parameters were set at disperse-dense waves of 2/100 Hz with an intensity of 1 mA, 2 Hz [12]. In Wistar + Sham group and SHR + Sham group, the animals received similar treatment as electroacupuncture groups but the electroacupuncture site was 1 cm and 2 cm from the root of the tail, respectively, to replace DU20 and ST36 [13]. The animals in Wistar group and SHR group underwent a similar procedure but without electroacupuncture.

2.3. Blood Pressure Measurement. Blood pressure was measured as described [14], with modification. The measurement was conducted once every 2 weeks at 8 am in a quiet room. After staying in a box at 29 ± 1°C for 10 min, the mean arterial pressure was measured with a blood pressure monitor (BP-98A, U0130163, Tokyo, Japan), taking the average of three consecutive measurements as the mean arterial pressure (MAP).

2.4. Assessment of CBF. CBF was measured using a laser Doppler perfusion imager (PeriScan PIM3; PERIMED, Stockholm, Sweden) at the end of the observation. For this purpose, an incision was made through the scalp, and the skin was retracted to expose the skull. The periosteal connective tissue adherent to the skull was removed with a sterile cotton swab. A computer-controlled optical scanner directed a low-powered He-Ne laser beam over the exposed cortex. The scanner head was positioned in parallel to the cerebral cortex at a distance of 18.5 cm. The scanning procedure took 4 sec for a measurement covering an area of 80 pixels. At each measuring site, the beam illuminated the tissue to a depth of 0.5 mm. A color-coded image to denote specific relative perfusion levels was displayed on a video monitor.

2.5. Morris Water Maze Test. Cognitive function was tested by the water maze at the end of the observation. The Morris water maze test was conducted according to Morris [15]. The water-filled (23 ± 1°C) black-colored tank (150 cm diameter, 60 cm depth) was divided into four quadrants of equal area arbitrarily. A round platform (10 cm in diameter) made of transparent perspex was submerged 1 cm below the water surface with its center 37.5 cm from the perimeter, in the middle of one quadrant (the target quadrant). A closed-circuit television camera was mounted onto the ceiling directly above the center of the pool to convey subject swimming trajectories and parameters to an electronic image analyzer.

2.6. Tissue Preparation for Histology. Animals in each group ($n = 6$) were anesthetized with pentobarbital sodium (0.1 g/kg body weight) intraperitoneally at 16 weeks and perfused transcardially with 0.9% saline followed by 4% paraformaldehyde in 0.1 M PBS (pH 7.4) for 40 min [16]. The brain was removed and cut into blocks, embedded in paraffin, and sectioned at 10 μm.

Three sections of cerebral hippocampus were collected in each animal. The sections were deparaffinized and rehydrated, sequentially, and examined by Nissl staining or immunohistochemistry as detailed below.

2.7. Nissl Staining. The sections were stained with cresyl violet and examined with a light microscope (BX512DP70, Olympus, Tokyo, Japan), according to the standard procedure [17]. Five fields of CA1 sector in hippocampus of each animal were randomly selected, and the number of surviving pyramidal cells per 2 mm of CA1 region was counted.

2.8. Immunohistochemistry. The sections were incubated with antibody against CD31 (Thermo Scientific, MA1-80069, Waltham, USA) after blocking with bovine serum albumin. The samples were then incubated with a biotinylated secondary antibody followed by avidin-biotin-peroxidase complex. As control, a consecutive section was treated similarly except that the primary antibody was omitted. Positive staining was visualized with diaminobenzidine. The images were captured by a digital camera connected to a microscope (BX512DP70, Olympus, Tokyo, Japan) and analyzed with Image-Pro Plus 5.0 software (IPP, Media Cybernetic, Bethesda, MD, USA). Five fields of CA1 region were examined for each animal.

2.9. ELISA. At 16 weeks, animals from each group ($n = 8$) were anesthetized and the hippocampus of brain was removed and homogenized in lysis buffer including protease inhibitor on ice. After being centrifuged at 20000 rcf for 60 minutes, the supernatant was collected for determination of endothelin-1 (ET-1) and NO content in cerebral tissues by ELISA, according to the manufacture's instruction (Abcam, Cambridge, UK).

2.10. Western Blot Analysis. Western blot analysis ($n = 3$) was performed as described previously [18]. Briefly, the brain was removed at week 16, and hippocampus was homogenized in lysis buffer including protease inhibitors. One hundred micrograms of the supernatant was mixed with 4× sample buffer. The protein samples were separated on Tris-glycineSDS-PAGE in a reducing condition. The rabbit primary antibodies used included those that directed against AT1R (1 : 300, Abcam, Cambridge, UK), AT2R (1 : 500, Abcam, Cambridge, UK), ETAR (1 : 500, Abcam, Cambridge, UK), eNOS (1 : 1000, BD, Franklin Lakes, USA), iNOS (1 : 200, Abcam, Cambridge, UK), and GAPDH (1 : 2000, Cell Signaling Technology, Boston, MA, USA). After washing with Tris-buffered saline containing 0.05% Tween-20, the membrane was incubated with horseradish peroxidase-conjugated goat anti-rabbit secondary antibody (1 : 3000, Santa Cruz Biotechnology, Santa Cruz, USA) at room temperature for 60 min. The membranes were analyzed using the enhanced chemiluminescence system, according to the manufacturer's protocol and exposed in a dark box. The protein signal was quantized by scanning densitometry in the X-film by bio-image analysis system (Image-Proplus 5.0, Media Cybermetrics, Bethesda, MD, USA). The results from each experimental group were expressed as relative integrated intensity compared with that from the sham group.

2.11. Statistical Analysis. All parameters are expressed as means ± SD. For comparison of >2 conditions a one-way analysis of variance (ANOVA) with Turkey post hoc test or a repeated measures ANOVA with Bonferroni post hoc test was used. A probability of less than 0.05 was considered to be statistically significant.

3. Results

3.1. Long-Term Stimulation with Electroacupuncture Reduces the MAP in SHR. Figure 1 shows the effect of long-term stimulation with electroacupuncture at DU20 and ST36 on MAP during the observation period. MAP in Wistar groups remained nearly unchanged from 8 through 16 weeks. In contrast, MAP in SHR group increased with time, from 130 mmHg at week 8 to 170 mmHg at week 16. MAP in SHR + Sham group changed over time similarly to that in SHR group, and no significant difference was observed at any time point between the two groups. Of notice, MAP in SHR + EA group was attenuated significantly at week 16, as compared to SHR group and SHR + Sham group ($P < 0.05$).

3.2. Long-Term Stimulation with Electroacupuncture Increases the CBF in SHR. The representative color images of rat CBF acquired at week 16 by Laser Doppler perfusion image system (PeriScan PIM3 System; PERIMED, Stockholm, Sweden) in the six groups are illustrated in Figure 2(a) wherein the different magnitude of CBF is indicated by distinct color, with the red (black arrow in a1) representing the highest CBF and black (white arrow in a4) representing the lowest. Figure 2(b) is statistical results of CBF in different groups, showing that as compared to Wistar group, CBF in SHR group decreased significantly. Electroacupuncture treatment

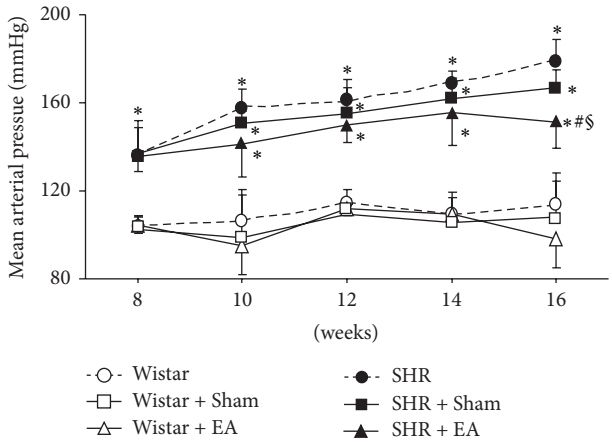

Figure 1: The effect of electroacupuncture on rat MAP. Wistar: Wistar rats without any treatment. Wistar + Sham: Wistar rats with stimulation at nonacupoints. Wistar + EA: Wistar rats with stimulation at acupoints. SHR: SHR without any treatment. SHR + Sham: SHR with stimulation at nonacupoints. SHR + EA: SHR with stimulation at acupoints. Data were expressed as mean ± SD from six animals. $^{*}P < 0.05$ versus 8 weeks; $^{\#}P < 0.05$ versus SHR group; $^{\S}P < 0.05$ versus SHR + Sham group.

at acupoints markedly relieved CBF in SHR. In contrast, electroacupuncture treatment at nonacupoints had no significant effect on CBF, although some trend to increase occurred. No significant difference was observed between SHR + Sham and SHR + EA groups either, probably due to the large standard deviation.

3.3. Long-Term Stimulation with Electroacupuncture Attenuates the Spatial Learning and Memory Impairment in SHR. Figure 3 illustrates the latency and swimming distances assessed by the Morris water maze for rats in different experimental groups. There was no significant difference observed among Wistar group, Wistar + EA group, and Wistar + Sham group in learning and memory potential. Longer latency and swimming distances were observed in SHR group compared to Wistar group. SHR rats that received electroacupuncture treatment displayed a significant improvement in spatial learning and memory impairment as compared with the rats in SHR, exhibiting a smaller mean latency and a shorter mean swimming distance. In comparison to SHR + Sham group, however, rats in SHR + EA displayed an improvement in mean latency but not in mean swimming distance. The impairment of spatial learning and memory was not alleviated by electroacupuncture at nonacupoints.

3.4. Long-Term Stimulation with Electroacupuncture Protects the Neuron in CA1 Region of Hippocampus in SHR. The number and morphology of neurons in hippocampal CA1 region (arrow) were assessed in different groups at week 16 by Nissl staining, and the results are presented in Figure 4. In Wistar group, the pyramidal cells existed in approximately three to four layers and packed regularly with the Nissl bodies being darkly stained (a1, b1). In contrast, the feature of CA1 region of SHR rats at week 16 was dramatically distinct, characterized by thinning of the cell layers, shrinkage and disintegration of neurons (a4, b4). These morphological changes were attenuated by electroacupuncture at DU20 and ST36 (a6, b6), but not at nonacupoints (a5 and b5). Figure 4(b) shows a quantitative evaluation of the cell number in CA1 region in various groups. As compared to Wistar rats, the neuron number decreased significantly in CA1 region in SHR and SHR + Sham groups, which was protected by electroacupuncture at DU20 and ST36.

3.5. Long-Term Stimulation with Electroacupuncture Increases the Number of Opening Microvessels in Hippocampus of SHR. To evaluate the number and morphology of microvessels, an immunochemistry staining for CD31 was performed to delineate the vessels (arrows). Figure 5(a) shows representative images of hippocampal CA1 region stained by immunohistochemisty for CD31 in the six groups. A survey at low power revealed that open microvessels in Wistar group, as well as in Wistar + EA group and Wistar + Sham group, were densely and uniformly distributed in a region between CA1 and dentate gyrus (a1, b1; a2, b2 and a3, b3). Impressively, in SHR and SHR + Sham groups, the density of open microvessels was reduced (a4 and a5), and their distribution became heterogeneous with obviously contractive vasculature and thickening vessel wall (b4 and b5). Compared to SHR and SHR + Sham rats, electroacupuncture at DU20 and ST36 attenuated the alteration in microvessels (a6 and b6), while electroacupuncture at nonacupoints had no effect (a5, b5). A quantitative evaluation of the number of open microvessels confirmed the survey results (Figure 5(b)).

3.6. Long-Term Stimulation with Electroacupuncture Reduces the ET-1 but Not NO Content in Brain Tissue of SHR. The brain content of ET-1 and NO, the two mediators with opposite action on blood pressure, was assessed by ELISA at week 16 in the different groups to explore the mechanism for electroacupuncture effect. As shown in Figure 6(a), there was no difference found in the content of ET-1 in brain homogenate among Wistar group, Wistar + EA group, and Wistar + Sham group. In contrast, ET-1 content increased significantly in SHR and SHR + Sham groups, as compared to Wistar group, which was attenuated by electroacupouncture at DU20 and ST36, but not at nonacupoints. On the other hand, the content of NO did not differ statistically in all the groups studied (Figure 6(b)), indicating that NO does not play a role in augmenting blood pressure in SHR, and is not a mechanism of the electroacupuncture effect.

3.7. Long-Term Stimulation with Electroacupuncture Attenuates the AT1R and ETAR but Not AT2R, Expression in Brain Tissue of SHR. To elucidate the pathogenesis of hypertension of SHR and the target for electroacupuncture effect observed in the present case, the expression of AT1R, AT2R, and ETAR in brain tissue was determined by Western blot in different conditions at week 16, and the results are presented in Figure 7. AT1R and ETAR expression did not differ obviously

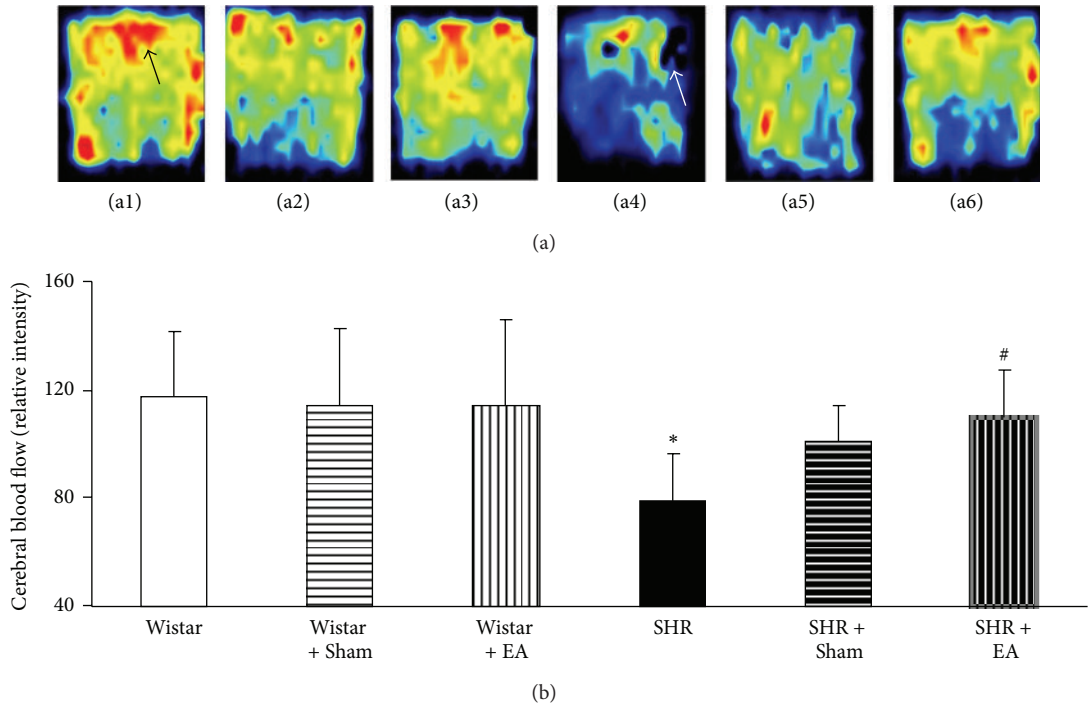

Figure 2: The effect of electroacupuncture on CBF in rat cerebral cortex. (a) Representative laser-Doppler perfusion images of Wistar (a1), Wistar + Sham (a2), Wistar + EA (a3), SHR (a4), SHR + Sham (a5), and SHR + EA (a6) group, respectively, acquired at week 16. Black arrow indicates the highest CBF, while white arrow indicates the lowest CBF. (b) Quantitative evaluation of CBF in six groups. Wistar: Wistar rats without any treatment. Wistar + Sham: Wistar rats with stimulation at nonacupoints. Wistar + EA: Wistar rats with stimulation at acupoints. SHR: SHR without any treatment. SHR + Sham: SHR with stimulation at nonacupoints. SHR + EA: SHR with stimulation at acupoints. Data were expressed as mean ± SD from six animals. $^{*}P < 0.05$ versus Wistar group; $^{\#}P < 0.05$ versus SHR group.

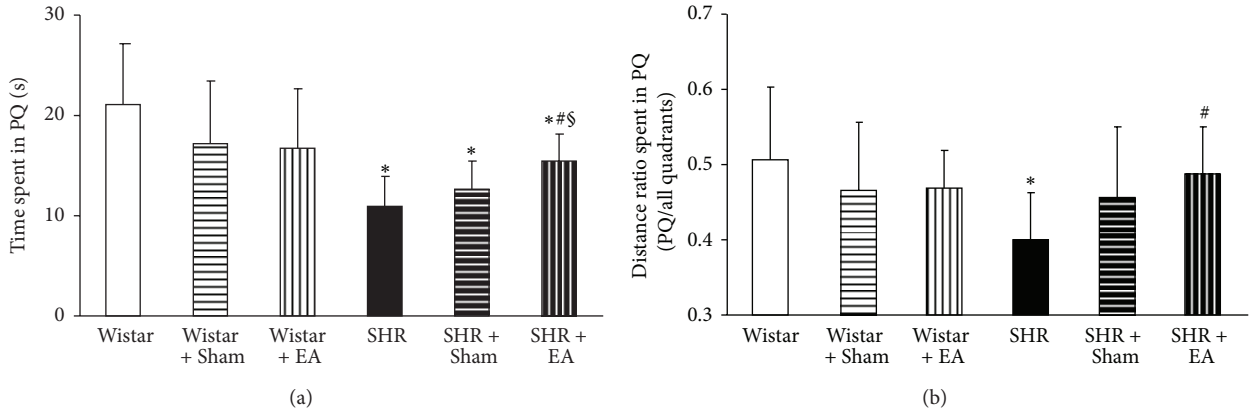

Figure 3: The effect of electroacupuncture on learning and memory capacity of rat. (a) The effect of electroacupuncture on time spent in PQ. (b) The effect of electroacupuncture on distance ratio spent in PQ. Wistar: Wistar rats without any treatment. Wistar + Sham: Wistar rats with stimulation at nonacupoints. Wistar + EA: Wistar rats with stimulation at acupoints. SHR: SHR without any treatment. SHR + Sham: SHR with stimulation at nonacupoints. SHR + EA: SHR with stimulation at acupoints. Data were expressed as mean ± SD from six animals. $^{*}P < 0.05$ versus Wistar group; $^{\#}P < 0.05$ versus SHR group; $^{\S}P < 0.05$ versus SHR + Sham group.

among the Wistar group, Wistar + EA group, and Wistar + Sham group, but increased significantly in SHR group, as compared to Wistar group. Electroacupuncture stimulation at acupoint DU20 and ST36 significantly suppressed the increased AT1R and ETAR expression of SHR rats, but had no effect at nonacupoints (Figures 7(a) and 7(c)). In contrast with AT1R and ETAR, there was no obvious difference in AT2R protein level among the six experiment groups (Figure 7(b)).

3.8. Long-Term Stimulation with Electroacupuncture Has No Effects on eNOS and iNOS Expression in Brain Tissue of SHR. Similar to AT2R, the expression of eNOS and iNOS proteins

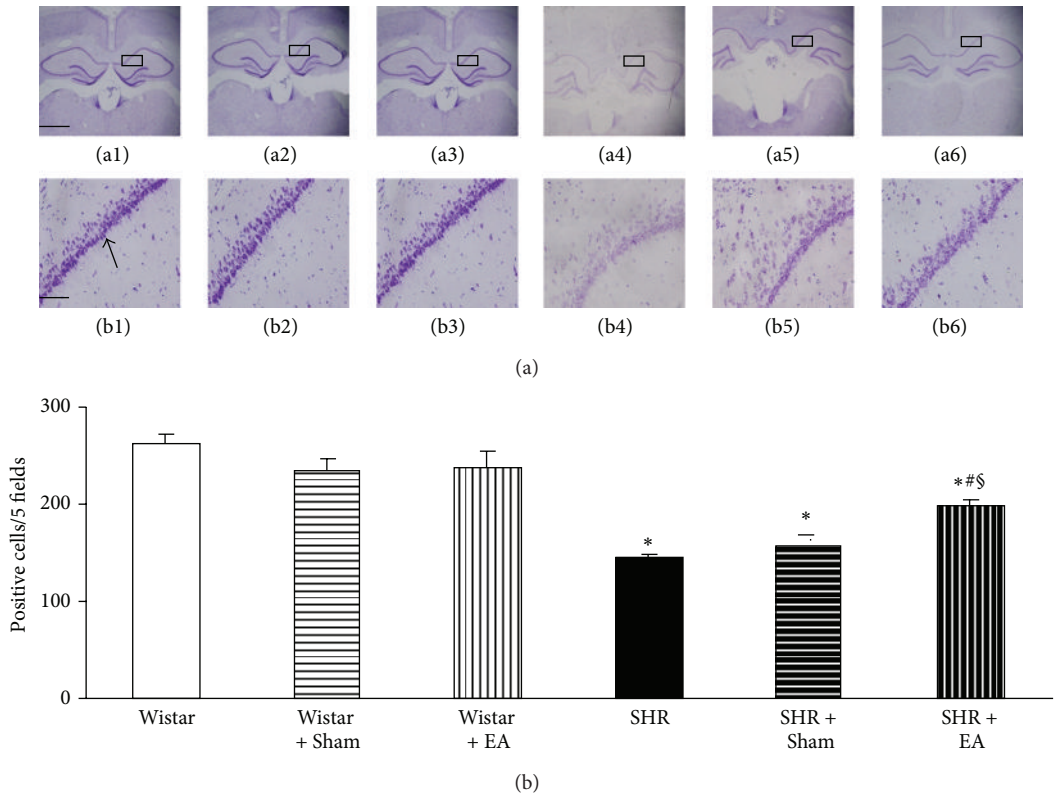

Figure 4: The effect of electroacupuncture on Nissl staining-positive neurons in rat hippocampal CA1 region. (a) Representative Nissl staining images at the end of observation in rat hippocampal CA1 region (arrow) of Wistar (a1), Wistar + Sham (a2), Wistar + EA (a3), SHR (a4), SHR + Sham (a5), and SHR + EA (a6) group, respectively. Bar = 50 μm. b1–b6, high magnification of a1–a6, respectively. Bar = 200 μm. (b) Quantitative evaluation of Nissl staining-positive neurons. Wistar: Wistar rats without any treatment. Wistar + Sham: Wistar rats with stimulation at nonacupoints. Wistar + EA: Wistar rats with stimulation at acupoints. SHR: SHR without any treatment. SHR + Sham: SHR with stimulation at nonacupoints. SHR + EA: SHR with stimulation at acupoint. Data were expressed as mean ± SD from six animals. $^{*}P < 0.05$ versus Wistar group; $^{\#}P < 0.05$ versus SHR group; $^{\S}P < 0.05$ versus SHR + Sham group.

in brain tissue did not change significantly among the six experiment groups, as shown in Figures 8(a) and 8(b).

4. Discussion

The present study revealed that SHR benefits from the long-term electroacupuncture stimulation at DU20 and ST36 significantly, including relief of hypertension, increase in the number of opening microvessels and cerebral blood flow, attenuation of neuron injury, and restoration of cognitive impairment.

Our preliminary experiments showed that compared to other acupuncture points, such as Yanglingquan (GB34), Hegu (LI4), Quchi (LI11), and Neiguan (PC6), electroacupuncture stimulation at DU20 and ST36 exerts a more apparent antihypertensive effect. Stimulation at ST36 alone was also reported to attenuate hypertension; however, the study regarding its ameliorating effect on cognitive impairment in hypertensive rats is limited [19]. On the other hand, acupuncture stimulation at DU20 is found more effective for improving cognitive impairment in clinic [20]. In the present study, electroacupuncture stimulation at DU20 combined with ST36 relieved hypertension in SHR as well as recovered cognitive impairment.

The morphological changes in the systemic microvasculature are the end result of established hypertension. This alteration may be ascribed to a rarefaction at the capillary level, which plays a significant role in the reduction of CBF induced by hypertension [21, 22]. It has been previously demonstrated that long-term cerebral arteriolar contraction causes the decrease in the number of open microvessels and diminishes the CBF in SHR [23, 24]. The clinical application of calcium channel blockers, diuretics, β-receptor blockers, angiotensin converting enzyme inhibitors, and AT1R antagonists can relieve vasospasm and reduce blood pressure [25]. However, these drugs have little effect on CBF. The present study showed that the decreased CBF could be significantly restored by long-term electroacupuncture stimulation therapy at two acupoints DU20 and ST36. In addition, using immunohistochemistry method, we revealed that long-term electroacupuncture could attenuate the reduction in the number of opening capillaries in hippocampus of SHR. The neurons in the hippocampus CA1 region are known to be vulnerable to ischemia and hypoxia. Ischemia and hypoxia induced by rarefaction during hypertension is the

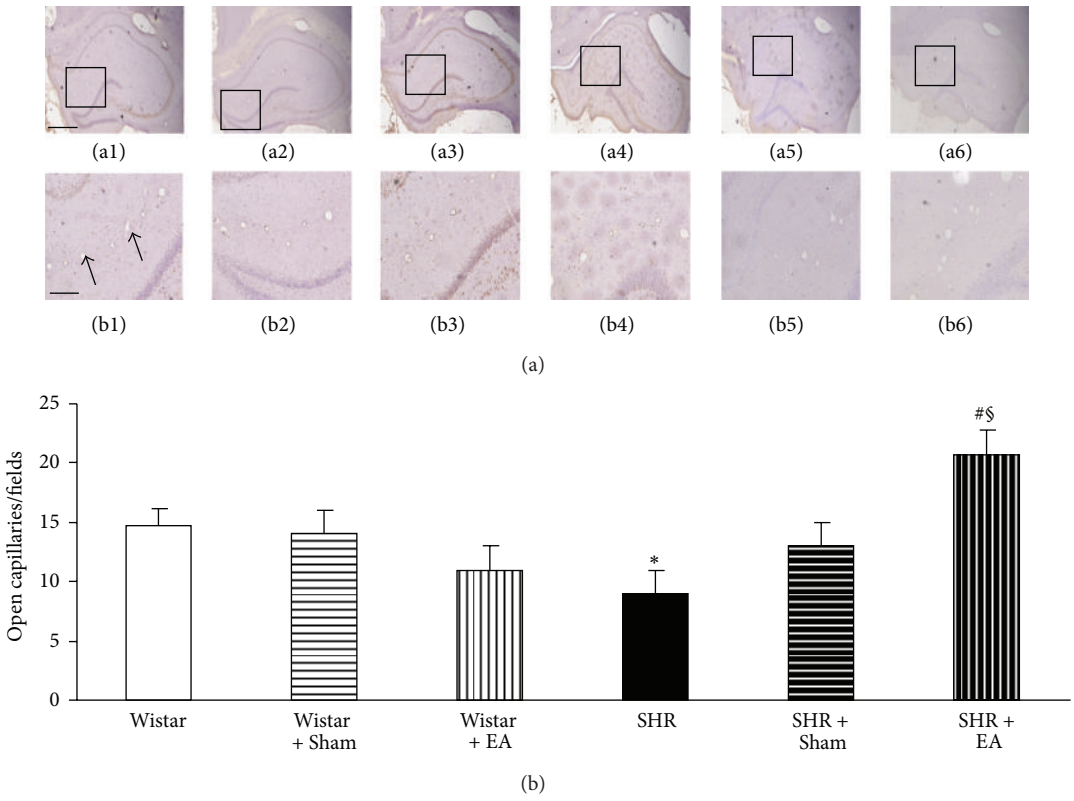

Figure 5: The effect of electroacupuncture on the number of opening microvessels in rat hippocampus. (a) Representative immunohistochemistry images at the end of observation in rat hippocampus of Wistar (a1), Wistar + Sham (a2), Wistar + EA (a3), SHR (a4), SHR + Sham (a5), and SHR + EA (a6) group, respectively. Bar = 50 μm. b1–b6, high magnification of a1–a6, respectively. Arrows indicate opening microvessels. Bar = 200 μm. (b) Quantitative evaluation of CD31-positive opening microvessels. Wistar: Wistar rats without any treatment. Wistar + Sham: Wistar rats with stimulation at nonacupoints. Wistar + EA: Wistar rats with stimulation at acupoints. SHR: SHR without any treatment. SHR + Sham: SHR with stimulation at nonacupoints. SHR + EA: SHR with stimulation at acupoints. Data were expressed as mean ± SD from six animals. $^{*}P < 0.05$ versus Wistar group; $^{\#}P < 0.05$ versus SHR group; $^{\S}P < 0.05$ versus SHR + Sham group.

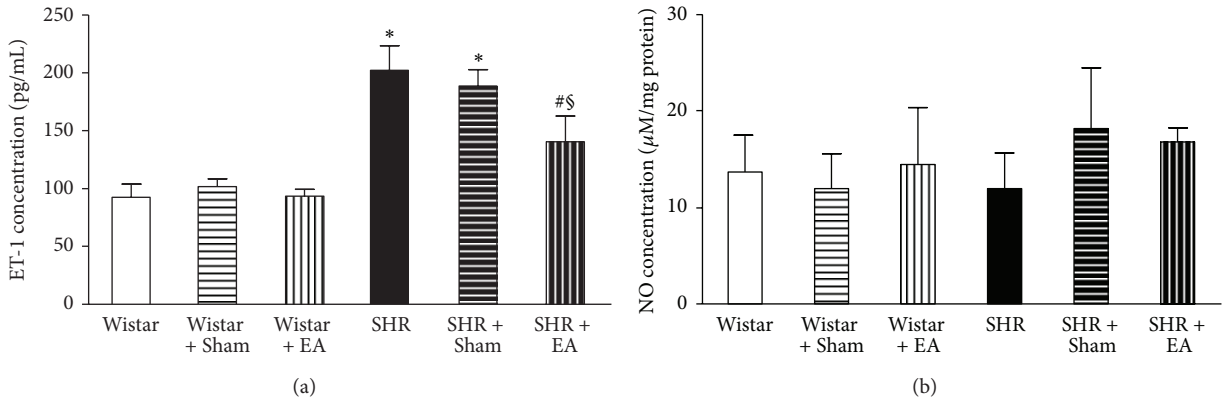

Figure 6: The effect of electroacupuncture on ET-1 and NO concentration in rat brain. (a) The effect of electroacupuncture on ET-1 concentration in rat brain. (b) The effect of electroacupuncture on NO concentration in rat brain. Wistar: Wistar rats without any treatment. Wistar + Sham: Wistar rats with stimulation at nonacupoints. Wistar + EA: Wistar rats with stimulation at acupoints. SHR: SHR without any treatment. SHR + Sham: SHR with stimulation at nonacupoints. SHR + EA: SHR with stimulation at acupoints. Data were expressed as mean ± SD of six animals. $^{*}P < 0.05$ versus Wistar group; $^{\#}P < 0.05$ versus SHR group; $^{\S}P < 0.05$ versus SHR + Sham group.

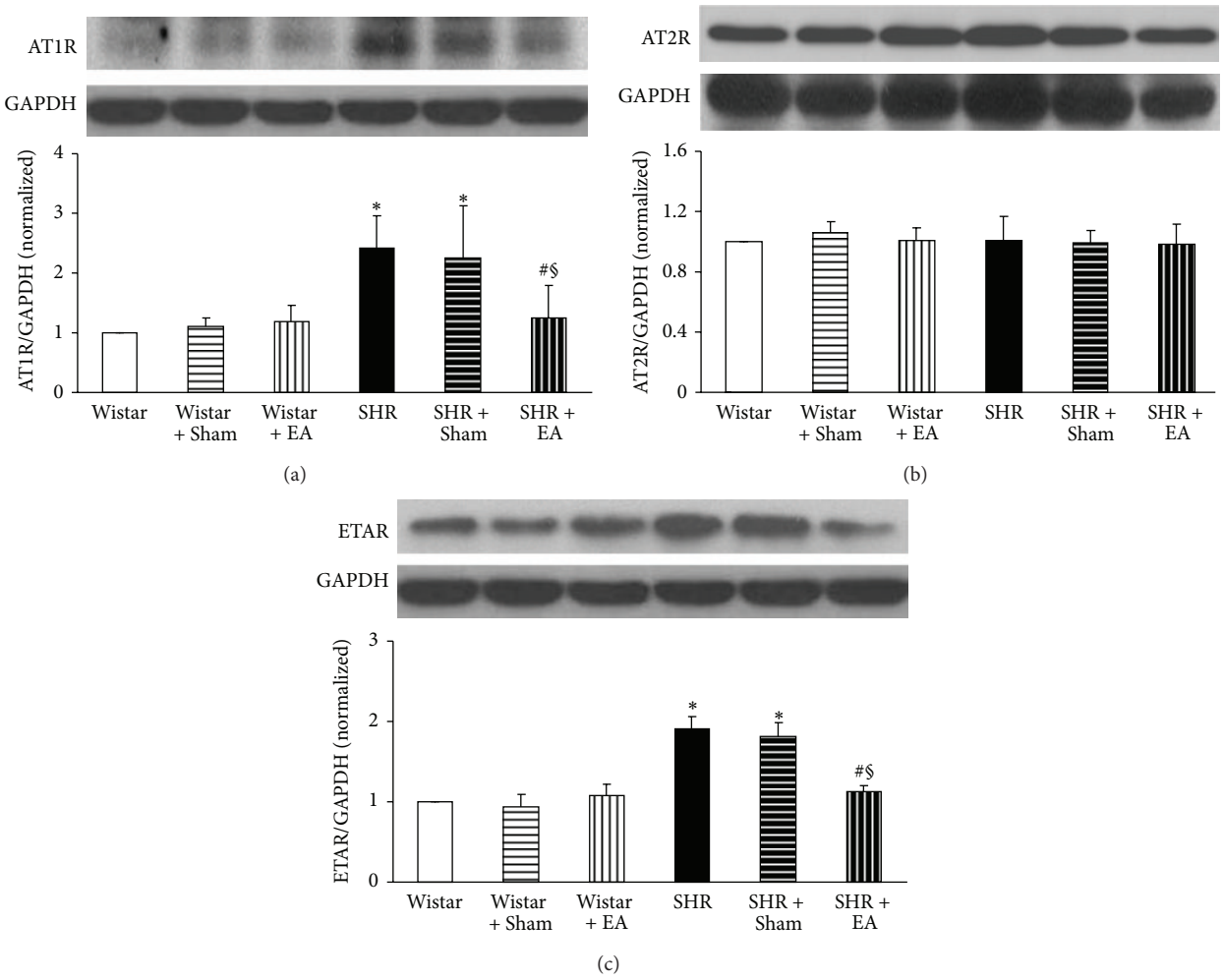

Figure 7: The effect of electroacupuncture on expression of AT1R (a), AT2R (b), and ETAR (c) in rat cerebral tissue. For each protein, the representative Western blot of each group is presented with the respective quantification showing below. Wistar: Wistar rats without any treatment. Wistar + Sham: Wistar rats with stimulation at nonacupoints. Wistar + EA: Wistar rats with stimulation at acupoints. SHR: SHR without any treatment. SHR + Sham: SHR with stimulation at nonacupoints. SHR + EA: SHR with stimulation at acupoints. Data were expressed as mean ± SD from three animals. $^{*}P < 0.05$ versus Wistar group; $^{\#}P < 0.05$ versus SHR group; $^{\$}P < 0.05$ versus SHR + Sham group.

major cause responsible for the damage of CA1 hippocampal region neurons and cognitive deficits in SHR [26, 27]. Therefore, ameliorating cerebral vasospasm is anticipated to reduce CA1 region neuron damage and alleviate the cognitive dysfunction. Previous studies showed that MAP increased from 6 weeks [28, 29] and learning and memory dysfunction occurred from 12 weeks in SHR [30]. By virtue of Nissl staining and Morris water maze detection, our work further demonstrated that electroacupuncture at DU20 and ST36 significantly offset hippocampus CA1 neuron lost and learning and memory impairment in SHR, the outcomes that are attributable to the relief of capillary rarefaction.

Existence of an AT1R-ET-1-ETAR pathway in hypertension pathogenesis is well recognized; that is, an increased interaction of AngII with AT1R stimulates the release of ET-1 in endothelial cells that enhances the binding of ET-1 with ETAR, leading to vasoconstriction [31]. Amelioration of AT1R and ETAR expression is thus pivotal for attenuating vasoconstriction and high blood pressure. Our study suggested an implication of AT1R-ET-1-ETAR pathway in alleviating MAP and CBF by electroacupuncture at DU20 and ST36, which suppressed the expression of AT1R and ETAR and reduced the content of ET-1 in SHR. On the other hand, as compared with Wistar rats, no change was observed in the expression of AT2R and the amount of NO. NO is an important molecule that plays a role in a variety of physiological functions, which is synthesized by NO synthase (NOS) [32]. Previous study has reported that therapeutic effects of acupuncture on hypertension are correlated with activation of NOS [9]. In contrast, our results precluded the involvement of AT2R-eNOS/iNOS-NO pathway in the present circumstance, which might be due to the difference in organ and acupuncture sites studied.

The present study has some limitations. Firstly, the finding of the present study was derived from the observation on the effect of simultaneous application of EA at DU20

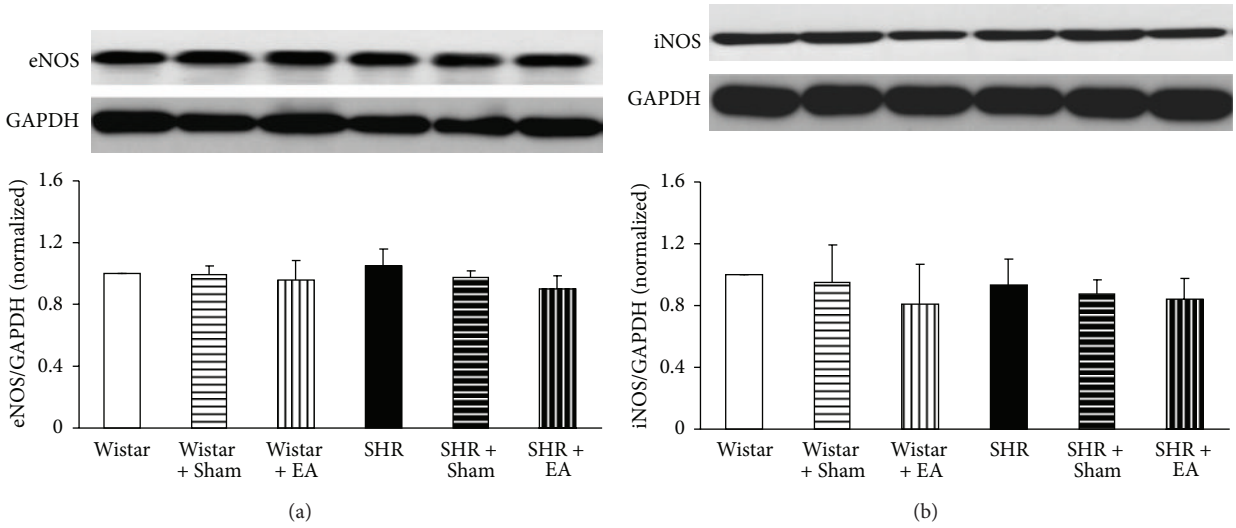

Figure 8: The effect of electroacupuncture on expression of eNOS (a) and iNOS (b) in rat cerebral tissue. For each protein, the representative Western blot of each group is presented with the respective quantification showing below. Wistar: Wistar rats without any treatment. Wistar + Sham: Wistar rats with stimulation at nonacupoints. Wistar + EA: Wistar rats with stimulation at acupoints. SHR: SHR without any treatment. SHR + Sham: SHR with stimulation at nonacupoints. SHR + EA: SHR with stimulation at acupoints. Data were expressed as mean ± SD from three animals.

and ST36. In a preliminary study, we evaluated the effect of EA on the MAP at 16 weeks by stimulating at either both DU20 and ST36 acupoints or only one of the two. The result showed a more pronounced effect of EA when applied at both acupoints than that at any single one. Since the objective of this study was to explore the mechanisms whereby EA attenuates hypertension, we thus chose a most effective application manner, that is, stimulation at both acupoints. The signaling pathway that mediates the effect of AE on DU20 or ST36 alone is at present unknown, and waits for further study. Secondly, EA is a strategy that combines the acupuncture with electrical stimulation. Researchers have reported that electrical and manual acupuncture stimulation affect glucose homeostasis through different mechanisms [33]. Whether or not the findings of the present study may be extrapolated to manual acupuncture remains to be verified. Finally, mean arterial pressure in SHR + EA group dropped obviously at week 16 compared with that at week 14. What was taking place in mean arterial pressure during the period between the two weeks is not clear. To localize the time point exactly when the effect of EA starts displaying, probably, one or two more time points between week 14 and 16 need to be examined.

In conclusion, the long-term electroacupuncture at acupoints DU20 and ST36 relieves the increased MAP and cerebral abnormality in both structure and function in SHR, this beneficial action is most likely mediated via inhibition of AT1R-ETAR-ET-1 pathway. However, two issues remain to be resolved in the future. The first is to confirm that MAP decrease is causative rather than epiphenomenal in the therapeutic effect of acupuncture at acupoints DU20 and ST36 on cerebral protection, and the second is to determine the relation of these findings with other vital pathways, such as endocrine system and meridian system.

Acknowledgment

This study was supported financially by the Tianjin Tasly Group (Grant no. 20050230), Tianjin, China.

References

[1] R. Düsing, "Optimizing blood pressure control through the use of fixed combinations," *Vascular Health and Risk Management*, vol. 6, pp. 321–325, 2010.

[2] G. Cohuet and H. Struijker-Boudier, "Mechanisms of target organ damage caused by hypertension: therapeutic potential," *Pharmacology and Therapeutics*, vol. 111, no. 1, pp. 81–98, 2006.

[3] J. M. Starr, L. J. Whalley, S. Inch, and P. A. Shering, "Blood pressure and cognitive function in healthy old people," *Journal of the American Geriatrics Society*, vol. 41, no. 7, pp. 753–756, 1993.

[4] H. B. Posner, M. X. Tang, J. Luchsinger, R. Lantigua, Y. Stern, and R. Mayeux, "The relationship of hypertension in the elderly to AD, vascular dementia, and cognitive function," *Neurology*, vol. 58, no. 8, pp. 1175–1181, 2002.

[5] O. Hanon, M. L. Seux, H. Lenoir, A. S. Rigaud, and F. Forette, "Hypertension and dementia," *Current Cardiology Reports*, vol. 5, no. 6, pp. 435–440, 2003.

[6] W. W. Zhang, K. C. Ma, O. Andersen, P. Sourander, P. O. Tollesson, and Y. Olsson, "The microvascular changes in cases of hereditary multi-infarct disease of the brain," *Acta Neuropathologica*, vol. 87, no. 3, pp. 317–324, 1994.

[7] E. B. Ringelstein and D. G. Nabavi, "Cerebral small vessel diseases: cerebral microangiopathies," *Current Opinion in Neurology*, vol. 18, no. 2, pp. 179–188, 2005.

[8] T. M. Zhu, H. Li, R. J. Jin et al., "Effects of electroacupuncture combined psycho-intervention on cognitive function and event-related potentials p300 and mismatch negativity in patients with internet addiction," *Chinese Journal of Integrative Medicine*, vol. 18, no. 2, pp. 146–151, 2012.

[9] D. D. Kim, A. M. Pica, R. G. Durán, and W. N. Durán, "Acupuncture reduces experimental renovascular hypertension through mechanisms involving nitric oxide synthases," *Microcirculation*, vol. 13, no. 7, pp. 577–585, 2006.

[10] I. K. Hwang, J. Y. Chung, D. Y. Yoo et al., "Effects of electroacupuncture at zusanli and baihui on brain-derived neurotrophic factor and cyclic AMP response element-binding protein in the hippocampal dentate gyrus," *Journal of Veterinary Medical Science*, vol. 72, no. 11, pp. 1431–1436, 2010.

[11] K. Okamoto and K. Aoki, "Development of a strain of spontaneously hypertensive rats," *Japanese circulation journal*, vol. 27, pp. 282–293, 1963.

[12] J. Zhang, D. Ng, and A. Sau, "Effects of electrical stimulation of acupuncture points on blood pressure," *Journal of Chiropractic Medicine*, vol. 8, no. 1, pp. 9–14, 2009.

[13] Y. S. Kim, C. Kim, M. Kang, J. Yoo, and Y. Huh, "Electroacupuncture-related changes of NADPH-diaphorase and neuronal nitric oxide synthase in the brainstem of spontaneously hypertensive rats," *Neuroscience Letters*, vol. 312, no. 2, pp. 63–66, 2001.

[14] O. H. Lee, K. I. Kim, C. K. Han, Y. C. Kim, and H. D. Hong, "Effects of acidic polysaccharides from gastrodia rhizome on systolic blood pressure and serum lipid concentrations in spontaneously hypertensive rats fed a high-fat diet," *International Journal of Molecular Sciences*, vol. 13, no. 1, pp. 698–709, 2012.

[15] Y. Liu, Z. Ye, H. Yang et al., "Disturbances of soluble N-ethylmaleimide-sensitive factor attachment proteins in hippocampal synaptosomes contribute to cognitive impairment after repetitive formaldehyde inhalation in male rats," *Neuroscience*, vol. 169, no. 3, pp. 1248–1254, 2010.

[16] N. Zhao, Y. Y. Liu, F. Wang et al., "Cardiotonic pills, a compound Chinese medicine, protects ischemia-reperfusion-induced microcirculatory disturbance and myocardial damage in rats," *American Journal of Physiology*, vol. 298, no. 4, pp. H1166–H1176, 2010.

[17] K. Sun, Q. Hu, C. M. Zhou et al., "Cerebralcare Granule®, a Chinese herb compound preparation, improves cerebral microcirculatory disorder and hippocampal CA1 neuron injury in gerbils after ischemia-reperfusion," *Journal of Ethnopharmacology*, vol. 130, no. 2, pp. 398–406, 2010.

[18] X. Chen, C. Zhou, J. Guo et al., "Effects of dihydroxylphenyl lactic acid on inflammatory responses in spinal cord injury," *Brain Research*, vol. 1372, pp. 160–168, 2011.

[19] J. I. Kim, Y. S. Kim, S. K. Kang et al., "Electroacupuncture decreases nitric oxide synthesis in the hypothalamus of spontaneously hypertensive rats," *Neuroscience Letters*, vol. 446, no. 2-3, pp. 78–82, 2008.

[20] H. X. Zhang, Q. Wang, L. Zhou et al., "Effects of scalp acupuncture on acute cerebral ischemia-reperfusion injury in rats," *Journal of Chinese Integrative Medicine*, vol. 7, no. 8, pp. 769–774, 2009.

[21] H. A. J. Struijker Boudier, "Microcirculation in hypertension," *European Heart Journal*, vol. 1, supplement L, pp. L32–L37, 1999.

[22] B. I. Levy, G. Ambrosio, A. R. Pries, and H. A. J. Struijker-Boudier, "Microcirculation in hypertension: a new target for treatment?" *Circulation*, vol. 104, no. 6, pp. 735–740, 2001.

[23] J. M. Saavedra, "Brain angiotensin II: new developments, unanswered questions and therapeutic opportunities," *Cellular and Molecular Neurobiology*, vol. 25, no. 3-4, pp. 485–512, 2005.

[24] R. L. Haberl, P. J. Decker-Hermann, and K. Hermann, "Effect of renin on brain arterioles and cerebral blood flow in rabbits," *Journal of Cerebral Blood Flow and Metabolism*, vol. 16, no. 4, pp. 714–719, 1996.

[25] B. Powers, L. Greene, and L. M. Balfe, "Updates on the treatment of essential hypertension: a summary of ahrq's comparative effectiveness review of angiotensin-converting enzyme inhibitors, angiotensin ii receptor blockers, and direct renin inhibitors," *Journal of Managed Care Pharmacy*, vol. 17, no. 8, supplement, pp. S1–S14, 2011.

[26] A. Tajima, F. J. Hans, D. Livingstone et al., "Smaller local brain volumes and cerebral atrophy in spontaneously hypertensive rats," *Hypertension*, vol. 21, no. 1, pp. 105–111, 1993.

[27] M. Sabbatini, P. Strocchi, L. Vitaioli, and F. Amenta, "The hippocampus in spontaneously hypertensive rats: a quantitative microanatomical study," *Neuroscience*, vol. 100, no. 2, pp. 251–258, 2000.

[28] H. Okano and C. Ohkubo, "Exposure to a moderate intensity static magnetic field enhances the hypotensive effect of a calcium channel blocker in spontaneously hypertensive rats," *Bioelectromagnetics*, vol. 26, no. 8, pp. 611–623, 2005.

[29] K. Okamoto, K. Yamamoto, N. Morita et al., "Establishment and use of the M strain of stroke-prone spontaneously hypertensive rat," *Journal of Hypertension*, vol. 4, no. 3, pp. S21–S24, 1986.

[30] N. Kato, T. Nabika, Y. Q. Liang et al., "Isolation of a chromosome 1 region affecting blood pressure and vascular disease traits in the stroke-prone rat model," *Hypertension*, vol. 42, no. 6, pp. 1191–1197, 2003.

[31] L. Naveri, C. Stromberg, and J. M. Saavedra, "Angiotensin II AT1 receptor mediated contraction of the perfused rat cerebral artery," *NeuroReport*, vol. 5, no. 17, pp. 2278–2280, 1994.

[32] Q. Xie and C. Nathan, "The high-output nitric oxide pathway: role and regulation," *Journal of Leukocyte Biology*, vol. 56, pp. 576–582, 1994.

[33] J. Johansson, L. Mannerås-Holm, R. Shao et al., "Electrical versus manual acupuncture stimulation in a rat model of polycystic ovary syndrome: different effects on muscle and fat tissue insulin signaling," *PLoS One*, vol. 8, no. 1, article e54357, 2013.

Hindawi Publishing Corporation
Evidence-Based Complementary and Alternative Medicine
Volume 2013, Article ID 291972, 10 pages
http://dx.doi.org/10.1155/2013/291972

Research Article

Spinal Serotonergic and Opioid Receptors Are Involved in Electroacupuncture-Induced Antinociception at Different Frequencies on ZuSanLi (ST 36) Acupoint

Chi-Chung Kuo,[1,2,3] Huei-Yann Tsai,[4] Jaung-Geng Lin,[5] Hong-Lin Su,[3] and Yuh-Fung Chen[4,6]

[1] *Department of Neurology, Tzu Chi General Hospital, Taichung Branch, Taichung 42743, Taiwan*
[2] *Department of Medicine, College of Medicine, Tzu Chi University, Hualien 97002, Taiwan*
[3] *Department of Life Sciences, National Chung Hsing University, Taichung 40227, Taiwan*
[4] *Department of Pharmacy, China Medical University Hospital, Taichung 40447, Taiwan*
[5] *Department of Chinese Medicine, College of Chinese Medicine, China Medical University, Taichung 40402, Taiwan*
[6] *Department of Pharmacology, College of Medicine, China Medical University, 91 Hsueh-Shih Road, Taichung 40402, Taiwan*

Correspondence should be addressed to Yuh-Fung Chen; yfchen@mail.cmu.edu.tw

Received 18 December 2012; Revised 18 February 2013; Accepted 25 February 2013

Academic Editor: Richard E. Harris

The present study was conducted to evaluate the effect of electroacupuncture-(EAc-) induced antinociception (EAA) at different currents and frequencies in rat spinal cord. We found that naloxone (0.05 μg i.t.) blocked EAA at different frequencies. Naltrindole (0.05 μg i.t.) blocked EAA on the 7th day after EAc of 100 Hz. 5,7-Dihydroxytryptamine (100 μg i.t.) significantly inhibited EAA at different frequencies on the 7th day after EAc. Pindobind (0.5 μg i.t.), a 5-HT_{1A} antagonist, notably attenuated EAA at different frequencies. Ketanserin (0.5 μg i.t.), inhibited EEA at a lower frequency (<10 Hz) than at a higher frequency (100 Hz). LY-278584 (0.5 μg i.t.) significantly inhibited EAA at a higher frequency (100 Hz) on the 7th day after EAc. The direction of effect of 8-OH-DPAT, on EAA was dependent on dosage. It had an inhibitory effect at a low dose (0.5 μg i.t.) and a high frequency (100 Hz) but enhanced EAA at a higher dose at lower frequencies (<10 Hz). DOI (10 μg, i.t.), did not affect EAA. These data indicate that the mechanism of EAA involves opioid receptors, and the serotonergic system, particularly, μ-, δ-opioid and 5-HT_{1A}, 5-HT_3 receptors and it is also dependent on the EAc frequency.

1. Introduction

Acupuncture, a traditional Chinese medicine, has been used to relieve pain for more than 2000 years, and it has been used in over 160 countries. Acupuncture has been proposed by an NIH consensus committee as a complementary medicine [1]. Treatment efficacy of acupuncture has been acknowledged worldwide. The physiological and biochemical mechanisms underlying acupuncture analgesia have been receiving increasing attention.

Analgesia by peripheral nerve stimulation, either transcutaneous nerve stimulation (TENS), acupuncture, or electroacupuncture (EAc), was demonstrated in anesthetized monkeys and in rodents [2–4]. In the spinal cord, substance P released by Aδ and C fiber while nociception entering the spinal cord posterior horn was blocked by naloxone. Not only substance P but also endorphin, encephalin, and dynorphin could be induced in the spinal cord. β-Endorphin predominantly synthetized in the arcuate nucleus of the hypothalamus has major analgesic effects via μ-, κ-opioid receptors in the periaqueductal gray region [5]. Enkephalins are ligands of both μ and δ receptors [6–8]. Dynorphin is a relatively specific ligand for κ receptors in the spinal cord of the rat [9].

Electroacupuncture antinociception (EAA) induced by low frequency may be mediated by endorphins. Effect of high frequency stimulation is not mediated by endorphin but may be due to either serotonin or dynorphins in the spinal

cord [10]. In previous studies, it was shown that 5-HT release from the spinal dorsal horn was significantly stimulated by somatostatin and substance P *in vitro*, but not by neurotensin or met-enkephalin [11]. The influence of EAc on serotonin release may cause activation of enkephalin-interneurons which presynaptically inhibit the primary sensory neurons in the spinal cord [12].

On the other hand, studies have shown that EAc-induced analgesia can be blocked by opioid receptor antagonists in human and animals [13–16]. One interpretation of those results is that an opioid mechanism is involved in mediating EAA. Antibody microinjection studies showed that 2/15 Hz EAA could be blocked by intrathecal (i.t.) injection of any one of the three categories of antibodies directed to met-enkephalin and leu-enkephalin [17], dynorphin A [18], and dynorphin B [9]. Moreover, different frequencies of EAc may be mediated by specific opioid receptors [19, 20].

Lumbar catheterization of the subarachnoid space in the spine is commonly used to study the rat spinal cord [21, 22]. The method (A-O method) involves freeing neck muscle from the occipital crest and sliding the catheter through a slit in the exposed atlanto-occipital (A-O) membrane, and caudally along the spinal cord [22]. Disadvantages of the A-O method are that some animals die during the first days after catheterization (3%–5%) and animals show signs of neurological impairment after implantation (10%–30%) [23–25]. In the present study, the operation procedure modified from Tsai et al. [11] was used to perform the intrathecal catheterization for drugs treatment when studying EAA.

2. Materials and Methods

2.1. Animals. Male Wistar rats weighing 240 to 260 g were purchased from National Taiwan University College of Medicine Laboratory Animal Center (NTU CMLAC). Animals were allowed at least 1 week of adaptation before the experiments, and they had free access to food and water. The laboratory had a 12 hr/12 hr light/dark cycle. The room temperature was controlled at 22 ± 1°C. The experimental protocol was approved by the Institutional Animal Care and Use Committee (IACUC), China Medical University, Protocol 101–250.

2.2. Drugs. Opioid receptor antagonists: naloxone, naltrindole (δ-opioid antagonist); serotonin neurotoxin: 5,7-dihydro xytryptamine (5,7-DHT); serotonin antagonists: pindobind (PDB, 5-HT1A antagonist), ketanserin tartrate (5-HT_2 antagonist), LY-278584 maleate (5-HT_3 antagonist), R(+)-8-hydroxy-dipropylaminotetralin (8-OH-DPAT, 5-HT_{1A} agonist), R(+)-2,5-dimethoxy-4-iodoamphetamine HCl (DOI, 5-$HT_{2/1C}$ agonist), 2-methylserotonin maleate (2-methyl-5-HT, 5-HT_3 agonist), all the aforementioned were from RBI Co., USA. Drugs were dissolved in artificial CSF (vehicle). The artificial CSF (ACSF) is a Krebs-bicarbonate solution (compositions: NaCl 120 mM, KCl 5 mM, $NaHCO_3$ 15 mM, $MgSO_4$ 1 mM, $CaCl_2$ 1.5 mM, and glucose 10 mM).

2.3. Intrathecal Catheterization. The operation procedures were modified from Tsai et al. [11]. The skin over the posterior cervical and lumbar region was shaved and prepared with povidone iodine (betadine). Rats were anesthetized with ether. The fifth spinal process was removed and the dura mater exposed. The dura was perforated with a short bevel no. 30-gauze needle, resulting in some leakage of CSF. A 16 cm in length polyethylene catheter (PE-10, i.d. 0.28 mm) previously filled with artificial CSF (ACSF) was immediately inserted 2 cm tangentially through the dura opening into the subarachnoid space, then anchored at the sixth spinal process with cyanoacrylic glue. The wound was irrigated with normal saline and closed in layers with silk streaks (no. 4). The left catheter was buried under the skin and the tip of catheter was threaded throughout the posterior cervical skin, also fixed with cyanoacrylic glue and tightened with silk threads (Figure 1).

2.4. The Acupoint, Electroacupuncture (EAc), and Tail-Flick Test. The procedure was carried out initially at 3 hrs after the rat recovered from ether anesthesia postintrathecal (i.t.) cannulation. Rats were placed in a transparent cylinder holder without body restriction. Acupuncture was performed by inserting fine stainless acupuncture needles (no. 36, 0.2 mm in diameter) at the bilateral acupoints ZuSanLi (ST36), 5 mm below the knee and 2 mm lateral to the tibia with 5 mm in depth. Electroacupuncture was applied with different currents (1 mA, 2 mA, and 3 mA) and different frequencies (2 Hz, 10 Hz, and 100 Hz) for 10 minutes using an electric stimulator (Coulbourn, C13-65). 1 mA current was chosen for the subsequent experiments in which drugs administration was held before electroacupuncture in this study.

The rat was placed in an acrylic holder to adapt for at least 15 minutes at ambient room temperature controlled at 22 ± 1°C. The pain threshold was determined by a tail-flick Analgesia Meter (Muromachi Kikai Co. MK-330). The nociceptive tail-flick (TF) reflex was evoked by noxious radiant heat (0.8 mm in diameter) by a 50 W projector lamp applied to the underside of the tail at 1 cm apart, with the distal site 2-3 cm from the end of the tail. TF latency was measured by a photocell timer circuit from the opening of a shutter until the rat withdrew its tail from the heat source. Intensity was set such that baseline TF latencies were typically between 2 and 4 seconds. The cut-off value of tail-flick latency was not over 10 seconds to avoid damaging the skin.

2.5. Experimental Protocol. The stable baseline TF latency was established in each experiment before intrathecal (i.t.) catheterization. Rats that exhibited neurological deficits or motor dysfunction following recovery from anesthesia after i.t. catheterization (described earlier) were sacrificed. The drugs were administered 2 minutes before electroacupuncture (except 5,7-DHT administered one week before experiments). 10 μL of drug or artificial CSF (vehicle) was injected via i.t. within 30 seconds, followed by flushing 10 μL of artificial CSF. The TF reflex latency was measured at 0, 15, 30, 60, 90, 120, and 150 minutes after a 10 min electroacupuncture.

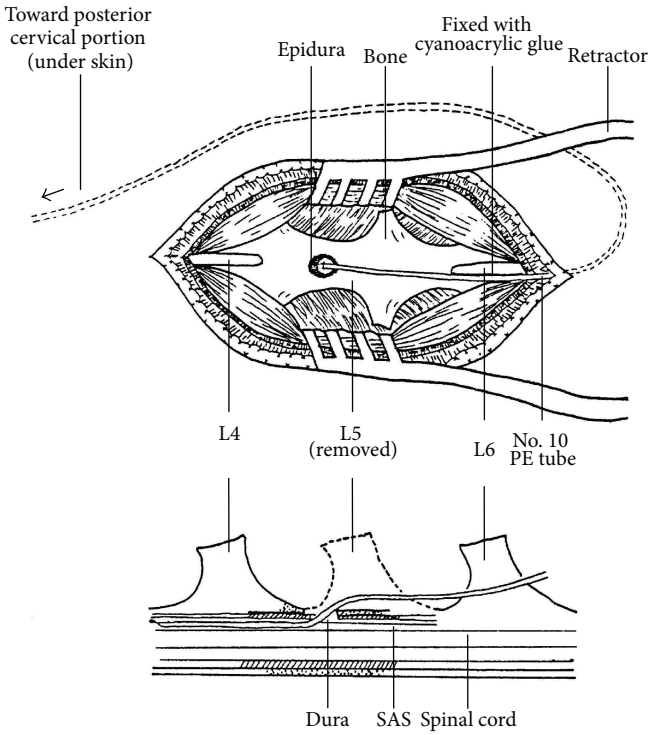

Figure 1: Diagram of intrathecal cannulation. A middle lumbar skin incision was performed, following the paravertebral muscle detached from the spinal process and retracted laterally. L5 spinal process was removed then opened the dura for exposing the spinal cord. The dura was perforated with a short bevel of no. 30 gauze needle following inserted 2 cm PE-10 into the subarachnoid space (SAS). A drop of cyanoacrylic glue was added for anchoring the PE-10 besides the L6 spinal process. The operation wound was irrigated with normal saline and closed in layers with silk streaks, no. 4.

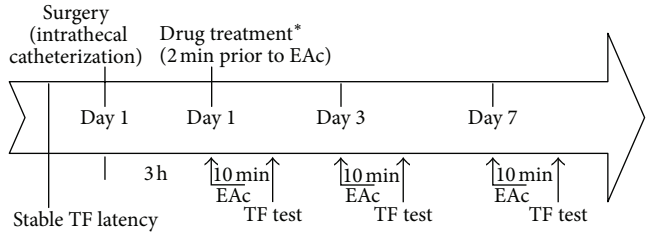

Figure 2: Schedule of drug treatment and experiment orders. Stable TF latency was carried out firstly before the surgery. EAc was performed 3 hrs after the rat recovered from ether anesthesia postintrathecal (i.t.) cannulation. Acupuncture was performed by inserting fine stainless acupuncture needles at bilateral acupoints ZuSanLi (ST36). EAc was applied with different currents (1 mA, 2 mA, and 3 mA) and different frequencies (2 Hz, 10 Hz, and 100 Hz) for 10 min, which was performed with electric stimulator. 1 mA current was chosen for the subsequent experiments in which drugs administration was held before electroacupuncture in this study. The pain threshold was determined by tail-flick Analgesia Meter. The basal TF latencies were typically between 2 and 4 seconds. EAc: electroacupuncture; *TF: tail-flick; 5,7-DHT: 5,7-dihydroxytryptamine, one week prior to EAc.

The same procedures (drugs administration, electroacupuncture, and TF latency measurement) were repeated on the 1st, 3rd, and 7th days after intrathecal catheterization was performed. Data for changes in TF latency are presented as percentage (%) change of pain threshold = [TF latency (after EAc) − baseline TF latency (before EAc)] × 100/[baseline TF latency (before EAc)]. The experimental protocol is shown in Figure 2.

2.6. Data and Statistical Analysis. Data were expressed as mean ± standard error (SE) and analyzed using one-way analysis of variance (ANOVA), followed by Scheffe's test. When the probability (P) was less than or equal to 0.05, differences were considered significant.

3. Results

3.1. The Effects of Electroacupuncture (EAc) at Different Frequencies on the 1st, 3rd, and 7th Days. The pain threshold increased by 51.41% in 30 minutes on the 1st day after 2 Hz, 1 mA EAc (Figure 3(a)). The antinociceptive effect occurred until 150 minutes after EAc. The pain threshold increased

Table 1: Effects of EAc in different currents on the 1st, 3rd, and 7th days.

Amp	Effect Percentage change of pain threshold Min						
	1st day						
	0 min	15 min	30 min	60 min	90 min	120 min	150 min
Control	−2.34 ± 3.96	−4.91 ± 2.56	−0.89 ± 3.44	−2.32 ± 2.77	−1.62 ± 2.47	−0.41 ± 3.52	2.73 ± 3.50
2 Hz, 1 mA	39.33 ± 5.14	44.60 ± 3.78	51.41 ± 4.49	41.64 ± 4.62	30.12 ± 5.94	30.78 ± 5.21	23.46 ± 3.99
2 mA	25.03 ± 6.88	28.97 ± 7.08	23.65 ± 6.25	25.71 ± 6.56	22.22 ± 3.40	18.55 ± 2.47	20.53 ± 2.67
3 mA	32.76 ± 14.96	9.40 ± 10.64	3.63 ± 11.61	2.57 ± 10.90	4.67 ± 8.96	11.07 ± 8.76	13.23 ± 7.76
10 Hz, 1 mA	30.68 ± 8.00	26.25 ± 7.92	37.47 ± 8.16	26.71 ± 6.39	27.38 ± 6.31	22.34 ± 5.38	20.65 ± 4.03
2 mA	17.30 ± 4.13	25.90 ± 3.78	28.72 ± 9.06	28.51 ± 8.02	26.92 ± 5.16	7.02 ± 3.77	2.37 ± 1.50
3 mA	10.58 ± 17.05	27.77 ± 7.04	13.87 ± 10.54	17.95 ± 9.68	16.40 ± 9.96	16.69 ± 8.80	16.62 ± 7.54
100 Hz, 1 mA	31.34 ± 10.43	22.05 ± 7.83	25.47 ± 8.81	19.96 ± 6.92	19.88 ± 7.69	23.14 ± 11.83	25.30 ± 9.13
2 mA	25.93 ± 8.17	20.27 ± 6.31	21.29 ± 7.47	14.54 ± 5.18	12.20 ± 5.03	2.31 ± 1.88	1.34 ± 3.24
3 mA	10.59 ± 10.34	3.78 ± 15.37	2.43 ± 14.96	−5.91 ± 6.01	−6.49 ± 9.32	−9.36 ± 6.79	−0.25 ± 5.29
	3rd day						
	0 min	15 min	30 min	60 min	90 min	120 min	150 min
Control	1.31 ± 2.74	1.09 ± 3.56	2.27 ± 3.63	0.03 ± 1.76	−1.42 ± 1.86	−0.96 ± 2.02	−0.97 ± 1.51
2 Hz, 1 mA	36.57 ± 5.46	28.70 ± 4.19	29.16 ± 6.49	25.19 ± 7.30	23.48 ± 6.10	19.30 ± 3.56	17.76 ± 4.54
2 mA	16.88 ± 4.01	17.66 ± 5.11	22.42 ± 3.86	11.78 ± 3.80	14.36 ± 3.62	16.53 ± 6.23	11.67 ± 7.02
3 mA	9.47 ± 8.53	4.01 ± 7.86	0.20 ± 9.56	−4.19 ± 6.64	−1.74 ± 5.01	2.98 ± 4.37	3.12 ± 4.07
10 Hz, 1 mA	32.53 ± 12.69	34.92 ± 6.99	61.73 ± 10.60	23.80 ± 5.49	27.27 ± 7.20	10.82 ± 3.75	12.41 ± 4.69
2 mA	22.21 ± 3.65	13.34 ± 5.82	16.51 ± 5.49	9.97 ± 5.26	4.32 ± 2.61	−0.87 ± 2.68	3.30 ± 4.53
3 mA	−5.36 ± 9.16	−3.85 ± 5.27	−5.38 ± 10.82	−9.10 ± 3.63	−6.81 ± 7.40	−2.76 ± 5.30	−2.73 ± 5.44
100 Hz, 1 mA	13.02 ± 9.21	28.95 ± 7.12	25.56 ± 7.96	19.35 ± 5.99	20.21 ± 7.46	16.44 ± 6.57	16.65 ± 6.40
2 mA	10.55 ± 3.38	16.18 ± 5.99	3.64 ± 3.01	5.43 ± 4.38	8.80 ± 3.51	−0.09 ± 3.60	0.69 ± 2.97
3 mA	18.32 ± 5.61	−2.27 ± 7.65	−5.62 ± 5.32	−0.30 ± 4.33	−0.13 ± 3.89	3.04 ± 3.90	3.63 ± 6.23
	7th day						
	0 min	15 min	30 min	60 min	90 min	120 min	150 min
Control	1.28 ± 2.83	1.05 ± 3.74	2.18 ± 3.68	0.05 ± 2.08	−1.38 ± 1.78	−0.94 ± 2.05	−0.94 ± 1.82
2 Hz, 1 mA	35.71 ± 5.33	36.47 ± 3.80	34.76 ± 5.79	35.38 ± 3.75	28.84 ± 3.82	28.08 ± 2.51	26.89 ± 6.12
2 mA	17.47 ± 3.78	12.43 ± 3.22	17.28 ± 3.85	9.98 ± 4.22	8.86 ± 4.91	3.36 ± 2.37	3.08 ± 3.49
3 mA	−1.93 ± 7.94	−4.40 ± 5.65	−2.61 ± 4.41	4.41 ± 6.80	−0.98 ± 3.22	−4.44 ± 4.35	2.06 ± 3.76
10 Hz, 1 mA	36.09 ± 5.90	35.30 ± 4.77	29.37 ± 7.23	29.23 ± 7.24	14.14 ± 3.86	9.52 ± 4.66	10.60 ± 4.23
2 mA	12.49 ± 2.31	8.92 ± 5.82	4.26 ± 5.29	5.07 ± 4.85	2.39 ± 3.71	4.08 ± 5.07	1.20 ± 3.62
3 mA	2.59 ± 1.84	−0.12 ± 5.12	−2.53 ± 3.44	−1.40 ± 3.67	−5.97 ± 4.91	3.89 ± 2.66	7.47 ± 4.41
100 Hz, 1 mA	7.80 ± 3.07	22.35 ± 6.00	29.82 ± 8.99	10.14 ± 3.16	14.32 ± 4.23	9.31 ± 2.89	13.80 ± 3.51
2 mA	8.35 ± 3.43	2.59 ± 1.71	1.72 ± 1.92	5.73 ± 3.48	20.47 ± 3.73	−1.43 ± 2.55	−3.41 ± 2.10
3 mA	25.43 ± 10.43	3.44 ± 5.76	−15.95 ± 4.78	−11.89 ± 4.11	−9.48 ± 2.67	8.59 ± 4.74	6.81 ± 5.90

Data are shown as mean ± S.E.

by 29.16% and 34.76% on the 3rd and 7th days, respectively. The duration of EAA revealed on the 3rd and 7th days was similar to the effect on the 1st day after intrathecal cannulation (Figures 3(b) and 3(c)). We also examined the effect of EAc at 2 mA and 3 mA. The pain threshold increased by 23.65% and 37.47% in 30 minutes and up to 150 min. Data on different currents and frequencies on the 1st, 3rd, and 7th days are shown in Table 1.

3.2. Effects of Naloxone and Naltrindole on EAc at Different Frequencies. Pretreatment with naloxone (0.05 μg/10 μL, i.t.), a μ-opioid antagonist, completely blocked the EAc-induced antinociception (EAA) at three different frequencies of EAc on the 1st, 3rd, and 7th days (Figures 4(a)–4(i)). Naltrindole (0.05 μg/10 μL, i.t.), a δ-opioid antagonist, significantly inhibited EAA at high (100 Hz) frequency on the 1st, 3rd, and 7th days (Figures 4(c), 4(f), and 4(i)).

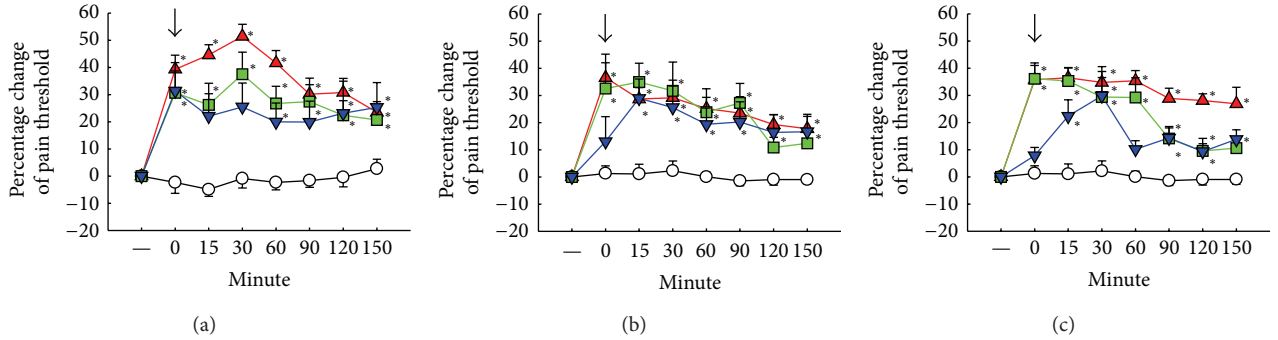

FIGURE 3: Antinociceptive effects of electroacupuncture (EAc) in different frequencies on the 1st, 3rd and 7th days after intrathecal cannulation by tail-flick test. ↓: initiation point of EAc except sham group. ○: sham group. ▲: 2 Hz, 1 mA. ▼: 10 Hz, 1 mA. ■: 100 Hz, 1 mA. (a) Determined on 1st day; (b) determined on 3rd day; (c) determined on 7th day (described as text). Data are shown as mean ± S.E. $^{*}P < 0.05$ compared with sham group ($n = 10$).

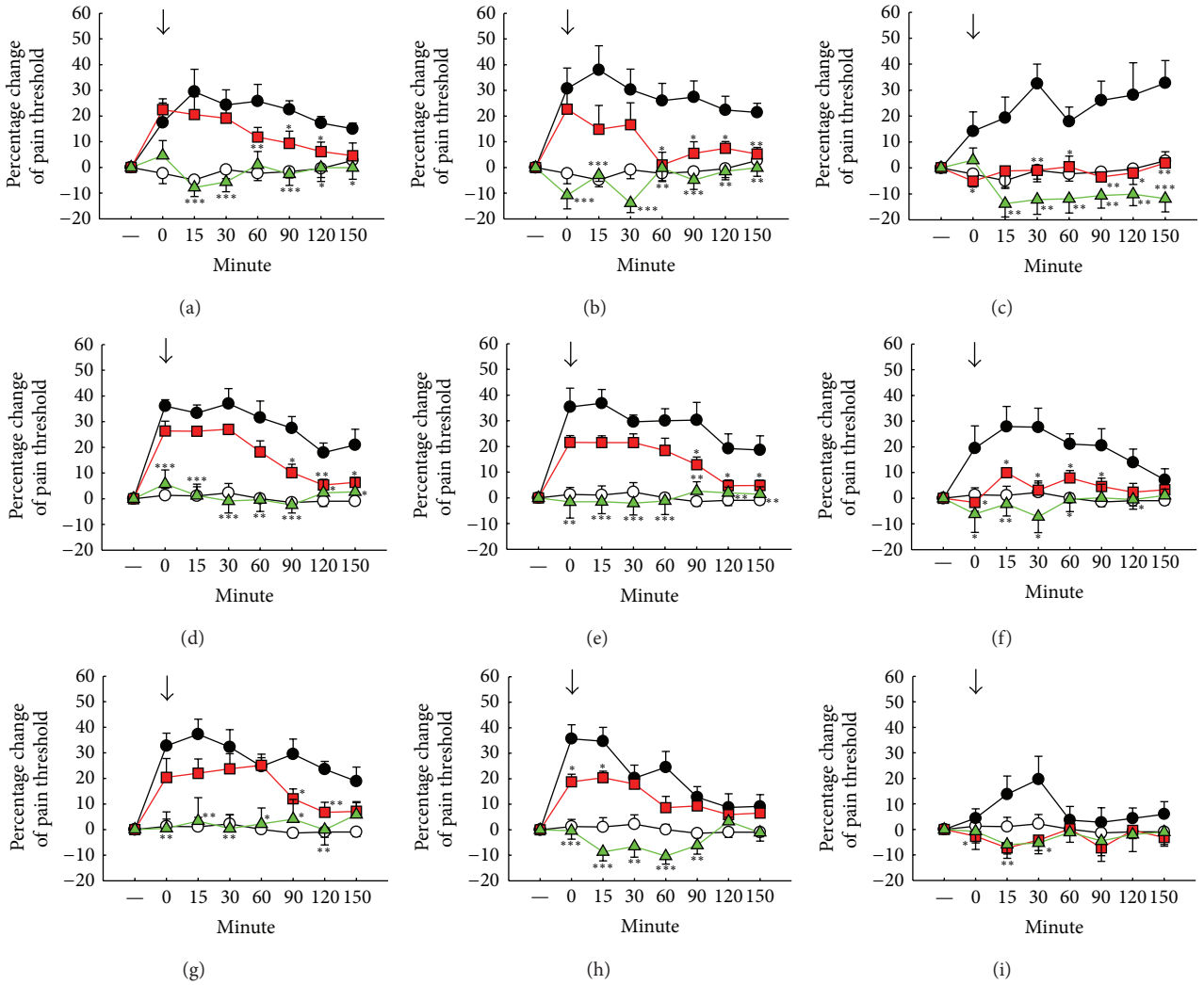

FIGURE 4: Pretreatment with opioid antagonists influences EAc-induced antinociception in different frequencies on the 1st (a, b, c), 3rd (d, e, f), and 7th (g, h, i) days after intrathecal cannulation. (a), (d), (g): 1 mA, 2 Hz EAc; (b), (e), (h): 1 mA, 10 Hz EAc; (c), (f), (i): 1 mA, 100 Hz EAc; ↓: initiation point of EAc except sham group. ○: sham group. ●: ACSF: artificial CSF. ▲: naloxone (0.05 μg/10 μL, i.t.). ■: naltrindole (0.05 μg/10 μL, i.t.). Data are shown as mean ± S.E. $^{*}P < 0.05$, $^{**}P < 0.01$, and $^{***}P < 0.001$ compared to the ACSF group ($n = 10$).

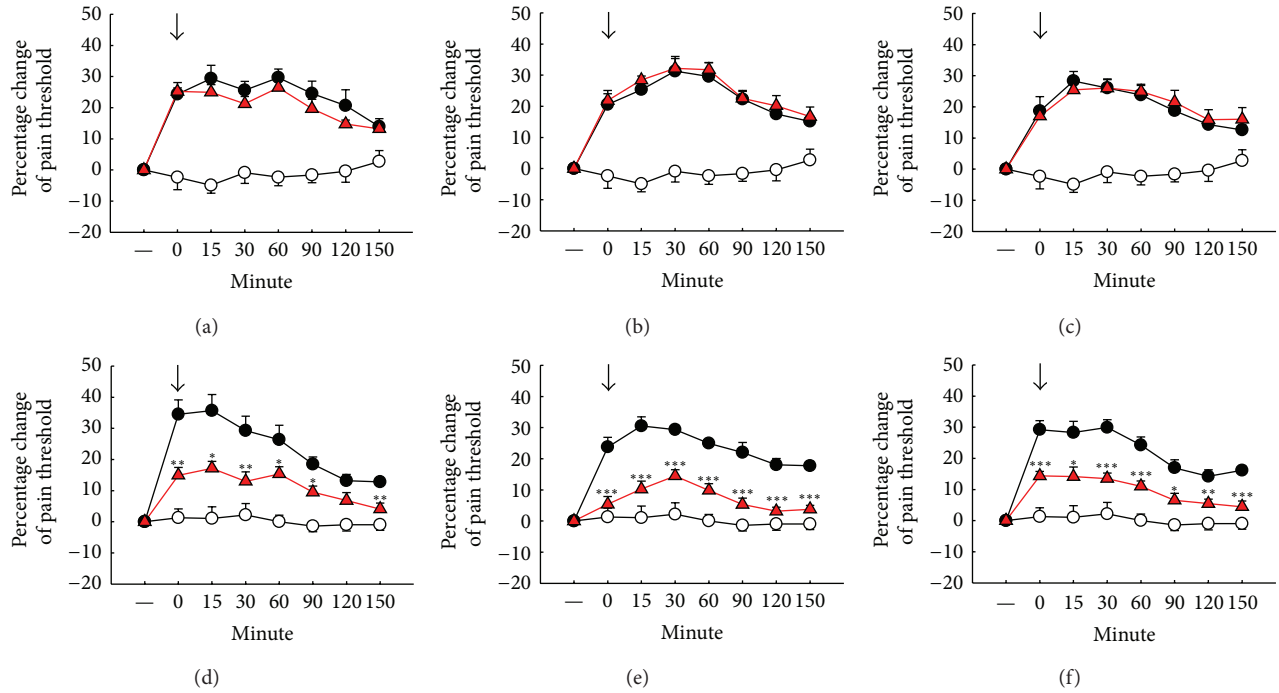

FIGURE 5: Pretreatment with 5,7-DHT influences EAc-induced antinociception in different frequencies on the 1st (a, b, c) and 7th (d, e, f) days. (a), (d): 1 mA, 2 Hz EAc; (b), (e): 1 mA, 10 Hz EAc; (c), (f): 1 mA, 100 Hz EAc; ↓: initiation point of EAc except sham group. ○: sham group. ●: ACSF (artificial CSF). ▲: 5, 7-DHT (5,7-dihydroxy tryptamine, serotonin neurotoxin, 100 μg/10 μL, i.t.). Data are shown as mean ± S.E. $^{*}P < 0.05$, $^{**}P < 0.01$, and $^{***}P < 0.001$ compared to the ACSF group ($n = 10$).

3.3. Effects of 5,7-Dihydroxytryptamine (5,7-DHT) Pretreatment on EAc at Different Frequencies. The pain threshold of EAc was not affected by 5,7-DHT (100 μg/10 μL) on the 1st day at different EAc frequencies of (Figures 5(a)–5(c)). Until one week after treatment with 5,7-DHT, the pain threshold of EAc was significantly inhibited by 5,7-DHT on the 7th day at three different frequencies (Figures 5(d)–5(f)).

3.4. Effects of 5-HT Antagonists on EAc at Different Frequencies. Figure 6 shows effects of pretreatment with 5-HT antagonists on EAc. Pindobind-5-HT_{1A} (PDB, 5-HT_{1A} antagonist, 0.5 μg/10 μL, i.t.) markedly blocked EAA at different frequencies on the 1st, 3rd, and 7th days (Figures 6(a)–6(i)). Pretreatment with ketanserin (5-HT_2 antagonist, 0.5 μg/10 μL, i.t.) reduced EAA at a lower frequency (<10 Hz) of EAc on the 1st, 3rd, and 7th days (Figures 6(a), 6(b), 6(c), 6(d), 6(g), and 6(h)). LY-278584 (5-HT_3 antagonist, 0.5 μg/10 μL) significantly inhibited high frequency EAA on the 1st, 3rd, and 7th days (Figures 6(c), 6(f), and 6(i)).

3.5. Effects of 5-HT_{1A} Agonist, 8-OH-DPAT on EAc at Different Frequencies. 8-OH-DPAT (DPAT), a 5-HT_{1A} agonist, inhibited EAA which was dependent on DPAT dose and EAc. DPAT (0.5 μg/10 μL, i.t.) inhibited the EAA at a high frequency (100 Hz) of EAc on the 1st, 3rd, and 7th days (Figures 7(c), 7(f), and 7(i)). However, a concentration of DPAT greater than 1 μg/10 μL (i.t.) potentiated the EAA at a lower frequency (<10 Hz) of EAc (Figures 7(a), 7(b), 7(d), 7(e), and 7(g)).

3.6. Effects of 5-HT_2 and 5-HT_3 Agonists on the EAc at Different Frequencies. R(+)-2,5-dimethoxy-4-iodoamphetamine HCl (10 μg/10 μL, i.t.), a 5-$HT_{2/1C}$ agonist, did not significantly affect EAA at different frequencies. However, pretreatment with 2-methy-5-HT (50 μg/10 μL, i.t.), a 5-HT_3 agonist, enhanced EAA at a lower frequency (<10 Hz) (Figures 8(a), 8(b), 8(d), 8(e), 8(g), and 8(h)).

4. Discussion

There has been increasing attention given to the use of EAc for treating pain both experimentally and clinically. Low and high electrical frequencies are an important component of EAc. A very low frequency of EAc at 0.4 Hz did not produce a desired analgesic effect, whereas 4 Hz or 200 Hz EAc could induce considerable analgesia [10]. In the present study, the relative lower frequencies of EAc (<10 Hz) may provide more stable and longer duration of antinociception when compared with a high EAc frequency (100 Hz). Similar results were present in another study that applied 2 Hz or 100 Hz EAc [26]. We found that EAA could be reobtained on different days in the present study. Similarly, repeated electroacupuncture had a cumulative effect on analgesia that may be associated with regulation of the hypothalamus-pituitary axis [27].

Earlier studies reported that μ- and δ-receptors were involved in EAc analgesia at a low frequency (2/15 Hz) [19, 20]. In the present study, the administration of drugs was intrathecally directed into the rat spinal cord. Effect of

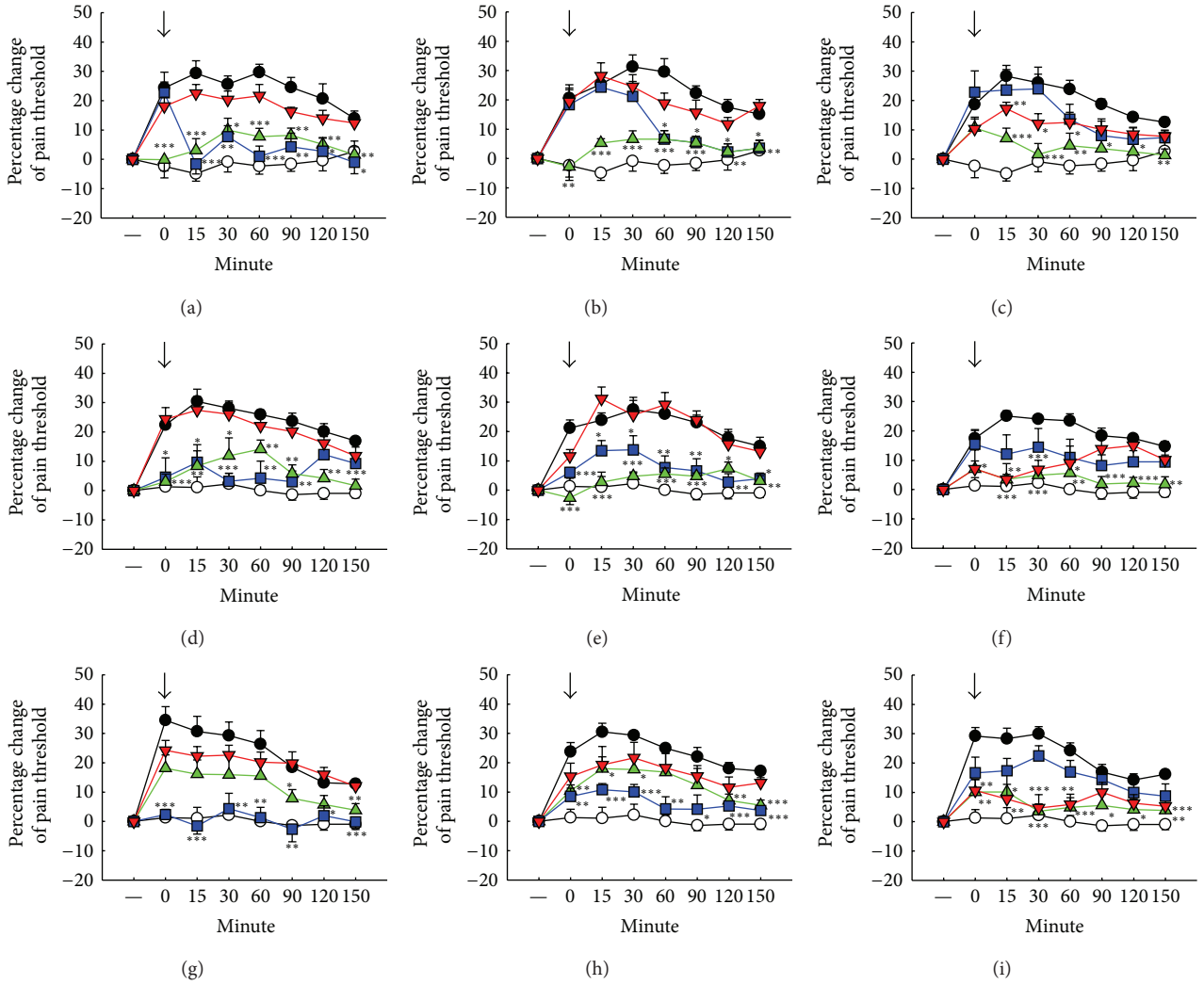

FIGURE 6: Pretreatment with 5-HT antagonist influences EAc-induced antinociception in different frequencies on the 1st (a, b, c), 3rd (d, e, f), and 7th (g, h, i) days. (a), (d), (g): 1 mA, 2 Hz EAc; (b), (e), (h): 1 mA, 10 Hz EAc; (c), (f), (i): 1 mA, 100 Hz EAc, ↓: initiation point of EAc except sham group. ○: sham group; ●: ACSF (artificial CSF). ▲: PDB: (pindobind, 5-HT_{1A} antagonist, 0.5 μg/10 μL, i.t.). ■: KTS (ketanserin, 5-HT_2 antagonist 0.5 μg/10 μL, i.t.). ▼: LY-278584 (5-HT_3 antagonist, 0.5 μg/10 μL, i.t.). Data are shown as mean ± S.E. $^{*}P < 0.05$, $^{**}P < 0.01$, and $^{***}P < 0.001$ compared to the ACSF group ($n = 10$).

drugs on EAA was determined by the tail-flick test. Naloxone, a μ-antagonist, completely abolished the EAA at different electrical frequencies. However, the δ-receptor participated in the EAA when the frequency of EAc was more than 100 Hz. The results were similar to a previous report [28]. Data from the present study suggested that EAA occurred via μ-opioid receptors at a low frequency (<10 Hz) and that activation of δ-opioid receptors was at a high frequency (100).

The present study also examined the role of the serotonergic pathway in mediating effect of EAc. EAA was blocked by pindobind, a 5-HT_{1A} antagonist, and by ketanserin, a 5-HT_2 antagonist at a low frequency (<10 Hz), and by LY-278584, a 5-HT_3 antagonist at a high frequency (100 Hz). On the other hand, EAA was potentiated by DPTA, a 5-HT_{1A} agonist at a high dose (>1 μg), and by 2-methyl-5-HT, a 5-HT_3 agonist at a low frequency (<10 Hz). Therefore, the effect of DPTA on EAA was dependent on drug dosage. It has been suggested that DPTA could decrease the turnover rate of 5-HT in presynaptic serotonergic neurons at a low dose (0.05 mg/kg, s.c.) and stimulate 5-HT receptors at a high dose (1.0 mg/kg) [29]. 2-Methyl-5-HT is not a selective 5-HT_3 receptor agonist but is associated with 5-HT_4 in pain pathway [30]. However, DOI, a 5-$HT_{2/1C}$, did not affect EAA in this study. These findings suggest that the 5-HT_{1A} and 5-HT_3 receptors may mediate predominantly EAA elicited at low EAc frequencies. There is evidence that brain serotonergic pathways, involving 5-HT_1 and 5-HT_3 receptors, contribute to the antinociceptive effect of EAc that 5-HT_2 may have a nociceptive function [31].

We found that 5,7-DHT (5,7-dihydroxytryptamine) reduced EAA up to 7 days following EAc. It has been reported that 5,7-DHT-induced lesions of the spinal cord serotonergic pathways reduced spinal cord 5-HT concentrations by 70%

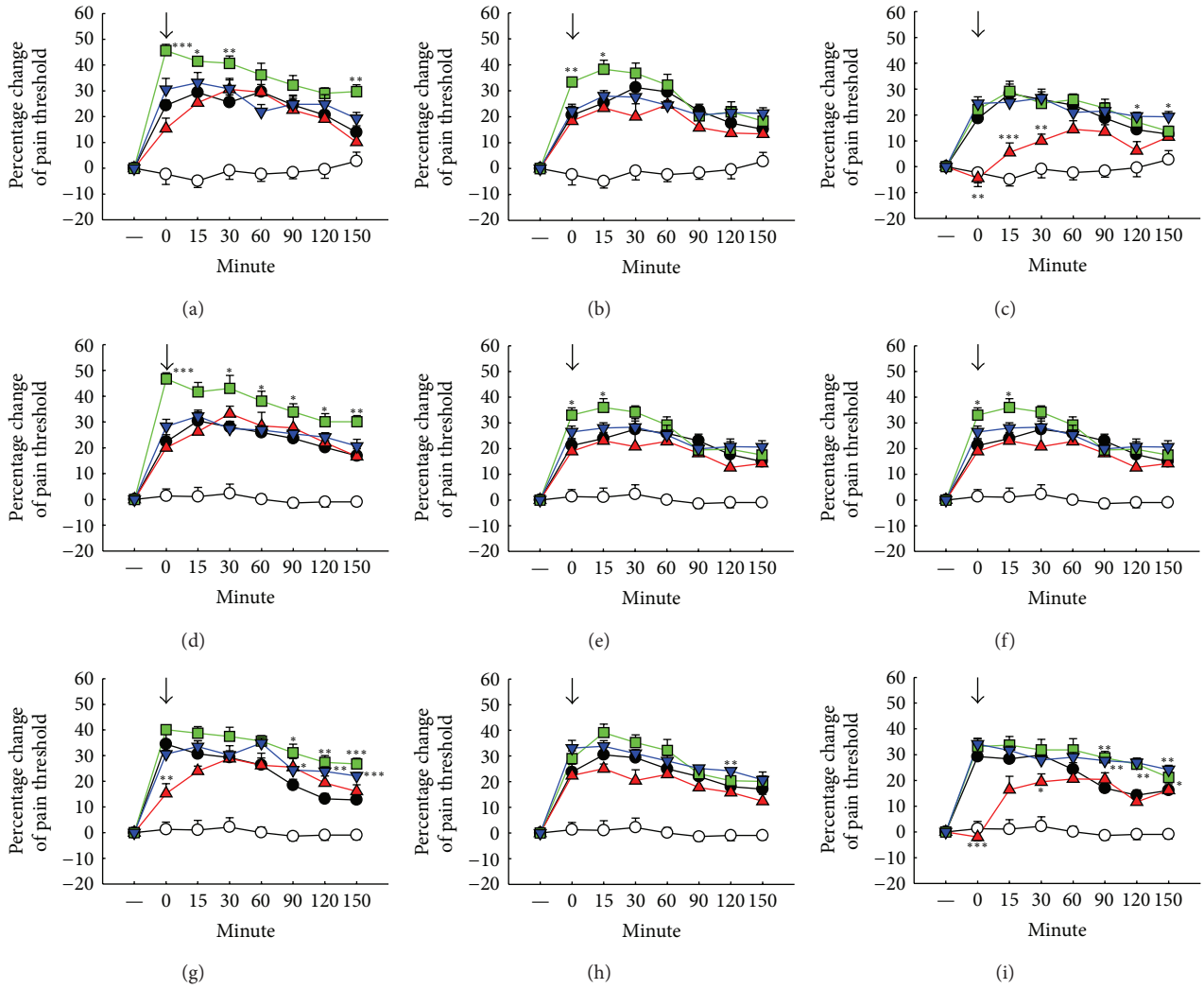

FIGURE 7: Pretreatment with 8-OH-DPAT influences EAc-induced antinociception in different frequencies on the 1st (a, b, c), 3rd (d, e, f), and 7th (g, h, i) days after intrathecal cannulation. (a), (d), (g): 1 mA, 2 Hz EAc; (b), (e), (h): 1 mA, 10 Hz EAc; (c), (f), (i): 1 mA, 100 Hz EAc, ↓: initiation point of EAc except sham group. ○: sham group. ●: ACSF (artificial CSF). ▲: 8-OH-DPAT (DPAT, 5-HT_{1A} agonist, 0.5 μg/10 μL, i.t.). ■: DPAT (1 μg/10 μL, i. t.); ▼: DPAT (2 μg/10 μL, i.t.). Data are shown as mean ± S.E. $^{*}P < 0.05$, $^{**}P < 0.01$, and $^{***}P < 0.001$ compared to the ACSF group ($n = 10$).

and notably reduced morphine analgesia as determined by the tail-flick test [32]. The delayed effect of 5,7-DHT on EAA may be related to its neurotoxic effect on serotonergic neuron.

The involvement of mu- and delta-opioid receptors as well as serotonin receptors has been previously described. The present study showed that EAc induced analgesia involvement serotonergic and opioid receptors at the superacute, acute, and subacute stages (1, 3, 7 days) of electroacupuncture-induced analgesia. We also found that responses of different serotonergic and opioid receptor subtypes were associated with electroacupuncture electrical frequencies. Lumbar catheterization of the subarachnoid space in the spine is commonly used in research to study spinal cord functions in rat models which can have a confounding effect on experimental outcomes. Direct lumbar catheterization has several advantages compared with the A-O method, such as decreasing the neurological disturbance and the interference with nociceptive functions of the spinal cord. In the present study, none of the animals died and no detectable signs of neurological impairment were detected after intrathecal catheterization.

We found that the μ opioid receptor participated at three different EAc frequencies, whereas the δ receptor was effective at a high EAc frequency (100 Hz). The 5-HT_{1A} and 5-HT_3 receptors were involved in EAA. 5-HT_{1A} agonist enhanced EAA which was significantly inhibited by 5-HT_{1A} antagonists. We did find that serotonergic and opioid receptors were involved at the superacute, acute, and subacute stage (1, 3, and 7 days) of electroacupuncture analgesia, and those receptors contributed to the antinociceptive effect of EAc. Although the sensitivities of various receptors to the low- and

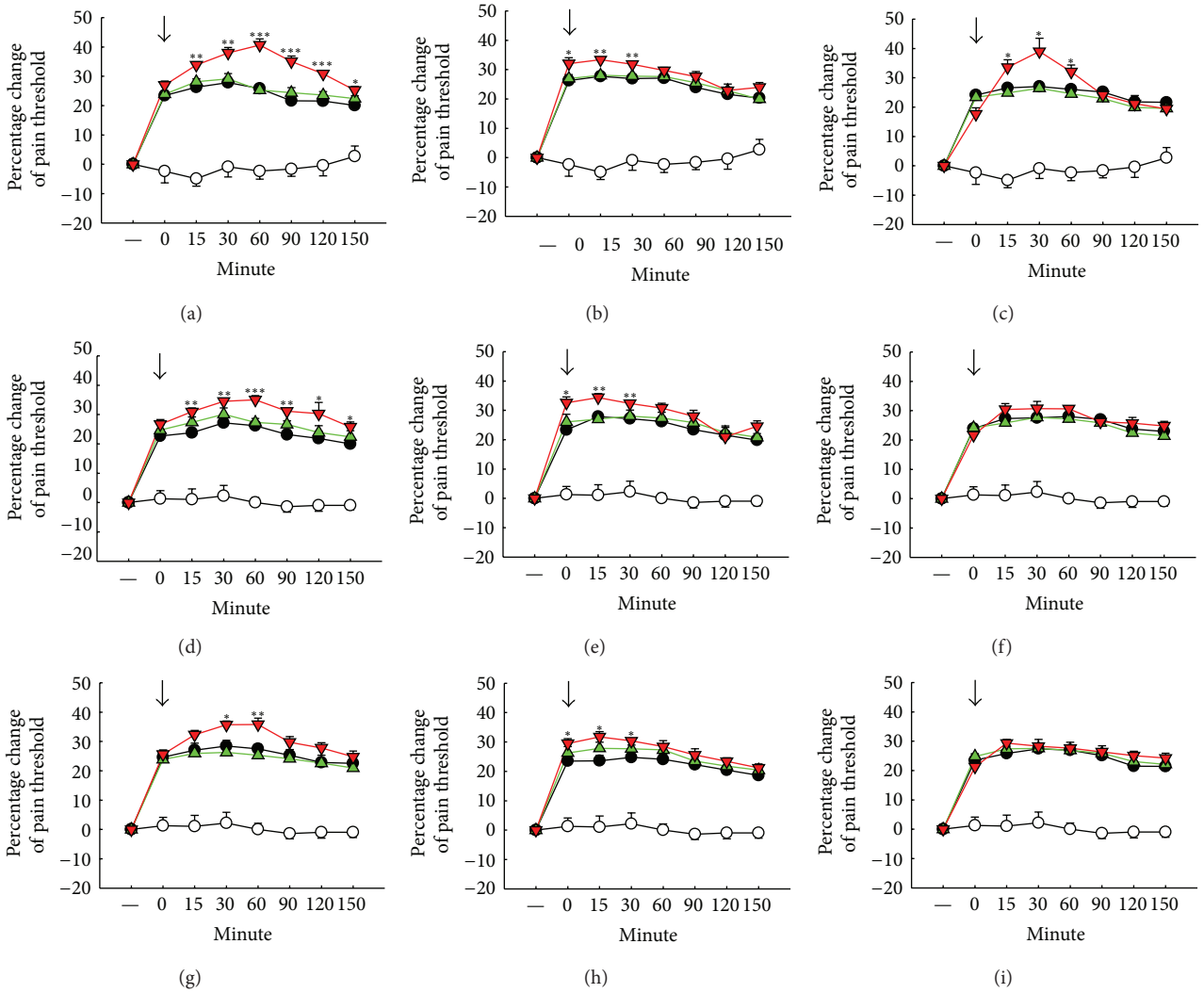

FIGURE 8: Pretreatment with 5-HT agonists influences EAc-induced antinociception in different frequencies on the 1st (a, b, c), 3rd (d, e, f), and 7th (g, h, i) days after intrathecal cannulation. (a), (d), (g): 1 mA, 2 Hz EAc; (b), (e), (h): 1 mA, 10 Hz EAc; (c), (f), (i): 1 mA, 100 Hz EAc; ↓: initiation point of EAc except sham group. ○: sham group. ●: ACSF (artificial CSF). ▲: DOI (R(+)-2,5-dimethoxy- 4-iodoamphetamine HCl, 5-$HT_{2/1C}$ agonist, 10 μg/10 μL, i.t.). ▼: 2-methyl-5-HT (2-methylserotonin maleate, 5-HT_3 agonist, 50 μg/10 μL, i.t.). Data are shown as mean ± S.E. $^{*}P < 0.05$, $^{**}P < 0.01$, and $^{***}P < 0.001$ compared to the ACSF group ($n = 10$).

high-frequency EAc are slightly different, the mechanisms of EAA are closely related to the activation of serotonergic and opioid neurons in spinal cord.

Acknowledgments

The authors would like to thank Professor W. Gibson Wood from Department of Pharmacology, University of Minnesota, USA, for his helpful comments and proofreading this revised paper. This work was partially supported by Grants from the National Science Council (NSC-101-2320-B-039-026) and Tzu Chi General Hospital (TCCRD-9811), Taiwan.

References

[1] National Institutes of Health, "Acupuncture," *NIH Consensus Statement*, vol. 15, no. 5, pp. 1–34, 1997.

[2] B. Pomeranz and D. Paley, "Electroacupuncture hypalgesia is mediated by afferent nerve impulses: an electrophysiological study in mice," *Experimental Neurology*, vol. 66, no. 2, pp. 398–402, 1979.

[3] K. Toda, "Effects of electro-acupuncture on rat jaw opening refelx elicited by tooth pulp stimulation," *Japanese Journal of Physiology*, vol. 28, no. 4, pp. 458–497, 1978.

[4] K. Toda, H. Suda, M. Ichioka, and A. Iriki, "Local electrical stimulation: effective needling points for suppressing jaw opening reflex in rat," *Pain*, vol. 9, no. 2, pp. 199–207, 1980.

[5] L. F. Tseng and K. A. Collins, "The tail-flick inhibition induced by β-endorphin administered intrathecally is mediated by activation of κ- and μ-opioid receptors in the mouse," *European Journal of Pharmacology*, vol. 214, no. 1, pp. 59–65, 1992.

[6] J. A. H. Lord, A. A. Waterfield, J. Hughes, and H. W. Kosterlitz, "Endogenous opioid peptides: multiple agonists and receptors," *Nature*, vol. 267, no. 5611, pp. 495–499, 1977.

[7] H. W. Kosterlitz, J. A. H. Lord, S. J. Paterson, and A. A. Waterfield, "Effects of changes in the structure of enkephalins and of narcotic analgesic drugs on their interactions with μ- and δ-receptors," *British Journal of Pharmacology*, vol. 68, no. 2, pp. 333–342, 1980.

[8] J. Magnan, S. J. Paterson, and H. W. Kosterlitz, "The interaction of [Met^5]enkephalin and [Leu^5]enkephalin sequences, extended at the C-terminus, with the μ-, δ- and κ-binding sites in the guinea-pig brain," *Life Sciences*, vol. 31, no. 12-13, pp. 1359–1361, 1982.

[9] G. X. Xie and J. S. Han, "Dynorphin: analgesic effect via kappa receptors in spinal cord of rats," *Zhongguo Yao Li Xue Bao*, vol. 5, no. 4, pp. 231–234, 1984.

[10] R. S. S. Cheng and B. Pomeranz, "Electroacupuncture analgesia could be mediated by at least two pain-relieving mechanisms; endorphin and non-endorphin systems," *Life Sciences*, vol. 25, no. 23, pp. 1957–1962, 1979.

[11] H. Y. Tsai, S. Maeda, K. Iwatsubo, and R. Inoki, "Effect of neuroactive peptides on labeled 5-hydroxytryptamine release from rat spinal slices in vitro," *Japanese Journal of Pharmacology*, vol. 35, no. 4, pp. 403–406, 1984.

[12] H. Y. Tsai, J. G. Lin, and R. Inoki, "Further evidence for possible analgesic mechanism of electroacupuncture: effects on neuropeptides and serotonergic neurons in rat spinal cord," *Japanese Journal of Pharmacology*, vol. 49, no. 2, pp. 181–185, 1989.

[13] B. Pomeranz and D. Chiu, "Naloxone blockade of acupuncture analgesia: endorphin implicated," *Life Sciences*, vol. 19, no. 11, pp. 1757–1762, 1976.

[14] D. J. Mayer, D. D. Price, and A. Rafii, "Antagonism of acupuncture analgesia in man by the narcotic antagonist naloxone," *Brain Research*, vol. 121, no. 2, pp. 368–372, 1977.

[15] B. H. Sjolund and M. B. E. Eriksson, "The influence of naloxone on analgesia produced by peripheral conditioning stimulation," *Brain Research*, vol. 173, no. 2, pp. 295–301, 1979.

[16] J. S. Han, X. Z. Ding, and S. G. Fan, "Frequency as the cardinal determinant for electroacupuncture analgesia to be reversed by opioid antagonists," *Sheng Li Xue Bao*, vol. 38, no. 5, pp. 475–482, 1986.

[17] J. S. Han, G. X. Xie, Z. F. Zhou, R. Folkesson, and L. Terenius, "Enkephalin and beta-endorphin as mediators of electroacupuncture analgesia in rabbits: an antiserum microinjection study," *Advances in Biochemical Psychopharmacology*, vol. 33, pp. 369–377, 1982.

[18] J. S. Han and C. W. Xie, "Dynorphin: potent analgesic effect in spinal cord of the rat," *Scientia Sinica B*, vol. 27, no. 2, pp. 169–177, 1984.

[19] X. H. Chen and J. S. Han, "All three types of opioid receptors in the spinal cord are important for 2/15 Hz electroacupuncture analgesia," *European Journal of Pharmacology*, vol. 211, no. 2, pp. 203–210, 1992.

[20] X. H. Chen and J. S. Han, "Analgesia induced by electroacupuncture of different frequencies is mediated by different types of opioid receptors: another cross-tolerance study," *Behavioural Brain Research*, vol. 47, no. 2, pp. 143–149, 1992.

[21] T. L. Yaksh and T. A. Rudy, "Chronic catheterization of the spinal subarachnoid space," *Physiology and Behavior*, vol. 17, no. 6, pp. 1031–1036, 1976.

[22] R. M. LoPachin, T. A. Rudy, and T. L. Yaksh, "An improved method for chronic catheterization of the rat spinal subarachnoid space," *Physiology and Behavior*, vol. 27, no. 3, pp. 559–561, 1981.

[23] P. Schoeffler, P. Auroy, J. E. Bazin, J. Taxi, and A. Woda, "Subarachnoid midazolam: histologic study in rats and report of its effect on chronic pain in humans," *Regional Anesthesia*, vol. 16, no. 6, pp. 329–332, 1991.

[24] Y. Igawa, K. E. Andersson, C. Post, B. Uvelius, and A. Mattiasson, "A rat model for investigation of spinal mechanisms in detrusor instability associated with infravesical outflow obstruction," *Urological Research*, vol. 21, no. 4, pp. 239–244, 1993.

[25] J. D. Kristensen, C. Post, T. Gordh Jr., and B. A. Svensson, "Spinal cord morphology and antinociception after chronic intrathecal administration of excitatory amino acid antagonists in the rat," *Pain*, vol. 54, no. 3, pp. 309–316, 1993.

[26] J. R. T. Silva, M. L. Silva, and W. A. Prado, "Analgesia induced by 2- or 100-Hz electroacupuncture in the rat tail-flick test depends on the activation of different descending pain inhibitory mechanisms," *Journal of Pain*, vol. 12, no. 1, pp. 51–60, 2011.

[27] J. L. Liu, S. P. Chen, Y. H. Gao, F. Y. Meng, S. B. Wang, and J. Y. Wang, "Effects of repeated electroacupuncture on β-endorphin and adrencorticotropic hormone levels in the hypothalamus and pituitary in rats with chronic pain and ovariectomy," *Chinese Journal of Integrative Medicine*, vol. 16, no. 4, pp. 315–323, 2010.

[28] K. A. Sluka, M. Deacon, A. Stibal, S. Strissel, and A. Terpstra, "Spinal blockade of opioid receptors prevents the analgesia produced by TENS in arthritic rats," *The Journal of Pharmacology and Experimental Therapeutics*, vol. 289, no. 2, pp. 840–846, 1999.

[29] L. G. Larsson, L. Renyi, S. B. Ross, and S. K. Angeby-Moller and, "Different effects on the responses of functional pre- and postsynaptic 5-HT$_{1A}$ receptors by repeated treatment of rats with the 5-HT$_{1A}$ receptor agonist 8-OH-DPAT," *Neuropharmacology*, vol. 29, no. 2, pp. 85–91, 1990.

[30] D. A. Craig, R. M. Eglen, L. K. M. Walsh, L. A. Perkins, R. L. Whiting, and D. E. Clarke, "5-methoxytryptamine and 2-methyl-5-hydroxytryptamine-induced desensitization as a discriminative tool for the 5-HT3 and putative 5-HT4 receptors in guinea pig ileum," *Naunyn-Schmiedeberg's Archives of Pharmacology*, vol. 342, no. 1, pp. 9–16, 1990.

[31] F. C. Chang, H. Y. Tsai, M. C. Yu, P. L. Yi, and J. G. Lin, "The central serotonergic system mediates the analgesic effect of electroacupuncture on ZUSANLI (ST36) acupoints," *Journal of Biomedical Science*, vol. 11, no. 2, pp. 179–185, 2004.

[32] J. F. Deakin and J. O. Dostrovsky, "Involvement of the periaqueductal grey matter and spinal 5-hydroxytryptaminergic pathways in morphine analgesia," *British Journal of Pharmacology*, vol. 63, no. 1, pp. 159–165, 1978.

Hindawi Publishing Corporation
Evidence-Based Complementary and Alternative Medicine
Volume 2013, Article ID 429186, 13 pages
http://dx.doi.org/10.1155/2013/429186

Research Article

The Possible Neuronal Mechanism of Acupuncture: Morphological Evidence of the Neuronal Connection between Groin A-Shi Point and Uterus

Chun-Yen Chen,[1] Rey-Shyong Chern,[2] Ming-Huei Liao,[2] Yung-Hsien Chang,[3] Jung-Yu C. Hsu,[1] and Chi-Hsien Chien[2]

[1] *Department of Cell Biology and Anatomy, College of Medicine, National Cheng-Kung University, Tainan, Taiwan*
[2] *Graduate Institute and Department of Veterinary Medicine, College of Veterinary Medicine, National Pingtung University of Science and Technology, 1, Shuefu Road, Neipu, Pingtung 912, Taiwan*
[3] *Graduate Institute of Chinese Medical Science, China Medical University, Taichung, Taiwan*

Correspondence should be addressed to Chi-Hsien Chien; chdvm@mail.npust.edu.tw

Received 8 November 2012; Accepted 25 January 2013

Academic Editor: Lixing Lao

Somatovisceral reflex suggested that the somatic stimulation could affect visceral function like acupuncture which treats diseases by stimulating acupoints. The neuronal connection between somatic point and visceral organ was not clear. Uterine pain referred to the groin region has long been recognized clinically. Wesselmann, using neurogenic plasma extravasation method, showed that uterine pain was referred to the groin region through a neuronal mechanism (Wesselmann and Lai 1997). This connection could be considered through the somatovisceral reflex pathway. However, the relay center of this pathway is still not clearly identified. In the present study, bee venom was injected in the groin region to induce central Fos expression to map the sensory innervation of groin region. Pseudorabies virus (PrV), a transneuronal tracer, was injected in the uterus to identify the higher motor control of the uterus. Immunohistochemistry staining revealed the Fos expression and PrV-infected double-labeled neurons in the nucleus of solitary tract (NTS), the dorsal motor nucleus of vagus (DMX), and the paraventricular hypothalamic nucleus (PVN). These results suggest a somatoparasympathetic neuronal connection (groin-spinal dorsal horn-NTS/DMX-uterus) and a somatosympathetic neuronal connection (groin-spinal dorsal horn-NTS-PVN-uterus). These two neuronal connections could be the prerequisites to the neuronal basis of the somatovisceral reflex and also the neuronal mechanism of acupuncture.

1. Introduction

The somatovisceral reflex was mentioned by Sato in 1995 and suggested that somatic stimulation could evoke sympathetic reflex response and, thereby, modulate functioning of visceral organ [1]. This phenomenon is in some way alike acupuncture that stimulates specific somatic points to relieve pain and treat many different diseases [2]. Many studies have shown that acupuncture can significantly modulate visceral function by stimulating specific acupoints [3–8]. Previous research suggested that the activation of the somatosensory pathway played an important role in the physiological effects of acupuncture [9]. Li et al.'s research showed that electroacupuncture-like stimulation diminishes regional myocardial ischemia triggered by sympathetical excitation [7]. Other studies have shown that electroacupuncture-like stimulation can activate a sympathetic inhibitory system in the brain to regulate cardiovascular responses [5, 10, 11]. Both the somatovisceral reflex and acupuncture stimulation suggest the neuronal connection between somatic acupoint and its corresponding organ. However, the neuronal connection of the somatovisceral reflex or acupuncture is still not clear.

Pervious report demonstrated that gynecological pain induced by dysmenorrhea, ascending genital infection, or cystic or hemorrhagic ovarian pathology usually refer pain to the low back, thighs, and abdominal wall [12]. Referred pain in the low back and abdominal wall was also reported by women in labor [13]. These reports suggested that the groin

region can account to the pain of uterine inflammation or diseases. According to traditional Chinese medicine, some acupoints, called A-shi points, do not have fixed specific locations and are usually pain-associated points [14–16]. Therefore, the groin region could be the A-shi point related to the uterus. In 1997, Wesselmann and Lai found that uterine inflammation in rats pretreated with Evans Blue Dye resulted in neurogenic plasma extravasation of dye in the skin over the abdomen, lower back, thighs, and groin, after antidromic stimulation of peripheral nerves [17]. This result suggested the possibility of a somatovisceral neural connection between the uterus and groin areas. Although these findings confirm the existence of a neural connection between the uterus and groin region, the exact location of this central neuronal connection remains unknown.

The Fos protein is an immediate-early gene transcription factor induced by short-term signals and alters target gene expression causing long-term change in cellular phenotype [18]. It has been used to map the activated neural cells after different types of stimulation and shows correlated anatomical neural pathways [19–21]. Pseudorabies virus (PrV) is a swine neurotropic herpes virus that has been used for transneuronal tracing in many studies [22–26]. The Pingtung (PT) strain of PrV has been demonstrated to label sympathetic pre- and postganglionic neurons after injection in the specific auricular kidney point [22]. The study showed that the PT strain of PrV was a useful transneuronal tracer in somatovisceral research. To establish the neural connection between the groin region and uterus, bee venom was injected in the groin region to induce c-Fos expression neurons innervating the groin region and PrV was injected in the uterus to infect the hierarchical motor neurons innervating the uterus. Furthermore, to evaluate central doubled Fos expression and PrV-infected neurons in order to identify the neuronal connection between the somatic point (groin region) and its related visceral organ (the uterus).

2. Materials and Methods

The study protocol was approved by Animal Care and Use Committee, and all experiments were conducted in accordance with the animal care guidelines of the National Institutes of Health and the International Association for the Study of Pain.

2.1. Animals. Sprague-Dawley adult virgin female rats (250–350 g) were used. Animals were housed on a 12 h-12 h light-dark cycle, and all animals had free access to standard food and water.

2.2. Bee Venom Injection in the Left Groin Region. The rats were anesthetized with ketamine (95 mg/kg) intraperitoneally. 50 μL of 1% bee venom (Sigma) were dissolved in normal saline and administrated subcutaneously into the midpoint between genital pore and apex of the left groin region ($n = 6$) according to Wesselmann and Lai's research [17]. Saline was injected as the control. After 90 minutes, the rats were sacrificed and perfused with 250 mL of saline intracardially, followed by 1000 mL of 4% paraformaldehyde in 0.1 M phosphate buffer solution (PBS). T10–S1 segments of spinal cord, brainstem, and brain were removed.

2.3. Pseudorabies Virus Injection in Left Uterine Horn. The rats were anesthetized with ketamine (1 mL/kg) intraperitoneally. A laparotomy was performed and 40 μL of Pingtung strain pseudorabies virus [22] was injected into the left uterus horn ($n = 9$). After the injections, the abdominal wall was sutured, the skin closed. The animals were sacrificed at 6 to 8 days after PrV injection (in the same way as described above). The spinal cord, dorsal root ganglion of T10–S2 segment, brainstem, and brain were removed.

2.4. Bee Venom Injection after PrV Injection. The rats were anesthetized and PrV was injected into the left uterus horn (in the same way as described above) ($n = 9$). After the injections, the abdominal wall was sutured, the skin closed, and the animals allowed to survive for 6 to 8 days. Before the rats were sacrificed, 50 μL of 1% bee venom was administrated subcutaneously into midpoint of left groin region and saline was injected as the control. After 90 minutes, the rats were sacrificed and perfused with 250 mL of saline intracardially, followed by 1000 mL of 4% paraformaldehyde in 0.1 M phosphate buffer solution (PBS). The spinal cord, dorsal root ganglion of T10–S1 segment, brainstem, and brain were removed.

2.5. Immunohistochemistry. Tissues of groin region-bee venom injection group and uterine horn-pseudorabies virus injection group were postfixed up to 4 hr in paraformaldehyde PBS and then cryoprotected in 10, 20, and 30% sucrose in PB solution. Serial 30 μm thick transverse sections of all dorsal root ganglia, spinal cord, brainstem, and brain were cut with a cryomicrotome. All sections from the ganglia and every five sections from other samples were collected in 0.01 M phosphate buffer saline (PBS). Floating sections were washed 30 min (10 min, 3 times) and incubated with blocking solution (5% normal goat serum, 0.05% Triton X-100, and 3% BSA in 0.1 M PB) for 1 hr. The sections were washed and incubated with the primary antibody (IgG of rabbit anti-FOS in 1 : 2000 or IgG of swine anti-PrV in 1 : 1000) in blocking solution for 72 hr at 4°C. After incubation, the sections were rinsed and incubated for 1 hr at 25°C with secondary antibody (biotin-conjugated IgG of goat anti-rabbit in 1 : 500 or goat anti-swine in 1 : 200) in blocking solution. The sections were washed three times for 30 min and incubated using ABC kit (Vector) for 1 hr. After rinsing, the sections were developed with GOD method followed by mounting on gelatin-coated slides and overslipped with mounting medium.

2.6. Immunofluorescence. Tissues of groin-uterus injection group were postfixed and sectioned in the same way described above. Floating sections were washed 30 min (10 min, 3 times) and incubated with blocking solution (5% normal goat serum, 0.05% Triton X-100, and 3% BSA in 0.1 M PB) for 1 h. The sections were washed and incubated with

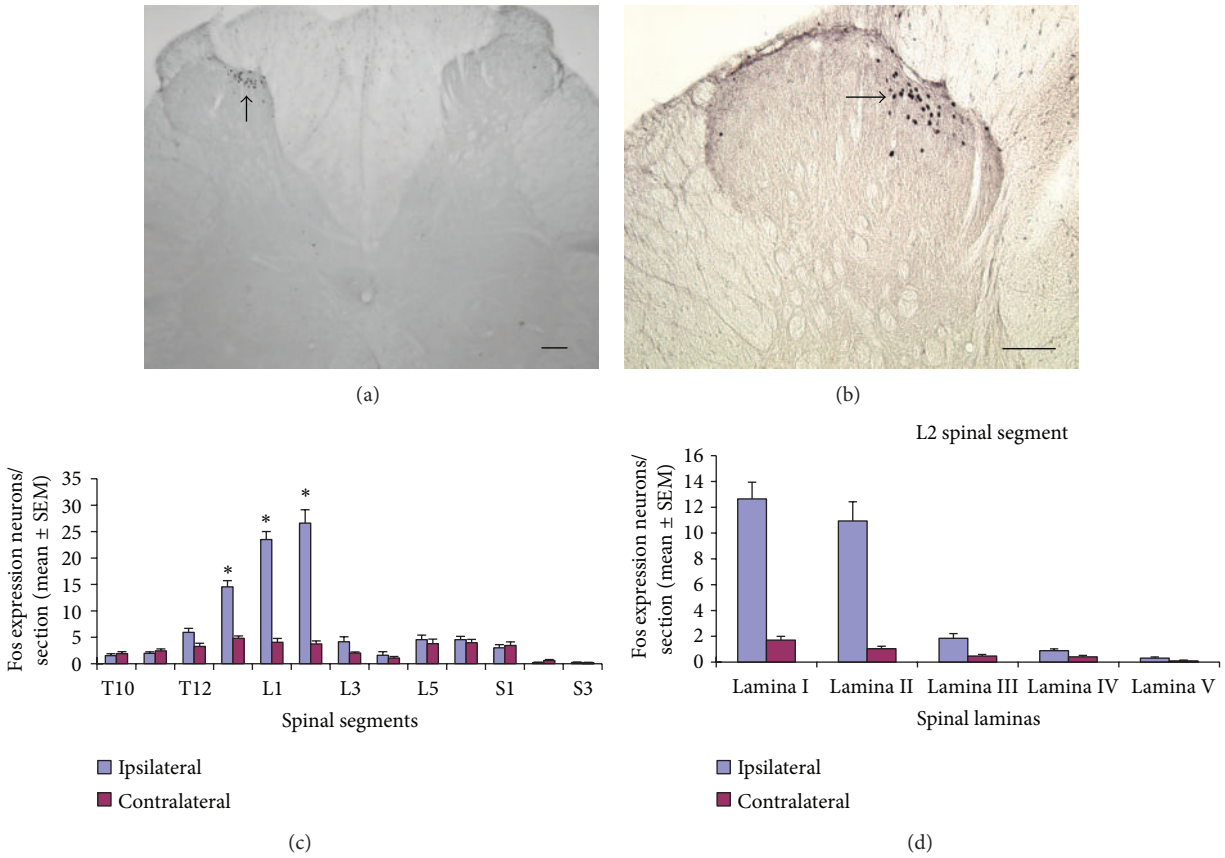

Figure 1: Fos expression neurons in the spinal cord after bee venom injection in the left groin region ($n = 9$). (a) Neurons express Fos protein (arrow) in ipsilateral L2 spinal dorsal horn. (b) Higher magnification of Fos expression neurons in (a) (scale bar: 100 um). (c) Mean number of Fos expression neurons in T10 to S3 spinal segments (±SEM). $^{*}P < 0.05$. (d) Mean number of Fos expression neurons in laminas I to V of L2 spinal segment.

two kinds of primary antibody (IgG of rabbit anti-FOS in 1 : 2000 and IgG of swine anti-PrV in 1 : 1000) in blocking solution for 72 hr at 4°C. After incubation, the sections were rinsed and incubated for 1 hr at 25°C with two secondary antibodies (FITC-conjugated IgG of goat anti-swine in 1 : 200 and TRITC-conjugated IgG of goat anti-rabbit in 1 : 500) in blocking solution. The sections were washed for 30 min and mounted on gelatin-coated slides followed by coverslipping with mounting medium.

2.7. Data and Statistical Analysis. Fos and PrV immunoreactivity neurons developed with GOD method in dorsal root ganglia, spinal cord, and brain were counted with bright field microscope. Fos and PrV double labeled neurons were observed with fluorescent microscope. Anatomical identification of brain structures was essentially based on the Rat Brain atlas of Paxinos and Watson [27]. All data were analyzed by t-test.

3. Result

3.1. Fos Expression Neurons after Bee Venom Stimulation in the Groin Region. Injecting bee venom in the left somatic groin region induces central Fos expression and the contralateral side as the control. In the spinal cord, Fos protein is predominantly (70%) apparent in ipsilateral T13 (14.5 ± 1.1), L1 (23.5 ± 1.5), and L2 (26.6 ± 2.5) spinal dorsal horn (Figures 1(a), 1(b), and 1(c)). Most of the c-Fos expression neurons are resided in laminas I (12.6 ± 1.2) and II (10.9 ± 1.4) of the dorsal horn (Figure 1(d)).

In the supraspinal area, c-Fos expression neurons appeared in numerous nuclei of the thalamus, hypothalamus, pons, and medulla. The c-Fos expression nuclei include the nucleus of solitary tract (NTS) (Figure 2(a)), parabrachial nucleus (PB), locus coeruleus (LC) (Figure 2(b)), raphe pallidus nucleus (RPa) (Figure 2(c)), paraventricular thalamic nucleus (PVT) (Figure 2(f)), lateral hypothalamic area (LH) (Figure 2(e)), and paraventricular hypothalamic nucleus (PVN) (Figure 2(d)). Table 1 listed the fos expression neurons in supraspinal areas of saline and bee venom groups. The NTS of bee venom group expressed significantly the difference between the fos expression neurons and the saline group.

3.2. The Appearance of PrV Infection Neurons after Virus Injection in the Uterus. PrV-infected neurons appeared in the central nuclei (Figures 3 and 4) 6–8 days after PrV injection in

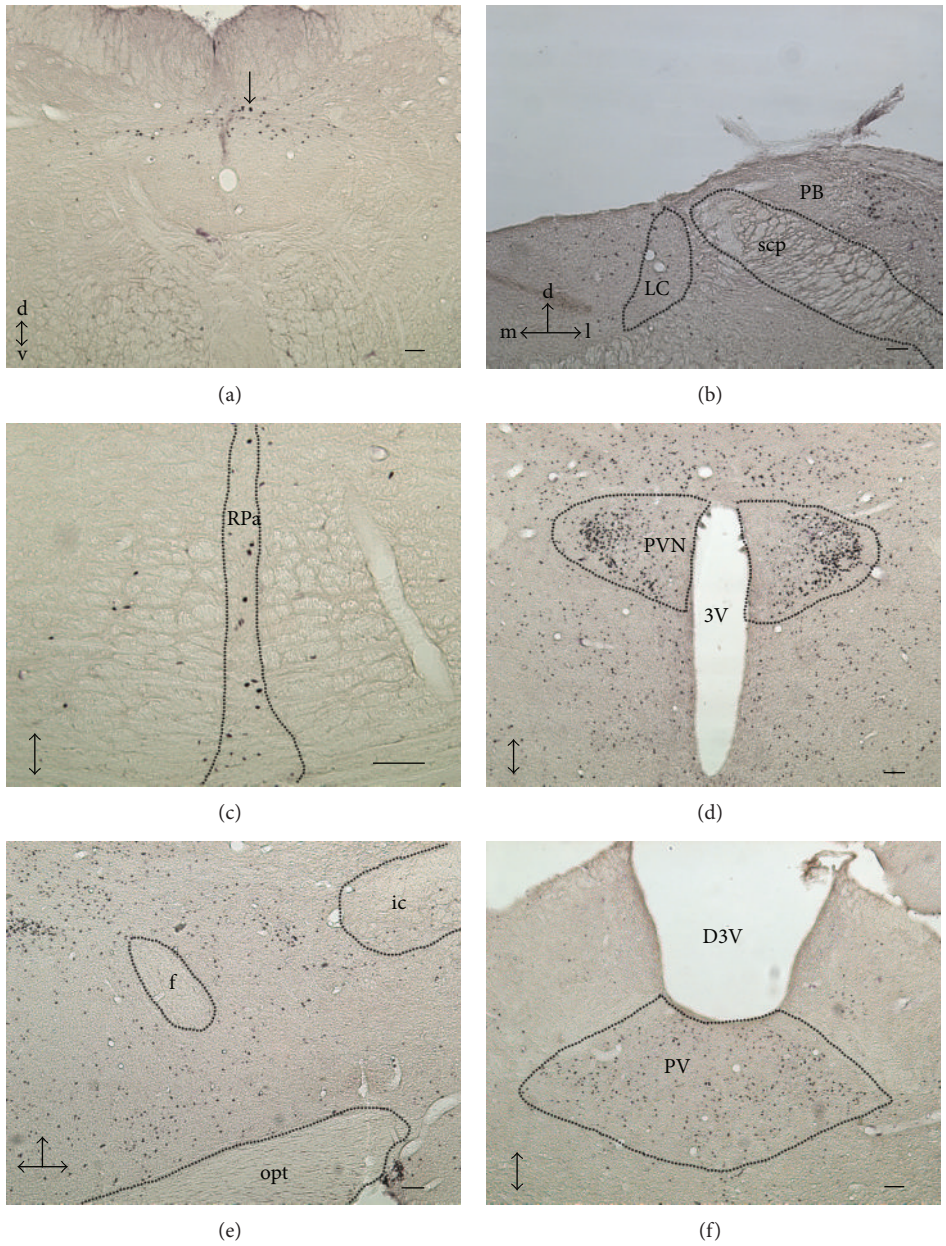

Figure 2: Fos expression neurons (arrow) in the supraspinal area after bee venom injection in the left groin region ($n = 9$). (a) Nucleus of solitary tract (NTS). (b) Locus coeruleus (LC), parabrachial nucleus (PB). (c) Raphe pallidus nucleus (RPa). (d) Paraventricular hypothalamic nucleus (PVN). (e) Lateral hypothalamic area. (f) Paraventricular thalamic nucleus (PV). 3V: third ventricle; 4V: fourth ventricle; D3V: dorsal third ventricle; d: dorsal; f: fornix; ic: internal capsule; l: lateral; m: medial; opt: optic tract; scp: superior cerebellar peduncle; v: ventral (scale bar: 100 um).

the left uterus horn. In the spinal cord, the most PrV-infected neurons were spotted in laminas IV and V of T11–L1 and L5–S2 spinal segments (Figures 3(a), 3(b), and 3(c)), rarely in the superficial laminas (laminas I, II).

In the supraspinal area, PrV-infected neurons were found in the hypothalamus, pons, and medulla, including the NTS, dorsal motor nucleus of vagus (DMX) (Figure 4(a)), intermediate reticular nucleus (IRt), ambiguus nucleus (Amb), lateral reticular nucleus (LRt), A5 noradrenaline cell group (A5) (Figure 4(b)), raphe pallidus nucleus (RPa) (Figure 4(c)), gigantocellular reticular nucleus (Gi) (Figure 4(d)), medial preoptic area (MPA), and PVN (Figure 4(e)). All PrV-infected neurons in supraspinal area were listed in Table 2.

3.3. Fos Expression and PrV-Infected Double Labeled Neurons in the NTS, DMX, and PVN. After uterine PrV injection and c-Fos expression of groin bee venom stimulation, double labeled neurons appeared in the hypothalamus, and specifically in the PVN (Figure 5(c1)). Some other double labeled neurons are apparent in the NTS and DMX (Figures 5(c2), 5(c3), and 5(c4)). Comparing saline and bee venom injection

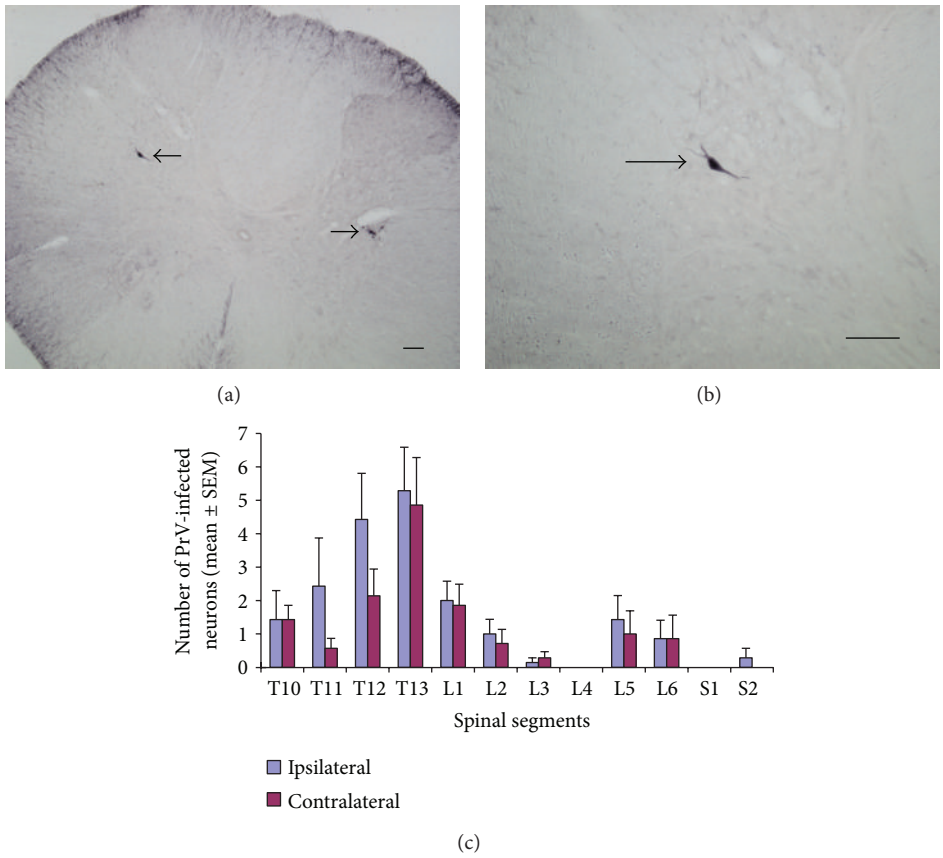

Figure 3: PrV-infected neurons in spinal cord after 6 to 8 d PrV injection in the left uterine horn ($n = 8$). (a) PrV-infected neuron (arrow) in T12 spinal segment. (b) Higher magnification of PrV-infected neuron in (a) (arrow) (scale bar: 100 um). (c) Mean number of PrV-infected neurons in T10 to S2 spinal segments (±SEM).

groups in PrV-infected neurons, the percentage of the double labeled neurons in PVN of bee venom injection group were significantly predominant ($P < 0.1$) (Figure 5(d)).

4. Discussion

After the application of bee venom to the left groin region, the c-Fos protein expression neurons were presented in the left spinal dorsal horn and certain supraspinal nuclei. PrV-infected uterine supraspinal neurons resided in the A5 noradrenaline cell group (A5), raphe pallidus nucleus (RPa), and gigantocellular reticular nucleus (Gi). Double labeled neurons located in the NTS, motor nucleus of vagus (DMX), and PVN (Figure 5). The neuronal connection between groin region and uterus suggests that the nuclei of PVN, NTS, and DMX not only receive somatic stimulation from groin region but also modulate the function of uterus. Those nuclei may play important roles in somatovisceral reflex [1] and could be the result of the neuronal mechanism of acupuncture.

4.1. Sensory Innervation of the Left Groin A-Shi Point. The stimulating acupoints elicit a composite of unique sensations called *dechi*. *Dechi* sensations including pressure, soreness, heaviness, and dull pain are essential for clinical efficacy [28]. Pain, as one of the *dechi* sensations, is a relatively strong and easily induced sensory modality in animal study. Panic stimulation can induce neurons expressing the Fos protein which could be used to investigate either somatic [29–31] or visceral [31–33] noxious afferent pathways. Takahashi and Nakajima [34] intravenously injected in the Evans Blue Dye and observed extravasation in the groin after electrical stimulation of the spinal nerves. This result proves that the sensory innervation of groin region comes from T13, L1, and L2 spinal nerves. The injection of bee venom in the left groin region in our study induced c-Fos expression in the ipsilateral spinal dorsal horn of T13, L1, and L2, and particularly in superficial laminas I and II (Figures 1(c) and 1(d)). This suggests that the spinal Fos expression neurons in our study were specifically activated by noxious stimulation of the groin region.

Fos expression neurons appeared in the NTS, gigantocellular reticular nucleus (Gi), raphe pallidus nucleus (RPa), and PVN after bee venom stimulated groin region (Figures 3 and 6). The NTS can be not only activated by somatic noxious stimulation but also triggered by vagal afferent activation as a physiological adaptation to pain [35]. Previous studies showed that Gi can be activated by noxious stimulation related to the activation of the descending antinociceptive pathway [36–39]. Electrically stimulating

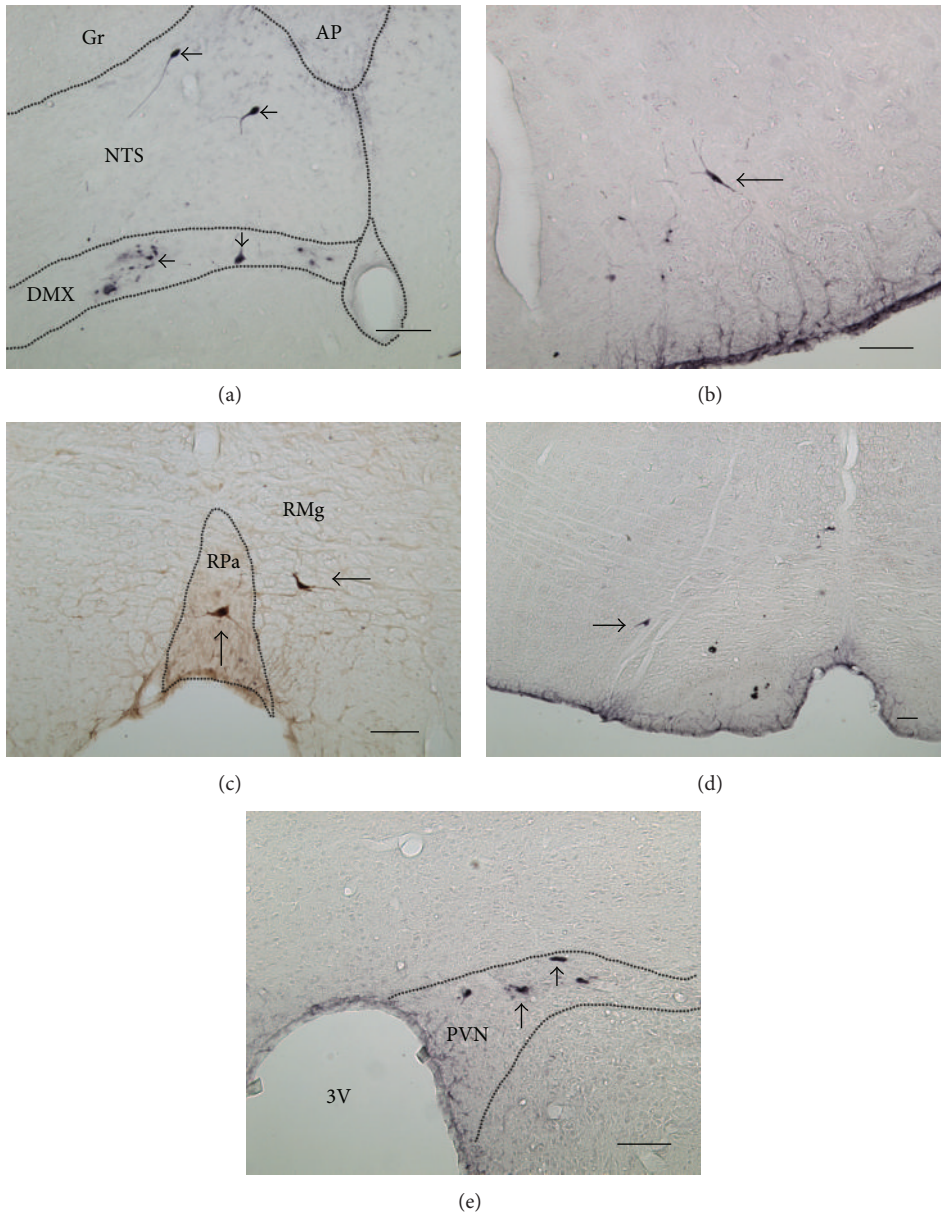

FIGURE 4: PrV-infected neurons (arrow) in the supraspinal area after 7-8 d PrV injection in the left uterus horn ($n = 8$). (a) PrV-infected neurons in the NTS and DMX. (b) PrV-infected neurons in the A5 noradrenaline cell group. (c) PrV-infected neurons in the RPa and RMg. (d) PrV-infected neurons in the Gi. (e) PrV-infected neurons in the PVN. 3V: third ventricle; AP: area postrema; DMX: motor nucleus of vagus; Gi: gigantocellular reticular nucleus; Gr: gracile nucleus; NTS: nucleus of solitary tract; PVN: paraventricular hypothalamic nucleus; RPa: raphe pallidus nucleus; RMg: raphe magnus nucleus (scale bar: 100 um).

the raphe nucleus could induce analgesia, proving that the raphe nucleus plays a crucial role in pain inhibition response [40, 41]. The thermal stimulation from hind feet inducing Fos expression in the PVN showed that the PVN can receive the noxious input [42]. The activation of PVN initiates the hypothalamus-pituitary-adrenal hormone cascade by releasing corticotropin-releasing factor (CRF) and arginine vasopressin from its parvocellular cells [43]. Fos expression neurons in those nuclei suggest that injecting bee venom in the groin region activates not only pain transmission pathway but also the nuclei regulating physiological responses and inhibiting pain in the central nervous system.

4.2. Hierarchical Innervation of the Uterus. The PrV transneuronal tracing method is widely used to detect the hierarchically central innervation of urethra, clitoris, penis, urinary bladder, and uterus [23, 24, 44–51]. In our previous study, the Pingtung strain of PrV applied to the auricular kidney point transneuronally and specifically infected sympathetic pre- and postganglionic neurons [22]. In order to investigate the highest central control of uterus, the survival time was proportionally extended to 6–8 days in this study. All PrV-infected nuclei in our study (Table 2) could be found in these nuclei reported by other strains of PrV transneuronal studies [23, 24]. This result confirms that the Pingtung strain

Table 1: Fos expression neurons in supraspinal area between saline and bee venom injection groups.

c-fos expression neurons in supraspinal area	Saline	Bee venom
Diencephalon		
Thalamus		
Paratenial thalamic nucleus (PT)	96.3 ± 49.5	105.8 ± 27.2
Precommissural nucleus (PrC)	69.6 ± 18.6	53.2 ± 17.4
Rhomboid thalamic nucleus (Rh)	44.9 ± 21.1	62.8 ± 15.2
Reuniens thalamic nucleus (Re)	112.6 ± 36.0	88.9 ± 24.3
Pretectal nucleus	89.9 ± 18.6	61.3 ± 16.0
Lateral dorsal thalamic nucleus (LD)	83.4 ± 25.9	72.6 ± 21.9
Mediodorsal thalamic nucleus (MD)	134.7 ± 56.9	163.5 ± 47.6
Paraventricular thalamic nucleus (PV)	98.9 ± 28.9	75.9 ± 17.8
Lateral habenular nucleus (LHb)	37.8 ± 5.0	44.4 ± 13.0
Lateral posterior thalamic nucleus (LP)	82.9 ± 30.6	89.5 ± 29.9
Lateral geniculate nucleus (LG)	82.7 ± 23.5	62.9 ± 13.3
Suprageniculate thalamic nucleus (SG)	97.0 ± 40.4	72.1 ± 18.2
Hypothalamus		
Medial preoptic area (MPA)	82.3 ± 17.2	94.9 ± 24.9
Suprachiasmatic nucleus (SCh)	67.0 ± 15.8	72.3 ± 13.7
Arcuate nucleus (Arc)	50.4 ± 15.3	50.8 ± 11.6
Supramammillary nucleus (SuM)	172.6 ± 17.3	189.2 ± 33.3
Lateral mammillary nucleus (LM)	94.3 ± 13.2	92.6 ± 29.0
Supraoptic nucleus (SO)	41.0 ± 19.5	86.7 ± 20.6
Lateral hypothalamic area (LH)	108.6 ± 20.3	121.0 ± 26.2
Premammillary nucleus (PM)	136.4 ± 13.0	96.1 ± 40.0
Posterior hypothalamic area (PH)	169.4 ± 33.1	149.4 ± 28.6
Ventromedial hypothalamic nucleus (VMH)	100.1 ± 44.8	86.9 ± 36.4
Dorsomedial hypothalamic nucleus (DM)	142.2 ± 30.2	150.4 ± 25.0
Anterior hypothalamic area (AHC)	100.1 ± 30.6	73.9 ± 15.6
Lateroanterior hypothalamic nucleus (LA)	118.4 ± 19.4	133.2 ± 55.5
Paraventricular hypothalamic nucleus (PVN)	82.3 ± 14.3	62.1 ± 9.7
Anterodorsal preoptic nucleus (ADP)	60.3 ± 20.3	60.9 ± 8.8
Mesencephalon		
Edinger-Westphal nucleus (EW)	30.7 ± 4.2	29.9 ± 3.1
Paranigral nucleus (PN)	51.6 ± 14.9	61.0 ± 13.2
Interfascicular nucleus (IF)	26.1 ± 6.6	30.4 ± 4.6
Pons		
Parabrachial nucleus (PB)	70.1 ± 15.9	52.6 ± 13.1
Dorsal raphe nucleus ventrolateral part (DRVL)	52.6 ± 35.8	90.6 ± 17.2
Dorsal raphe nucleus (DR)	37.3 ± 16.1	16.1 ± 4.3
Pontine nuclei (Pn)	277.1 ± 107.9	298.7 ± 68.2
Nucleus of lateral lemniscus (LL)	58.0 ± 22.7	64.8 ± 12.0
Locus coeruleus (LC)	73.4 ± 14.8	31.4 ± 5.7
Prepositus nucleus (Pr)	13.7 ± 8.0	22.3 ± 6.4
Area postrema (AP)	21.8 ± 8.3	31.4 ± 11.9
Medulla		
Gigantocellular reticular nucleus (Gi)	16.4 ± 2.2	14.7 ± 4.9
Raphe magnus nucleus (RMg)	20.6 ± 1.7	11.9 ± 3.3
Raphe pallidus nucleus (RPa)	12.6 ± 2.3	19.1 ± 4.8
Medial vestibular nucleus (MVe)	33.5 ± 3.9	45.7 ± 7.1
Inferior olivary nucleus (IO)	40.7 ± 10.7	39.5 ± 8.2
Caudoventrolateral reticular nucleus (CVL)	18.8 ± 4.9	18.9 ± 3.9
Nucleus of solitary tract (NTS)	17.1 ± 4.0	33.8 ± 5.0*

* Significant difference between saline and bee venom injection groups, $P < 0.1$.

Table 2: PrV-infected neurons in supraspinal area.

PrV-infected neurons in supraspinal area	
Hypothalamus	
Medial preoptic area (MPA)	+
Arcuate nucleus (Arc)	+
Ventromedial hypothalamic nucleus (VMH)	+
Dorsomedial hypothalamic nucleus (DM)	+
Paraventricular hypothalamic nucleus (PVN)	++
Pons	
Locus coeruleus (LC)	+
Medulla	
Gigantocellular reticular nucleus (Gi)	+++
Raphe magnus nucleus (RMg)	++
Raphe pallidus nucleus (RPa)	+
Caudoventrolateral reticular nucleus (CVL)	++
Nucleus of solitary tract (NTS)	+++
Dorsal motor nucleus of vagus (DMV)	+++
A5 noradrenaline cells (A5)	++
Lateral reticular nucleus (LRt)	++

+: 1–3 infected neurons, ++: 4–8 infected neurons, and +++: >9 infected neurons.

of PrV was a sustainable strain as a transneuronal tracer in hierarchical innervation studying.

Lee and Papka discovered PrV-infected sympathetic and parasympathetic preganglionic neurons at T11–13 and L6–S1 spinal segments, after PrV injection in the uterine cervix [23, 24]. The results indicate the visceral efferent of the uterus are mainly from T11–T13 and L6–S1 segments. In our study, PrV-infected preganglionic neurons are mainly in the intermediolateral nucleus (IML) and sacral parasympathetic nucleus of T10–L2 and L6–S1 spinal segments (Figure 2). Our result is in accord with previous studies [23, 24, 50].

Supraspinal PrV-infected high hierarchical uterine neurons are located in the NTS, dorsal motor nucleus of vagus (DMX), A5 noradrenaline cell group (A5), raphe pallidus nucleus (RPa), gigantocellular reticular nucleus (Gi), and PVN (Figure 4). The NTS is the major brainstem structure receiving both general and special visceral sensory inputs, including visceral pain [52, 53]. Electrophysiological and HRP studies have shown that the NTS contains neuronal connection with the uterus [54, 55]. The DMX is generally recognized as parasympathetic preganglionic neurons that innervate various visceral organs. Retrograde tracer studies have shown that the DMX innervates the cecum, uterus, and colon directly or indirectly [50, 52, 55–57]. The neurons in the A5 cell group, RPa, and Gi innervating the uterus were also confirmed by previous PrV tracing researches [23, 24, 50]. Therefore, the PVN function is not only a uterus-related hormone regulation center [58], but also a direct neuronal connection to the uterus [23, 24]. After PHA-L injection in the PVN, terminal varicosities appeared in the IML of the thoracic spinal cord [59]. Retrograde tracer studies also showed a neuronal connection between the PVN and the uterus [23, 24, 50]. In summary, all these results suggest that the PVN has either a direct or indirect neuronal connection and it regulates the uterus through both hormonal and neuronal innervations.

4.3. Somatovisceral Neuronal Connection Nuclei between the Groin A-Shi Point and the Uterus Located in the NTS, DMX, and PVN. Retrograde tracer injection in the NTS suggests that the spinal superficial dorsal horn neurons (lamina I) directly project to the NTS [60]. Our result (Figure 2(a)) and a previous study [35] also showed that the NTS can be activated by somatic noxious stimulation. Several anatomical and electrophysiological studies have shown the neuronal connection between the uterus and NTS and DMX through the vagus nerve [23, 24, 50, 54, 55]. The PrV-infected neurons in the NTS and DMX (Figure 4(a)) also confirmed the efferent innervation of the NTS and DMX to the uterus as in a previous study [55]. Neurons with cell bodies in the DMX send their dendrites into the gelatinosus solitary nucleus, where they receive synaptic inputs from gastric sensory afferents [61]. These researches suggested that the NTS and DMX play important roles in visceral innervation, including the digestive functions of the stomach and baroreceptor reflex [61–66]. The double labeled NTS and DMX neurons in our study suggest that the nuclei may be one of the relay centers of the somatovisceral reflex of the groin A-shi point and uterus.

Retrograde labeling study shows that the NTS receives spinal projections from the superficial dorsal horn [60] and projects to the PVN [42]. Fos expression studies also suggested that the PVN could be activated by somatic noxious stimulations [42, 67]. Swanson proved that the PVN, a higher hormonal regulation center, projects neuronal fibers to the pituitary gland, medulla, and spinal cord [68]. The neuronal connection between the PVN and the uterus was also proved by previous indicators [23, 24, 50] and our studies (Figure 4(e)). Noxious stimulation and retrograde tracer injection in different visceral organs showed that the PVN was not only receive noxious afferent but also innervate visceral organs as well [24, 69–72]. The reflex inhibition of the heart rate elicited by acupuncture-like stimulation likely occurs through the activation of the hypothalamic nucleus, which inhibits the activity of premotor sympathetic neurons in the rostral ventrolateral medulla (rVLM) [73, 74]. Although bee venom stimulation in groin A-shi point induced less neuronal activity in the PVN, comparing to saline group (Table 1) in our study, there was higher percentage of double labeled neurons in the PVN than saline injection group (Figure 5(d)). Those previous researches and our result suggest that the PVN may be another relay center of the somatovisceral reflex between the groin and uterus.

Although the electrophysiological studies show laminas I and V of the spinal dorsal horn receive afferent information from both somatic and visceral tissues [75–79], no double labeled spinal dorsal neurons can be detected in our study. This solid evidence shows the neuronal connection between the groin region and the uterus is not admitted through the spinal cord.

4.4. The Morphologic Evidence of Somatovisceral Reflex: A Possible Neuronal Pathway of Acupuncture. A previous study suggested that acupuncture may influence visceral

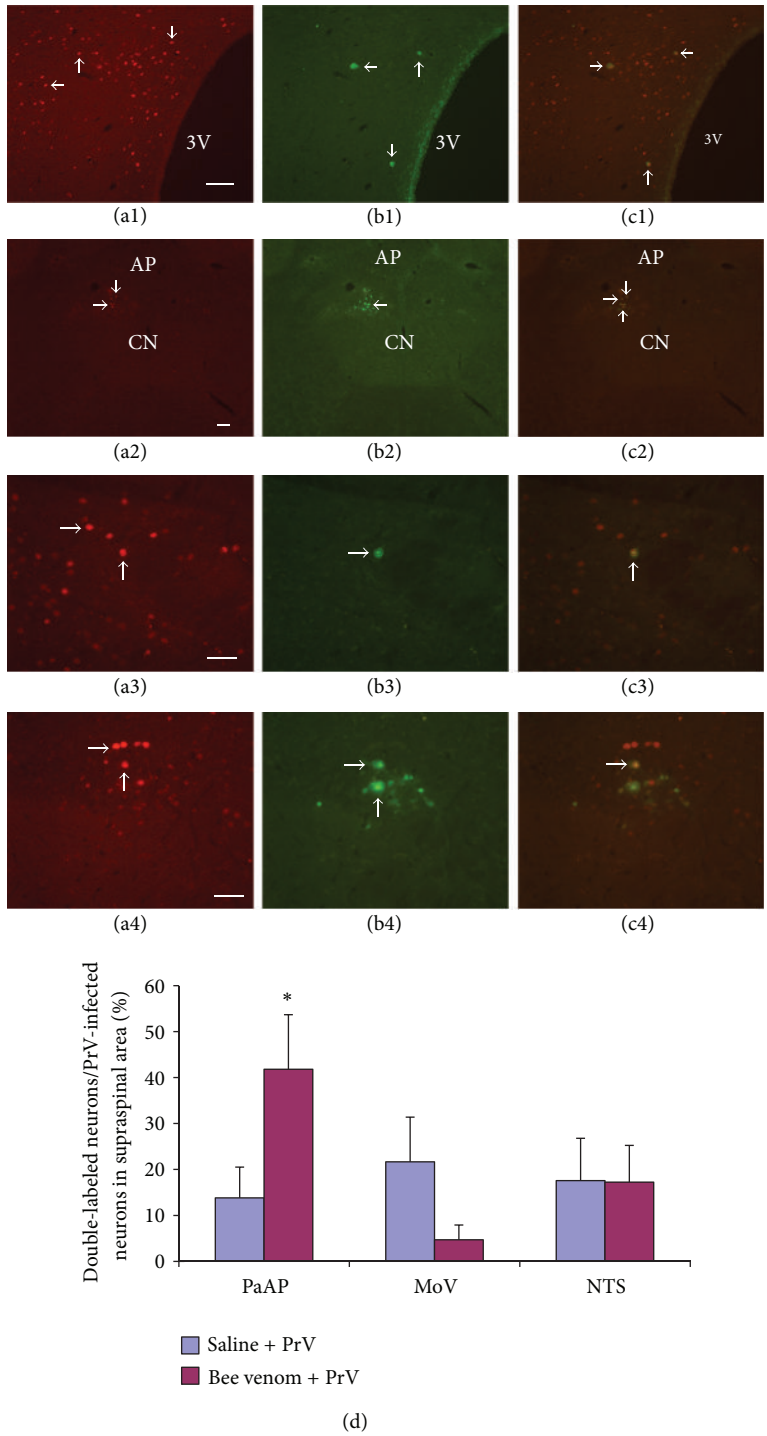

Figure 5: Double-labeled neurons of Fos expression and PrV infection ($n = 8$). Fos expression neurons ((a), red, arrow) in the PVN (a1), NTS ((a2), (a3)), and DMX ((a2), (a4)). PrV-infected neurons ((b), green, arrow) in the PVN (b1), NTS ((b2), (b3)), and DMX ((b2), (b4)). Merged double labeling Fos expression and PrV-infected neurons ((c), yellow, arrow) in the PVN (c1), NTS ((c2), (c3)), and DMX ((c2), (c4)) (scale bar: 1000 um). (d) The percentage of double labeled neurons in PVN, DMX, and NTS between saline and bee venom injection groups ($^{*}P < 0.1$).

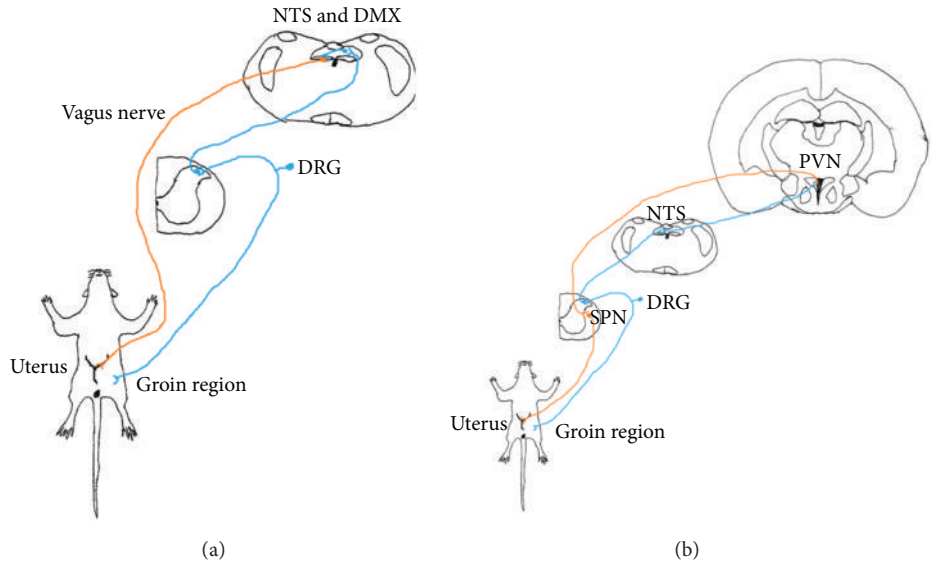

Figure 6: Schematic drawing of three neuronal pathways of somatovisceral reflex. (a) Somato-parasympathetic reflex pathway through the vagus nerve. (b) Somato-sympathetic reflex pathways through the NTS and PVN. DMX: dorsal motor nucleus of vagus; DRG: dorsal root ganglia; NTS: nucleus of solitary tract; SPN: sympathetic preganglionic neurons; PVN: paraventricular hypothalamic nucleus; blue: somatic afferent; red: visceral efferent.

function via the activation of the somatosensory neurons [9]. However, most researches focused on the physiological responses induced by acupuncture [5, 10, 11]. The purpose of our study is to investigate and provide the morphological evidence of somatovisceral reflex and possible neuronal pathway of acupuncture. Our result suggests that the PVN, NTS, and DMX could be the relay center of the somatovisceral reflex. The visceral organs usually receive sympathetic and parasympathetic dual interacted and the interaction is antagonistic. Therefore, our study proved morphological evidence of both sympathetic and parasympathetic pathways of somatovisceral reflex between the groin A-shi point and the uterus (Figure 6). The somato-parasympathetic pathway starts from the stimulation of the groin A-shi point, which activates neurons in the spinal dorsal horn. The signal in turn elicits noxious input to the NTS [60]. Neurons in the NTS relay the information and project to the DMX [80], which innervates the uterus through the vagus nerve [55] (Figure 6(a)). The somato-sympathetic pathways from the neurons in the spinal dorsal horn project to the NTS [60] then direct connection to the PVN [81]; it innervates the visceral organ through the sympathetic pre- and postganglionic neurons [59] (Figure 6(b)). These complementary somato-sympathetic and somato-parasympathetic systems coincidentally match the concept of Yin-Yang theory in traditional Chinese medicine [2, 82].

In conclusion, the present study provides the morphological evidence of the neuronal connection between somatic groin A-shi point and its corresponding visceral organ uterus. Therefore, we come up to the conclusion that the somato-sympathetic/somatoparasympathetic pathways are the morphological basis of somatovisceral reflex and also the neuronal substrate of acupuncture pathways.

Abbreviations

PrV: Pseudorabies virus
NTS: Nucleus of solitary tract
PVN: Paraventricular hypothalamic nucleus
DMX: Dorsal motor nucleus of vagus
PB: Parabrachial nucleus
LC: Locus coeruleus
RPa: Raphe pallidus nucleus
PVT: Paraventricular thalamic nucleus
LH: Lateral hypothalamic area
IRt: Intermediate reticular nucleus
Amb: Ambiguus nucleus
LRt: Lateral reticular nucleus
A5: A5 noradrenaline cells group
Gi: Gigantocellular reticular nucleus
MPA: Medial preoptic area
CRF: Corticotropin-releasing factor
IML: Intermediolateral nucleus
SPN: Sympathetic preganglionic neurons.

Acknowledgment

This study is supported by research Grants (no. NSC-92-2320-B-006-078- and no. NSC-93-2320-B-006-075-) from the National Science Council.

References

[1] A. Sato, "Somatovisceral reflexes," *Journal of Manipulative and Physiological Therapeutics*, vol. 18, no. 9, pp. 597–602, 1995.

[2] World Health Organization. Regional Office for the Western Pacific, *Standard Acupuncture Nomenclature: A Brief Explanation of 361 Classical Acupuncture Point Names and Their Mul-*

tilingual Comparative List, WHO Regional Office for the Western Pacific, Manila, Philippines, 1993.

[3] S. Ballegaard, G. Jensen, F. Pedersen, and V. H. Nissen, "Acupuncture in severe, stable angina pectoris: a randomized trial," *Acta Medica Scandinavica*, vol. 220, no. 4, pp. 307–313, 1986.

[4] Y. X. Bao, G. R. Yu, H. H. Lu, D. S. Zhen, B. H. Cheng, and C. Q. Pan, "Acupuncture in acute myocardial infarction," *Chinese Medical Journal*, vol. 95, pp. 824–828, 1982.

[5] D. M. Chao, L. L. Shen, S. Tjen-A-Looi, K. F. Pitsillides, P. Li, and J. C. Longhurst, "Naloxone reverses inhibitory effect of electroacupuncture on sympathetic cardiovascular reflex responses," *American Journal of Physiology*, vol. 276, no. 6, pp. H2127–H2134, 1999.

[6] M. Ho, L. C. Huang, Y. Y. Chang et al., "Electroacupuncture reduces uterine artery blood flow impedance in infertile women," *Taiwanese Journal of Obstetrics and Gynecology*, vol. 48, no. 2, pp. 148–151, 2009.

[7] P. Li, K. F. Pitsillides, S. V. Rendig, H. L. Pan, and J. C. Longhurst, "Reversal of reflex-induced myocardial ischemia by median nerve stimulation: a feline model of electroacupuncture," *Circulation*, vol. 97, no. 12, pp. 1186–1194, 1998.

[8] A. Richter, J. Herlitz, and A. Hjalmarson, "Effect of acupuncture in patients with angina pectoris," *European Heart Journal*, vol. 12, no. 2, pp. 175–178, 1991.

[9] M. H. Kim, Y. C. Park, and U. Namgung, "Acupuncture-stimulated activation of sensory neurons," *Journal of Acupuncture and Meridian Studies*, vol. 5, pp. 148–155, 2012.

[10] L. Peng, "Neural mechanisms of the effect of acupuncture on cardiovascular diseases," *International Congress Series*, vol. 1238, pp. 71–77, 2002.

[11] X. Y. Sun and T. Yao, "Inhibitory effect of electric needling on the defence reaction produced by hypothalamic stimulation in awake rabbits," *Sheng Li Xue Bao*, vol. 37, no. 1, pp. 15–23, 1985.

[12] M. A. Giamberardino, K. J. Berkley, S. Iezzi, P. De Bigontina, and L. Vecchiet, "Pain threshold variations in somatic wall tissues as a function of menstrual cycle, segmental site and tissue depth in non-dysmenorrheic women, dysmenorrheic women and men," *Pain*, vol. 71, no. 2, pp. 187–197, 1997.

[13] R. Melzack and E. Belanger, "Labour pain: correlations with menstrual pain and acute low-back pain before and during pregnancy," *Pain*, vol. 36, no. 2, pp. 225–229, 1989.

[14] G. F. Yang, C. N. Ji, and S. Q. Yuan, "Modern medical explanation on Ashi points," *Zhongguo Zhen Jiu*, vol. 32, pp. 180–182, 2012.

[15] T. Liu, "Rethinking on Ashi points," *Zhongguo Zhen Jiu*, vol. 31, pp. 929–931, 2011.

[16] R. D. Xu and H. Li, "Conception of Ashi points," *Zhongguo Zhen Jiu*, vol. 25, pp. 281–283, 2005.

[17] U. Wesselmann and J. Lai, "Mechanisms of referred visceral pain: uterine inflammation in the adult virgin rat results in neurogenic plasma extravasation in the skin," *Pain*, vol. 73, no. 3, pp. 309–317, 1997.

[18] T. Curran and J. I. Morgan, "Fos: an immediate-early transcription factor in neurons," *Journal of Neurobiology*, vol. 26, no. 3, pp. 403–412, 1995.

[19] M. A. de Medeiros, N. S. Canteras, D. Suchecki, and L. E. A. M. Mello, "Analgesia and c-Fos expression in the periaqueductal gray induced by electroacupuncture at the Zusanli point in rats," *Brain Research*, vol. 973, no. 2, pp. 196–204, 2003.

[20] A. Ghanima, M. Bennis, and O. Rampin, "c-Fos expression as endogenous marker of lumbosacral spinal neuron activity in response to vaginocervical-stimulation," *Brain Research Protocols*, vol. 9, no. 1, pp. 1–8, 2002.

[21] C. Luo, J. Chen, H. L. Li, and J. S. Li, "Spatial and temporal expression of c-Fos protein in the spinal cord of anesthetized rat induced by subcutaneous bee venom injection," *Brain Research*, vol. 806, no. 2, pp. 175–185, 1998.

[22] C. H. Chien, J. Y. Shieh, M. H. Liao, E. A. Ling, and C. Y. Wen, "Neuronal connections between the auricular skin and the sympathetic pre- and postganglionic neurons of the dog as studied by using pseudorabies virus," *Neuroscience Research*, vol. 30, no. 2, pp. 169–175, 1998.

[23] J. W. Lee and M. S. Erskine, "Pseudorabies virus tracing of neural pathways between the uterine cervix and CNS: effects of survival time, estrogen treatment, rhizotomy, and pelvic nerve transection," *Journal of Comparative Neurology*, vol. 418, pp. 484–503, 2000.

[24] R. E. Papka, S. Williams, K. E. Miller, T. Copelin, and P. Puri, "CNS location of uterine-related neurons revealed by transsynaptic tracing with pseudorabies virus and their relation to estrogen receptor-immunoreactive neurons," *Neuroscience*, vol. 84, no. 3, pp. 935–952, 1998.

[25] M. Rothermel, N. Schöbel, N. Damann et al., "Anterograde transsynaptic tracing in the murine somatosensory system using Pseudorabies virus (PrV): a "live-cell"-tracing tool for analysis of identified neurons in vitro," *Journal of NeuroVirology*, vol. 13, no. 6, pp. 579–585, 2007.

[26] M. L. Weiss and S. I. Chowdhury, "The renal afferent pathways in the rat: a pseudorabies virus study," *Brain Research*, vol. 812, no. 1-2, pp. 227–241, 1998.

[27] G. Paxinos and C. Watson, *The Rat Brain in Stereotaxic Coordinates*, Academic Press, San Diego, Calif, USA, 4th edition, 1998.

[28] K. K. S. Hui, E. E. Nixon, M. G. Vangel et al., "Characterization of the "deqi" response in acupuncture," *BMC Complementary and Alternative Medicine*, vol. 7, article 33, 2007.

[29] M. Pinto, D. Lima, and I. Tavares, "Correlation of noxious evoked c-fos expression in areas of the somatosensory system during chronic pain: involvement of spino-medullary and intramedullary connections," *Neuroscience Letters*, vol. 409, no. 2, pp. 100–105, 2006.

[30] D. H. Roh, H. W. Kim, S. Y. Yoon et al., "Bee venom injection significantly reduces nociceptive behavior in the mouse formalin test via capsaicin-insensitive afferents," *Journal of Pain*, vol. 7, no. 7, pp. 500–512, 2006.

[31] I. Tavares, D. Lima, and A. Coimbra, "Neurons in the superficial dorsal horn of the rat spinal cord projecting to the medullary ventrolateral reticular formation express c-fos after noxious stimulation of the skin," *Brain Research*, vol. 623, no. 2, pp. 278–286, 1993.

[32] V. Martínez, L. Wang, and Y. Taché, "Proximal colon distension induces Fos expression in the brain and inhibits gastric emptying through capsaicin-sensitive pathways in conscious rats," *Brain Research*, vol. 1086, no. 1, pp. 168–180, 2006.

[33] H. Mönnikes, J. Rüter, M. König et al., "Differential induction of c-fos expression in brain nuclei by noxious and non-noxious colonic distension:: role of afferent C-fibers and 5-HT3 receptors," *Brain Research*, vol. 966, no. 2, pp. 253–264, 2003.

[34] Y. Takahashi and Y. Nakajima, "Dermatomes in the rat limbs as determined by antidromic stimulation of sensory C-fibers in spinal nerves," *Pain*, vol. 67, no. 1, pp. 197–202, 1996.

[35] G. J. Ter Horst, W. J. Meijler, J. Korf, and R. H. A. Kemper, "Trigeminal nociception-induced cerebral Fos expression in the conscious rat," *Cephalalgia*, vol. 21, no. 10, pp. 963–975, 2001.

[36] M. Zhuo and G. F. Gebhart, "Characterization of descending inhibition and facilitation from the nuclei reticularis gigantocellularis and gigantocellularis pars alpha in the rat," *Pain*, vol. 42, no. 3, pp. 337–350, 1990.

[37] M. Zhuo and G. F. Gebhart, "Characterization of descending facilitation and inhibition of spinal nociceptive transmission from the nuclei reticularis gigantocellularis and gigantocellularis pars alpha in the rat," *Journal of Neurophysiology*, vol. 67, no. 6, pp. 1599–1614, 1992.

[38] P. L. Goldman, W. F. Collins, A. Taub, and J. Fitzmartin, "Evoked bulbar reticular unit activity following delta fiber stimulation of peripheral somatosensory nerve in cat," *Experimental Neurology*, vol. 37, no. 3, pp. 597–606, 1972.

[39] H. Burton, "Somatic sensory properties of caudal bulbar reticular neurons in the cat (Felis domestica)," *Brain Research*, vol. 11, no. 2, pp. 357–372, 1968.

[40] M. B. Llewelyn, J. Azami, and M. H. T. Roberts, "Brainstem mechanisms of antinociception. Effects of electrical stimulation and injection of morphine into the nucleus raphe magnus," *Neuropharmacology*, vol. 25, no. 7, pp. 727–735, 1986.

[41] J. L. Oliveras, F. Redjemi, G. Guilbaud, and J. M. Besson, "Analgesia induced by electrical stimulation of the inferior centralis nucleus of the raphe in the cat," *Pain*, vol. 1, no. 2, pp. 139–145, 1975.

[42] B. Pan, J. M. Castro-Lopes, and A. Coimbra, "Central afferent pathways conveying nociceptive input to the hypothalamic paraventricular nucleus as revealed by a combination of retrograde labeling and c-fos activation," *Journal of Comparative Neurology*, vol. 413, pp. 129–145, 1999.

[43] M. H. Whitnall, "Distributions of pro-vasopressin expressing and pro-vasopressin deficient CRH neurons in the paraventricular hypothalamic nucleus of colchicine-treated normal and adrenalectomized rats," *Journal of Comparative Neurology*, vol. 275, no. 1, pp. 13–28, 1988.

[44] J. S. Kim, L. W. Enquist, and J. P. Card, "Circuit-specific coinfection of neurons in the rat central nervous system with two pseudorabies virus recombinants," *Journal of Virology*, vol. 73, no. 11, pp. 9521–9531, 1999.

[45] L. Marson, K. B. Platt, and K. E. McKenna, "Central nervous system innervation of the penis as revealed by the transneuronal transport of pseudorabies virus," *Neuroscience*, vol. 55, no. 1, pp. 263–280, 1993.

[46] R. Y. Moore, J. C. Speh, and J. P. Card, "The retinohypothalamic tract originates from a distinct subset of retinal ganglion cells," *Journal of Comparative Neurology*, vol. 352, no. 3, pp. 351–366, 1995.

[47] I. Nadelhaft, P. L. Vera, J. P. Card, and R. R. Miselis, "Central nervous system neurons labelled following the injection of pseudorabies virus into the rat urinary bladder," *Neuroscience Letters*, vol. 143, no. 1-2, pp. 271–274, 1992.

[48] M. Park, J. Kim, Y. Bae et al., "CNS innervation of the urinary bladder demonstrated by immunohistochemical study for c-fos and pseudorabies virus," *Journal of Korean Medical Science*, vol. 12, no. 4, pp. 340–352, 1997.

[49] M. A. Vizzard, V. L. Erickson, J. P. Card, J. R. Roppolo, and W. C. de Groat, "Transneuronal labeling of neurons in the adult rat brainstem and spinal cord after injection of pseudorabies virus into the urethra," *Journal of Comparative Neurology*, vol. 355, no. 4, pp. 629–640, 1995.

[50] O. Wiesel, I. E. Tóth, Z. Boldogkoi et al., "Comparison of transsynaptic viral labeling of central nervous system structures from the uterine horn in virgin, pregnant, and lactating rats," *Microscopy Research and Technique*, vol. 63, no. 4, pp. 244–252, 2004.

[51] L. Marson, "Central nervous system neurons identified after injection of pseudorabies virus into the rat clitoris," *Neuroscience Letters*, vol. 190, no. 1, pp. 41–44, 1995.

[52] S. M. Altschuler, D. A. Ferenci, R. B. Lynn, and R. R. Miselis, "Representation of the cecum in the lateral dorsal motor nucleus of the vagus nerve and commissural subnucleus of the nucleus tractus solitarii in rat," *Journal of Comparative Neurology*, vol. 304, no. 2, pp. 261–274, 1991.

[53] F. Appia, W. R. Ewart, B. S. Pittam, and D. L. Wingate, "Convergence of sensory information from abdominal viscera in the rat brain stem," *American Journal of Physiology*, vol. 251, no. 2, pp. G169–G175, 1986.

[54] C. H. Hubscher and K. J. Berkley, "Responses of neurons in caudal solitary nucleus of female rats to stimulation of vagina, cervix, uterine horn and colon," *Brain Research*, vol. 664, no. 1-2, pp. 1–8, 1994.

[55] M. Ortega-Villalobos, M. Garcia-Bazan, L. P. Solano-Flores, J. G. Ninomiya-Alarcon, and R. Guevara-Guzman, "Vagus nerve afferent and efferent innervation of the rat uterus: an electrophysiological and HRP study," *Brain Research Bulletin*, vol. 25, no. 3, pp. 365–371, 1990.

[56] J. J. Collins, C. E. Lin, H. R. Berthoud, and R. E. Papka, "Vagal afferents from the uterus and cervix provide direct connections to the brainstem," *Cell and Tissue Research*, vol. 295, no. 1, pp. 43–54, 1999.

[57] M. A. Vizzard, M. Brisson, and W. C. de Groat, "Transneuronal labeling of neurons in the adult rat central nervous system following inoculation of pseudorabies virus into the colon," *Cell and Tissue Research*, vol. 299, no. 1, pp. 9–26, 2000.

[58] H. B. Patisaul, M. Melby, P. L. Whitten, and L. J. Young, "Genistein affects ERβ- but not ERα-dependent gene expression in the hypothalamus," *Endocrinology*, vol. 143, no. 6, pp. 2189–2197, 2002.

[59] Y. Hosoya, Y. Sugiura, N. Okado, A. D. Loewy, and K. Kohno, "Descending input from the hypothalamic paraventricular nucleus to sympathetic preganglionic neurons in the rat," *Experimental Brain Research*, vol. 85, no. 1, pp. 10–20, 1991.

[60] F. Esteves, D. Lima, and A. Coimbra, "Structural types of spinal cord marginal (lamina I) neurons projecting to the nucleus of the tractus solitarius in the rat," *Somatosensory and Motor Research*, vol. 10, no. 2, pp. 203–216, 1993.

[61] L. Rinaman, J. P. Card, J. S. Schwaber, and R. R. Miselis, "Ultrastructural demonstration of a gastric monosynaptic vagal circuit in the nucleus of the solitary tract in rat," *Journal of Neuroscience*, vol. 9, no. 6, pp. 1985–1996, 1989.

[62] R. A. Travagli, G. E. Hermann, K. N. Browning, and R. C. Rogers, "Brainstem circuits regulating gastric function," *Annual Review of Physiology*, vol. 68, pp. 279–305, 2006.

[63] E. J. Spary, A. Maqbool, and T. F. C. Batten, "Expression and localisation of somatostatin receptor subtypes sst1-sst5 in areas of the rat medulla oblongata involved in autonomic regulation," *Journal of Chemical Neuroanatomy*, vol. 35, no. 1, pp. 49–66, 2008.

[64] C. Streefland, F. W. Maes, and B. Bohus, "Autonomic brainstem projections to the pancreas: a retrograde transneuronal viral tracing study in the rat," *Journal of the Autonomic Nervous System*, vol. 74, no. 2-3, pp. 71–81, 1998.

[65] M. A. Herman, M. Niedringhaus, A. Alayan, J. G. Verbalis, N. Sahibzada, and R. A. Gillis, "Characterization of noradrenergic transmission at the dorsal motor nucleus of the vagus involved

in reflex control of fundus tone," *American Journal of Physiology*, vol. 294, no. 3, pp. R720–R729, 2008.

[66] H. Y. Chang, H. Mashimo, and R. K. Goyal, "Musings on the wanderer: what's new in our understanding of vago-vagal reflex? IV. Current concepts of vagal efferent projections to the gut," *American Journal of Physiology*, vol. 284, no. 3, pp. G357–G366, 2003.

[67] B. Pan, J. M. Castro-Lopes, and A. Coimbra, "C-fos expression in the hypothalamo-pituitary system induced by electroacupuncture or noxious stimulation," *NeuroReport*, vol. 5, no. 13, pp. 1649–1652, 1994.

[68] L. W. Swanson and H. G. J. M. Kuypers, "The paraventricular nucleus of the hypothalamus: cytoarchitectonic subdivisions and organization of projections to the pituitary, dorsal vagal complex, and spinal cord as demonstrated by retrograde fluorescence double-labeling methods," *Journal of Comparative Neurology*, vol. 194, no. 3, pp. 555–570, 1980.

[69] L. Wang, V. Martínez, M. Larauche, and Y. Taché, "Proximal colon distension induces Fos expression in oxytocin-, vasopressin-, CRF- and catecholamines-containing neurons in rat brain," *Brain Research*, vol. 1247, no. C, pp. 79–91, 2009.

[70] R. J. Traub, E. Silva, G. F. Gebhart, and A. Solodkin, "Noxious colorectal distention induced-c-Fos protein in limbic brain structures in the rat," *Neuroscience Letters*, vol. 215, no. 3, pp. 165–168, 1996.

[71] V. Sinniger, C. Porcher, P. Mouchet, A. Juhem, and B. Bonaz, "c-fos and CRF receptor gene transcription in the brain of acetic acid-induced somato-visceral pain in rats," *Pain*, vol. 110, no. 3, pp. 738–750, 2004.

[72] I. Gerendai, I. E. Tóth, K. Kocsis, Z. Boldogköi, I. Medveczky, and B. Halász, "Transneuronal labelling of nerve cells in the CNS of female rat from the mammary gland by viral tracing technique," *Neuroscience*, vol. 108, no. 1, pp. 103–118, 2001.

[73] P. Li and J. C. Longhurst, "Neural mechanism of electroacupuncture's hypotensive effects," *Autonomic Neuroscience: Basic & Clinical*, vol. 157, no. 1-2, pp. 24–30, 2010.

[74] S. Uchida, F. Kagitani, and H. Hotta, "Mechanism of the reflex inhibition of heart rate elicited by acupuncture-like stimulation in anesthetized rats," *Autonomic Neuroscience: Basic & Clinical*, vol. 143, no. 1-2, pp. 12–19, 2008.

[75] D. C. Bolser, S. F. Hobbs, M. J. Chandler, W. S. Ammons, T. J. Brennan, and R. D. Foreman, "Convergence of phrenic and cardiopulmonary spinal afferent information on cervical and thoracic spinothalamic tract neurons in the monkey: implications for referred pain from the diaphragm and heart," *Journal of Neurophysiology*, vol. 65, no. 5, pp. 1042–1054, 1991.

[76] J. Ellrich, O. K. Andersen, K. Messlinger, and L. Arendt-Nielsen, "Convergence of meningeal and facial afferents onto trigeminal brainstem neurons: an electrophysiological study in rat and man," *Pain*, vol. 82, no. 3, pp. 229–237, 1999.

[77] R. D. Foreman, R. W. Blair, and R. N. Weber, "Viscerosomatic convergence onto T2-T4 spinoreticular, spinoreticular-spinothalamic, and spinothalamic tract neurons in the cat," *Experimental Neurology*, vol. 85, no. 3, pp. 597–619, 1984.

[78] S. F. Hobbs, M. J. Chandler, D. C. Bolser, and R. D. Foreman, "Segmental organization of visceral and somatic input onto C3-T6 spinothalamic tract cells of the monkey," *Journal of Neurophysiology*, vol. 68, no. 5, pp. 1575–1588, 1992.

[79] M. Takahashi and T. Yokota, "Convergence of cardiac and cutaneous afferents onto neurons in the dorsal horn of the spinal cord in the cat," *Neuroscience Letters*, vol. 38, no. 3, pp. 251–256, 1983.

[80] R. Norgren, "Projections from the nucleus of the solitary tract in the rat," *Neuroscience*, vol. 3, no. 2, pp. 207–218, 1978.

[81] G. J. ter Horst, P. de Boer, P. G. M. Luiten, and J. D. van Willigen, "Ascending projections from the solitary tract nucleus to the hypothalamus. A phaseolus vulgaris lectin tracing study in the rat," *Neuroscience*, vol. 31, no. 3, pp. 785–797, 1989.

[82] J. F. R. Paton, P. Boscan, A. E. Pickering, and E. Nalivaiko, "The yin and yang of cardiac autonomic control: vago-sympathetic interactions revisited," *Brain Research Reviews*, vol. 49, no. 3, pp. 555–565, 2005.